bulletin 43

guide to good practice

Structural connections for precast concrete buildings

Structural connections for precast concrete buildings

Guide to good practice prepared by

Task Group 6.2

February 2008

Subject to priorities defined by the Technical Council and the Presidium, the results of ***fib***'s work in Commissions and Task Groups are published in a continuously numbered series of technical publications called 'Bulletins'. The following categories are used:

category	minimum approval procedure required prior to publication
Technical Report	approved by a Task Group and the Chairpersons of the Commission
State-of-Art Report	approved by a Commission
Manual, Guide (to good practice) or Recommendation	approved by the Technical Council of ***fib***
Model Code	approved by the General Assembly of ***fib***

Any publication not having met the above requirements will be clearly identified as preliminary draft.

This Bulletin N° 43 was approved as an ***fib*** Guide to good practice by the Technical Council of ***fib*** in June 2006

This report was drafted by Task Group 6.2, *Structural connections for precast concrete*, in Commission 6, *Prefabrication*:

Björn Engström (Convener, Chalmers Univ. of Technology, Sweden)

Sven Alexander (Norway), Andrzej Cholewicki (Building Research Institute (ITB), Poland), André De Chefdebien (LB7, France), Bruno Della Bella (Precompressi Centro Nord SpA, Italy), Kim S. Elliott (Univ. of Nottingham, United Kingdom), David Fernández Ordoñez (Prefabricados Castelo S.A., Spain), Marco Menegotto (Univ. La Sapienza, Roma, Italy), Michael Newby (Holmes Consulting Group, New Zealand), Gunnar Rise (Sweden), Harry Romanes (Unicast Concrete Ltd.), Arne Skjelle (Construction Products Association, Norway), Spyros Tsoukantas (Greece), N. Jan A. Vambersky (Corsmit Consulting Engineers, The Netherlands), Arnold van Acker (Belgium), Leidulv Vinje (Spenncon AS Trondelag, Norway)

Full address details of Task Group members may be found in the ***fib*** Directory or through the online services on ***fib's*** website, www.fib-international.org.

Cover image: Beam-column connection and floor-beam connection in precast concrete skeletal frame

First published in 2008 by the International Federation for Structural Concrete (*fib*)
Postal address: Case Postale 88, CH-1015 Lausanne, Switzerland
Street address: Federal Institute of Technology Lausanne - EPFL, Section Génie Civil
Tel +41 21 693 2747 • Fax +41 21 693 6245
fib@epfl.ch • www.fib-international.org

ISSN 1562-3610
ISBN 978-2-88394-083-3

Printed by Sprint-Digital-Druck, Stuttgart

Foreword

Connections are among the most essential parts in precast structures. Their performance relates to the structural limit states, as well as to manufacture, erection and maintenance of the structure itself. Proper design of connections is one major key to a successful prefabrication.

The literature on this matter mostly illustrates classical solutions, often well known, but an explanation of a general design philosophy for the design of connections was necessary. In fact, the engineer, confronted with particular problems in his daily practice, does not always have the theoretical basis to find the most appropriate solutions.

fib Commission 6 "Prefabrication" therefore formed a Task Group – TG 6.2 – who drafted this Guide to Good Practice with the goal of filling this gap. Its philosophy focuses on the knowledge of the behaviour of a whole structure, of the mechanisms and paths of force transfer within the connections and of their interaction with the structural members. Indeed, such knowledge is the base for assessing the safety and reliability of usual types of connections and to develop innovative design.

The Task Group has been working during several years, to collect and discuss information and studies about the different aspects intervening in the design of structural connections for precast concrete structures. The result is a voluminous document, with a comprehensive survey of basic principles and design guidelines, illustrated by several examples of adequate solutions.

Throughout these years, the Commission, chaired by the undersigned persons, supported the activity of the Task Group with comments and discussion. However the merit for the finalization of the work into this Guide must be acknowledged as mainly due to the tenaciousness of its Convener, Prof. Björn Engström of Chalmers University, Sweden.

Arnold Van Acker
Past Chairman

Gunnar Rise
Past Chairman

Marco Menegotto
Chairman

Commission 6 - Prefabrication

Acknowledgement

Several figures in this publication have been provided by the Norwegian Association for Precast Concrete, "Betongelementforeningen" and Chalmers University of Technology. A considerable number of sketches have been redrawn by Holmes Consulting Group in Auckland, New Zealand. This valuable support is gratefully acknowledged. Other figures and photos have been provided by the Task Group members.

Contents

PART II Basic force transfer mechanisms

Part I

General considerations and design philosophy

1 Introduction

1.1 The role of structural connections in prefabricated concrete building structures

Precast concrete systems enable fast and effective completion of many different types of buildings and other structures. The type of structures referred to in this document is shown in Fig. 1-1. These are skeletal frames, wall frames and portal frames.

Fig. 1-1: Examples of skeletal, wall and portal frames

It is a misconception to think of precast technology only as a mere translation of cast *insitu* into a number of precast elements that are assembled on the site in a manner such that the initial cast *insitu* concept is obtained. This misconception is due to a lack of understanding of the design philosophy and the special characteristics and rules associated with precast concrete design and construction.

Effective design and construction is achieved through the use of suitable connections to cater for all service, environmental and ultimate load conditions. The structural systems are composed of precast concrete elements that are joined together in a mechanical way, for example using bolts, welds, reinforcing steel, and grout and concrete in the joints, as shown in Fig. 1-2. However, connecting the elements together is not just a question of fixing the elements to each other, but it is to ensure the structural integrity of the whole structure.

Fig. 1-2: Grouted dowels (left) and bolted steel plates are just two ways of making mechanical connections

In the completed building the structural connections will form an essential part of the structural system. The structural response will depend on the behaviour and the characteristics of the connections. The structural layout, the arrangement of stabilising units, the design of the structural system (and its sub-systems) and the design and detailing of the connections must be made consistently and with awareness of the intended structural behaviour. To achieve a satisfactory design the designer should understand how the connections influence the flow of forces through a structure under vertical and /or horizontal loads. The main purpose of the structural connections is therefore to transfer forces between the precast elements in order to enable the intended structural interaction when the system is loaded.

The structural connection interacts closely with the adjacent structural elements, and the design and detailing of the connection is influenced by the design and detailing of the adjacent elements that are to be connected. Therefore, the connections and elements must be designed and detailed implicitly so that the flow of forces is not only logical and natural, but the forces to be resisted by the connection can be transferred into the element and further on to the overall load-resisting system.

Connections can be classified in different ways depending on, for instance, the type of elements that are to be connected, or the principal force that should be resisted. Standardised types of structural connections are often listed in design handbooks or catalogues from precast element producers, although this is not just a question of selecting an appropriate solution from listed standard solutions. To improve the detailing, to find proper connections in specific situations when the standard solutions do not fit, and to develop innovative solutions, the designer must be prepared to work with connections in a more creative way.

Within a single connection there may be several load transmitting joints, and so it is first necessary to distinguish between a ‘joint’ and a ‘connection’. A ‘joint’ is the interface between two or more structural elements, where the action of forces (e.g. tension, shear, compression) and or moments may take place. A ‘connection’ is an assembly, comprising one or more interfaces and parts of adjoining elements, designed to resist the action of forces or moments. The design of the connection is therefore a function of both the structural elements and of the joints between them. This is explained in Fig. 1-3,

for the case of a beam-to-column connection, where the zone of the connection may extend quite far from the contact surfaces. In addition to the actions of forces connection design must consider the hazards of fire, accidental damage, effects of temporary construction and inaccurate workmanship, and durability.

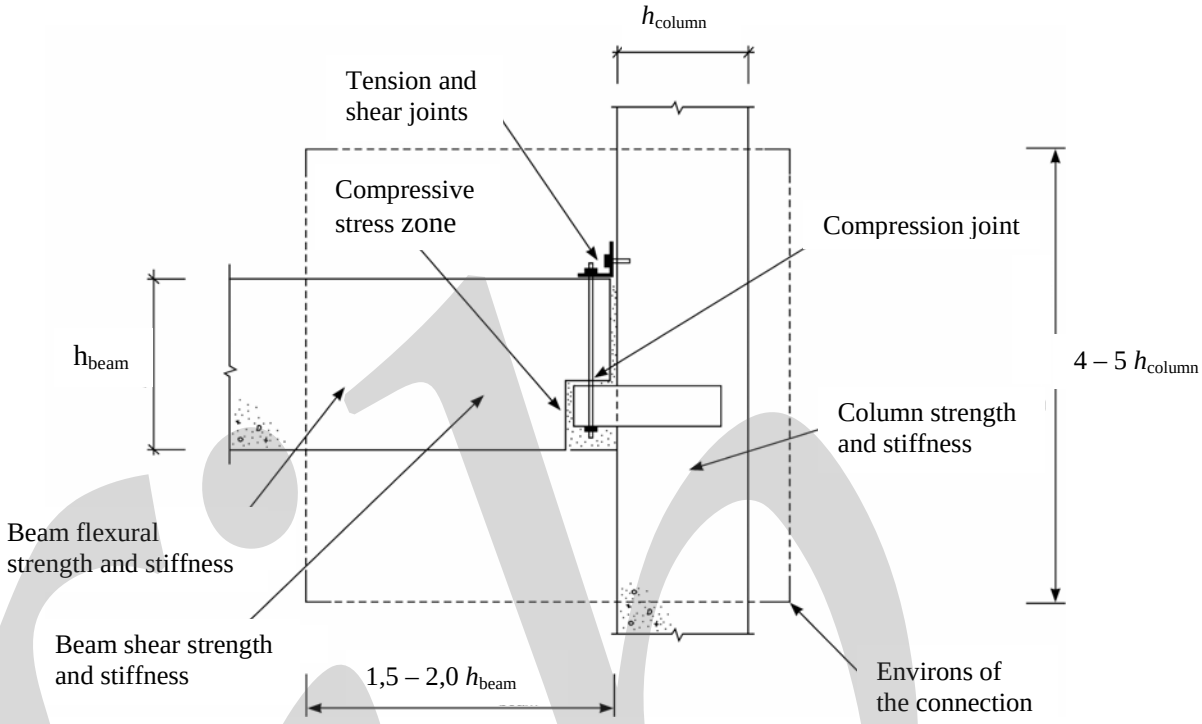

Fig. 1-3: Definition of 'joints' and 'connections'

Unlike cast *insitu* concrete work, the design philosophy for precast connections concerns both the structural requirements and the chosen method of construction. In many instances the working practices in the factory strongly influence connection design! Design philosophy depends on several factors, some of which may seem unlikely to the inexperienced:
the stability of the frame. Unbraced portal and skeletal precast frames require moment resisting foundations, whereas braced frames and cross-wall frames do not

- the structural layout of the frame. The number and available positions of columns, walls, cores and other bracing elements may dictate connection design
- moment continuity at ends of beams or slabs. Cantilevered elements always require moment resisting end connections (or otherwise beam continuity) whereas beams simply supported at both ends do not. Unbraced frames up to a certain height may be designed using rigid (or semi-rigid) end connections
- fire protection to important bearings and rebars
- appearance of the connection and minimising structural zones, e.g. 'hidden' connections must be designed within the dimensions of the elements, whereas 'visible' connections are outside the elements
- ease and economy of manufacture
- the requirements for temporary stability to enable frame erection to proceed, and the need for immediate fixity/stability, e.g. torsional restraint at the ends of beams during floor erection
- site access, or lack of it, may influence structural design, and hence connection design
- the chosen method(s) of making joints, e.g. grouting, bolting, welding, and the type of bearing(s) used
- the plant capabilities of hoisting and lifting

1.2 Aim and scope

The principal aim of this guide is to encourage good practice in the design of structural connections in precast concrete structures. This is achieved through a basic understanding of structural connections as parts of the overall structural system and subsystems, such as floors diaphragms, walls, cores and moment-frames.
The general design philosophy for concrete structures outlined in the CEB-FIP Model Code 1990 [CEB-FIP (1992)] is used as a basis for this design guide and models appearing in this Model Code is generally applied and further explained and developed.
This design guide is limited to structural connections that are essential parts of the overall structural system and structural subsystems. Non-structural connections are outside the scope of this publication. For fasteners in general reference is made to CEB (1994, 1997). The basic force transfer mechanisms presented here are, however, very often of major importance also in non-structural connections, and so the information is relevant at least for some types of non-structural connections.
This design guide is prepared for precast concrete buildings. This means that the general design philosophy presented here is meant for building structures and not for other types of structures like bridges, foundations, containers, etc. Of course, the information of basic force transfer mechanisms can also be applicable to other types of prefabricated structures.
The main focus is on the design of structural connections with regard to their structural function in ordinary design situations in the serviceability and ultimate limit states, and in accidental/abnormal design situations, like fire, lack of fit and impact/accidental loads. Other aspects considered include production methods, handling and site erection of elements, building physics, durability and maintenance. One section is devoted to the behaviour of connections under cyclic action; however the detailed dynamic and seismic design of connections is beyond the scope of this publication. Here instead reference is made to fib (2003b).

1.3 Outline of the document

This design guide consists of two parts; the first part concerns general considerations and philosophy in the design of structural connections, and the second part deals with basic force transferring mechanisms within structural connections.

The approach in Part I is to first identify the role of the connections in the structural system in order to reach the intended structural behaviour. Therefore Chapter 2 presents the major structural systems and subsystems, together with the conceptual design of the structural systems. Chapter 3 introduces the general design considerations and design philosophy at the local level. Other aspects that normally influence the design specification are outlined in Chapter 4. These include production, transportation and erection of the precast elements, aesthetics, and the service function and durability of the completed building. Chapter 5 concerns structural integrity in the event of fire, accidental loads or seismic action.

Part II is devoted to basic force transferring mechanisms; transfer of compressive forces in Chapter 6, of tensile forces in Chapter 7, of shear forces in Chapter 8, and of flexural and torsional moments in Chapter 9. In each of these chapters various examples of structural connections are included and discussed.

2 Precast structural systems and structural interaction

2.1 Basic precast concrete systems

Precast concrete building structures are composed of some basic types of structural systems. These systems can be combined in different ways to obtain an appropriate and effective structural concept that fulfils the needs of specific buildings. The most common systems are:

- beam and column systems (beam elements, column elements, connections)
- floor and roof systems (floor elements, roof elements, connections)
- bearing wall systems (wall elements, connections)
- façade systems (façade wall elements, connections)

The above list is not unique as there are many variations possible to achieve the same objectives that architects and engineers are now successfully exploring, such as the use of arches and rigid portal frames. Façades are sometimes load-bearing, providing also the lateral stability, but they can also be used without a load-bearing function. Other less common precast systems are:

- frame systems (frame elements, connections)
- cell systems (cell elements, connections)

2.1.1 Beam and column systems

Beam and column systems are composed of columns and beams, although the beams are more like rafters in the case of Fig. 2-1 a where the column height may correspond to more than one storey. The system in Fig. 2-1 b forms the basis of the skeletal frame. The connections in these systems are:

- beam to column
- beam to beam
- column to column
- column to base

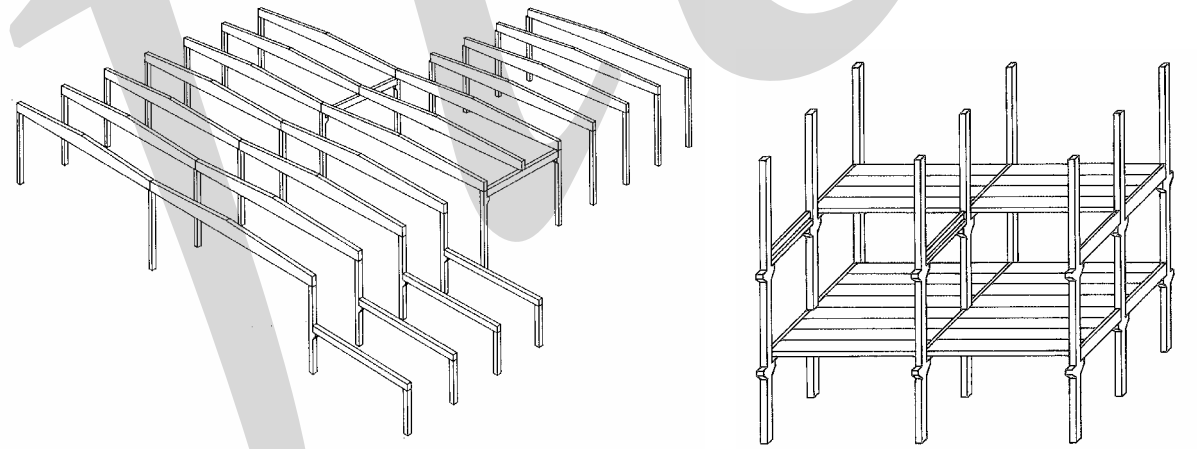

a) b)

Fig. 2-1: Beam/column systems, a) single storey columns, b) multi-storey columns

2.1.2 Floor and roof systems

The main purpose of floor and roof systems is to carry vertical load to the vertical load-resisting structural elements. Besides, precast floors and roofs are often used as essential parts of the stabilising system to transfer horizontal loads by diaphragm action to the stabilising units, see Sections 2.2.2 and 2.3.1. The most common floor systems are hollow-core floors and double-tee floors, see Fig. 2-2. Double-tee units are also used in roof systems. The connections of these systems are:

- slab to slab at longitudinal interior joints
- slab to edge element at longitudinal edge
- slab to slab at interior support
- slab to end support

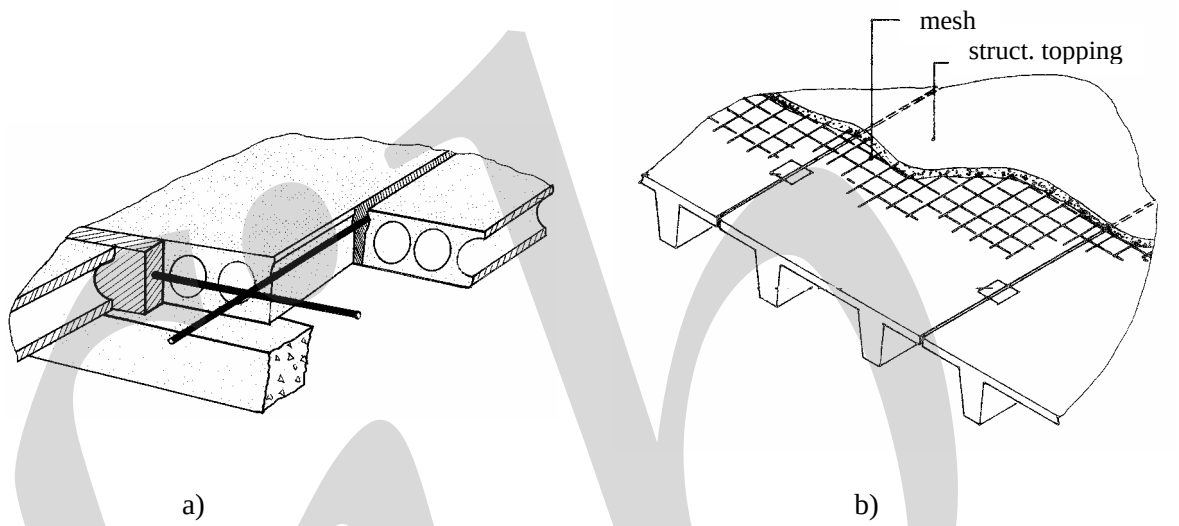

Fig. 2-2: Typical floor systems, a) hollow core floor system, b) double-T floor system

The elements in a floor system will not resist loads separately from each other, but a degree of interaction between adjacent elements is desired. To obtain a transverse distribution of load effects in case of concentrated loads and prevent uneven vertical displacements at the longitudinal joints, the floor connections must be designed to develop *shear key action* that ensures the interaction between adjacent elements, see Fig. 2-3.

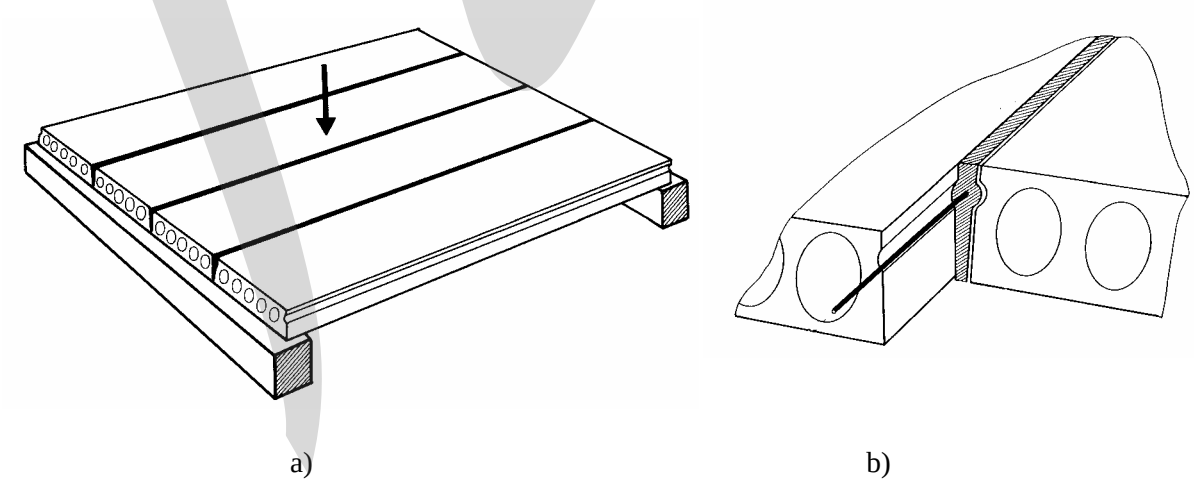

Fig. 2-3: Interaction and transverse distribution of load effects between adjacent precast hollow core floor elements are achieved by shear transfer across the longitudinal joints, a) transverse load distribution, b) joint detail with longitudinal shear key

In composite floor plate floors (also known as *half-slab*), precast concrete floor plates are used as formwork for the cast *insitu* part and remain integrated in the composite floor section, see Fig. 2-4. Composite action depends on the shear transfer in the horizontal joint between the precast plate and the cast insitu concrete part, see Section 2.3.4. There is no requirement for design of longitudinal joint between the plates as the topping is continuous over the precast joint lines.

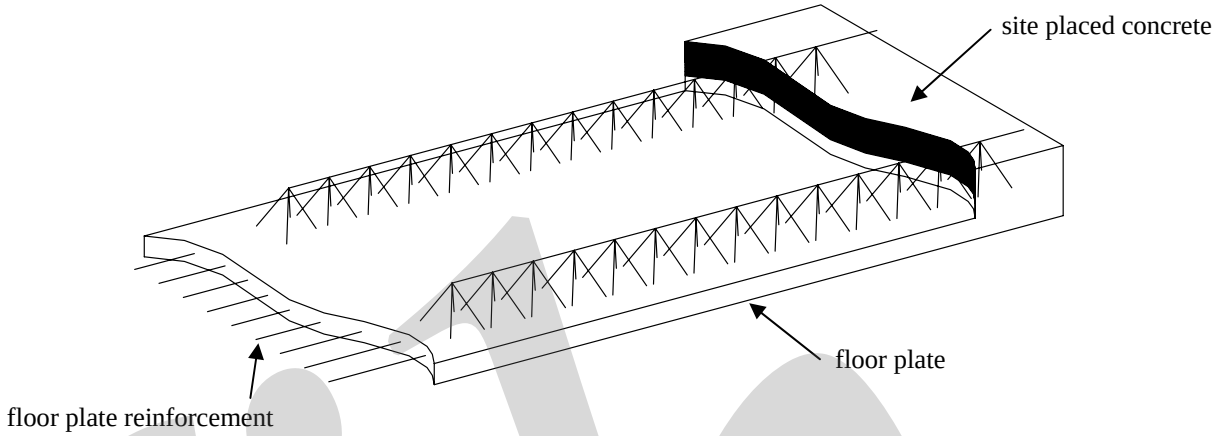

Fig. 2-4: Composite floor plate floor system with lattice girders

2.1.3 Wall systems

The main types of precast concrete wall systems are shown in Fig. 2-5 as façades and interior cross-walls. Walls can be classified as bearing and non-bearing walls. Bearing walls are used to support bridging components like floors, roofs or beams, see Fig. 2-5. Examples of non-bearing walls are shown in Fig. 2-6.

The connections of these systems are:

- wall to wall at interior and exterior vertical joints
- wall to wall at interior and exterior horizontal joints
- wall to base/foundation

a) b)

Fig: 2-5: Examples of bearing wall systems, a) load-bearing façade wall, b) load-bearing cross-walls

The connections of non-bearing wall systems are mainly façade to beam – rarely are they connected to columns.

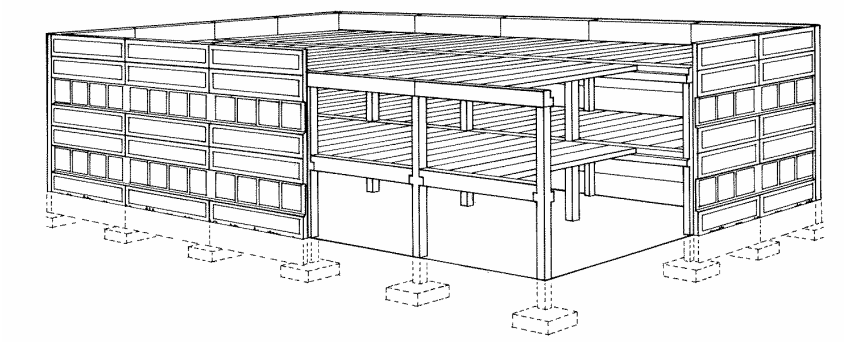

Fig. 2-6: Example non-bearing façade walls

Non-bearing walls are normally designed to carry their dead weight, which means that the connections at horizontal joints need to resist the weight of the wall elements above this level of the wall. However, as an alternative, non-bearing façade walls might be fixed to the adjacent load bearing system in such a way that the dead weight of each wall element is supported by the main system.

Prefabricated walls can be used as part of the stabilising system to resist horizontal loads in its own plane. In that case the prefabricated wall should behave as one structural unit composed of interacting wall elements, see Fig. 2-7. This structural interaction within the wall needs to be secured by structural connections that resist the required shear forces, tensile forces and compressive forces.

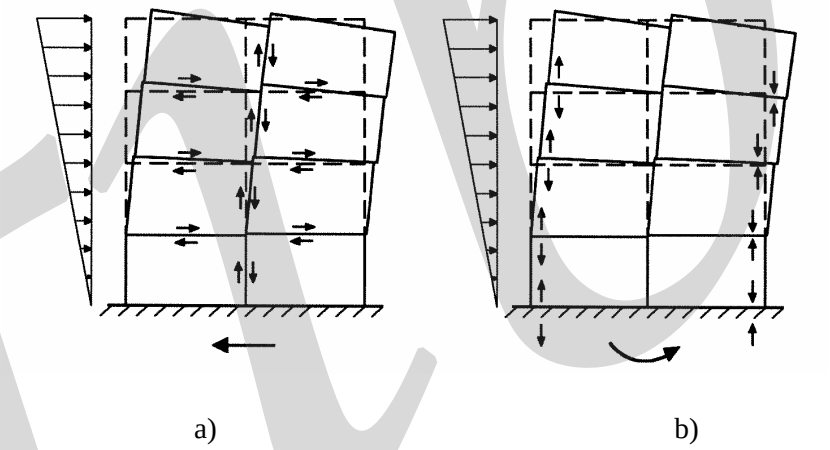

Fig. 2-7: In-plane action of prefabricated wall, a) shear forces, b) tensile and compressive forces

2.1.4 Moment resisting frame systems

Precast concrete moment-resisting frame systems are found in skeletal or portal systems where ‘frame action’ is used for the stabilisation. This is obtained by combining spatial H-shaped elements, L-shape elements, or portal frames, etc. with monolithic connections at the intersections between beams and columns within the element. The elements are connected in locations where flexural resistance is not required at points at contraflexure.

Alternatively the connections between beam and column elements may be designed and detailed to obtain the required continuity and moment resisting capacity. However, this often makes the connections complicated and costly, and such solutions seldom appear in practice.

2.1.5 Cell systems

Precast concrete cell systems are composed of closed cell elements or open cell elements with U- or L-section, see Fig. 2-8. Complete structures can be made by combining cell elements. However, it is more common to use cell elements for specific parts of a structure, for instance wet areas, and combine these with ordinary walls and floor systems.

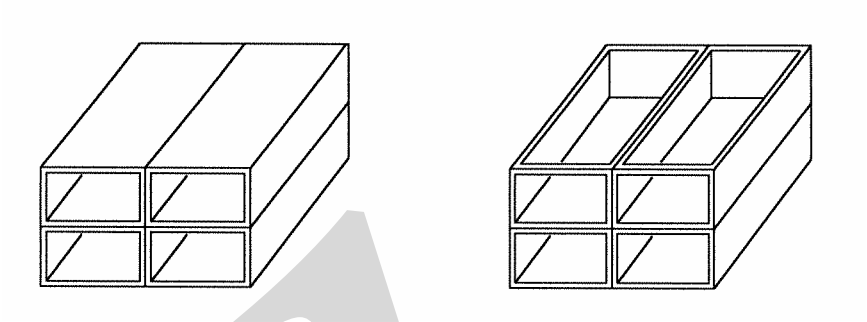

a) b)

Fig. 2-8 Prefabricated cell systems, a) closed cell elements, b) open cell elements with U-section

2.2 Structural systems

2.2.1 Conceptual design

One of the biggest advantages of precast concrete technology is the speed of construction – fixing rates of up to 1000 m^2 floor area per week are common. But to achieve this it is essential that simple and easy to handle solutions are pursued at all stages of the construction process, from design to manufacture, transportation and erection. This is even more important with regard to connections where the use of pinned jointed connections and simply supported beams is the most favoured solution for framed structures. In wall frames and cell structures, the connections are too pinned in the out-of-plane directions, but are moment resisting in-plane.

The main structural difference between cast *insitu* and precast structures lies in their structural continuity. The inherent continuity of cast *insitu* buildings is an automatic consequence of the construction process. For precast structures, there must be a conscious effort undertaken to ensure structural continuity when precast elements are put in place. The connections act as bridging links between the elements, forming together structural chains linking every element to the stabilising elements, such as shear walls and cores.

For example in the braced frames shown in Fig. 2-9 between them the elements and connections form a chain of horizontal forces and reactions to transmit the horizontal load to the ground. The reactions at each floor level are determined as shown in Fig. 2-10 such that the entire design method for the stability of a precast structure is described in these four diagrams.

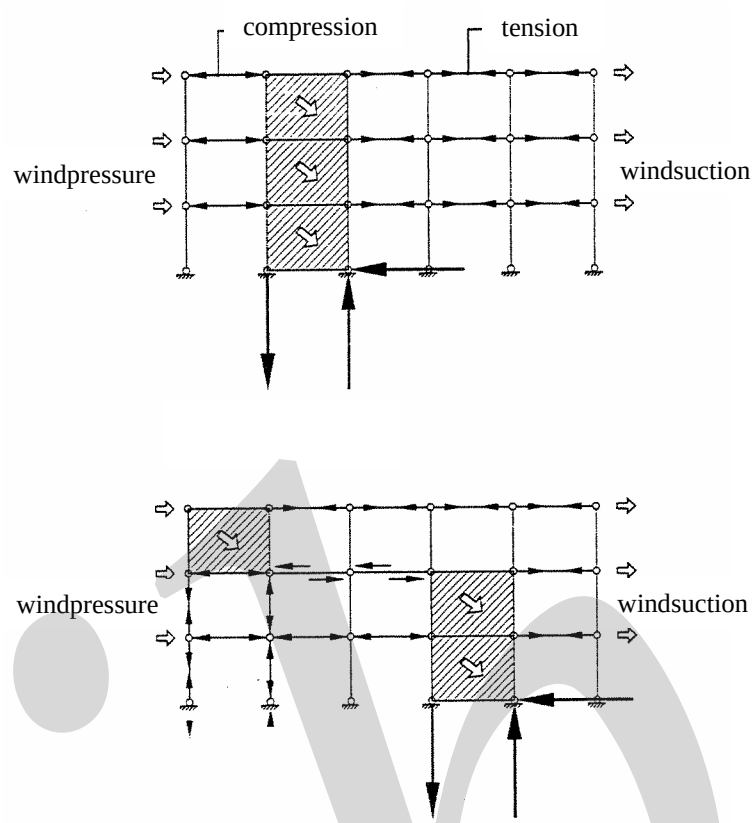

Fig. 2-9: Braced frame. The stability in precast concrete technology requires continuous attention

Finally, the precast structure must be robust and adequately designed against progressive collapse, structural failure, cracking and unacceptable deformations The stability of the system and its parts has to be ensured at all stages during the erection as during its service life.

As in every design process the steps are iterative and cyclic, starting with rough conceptual lines and decisions and ending up with design of details and fine-tuning adjustments.

The first and very important part is the choice of structural concept as envisaged by the architect. The primary functional aspects of the building, its form, mass and the desired architectural appearance have to be considered. Early consultation with the architect is very important in order to bring the structural and precast concrete concepts in time to make concessions where necessary.

At this stage the important decisions are:

- position and the approximate requirements for the stabilising elements
- the need for expansion joints
- grid distances
- span directions of slabs and beams
- positions of columns and walls
- use of load bearing walls and/or facades

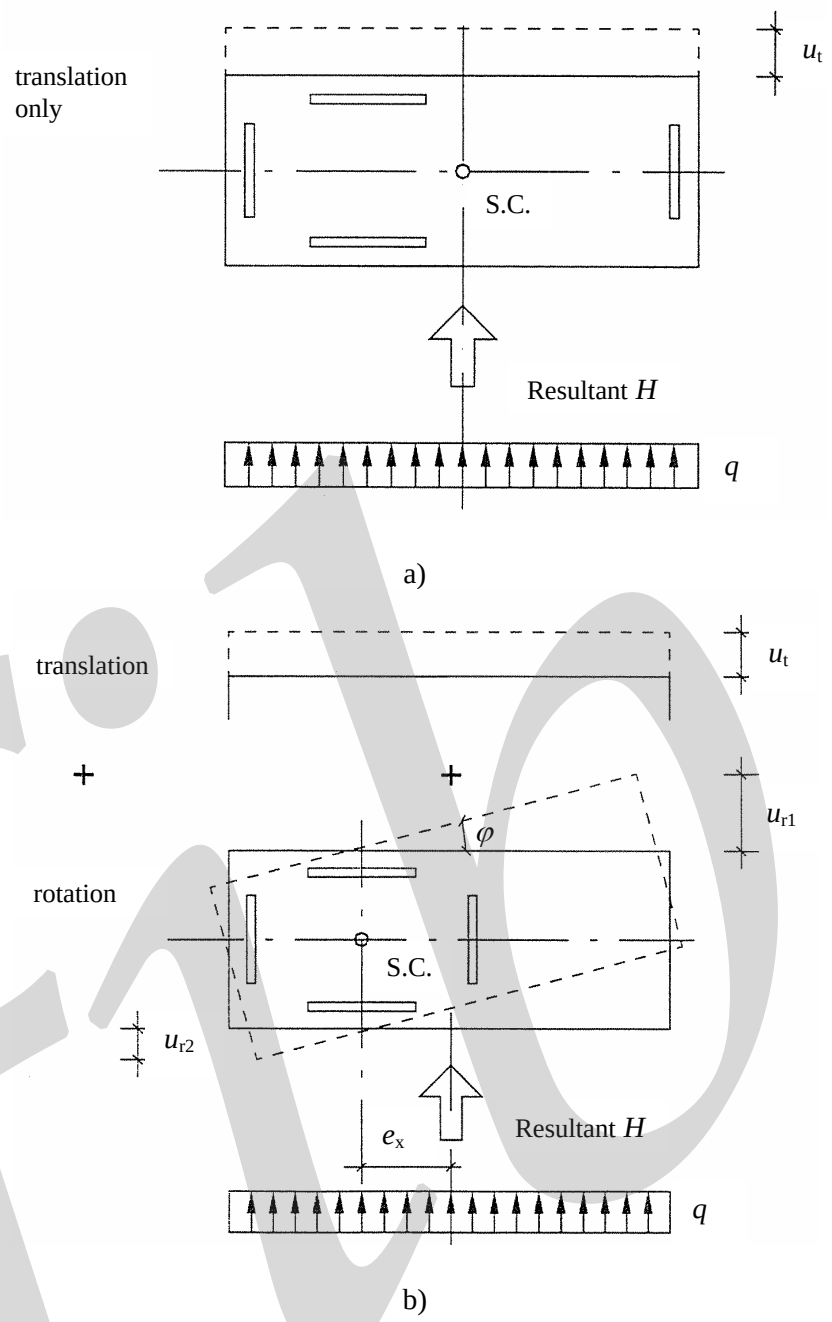

Fig. 2-10: Reactions in shear walls due to horizontal load, a) when the resultant H of the horizontal load passes through the shear centre (S.C.), there is only translation, b) rotation is due to eccentric positioning of the stabilising elements (the horizontal load resultant does not pass through the shear centre), the total deformation is translation + rotation

The positions of shear walls and cores should be according to Fig. 2-10 a, rather than Fig. 2-10 b, in order to avoid torsional sway, which will eventually lead to large connection forces around the walls. In this way evenly distributed stresses in the stabilising elements can be achieved resulting in:

- balanced design and repetition of connections in the stabilising elements
- equal horizontal sway
- equal angle of rotation of the structural elements such as columns, walls etc. following the horizontal deformation of the stabilising elements
- uniform detailing.

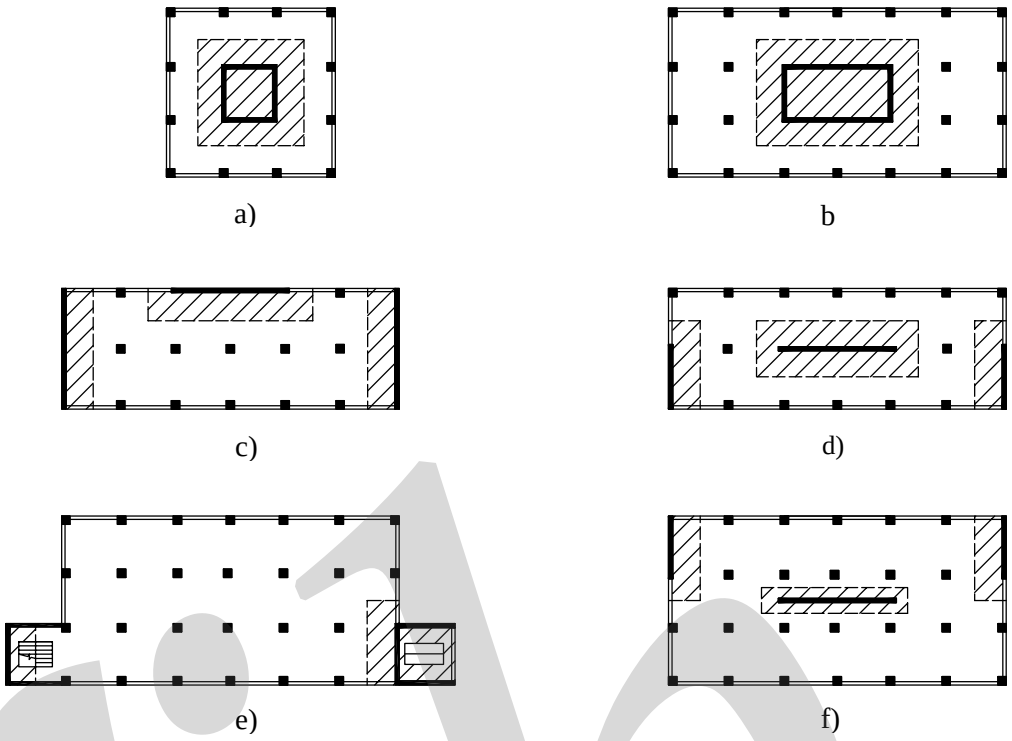

Fig. 2-11: Position of cores/shear walls in the plan of the building, a) good, b) good, c) good, d) satisfactory, two transversal walls have already moments due to eccentricity of the vertical load, e) bad, almost no vertical load, and/or eccentric vertical load, f) bad, almost no vertical load on the longitudinal shear wall

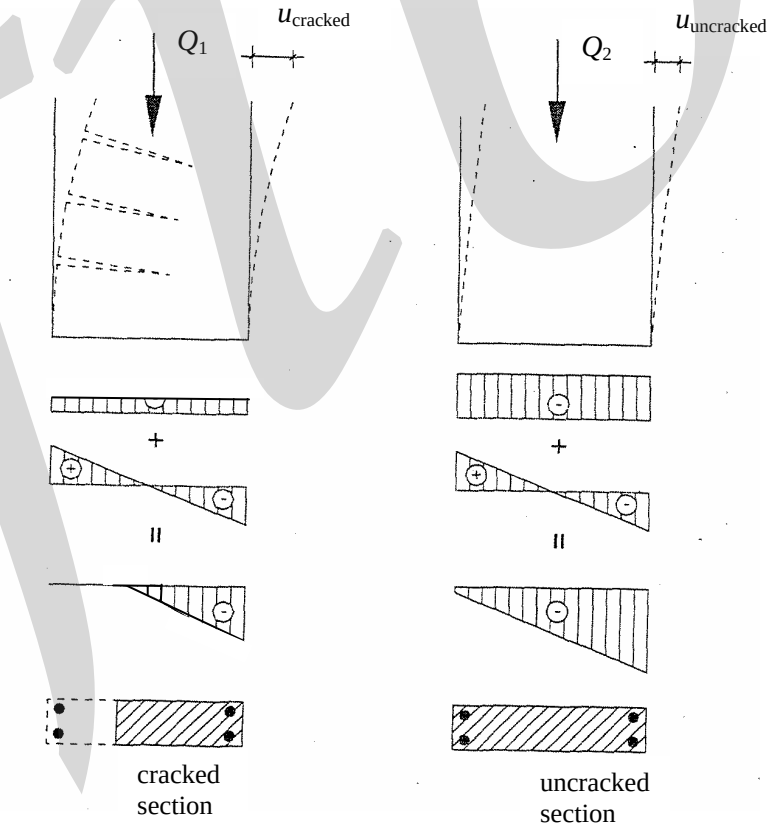

Fig. 2-12: In the case of a small vertical load on shear wall or core the concrete section will crack resulting in larger deformations or more reinforcement needed

It is the choice of the right force paths and the main structural scheme, which makes the further development of the precast concrete system and details a success or failure.

The structural engineer still has the freedom to position shear walls and cores and to choose spans of floors and beams in such a way that the gravity load acting on the cores and shear walls is large enough to eliminate uplifting forces and tensile stresses due to bending, see Fig. 2-11.

Tensile forces require more complicated and time-consuming connections, using for example reinforcing bars passing from one element to another, welding steel plates, bolted connections, post-tensioning, etc. Tensile stresses will cause opening of the joints or even cracking of the concrete in stabilising elements before the reinforcing steel bars will be activated to take the resulting force. Also the second moment of area of the cracked sections will be less than in the uncracked state, see Fig. 2-12. This leads to larger deformations of the stabilising elements and of the whole building. Compression forces on the other hand can be easily transferred from one element to another through, for instance insitu mortar joints, which are easy and cheap to make.

2.2.2 Force paths

For every external load applied to a structure it must be possible to identify a force path that links this load to its reaction in the foundation. This force must pass through structural elements and connections that can be regarded as a chain of components. When several loads act simultaneously there will be several force paths running side by side, and this makes it possible to speak about a flow of forces, see Figs. 2-10 and 2-11.

It is appropriate to examine the flow of forces under the vertical and horizontal loads separately and to superimpose the two solutions in the development of the structural system. The vertical loads are resisted by bridging elements roof and floor elements, beams, stairs) and supporting elements (columns and load-bearing walls)

For horizontal forces the structure must be provided with stabilizing units that are capable to resist the horizontal loads and link them to the reactions in the foundation.

The following components can be part of the stabilising system:

- fixed-end column (cantilever action)
- fixed-end core (cantilever action)
- fixed end slender wall (cantilever action)
- non-slender wall (diaphragm action)
- frames with moment-resisting joints (frame action)
- boxes (frame and diaphragm action)
- floor (diaphragm action)
- roof (diaphragm action)

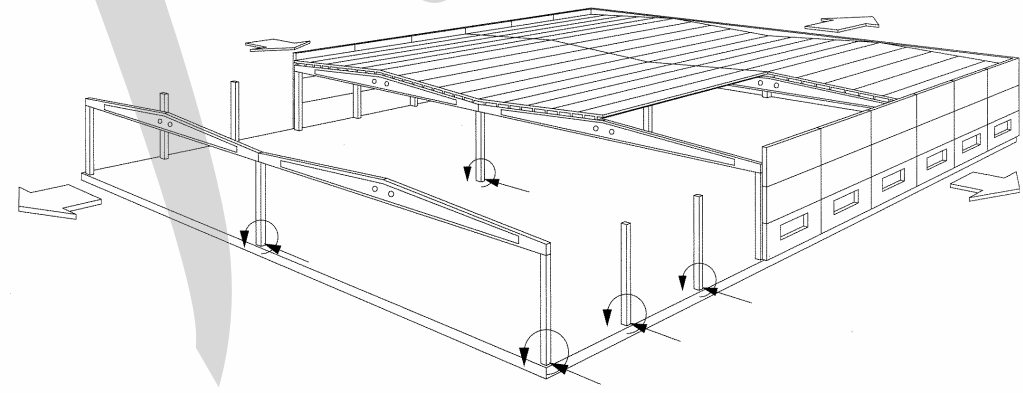

Fig. 2-13: Precast structure with fixed-end columns

A fixed-end moment-resisting column behaves as a cantilever when loaded horizontally as shown in Fig. 2-13. (It should be noted that the response of the system depends on how the wall elements are arranged and supported, compare with Fig. 3-8.) Reference is made to Section 9.5 for column base connections

In multi-storey structures the cores, staircase shafts or high slender walls can be used as stabilising units, Fig. 2-14. Such stabilising units are often composed of precast concrete wall elements designed as huge fixed-end cantilevered walls, secured by connections between the units. Staircase shafts can be composed by wall elements that are connected to become an interacting substructure. Solutions also exist where storey-high cell-elements are placed in open box format as shown in Fig. 2-15.

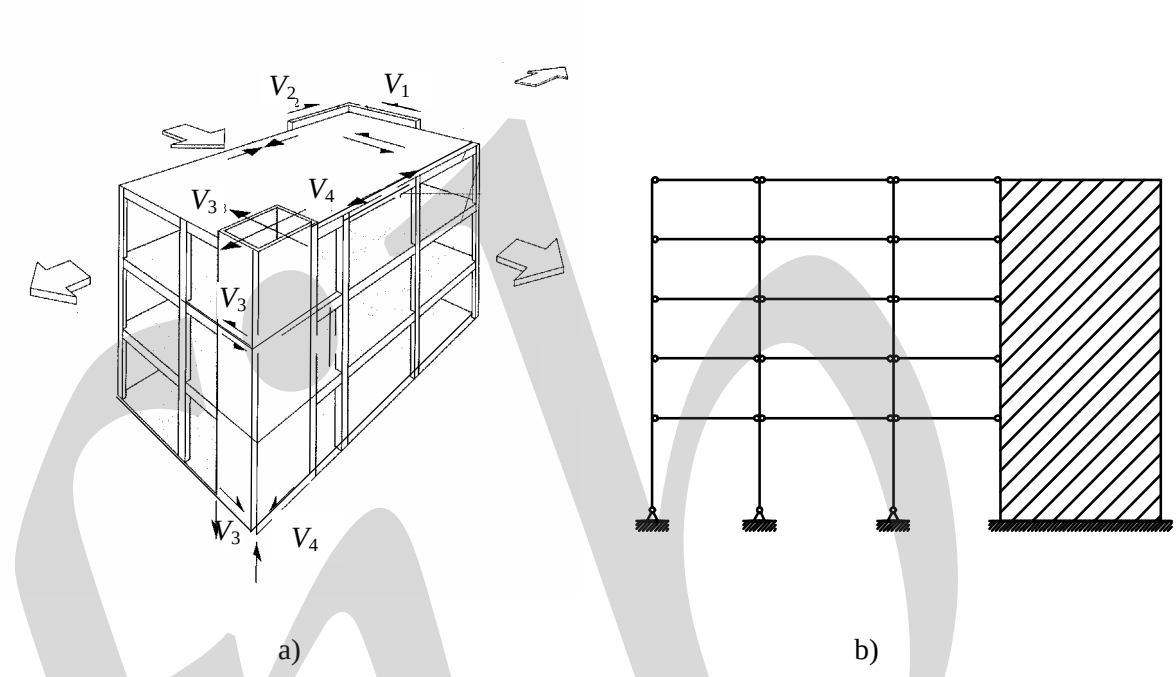

Fig. 2-14: Precast beam/column system stabilised by bracing units, a) multi-storey building b) calculation model

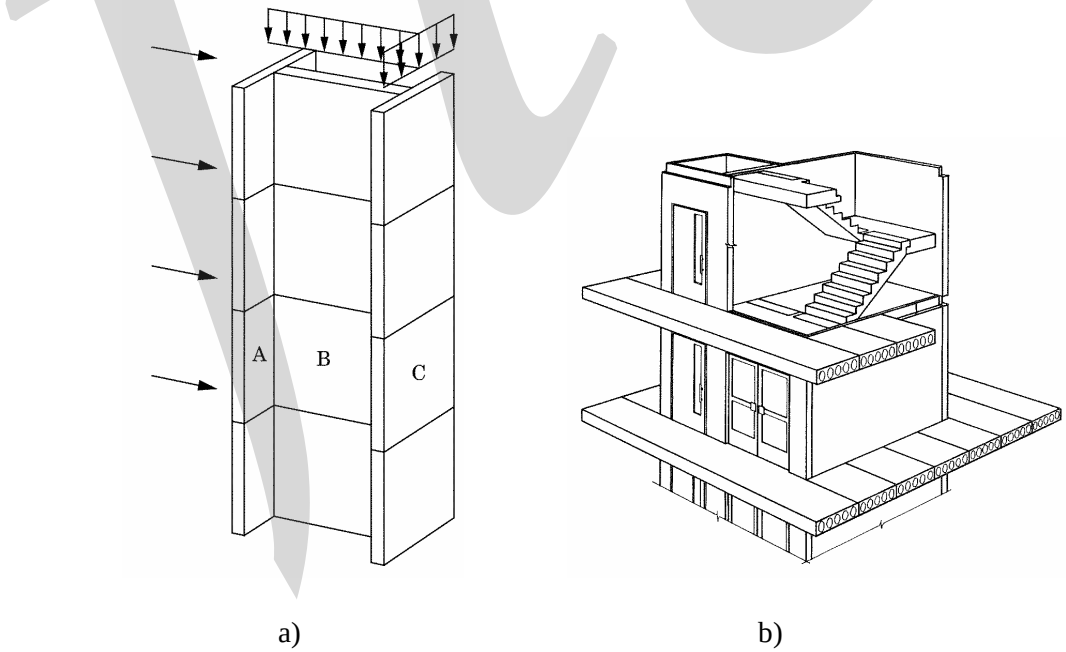

Fig. 2-15: Prefabricated slender stabilising units, a) precast shear wall, b) precast staircase

For less slender walls the flexural mode of behaviour is not as pronounced as in more slender walls, which resist horizontal load by cantilever action, Fig. 2-16. In less slender walls the shear capacity in joints and in the connections to the foundation can with relatively small measures be sufficient for stabilisation by diaphragm action. For this reason precast walls and façade walls are often used as stabilising units. In this respect it is favourable that the walls are load bearing, since the vertical load, which gives compression in the horizontal joints, reduces the need for tensile force transfer across the joints.

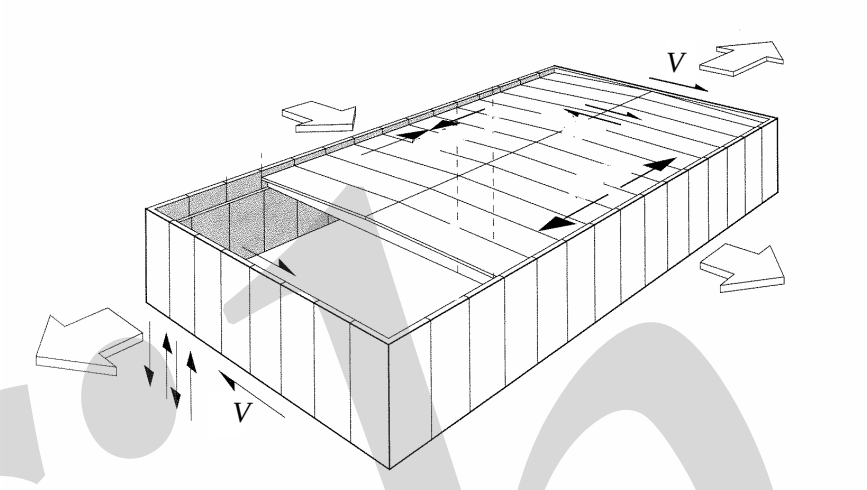

Fig. 2-16: Stabilisation with diaphragm action in non-slender walls

Frames with moment resisting beam-column connections can adopt frame action, which can also be used with façade panels, as shown in Fig. 2-17.

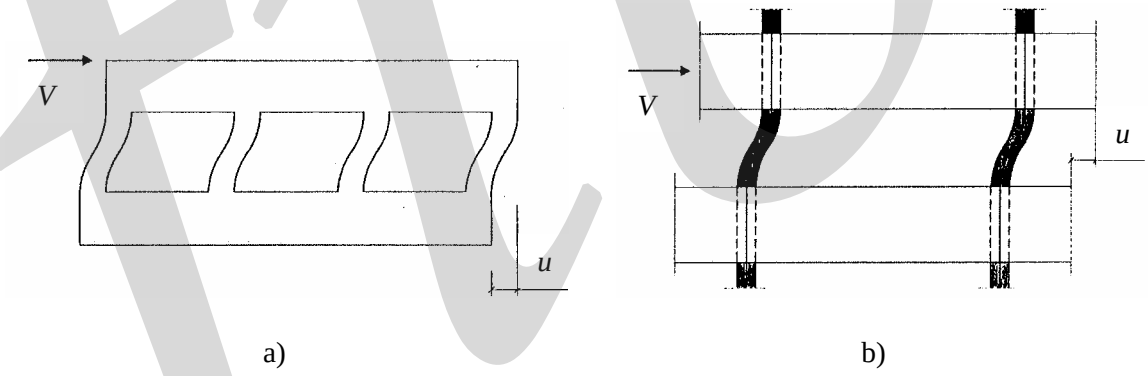

Fig. 2-17: Stabilisation by frame action in façades, a) frame action in façade elements, b) frame action in spandrel beams and continuous columns, adopted from Westerberg (1999)

Horizontal load must be transferred by diaphragm action in precast floors (and roofs) to the stabilising units - an essential part of the stabilising system. Connections between the floors or roofs and the stabilising units interact to resist the horizontal load as shown in Fig. 2-18. Precast floors or roofs that will obtain considerable stiffness in their plane where they are normally considered as being fully-rigid in design, i.e. the joints do not slip.

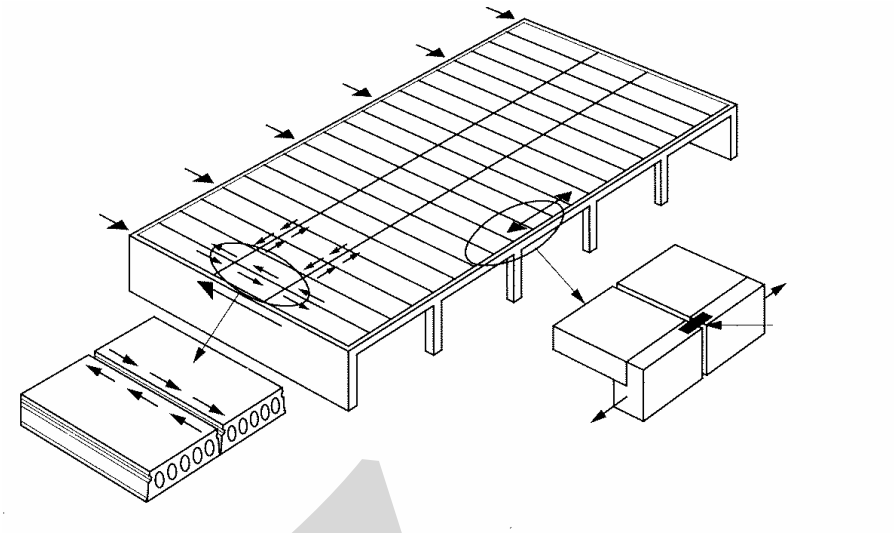

Fig. 2-18: Diaphragm action in precast floors and roofs

2.2.3 Structural movements

Concrete structures must be designed considering the need for movements due to temperature variations, and concrete creep and shrinkage. This need for movement will influence the structural design as well as the design of the connections. Reference is made to Section 3.5.1 for the connection design.

Temperature variations and shrinkage give rise to stress-independent strains, which if they are not prevented will result in deformations and movements without any stresses occurring. However, if free deformations are prevented by global or local restraints, stresses and associated stress-dependent strains will appear. In practice the need for movements cannot be fully prevented by restraints, even if this is often assumed in calculations as extreme cases. In practice the restraints will only partially prevent the free deformations. The actual deformation will be smaller than the free deformations and is determined as the numerical sum of stress-dependent and stress-independent strains.

With regard to thermal deformations the possible difference in the ambient temperature range following the day of erecting the elements and during service life should be considered. The maximum temperature variation is obtained in outdoors structures. The maximum need for thermal expansion will occur if the elements are erected when it is cold, or vice versa for thermal contraction if the elements are erected when it is hot.

In order to reduce possible horizontal restraint forces the following options are available:

- reduce the restraint at supports by provision of rubber bearings (or similar) or sliding bearings,
- reduce the restraint at supports by decreasing the stiffness of adjacent structures, e.g. the flexural rigidity of columns,
- reduce the global restraint by rearrangement of the stabilizing units,
- reduce the global restraint by introduction of movement joints.

Independently of the measures taken, actual restraint forces should be considered in the structural analysis. Movement joints can be arranged in different ways:

1) The whole structure can be divided in isolated parts by separate foundations and separate structural systems. With this approach no forces will be transferred in any direction between the separated systems.
2) The vertical load bearing system is not split by movement joints, but movement joints are introduced in beams and floors. This can be achieved by providing sliding joints at one side of the connections. In this case contraction/expansion induced forces cannot be transferred, but still shear forces can be resisted in the connections when needed, for instance by horizontal dowels.

Fig. 2-19 shows indicative values of appropriate spacing of movement joints for beam/column systems in heated buildings where the columns are hinged at the base, [BLF (1995)]. For a building that is not heated the values should be reduced by 33 %. In case of fixed end columns, the values should be reduced by 15 %. When a considerable part of the stabilizing system is concentrated to one end of the building, the values should be reduced by 25 %.

It should be noted that the equivalent temperature variation given in the figure should include the effect of concrete shrinkage. The actual temperature variation should be increased with a fictitious value that results in the same thermal strain as the shrinkage strain.

Movement joints might cause problems with leakage, which has to be considered in the detailing.

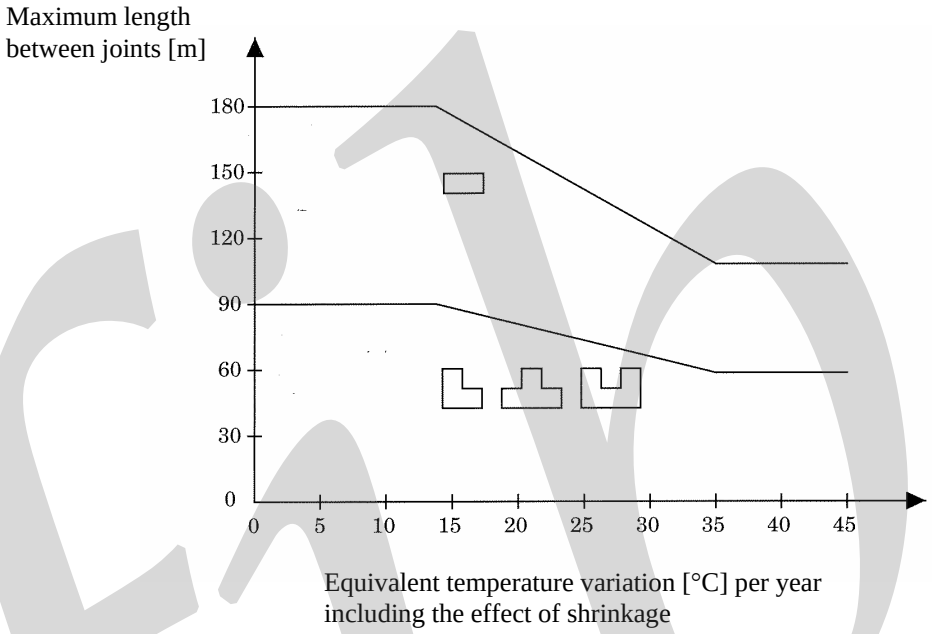

Fig. 2-19: Recommended spacing of expansion joints

It is essential to arrange the bracing units appropriately in wall and moment-resisting frame structures. When bracing units are arranged as shown in Fig. 2-21 a and b, they offer less resistance in the longitudinal direction, but when placed as shown in Fig. 2-21 c and d, the restraint forces will be of considerable magnitude and will probably cause cracking.

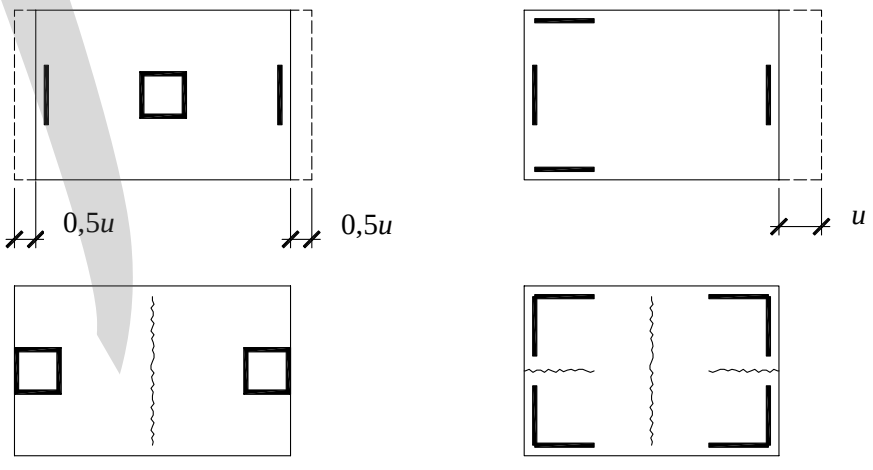

Fig. 2-21: Alternative arrangements of bracing units

2.3 Structural sub-systems

2.3.1 Precast floors

The same approach to the flow of forces, which was described for the structural systems, has also to be considered for structural sub-systems.

As an example the longitudinal joint between hollow core units is provided with a shear key, shown in Fig. 2-22, to enable a spreading of concentrated loads over adjacent slabs and to increase the stiffness of the total floor in comparison with the solitary slabs. The shear force across the joint results in principle tensile and principle compressive stresses in the joints. In the ultimate state the principle tensile stresses cause inclined cracking and the shear force is mainly transferred by an inclined compressive strut, of which the vertical component equals the shear force.

The connection will be able to fulfil its requirement only if the floor elements are prevented to part from each other in the horizontal direction, i.e. the horizontal component of the inclined compressive force must be balanced. The magnitude of the shear force, which has to be transferred over the joint, together with the angle of the compression strut in between the two adjacent slabs, will determine the resulting horizontal force *H* and the necessary reinforcement, to keep the slabs together, see Fig. 2-22. This mechanism reminds of the so-called shear friction mechanism, Fig. 2-23, which is further explained in Section 8.3. For grouted joints between floor elements reference is also made to Section 8.4.2

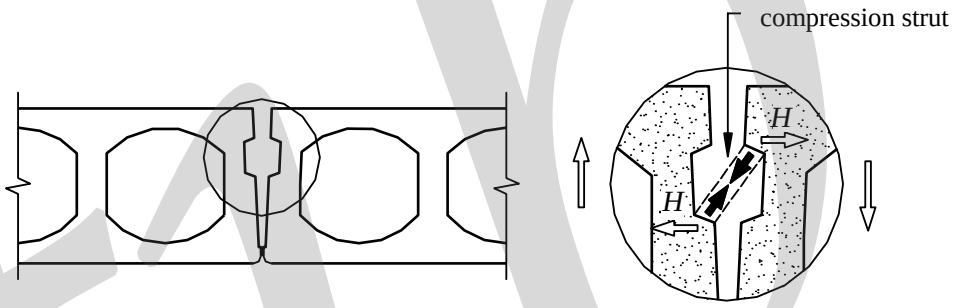

Fig. 2-22: Shear transfer mechanism in keyed joint between hollow core slabs. The resulting horizontal force H has to be resisted to prevent the slabs parting from each other

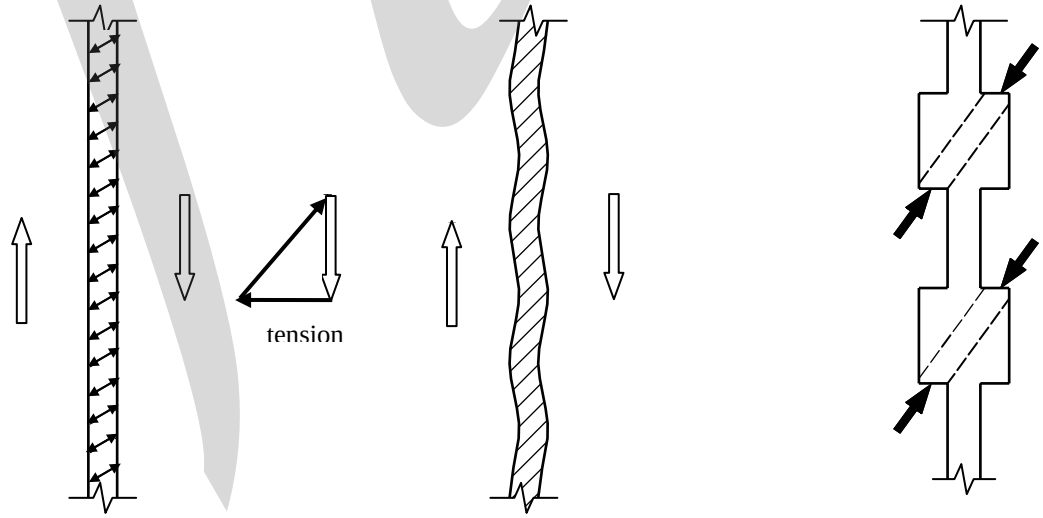

Fig. 2-23: Shear transfer mechanism

In joints with distributed projecting bars or loops along the joint faces, the horizontal force could be balanced continuously along the joint where the force originates, as shown in Fig. 2-24.

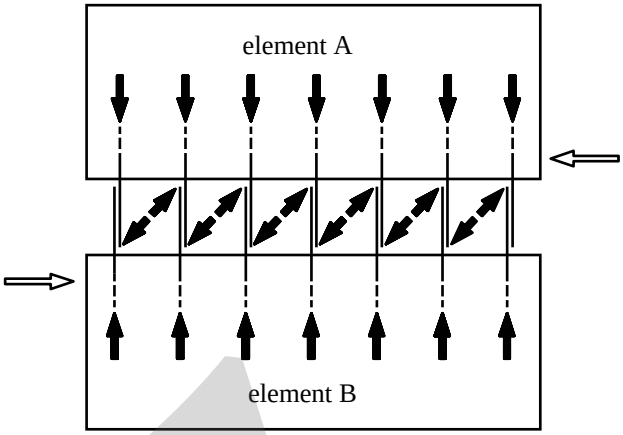

Fig. 2-24: Connecting bars equally distributed along the sides of the precast concrete elements

However, because of the techniques used to manufacture hollow core floor units, extrusion or slip-forming, preclude projecting reinforcement, the reinforcement required to resist the force *H* (Figure 2-22) will be concentrated in the transversal joints at the ends of the units, see Fig. 2-25. As the in-plane stiffness of the units is large, this detail is adequate for the transfer of longitudinal as well as transversal shear forces. The force *H*, generated at the places where the compression struts develop, is not resisted at the same place, but is transferred by the floor unit in its plane to its ends, where it is taken by the concentrated reinforcement. This mechanism is further explained in Section 8.5.1.

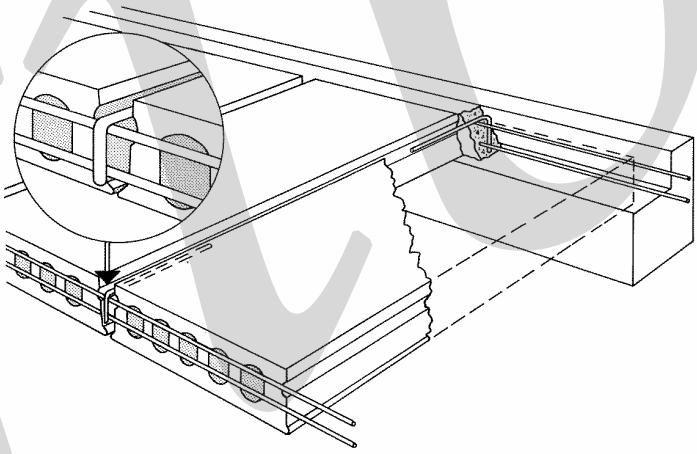

Fig. 2-25: Example of concentrating coupling reinforcement to the transversal and longitudinal joints

In case of a floor diaphragm transferring horizontal wind forces to the shear walls at both ends of the diaphragm, see Figs. 2-18 and 2-26, concentrated reinforcement is satisfactory for the shear force transfer between the slabs, but not for the transfer between the floor and the shear wall.

If the shear wall in the direction perpendicular to its plane is not stiff enough to resist the horizontal force components of the compression struts at the place of the intended shear transfer, it will deform as shown in Fig. 2-27. Loosing sufficient contact because of this deformation, the contact planes can slip and the shear transfer will not be effective.

The force path model, shown in Fig. 2-26, which is appropriate for shear transfer between hollow core units that are stiff and strong in their plane, is therefore not valid for the shear transfer to insufficiently stiff shear wall elements. To transfer these forces, the reinforcement necessary to resist

the horizontal component *H* must be placed directly where the compression struts develop. Some details of how to solve this are shown in the Figs. 2-28 and 2-29.

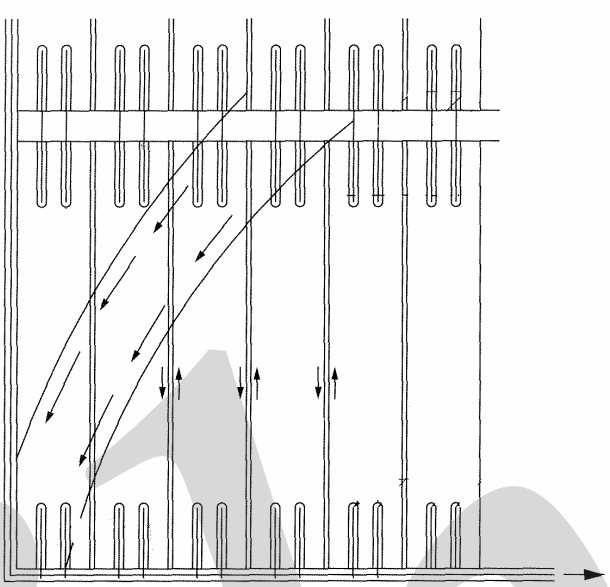

Fig. 2-26: Flow of forces in a floor diaphragm, adopted from Bruggeling and Huyghe (1991)

This is an example, illustrating the importance of the flow of forces in the joint, on the proper functioning of the total. This explains also why the structural engineer, when designing in precast concrete, should always be aware of the flow of forces and its consequences.

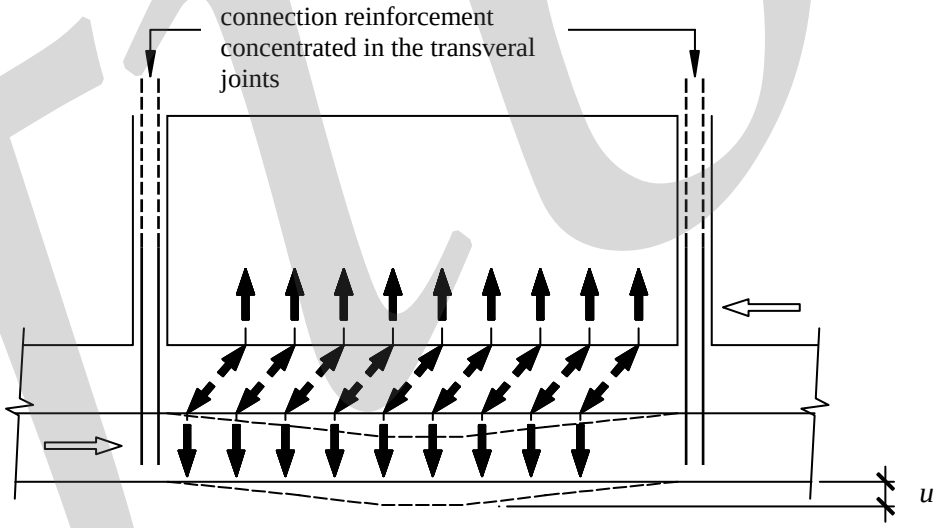

Fig. 2-27: Concentrated reinforcement in the transversal joints in combination with relatively flexible wall will result in poor shear transfer

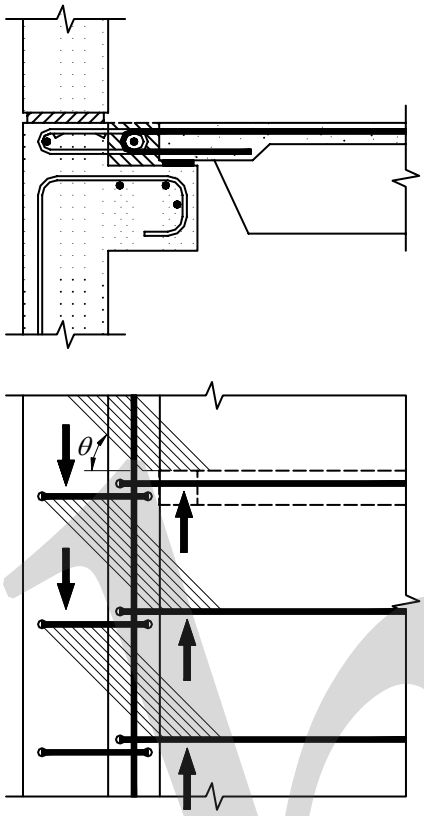

Fig. 2-28: Connection between a double-T floor unit and a wall. Connecting reinforcement is placed directly there where the compression strut is meant to develop

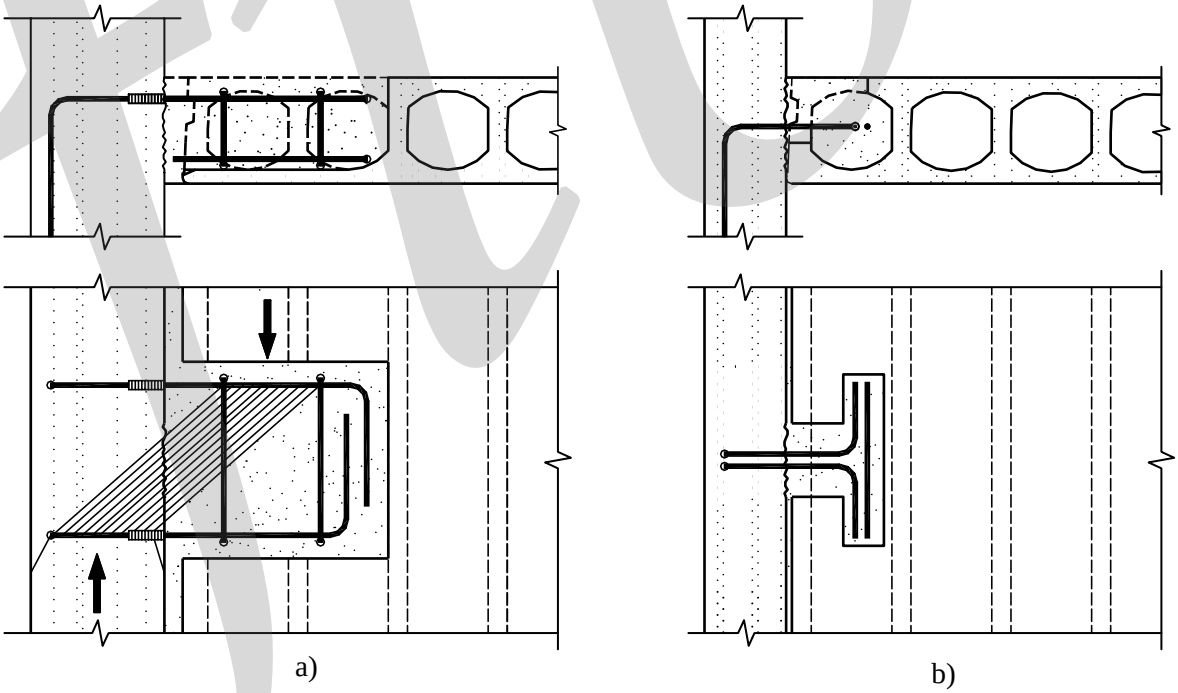

Fig. 2-29: Longitudinal connection of a hollow core slab with a wall

In general strut-and-tie models are valuable tools in understanding the flow of forces within the floor and between the floor and the stabilising units and find how tie bars should be arranged and anchored so that a safe equilibrium system is obtained.

It should be noted that a precast floor diaphragm does not behave like a deep beam placed directly on supports. This is because the support reactions are transferred by shear continuously along the joints between the floor and the stabilising units. Hence, the tying system should secure that the in-plane forces can safely be transferred through the floor to these supports. In the case of a structural topping the tying system can be arranged freely almost without restriction. In that case it is natural to transfer the load successively the shortest way to the support and arrange the tie bars continuously so that equilibrium is fulfilled, as shown in Fig. 2-30. This results in a tying system of well-distributed tie bars.

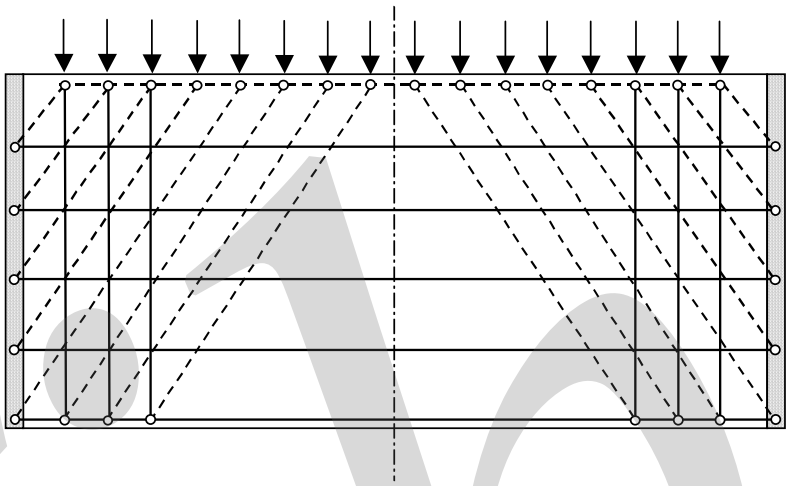

Fig. 2-30: A distributed tying system is used to balance the inclined in-plane forces. Such a distributed system can be used in case of a structural topping where the tie bars can be placed without restrictions.

However, in many cases structural toppings are avoided and the arrangement of tie bars is restricted to the joints. In this case the in-plane forces must be concentrated to the nodes where the tie bars are placed as shown in Fig. 2-31. From these nodes the in-plane forces must be activated by suspension ties so that the forces can finally be transferred by shear to the stabilising systems.

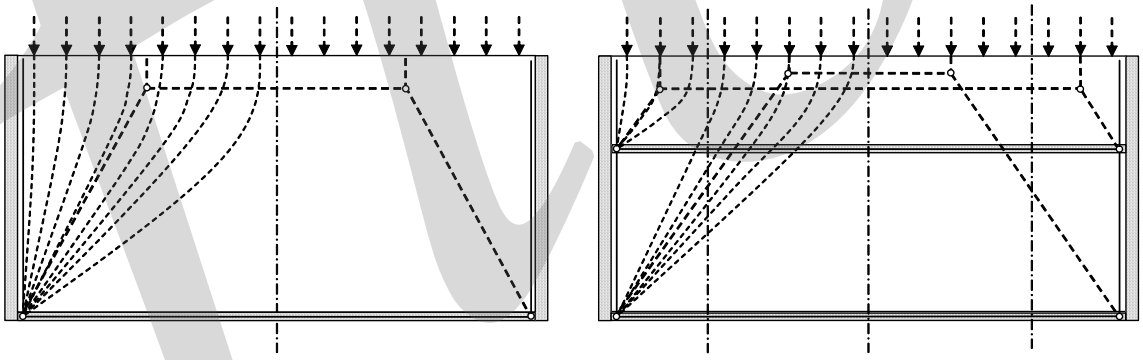

a) b)

Fig. 2-31: A concentrated tying system is used to balance the inclined in-plane forces, a) tie bars placed at the tensile chord only, b) tie bars are placed both at the tensile chord and in an intermediate joint

Some examples of strut-and-tie models for floors with regular geometry are shown in Figs. 2-32 – 2-33.

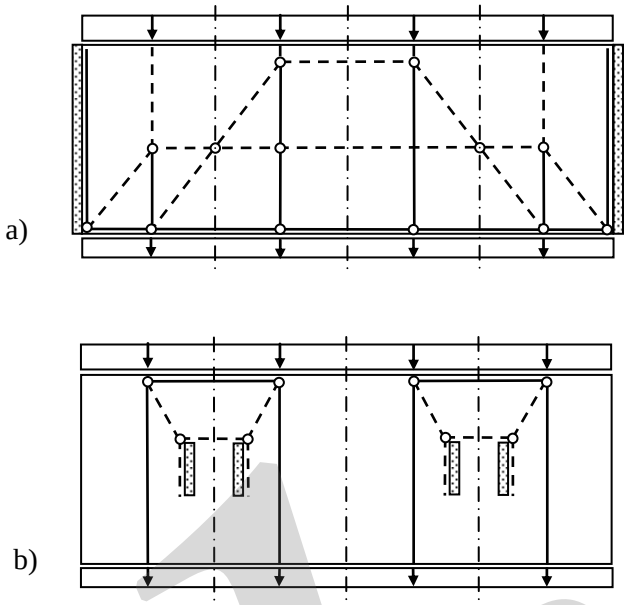

Fig. 2-32: Examples of strut-and-tie models representing the in-plane action of a floor, a) shear walls at the short ends, b) interior shear walls

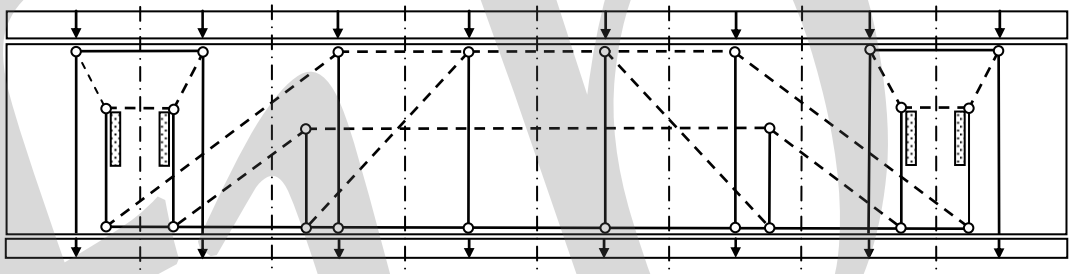

Fig. 2-33: Example of strut-and-tie model representing the in-plane action of a floor

Special attention is required in case of floors and stabilising elements with an irregular arrangement. For example, at inner corners the tie reinforcement needs to be anchored on both sides as shown in Fig. 2-34.

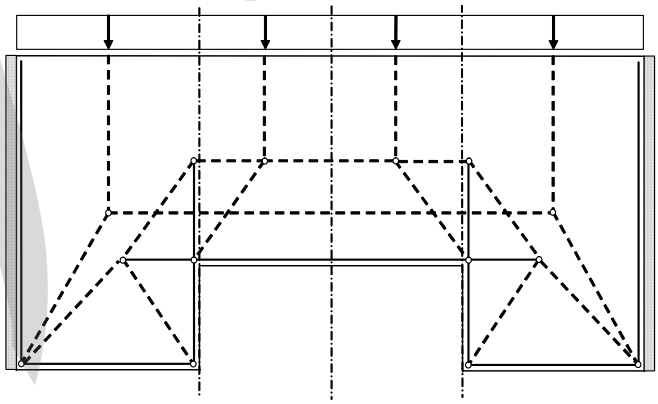

Fig. 2-34: Strut-and-tie model representing the in-plane action of a floor with inward corners

2.3.2 Precast walls

Precast concrete walls are often used to stabilise precast buildings, thanks to their large in-plane stiffness, obtained by a combination of shear and flexural stiffness. Such walls can be short or slender depending on their geometry. Slender shear walls must be checked with regard to global in-plane buckling with due regard to second order effects and flexibility of the foundation (partial fixity). Out-of plane buckling is normally restricted, but must be checked at least within a storey height. Even if the flexural stiffness dominates in slender walls, such walls are referred to as 'shear walls' due to their ability to resist horizontal loads.

For the overall structural behaviour and the stabilisation the interaction between the precast floors and the stabilising shear walls is essential. To reach the intended behaviour the connections between the floors and the walls are very important.

Diaphragm action of precast walls is obtained by interaction of the wall elements and hence the transfer of shear and tensile forces across the joints is essential. The equilibrium system can be studied by strut and tie models, and the connections should be designed consistently and in accordance with the intended structural behaviour.

Stabilising wall diaphragms are normally subjected to axial load and have higher stresses than precast floor diaphragms. The stiffness is an important parameter of shear walls. If cracks develop in horizontal joints, this influences the stiffness significantly. Whenever possible, shear walls should be designed in such a way that tensile stresses are avoided in horizontal joints or only small tensile stresses occur. It is often economical to have as much vertical load on the shear walls as possible to suppress tensile forces, see Fig. 2-12. To have a good interaction of wall elements, the elements have to be connected to the foundation, to each other and to the adjacent floor diaphragms. An example of this is the grouted starter bar connection. The starter bar is (usually) protruding out of the lower element and the upper element is provided with a sleeve that is filled with grout by pouring. This provides a well proven connection, which has a high reliability, requires no skilled labour, has a relative high fitting tolerance, and can carry over the full steel stress of the starter bar.

The walls in precast shafts can be designed either as individual shear walls or connected along the vertical joints to form a closed or open cross-section, see Fig. 2-35. Then the shaft will act as one unit in the stabilising system. If this interaction between the walls is accounted for in the stabilising system, the connections along the vertical joints must be able to resist the corresponding shear forces and must be designed and detailed accordingly.

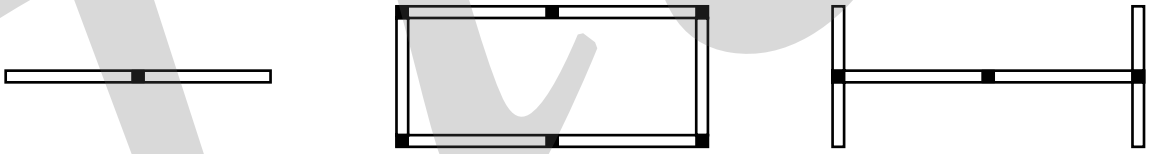

Fig, 2-35: Examples of stabilising units composed of interacting precast wall elements

Besides solutions with welded connections and concrete filled joints, one possibility is also to interlock elements (like bricks in masonry), see Fig. 2-36. This provides a connection with a high shear capacity.

When the connection at a vertical joint between wall elements is loaded in shear, it will deform according to shear stress *vs* slip characteristics. This will influence the structural response and, depending on the effectiveness of the connection to prevent shear deformation, the interaction between the wall elements can be classified as full or partial, see Fig. 2-37.

The connections at vertical joints are mainly of two types, cast *insitu* concrete joints with transverse reinforcement, or welded connections. In the concrete filled joint there is a continuous shear transfer along the joint, but with welded connections the shear transfer is intermittent. The concrete filled joint can be plain or castellated, see Sections 8.4.2. The transverse reinforcement can be well distributed or concentrated at the horizontal joints. Concrete filled joints may be difficult to execute especially when elements meet at a corner, or that they need propping during casting. However, these

connections are generally stiffer and stronger than welded connections, and may be required with regard to stress and deformation restrictions.

Welded connections become active directly after mounting and will then contribute to the stabilising system, see Section 8.4.1. This type of connection requires protection for fire resistance and durability and may need finishing with regard to aesthetics. Protection can be achieved by grout/mortar or paint. The reliability of the connection is very much influenced by the quality of the field welding. This means that the conditions during welding and the skill of the welder are crucial for the reliability of the connection. Welded connections are in most cases much less stiff (for the same strength) than concrete filled or 'interlocking element' connections (Delft University and 'Stufib' – The Netherlands).

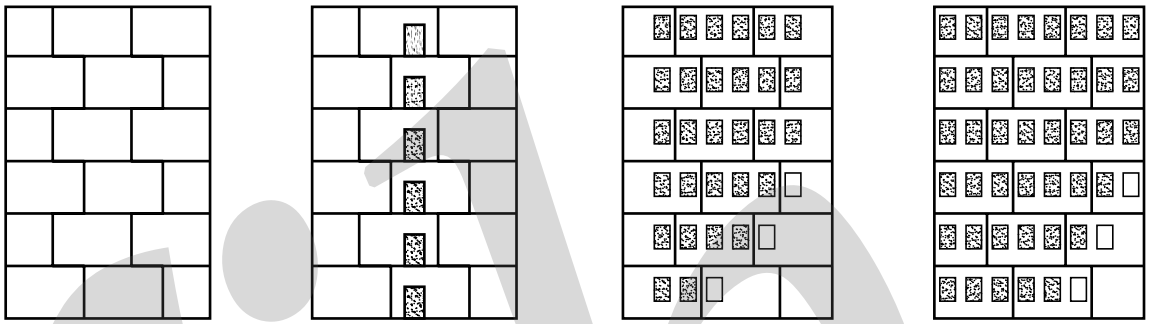

Fig, 2-36: Connection between wall elements by interlocking the elements

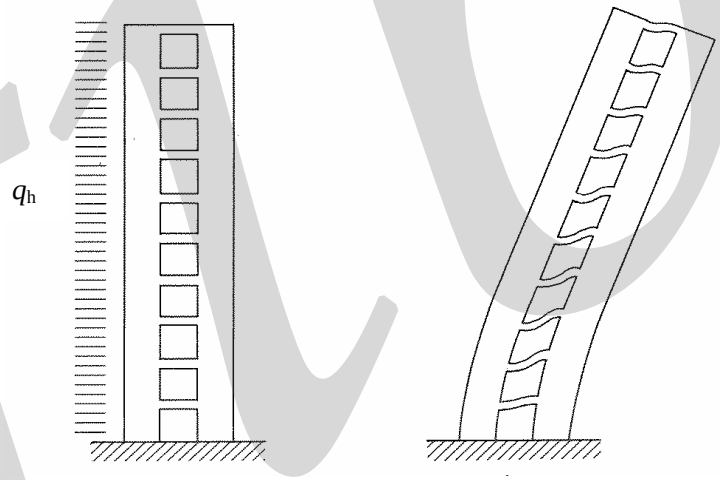

Fig. 2-37: Shear deformation of connection between wall elements influences the degree of interaction and the structural response

Façade walls can be established by 'standing' multi-storey wall elements, or 'laying' storey-high wall elements, see Fig. 2-38. The elements can carry vertical floor loads, or they can be non-loadbearing cladding. Both types can be designed as shear walls or not. In case they are used as shear walls the elements must be connected at the joints to transfer shear forces. Otherwise, the joints are non-structural just fulfilling tightness for climate protection

When stabilising and non-stabilising walls appear in the same structural systems, it is important to consider the actual stiffness appropriately. If a wall considered as non-stabilising attracts load due to its real stiffness, the structural behaviour may deviate from the intended in an unfavourable way.

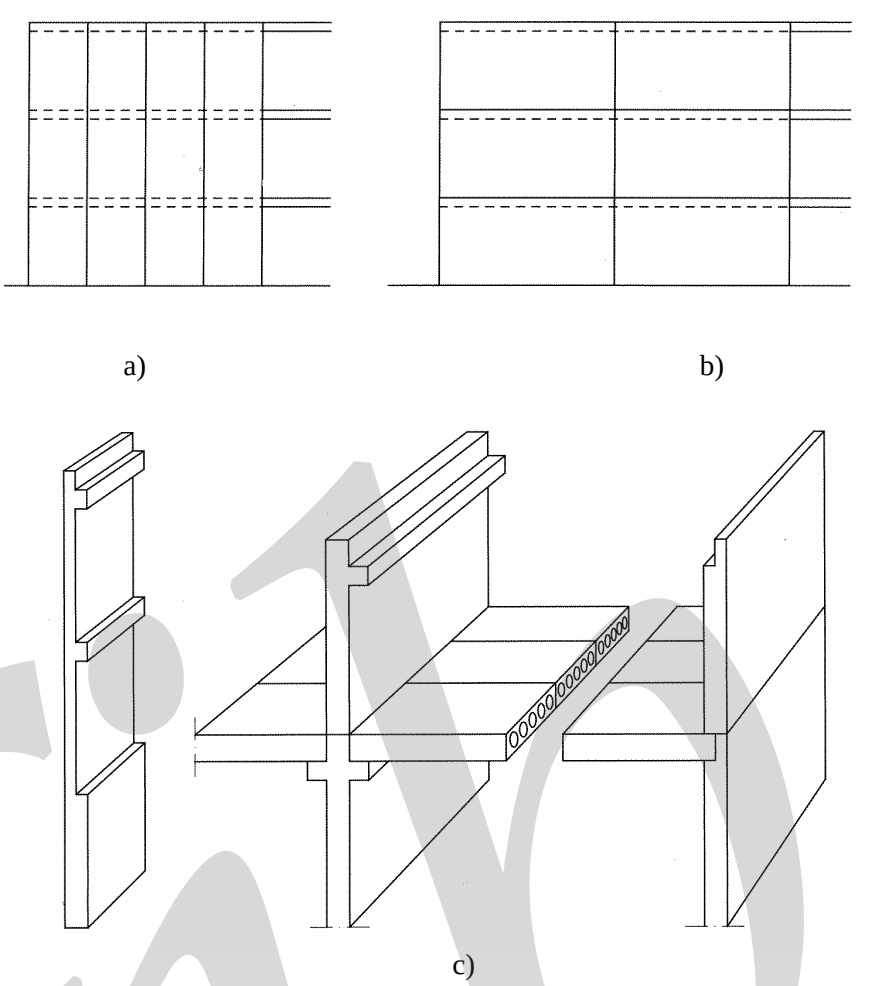

Fig. 2-38: Possible alternative arrangements of façade wall elements, a) standing multi-storey wall elements, b) laying single-storey wall elements, c) examples

2.3.3 Moment resisting frames

Moment-resisting precast frame systems typically include moment-resisting connections. For design of connections for moment transfer reference is made to Sections 9.1 – 9.5. Moment resisting frames can be classified as skeletal, portal and wall framed structures. They can be unbraced or partially braced. (Where a structure is fully braced, the need for moment-resisting connections is eliminated, and the designer must therefore exploit this fact in the ease and simplicity of making pinned jointed connections.)

When the moment resisting connections are assumed to have at least the same moment resistance as the structural members and substantial stiffness, structural analysis of precast frames is best approached by classical frame analysis assuming a continuous frame. Fig. 2-39 shows the approximate deflected shapes and bending moment distributions for a continuous frame subjected to gravity and horizontal loads. The relative magnitudes of the moments in the beams and columns depend on the relative stiffness of the columns and beams meeting at a joint.

There are many ways in which the framework in Fig. 2-39 may be designed in practice as a precast frame without compromising its stability or continuity. If the joints at the ends of some of the beams or columns are designed as pinned joints, the remaining joints may be factory cast monolithically, as shown in Fig. 2-40 a. Pinned column splices at the mid-storey height position leads to the so-called H-frame, Fig. 2-40 b, popular in grandstands where terracing beams are cantilevered from the H-framework, as shown in Fig. 2-41. Forming pinned joints at the point of beam contraflexure allows both the beams and the framework to be continuous, as shown in Figs. 2-40 c and d, the latter using monolithic T-columns.

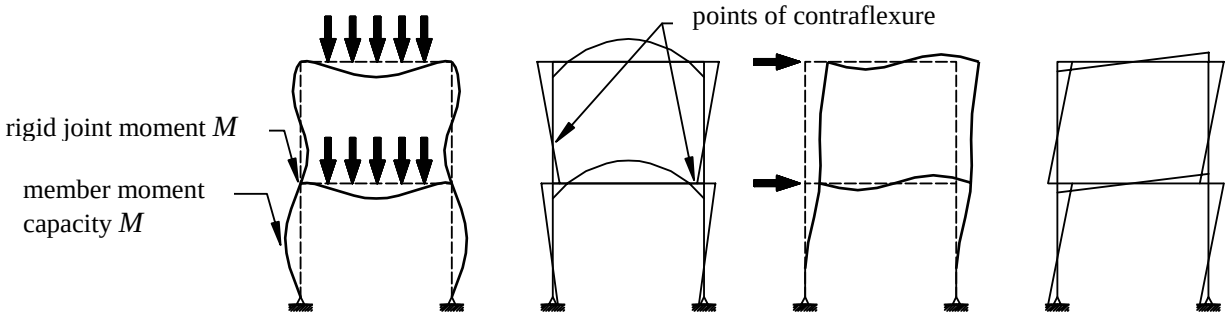

Fig. 2-39: Behaviour of rigid framework with moment-resisting connections

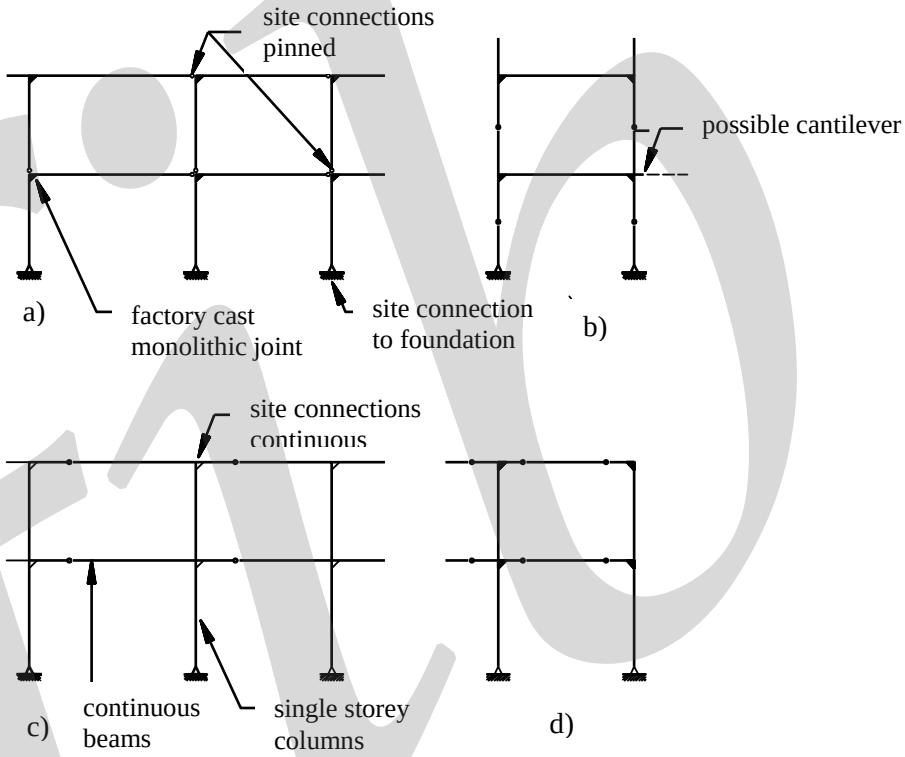

Fig. 2-40: Moment resisting frames using precast elements, a) precast monolithic beam-column elements, b) precast H-frames, c) precast continuous beams, d) precast T-columns

The connections between the precast elements themselves can also be designed to be moment-resisting, see Sections 9.1 – 9.5. Note that not all precast frames lend themselves to having moment-resisting connections.

The connections between beam and column elements may be designed to transfer bending moments. Depending on the moment resistance and stiffness of the connection relative to that of the structural members, the connection can be classified as pinned, semi-rigid or rigid, see Section 3.5.4. The frame analysis should be made accordingly. In relation to a pinned joint a moment resisting connection is in general more complicated to execute. Therefore, the advantages of having moment resisting connections must be weighted against the ease in design and execution using pinned joints and stabilising the structure by other means, for instance bracing by shear walls.

It should be noted that a connection assumed to be pinned in the structural analysis and in the design and detailing of the connection itself, still can possess a certain ability to transfer a bending moment. In this case there is a so-called unintended restraint and the possible negative effects of this with regard to cracking and resistance should be carefully examined, see Section 3.5.2.

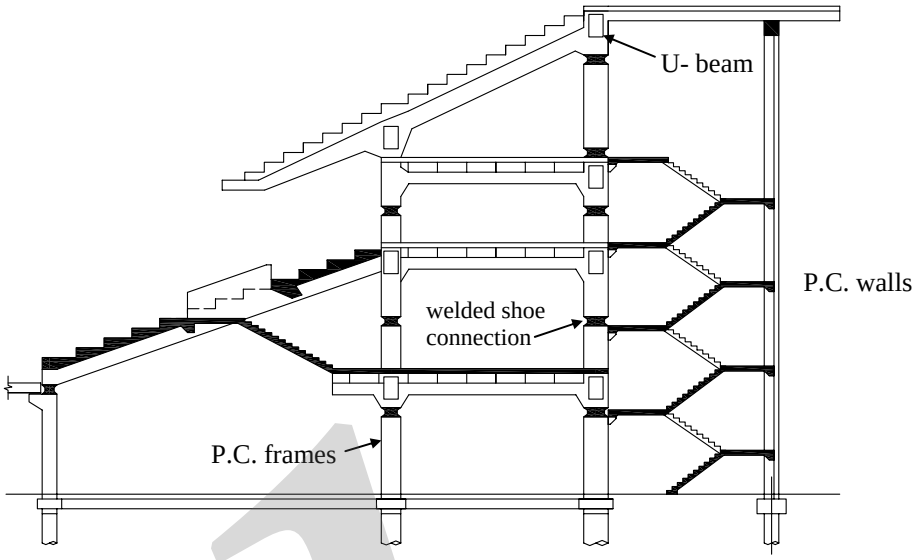

Fig. 2-41: H-frames used in multi-storey moment resisting frames for grandstands

2.3.4 Composite action and composite members

When a section is composed of more than one structural material that structurally acts together when the section is strained, this is referred to as 'composite action'. This definition is also used in the case when *insitu* concrete is added on top of a precast section, where in this case the two types of concrete are considered as *different* structural materials.

Composite action can be used to increase the flexural strength and stiffness of structural members and to utilize the material more effectively. Typical precast composite sections could be a hollow core element or double-T unit with a structural topping, or composite floor-plate floors as shown in Fig. 2-42. Composite beams can be precast beams or steel beams with a cast *insitu* topping or infill.

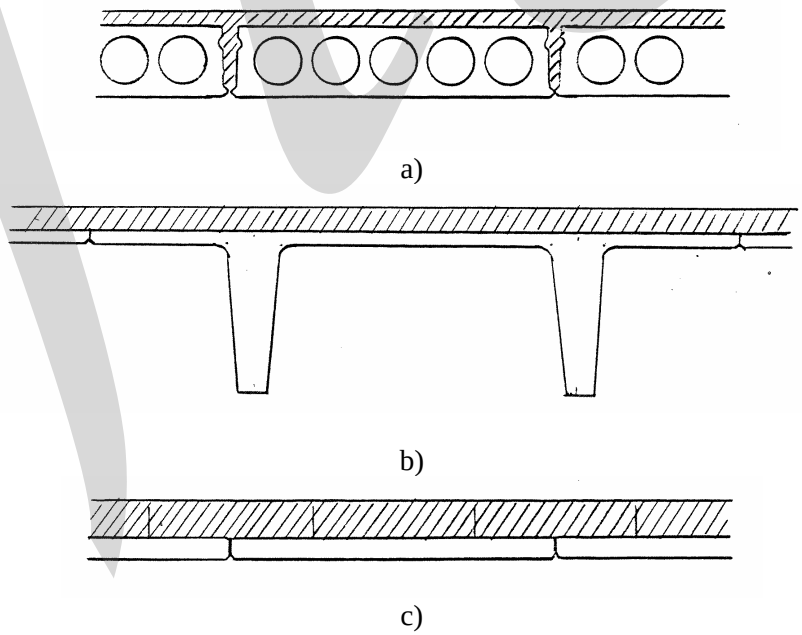

Fig. 2-42: Composite sections of floor elements, a) hollow core element, b) double-T element c) composite floor-plate floor

Composite action relies on the transfer of shear stresses at the interface from one layer of material to another. The interface must be able to resist the corresponding shear stresses and the interface must be designed as a connection for shear transfer, see Section 8.4.3. In this respect 'low' and 'high' shear situations are distinguished [FIP (1982)]. In low shear situations the shear stresses are small and it may be possible to relay on the bond at the interface provided that the roughness and cleanness of the joint interface are satisfactory. In high shear situations reinforcement or other connection devices across the joint interface are required, see Section 8.5.2.

Beams in precast structures typically support floor elements. When the joint between the floor elements is filled with cast *insitu* concrete a composite section is formed, which includes not only the cast *insitu* topping but also part of the floor elements. Because of the joint fill, the floor elements are forced to follow the movements of the beam when it deflects. Hence, the floor elements will contribute to the stiffness of the beam cross-section and take part in the composite action, see Fig. 2-43. However, in this case the composite action influences the state of stresses in the floor elements, which must be considered in the design.

Composite action can be utilized in design when it is needed. However, composite action can also develop without intention, if the elements are arranged and jointed in such a way that they interact when the beam is deflecting. This case can be regarded as unintended restraint, which should be carefully examined in the design, see Section 3.5.3.

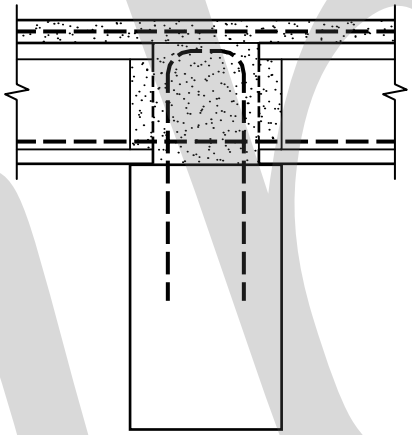

Fig. 2-43: Composite beam in precast floor system

3 Basic considerations for the design of structural connections

3.1 Principal arrangement and definitions

A structural connection consists of several components that interact when the connection is loaded. Typical components are joints with joint fills, tie bars, anchor bars and other coupling devices, and the connection zones of the connected precast concrete elements, see Fig. 3-1.

The joint refers to the opening between adjacent concrete elements. Often the joint is provided with a joint fill of grout, mortar or concrete, depending on the width of the gap to be filled. The structure formed by this joint fill itself is sometimes referred to as a 'joint'. Various types of soft or hard bearings placed in the joints can also be considered as 'joint fills'.

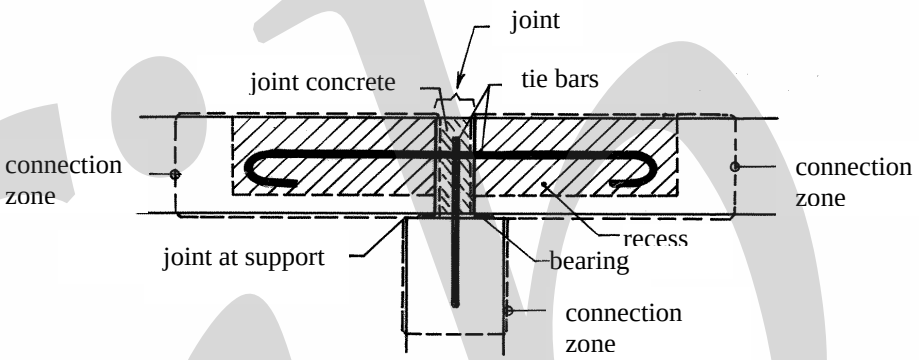

Fig. 3-1: A structural connection consists normally of several components. The structural behaviour and the performance of the connection depend on the interaction between these components

The connection zones are the end regions of the structural elements that meet and are connected at the joint. Often considerable concentrated forces are introduced in the concrete elements through the joints and the connection zones will be strongly influenced by this force transfer. For instance, tie bars, anchor bars etc. need to be anchored in the connection zones. The connection zones must be designed to transfer the forces, originating from the joint, to the principal load resisting system of the structural member. This influences the geometry of the connection zone and the reinforcement arrangement in it. Therefore the connection zones should be considered as essential parts of the structural connection. For design of connection zones reference is made to Section 3.4.

One essential part of the connection zone is the joint face itself, i.e. the surface of the concrete element towards the joint. The geometry of the joint face and its surface characteristics will influence both the grouting operation and the force transfer ability across the joint.

3.2 Design philosophy

3.2.1 Design for the structural purpose

The main purpose of the structural connections is to transfer forces between the precast concrete elements in order to obtain a structural interaction when the system is loaded. By the ability to transfer forces, the connections should secure the intended structural behaviour of the superstructure and the precast subsystems that are integrated in it. This could for instance be to establish diaphragm action in precast floors and walls, or cantilever action in precast shafts. For this reason the structural connections should be regarded as essential and integrated parts of the structural system and they

should be designed accordingly and with the same care as for the precast concrete elements. It is insufficient just to consider the connections as details for site erection. The advantages that normally are obtainable with prefabrication can be lost with an inappropriate design and detailing of the structural connections.

The design of the structural connections is not just a question of selecting appropriate dimension of the connection devises, but the force path through the connection must be considered in a global view of the whole connection and the adjacent structural members. Examples of the flow of forces through connections are shown in Section 3.7. This means for instance that the anchorage of tie bars, the connection zones of the adjacent structural members, the joints with joint fill must be considered in the design of structural connections. The force transfer from tying devices, support bearings etc. into the adjacent precast concrete elements must be secured by proper design and detailing of the connection zones. Hence, it may be necessary to design and reinforce the connection zones with regard to the action of concentrated forces and the corresponding risk of cracking, see Section 3.4.

The various aspects that should be considered in the design and detailing can be related to the following groups:

- the structural behaviour for ordinary and excessive loads, see Sections 3.3 and 5.2
- the appearance and function of the building in the service state, see Section 4.2
- structural fire protection, see Section 5.1
- production of the concrete elements, see Section 4.1.1
- handling, storage, and transportation of the concrete elements, see Section 4.1.2
- erection of the prefabricated structural system, see Section 4.1.3

With regard to the structural behaviour, the ability of the connection to transfer forces is the most essential property. Demands can be raised with regard to the transfer of compressive forces, tensile forces, shear forces, bending moments and torsional moments. The ability to transfer forces should fulfil needs in the ultimate as well as in the serviceability limit states. In the ultimate limit state the connection should secure the intended structural interaction and possess sufficient deformation capacity and ductility. It is obvious to consider forces due to dead load, live load, wind load, snow load and pressures from soil and water. Additional forces that might appear due to unintended inclination of load bearing columns and walls and unintended eccentricities should also be considered.

It is not as obvious to consider forces that develop when deformations, due to temperature variations, shrinkage and creep of concrete, are prevented from developing freely. Very often observed damages in precast concrete structures can be related to unforeseen or underestimated needs of deformations, which is further explained in Section 3.5.1.

Some elements may be subjected to actions during erection, which are larger than those under service conditions. When designing the connections this has to be considered, unless special measures are taken (such as temporary supports).

Additional capacity may be required to resist accidental loads. Such loads may be foundation settlements, explosions or collisions. Such loads may be accommodated in the connections with a capacity for overload, by ductility within the connection, or by redundancy (alternate load paths) in the total structure or within the connection, see Section 5.2. In seismic regions the connections must be designed with regard to the possible risk of earthquake. Some aspects of such design are presented in Section 5.3. Otherwise, reference is made to fib (2003b).

3.2.2 Design aspects

(1) Standardisation

A standardised connection system will always be beneficial. Structural connections are supposed to transfer forces, and the magnitude of these forces will vary. Therefore the idea can be to standardize a light, medium and heavy-duty type of the same principal solution, each with a given capacity for force transfer. This makes it easy for the designer to choose a standard solution (saves time and eliminates possibilities of errors in the calculation), and creates repetition for the workmen (less

chance of mistakes). The necessary components for a standardised connection can also be kept in stock at the plant.

(2) Simplicity

Simplicity is important to achieve a connection detail that is inexpensive and least likely to be used incorrectly.

Consequently all connection arrangements should consist of the least possible number of pieces not embedded in the element. Furthermore, if the same unit can be used for different purposes, the chance of mistakes is greatly reduced.

(3) Tensile capacity

If a connection must have a tensile force capacity, then, consequently all embedded units must have sufficient anchorage, and friction can never be part of the utilised force transfer mechanism. The connection between anchored units must also have a tensile force capacity.

(4) Ductility

Connections should preferably behave in a ductile manner. Ductility can be defined as the ability to have large plastic deformations before failure, see Section 3.3.2. In structural materials ductility is measured as the magnitude of the deformation that occurs between yielding and ultimate failure. Ductility in building frames is usually associated with moment resistance. In concrete members with moment-resisting connections, the flexural tension is normally resisted by steel components, either reinforcing bars or structural steel members. Ductile joints can be achieved by giving the brittle parts of the joint an extra capacity, for example by calculating with reduced allowable stress in these components, see Section 3.6. Typical brittle components are welds, short bolts in tension, bolts subjected to shear, reinforcement anchorage zones, etc.

(5) Movements

Connections must not hamper necessary movements in the structure. Necessary movements will in most cases be the deformation of beams and slabs due to loads and/or prestressing forces. Typically this problem arises when a vertical facade panel is connected to a beam or slab somewhere in the span (away from the support). If the connection detail makes the vertical movement of the beam or slab impossible, this may cause damage to the connection detail itself, or to the elements. Even if there is no damage, unwanted forces may be introduced in the elements, causing unwanted deformations. The solution is to construct the connection detail with a sliding arrangement, or it can be made as a hinge. How to consider the need for movement and restrained deformation is further explained in Section 3.5.

(6) Fire resistance

Many precast concrete connection details are not vulnerable to fire, and require no special treatment. Connection where weakening by fire would jeopardize the structure's stability should be protected to give the same resistance as the structural frame. A typical example is an exposed steel corbel supporting a beam. Methods of fire protection include encasing in concrete, covering with gypsum boards, coating with intumescent mastic, or spraying with a fire protective paint. There is evidence that exposed steel used in connections is less susceptible to fire related strength reduction than fully exposed steel members. This is because the concrete elements provide a 'heat sink', which draws off the heat and reduces the temperature of the steel. Design of connections with regard to fire resistance is treated further in Section 5.1.

(7) Durability

Evidence of poor durability usually appears as corrosion of exposed steel details, or by cracking and spalling of concrete. Connections subjected to corrosion must have steel details adequately covered with concrete, or should be corrosion protected. Alternatively non-corrosive materials can be used. Design with regard to durability is treated in Section 4.2.6.

(8) Aesthetics

It must be kept in mind that aesthetics is important. Any structural connection that will not be hidden, can either be emphasized and become part of the architecture, or should be made in a way that demonstrates how it functions without being dominating, see Section 4.2.7.

3.2.3 Aspects on connection methods

There are several ways to obtain tensile capacity in connections. Considering the safety aspect only, the order of preference is as follows:

1) Bolting
2) Grouting reinforcing bars at the site
3) Embedding reinforcing bars in epoxy or polyester at the site
4) Welding

The use of bolts is a simple way to establish a safe connection, but it generally puts strict requirements on the tolerances. The bolts can be threaded rods or regular bolts.

Grouting at the site will to some extent depend upon the weather to be successful. Generally the requirements on tolerances are not severe. When the result from a casting operation is successful, a very sound connection is established. It also provides fire and corrosion protection for the steel details.

Mix proportions, aggregate size and casting procedures will vary with the size, location and orientation of the operation. Patches permanently exposed will often not be acceptable. Anchoring the grout to relatively large steel surfaces is a problem that is often overlooked. Large elements such as steel haunches can be wrapped with mesh or wire. For recessed plates and similar elements headed studs or wiggled refractory anchors can be welded to plate to provide anchorage for the grout. Gluing with epoxy or polyester is very dependent upon weather conditions to be successful, especially temperature. Also the workmanship is of great importance to secure a satisfactory result, like the mixing of the ingredients and the preparatory cleaning and drying of the contact surfaces. Some types of glued connections also put some requirements on tolerances. Most types of glue loose most of their strength when heated to about 80^{o}C.

Welded connections will in most cases fit without any problems, but the quality of the weld is totally dependent upon the skill of the welder. When welding outdoors the welder must have extensive knowledge about what kind of electrodes to use under different weather conditions on different material qualities, and of treatment of the electrodes and materials prior to welding. Also the actual work may be difficult and laborious to perform; like when fixing a small plate with only ladder access, with heavy cables and no place to put the clamp. The heat generated when welding may also damage the quality of the concrete close to the weld. Welded connections will in many cases have to be fire protected.

3.3 Force transfer mechanisms and the mechanical behaviour

3.3.1 Force transfer types

The connection characteristics can be categorised by the type of action it is designed to resist:
- shear
- tension
- compression
- flexure
- torsion

For many structural connections the behaviour is dominated by one of the actions above. Sometimes connections are classified by this dominating action as 'shear connections', 'compression connections' etc. However, very often the structural connections should be capable to transfer a combination of these basic actions.

Shear transfer is required at joints between precast wall elements and between floor elements. At longitudinal joints between hollow core units shear transfer is required horizontally as well as vertically. Connections between precast beam elements or floor elements and a cast *insitu* topping may require shear resistance to obtain an adequate behaviour in the final state.

The ability to transfer tensile forces is normally secured by means of various types of tie bars, anchor bars and other connecting devices of steel. Tensile capacity is often required between wall elements used for stabilisation, between floor elements and between precast floors and their supports. Depending on the position of the ties these connections can be more or less capable of transferring bending moments, even if this was not intended by the design. Unintended tensile resistance can sometimes appear in connections, for instance due to bond between the short end face of a floor element and the joint concrete in the support joint nearby. Unintended tensile or flexural resistance may result in undesirable restraints that must be considered in the design, see Section 3.5.2.

Transfer of compressive forces is an important function of connections at horizontal joints in precast walls, in connections between precast column elements, and at support connections of precast beams.

Flexural resistance is required for instance when a precast column is fixed at the base, or when continuity is needed at interior supports of beams or floors. Also for beam/column connections in moment resisting frames, flexural resistance may be required.

Torsional capacity is needed at support connections of simply supported beams that are loaded eccentrically with respect to the sectional shear centre. This may for instance be the case for one-sided ledge beams used for precast floors.

Many structural connections should be able to transfer more than one type of basic action. For instance connections at the short ends of floor elements may need, besides the primary support action, both shear resistance along the support and tensile resistance across the joint. In support connections it may also be necessary to combine the ability to transfer forces with the need for movement.

Design of connections with regard to the ability to transfer forces must be based on the knowledge and understanding of basic force transfer mechanisms. Some of these are specific in precast structures. Basic force transfer mechanisms are presented in Chapters 6 - 9 together with typical connections where they are utilised.

3.3.2 Mechanical characteristics

The mechanical behaviour of a structural connection can be characterised by the relationship between transferred force (principal action) and the corresponding displacement, for instance relations between tensile force and elongation (crack opening), bending moment and rotation, shear force and shear displacement (slip).

A principal load-displacement relationship is shown in Fig. 3-2. In ordinary design, the maximum resistance S_{max} and the stiffness $K=S/u$ in the service state are of primary interest. Very often the load-displacement relationship is non-linear and a characteristic stiffness to be used for service state verification can be defined by the secant modulus of a certain appropriate load level.

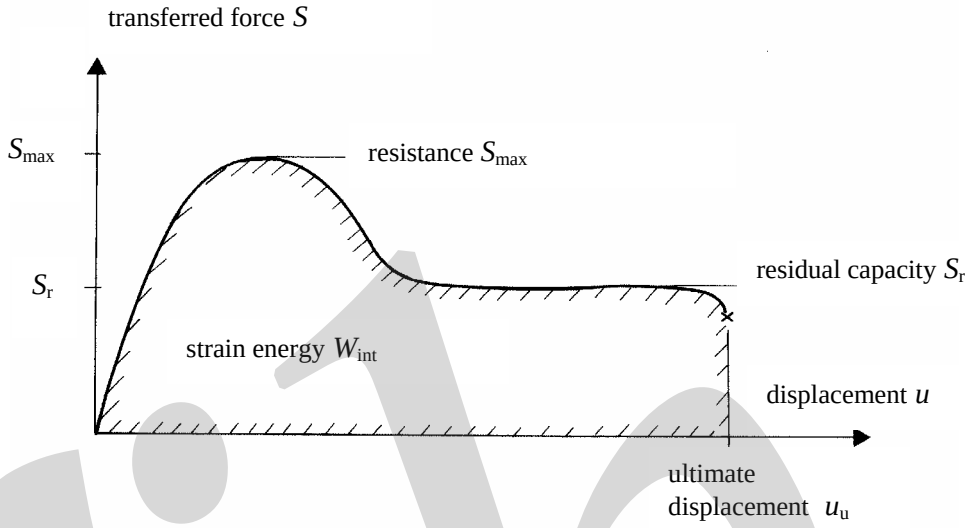

Fig. 3-2: The mechanical behaviour of a structural connection can be characterised by a load-displacement relationship for the primary action

To evaluate the effect of deformations, movements and possible restraints in the structural system, it is necessary to have knowledge about the displacements that develop in the structural connections when they are loaded. In case of excessive loading, due to unexpected restraint forces or accidental actions, a ductile behaviour of the structural connections is most desirable.

The parameters 'deformation capacity' and 'ductility' are often misunderstood and confused. The deformation capacity of a connection refers to the maximum displacement that is possible to reach before a total degradation, but says nothing about the shape of the load-displacement relationship. Ductility is the ability of the connection to undergo large plastic deformations without a substantial reduction of the force that is resisted. The ductility is often expressed by the ductility factor μ, see also Fig. 5-20.

$$\mu = \frac{u_{max}}{u_y} \tag{3-1}$$

where u_{max} = maximum deformation without a substantial reduction of the resisted force
u_y = deformation when a plastic behaviour is reached

Various parameters describing deformations can be used to determine the ductility factor, for instance displacement, rotation, slip, strain, and curvature. The ductility factor says something about the shape of the load-displacement relationship, but not about the deformation capacity as such. Connections may have different deformation capacities but still the same ductility.

However, the ductility factor is a rather primitive measure to express the ductility, since it is in fact anticipated that the load-displacement relationship is ideally elastic-plastic. For general non-linear load-displacement relationships, there will be problem to define the characteristic deformations u_y and u_{max} that cannot be determined precisely from the curve.

The parameter 'relative strain energy' $\xi(u)$ is proposed as a more general measure to express the ductility numerically, [Engström (1992)]. This parameter can easily be defined for any type of load-displacement relationship.

The strain energy W_{int} that is consumed when the connection is strained corresponds to the area defined by the load-displacement relationship. For any value of the displacement u the strain energy can be expressed as

$$W_{int}(u) = \int_0^u S(u)du \tag{3-2}$$

For the same displacement u the relative strain energy is defined as

$$\xi(u) = \frac{W_{int}(u)}{S_{max} \cdot u} \tag{3-3}$$

Hence, the expression (3-3) is the ratio between the average force applied during the displacement u and the maximum resistance S_{max}. This ratio, determined for the ultimate displacement u_u (deformation capacity), defines the final strain energy or the strain energy capacity $\xi(u_u)$.

$$\xi(u_u) = \frac{W_{int}(u_u)}{S_{max} \cdot u_u} \tag{3-4}$$

The relative strain energy capacity will always have a value $0 \le \xi(u_u) \le 1{,}0$ and an ideally plastic behaviour gives $\xi(u_u) = 1$, see Fig. 3-3. An ideally elastic behaviour, which is not ductile at all, gives the value $\xi(u_u) = 0{,}5$. The higher value of the ratio (3-4), the higher is the ductility of the considered connection.

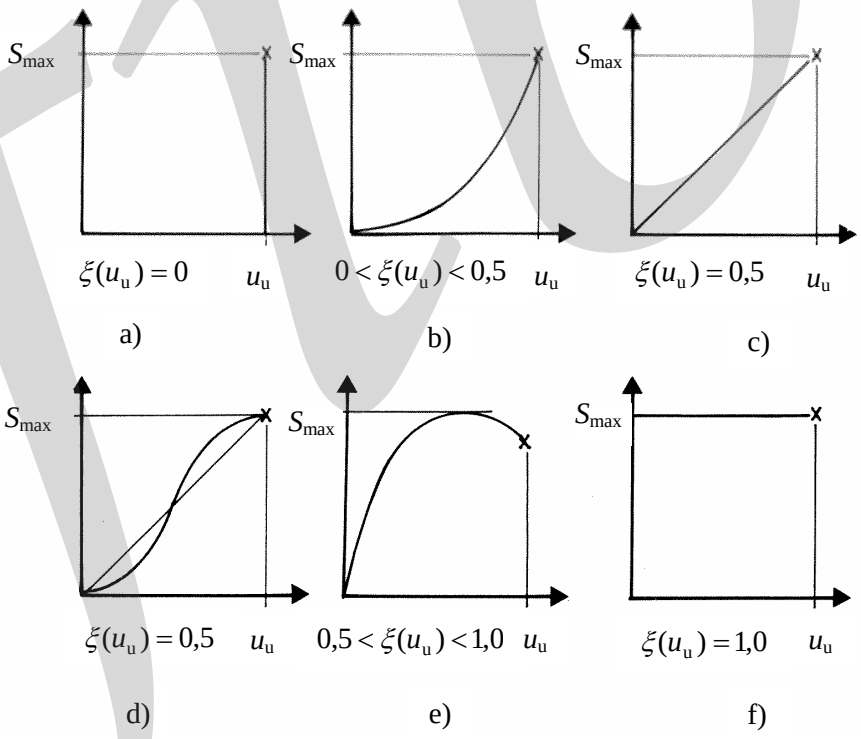

Fig. 3-3: Examples of how the relative strain energy capacity depends on the shape of the load-displacement relationship, according to Engström (1992)

In connections with a brittle (non-ductile) behaviour, failure typically appears when or very soon after the maximum resistance is reached, while ductile types of connections can withstand further

deformations after reaching a resistance corresponding to yielding. This is a very favourable behaviour in case of overloading by restraint forces. The restraint force depends on the deformations and is reduced when the connection is yielding. Due to the ductile behaviour, the resistance still remains after some plastic deformations. In case of accidental actions, fire etc, the plastic deformations due to overloading make it possible to get favourable force redistribution.

3.4 Design of connection zones by the strut-and-tie method

Structural connections and connection zones of precast concrete elements are often subjected to high concentrated forces. When these forces are transferred through the connection and further into the adjacent elements, they are spread across the sections into wider stress distributions. The deviation of forces (i.e. change of directions) and spread of stresses often lead to high transverse stresses. If the concrete tensile strength is reached, cracks will appear in these zones. In case of improper detailing these cracks might result in damages, which in turn may limit the capacity of the connection, for instance due to splitting failure in a support region.

In this context it is appropriate to distinguish the B-regions and the D-regions of the precast concrete elements, see Fig. 3-4. In the B-regions, the hypothesis of Bernoulli of a linear strain distribution across the section can be applied. Here the sections can be analysed and designed according the traditional approach for reinforced or prestressed concrete cross-sections subjected to bending moment with or without an axial force. In the D-regions (discontinuity or disturbed regions) the strain distribution can deviate considerably from a linear one and other methods are required for analysis and design. Because of geometrical and static discontinuities in the structural connections, the connections zones should be considered to be discontinuity regions. In fact, the connection zone of a precast concrete element could be defined as being the discontinuity region.

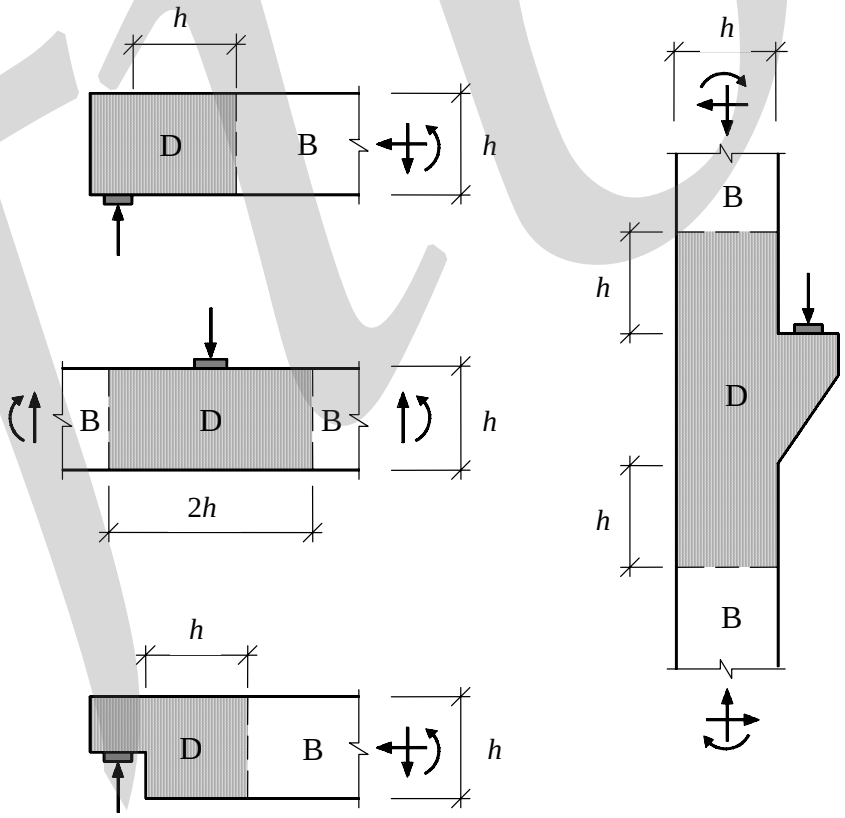

Fig. 3-4: Examples of D-regions of structural elements, adopted from Schlaich and Schäfer (1991)

It is quite normal that reinforced concrete structures crack when they are subjected to load. However, the cracking can be controlled by an appropriate amount and arrangement of reinforcing steel. In the service state cracking should be controlled and crack widths kept to allowable values with regard to the risk of corrosion and appearance. In the ultimate limit state the resistance should be sufficient in spite of the cracks. The reinforcement should be designed and arranged so that the stress field that develops in the cracked reinforced concrete can stay in equilibrium with the applied loads.

The 'strut-and-tie method' is an appropriate tool to design the connections zones and check that the equilibrium conditions are satisfied in the ultimate limit state. The method also reveals the flow of forces through the structural connection and, thus, helps the designer to understand the behaviour and find a proper detailing, which is consistent with the intended behaviour.

The strut-and-tie method is based on theory of plasticity and gives theoretically a lower bound solution, i.e. the failure load calculated on basis of the chosen strut-and-tie model will be smaller than or equal to the theoretically correct failure load. Under the condition that the critical regions within the connection zones have sufficient plastic deformation capacity, the solution will be on the safe side.

The designer will choose a strut-and-tie model that simulates the stress field in the reinforced cracked concrete and stays in equilibrium with the design load and design and detail the connection zones consistently, see Fig. 3-5.

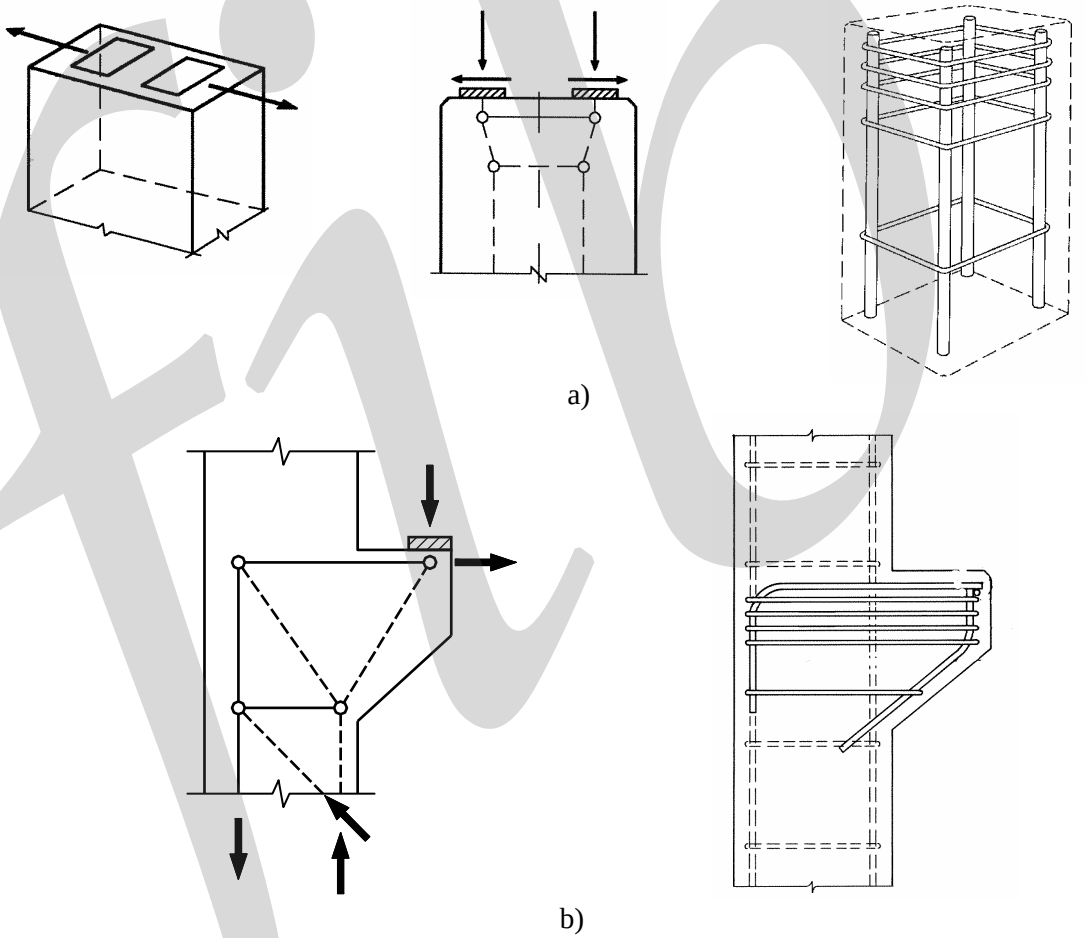

Fig. 3-5: The connection zones of precast concrete elements are typical discontinuity regions. The strut-and-tie method can be used to study the flow of forces and as a basis for design and detailing, a) design and detailing of a column head, b) design and detailing of a column corbel

The members of the strut-and-tie system, i.e. ties, struts and nodes, are checked with regard to their strengths. As long as the chosen stress field is in equilibrium with the applied load and no critical regions are overstressed above their strengths, the stress field is theoretically a possible one. However, the actual stress-field in the structure under the applied loads may be different, since the structure

itself, by means of the detailing that the designer has provided, can find a more effective way to carry the load. In this way the actual solution will theoretically be on the safe side.

For small loads the concrete remains uncracked and the reinforcement has only a very small influence on the behaviour. In this stage the concrete has an almost linear elastic response and the behaviour of the connection zone could be examined by linear analysis based on theory of elasticity for a homogenous material. Linear analysis results in one unique solution, i.e. a stress field. Typical for this solution is that when the load increases, the stress field configuration remains the same and the magnitude of the stresses increases in proportions to the applied load.

However, when the load increases the concrete will crack. The reinforcement placed across cracks will now have a significant influence on the behaviour. The stiffness properties before and after cracking will be quite different. The actual stress field will depend on the actual stiffness properties, which in turn will depend on the actual state of cracking and the reinforcement arrangement. Therefore, different reinforcement arrangements will result in different stress fields, which in turn will deviate from the one, found by linear analysis. Under increasing loads the cracking will develop more and more, which results in a continuous change of the stiffness properties and of the corresponding stress field configuration. This is known as stress redistribution due to cracking.

At high loads critical points in the connections zone will be stressed to their strengths. Both concrete in compression and steel has a plastic behaviour at high strains. Due to this plastic behaviour in some critical points, the stiffness properties of the connection zone will change again, which results in a change of the stress field. When the load increases further, the stresses of these critical points cannot increase any more, but will be limited to the strength that was provided by the designer. This change of the stress field configuration is known as plastic stress redistribution. Plastic redistribution continues with increasing load until the plastic strength is reached in so many critical points that the load cannot be increased further. This load should correspond to the design load and the final stress field will be the one that was simulated by the strut-and-tie model. It is finally reached by successive stress redistribution. Hence, the structure has to follow the intention of the designer by using the capacities that are provided. For this reason the design problem can be solved by alternative designs, as long as they all fulfil the basic equilibrium conditions.

The plastic stress redistribution will require substantial plastic deformation capacity of the critical points that reach their strength early. The theory of plasticity assumes that the materials have an ideally plastic behaviour with unlimited plastic deformation capacity. In this respect there is a deviation between theory and reality. Reinforced concrete has a limited plastic deformation capacity. The knowledge about the plastic redistribution, need for plastic deformations, and plastic deformation capacity in connection zones with alternative designs is very limited. For this reason the designer should be careful in the choice of strut-and-tie models to avoid models that will require large plastic redistribution.

Therefore, it is generally recommended not to deviate too much from the elastic stress field found by linear analysis. However, it is not at all necessary to accurately follow the elastic stress field, as this will never be the actual one in cracked reinforced concrete. Instead the freedom allowed should be used to find strut-and-tie models that result in practical reinforcement arrangements.

For more information about the strut-and-tie method and check of struts and nodes, reference is made to Schäfer (1999a, b).

3.5 Need for movement and restrained deformation

3.5.1 Consideration of the need for movement

The needs for movement in a structural system are due to the service load, concrete creep and shrinkage, temperature variations, support settlements etc. This is very important at connections where various structural elements meet and may be restrained by each other. If the need for movement is not considered there will be a risk of damage to the connection zones. Such damage can be especially dangerous when it appear in support regions, see Fig. 3-6. The need for movement can be considered in two principally different ways.

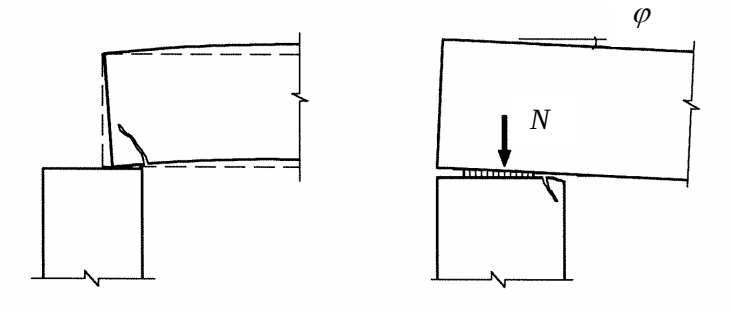

Fig. 3-6: Examples of how connection zones can be damaged because of movements of the of the precast elements

One extreme way is to fully satisfy the need for movement by detailing the connection so that the corresponding movement can fully take place without restraint. Freedom for movements can be achieved by providing sliding bearings, hinge details etc. Force transferring details can be provided with gaps, slots etc., so that force is not transferred before the need for movements becomes greater than expected, for instance in case of accidental actions and other extreme load cases. Design of connections with soft bearings is treated in Section 6.5.

The other extreme alternative is to fully prevent movements between adjacent precast elements. In this case the connection and the elements must be designed to resist the corresponding restraint forces that will develop. The restraint forces can be considerable and it is in practice not possible to fully prevent movements to occur.

In practice structural connections where movements are prevented will give partial restraint. The restraint forces may develop before and whilst movements are taking place, for instance frictional forces before and whilst a precast element slides on its support or when a rubber bearing deforms. When some little movement is possible by deformation of connection details and of the connection zones, the restraint forces will be considerably smaller than the theoretical ones calculated under the assumption of full restraint. Therefore it is worthwhile to consider such flexibility of the strained components. However, an accurate consideration requires knowledge about the load-displacement relationship of the structural connections. This knowledge is often missing and the analysis must be based on reasonable estimates.

A design on the basis of partial restraint in the connections will result in a distribution of movements in the structural system instead of a concentration of movements to special movement joints. This may result in limited cracking in grouted joints or in cast *insitu* concrete toppings. In this case the structural connections should be designed in such a way that single, wide cracks are prevented. Special concern is required in areas where cross-sections are changed abruptly and where the need for movements can be especially large.

In simply supported structural members the prestressing force is applied in the lower part of the section, and consequently the creep deformation under the prestressing force results in an overall shortening of the member and a negative curvature. The vertical load results in a positive curvature. As a result the end face of the precast element will both move and rotate. When these displacements are added, it is often found that the bottom edge needs to move more than the upper edge. Hence, in order to avoid restraint from connection details it is better to place the connecting devices at the upper edge, see Fig. 3-7. This might be of importance for beams and slabs with substantial depth.

Beams in buildings are often bolted at the supports or connected by dowel pins. Deformations, caused by shrinkage or thermal strain, result in a need for movements at the supports. When the bolthole is left open without grout, the need for movement may be restrained by friction but not by the bolted connection itself. When the bolthole is grouted, the restraint force is more effectively transferred to columns and other parts of the structure. The actual restraint forces depend on the stiffness of the beam as well as the stiffness of the supporting members. This results in an intermediate situation where the need for movement will not be fully satisfied, but the actual movement that occurs is transferred to the columns. These movements are normally not taken into account in the design if there are expansion joints at regular distances. In some cases, when the expansion joints are placed at long distances or when the plan of the building is not symmetrical, or has a not normal shape, some problems might arise in the structure induced from these movements.

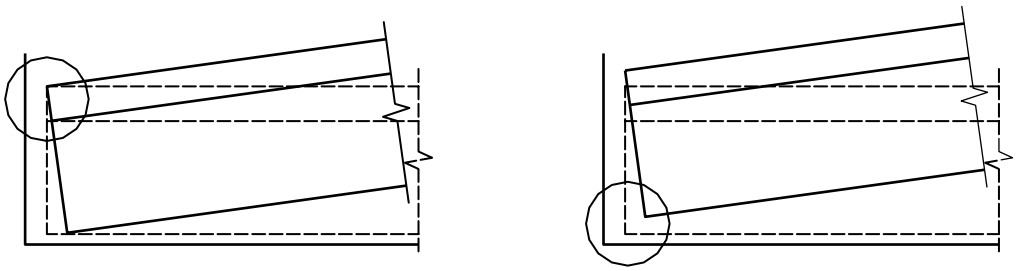

Fig. 3-7: The movement of the end face of a precast prestressed element can often be greater in the bottom edge than in the top edge. To avoid restraint connection devices should better be placed at the top

Non-structural façade panels can be placed in the buildings horizontally between vertical supports, or vertically between horizontal supports, see Fig. 3-8. When the wall elements are placed vertically, all columns in one single frame will get their horizontal loads from the roof. However, when the wall elements are placed horizontally, the column at the facade is loaded by a distributed wind load, while the other columns in the single frame get their horizontal loads from the beam only. This leads to different types of moment diagrams for different columns in the frame, see Fig. 3-8.

In both cases the panels are tied to the main structural system. Vertical panels are supported on a small linear foundation and tied normally to a horizontal beam on top. The support connection at the foundation has to allow rotation of the panel and the tie connection at the top has to allow vertical movement. The panels have thermal movements, which can be large in high temperature. The panels have a need to curve due to the temperature gradient, which normally develop in insulated panels. However, if the ties at the top do not allow the panel to move vertically, the panel is clamped and the prevented need for expansion will lead to bending stresses and further curvature.

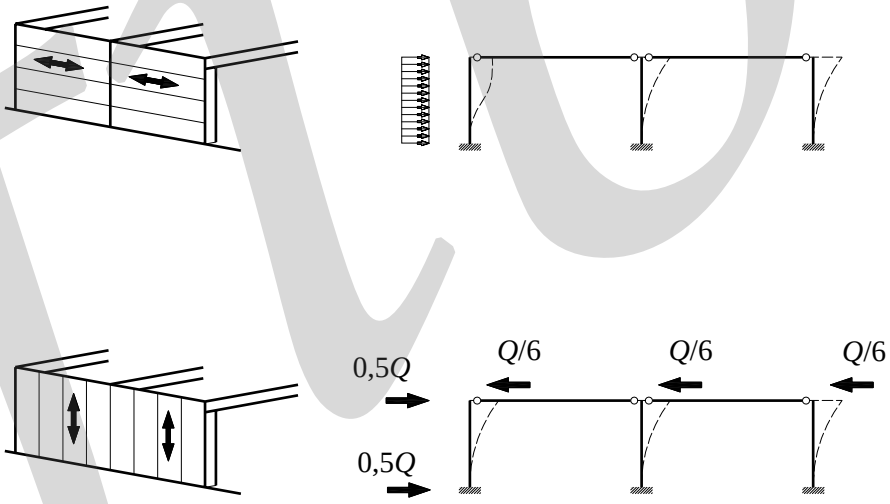

Fig. 3-8: Non-structural cladding panels can be placed horizontally or vertically

In horizontal panels a similar phenomenon may occur. The panels are normally connected to the columns of the main structural system. It is desirable that the panels can move in relation to the fixation points so that thermal movements can take place without restraint. However, if the panels also are connected longitudinally to each other, the need for thermal movements will increase as in this case the whole wall needs to move as one unit.

Because of the uncertainties, both in the estimation of the need for movements and in the estimation of the flexibility of the structural connections, the real need for movements may exceed the calculated one. Therefore, the connections should preferably be designed and detailed so that brittle

failures are avoided, if the connections are overstressed due to an unexpectedly high restraint force or in case of fire or accidental action. In this case a ductile behaviour is favourable. When overstressed, a brittle connection will fracture, but a ductile connection will yield under more or less constant force. This means that the resistance of the ductile connection remains. When this connection deforms, the need for movement decreases and so will the restraint force until a new state of equilibrium is obtained. Large movements may occur but the resistance of the connection remains without damages to the connection zones. In order to have a ductile behaviour in structural connections, the strengths of the various components of the connection must be balanced to each other. The principles for this are presented in Section 3.6.

3.5.2 Unintended restraint

3.5.2.1 Risk of unintended flexural cracks

Although precast elements are normally designed as simply supported to aid fast erection, there is normally a difference between the conceptual idea of the connection behaviour and the real conditions in the completed connection – a typical example is shown in Fig. 3-9. In design a simple mechanical model has been used assuming 'pinned' conditions at the supports. However, for several reasons, such as the need for structural interaction between walls and floors, and need for structural integrity and robustness, the connections are completed with small quantities of reinforced concrete sufficient to cause a so-called 'unintended' restraint.

The elements can also be 'clamped' in the connection between other elements. Restraint forces can also occur due to intrinsic effects, such as shrinkage, creep and thermal strains, where there would be no stress if the deformation of the precast element develops freely. Even if the unintended restraint is ignored in the design of the elements themselves, the consequences must be evaluated and appropriate measures should be taken to avoid possible problems.

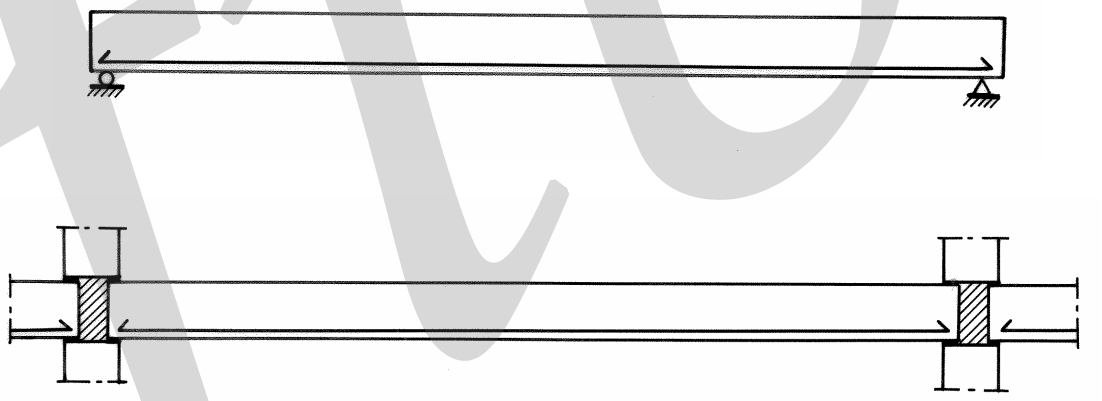

Fig 3-9: Differences between the mechanical model used in the design (top) and the real condition in the completed connection (bottom).

In many cases the precast elements are strong enough to resist the stresses arising from unintended restraint. In other cases the tensile strength may be reached and cracks develop as a consequence. Often limited cracking can be accepted, but in certain cases cracking can be dangerous with regard to the load-bearing capacity of the elements. For example, when the connection zone is not provided with reinforcement in the upper part of the section, flexural cracks starting from the top can open up considerably and significantly reduce the shear capacity of the section. Especially dangerous are cracks in locations away from the support, since the bottom concrete cover might spall off when the shear force is resisted mainly by dowel action of the bottom reinforcement as shown in Fig. 3-10 a. Such crack locations are therefore considered as unfavourable in relation to crack positions at the edge

of the support, see Fig. 3-10 b. In the latter case the shear transfer by dowel action of the bottom reinforcement can be balanced by the support pressure.

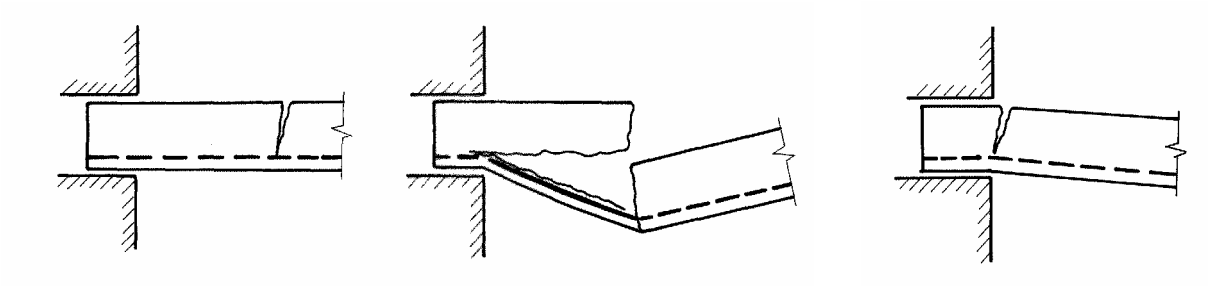

a) b)

Fig 3-10: Various locations of a flexural restraint crack, a) unfavourable location where shear transfer by dowel action of the bottom reinforcement might spall off the bottom concrete cover, b) preferred location where shear can be transferred by dowel action balanced by the support pressure

Restraint stresses can occur due to load-imposed deformations, for instance when the support rotation due to the service load cannot develop freely but a negative moment arises, see Fig. 3-11.

The bond between the joint face of the precast element and the joint fill can be significant. It has been observed that the bond in joint interfaces can be of the same magnitude as the tensile strength of the joint filling material, grout or concrete, [Lundgren (1995)]. Since the bond across a joint interface is normally a brittle and unreliable parameter, it cannot be utilized in design. Consequently, the joints are assumed to be cracked. However, in practise they can often remain uncracked and transfer considerable tensile stresses that were not accounted for in the design.

Fig. 3-11: A negative moment at the support may develop when the element is subjected to service load because the support rotation is fully or partly prevented

3.5.2.2 Unintended restraint of hollow core floor units

Hollow core floor units are normally designed to be simply supported and to resist shear and bending mainly in the longitudinal direction. However, the design and detailing of the support connections often result in restraining effects. Since hollow core elements normally have no top reinforcement and no shear and transverse reinforcement, it is necessary to carefully consider the risk that cracks caused by unintended restraint reduce the shear capacity of the element.

Some possible causes for restraint at floor-wall connections are shown in Fig. 3-12. The causes can be clamping between wall elements at the end of the hollow core element, frictional forces developing between the floor and wall elements, bond stresses between the end face of the hollow core unit and the joint grout/joint concrete, dowel action from the concrete that is allowed to fill the cores at the end of the hollow core unit, tie bars.

As described in Section 3.5.1 (Fig. 3-7), the end displacement of a prestressed slab varies with the amount of prestressing, dead loads, live loads, slab thickness, span length etc. It should be noted that the result is often as shown in Fig. 3-7 and not as shown in Fig. 3-12.

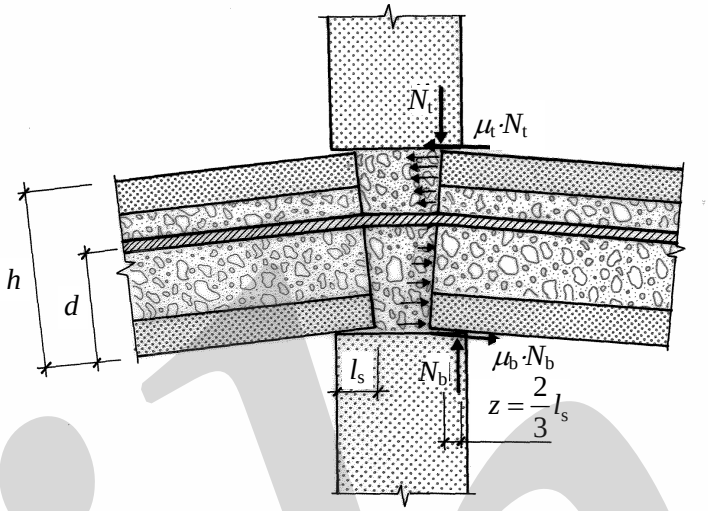

Fig. 3-12: Possible causes for unintended restraint of hollow core units at the support connection

The actual restraint moment M_{restr} in the connections depends on the actual need for deformation (rotation and overall shortening) and the stiffness of the elements involved. The restraint moment can never exceed the capacities of the connection details. To estimate the restraint moment, the following expressions (3-5) and (3-6) are recommended, [EN 1168 (2005)]. It is not necessary to consider the effect of friction or of the tie bar when the joint interface is still uncracked. The total normal force is used as a conservative assumption.

End face assumed to be uncracked:

$$M_{restr} = \frac{2}{3} N_t \cdot l_s + f_{ctj} \cdot W_{cj} \tag{3-5}$$

End face assumed to be cracked:

$$M_{restr} = \frac{2}{3} N_t \cdot l_s + f_y \cdot A_s \cdot d + \mu_t N_t \cdot h \tag{3-6}$$

where μ_t = frictional coefficient at top edge
f_{ctj} = tensile strength of joint concrete
N_t = total normal force in the wall at the top edge
W_{cj} = sectional modulus of the joint interface (the whole joint interface including the cores)

To estimate the maximum axial restraint force N_{restr} that can develop, the following expressions are recommended.

End face assumed to be uncracked:

$$N_{restr} = f_{ctj} \cdot A_j \tag{3-7}$$

End face assumed to be cracked:

$$N_{\text{restr}} = \frac{\mu_t N_t + \mu_b N_b}{2} + f_y \cdot A_s \tag{3-8}$$

where A_j = full area of joint interface (including the cores)
μ_b = frictional coefficient at bottom edge
N_b = total normal force in the wall at the bottom edge

The end zone of the hollow core unit should be analysed with regard to the risk of cracking taking into account the restraint effect, ordinary loading and the effective prestressing force. Within the transfer length the development of the prestressing force must be considered. Near the support the prestressing force may be insufficient to prevent a possible crack, starting from the top, from propagating deeply into the section. A deep crack may result in a considerable reduction of the shear capacity. There are in principle three ways to handle this risk:

- the connection can be designed to be effectively simply supported, see Fig. 3-23
- the restraint moment can be reduced or limited so that restraint cracks are avoided
- a restraint crack in the preferred location, see Fig. 3-10 b, is permitted and the connection zone is strengthened so that the shear capacity is sufficient in spite of this crack

In the two last cases the following measures should be taken to reduce the risk of cracking in unfavourable positions (Fig. 3-10 b) within the critical region where there is a significant tensile stress in the top of the section:

- transverse slots or other weaknesses should be avoided
- the concrete fill in cores without tie bars should not extend outside the wall in case of straight ends of the hollow core units (Fig. 3-13 a), or not outside the transverse recess in case of slanted ends (Fig 3-13 b)
- tie bars anchored in cores or longitudinal joints should not be cut off within the critical region

The restraint moment can be reduced by limiting the load on the wall, i.e. limiting the number of floors or providing soft joint fill that prevents wall load from entering the end zones of the hollow core unit(s), see Fig. 3-13 a. To avoid direct loading from the wall and facilitate crack formation in the preferred location, the hollow core unit(s) could be provided with slanted ends as shown in Fig. 3-13 b

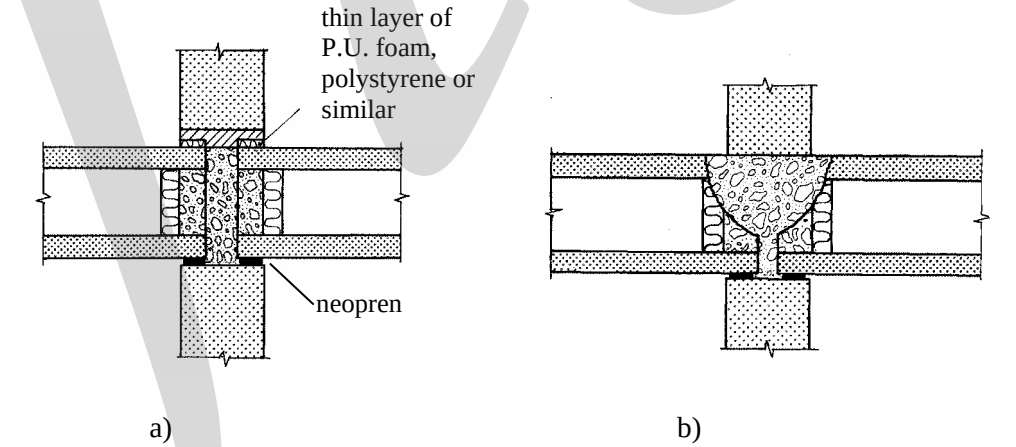

Fig. 3-13: Measures to limit or avoid restraint moment at the support connection of hollow core elements, a) use of soft joint fill, b) slanted ends

In case of high wall loads restraint cracks can not be avoided and the elements need to be strengthened by placing additional reinforcement bars in concreted cores or grouted joints, see Fig. 3-14. The purpose of the tie bars is to increase the shear capacity of a cracked section in the favourable position (Fig. 3-10b). The following aspects should be considered:

- The reinforcement used for strengthening should be placed in the upper part of the section (above mid-depth) in addition to the ordinary tie bars, which are placed in the lower part of the section.
- The additional reinforcement bars should be anchored so that they are able to transfer their yield load in the assumed crack section.
- The amount of reinforcement in the upper part should be limited so that no further flexural cracks (from a negative bending moment) appear in unfavourable locations after formation of the first crack in the preferred location.

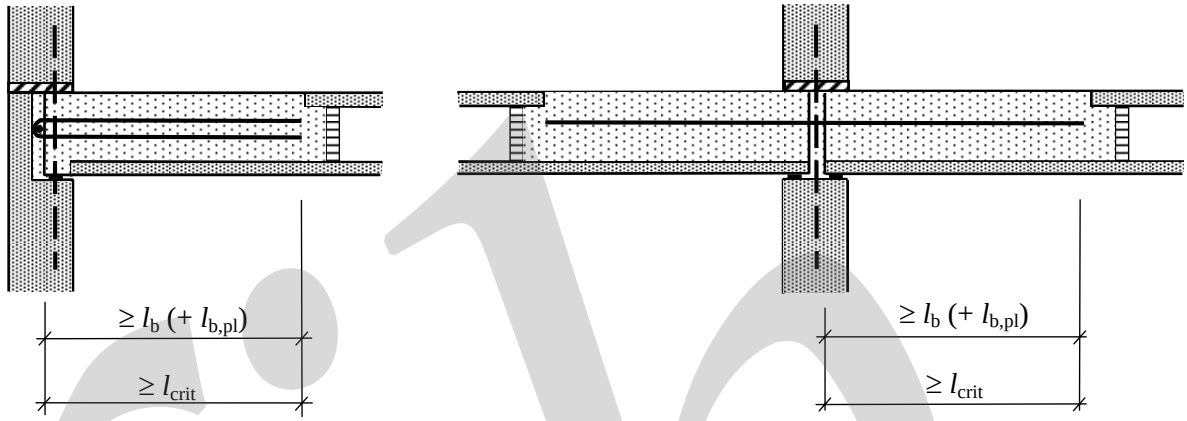

Fig. 3-14: Strengthening of the end zones of the hollow core elements by tie bars placed in concreted cores

Test results [VTT(2002, 2003)] show that there is a considerable shear capacity of a cracked section when the crack is in a favourable position. This can be explained by the following mechanisms:

- Shear capacity of the bottom compressive zone below the tip of the crack
- Dowel action of the bottom strands balanced by the support reaction
- Friction and interlocking effects along the crack as long as the crack is kept together by reinforcement in the upper part of the section.

Another case of unintended restraint of hollow core floors appears when the floor is connected to a stabilising unit, e.g. an elevator shaft, along the longitudinal edge of a hollow core unit. Then the hollow core units near this connection will act as supported on three sides and the restraint may result in unexpected cracking.

3.5.3 Unintended composite action

Where composite action between the precast element(s) or cast *insitu* infill is used, unintended restraint can occur in the precast elements. The most common situation is a negative moment capacity provided in a reinforced concrete topping, which is not accounted for in the precast element. Similarly, where floor elements are connected to a supporting beam, they will increase the overall flexural stiffness of the beam and they can to some extent be included in the composite beam section. In such cases the elements, their connection and details should be designed consistently in accordance with the assumed structural behaviour.

However, it is not possible to draw the conclusion that composite action will not be there if it was not utilized in design. For example, where precast floor elements are placed on slender beams and connected together composite action will follow by intention or not. It is thus possible to speak about ‘unintended composite action’ in a similar way as for ‘unintended restraint’.

Hollow core units are normally designed according to a simplified model assuming simply supported ends on rigid supports. However, in the real situation the supporting beam may be flexible and the hollow core units are grouted and connected together and to the supports. Hence, when the

beam is loaded and deflects, the hollow core elements will, due to compatibility reasons, increase the stiffness of the beam. However, transverse tensile stresses appear in the hollow core elements when they too deform, as shown in Fig. 3-15. These stresses are added to other stresses that normally appear and as a consequence cracks may appear and the shear capacity of the hollow core units may be reduced. This matter of 'unintended composite action' is addressed in *fib* (2000a). Reference is also made to Pajari and Kloukkari (1998) and Pajari (1998).

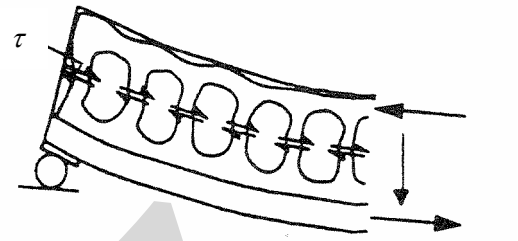

Fig. 3-15: Unintended composite action results in tensile stresses in hollow core units when they are placed on flexible supports, adopted from Leskelä and Pajari (1995)

3.5.4 Full and partial continuity

The connections in a precast concrete structures will give a certain restraint that in most cases is 'unintended', even though they are designed as simply supported. The connections have finite stiffness and moment capacity, but are normally weaker than the connected elements, often considered to be so small that they are ignored.

In some cases full continuity of the precast structure is aimed at, trying to simulate a cast *insitu* structure. This leads as a rule to rather complicated connections as it is difficult to obtain full continuity across joints, particularly in the soffit and exterior sides.

Intermediate situations, known as 'semi-rigid', often occur in precast construction. Although the stiffness and capacity of the connection may be considerably smaller than in the elements, the stiffness and the resistance of the connection are accounted for in design. Fig. 3-16 shows how a moment resisting connection can be classified as fully rigid, semi-rigid, or pinned depending on its moment-rotation characteristics in relation to the strength and stiffness of the structural elements.

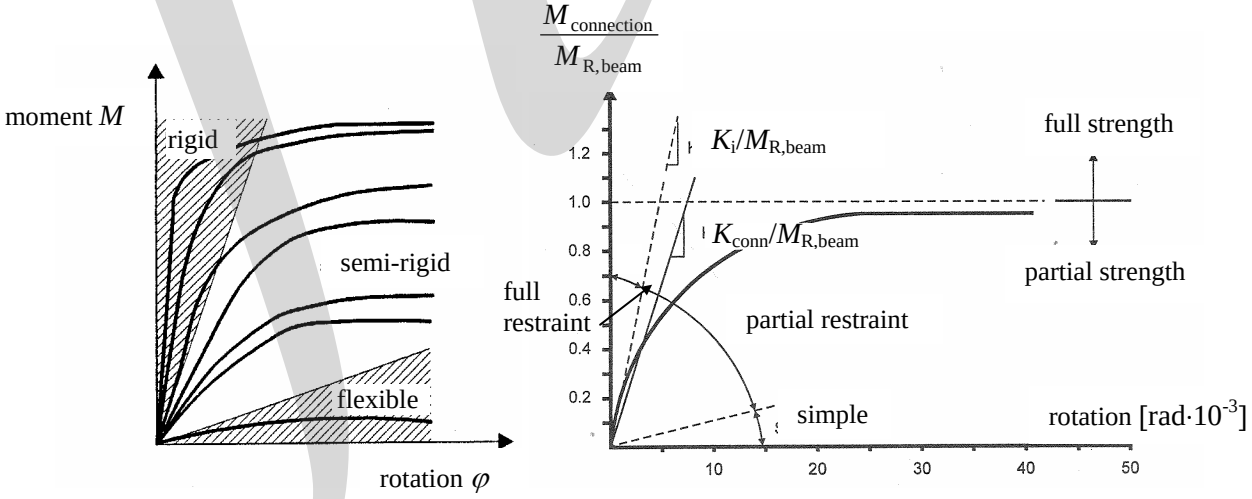

Fig. 3-16: Classification of moment-resisting connections as fully rigid, semi-rigid or pinned/flexible, adopted from Leon (1998)

Partial continuity occurs in composite precast floors with multiple spans. The floor elements are erected as simply supported and will carry its dead weight in this way. Then the floor is completed

with structural connections or a structural topping to resist negative bending moment that appears at interior supports for imposed service load. Therefore reinforcement is only placed in the topping and no reinforcement is used in the bottom of the slab at these sections.

In some cases it may happen that positive moments are to be resisted at internal supports due to wind, thermal, creep or redistribution effects. Therefore, when only negative reinforcement is used at the support, the designer has to check that no positive moments will be expected due to the conditions mentioned above. Design of floor connections for partial or full continuity is treated further in Section 9.6.

Another case of partial continuity is when connections in beam-column systems are very deformable in relation to the structural members. In that case the deformations of the connections must be considered as concentrated rotations in the structural analysis. When connections are weak in relation to the structural members that they connect, they are classified as 'semi-rigid connections'.

Often connections that are considered as pinned could be treated as 'semi-rigid', if the restraint that they normally provide is accounted for in the design. One example of such connection is shown in Fig. 3-17. More examples of semi-rigid connections in precast structures are given in COST C1 (1998).

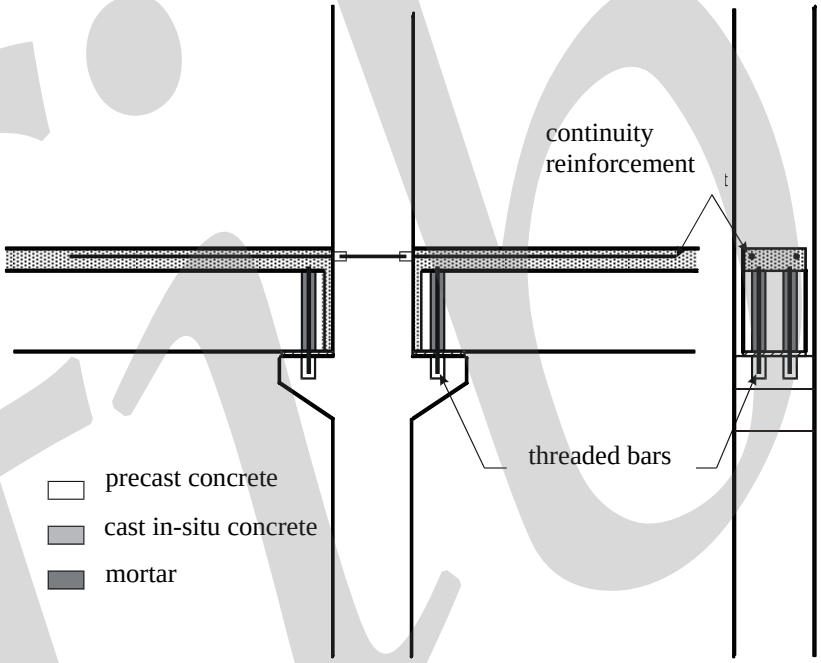

Fig. 3-17: Example of bolted connection that is often considered as pinned, but which could in many cases be treated as a semi-rigid connection

3.6 Balanced design for ductility

Even an uncomplicated connection, like the tie connection shown in Fig. 3-18, in which the tensile force is transferred across the transverse joint by one tie bar only, can be considered as links of a force path. All the links contribute to the global load-displacement relationship of the tie connection. However, normally only certain components of the connection can contribute to the global displacement with large plastic deformations. These elements can be identified as the ductile ones. In the single tie bar connection in Fig. 3-18, the tie bar and the anchorage at each side of the joint can be considered as force transferring links, where the tie bar is the ductile component.

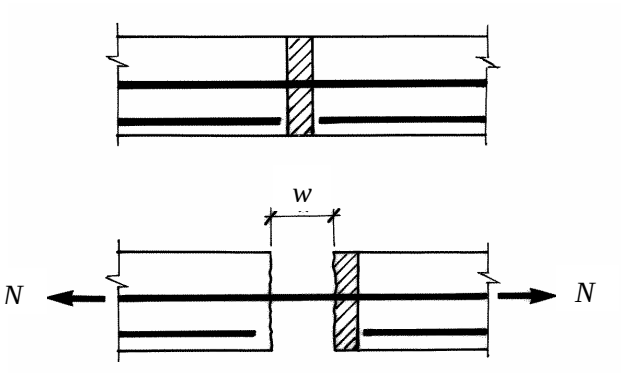

Fig. 3-18: Tie connection between precast concrete elements

The aim of a balanced design for ductility is to ensure that the full deformation capacity of the ductile links can be mobilised. Brittle failures in the other elements should be prevented before the full plastic deformation is obtained in the ductile ones. Hence, the other links should be designed to resist not only the yield capacity, but also the ultimate capacity of the ductile ones with a sufficient margin. In this respect, an unexpectedly high value of the ultimate strength of the ductile component is unfavourable and should better be considered in the design by introduction of characteristic high values.

The principle for a balanced design is illustrated in Fig. 3-19 on a more complex tie connection. The ribbed anchorage bars are identified as the ductile elements and presumed to have the most important contribution to the plastic displacement. All the other components, i.e. the anchorage of the embedded bars, the steel angles, the transverse steel rod and the welds, should be designed to resist an unexpectedly high value of the ultimate capacity of the anchor bars.

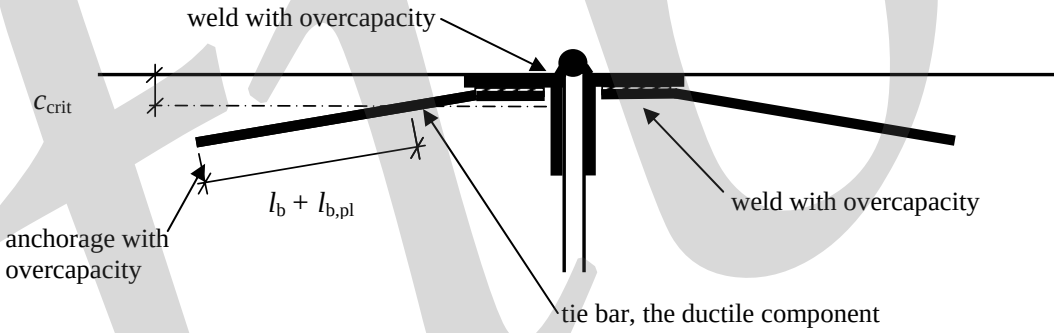

Fig. 3-19: Example of balanced design for ductility of a tie connection. The anchor bars are the ductile components. The other components, including the anchorage of the bars in the concrete elements, should be designed in order to resist an unexpectedly high value of the ultimate capacity of the anchorage bars

The anchorage capacity of tie bars should be subjected to certain attention. In order to avoid brittle failures initiated be splitting cracks, sufficient transverse confinement should be provided, for instance by transverse reinforcement or a concrete cover exceeding a critical value c_{crit}. For straight bars, the anchorage length should be sufficient to prevent brittle pullout failure. In this respect, the possible yield penetration in the plastic stage should be considered. When connection details are placed near free edges of the element, the concrete cover of the anchorage bars may be less than the critical value concerning brittle splitting failure. In such cases the bar could be bent into a zone with sufficient concrete cover and anchored by a sufficient anchorage length within the safe zone. The principle is illustrated in Fig. 3-20. Alternatively, transverse reinforcement can be provided in the anchorage zone.

Furthermore, the detailing should facilitate welding of high quality and a sound and safe force path through the entire connection. The tendency of bent bars to straighten when loaded should be observed. The strut and tie method could be used to check the equilibrium system, see Section 3.4. More information on anchorage and detailing of anchor bars is given in Section 7.2.4

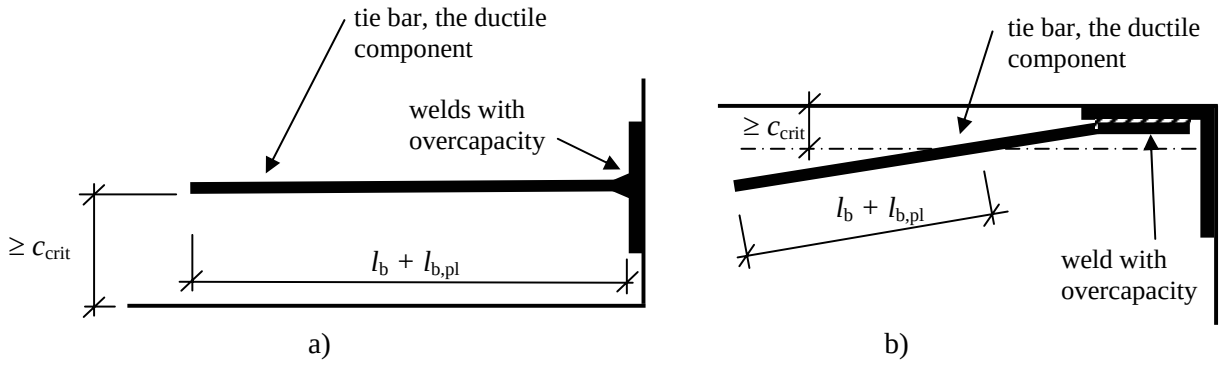

Fig. 3-20: Examples of balanced design for a ductile behaviour. The bar is anchored is a safe region to prevent splitting failure. Furthermore, the anchorage length is increased with an additional amount $l_{b,pl}$ compensating for the yield penetration in the plastic stage; a) the concrete cover exceeds the critical value with regard to splitting; b) the bar is bent into the safe zone where it is properly anchored by a sufficient anchorage length

When tie bars are anchored in narrow joints or recesses, additional precautions are needed to ensure efficient anchorage. This is especially true when there is a risk of improper encasing of the bar or uncompleted fill of grout or concrete in the joint or recess, see Section 7.2.5 for more information on the subject.

3.7 The flow of forces through connections - examples

The term *structural connection* is not limited only to the area where two (or more) elements meet - it includes the zones adjacent to both elements in which the transfer of the forces takes place. In these congested zones, the forces have to be safely transferred and the reinforcement sufficiently anchored, otherwise the connection will not work properly.

The designer should draw an engineering model (scheme) of the path of the forces in the connection, for example as shown in Fig. 3-21, and design the joint and the adjacent zones accordingly.

The strut-and-tie model is in this respect a simple and convenient tool, see Section 3.4. The designer should check that the path of the forces is uninterrupted and that the forces can be generated and resisted in every location along the path, including anchorage of tensile forces. If deformations due to shrinkage, creep, or other reasons are expected, it should be checked whether they could be allowed to freely take place. If these deformations are restrained, or partly restrained, the resulting forces have to be added to other acting forces in the connection and incorporated in the design of the connection to prevent damage or cracks. The designer should also keep in mind the influence of the execution and the workmanship on the performance, quality, and the intended flow of forces in the connection. Three examples are given to demonstrate these principles:

Fig. 3-22 shows a compression loaded mortar joint for the columns and a half-joint for the beams. Solution A will give an excellent performance - the joints are easily accessible for workers and the large forces in the columns are readily transferred from one column to another. Solution B, with a beam passing over the column and one half beam joint, say at one fifth of the span, will give better moment distribution over the beams, but most probably a poorer performance at the column connection. The column connection, which now consists of two mortar joints, will have to overcome the following two handicaps:

- As the beam passes over the column and has a certain negative moment, its top filaments will elongate. This elongation transferred through the mortar joint to the underside of the upper column will negatively influence the bearing capacity of this column, as it will tend to undergo the same deformation and split
- The joint at the underside of the beam is in turn difficult to reach. Placing of the mortar is difficult, resulting (most probably) in bad quality and subsequent poor force transfer.

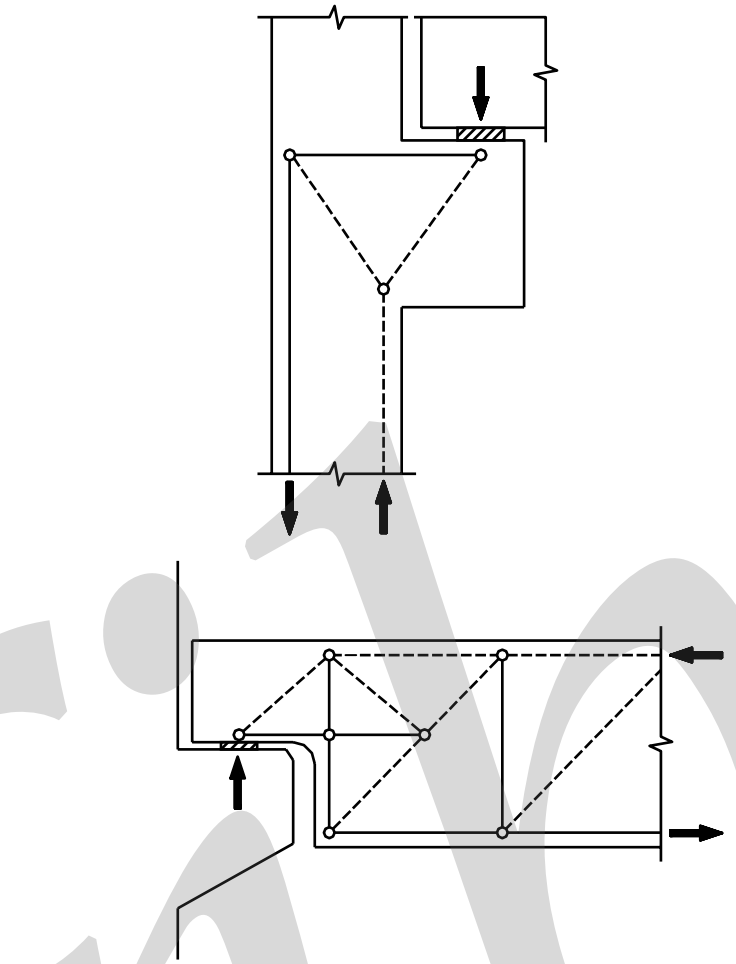

Fig. 3-21: Engineering strut and tie model for column-beam connection

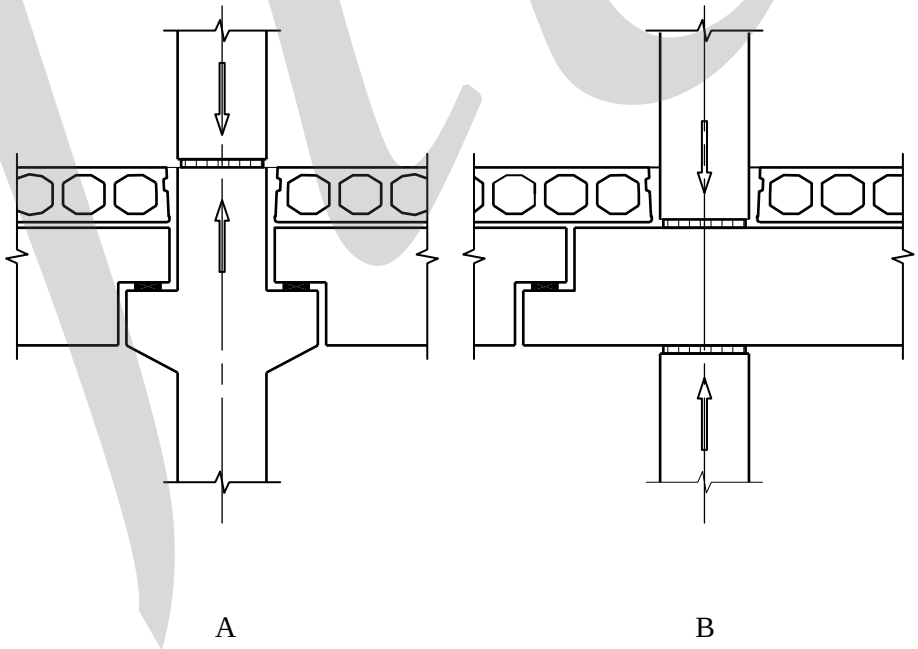

Fig. 3-22: Two alternative solutions for column-beam detailing in precast concrete. Solution A. will perform better than solution B

Fig. 3-23 gives an example between wall elements and two hollow core floor units. Solution A will give the best structural result. The prestressed floor units, which are normally designed for positive moments only, are free to deform and rotate at their bearings and the generally large forces in the wall elements can be directly transferred from one wall element to another.

Solution B has the following disadvantages:

- The precast prestressed hollow core slabs might be clamped in between the wall elements. Because of this the hollow core units might be exposed to negative moments, see Section 3.5.2.
- The lower joint will have a much smaller effective area to carry the vertical wall load due to the area taken by the supports of the hollow core slabs.
- The load from the upper wall will be forced to squeeze in the concrete wedge formed by the concrete fill in between the hollow core slabs. This change in the flow of the stress trajectories will cause splitting forces in both ends of the wall elements.
- There is a significant risk that the quality of the concrete fill in between the hollow core slabs, because of the limited space, will be less then required.

This means that only smaller forces can be transferred over this joint from one wall element to another, see design example in Section 6.7.2.

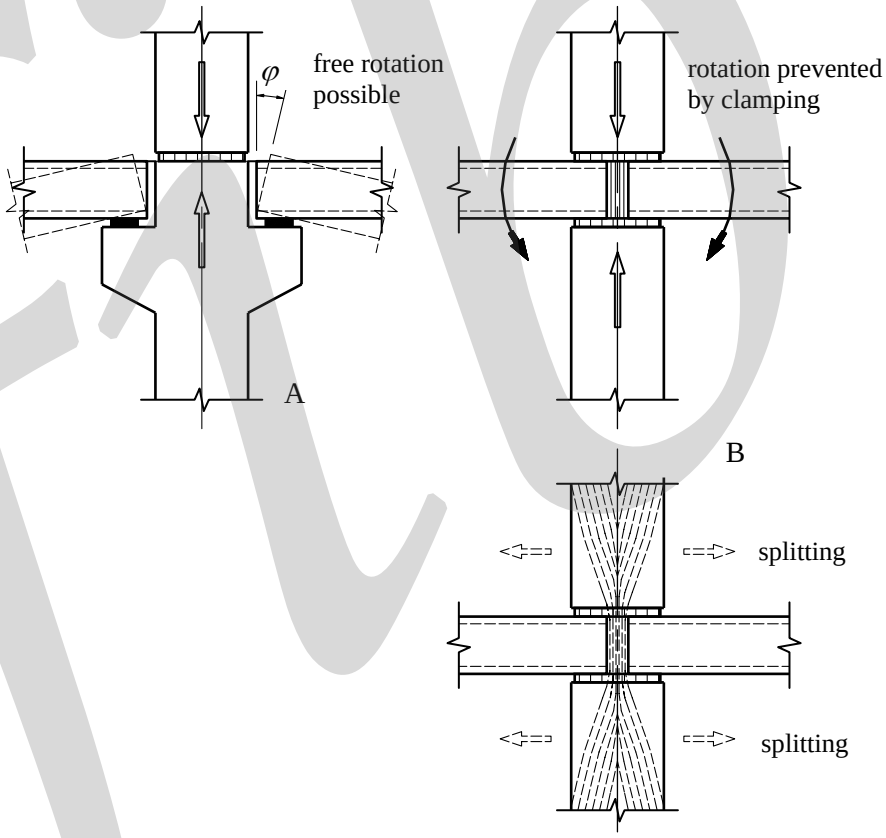

Fig. 3-23: Two alternative details for wall-hollow core floor connection

These two examples show how important it is to keep in mind the flow of forces through the connection and to relate this to the influence it may have on the performance of other structural elements.

The third example in Fig. 3-24 shows a patented[(1)] connection between precast beams and columns. The main advantage of the so-called 'sliding plate' connector is that a hidden plate inside a steel casing in the beam is pushed out and into the column unit when the beam is in its correct position. The strut and tie model in Fig. 3-25 a shows the principal function of the vertical tie bars welded to the end plate and the vertical stirrups illustrated in Fig. 3-25 b.

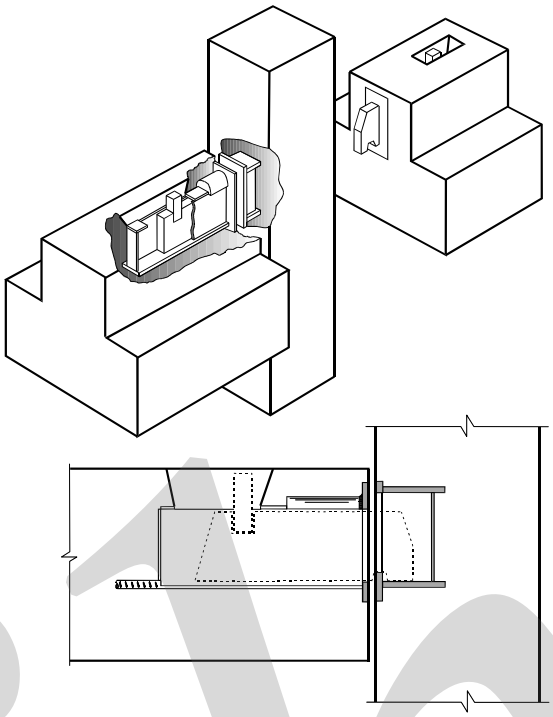

Fig. 3-24: Beam-to-column connection with hidden movable steel plate, developed by Spenncon AS Hønefoss, Norway[(1)]

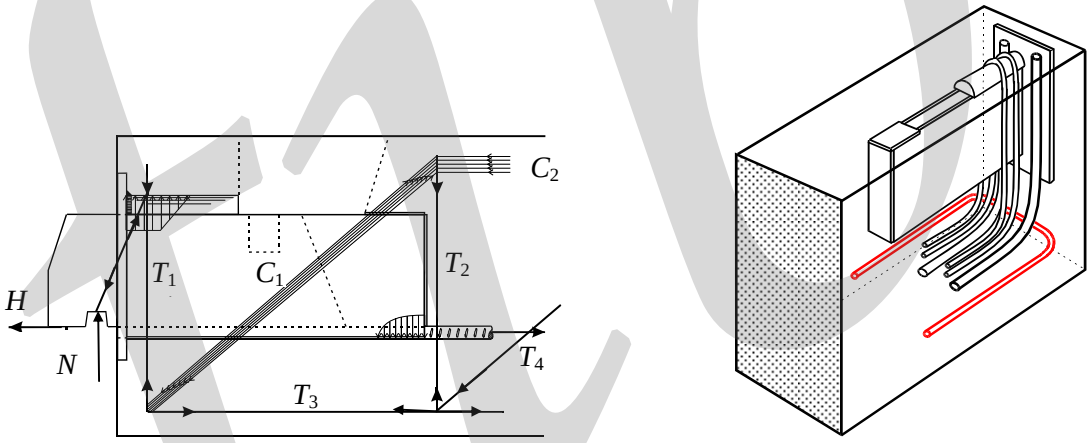

a) b)

N = Vertical support load
H = Horizontal support load
T_1 = Resulting tensile force at the front of the beam unit
T_2 = Resulting tensile force at the rear of the beam unit
T_3 = Resulting tensile force at the bottom of the beam
T_4 = Tensile force caused by restraint from the column unit
C_1 = Resulting compressive struts on each side of the beam unit
C_2 = Resulting compressive force in the top of the beam

Fig. 3-25: Design of connection zone in the beam element, a) strut and tie model representing the flow of forces through the connection, b) arrangement of reinforcement in the connection in consequence of the model

(1) Patent holder is SB Produksjon AS, Åndalsnes, Norway

4 Other design aspects

4.1 Production, transportation and erection

4.1.1 Considerations in production

The general rule is that the connection device must be as 'foolproof' as possible. It should be possible to place it in the mould correctly oriented and within the necessary tolerances, with a minimum of effort.

(1) Avoid congestion

At the location of connections additional reinforcing steel, embedded plates, inserts, block-outs etc. are frequently required. It is not unusual that so many items are concentrated in a small location that very little room is left for the concrete. It must be kept in mind that reinforcing bars and prestressing strands, which appear as lines on the drawing, take up real space in the elements. Reinforcing bars require more space than their nominal diameter, and there must be room for the curvature of bent bars. If congestion is suspected, it is helpful to draw large-scale details of the region in question.

(2) Avoid penetration of the forms

Units requiring holes in the forms should be avoided if possible, especially in steel moulds. Exceptions to this rule can be made if there is a substantial amount of repetition in the production. Holes in the forms may be necessary not only because the units are protruding from the elements, but also for the arrangement used to keep the units in place during casting.

The units must also be designed so that they do not make the dismantling of the form impossible without damage to the form. Most forms are supposed to be used more than once.

Connection units to be placed in the top surface during casting should be secured against the edges of the mould using purpose made holding devices. These devices are mostly costly, make it more difficult to obtain a smooth surface, or the holding device may hamper the placement of concrete or other surface material. The various disadvantages have to be evaluated before selecting the method. However, if the same steel plate is placed in the bottom of the form, it can be located with great accuracy, as it can be fixed to the bottom directly.

(3) Reduce post-stripping work

A plant casting operation is most efficient when the product can be taken directly to the storage area immediately after removal from the form. Any operations required after stripping and before erection, such as special cleaning or finishing, welding on projecting hardware etc. should be avoided. These operations require additional handling (increased possibility of damage to the elements), extra workspace and added labour, often with skilled trades. Sometimes a trade-off is necessary between penetration of the forms and post-stripping work.

(4) Use repetitious details

It is very desirable to repeat details as much as possible. Similar details should be identical, even if it results in a slight over-design.

(5) Use standard items

Hardware items such as inserts, studs, steel elements, etc., should be readily available standard items that are preferably from more than one supplier. Custom fabricated or specialised proprietary

items add cost and may cause delays. It also simplifies fabrication if similar product items are standardised as to size and shape. There is also less chance of error. The same principle applies to reinforcing bars, embedded plates, etc.

(6) Be aware of material limitations

Examples of this are the radius requirements for bending reinforcing bars, standard lengths for certain sizes of inserts, etc.

(7) Avoid non-standard tolerances

Dimensional tolerances, which are specified to be more rigid than industry standards, are difficult to achieve. Connections, which require close-fitting parts without provision for adjustment, should be avoided as much as possible.

(8) Allow alternatives

Very often precasters will prefer certain details. The producer should be allowed to use alternative methods or materials, provided the design requirements are met. Allowing alternative solutions will often result in the most economical and best performing connections.

4.1.2 Considerations for transportation

During transportation any units protruding from the concrete element must be shielded in order not to create a hazard to people. Protruding units must be able to withstand any shocks they can be subjected to during handling. Protruding units, like reinforcing bars, can in many cases be difficult to handle during transportation. For example, a wall panel shall be transported standing at the edge, but has reinforcing bars protruding at the bottom. This will make it necessary to build up the support on the trucks, which is costly, takes time, and makes the load less stable. This problem can be solved by letting the bars protrude from the top of the element, but then the total height may make it difficult to negotiate the underpasses en route. The solution may then be to have the protruding bars replaced by insert and threaded bar, to screw in after the element has been transported to the site.

If protruding units do not create the kind of problems described above because they do not stick out that much, there still may be some difficulties. For example: corbels pointing down during transport may necessitate a lot of additional support provisions for the columns on the trucks. The consequence can be a less stable load, or decreased loading capacity of the truck. This kind of problem can be solved by making columns with the corbels in one plane only, and then place every second column ‘top-to-bottom’ on the trucks. Otherwise it is also possible to look for a corbel-free solution.

4.1.3 Considerations for erection

To fully realise this benefit of fast erection of a precast structure, and to keep the costs within reasonable limits, field connections should be kept simple. In order to fulfil the design requirements, it is sometimes necessary to compromise fabrication and erection simplicity.

(1) Use connections that are not weather sensitive

Materials such as grout, dry pack, cast-in-place concrete and epoxies need special provisions to be placed in cold weather. Welding is slower when the ambient temperature is low. If the connections are designed so that these processes must be completed before erection can continue, costly delays may result.

(2) Plan for the shortest possible hook-up time

Hoisting the precast element is usually the most expensive and time-critical process of the erection. Connections should be designed so that the unit can be lifted, set and unhooked in the shortest possible time. Before the hoist can be unhooked, the precast element must be stable and in its final position.

(3) Stability of the elements

Some elements may require propping, shoring, bracing or fastening before the hoist can be unhooked. Planning for the fewest, quickest and safest possible operations to be executed before releasing the hoist will greatly facilitate the erection.

Bearing pads, shims, or other devices, upon which the piece is to be set, should be placed ahead of hoisting. Loose hardware that is required for the connection should be immediately available for quick attachment. In some cases, it may be necessary to provide temporary fasteners or levelling devices, with the permanent connection made after the hoist is released. For example, if the permanent connection requires field welding, grouting, dry packing, or cast-in-place concrete; erection bolts, pins, or shims can be used.

These temporary devices must be given careful attention to assure that they will hold the piece in its proper position during the placement of all pieces that are erected before the final connection is made.

(4) Stability of the structure

In every stage of the erection process the stability of the structure as a whole must be planned and assured. If not, costly additional measures may have to be taken. The type of connection used may play a decisive role in this.

(5) Be aware of possible different loading conditions during erection

During erection loading conditions can occur, which induce stresses or deformations, as well in the precast concrete units as in the connections, which are higher than those under service conditions. When designing the connections due consideration has to be paid to these effects unless special measures are taken during the erection, such as temporary supports etc., to prevent such situations.

(6) Standardize connection types

All connections, which serve similar functions within the building, should be standardised as much as possible. As workmen become familiar with the procedures required to make the connection, productivity is enhanced, and there is less chance for error.

Some types of connections require skilled craftsmen to accomplish, for example welding and post tensioning. The fewer of these skilled trades required, the more economical the connection will be.

(7) Standardize sizes of components

Whenever possible, such things as field bolts, loose angles, etc., should be of common size for all connections. This reduces the chance for error, and the time required searching for the proper item.

(8) Use connections that are not susceptible to damage in handling

Reinforcing bars, steel plates, dowels and bolts that project from the precast piece will often be damaged in handling, requiring repair to make them fit, especially if they are of small diameter or thickness.

(9) Plan the movements

The connection detail must permit the element to be lowered into place as directly as possible – for example bars protruding in two directions make an element impossible to erect, see Fig. 4-1. A support or connection detail that makes it necessary to move the element horizontally in the last part of the erection sequence is difficult to perform, and is playing hazard with the possibilities of damage to the supports.

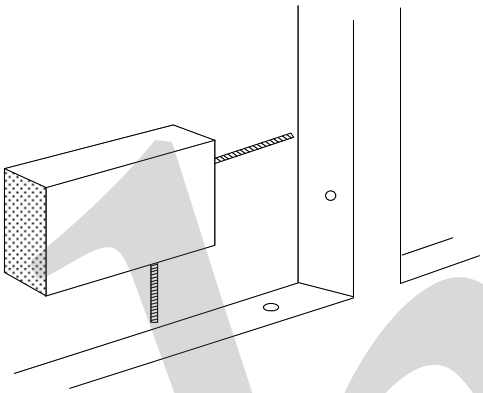

Fig. 4-1: Connection detail that makes erection impossible

Connection details that make it necessary to hoist the element at an angle other than horizontal should not be permitted. The hoisting operation in itself is rather hazardous, and to manoeuvre an element into position at a skewed angle is very difficult.

A support detail that is based on horizontal movement of the element during erection can only be used in one end of the element; otherwise it will be impossible to erect. An example is shown in Fig. 4-2.

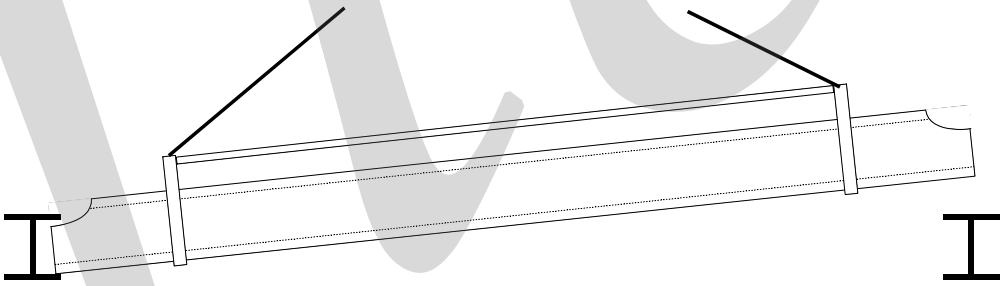

Fig. 4-2: Support solution that makes erection impossible

(10) Consider the reinforcement bar positions

Where protruding reinforcement bars or loops out of precast elements interlock or overlap with other reinforcement bars, care should be taken to ensure that the bars do not interfere with each other and that there is enough space (including the necessary tolerances) to place the elements in their final position in one single operation.

This aspect should be especially looked at where precast concrete elements are connected to or integrated in cast *insitu* concrete structures, since it is not a common use in the cast *insitu* concrete technology to position every reinforcement bar in plan to exact measurement. See example in Fig. 4-3 where a cast *insitu* loop connection of precast parapet panel to cast *insitu* concrete floor is shown.

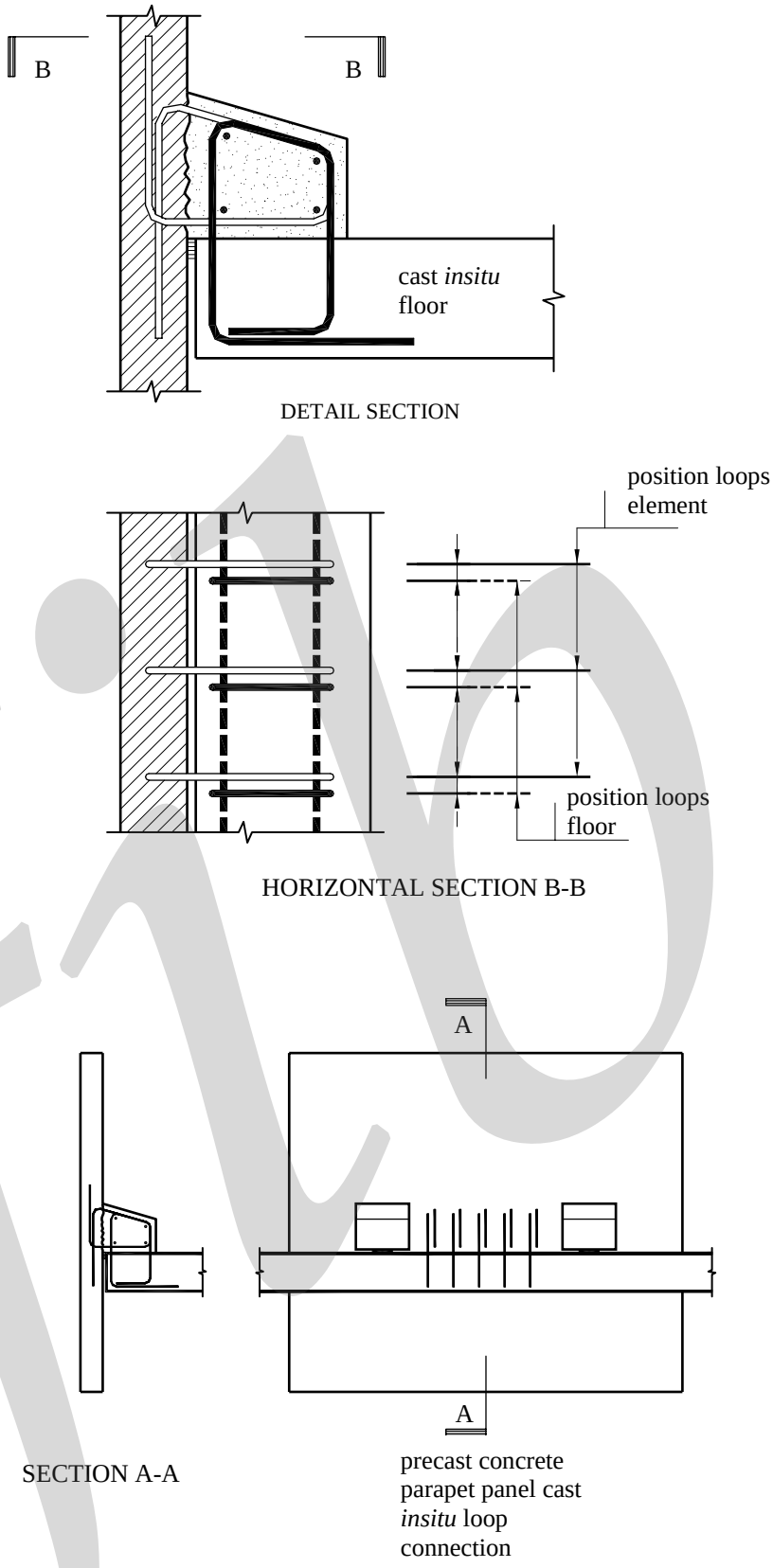

Fig. 4-3: Loop connection between precast concrete parapet and cast insitu concrete floor. Care should be taken that correct position of loops is ensured

(11) Accessibility

The connection detail must be accessible when the element is in its final position, see Fig. 4-4. It is often necessary to gain access to a connection after erection; to adjust a bolt, do some welding, put in some shims, check alignment, etc. The place where this is most often forgotten is the connection detail that connects a façade panel to the outside of a column. It must always be possible to enter bolts, see Fig. 4-5.

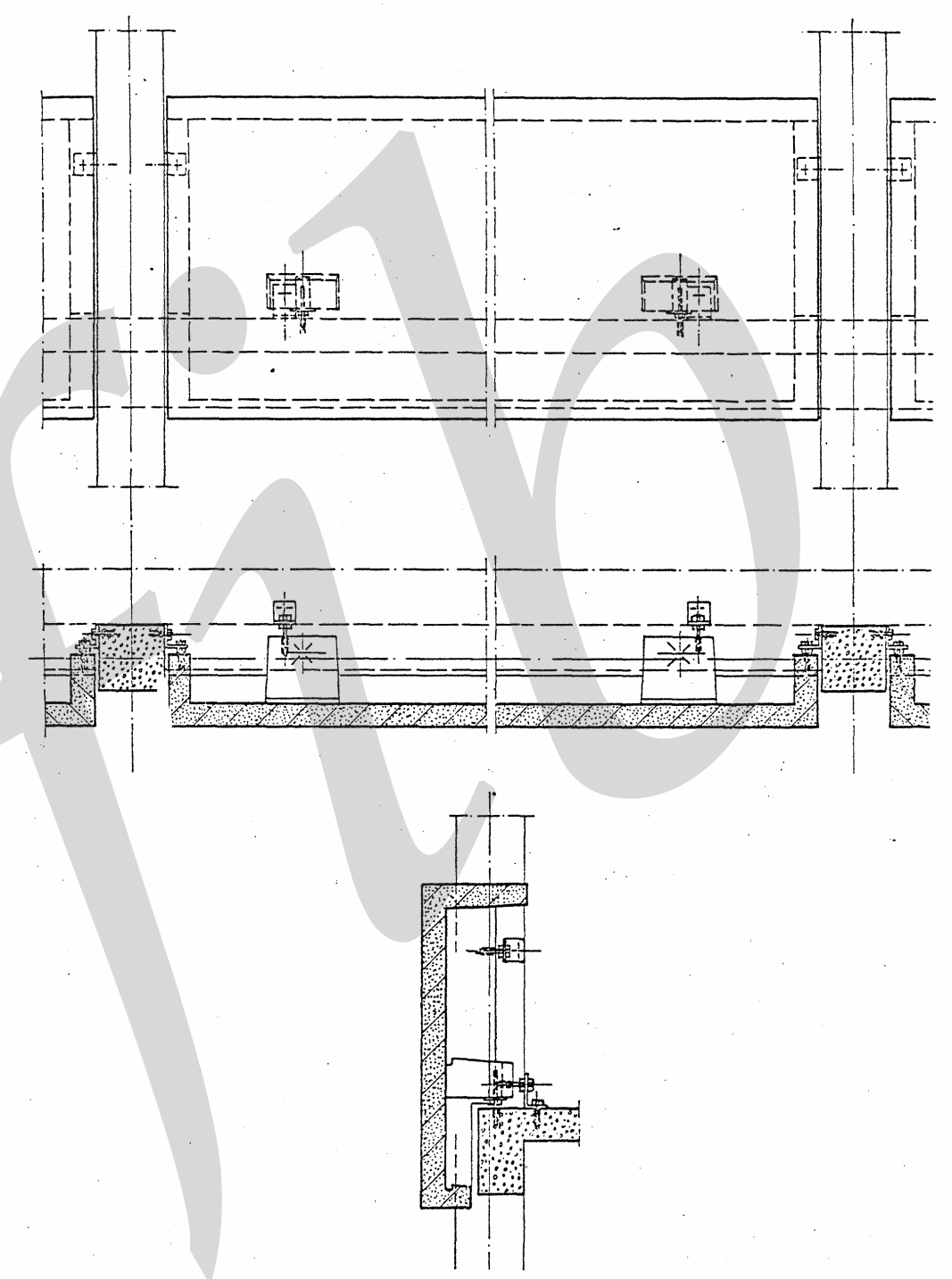

Fig. 4-4: The connection detail must be accessible when the element is in its final position

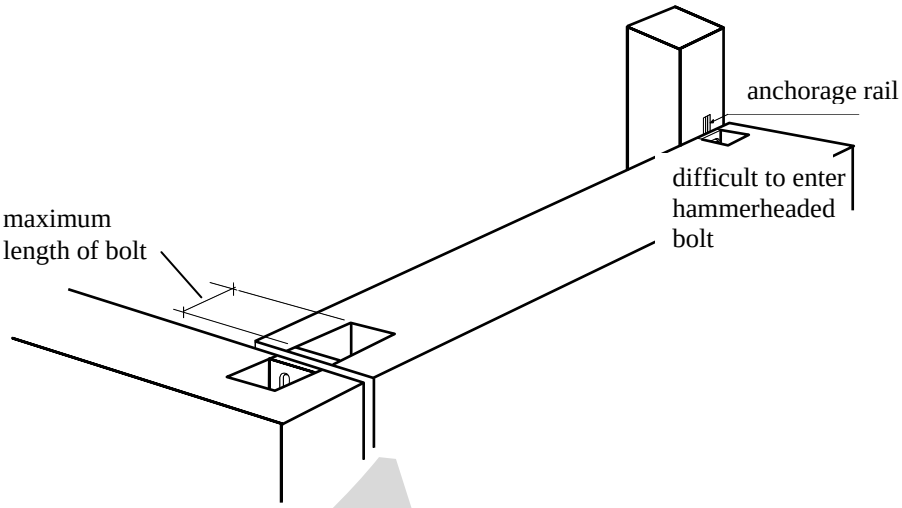

Fig. 4-5: Allow room for placing of loose components

4.1.4 Modular co-ordination

It is important to keep the modular system in mind when the connection detail is designed. If the connection details are adjusted for the best individual solutions in all joints, this may not be beneficial for the overall system. It may create variations on elements that otherwise could have been the same, and the benefit of repetition is lost. The advantages of repetition are obvious in the drafting and production process, but it is also of importance not to loose the freedom to interchange elements at the site. A typical example is erection of coloured facade panels, where it is sometimes necessary to be able to sort the panels according to the shade of colour in order to achieve the best possible result.

It used to be rather common to make the corner solution for horizontal facade panels as shown in Fig. 4-6 a. However, this solution makes it impossible to use a corner element at any other location in the facade. The solution shown in Fig. 4-6 b can in many cases be recommended to be used instead. This solution will necessitate one extra corner element, or some other facade material around the column, to cover it and to insulate. However, this solution will make all facade panels of the same length, and this advantage will probably more than outweigh the cost of the extra corner element.

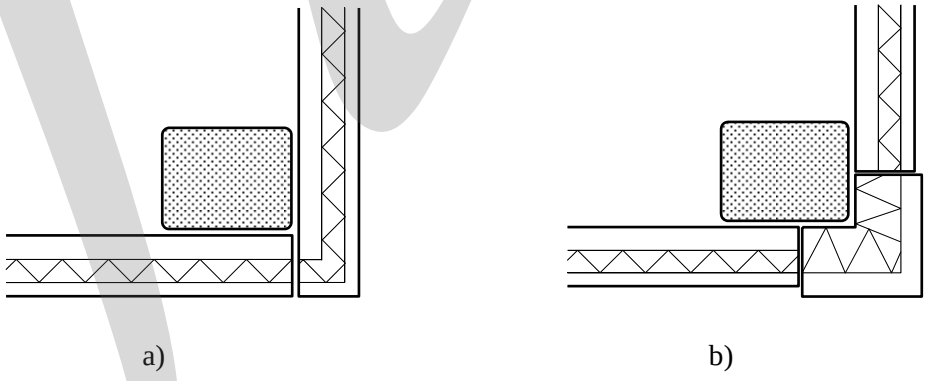

Fig. 4-6: Corner solution for façade panels, a) traditional solution with one special façade element, b) alternative solution with specially designed corner piece and otherwise identical elements

Another example concerns the same facade used in the previous example, in which the columns may have concrete corbels to support the panels. In order to permit the corner columns to be cast in the same mould as the other columns, it may be advantageous to have the panels in the gable supported by corbels made after the column is cast. These corbels can be made of steel, welded to an embedded

steel plate, or concrete corbel cast as an extra operation. The important thing is to achieve a corbel without having to do any extra formwork on the mould, and to have the extra corbel fixed in the factory and not on site. In this way the corner columns can be cast in the same form as the rest of the columns.

4.1.5 Tolerances

Tolerances can be defined as the maximum allowable deviation. Deviations have basically two reasons:

- Inaccuracies caused by humans, e.g. inaccurate reading of the tape measure, or a column erected slightly at an angle.
- Physical reasons, like the tape measure's change of length due to temperature, or a column's change of length due to axial loads, temperature, or expansion of wood due to moisture.

Deviations must not be confused with outright errors, or with a planned erection clearance. The total deviation in a prefabricated structure is the result of the following part deviations:

- product deviation,
- erection deviation,
- deviation of the work done at the site (foundations).

The reasons for the total deviation are the same for any structure where the units are produced off site, regardless of material. However, if something is not quite right, concrete is a little more difficult to alter or adjust compared to for instance steel or wood. Therefore one has to pay more attention to tolerances in prefabricated concrete structures, and to develop connection details that have the necessary room for adjustments.

A key element when designing a connection detail should always be an emphasis on making it as adjustable as possible. Preferably the connection detail should be adjustable in three directions. This may be difficult to combine with a requirement for simplicity, so the engineer has to use his judgement to decide on the priorities in each case. The easiest way to make a connection adjustable is by welding; a welded connection is automatically adjustable in two directions, limited only by the size of the steel units. However, welding is not a desirable solution due to the reasons mentioned before: necessity of skilled labour, different levels of quality control etc.

Fig. 4-7 shows an example of how bolted connections can be made adjustable.

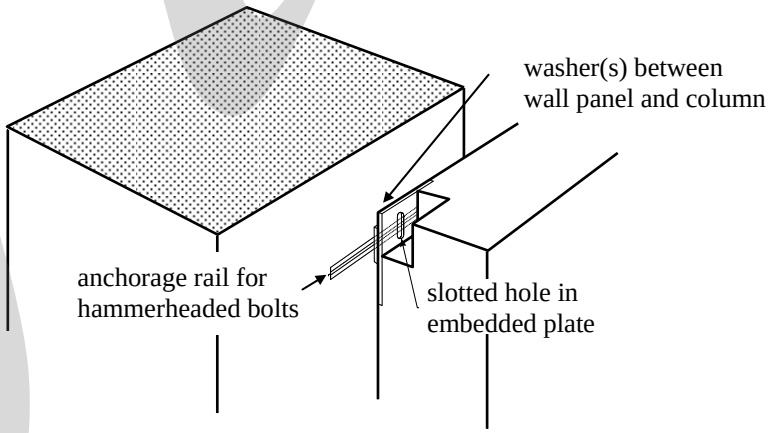

Fig. 4-7: Adjustable bolted connection for façades

4.1.6 Quality control

For precast concrete structures, connections are very important. The ability of the connections to transfer the acting forces is vital to the stability and load carrying capacity of the entire structure. Consequently, emphasis has to be placed upon the quality control of the connection details, and at the execution of the connections at the site.

All precasters should have a quality control scheme, and for connection details this quality control should focus on the following items.

(1) Material control

A system is required at the plant to ensure that all incoming units are checked to be of both the correct quality and that the dimensions are within the prescribed tolerances. Furthermore, a storing system that prevents later mix-up of the parts is needed.

(2) Production control

Production control of the connection units includes a scheme of education that guarantees that the workman knows the importance of using the right dimension and material quality. For example, is it not satisfactory to ask for a 20 mm bolt, but to also specify the grade of the bolt. If the quality information is not provided, for example at the drawings, this information must be demanded in order to carry out the job. Welding done to produce a connection unit should always have some sort of control, ranged according to the load-carrying importance of the weld. A visual inspection may be good enough in many cases, while for the most important parts X-raying may be necessary. Welding on galvanised steel should be avoided, but if it is necessary the size of the weld should be 30% larger than calculated.

(3) Production of the elements

One major aspect of the quality control system is the control of the connection units. This must be specified as a separate item, and include the placement of the parts, a check of the material quality and the anchorage. In the documentation of the production control the result of the control of the connection units must be specified separately.

(4) Site control

All connections must be checked at the site. In principle this just means that all connections must be checked twice, even though it may not be all that easy in practice.

For bolted connections the control will be to check that all nuts and bolts are properly fastened. For connections involving grouting or gluing with epoxy the control must include both a quality control of the grout and a check that the grout has filled all cavities properly. For welded connections the quality control is especially important, as welding at the site is very dependent upon climatic conditions and the skill of the welder. According to the importance of the connection, the control may vary from visual inspection to X-raying.

4.1.7 Economy

The costs of the connection itself depend on the magnitude of the forces to be carried over and the repetition (number of the same connections) involved. For the economically justified choice it is also important to consider the influence, which the connection has on the total cost of the prefabricated structure as a whole. The direct costs of the connection should be weighted against the costs of the element manufacturing, storage, transport, erection, and finishing.

4.2 Serviceability, functionality and durability of the building

4.2.1 Requirements in the serviceability limit state

Beside their structural function connections have to fulfil also other requirements. The choice of connection is essential to the behaviour of the total structure. The following requirements are the most important in the serviceability limit state:

- structural behaviour
- moisture and water tightness
- sound insulation and dynamic behaviour
- heat insulation
- durability
- aesthetic aspects and tolerances
- demountability

4.2.2 Structural behaviour

The connection must primarily comply with all requirements in the serviceability limit state (SLS) regarding transmission of forces, moments and permissible deformations and/or rotations. The distribution of forces and moments should agree with the intended behaviour of the structure in the SLS. Linear analysis is usually applied.

It is important that the deformations due to loading, creep, shrinkage, relaxation and temperature are considered when choosing a support. If the deformations are restrained, the structure and its connections must be designed to withstand the restraint forces. It is obvious that different connections will have different degree of restraint to different types of stresses. Many connections will have a high degree of resistance to one type of stress, but little or no resistance to others. In many cases it may be unnecessary, or even undesirable, to provide a high capability to resist certain types of stresses.

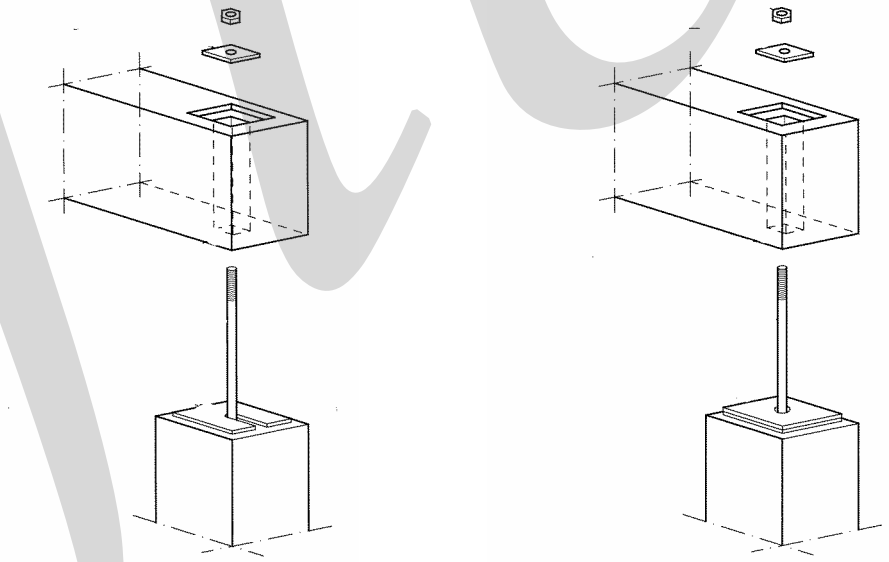

Fig. 4-8: Beam-column connection with bearing pad fixed in position by dowel

For load bearing parts of the structure normal crack width criteria for concrete have to be satisfied. For other parts the acceptable crack width is dependent on moisture penetration, tightness, sound insulation, aesthetic aspects etc.

Support pads of steel, neoprene or rubber, mortar joints etc. have to be designed with regard to relevant codes, recommendations from the producers or the authorities. When designing the support, actual tolerances must be considered.

In case of bearing pads, it is important that the bearing pad is not dislodged. A common solution is to use a dowel passing through the pad, preventing in this way the displacement of the pad. In other cases the pad can be glued to the bearing etc., see Fig. 4-8.

Design of connections with hard bearings is treated in Sections 6.4 and 6.7.1, and with soft bearings in Section 6.5.

4.2.3 Moisture and water ingress control

Prevention of moisture and/or water penetration is sometimes required. Joints between façade elements, floor elements in parking garages, roof elements etc. are typical examples.

In each case the movements from loads, temperature, creep, shrinkage etc. must be considered in order not to impair the water tightness of the provisions that were taken. For instance the roofing membrane must be able to follow the deformation of the joint without cracking and the mastic seal sealing the joint must be able to elongate and shorten in accordance with the movement of the joint without tearing off the sides or breaking.

4.2.4 Sound insulation and dynamic response to vibrations

Sound insulation between adjacent rooms in a building is dependent on both the direct transmission between separating structural elements and the indirect transmission by the flanking elements. In addition to this the sound insulation is also dependent on the size and sound absorption properties of the rooms. The type of sound in a building is normally characterised as airborne or impact sound. Both of these characteristics have to be controlled within certain limits to provide a certain sound insulation quality in a building.

The verification of sound insulation is made by a standardized type of measuring of both airborne and impact sound insulation. For design purpose it is important to derive methods to predict or estimate the sound insulation properties. A method to calculate sound insulation is described in the European standard EN 12354. It describes calculation methods designed to estimate sound insulation between rooms in a building primarily using measured data of the participating building elements as input to derive the effect of direct or indirect flanking transmission. The model also includes the effect of additional layers both on the separating and flanking elements. The properties of structural connections are included by the vibration reduction index, which describes the velocity level difference over different type of connections.

The calculation model is rather complicated and a lot of laboratory values are needed to make an analysis, which makes the procedure suited for computer methods. The most spread computer program in Europe based on this standard is named BASTIAN, which contains a database of a lot of structural building elements and different connections.

The dynamic response of a structure is an interaction effect due to the type of loading in time and the structural properties, both static and dynamic. The influence from connections on the response is primarily through the possible stiffening effect of the connection. By changing from simply supported to rigid connections the mode shapes and the natural frequencies are influenced. To evaluate the structure from vibration point of view it is important to have knowledge of both the loading type and the acceptance level of vibration. The acceptance level is normally expressed as an acceleration level, which may vary for different frequencies. The human body has an acceptance level for peak accelerations ranging from 0,05 % to about 5,0 % of gravity in frequency range 4 – 8 Hz. The large range, a factor 100, is depending of the human activity when subjected to the vibration. Recommendations for permissible peak vibrations for human comfort are found in ISO Standard 2631-2. As a general recommendation floors with natural frequencies less than about 6 Hz need to be evaluated from a dynamic point of view, having in mind the type of loading and acceptance level for the intended use. Simple guidelines of floor vibration control are available in the ATC Design Guide 1

with title 'Minimizing floor Vibration', issued from the US Applied Technology Council. There are also given some recommendations on damping values to use for different type of structures.

For preliminary design purpose the natural frequency of a floor or a beam can be estimated by the simple expression

$$f_n = \frac{18}{\sqrt{u}} \text{ [Hz]}$$

where u = deflection in [mm] taken as the maximum deformation due to the distributed load and self-weight

4.2.5 Heat insulation

The heat insulation in the precast building is strongly dependent on the detailing of the joints. To reach small energy consumption (heating or cooling), it is important that the air leakage through the joints is low and that the exposed elements including the joints are well insulated. Cold bridges are to be avoided as far as possible, especially in a cold climate.

The leakage factor for the façade is normally limited to a certain value at 50 Pa pressure difference.

4.2.6 Durability

4.2.6.1 Design with regard to durability

The connections in a precast concrete structure should be designed in such a way that their durability achieved in the actual environment is the same as that required for the total structure. If the connection is exposed to freezing and thawing cycles, the concrete should comply with the corresponding general requirements. When there is a risk of chemical or mechanical attack, a special investigation should be made concerning the effect of such an attack on the connection.

Evidence of poor durability is usually exhibited by corrosion of exposed steel elements, or by cracking and spalling of concrete.

4.2.6.2 Steel components

Steel parts like plates, bolts, slotted inserts etc have to be designed for the actual exposure class. The steel elements should be adequately covered with concrete, or should be upgraded for corrosion resistance by painting, electrolytic galvanizing, hot dip galvanizing, joint caulking, concrete grouting etc. If not, non-corrosive materials should be used like stainless steel, acid resistant steel, etc. A guideline is given in BLF (1997).

All-weather or other aggressive environment exposed connections should be periodically inspected and maintained. If maintenance of the exposed steel is not possible, stainless steel is recommended. Good experiences have also been reported with hot dip galvanising in combination with epoxy coal tar paint.

The preferred method of protecting exposed steel connection elements is to cover them with concrete, mortar or grout. Mix proportions, aggregate size and application procedures will vary with the size, location and orientation of the element to be covered. Mixes containing chlorides should be avoided.

Patches in architectural panels and others that will be permanently exposed to view will often not be accepted. Anchoring the concrete or grout to the relatively large steel surfaces is a problem that is often overlooked. Larger elements such as steel haunches can be wrapped with mesh or wire. For recessed plates and similar elements, connections such as those shown in Fig. 4-9 can be used.

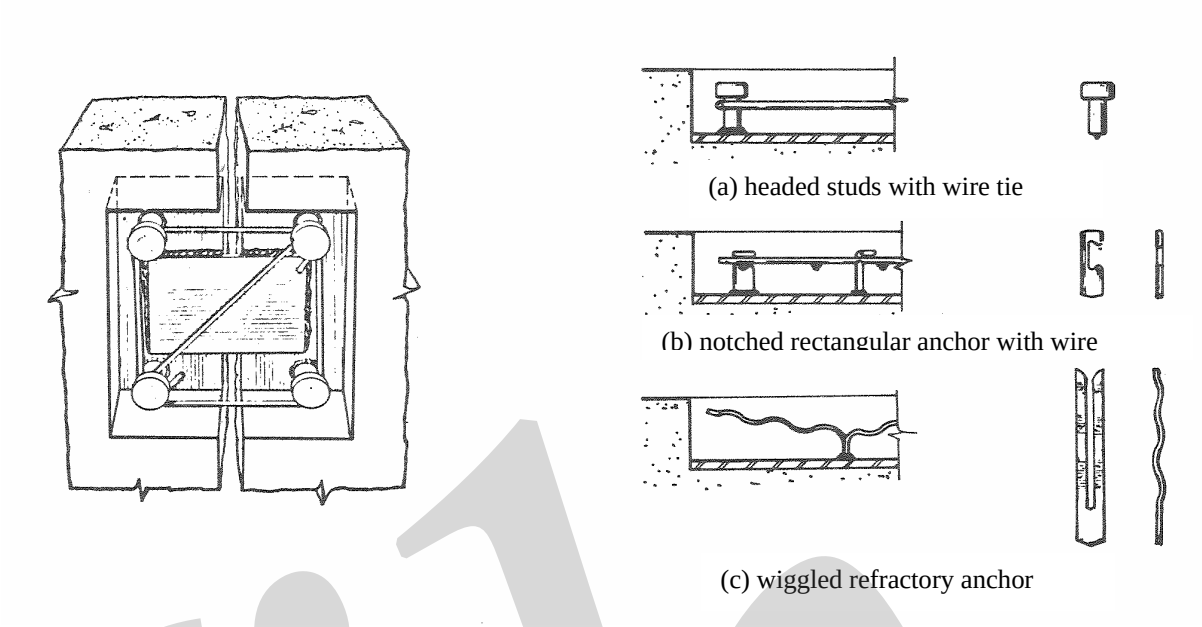

Fig. 4-9: Methods of anchoring patches to recessed plates

4.2.6.3 Bearings

Design of grouting regarding durability may in most cases be disregarded due to the fact that the grout is not reinforced, and the exposed surface is very small.

Bearing pads have also a very small exposed surface. Outdoor use or exposure to oil or other chemicals requires Chloroprene quality.

4.2.6.4 Cracking of concrete in connection zones

Most precast concrete elements are of high quality and cracking is seldom a serious problem, provided crack widths are limited. However, local cracking or spalling can occur when improper details result in restraint of movements or stress concentrations.

With regard to durability, crack width limitations for different types of exposure classes should be satisfied. In connection zones cracks might appear due to the transfer of forces through the connection, see Fig. 4-10.

However, general recommendations are normally not applicable for the connection areas. The basic rule is to reduce the allowable tensile stress in the connection zone reinforcement for severe exposure classes. Simplified relations between steel stress and crack width given in Section 7.2.3 can be used to find appropriate limitations of the steel stress. General guidelines for steel stress limitations with regard to durability are given in BLF (1996).

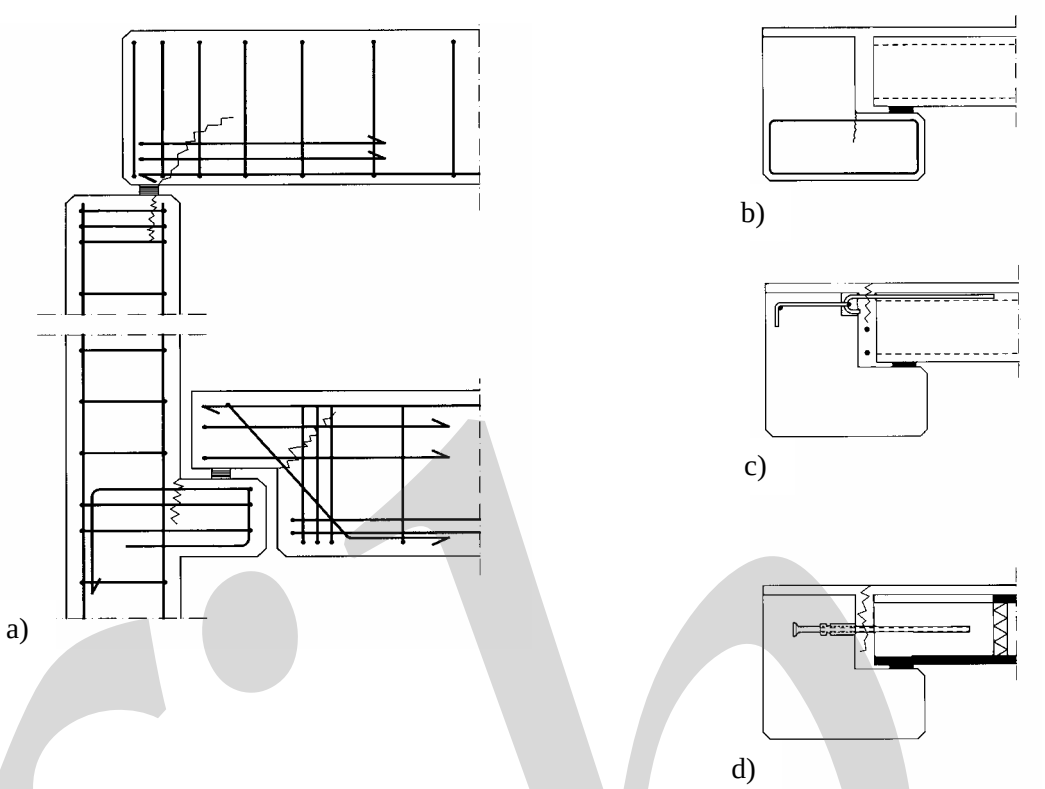

Fig. 4-10: Examples of cracks in support connections, according to BLF (1994-1997), a) beam-column-reinforcement, b) slab-beam-reinforcement, c) slab-beam-steel component, d) slab-beam-steel component

4.2.7 Aesthetic aspects and tolerances

When choosing an exposed connection the aesthetic aspects ought to be considered. It is sometimes necessary to compromise fabrication and erection simplicity, and hence, increase the cost, to provide a satisfactory appearance.

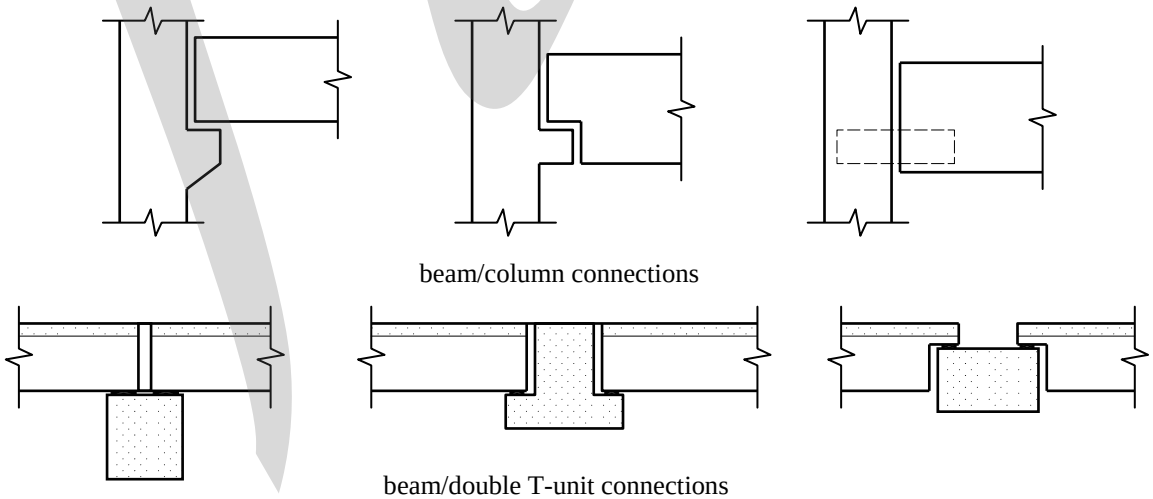

Fig. 4-11: Examples of alternative connections with various aesthetic appearances, a) beam-column connection, b) double-T-beam connection

Examples of alternative solutions for a beam-column connection and a double-T-beam connection are shown in Fig. 4-11. In Fig. 4-11 a the exposed corbel connection can be replaced by hidden corbels or internal inserts (Fig. 3-24 shows a good example of a connection with a hidden corbel). Clearly the cost and disruption to manufacturing a plain beam or column where the hidden inserts are specified must be balanced against the aesthetic effect.

Always when choosing a connection, the tolerances must be considered, not only for structural reasons but also with regard to the aesthetic appearance. Especially notched ends are sensible when exposed.

4.2.8 Transient situations

Connections can be exposed to special loading cases or special environmental conditions during handling, transport and erection. Temporary supports, eccentric loading during erection, wind loads, lifting and transportation etc. are examples of transient situations.

Steel details must often be protected during storing and erection to prevent corrosion before being placed in the final environment.

4.2.9 Demountability, recycling and environmental care

By way of the manner of detailing and assembling the connections, precast concrete structures offer more possibilities when it comes to removal of these buildings at the end of their life cycle [*fib* (2003a)]. In many cases the precast concrete structures can be demounted rather than demolished, and in some cases elements can be reused. This is of course possible provided that the connections are made in such way that dismantling can easily take place.

It is obvious that in this respect precast concrete is more friendly to the environment than many other traditional ways of building. It can save basic materials, energy and prevent, or partially prevent, destruction of capital invested in the building in the past.

Growing environmental awareness in The Netherlands has lead to the development of more or less demountable precast concrete systems - some typical details are shown in Figs. 4-12 to 4-14.

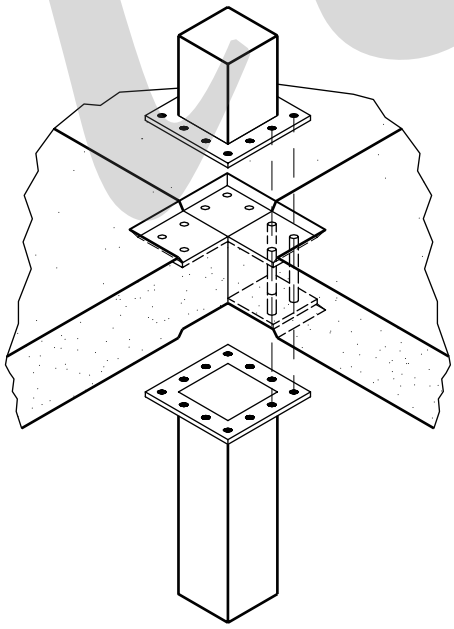

Fig. 4-12: Principal detail connection of demountable precast concrete system 'Matrixbouw', The Netherlands

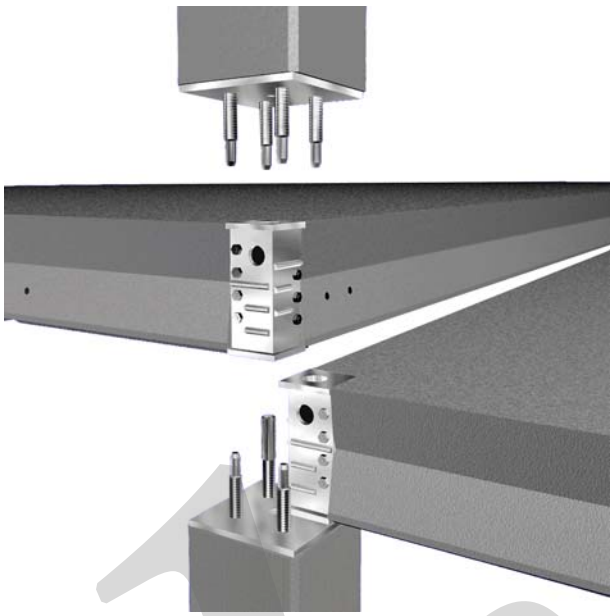

Fig. 4-13: Principle detail connection of demountable precast concrete system CD20, The Netherlands

It should be noted that except for the system 'Matrixbouw' these demountable systems require a certain invasive treatment like drilling holes in the dowel/mortar fill areas to enable the disassembly of the concrete units. These handlings are however rather simple.

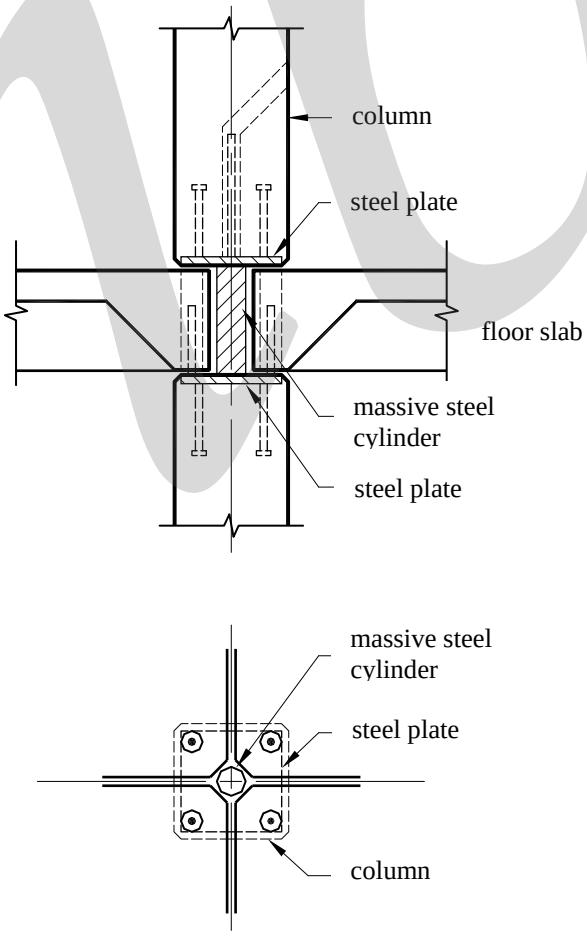

Fig.4-14: Principle detail connection of demountable precast concrete system 'BESTCON30', The Netherlands

5 Structural integrity

5.1 Fire resistance

5.1.1 General

Connections are vital parts in the performance of precast concrete structures. They shall be designed, constructed and maintained in such a way that they fulfil their functions and display the required performances also in case of fire.

The following performance requirements shall be satisfied under fire conditions:

- the load bearing function, i.e. the capacity of the connection to take up the different actions in the structure,
- the separating function, namely the ability to prevent fire spread by passage of flames or hot gases or ignition beyond the exposed surface during the relevant fire.

5.1.2 Load bearing function

The capacity of a precast concrete structure to assume its load bearing function during a fire can be expressed as follows:

$$E_{d,fi}(t) \leq R_{d,fi}(t)$$

where $E_{d,fi}(t)$ = design effect of actions in the fire situation at time t
$R_{d,fi}(t)$ = corresponding design resistance at elevated temperatures.

5.1.2.1 Effect of actions

The distinction is made between permanent and variable actions on one hand, and indirect actions resulting from the effects of thermal expansion and deformations on the other.

In general, the normal permanent and variable actions on a structure will not give rise to specific design problems for connections, since the load level is mostly smaller at fire than in the normal situation and also lower safety factors are used for the ultimate state design because of the accidental character of a fire. However this is not the case for indirect actions, where important alterations may occur, mainly affecting the connections. Some classical examples of such alterations are explained hereafter.

(1) Increase of the support moment for restrained continuous structures

The thermal dilatation of the exposed underside of a beam or a floor, forces the member to curve, which in turn results in an increase of the support moment at the colder top side of the member (Fig. 5-1), see also CEB (1991). The effect on the connections can be important, since the thermal restraint may lead to the yielding of the top reinforcement. However, precast structures are generally designed for simple supporting conditions where the rotational capacity is large enough to cope with this action.

(2) Forces due to hindered thermal expansion

When a fire occurs locally in the centre of a large building, the thermal expansion will be hindered by the surrounding floor structure, and very large compressive forces will generate in all directions (Fig. 5-2). Experience from real fires has shown that the effect of hindered expansion is generally less

critical since concrete connections are generally capable to take up large forces. In any case it is recommended to take account of the phenomenon at the design stage.

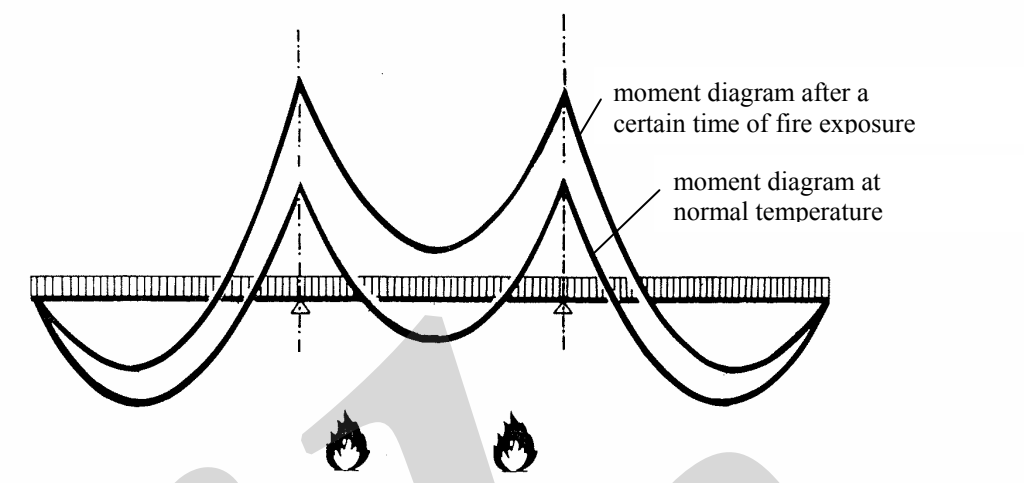

Fig. 5-1: Moment distribution in a continuous structure at normal temperature and in fire condition

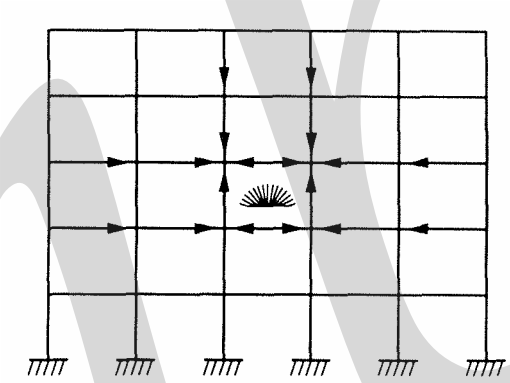

Fig. 5-2: Compressive forces in a frame structure due to hindered thermal dilatations

(3) Large deformations due to cumulated thermal dilatations

When a fire covers a wide building surface and lasts for a long period, it may lead to large cumulative deformations of the fire exposed floors and beams at the edge of the building structure. It is not unrealistic to assume that, in a large open store hall, the cumulated longitudinal deformation of a bay during a long fire, may amount to 100 mm and more. The rotational capacity of the connection between, for example, beams and columns at the edge of a building is a critical parameter for the stability of the entire structure.

(4) Local damage at the support

The deflection of beams and floors during a severe fire may have an influence on the support connection (Fig. 5-3). The edge of the supporting member might split off, when the contact between the supported and the supporting member is moving towards the edge of the latter. The problem can be solved by increasing the thickness of the bearing pad.

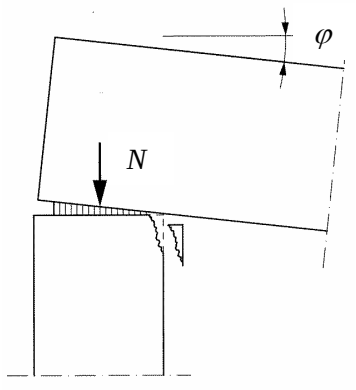

Fig. 5-3: Possible effects of curvature of beams or floors during a fire

(5) Cooling effect after a fire

The cooling of a structure after a long fire may introduce tensile forces on the connections between long structural members. However, these effects are normally not taken into account in the design.

5.1.2.2 Structural fire resistance

The principles and solutions valid for the fire resistance of structural concrete elements, apply also for the design of connections: minimum cross-sectional dimensions and sufficient cover to the reinforcement. This design philosophy is based on the large fire insulating capacity of concrete. Most concrete connections will normally not require additional measures. This is also the case for supporting details such as bearing pads in neoprene or another material, since they are protected by the surrounding components.

The most important analysis concerns the resistance against indirect actions due to thermal dilatations and deformations. In the following, some examples are given of how to cope with this.

(1) Bolted connections

Simply supported connections perform better during a fire than heavy continuous ones because of their large rotational capacity. Dowel connections are a good solution to transfer horizontal forces in simple supports. They need no special considerations since the dowel is well protected by the surrounding concrete. In addition, dowel connections can provide additional stiffness to the structure because of the semi-rigid behaviour. After a certain horizontal deformation, an internal force couple is created between the dowel and the surrounding concrete, giving additional stiffness in the ultimate limit state. This is normally not taken into account in the design, but constitutes nevertheless a reserve in safety.

(2) Connections between superposed columns

Columns are often intervening in the horizontal stiffness of low rise precast concrete structures. This is generally the case for industrial buildings, where the horizontal stability is ensured by portal frames composed of columns and beams. The columns are restrained into the foundations and have a dowel connection with the beams. The horizontal blocking of possible large deformations depends on the stiffness of the column and the rigidity of the restraint. Experience with real fires has shown that such column connections behave rather well in a fire and do not lead to structural incompatibility.

In multi-floor precast structures, columns generally transfer only vertical forces, the horizontal rigidity being assumed by central cores and shear walls. The question to be answered with regard to the fire resistance concerns the choice whether to use single storey columns or continuous columns

over several storeys. When a fire occurs at an intermediate floor, the horizontal blocking will be smaller in the case of single storey columns than with continuous columns (Fig. 5-4). The blocking in itself is not so dangerous, since it provides a kind of prestressing to the heat exposed structure, but the forces may lead to shear failure of the column itself. The latter phenomenon has effectively been observed in a real fire in a rigid cast *insitu* structure. The example shows that the connection between superposed columns may influence the indirect actions on the column.

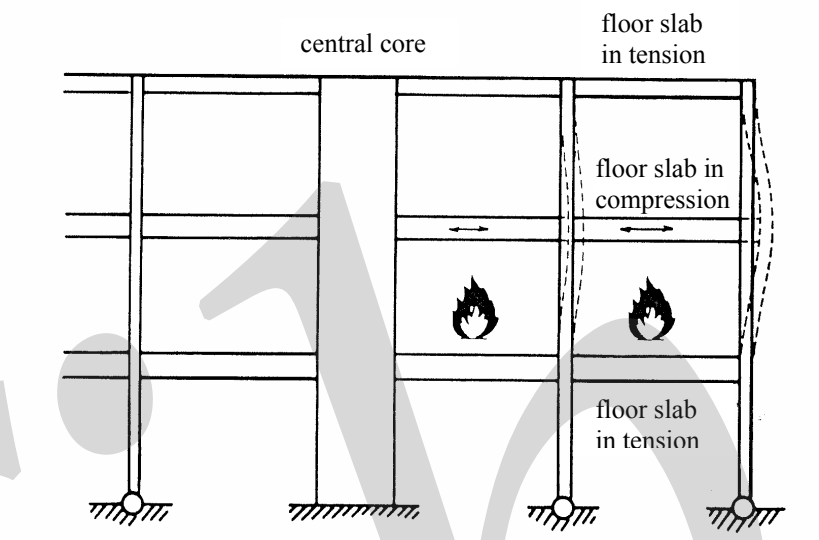

Fig. 5-4: Large horizontal forces on continuous columns due to thermal deformation of floor

(3) Floor-beam connections

The connections between precast floors and supporting beams are situated within the colder zone of the structure, and hence less affected by the fire. The position of the longitudinal tie reinforcement (longitudinal means in the direction of the floor span) should preferably be in the centre of the floor thickness, or a type of hairpin connecting reinforcement, see Fig. 5-5.

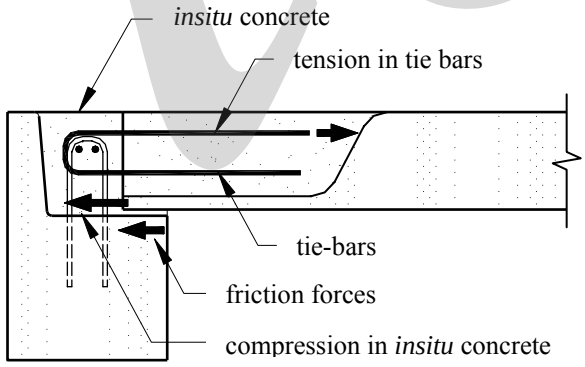

Fig. 5-5: Hair-pin connection at floor-wall or floor-beam support

In case of restrained support connections, the Eurocode [CEN (2005)] prescribes to provide sufficient continuous tensile reinforcement in the floor itself to cover possible modifications of the positive and negative moments.

(4) Floor-wall connections

Walls exposed to fire at one side will curve because of the differential temperature gradient. At the same time the supported floor will expand in the longitudinal direction. Both phenomena will lead to an increasing eccentricity of the load transfer between floor and wall, with a risk of collapse (Fig. 5-6). A possible solution is to increase the rigidity of the wall. (The situation is most critical for masonry walls since they cannot resist large bending moments.)

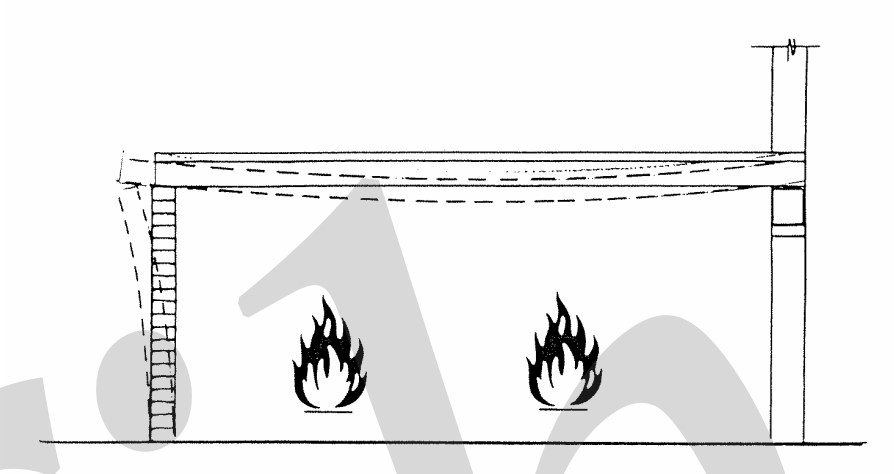

Fig. 5-6: Wall curvature and floor expansion may lead to large support eccentricity

(5) Hollow core floor connections

Experience during fire tests in laboratories has shown that the structural integrity and diaphragm capacity of hollow core floors through correctly designed connections, which as a matter of fact constitutes the basis for the stability of the floor at ambient temperature, are also essential in the fire situation. Due to the thermal dilatation of the underside, the slab will curve. As a consequence, compressive stresses appear at the top and the bottom of the concrete cross-section and tensile stresses in the middle (Fig. 5-7). The induced thermal stresses may lead to internal cracking. In principle, cracked concrete sections can take up shear as good as non-cracked sections on condition that the cracks are not opening. In fact, the crack borders are rough and shear forces can be transmitted by shear friction and aggregate interlocking (Fig. 5-8). The figure illustrates the generation of transverse forces due to the wedging effect. In hollow core floors, this transversal force is taken up by the transversal tie reinforcement at the support.

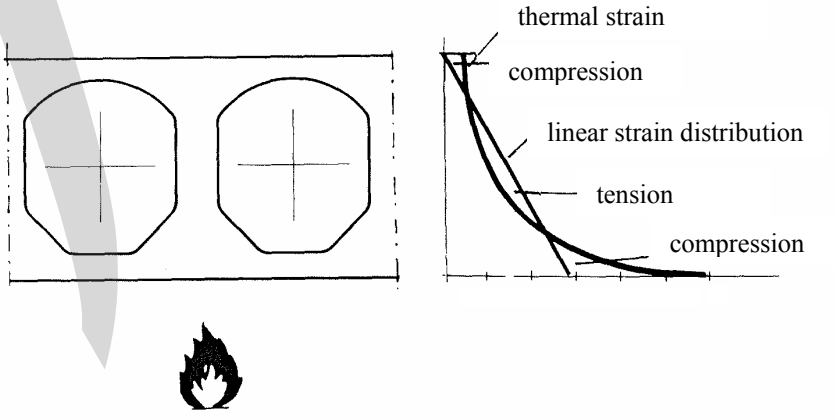

Fig. 5-7: Induced thermal stresses due to slab curvature

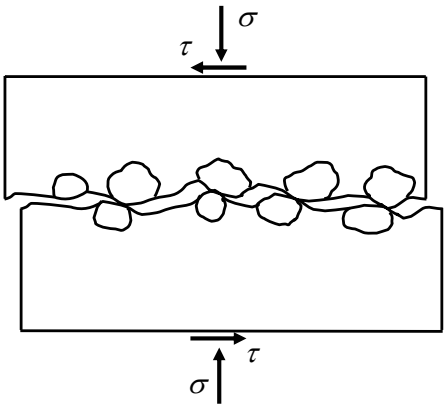

Fig. 5-8: Shear friction and interlocking

The decrease of the concrete strength at higher temperatures is hardly playing a role. Such temperatures appear only at the bottom part of the concrete section, and much less in the centre. From the foregoing, it appears that at the design stage, provisions are to be taken to realize the necessary connections between the units in order to obtain an effective force transfer through cracked concrete sections. The fact that shear failures have not been observed in real fires shows that there exist enough possibilities to realize the connections between the units. (This has also been proven in numerous fire tests in different laboratories.) The possible design provisions are explained hereafter.

- Reinforcing bars in cast open cores

The reinforcing bars are first designed to connect the floor units at the support. The reinforcing bars are placed centrally in the section, where the thermal stresses appear, in order to keep the cracks closed. The effectiveness of such reinforcement in the preservation of the shear capacity of the units at fire has been proven in many full-scale tests.

- Reinforcing bars in the longitudinal joints

This is a variant solution of the above. Good anchorage of the bars in the longitudinal joint between units is required. This presupposes that the joints remain closed, which can be achieved by the tying effect of peripheral tie reinforcement. The real function of the latter is to ensure the diaphragm action of the floor and the lateral distribution of concentrated loading, even through cracked joints by shear friction. The anchorage capacity of steel bars in cracked longitudinal joints between hollow core units has been extensively studied [Engström (1992)]. It is recommended to limit the diameter of the bars to 12 mm maximum and to provide a larger anchorage length than normally needed, e.g. 1500 mm for a bar of 12 mm, see Section 7.2.5 for more information. When the above conditions are met, the reinforcing bars in the joints ensure the interlocking effect of the possible cracked concrete section, and hence the shear capacity of the units at fire. Also this case has been proven repeatedly in many ISO fire tests.

- Peripheral ties

The peripheral ties contribute to preserving the shear capacity of the units when exposed to fire by obstructing, directly and indirectly, the expansion of the floor through the rigidity of the tie beam itself, and through the coherence between neighbouring floor units.

When fire occurs in the central part of a large floor, the thermal expansion of the units will be practically completely blocked by the rigidity of the surrounding floor. The blocking will mobilize important compressive forces in the fire exposed floor units. (This has been observed in real fires, where large spalling sometimes occurs under the high compressive forces.) In such cases, the central part of the cross-section will not be cracked because of the differential thermal stresses, but the whole section will be subjected to compression. The shear capacity will therefore be unaffected.

(6) Steel connections

Steel connections, such as steel corbels and similar, shall be protected against the effect of fire, either by encasing them into concrete/mortar (containing an expansive agent) or by an adequate fire insulation.

The concrete cover should be at least 30 mm for 1 hour of fire resistance and 50 mm for two hours. Precautions are to be taken to prevent spalling of the concrete cover by adequate reinforcement.

In case of partially encased steel profiles, for example in slim floor structures, the temperature rise in the steel profile will be slower than in non-encased unprotected profiles, due to the effect of the thermal conductivity of the surrounding concrete. However, it is recommended to protect the exposed steel flange by a fire insulating material, Fig. 5-9.

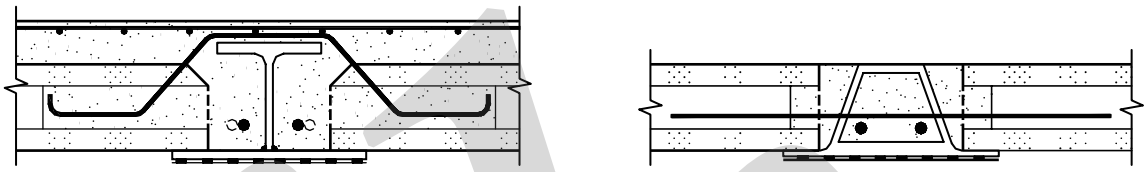

Fig. 5-9: Examples of slim floor structures

5.1.3 Separating function

Requirements, with respect to the separating function, are expressed as limit states of thermal insulation and structural integrity against fire penetration. They apply mainly for joints between prefabricated floors, walls, or walls and columns, which should be constructed to prevent the passage of flames or hot gases.

Longitudinal joints between precast floor elements generally do not require any special protection. The precondition for thermal isolation and structural integrity is a minimum section thickness (unit plus finishing) according to the required fire resistance. Minimum dimensions are given in Table 5-1, according to CEB (1991). The joint should also remain closed. The latter is realized through the peripheral tie reinforcement. When the section is too small, for example due to the limited thickness of flanges of TT-floor elements, a special fire insulating joint strip can be used.

standard fire resistance	minimum joint height (sectional thickness) [mm]	
	dense aggregate concrete	lightweight aggregate concrete ($1200 kg/m^3$)
Rf 30	60	60
Rf 60	80	65
Rf 90	100	80
Rf 120	120	95

Table 5-1: Minimum joint height (sectional thickness) h_s [mm], according to CEB (1991)

Joints between walls and columns can be made fire tight by either providing connecting reinforcement at half height, or through a special profile of the column cross-section (Fig. 5-10).

Fig. 5-10: Connection between column and wall

5.2 Prevention of progressive collapse

5.2.1 General

The safety of a structure is determined by its ability to withstand loads and other actions or influences of phenomena like weather, moisture, ageing, etc. which can occur during the construction time and the rest of the structure's lifetime. 'Safety is the ability of a structure to sustain actions and other influences liable to occur during construction and use and to maintain sufficient structural integrity during and after accidents', [IABSE (1981)].

To carry the loads and the said influences, beams, columns, floor, walls and other elements are used. The sufficient strength and stiffness of these components alone, however, does not yet guarantee a safe structure. The components have to be connected to each other in such a way that a coherent entity is formed, which as a total is sufficiently strong, stiff and stable.

Construction practice has learned that the chance of complete failure of a structure is mostly determined by the factors that were not counted on in the original design. These factors, mostly called accidental loadings, include, but are not limited to: errors in design and construction; local overloading; service system (gas) explosions; vehicular and aircraft collisions; tornadoes; flooding; bomb explosions; fire loads and foundation settlements. This means that in every design the possibility that during its lifetime the structure can be damaged should be considered.

Codes of practice refer to this topic as 'robustness' and require that: '…Situations should be avoided where damage to small areas of a structure or failure of single elements may lead to collapse of major parts of the structure' [BSI (1985)]. Another popular term for this is 'structural integrity', meaning also that the design aspects involve all the items like element design, connections, diaphragm action and structural stability, as these items cannot be dealt with in isolation.

Further, the term 'progressive collapse' was first used in the United Kingdom following the partial collapse of a precast concrete wall structure at Ronan Point in 1968, see Fig. 5-11.

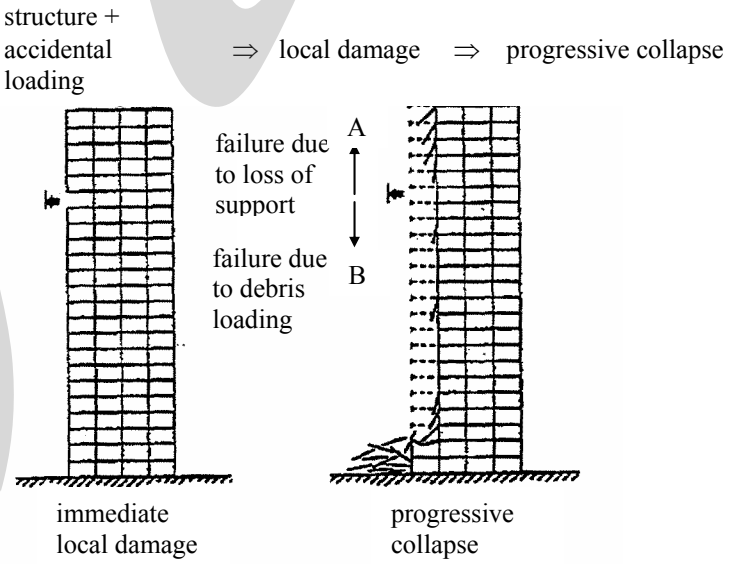

Fig. 5-11: Example of progressive collapse (Ronan Point, England)

A gas explosion in a corner room on the eighteenth floor blew out one of the external wall panels and because of inadequate structural continuity between the wall and floor elements, the removal of one wall element was sufficient to cause the total collapse of about 23 m^2 of floor area per storey over the entire height of the building. The investigations found deficiencies in the manner in which the precast elements were tied to each other. Poor detailing and unsatisfactory workmanship were blamed for the disproportionate amount of damage. However, the most crucial factor was that there was no suitable design information to guide the designer towards a robust solution [Elliott (1996)].

Frame stability is a crucial issue in multi-storey precast construction. To guarantee this frame stability an adequate stiffness, strength and the provisions to guard against the possibility of a collapse, which is disproportionate to its cause, must be provided. Tie forces between the precast elements must be mobilised in the event of accidental damage or abnormal loading and alternative means of transferring loads to the foundations must be sought if an element is rendered unserviceable.

5.2.2 Design considerations

Today three alternative measures are used (often in combination) to reduce the risk of progressive collapse. These measures are:

1) designing the structure to withstand accidental loading
2) reducing the possibility of occurrence of accidental loading
3) preventing the propagation of a possible initial failure and increasing redundancy

(1) Designing the structure to withstand accidental loading

This method is classified as 'direct' method because an appreciation of the severity and possible location of any accidental load is known or assumed. An adequate resistance for one accidental loading condition will not necessarily provide strength to resist all other possible accidental loadings.

(2) Reducing the possibility of occurrence of accidental loading

Eliminate sources of accidental loadings, e.g. gas installations can be prohibited to place, barriers can be placed to prevent vehicular collisions. In general not all accidental loads can be eliminated. Since any realistic solution must deal with all abnormal loading conditions to some extent, this method of eliminating the hazards cannot be deemed to provide an overall solution. However, in design all efforts should be made to reduce the occurrence of accidental loadings as much as possible, as this is the most direct way to an effective solution.

Reduce the chance of errors in design, construction and operation:

- establish and maintain quality control systems,
- make the tasks and responsibilities clear,
- take care that design and construction is thoroughly checked,
- give instruction for inspection and maintenance,
- give instructions for later demolition or dismantling.

(3) Preventing the propagation of a possible initial failure and increasing redundancy

- Pursue balanced design
  - reduce weak links
- Limit the primary damage to confined areas
  - apply discontinuities like expansion joints, etc.
- Prevent large loads caused by (falling) debris
  - take care for good and ductile interconnection of elements

– Increase the redundancy
  - use ductile connections,
  - provide alternative load paths,
  - apply ties (minimum detailing practice) to increase structural integrity.

Where possible (practically and economically), an alternative path should be provided to prevent progressive collapse when local damage occurs. If it is not possible (for practical or economic reasons) the structure should be designed in such a way that the chance of local failure is kept to an acceptable minimum. Minimum detailing prescribed by requirements has been adopted by several countries and concerns mainly the execution of connections and ties and the resistance of local parts to described accidental loads, increasing in this way the structural integrity.

5.2.3 Structural integrity

Structural integrity and interaction between elements are obtained by the use of horizontal floor and vertical column and wall ties, Fig. 5-12. Peripheral ties (A) enclosing the floor fields and the internal ties (B) and (C) are essential for the diaphragm action of the floor.

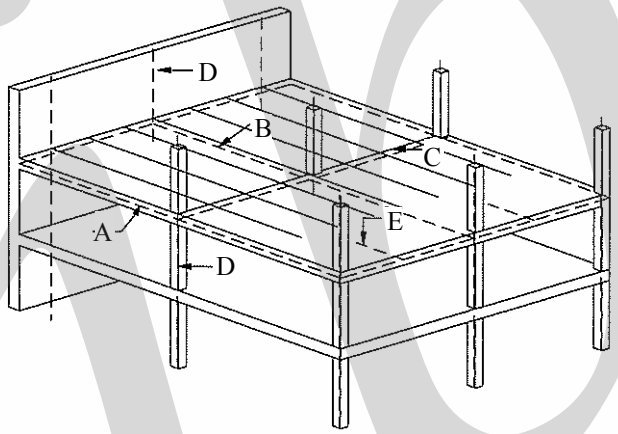

Fig. 5-12: Example of fully tied precast concrete structure

The vertical ties (D) are connecting the separate wall and column elements together providing vertical continuity. The ties (E) are connecting the floor elements to their supports (beams or walls) to prevent loss of those supports in case of accident.

It is essential that the ties and connections are ductile (possess large plastic deformation capacity) to be able to dissipate the energy when damage occurs.

Tying the large panel structure together horizontally and vertically utilises the following structural mechanisms to bridge local failures, which are illustrated in Fig. 5-13:

(a) cantilever action of the wall panels
(b) beam and arch action of the wall panels
(c) partial catenary and membrane action of successive spans of the floor planks
(d) vertical suspension of the wall panels
(e) diaphragm action of the floor planks.

Examples of how some of the mechanisms can be analysed are given in Appendix A.

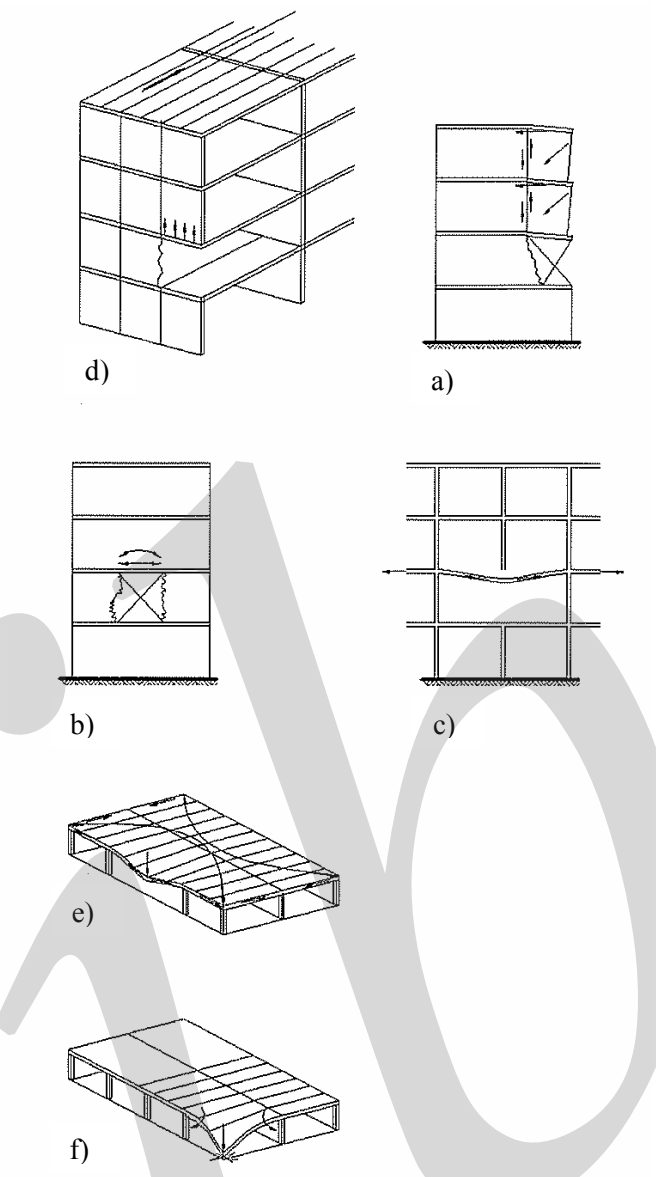

Fig. 5-13: Some examples of alternative load paths, a) cantilever action of wall panels, b) beam and arch action of wall panels, c) catenary and membrane action of floor panels, d) suspension of wall panels, e) diaphragm action of floor system (note that it is not always possible or easy to find a practical alternative load path such as for instance in the case of collapse of a corner column (f)

(1) Minimum requirements

The goal is to achieve a certain minimum structural integrity, which guarantees enough safety for accidental loadings. In the event of accidental loading, a notional tie force is capable of being activated at every location in the structure. Because the severity and possible location of the loads are not known, this method is classified as 'indirect' and the forces for which the ties have to be minimally designed for are arbitrarily chosen, based on experience in practice. These forces are minimum forces.

(2) Ties in the floor

Ties in floors are primarily designed with regard to diaphragm action according to the needs identified in the structural analysis of the stabilising system. For instance, the peripheral tie in the floor has to act as tensile reinforcement in the floor diaphragm to resist the in-plane moments caused by wind and horizontal forces due to possible leaning of the building, columns out of plumb, second order effects etc.

This means that the following ordinary effects need to be considered:

- horizontal wind load resisted by the floor diaphragm,
  - tie forces necessary to resist the resulting in-plane bending moments,
  - tie forces necessary for sufficient shear capacity of the floor diaphragm (this is as well in the plane as perpendicular to the plane), see Section
- initial out of plumb position of columns, see Fig. 5-14 b,
- second order effects due to the horizontal sway of the building.

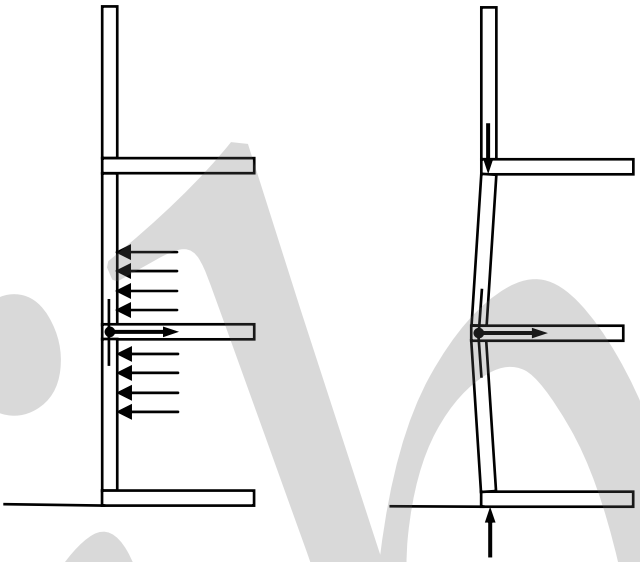

1. Tie force required to withstand (explosion) pressure from inside
2. Tie force required to deal with imperfections (misalignments)

Fig. 5-14: Different reasons for tying systems

Furthermore, it should be checked that the ties so designed also fulfil the minimum tensile capacities with regard to structural integrity. If not additional steel must be provided. Various values of minimum tensile capacities have been recommended in codes and handbooks in the past. Table 5-2 gives some examples of recommendations for minimum horizontal tie forces in floors.

The basic horizontal tie forces as given in different codes and reports [CUR (1988)]		
PCI	$F_{tie} = 23$ kN/m	
FIP	$F_{tie} = 20$ kN/m	
BS8110	$F_{tie} = 20 + 4\,n \leq 60$ kN/m	where: n = number of storeys

Table 5-2: Minimum tensile capacity of ties in floors

According to CEB-FIP Model Code 1990 [CEB-FIP (1992)] the minimum capacity of internal ties in floors should be 20 kN per metre width and of peripheral ties 60 kN (design values) and the floor elements should be directly or indirectly tied to the supports at both ends. In Eurocode 2 [CEN 2004] the following minimum tensile capacities are generally recommended. However, the actual values may vary between countries and are given in National Annex.

- peripheral ties in floors and roofs (along external and internal edges)

$F_{\text{tie,per}} = l_1 \cdot q_1 \le q_2$ with $q_1 = 10$ kN/m and $q_2 = 70$ kN (recommended values)

where l_1 = length of end-span

- internal ties in two direction in floors and roofs

$F_{\text{tie,int}} = 20$ kN/m (recommended value per metre width)

The internal ties can be distributed evenly or concentrated, for instance along beam lines, see Fig. 5-15. The tensile capacity of concentrated ties is determined as

$$F_{\text{tie}} = \frac{l_1 + l_2}{2} \cdot q_3 \le q_4 \quad \text{with } q_3 = 20 \text{ kN/m and } q_4 = 70 \text{ kN} \quad \text{(recommended values)}$$

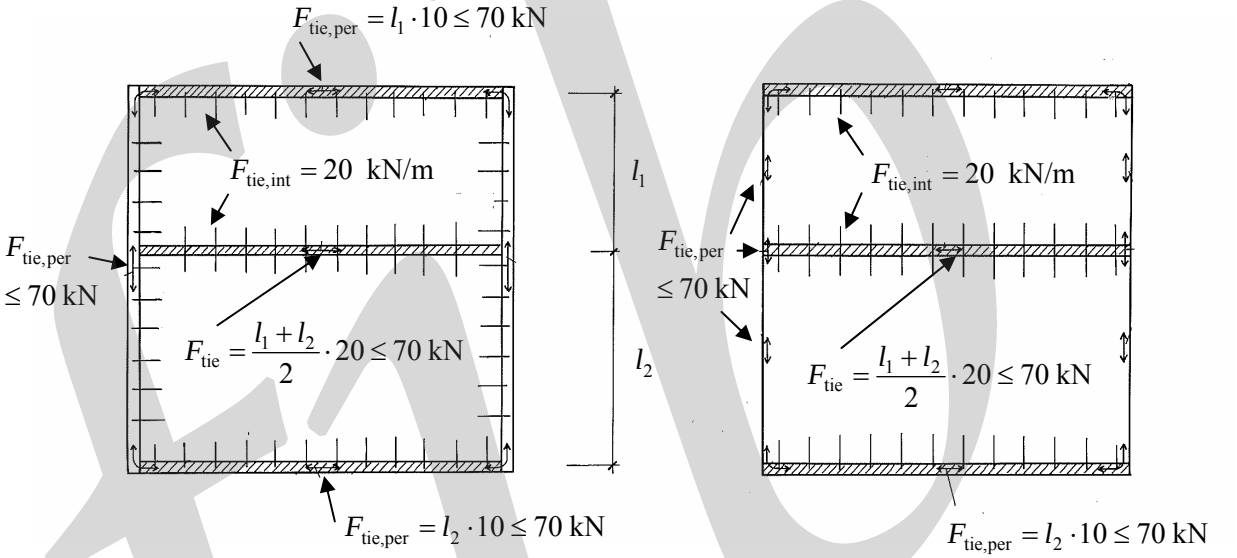

Fig. 5-15: Example of concentrated and distributed internal ties in floors

(3) Connection of the columns and walls to the floor

It is necessary to connect the edge and corner columns to the floor diaphragms to prevent their detachment from the floor under the influence of accidental loading like explosions, vehicular collisions or the possible out of plumb position of the columns, as shown in Fig. 5-14 b. Corner columns should be tied to the structure in two mutually perpendicular directions with the vertical force. The following minimum capacities are generally recommended in Eurocode 2, however, actual values may vary between countries.

- horizontal ties to edge columns and/or walls

$F_{\text{tie,fac}} = 20$ kN/m (recommended value per metre width of the facade)

For columns the force needs not to exceed the value

$F_{\text{tie,col}} = 150$ kN

Examples of arrangement of tying systems in floors and how the floor is tied to the supports are shown in Fig. 5-16.

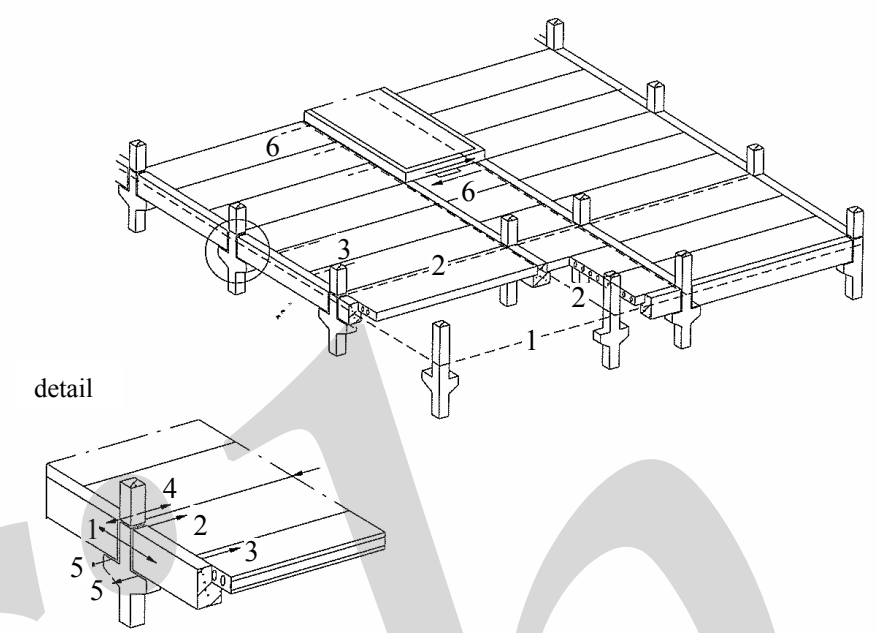

1. peripheral tie (beam)
2. connection of the edge column to the floor and internal floor tie
3. connection of the floor elements to the edge beams
4. connection of upper column to the underneath column
5. connection beam-column
6. connection of floor diaphragm to the core

Fig. 5-16: Example of ties in a precast floor

(4) Vertical ties in columns and walls

Vertical ties in columns and walls should be provided in order to limit the damage of a floor if a column or wall is lost below this floor. These ties should be able to carry (part of) the load to the upper levels so as the structure seeks the alternative path for load transfer. According to Eurocode 2 this type of ties should be provided in panel buildings of 5 storeys or more. Various alternative load paths may be used in the design.

5.2.4 Analysis of collapse mechanisms

The design approach, aiming at preventing the propagation of a possible initial failure, implies that the overall structural stability must be preserved after the occurrence of the primary failure. Furthermore, a local alternative load-bearing system must be able to bridge over the damaged area, see Fig. 5-17. The local bridging system is essential for prevention of an uncontrolled extension of the damage. In this respect it is most important to prevent structural members from falling, thus initiating further damage by debris loading.

An alternative load-bearing system can be comprised by ordinary structural members acting in an alternative mode of behaviour, or by non-bearing elements that take over the load from the damaged structural members.

For a certain presupposed local damage in a precast structure, possible collapse mechanisms and the corresponding alternative bridging systems will be determined by the actual joint locations and detailing. The deformation that follows the primary failure may be concentrated to the joints and characterised as joint slips, joint openings and rotations. Accordingly, the resistance of the

bridging system will mainly depend on the behaviour of the structural connections that are strained, for instance tie connections across joints that open up.

The collapse mechanism may be more or less complex depending on the number of interacting elements and connections and in what locations large plastic deformations are obtained. As idealizations it is possible to distinguish pure rotation mechanisms, joint slip mechanisms and suspension mechanisms. In practice composed forms may occur. However, it should be noted that the behaviour of the collapse mechanism could be controlled to some extent by a balanced design for ductility and a consistent detailing of the components in the bridging system.

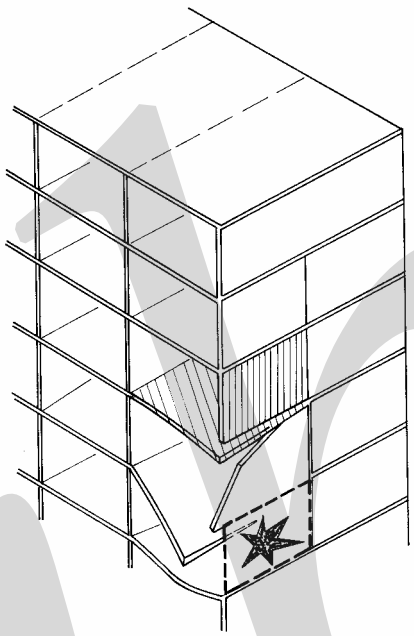

Fig. 5-17: A wall structure that is partially damaged by accidental loading. In order to prevent an extension of the damage and a total collapse, the damaged structure must remain stable and an alternative load-bearing system must bridge over the damaged area

In the design of alternative load-bearing systems it is possible to take advantage of large displacements and a ductile behaviour. For such a system the resistance can be expected to be considerably affected by dynamic effects during the transition to the alternative mode of action, and the non-linear behaviour of the strained connections. In an appropriate model for the design and analysis these effects must be considered. A simplified approach for such analysis was proposed by Engström (1992) and is presented and exemplified in Appendix A. The model is applied on alternative bridging systems where the resistance is determined by the action of tie connections loaded mainly in tension. However, the basic principles can be adopted also in the analysis of other types of collapse mechanisms where the deformations are localised to ductile connections, e.g. joint slip mechanisms.

5.2.5 Conclusion

To design for robustness and structural integrity when designing precast concrete structures is important. Precast structures, when designed properly, will have the same redundancy as cast *insitu* ones. Tests on Dutch precast concrete system Matrixbouw so as shown in Fig. 5-18 testify that this is the case.

Fig. 5-18: Test of demountable precast concrete system 'Matrixbouw', The Netherlands for alternative load path and redundancy

5.3 Seismic structures

5.3.1 General

The following section gives basic information concerning response and design of seismic structures. The purpose is to explain that seismic structures require special attention and specific approaches in their design. The detailed dynamic and seismic design of connections is beyond the scope of this publication. Here instead reference is made to fib (2003b).

5.3.1.1 Seismic action

The main difference in case of seismic action is that it is dynamic and does not consist of defined forces applied to the structure. The forces that arise in consequence depend on the structural behaviour. Earthquakes are motions of the ground, transmitted to the masses that lay on it. Various parameters are involved in the motion, the most relevant, with respect to the effects on structures, is the ground acceleration.

Ignoring, for sake of simplicity, problems such as differential accelerations at the base supports of the structure or the soil-structure interaction (important in some cases) the seismic action can be represented as a given accelerogram, applied uniformly at the base of the structure.

Accelerations are both horizontal and vertical. The first are generally greater in intensity and, although they have orientations, in current design rules they are assumed to act possibly in any direction with the same features.

A given accelerogram may be synthesized by two parameters: the intensity, in terms of effective peak ground acceleration, reaching up to 0,5*g (g = gravity acceleration)*, and the shape, in terms of frequencies content (*PSD Spectrum*).

5.3.1.2 Response of the structure

Rigid body structures would follow the ground acceleration in their whole, instant by instant (Fig. 5-19 a). Instead, in deformable structures, each point follows its own motion path: displacements, velocities and accelerations are different from point to point and vary during time (Fig. 5-19 b). This motion is called the *response* of the structure to the excitation from the ground. The response is governed by the exciting motion, the stiffness of the structure and the masses involved. It is proportional to the peak ground acceleration and, in the majority of cases, is amplified with respect to the ground motion (up to 4÷5 times and more).

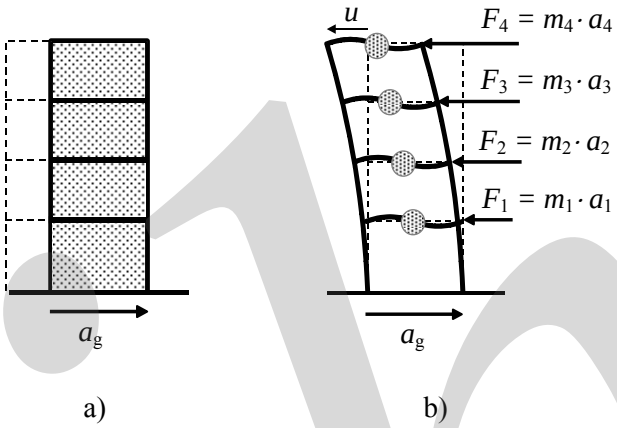

Fig. 5-19: Structural response, a) rigid structure, b) deformable structure

The masses bearing on the structure undergo the local acceleration and generate inertial forces, continuously changing with time. Several intense shocks of alternate sign may occur in a few seconds. The stiffness itself may change during the motion, thus altering the response. This occurs under major earthquakes when for instance some structural elements yield, thus 'softening' the structure, which is accepted by seismic design criteria.

5.3.1.3 Design criteria

Seismic design codes give the main parameters of the ground motion to be accounted for, as well as criteria for designing and detailing the structure. Nevertheless, data on quakes to be expected being rather uncertain. It is accepted there is a risk of severe structural damages by high intensity events, just avoiding collapse. In fact, to keep the structure within elastic state by those events is unpractical: such a criterion would require extremely high resistance, considering that the resulting total horizontal force might be greater than the weight of the building! Indeed, the response to high intensity quakes is foreseen to involve inelastic deformations of selected structural elements, in order to have plastic dissipation of energy. This reduces the accelerations and, consequently, the resistance demanded, in terms of force, reduces too.

A rough criterion – derived for one-degree-of-freedom elasto-plastic structures – sets the above reduction as proportional to the *ductility factor*, i.e., to the ratio of the maximum displacement capacity to the displacement at yielding, $\mu = u_{max} / u_y$ (Fig. 5-20).

The ductility reveals a design parameter of resistance as important as the strength, being somehow interchangeable with it. It is not immediately definable numerically, for complex structures; however its concept is clear. Simplified design methods allowed by codes, as for instance the use of static equivalent forces, account for given ductility factors available in the structures. Those forces are then several times (μ) lower, than if the structure should remain elastic, where μ is the ductility factor as defined in Fig. 5-20.

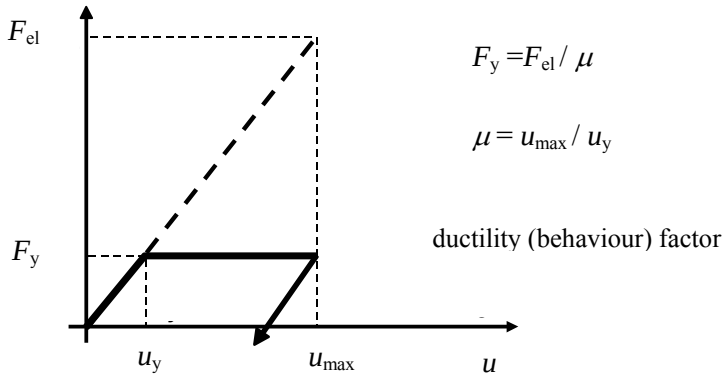

Fig. 5-20: Ductility-based force reduction factor

5.3.2 Actions on structural elements

5.3.2.1 Horizontal elements

With the need for large structure-free spaces, building layouts trend toward large span floors. This has given more and more relevance to the structural properties of prestressed concrete floors, including their performance in seismic conditions. The primary function of a building structure is to sustain gravity loads, located mainly on floors and roofs, which deform out of their plane (Fig. 5-21 a). The floor deck is also required to perform the function of an in-plane horizontal diaphragm in common with 'rigid' (or nearly rigid) horizontal displacement (Fig. 5-21 b).

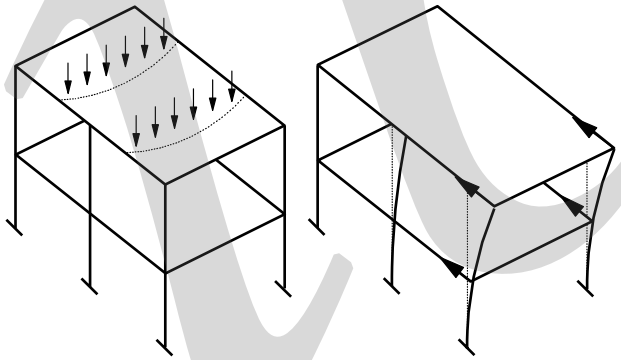

Fig. 5-21: Various actions of the floors, a) slab action, b) diaphragm action

Creep, shrinkage, thermal variations, deflections of columns and walls (due to loading and settlements) strain the floor decks in their plane. Floor decks are even called to work as tying elements in subsidiary statical systems, providing alternative load paths, after an accident may have destroyed the principal one. Compatibility at nodes gives rise to restraining in-plane forces (Fig. 5-22 a). External horizontal forces also act on floors, resulting from wind and earthquake loading (Fig. 5-22 b) - the first are applied at upwind and downwind edges by façades. The latter appear where the masses are located.

Horizontal seismic action is much more relevant on decks, than the vertical one. This is often neglected, for it is lower; moreover, buildings respond to it with lower amplification and are not much affected by the addition of an up- or down-wards force that is only a fraction of the actual gravity loads. Thus, floors are mobilized by seismic action in their diaphragm function more than in the slab function, although the latter must be taken into account, as out-of-plane deflections affect the in-plane behaviour.

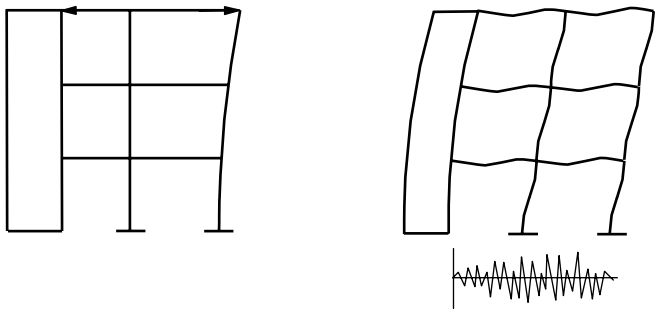

Fig. 5-22: Action on floors, a) internal action, b) external action

When the layout of a building or the distribution of masses and stiffness are not regular, also the diaphragm forces may increase much more under seismic conditions, due to the increased influence of torsional modes.

When a horizontal force acts at one level of a building, all the floor diaphragms intervene (Fig. 5-23). In fact, they not only transmit the horizontal forces applied at their own level but also make the displacements of the nodes, due to overall forces, compatible.

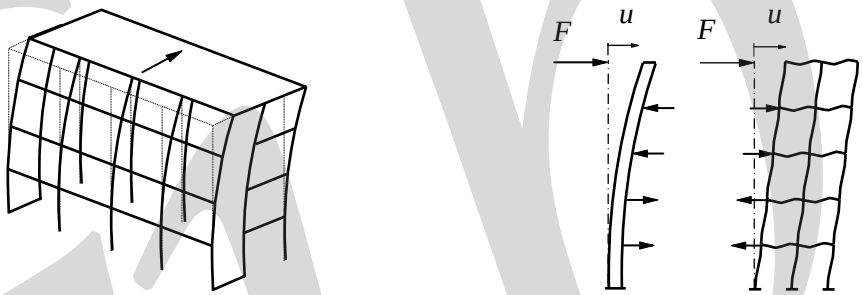

Fig. 5-23: Interaction of all storey diaphragms

5.3.2.2 Vertical elements

The seismic forces, mainly arising at floors levels, are transmitted to the foundations via frames and/or walls.

The structural system can be a framework, made of beams and columns, rigidly connected at their nodes; or a pure wall system, where all vertical bearing elements are walls; or a so called *dual* system, where vertical actions are mainly carried by columns and horizontal actions only by shear walls (Fig. 5-23). In the latter case, columns and beams do not form frames but are theoretically pin-jointed at their nodes or, equivalently, columns are extremely flexible, so that practically they are subject only to compression and the entire horizontal action is carried by the shear walls. Dual systems are the better suited for precast seismic structures.

The energy dissipation in frames is assigned deliberately to beams, which are much more ductile than columns, by means of a design based on capacity, i.e., which makes the beams weaker and yield first. It relies on ductility of cross-sections under bending. In precast structures, it can occur either in the joints or in cross-sections within the jointed members. In the latter case, joints are either placed far from the most stressed sections (beam ends) or they are made strong enough not to yield first.

In shear walls, the dissipation takes place in the most stressed section in bending. In precast walls, it can take place also in the vertical joints between panels, due to shear-friction mechanisms. Generally, walls are less ductile altogether than frames and require greater strength. On the other hand, they are much stiffer, which better prevents damage under low intensity quakes.

5.3.2.3 Applied forces

The typical actions a diaphragm undergoes are in-plane forces coming from the deep beam action (shear and bending of the diaphragm), but also compression and tension (Fig. 5-24). The seismic inertial forces are applied along its body and may have any direction. Other forces are applied at the nodes with columns and walls, i.e., the reactions to the former and self-equilibrated forces due to restrained deformations.

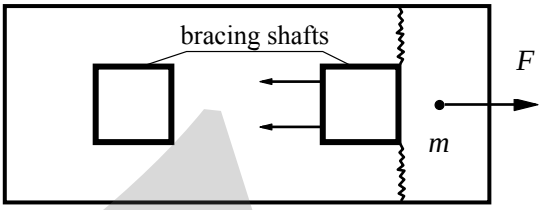

Fig. 5-24: Example of tensile action on floor diaphragm

Seismic codes give the combination of loads to be considered with earthquake and conventional displacement of the masses for exciting unsymmetrical modes of vibration.

Consequently actions are generally well controlled, when the structure has a regular layout in plan (compact, bi-symmetric: Fig 5-25) and in elevation (continuous vertical element), a uniform distribution of stiffness and masses, and floors are continuous and well tied.

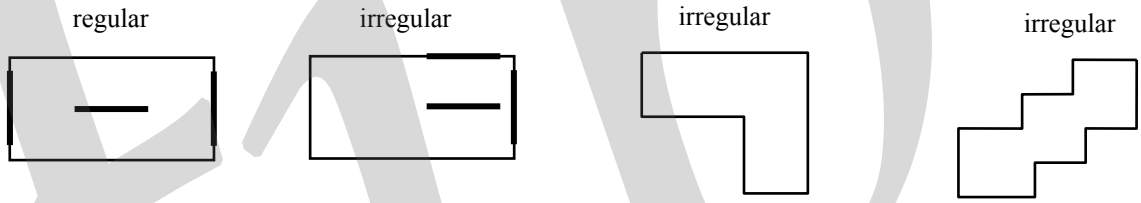

Fig. 5-25: Plan regularity of floors

On the contrary, stresses increase, when the layout is not compact, vertical elements are interrupted, large openings, inlets, concave corners are present, mechanical gaps (of special interest in prefabrication) or cracks of any origin (due to slab action, shrinkage, temperature) are formed, and few stiff bracing elements (shear walls) carry most of horizontal action (Fig. 5-26). In this case, the increase of stresses may run out of control, becoming locally critical.

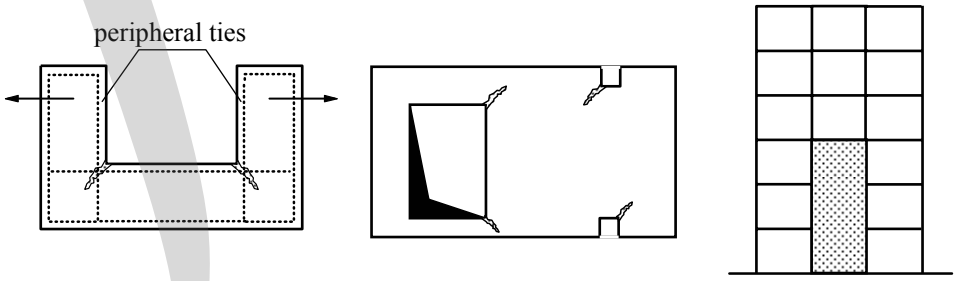

Fig. 5-26: Causes of local stress concentrations

5.3.3 Connections

From the above considerations, it is clear that the connections for precast seismic structures are designed to transfer the same kind of forces as from static actions. Therefore they do not differ basically from non-seismic, as function of different action effects examined in the previous sections but additional features are requested, above design strength. It must be taken into account that the philosophy is specific and leads to some important peculiarities that can be summarized as follows.

(1) Action effects

Action effects are derived from very conventional input assumptions and analysis. Therefore they are affected by large uncertainties and are far from exact. Intrinsic robustness and ductility are as relevant as dimensioning.

(2) Location

Connections are located in the structure according to practicality and to action effects, taking into account 'capacity design'. This means that not only are the forces to be transmitted according to the structural analysis to be examined, for selecting the location, but also a hierarchy of weaker zones in structural elements to dissipate energy.

(3) Design

As for any connection, devising and dimensioning must be done first conceptually, bearing in mind the performance requirements. Seismic structures have some additional ones, as follows.

- Connections must behave in a ductile manner. They can be either designed for only force transmission or also for dissipating energy, according to the hierarchy said above. For force transmission, ductility provides the capability of undergoing large displacement without breaking failure. For dissipation of energy, ductility is to fulfill the capability of dissipating energy under large amplitude straining cycles (by hysteretic loops of plastic material, or by controlled friction).
- Friction relying on gravity loads (e.g. at supports) cannot be accounted for, neither for force transmission nor for energy dissipation.
- In dimensioning connections, the resistance is to be evaluated not only with usual models giving the design strength in terms of monotonic action effects, but also in degraded conditions, after several alternations of large intensity straining.
- Detailing must be such to ensure for reinforcement, adequate anchorage under yield reversals and stirrups to avoid buckling at yield stress; and for concrete, confinement to prevent loss of material under extreme reversed compression and tension.

(4) Examples

- Uncertainties on intensity of earthquakes and on the structural response necessitate resistance for full reversals of stress. Thus, connections to transfer compressive forces must have a tensile capacity, and continuous beams must be connected to columns with top and bottom reinforcement even if the analysis, including seismic action, shows that only negative bending moments arise.
- Concrete under alternate large compression and tension deteriorates. Thus, confinement is required in wet cast connections (not for increasing the strength but at least for keeping it).
- Bond strength reduces considerably after several stress reversals. Thus, connection made by overlapping is not relied upon, if not provided with an increased length and a tight tying. Overlapping within grouted joints is not allowed.
- Reversed shear stresses reduce friction. Although in non-seismic buildings joints between slabs may be justified only about strength, in seismic ones the ductility (even if not accompanied with energy dissipation) is also necessary in order to avoid sudden diaphragm

failures. Thus, grouted joints of precast slabs cannot be plain or indented, but must maintain load after loading cycles.

For the detailed dynamic and seismic design of connections reference is made to fib (2003b).

Part II

Basic force transfer mechanisms

6 Transfer of compressive force

6.1 Principles for compressive force transfer connections

6.1.1 Typical joints with compressive forces

Every precast concrete element has to be supported at one or several locations in order to transfer its own weight and imposed loads down to the foundations. These forces will normally be compressive forces. Typical connections with compressive forces are shown in Fig. 6-1.

In most cases dead loads from other elements and live loads will increase the compressive forces. The main task for the designer is to optimise the size of the concrete member with regard to axial load, moment and shear, and afterwards to design the connections with proper components and materials in such a way that the load capacities are adequate.

Small bearing areas lead to small eccentricities, which is normally of great advantage. Large forces, or practical considerations, may however, require larger bearing areas.

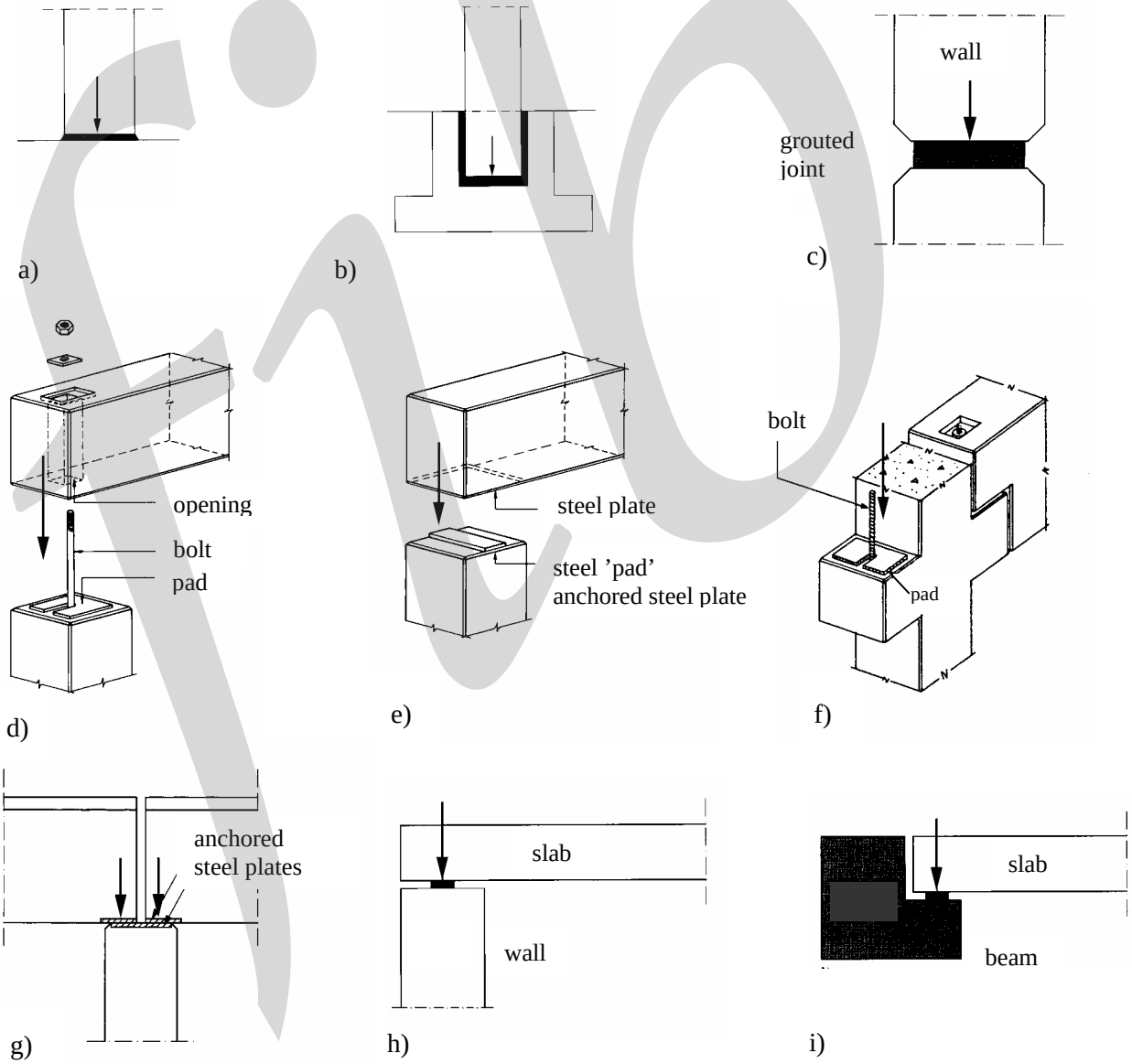

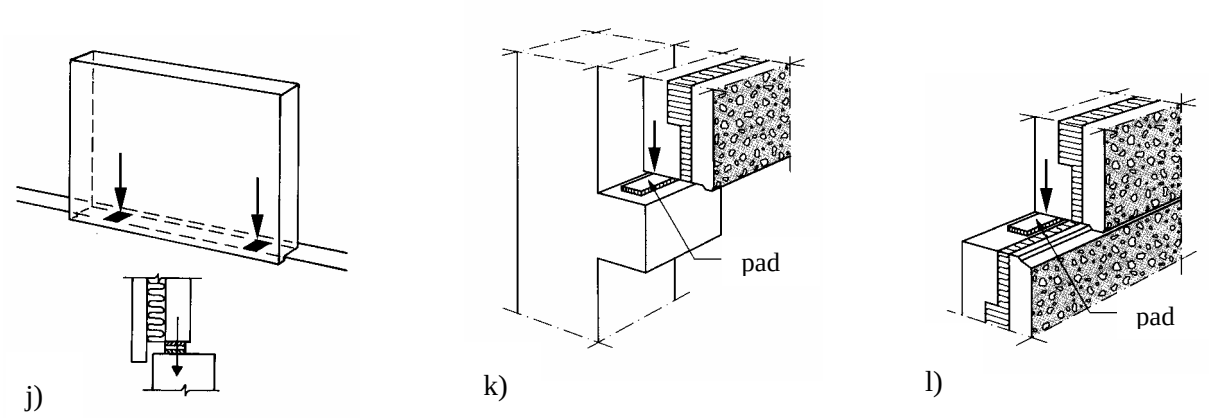

Fig. 6-1: Typical connections with compressive forces, a) column-foundation (grout), b) column-foundation (grout), c) wall (column)-wall (column) (grout), d) beam-column (pad), e) beam-column (steel), f) beam-corbel (pad), g) double tee-wall (steel), h) slab-wall (strip), i) slab-beam (strip), j) wall-foundation (steel), k) wall-corbel (plastic), l) wall-wall (plastic)

6.1.2 Typical compression joints with combined actions

Wind loads and/or earth pressure, will in some cases change the compressive forces into tensile forces, or impose horizontal (shear) forces on the connection. A connection will also often consist of not only two, but also three or four concrete members. Thus, compression joints must often be checked for shear forces, and require reinforcement or other steel components across the joint in addition to the joint bearing material. Typical connections where compression is combined with other action(s) are shown in Fig. 6-2.

Long horizontal members, such as beams or slabs, will rotate at the support following the variation due to temperature change, creep and shrinkage. The rotation often requires bearing pads and strips with special attention to detailed design of pad thickness and edge distances.

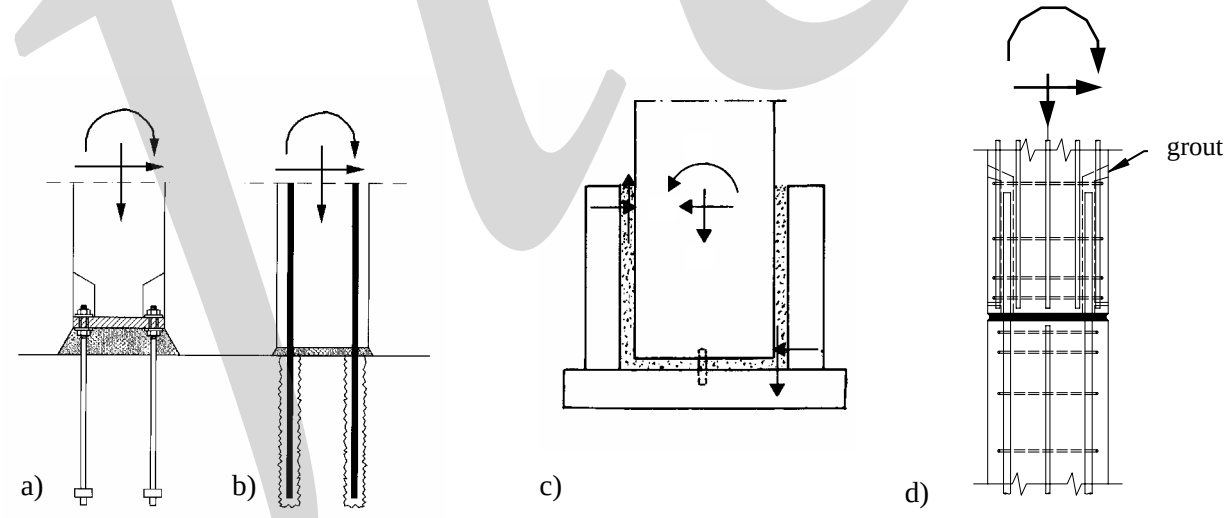

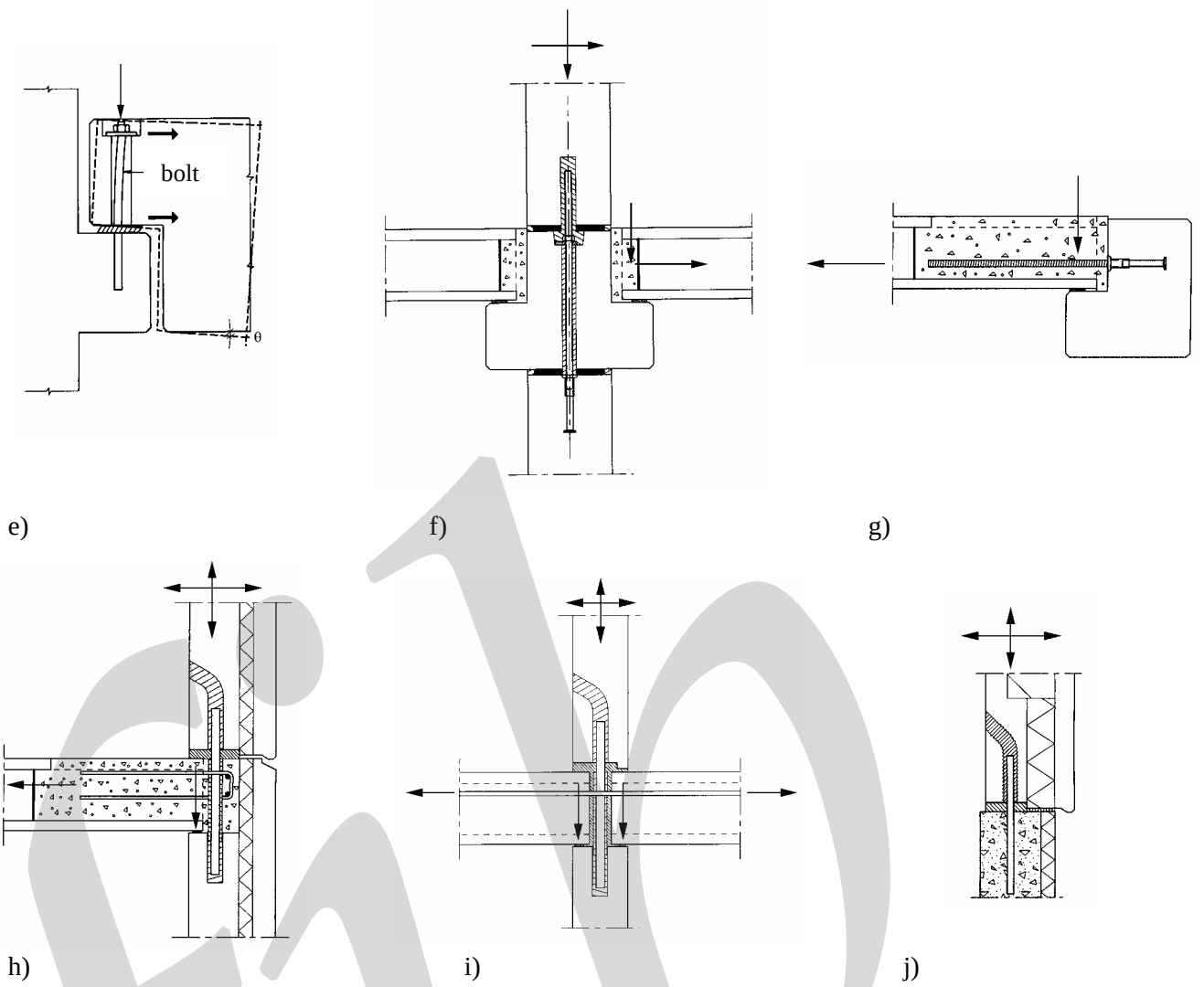

Fig. 6-2: Typical connections with combined actions, a) column-foundation (grout, steel), b) column-foundation (grout, reinf.), c) column-foundation (grout), d) column-column (grout, reinf.), e) beam-corbel (pad, bolt), f) column-beam-slab (grout, steel, reinf.) g) slab-beam (strip, grout, steel), h) slab-wall-wall (strip, grout, steel, reinf.), i) slab-wall-wall (strip, grout, steel, reinf.), j) wall-foundation (grout, steel)

6.1.3 Selection of bearing type and material

The bearing material is mainly designed for vertical and horizontal loads, and for rotation and lateral movements. The size of the bearing area and joint openings are, however, very often determined by the size of the concrete elements, erection tolerances and architectural considerations. The type of bearing material is also depending upon local availability and economy.

6.1.3.1 High compressive force without lateral movement and/or rotation

Connections with high compressive forces without lateral movement and/or rotation require construction steel (steel plates or bars) across the joint with properly designed field-bolting or welding in the connection area, see Fig. 6-3. The steel components should be properly anchored in the concrete member to secure transfer of the compressive forces to the main reinforcement. This type of solution is mostly needed for connections such as: beam-column, column-column, column-foundation, moment resisting frames or lateral bracing. The basic idea is to achieve a monolithic joint, see Section 9.4. If it

is possible, it is normally economical to avoid field welding with direct steel bearing, but to use steel base plates combined with anchor bolts and grouting instead.

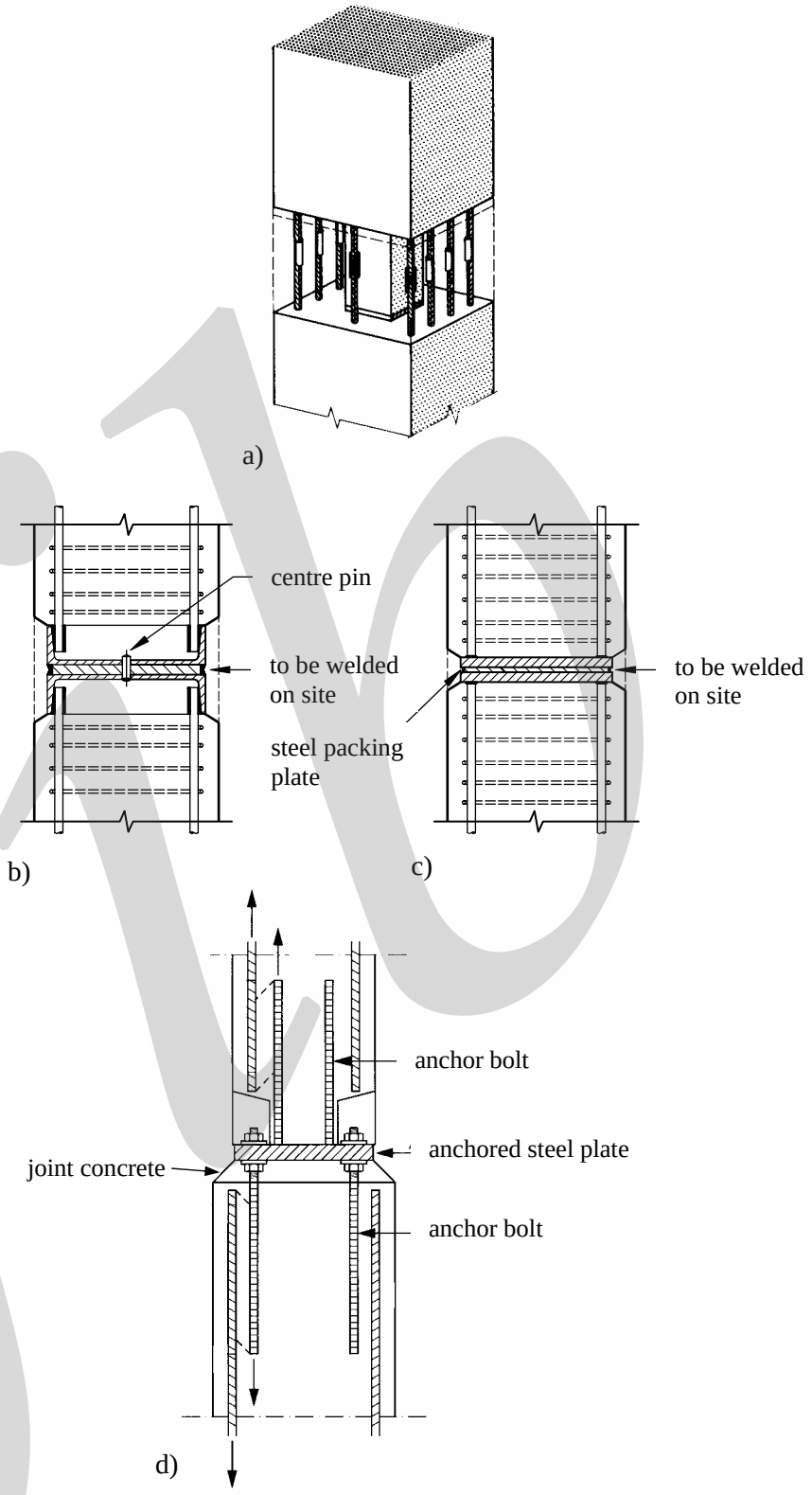

Fig. 6-3: High compressive forces without movement/rotation, a) steel member, reinforcement, welding, concrete, b) steel member, welding, patching, c) steel plates, welding, patching, d) steel plates, anchor bolts, grouting

6.1.3.2 Medium compressive force without lateral movement and/or rotation

Connections with medium compressive forces without lateral movement and/or rotation are typical for one-story columns and load bearing walls. Normally the column or wall is placed on erection shims and the joint is 90 – 100 % grouted. Steel bars or reinforcement across the joint are normally designed for tensile- or shear forces only, but they can also be utilized as compressive reinforcement. Typical solutions are shown in Fig. 6-4.

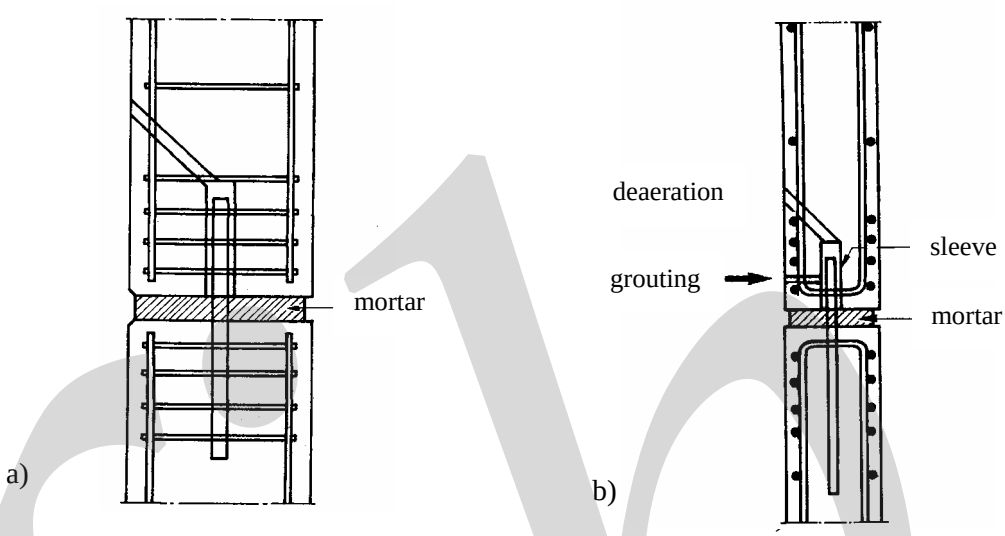

Fig. 6-4: Connections subjected to medium compressive forces without movement/rotation, a) column with grouting, steel bar, b) wall with grouting, steel bar

6.1.3.3 High and medium compressive forces with lateral movement and/or rotation

Connections with high and medium compressive forces with lateral movement and/or rotation are typical for the support of all types of beams, girders and T-shaped slabs (double tees and single tees), see typical examples in Fig. 6-5. Typically, this type of connections is provided with bearing pads. The reasons for this are illustrated in Fig. 6-6.

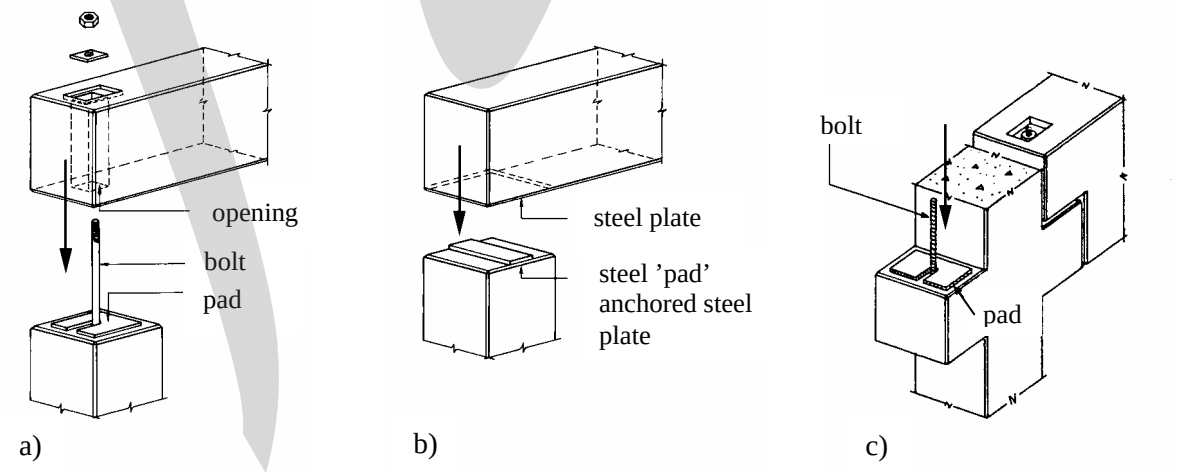

Fig. 6-5: Medium compressive forces with movement/rotation, a) beam-column with elastomeric pad, bolt, b) beam-column with cast in place plates, steel plate 'pad', welding, c) beam-corbel with plain elastomeric pad, bolt

Cast in steel plates in the concrete members with a steel plate 'pad' will provide large compressive capacity, but the rotation ability is limited. Lateral movement will only occur as slippage, which means that a horizontal force $H = \mu N = 0{,}2N$ to $0{,}5N$ might be imposed on the supporting member.

Elastomeric bearing pads are available in many types of materials, compositions and cost. They may be designed to accommodate almost any magnitude of forces, movement and rotation. The resisting horizontal force against movement is normally $H = \mu N = 0{,}05N$ to $0{,}2N$.

Two layers of hard plastic will provide a more predictable thickness of the joint than an elastomeric pad, but the rotation ability is limited. Lateral movement will occur by sliding with a resisting friction (horizontal) force $H = \mu N = 0{,}1N$ to $0{,}2N$.

There is also a large availability of different types of special sliding bearings. Bearings with Teflon layers may produce friction forces as low as $H = 0{,}02N$.

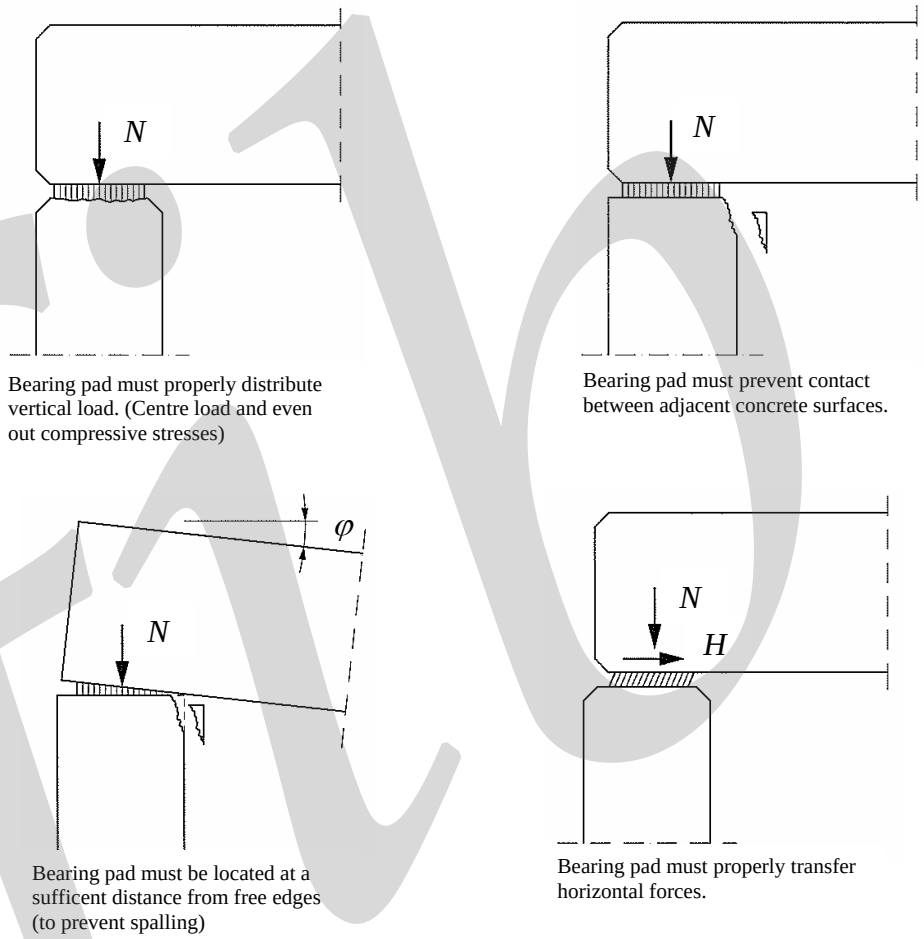

Fig. 6-6: Reasons for using bearing pads

6.1.3.4 Moderate compressive forces with little rotation and separate transfer of horizontal forces

Connections with moderate compressive forces with little rotation and separate transfer of horizontal forces are typical for the support of compact slabs or hollow core slabs and smaller double tees, see Fig. 6-7.

Compact or hollow core slabs will often require bearing strips sustaining compressive stresses of magnitude 1 to 4 N/mm^2. Used materials are for example moulded sponge rubber, neoprene and hard plastic. Small double tees are sometimes provided with cast in steel plates at the end, and placed directly upon cast in steel plates in the supporting member.

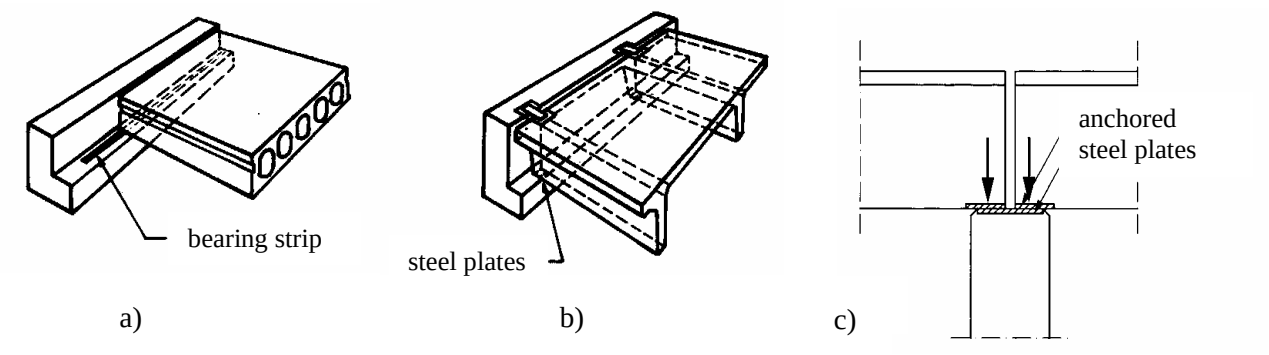

Fig 6-7: Moderate compressive forces, movement and rotation, a) slab-beam with bearing strip, b) double-tee beam with steel plates, c) double-tee wall with steel plates

6.1.3.5 Small compressive forces with negligible rotation and horizontal forces

Connections with small compressive forces with negligible rotation and horizontal forces are typical for the support of short slabs. The support reactions may be of magnitude 3 – 10 kN/m. In some cases the slabs are supported directly by the substructure without any bearing strips. In other cases strips of cardboard or felt may be used. The required minimum support length must still be present.

6.1.4 Design

Basic design rules for local concrete compression and corresponding local reinforcement in the splitting zones are given in Section 6.2. Basic design rules for the bearing material are given in Sections 6.3 – 6.5.

Bearing materials harder than concrete are checked at the ultimate limit state (ULS), whereas bearing materials softer than concrete are checked at the serviceability limit state (SLS). The most important issue in this case is to have satisfactory service load behaviour. In most cases the concrete itself with the splitting reinforcement will govern the ultimate limit state.

The design and dimensioning of the supporting and supported members at a bearing should take into account the anchorage requirements and the necessary dimensions of bends of the reinforcement in the members. Bearings must be dimensioned and detailed in order to assure correct positioning, accounting for production and assembling tolerances.

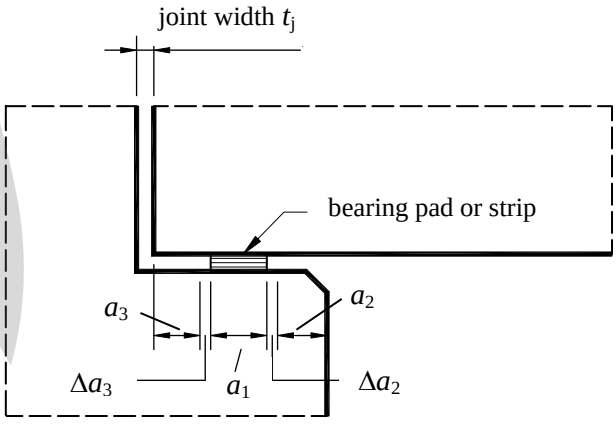

Fig. 6-8: Support length and tolerances, according to Eurocode 2 [CEN (2004)]

The position of the support load must account for eccentricities due to rotation and tolerances. Rules for this are given in Eurocode 2 [CEN (2004)], see Fig. 6-8.

6.2 Effect of local compression in concrete

A connection designed for compressive forces must include the design and detailing of the splitting reinforcement (local reinforcement) following the force paths from the joint to the main member reinforcement. The main factors to consider are the effect of lateral expansion through different materials, the effect of concrete and reinforcement lateral confinement (bi - or tri-axial effect) on the local compressive resistance (concentrated loads) and the local tension effects in the transition zones.

6.2.1 Lateral expansion

6.2.1.1 General formulas for lateral expansion

The concrete cube shown in Fig. 6-10 is subjected to uni-axial compression.

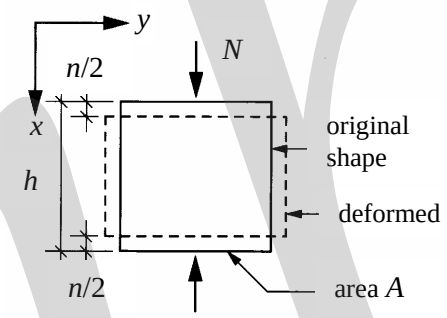

Fig. 6-10: Uni-axial compression of concrete cube

Formulas for uni-axial compression:

Original thickness	$= h$
Measured deformation	$= n$
Strain (x-direction)	$= \varepsilon = n/h$ or $\varepsilon_x = \sigma_x / E$
Compressive stress	$= \sigma_x = N/A$
Lateral stress	$= \sigma_y = 0$
Poisson's ratio	$= \nu = \varepsilon_y / \varepsilon_x$
Lateral strain	$= \varepsilon_y = \nu \cdot \varepsilon_x = \nu \cdot \sigma_x / E$
(y-direction)	(6-1)

The value of Poisson's ratio ν is different for various materials; for steel it varies from 0,25 to 0,33; for rubber it is slightly less than 0,50. For concrete it varies from 0,15 to 0,25 depending on the type of aggregate and other concrete properties. Generally ν = 0,2 is an accepted value used for concrete.

Small values for ν/E (steel) results in very small lateral expansion, while high values (rubber) results in large lateral expansion (almost constant volume).

General formulas for bi-axial compression:

$$\varepsilon_x = \left(\sigma_x - \nu\sigma_y\right)/E$$
$$\varepsilon_y = \left(\sigma_x - \nu\sigma_x\right)/E$$
$$\sigma_x = E\left(\varepsilon_x + \nu\varepsilon_y\right)/\left(1-\nu^2\right)$$
$$\sigma_y = E\left(\varepsilon_y + \nu\varepsilon_x\right)/\left(1-\nu^2\right) \qquad (6\text{-}2)$$

6.2.1.2 Formulas for compression through layers of different materials

Compression joints will always be composed of several layers of materials with different properties. These layers will have different compressive stresses σ, different elastic modules E and Poisson's ratios ν, leading to different lateral expansion ε_y, see Fig. 6-11.

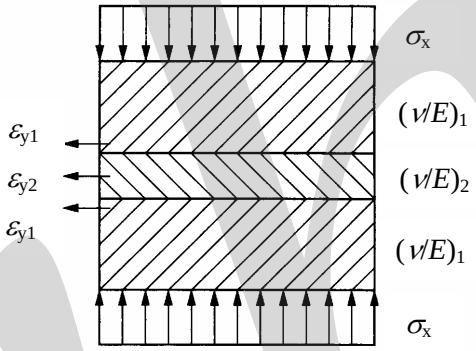

Fig. 6-11: Compression through several layers of different materials

Formulas for compression through several layers of different materials:

Lateral strain:	$\varepsilon_y = \nu \cdot \varepsilon_x = \nu \cdot \sigma_x / E$
Material 1:	$\varepsilon_{y1} = \nu_1 \cdot \sigma_x / E_1$
Material 2:	$\varepsilon_{y2} = \nu_2 \cdot \sigma_x / E_2$
Difference in lateral strain:	$\varepsilon_{y1} - \varepsilon_{y2} = \left[\left(\nu/E\right)_1 - \left(\nu/E\right)_2\right] \cdot \sigma_x$ (6-3)

Lateral stress σ_y if there is no sliding between the different layers:

$$\sigma_{y1} = \left(\varepsilon_{y1} - \varepsilon_{y2}\right) \cdot E_1 = \text{const.} \cdot E_1 \cdot \sigma_x$$
$$\sigma_{y2} = \left(\varepsilon_{y1} - \varepsilon_{y2}\right) \cdot E_2 = \text{const.} \cdot E_2 \cdot \sigma_x$$

This shows that a variation of σ_y will have a corresponding effect upon σ_x. In other words, the compressive stresses can only be uniformly distributed through the different layers if ν/E is constant. The lateral stress σ_y will produce corresponding lateral shear stresses between the different material layers. These shear stresses will effect the joint capacities (stresses) depending on the function ν/E.

6.2.1.3 Steel joint

Steel has a lower value for ν/*E* than concrete and will therefore impose lateral compressive stresses σ_y on the concrete, as shown in Fig. 6-12. These compressive stresses will increase the concrete bearing capacity. This is similar to the effect observed by cube testing, see Section 6.2.2. However, these effects are small, and are normally neglected for both concrete and steel in connection design, see Section 6.4.

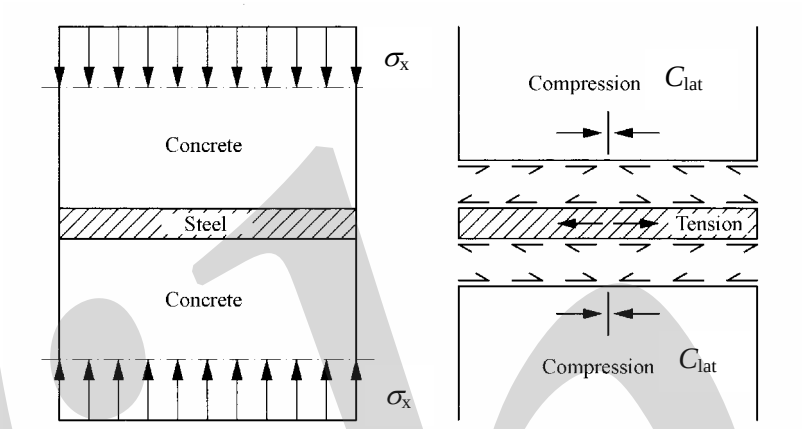

Fig. 6-12: Compression through concrete and steel plate, adopted from BLF (1995)

6.2.1.4 Mortar joint

The mortar quality will normally be of poorer quality than the concrete elements. The mortar, thus having a higher lateral strain *ν/E* than the concrete elements, will cause lateral tensile stresses in the elements close to the joint, and cause lateral compressive stresses in the mortar as shown in Fig. 6-13. The tension effect on the concrete element is normally very small compared to other effects, and is normally neglected in connection design. The compression effect on the mortar is of great importance, and will normally increase the bearing capacity σ_x to the level of the concrete element, see Section 6.3.

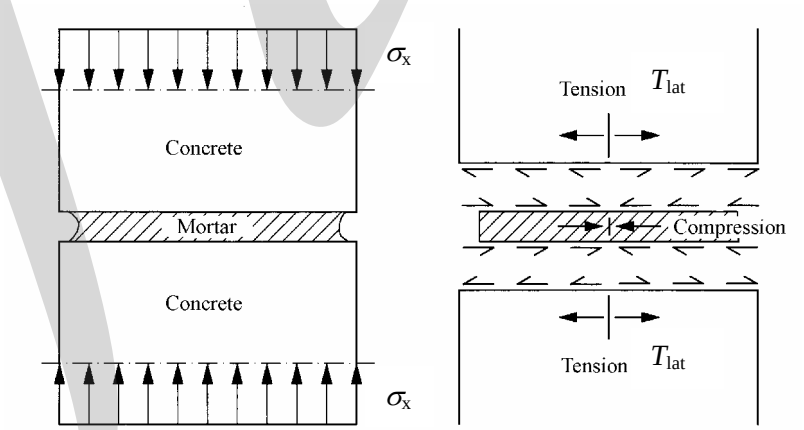

Fig. 6-13: Compression through concrete and mortar joint, [Basler and Witta (1966)]

6.2.1.5 Joint with soft materials

Soft materials, like plain elastomeric bearing pads, have much larger values for ν/E than concrete. The effect will be the same as for mortar, but with much higher values, see Fig. 6-14. The lateral strain is often so large that the pad will slide along the concrete surface. The friction is a function of the surface roughness and the type of pad [Vinje (1985a,b)].

The tension effect on the concrete element is often of such degree that it should be included in the design of splitting reinforcement. The compression effect on the bearing pad is essential for the bearing pad behaviour, and is always included in the design, see Section 6.5.

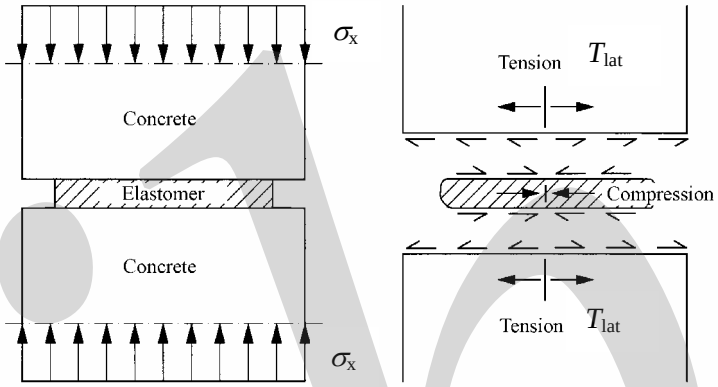

Fig. 6-14: Compression through concrete and plain bearing pad [Vinje (1985a, b)]

6.2.2 General failure modes of concrete

Concrete is a complex composition of aggregate, sand, cement, water and other additives. The failure mechanism is simply described as a function of the cohesion between the paste and the aggregate (shear, tension) and the strength of the weakest components themselves. When the concrete is subjected to compressive stresses, the first micro-cracks will appear between the paste and the aggregate. If the surrounding concrete prevents the corresponding deformation, the concrete will end up 'breaking' as the weakest components are crushed. If the surrounding concrete does not prevent deformation, a shear/tension failure will occur.

Compression cylinder or cube tests clearly demonstrate that the concrete specimen is splitting due to lateral tensile stresses. The tests also demonstrate the effect of friction between the concrete and steel plates, see Fig. 6-15. Reference is made to Section 6.2.1 for theoretical formulas.

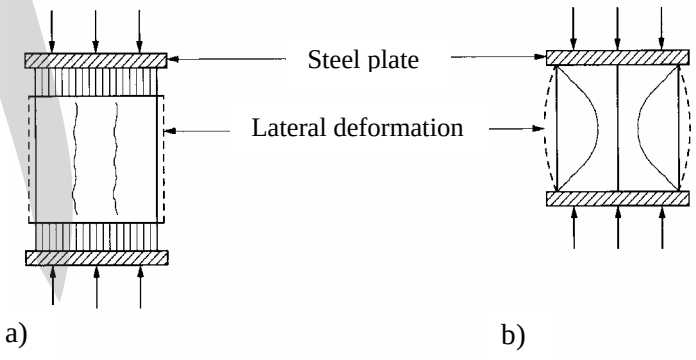

Fig. 6-15: Cylinder compressive testing [Leonhardt (1975)], a) minimal friction on loading area, b) normal friction on loading area

The concrete is much weaker for tension than compression (the tensile strength is 5 – 10 % of the compressive strength) and the failure mode will always be due to secondary tensile stresses.

6.2.2.1 Crushing

The bearing capacity f_{cc}^{*} of locally compressed concrete associated with **compressive failure** directly under the load, may be estimated by means of soil mechanics models for strip, square or circular footings. The triaxial state of stresses under the loaded area is favourable and may result in very high bearing capacity. However, if limited penetration is to be considered the following expression is recommended in Model Code 90 [CEB-FIP (1992)] for the bearing capacity.

$$f_{cc}^{*} = 4\, f_{cc} \qquad \text{for circular or square loaded areas} \tag{6-4}$$

where f_{cc}^{*} = bearing capacity of concrete under local compression
f_{cc} = compressive strength of concrete under uniaxial stress

6.2.2.2 Splitting

Lateral dilatation of locally compressed concrete is hindered by the surrounding mass of the non-loaded concrete (and, sometimes, by the presence of surrounding stirrups or helical reinforcement), which provides lateral confinement to the loaded strut, see Fig. 6-16. The increase of the strength due to the confinement is as approximately described by the following formulas (for plain concrete) according to Model Code 90 [CEB-FIP (1992)]:

Equilibrium before splitting, notations according to Fig. 6-16:

$$p \cdot d_1 = f_{ct}\left(d_2 - d_1\right) \qquad d_2 > d_1$$

$$p = \frac{f_{cc}}{10} \cdot \frac{d_2 - d_1}{d_1}$$

Triaxial effect:

$$f_{cc}^{*} = f_{cc} + 5p = f_{cc} + 0{,}5\, f_{cc}\, \frac{d_2 - d_1}{d_1}$$

with $d_2 \approx 2d_1$ to $4d_1$

$$f_{cc}^{*} = 0{,}7 \cdot \left(1{,}3\, f_{cc}\right)\sqrt{A_2 / A_1} = f_{cc}\sqrt{A_2 / A_1} \tag{6-5}$$

where A_1 = loaded area
A_2 = cross section of the surrounding concrete where the stress field is developed (leading to a final uniform longitudinal stress distribution) where, due to favourable size effects, the basic concrete strength has been taken as $1{,}3 f_{cc}$

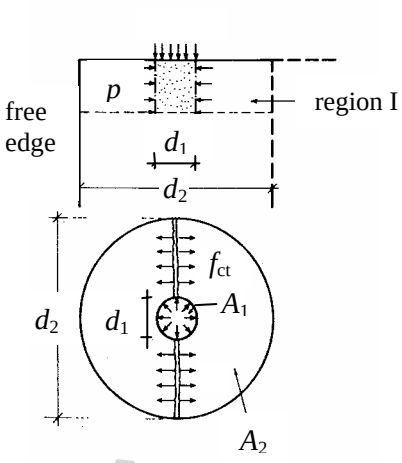

Fig. 6-16: Mechanism of 'confinement' offered by the surrounding mass of concrete, [CEB-FIP (1992)]

6.2.3 Compressive stress control

6.2.3.1 Stress limitations

Based upon Leonhardt (1975) and CEB-FIP (1992), the following formulae may be used for compressive stress control of concrete directly under local concentrated loads. The loading areas must correspond geometrically and have the same centre of gravity, see Fig. 6-17.

$$f_{cd}^{*} = f_{cd}\sqrt{A_2/A_1} \le 4{,}0\, f_{cd}$$

$$N_{Rd} = f_{cd}^{*} A_1 = f_{cd}\sqrt{A_1/A_2} \le 4{,}0\, f_{cd} \cdot A_1 \qquad (6\text{-}6)$$

where $A_1 = a_1 \cdot b_1$ (effective loading area)
$A_2 = a_2 \cdot b_2$ (distribution area)
$f_{cd} =$ concrete design compressive strength
$f_{cd}^{*} =$ bearing capacity

Fig. 6-17 b shows that in order to obtain the maximum allowable compressive stress, the edge distances must be at least given as follows:

$c_a \ge a_1$ and $h \ge 2a_1$, which leads to $a_2 \ge 3 \cdot a_1$ (Fig. 6-17 b)

$c_b \ge b_1$ and $h \ge 2b_1$ which leads to $b_2 \ge 3 \cdot b_1$ (Fig. 6-17 b)

Several concentrated loads close to each other will have reduced distribution areas, see Fig. 6-17 c:

$$\sum A_1 = 2a_1 \cdot b_1 \text{ and } \sum A_2 = a_2 \cdot b_2$$

$$f_{cd}^{*} = f_{cd}\sqrt{\sum A_2 / \sum A_1} \qquad (6\text{-}7)$$

When b_1 is much larger than a_1 (bearing strips for slabs), the compressive stress capacity is reduced:

$$f_{cd}^{*} = f_{cd}\sqrt[3]{A_2/A_1} \le 2{,}5\, f_{cd} \tag{6-8}$$

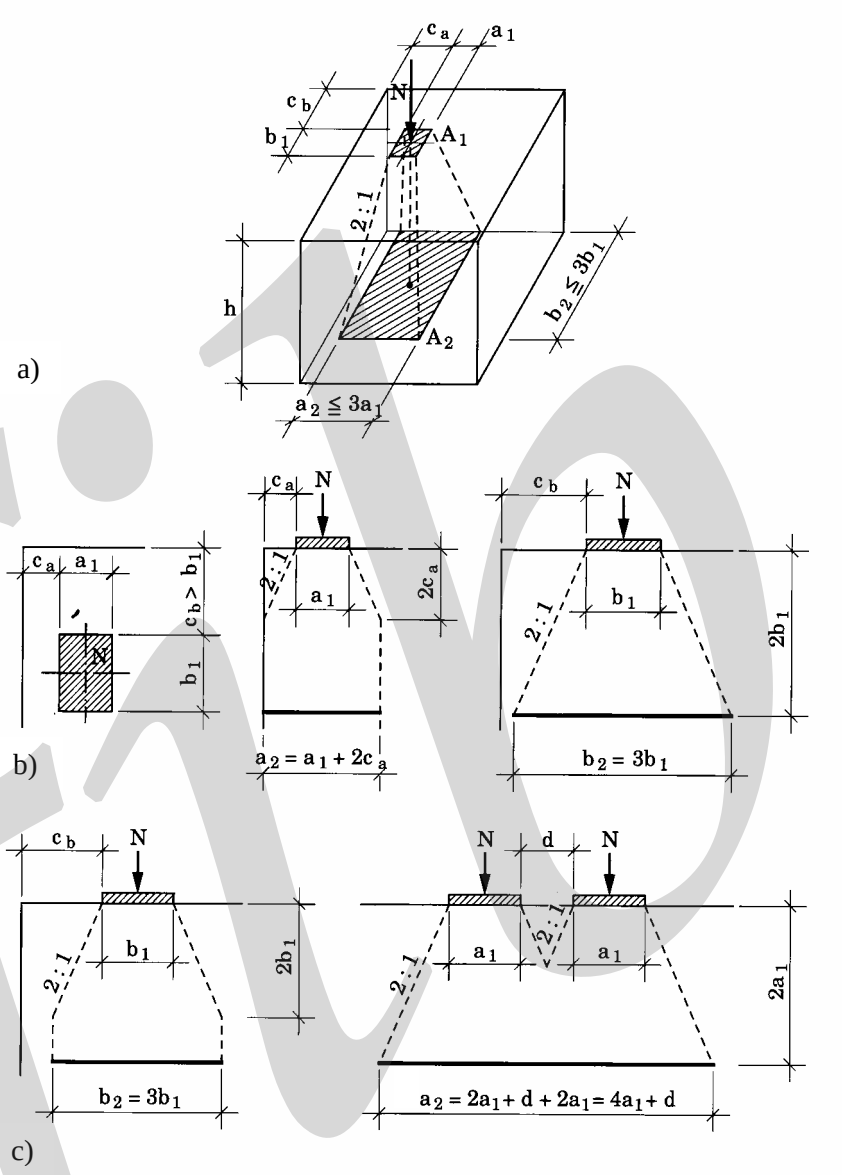

Fig. 6-17: Compressive stress control, adopted from BLF (1995), a) general load distribution, b) edge distance, c) overlapping loads

6.2.3.2 Definition of effective loading area and design stress:

If the concentrated load is transferred through a joint material (pad, plate) the stress will vary across the surface. The recommended procedure is to define the loading stress σ_m with the corresponding effective loading area $a_1 \cdot b_1$ as a mean value when checking the **concrete** compressive stresses, see Fig. 6-18.

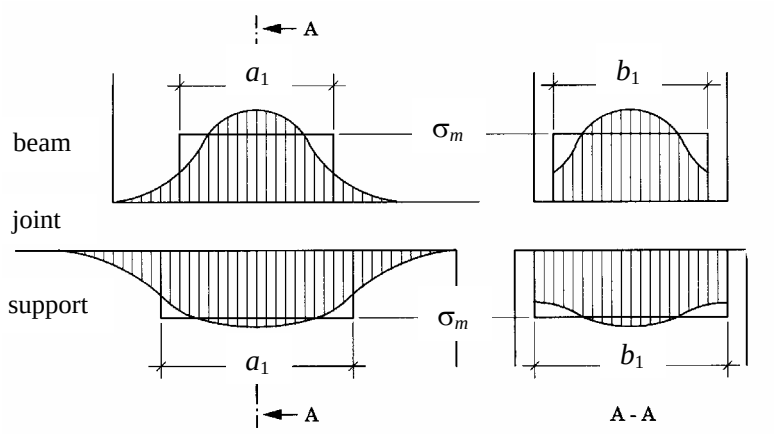

Fig. 6-18: Effective loading area above and below a joint

Peak values of the loading stress and loading areas will always vary with the joint type, joint material and the alignment of the concrete surfaces.

$\sigma_m = N/(a_1 \cdot b_1)$ is to be used in eqs. (6-6, 6-7, 6-8)

6.2.3.3 Hard materials

Joint material harder than concrete is generally composed of embedded steel plates with dimensions $a \cdot b$ and with a steel 'pad' with dimensions $a_0 \cdot b_0$, which is much smaller than the embedded plates, see Fig. 6-19.

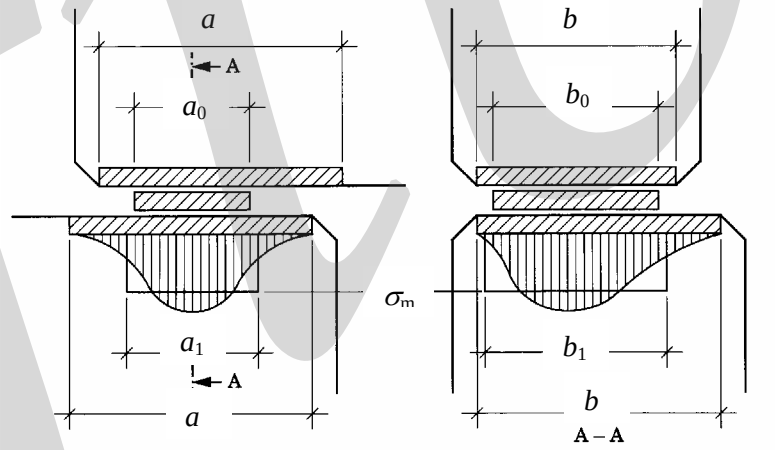

Fig. 6-19: Connections with steel plates as 'pads'

There are very few test results indicating correct values for stress and loading areas, but, as repeated later on, the local compression values will normally be of less importance than the local splitting (tensile) forces in the concrete further away from the loading area.

Within certain limits regarding rotation, the effective loading area for **concrete** stress control is:

Steel 'pad' area = $a_0 \cdot b_0 < a_1 \cdot b_1 <$ embedded steel plate area = $a \cdot b$, see Section 6.4.

6.2.3.4 Soft materials

Joint materials much softer than concrete are mostly different types of elastomeric bearing pads. Within certain limits regarding rotation, the effective loading area for **concrete** stress control can be taken equal to the bearing dimensions, see Fig. 6-20, i.e.

$$a_1 \cdot b_1 = a_0 \cdot b_0$$

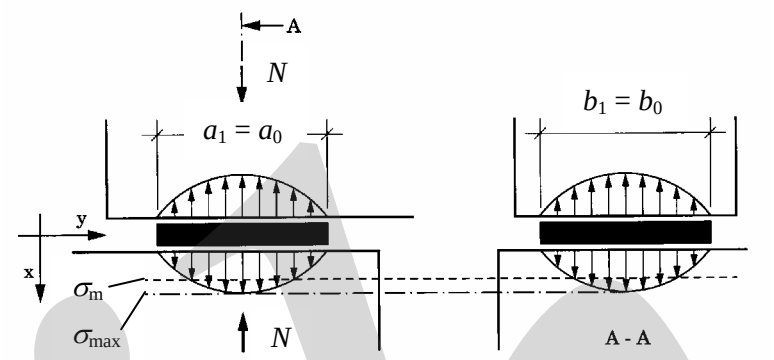

$\sigma_x \approx \sigma_y \approx \sigma_z$ (within pad)

$\sigma_{max} \approx 1{,}5\ \sigma_m$

Fig. 6-20: Rubber pad with centric loading

With larger rotation, the effective loading area has to be reduced, see Fig. 6-21.

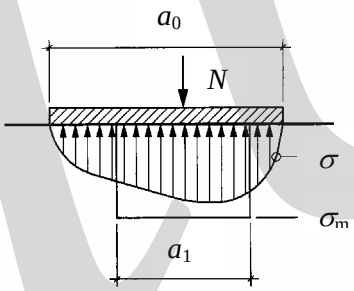

Fig. 6-21: Rubber pad with eccentric loading

6.2.4 Lateral tensile forces in the transition zones

Testing and practical experience indicate that the design and detailing of the local lateral tensile reinforcement in the transition zone is the most important factor when designing for concentrated loads. The tensile forces transversal to the axial loads and are often referred to as ‘splitting’ forces. The Model Code, [CEB-FIP (1992)], refers to ‘splitting’ forces close to the load, and ‘bursting’ forces in the transition region.

In these areas where Bernoulli’s hypothesis does not apply, it is not possible to design with standard formulas for moment and shear force capacities. The following procedure is recommended if there are no relevant formulas available:

- Start with test results that are relevant for this type of connection.
- If there are no test results available, apply theoretical linear analysis with FEM or elastic stress figures.

- Try to idealise test results or analysis by developing formulas or strut and tie models (compression and tension) from the external loading to the main member reinforcement, see Section 3.4.
- Provide local reinforcement for the local tensile forces and check the anchorage at both ends.

The basis for calculating the tensile (splitting) forces with one centric load is shown in Fig. 6-22, according to Leonhardt (1975).

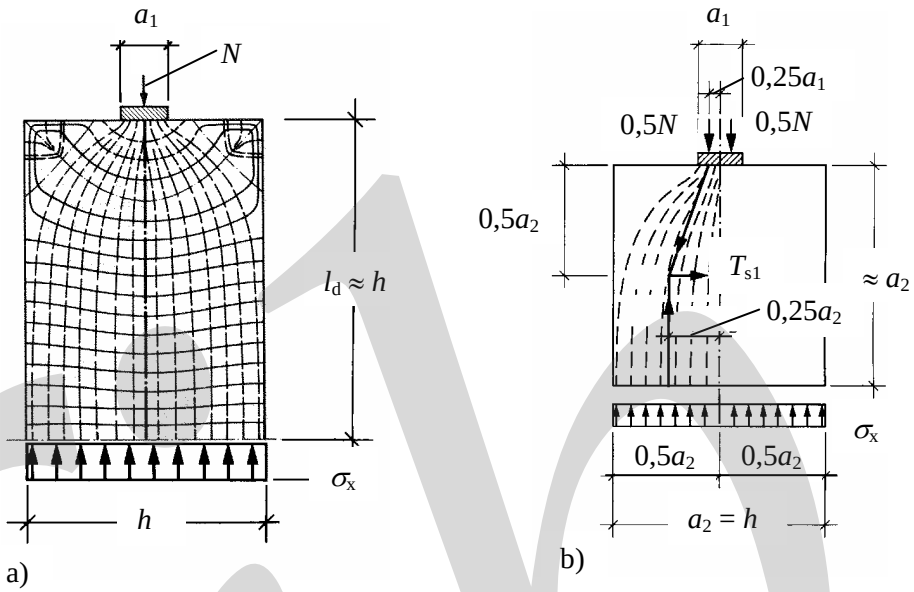

Fig. 6-22: Stress field under one centric load according to linear analysis, from Leonhardt (1975)

Resulting tensile force in a-direction:

$$T_{s1} = 0{,}5N\left[\left(0{,}25a_2 - 0{,}25a_1\right)/0{,}5a_2\right] = 0{,}25N\left(1 - a_1/a_2\right) \tag{6-9}$$

An eccentric load will increase the tensile forces close to the load, and reduce the tensile forces in the transition zone, see Fig. 6-23.

One simplified approach to estimate these forces may be to treat these forces separately, see Fig. 6-24. First the tensile force T_{s1} in the transition zone is determined by using eq. (6-9), considering the force distribution symmetrically around the load:

$$T_{s1} = 0{,}25N\left(\left(1 - a_1/a_2\right)\right)$$

Secondly, the tensile force T_{s2} close to the load is determined by using the following empirical formula instead of a strut and tie model:

$$T_{s2} = 0{,}015\,N\Big/\left(1 - \sqrt{2e/h}\right) \tag{6-10}$$

This formula results in forces $T_{s2} = 0{,}027N$ when $e/a = 0{,}1$ and $T_{s2} = 0{,}075N$ when $e/a = 0{,}4$. The total tensile force is

$$T_s = T_{s1} + T_{s2} \tag{6-11}$$

Alternatively the tensile forces T_{s1} and T_{s2} can be determined by a general strut and tie model.

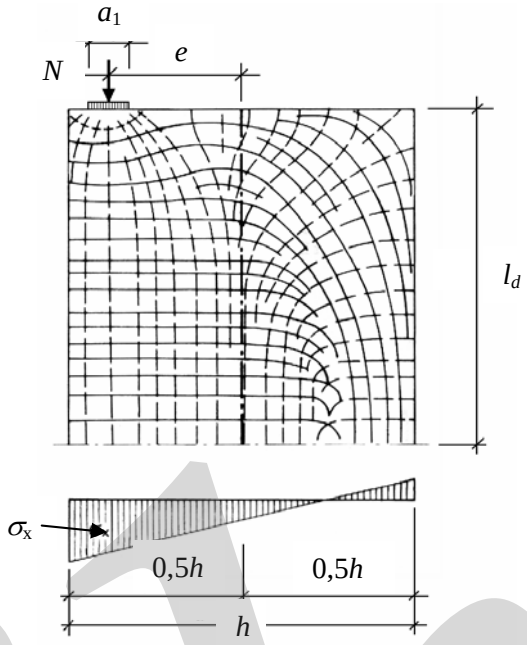

Fig. 6-23: Stress field under one eccentric load according to linear analysis, from Leonhardt (1975)

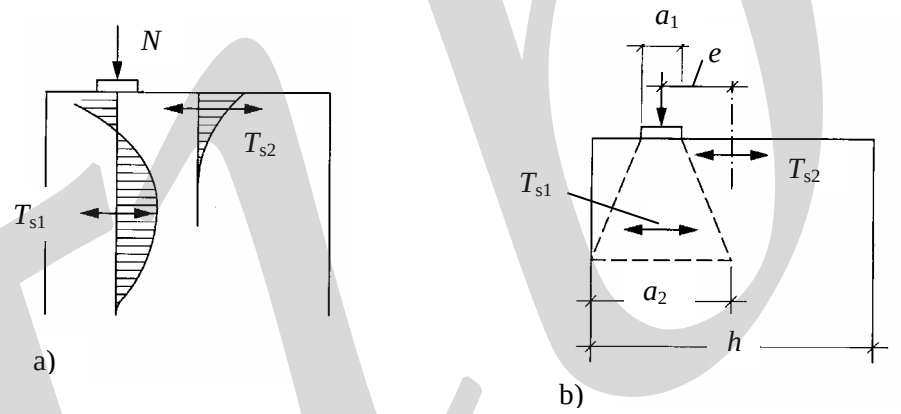

Fig. 6-24: Simplified approach to consider eccentric load, a) transverse stresses and resultants, b) notation

As discussed later, it is vital to provide local reinforcement for these tensile forces.

One simple conservative way of estimating the tensile force due to several point loads with the total of ΣN, is to use the same distribution values for a_1 and a_2 as shown in Fig. 6-17.

$$T_s = 0{,}25 \cdot \sum N \left(1 - \sum a_1 / \sum a_2\right) \tag{6-12}$$

The same procedure has to be done in the b-direction, see Fig. 6-17, to check the tensile forces in the b-direction.

In addition to these tensile forces there will always be lateral forces T_{lat} due to the difference in lateral strain for the joint material (Figs. 6-12 – 6-14), and lateral forces due to horizontal loads H (perpendicular to the axial concentrated load N).

6.2.5 Conclusion

1) The concrete compressive failure mode will practically always be due to secondary tensile stresses. It is therefore emphasised that the lateral tensile (splitting) forces in the concrete in the transition zone normally are of much greater importance than the local concrete compressive stresses directly under the load bearings.

2) Provide local tensile reinforcement for the design force:

$$T = T_s + T_{lat} + H \tag{6-13}$$

Proper detailing of this reinforcement with adequate anchorage at both ends is of vital importance.

3) The ultimate load capacity of reinforced concrete is depending upon tri-axial stress distributions. Simple 2-D strut-and-tie models, assuming that concrete has no tensile capacity, may lead to conservative or misleading models (example: hollow core floor unit end supports). FE analyses are very helpful as basis for optimising innovative connection design.

6.3 Joints filled with mortar, grout or concrete

Joints filled with mortar, grout and concrete are typical wall- and column connections, see Figs. 6-2 a, b, c, d, h, i, j, 6-3 d, 6-4. Horizontal movement is not allowed, and only very small rotation is permitted [Basler and Witta (1966)], [Vambersky and Walraven (1988)], [Paschen *et al.* (1981)], [Paschen and Zillich (1980)], [Brüggeling and Huyghe (1991)].

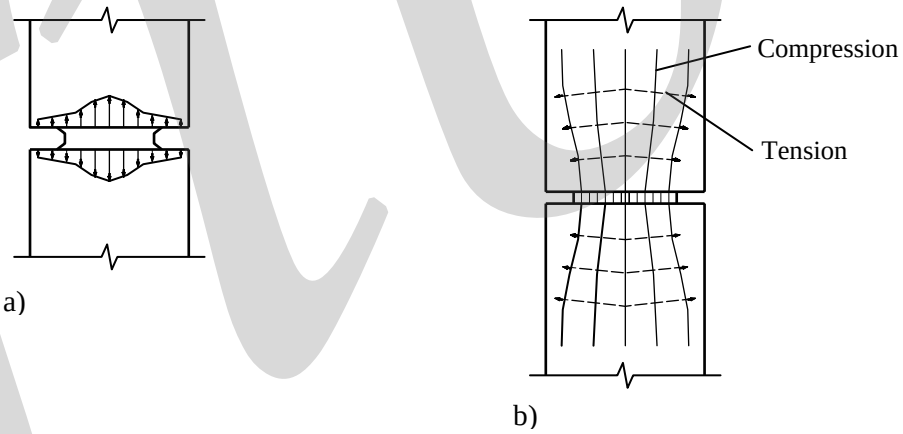

Fig. 6-25: Mortar joint according to Paschen and Zillich (1980), a) axial stress distribution, b) stress analysis

The basic behaviour of this type of joint is explained in Fig. 6-13 and corresponding text. The influence of the joint geometry on the joint compressive capacity is shown in the following formulas and Fig. 6-26.

$$N_{Rd,joint} = f_{cd,joint} \cdot A_{joint} = \beta \cdot f_{cd,wall} \cdot a_1 \cdot l \qquad \text{(joint bearing capacity)} \tag{6-14}$$

where $f_{cd,wall}$ = design compressive strength of wall concrete cylinder
$f_{cd,mortar}$ = design compressive strength of joint mortar cylinder
$f_{cd,joint}$ = design compressive strength of actual joint

$$\beta_0 = f_{cd,mortar} / f_{cd,wall}$$
$$\beta = f_{cd,joint} / f_{cd,wall}$$

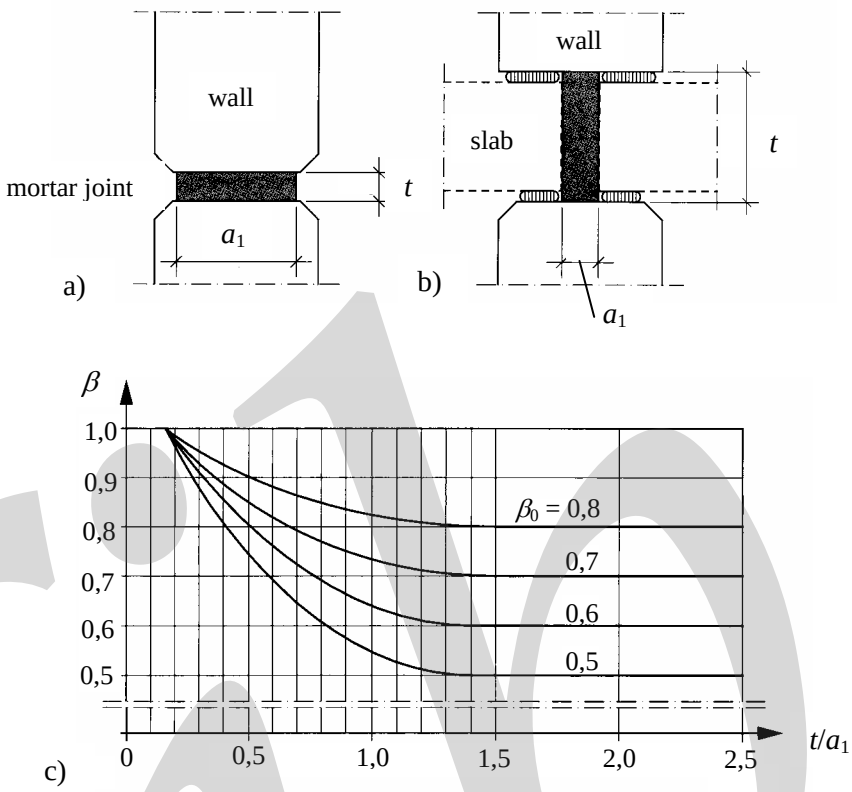

Fig. 6-26: Capacity of mortar joint, according to BLF (1995), a) wall-wall joint, b) wall-slab-wall joint, c) strength – geometry diagram

The mortar strength has to be at least 50% of the wall strength,

$$f_{cd,mortar} \geq 0{,}5\, f_{cd,wall}$$

The effective joint area is also depending on the mortar type and execution procedures (colloidal pouring mortar, dry packed mortar, mortar bed etc), [Vambersky and Walraven (1988)].

The mortar strength used in calculations should also take into account the actual strength of the mortar prepared in site conditions. The diagram indicates that for 'normal' wall to wall joints with $t/a_1 < 0{,}15$, the joint capacity will be equal to the wall capacity.

The joint between walls is subjected to a bi-axial effect, while column joints should be analysed with tri-axial effects. With 'normal' joint geometry the curves can be used for columns with centric loading when the smallest dimension is used for a_1.

Example 6-1

Geometry as shown in Fig. 6-27.

Effective loading area: $A_1 = a_1 \cdot l = 170 \times 1000 = 170000\ \text{mm}^2$

Wall strength: $f_{cd,wall} = 20\ \text{N/mm}^2$

Mortar strength: $f_{cd,mortar} = 12\ \text{N/mm}^2$

$\beta_0 = 12/20 = 0{,}6$
$t/a_1 = 50/170 = 0{,}29$

In Fig. 6-26 c we find $\beta = 0{,}92$.

Joint bearing capacity: $N_{Rd,\,joint} = 0{,}92 \times 20 \times 170000 = 3128 \cdot 10^3$ kN/m

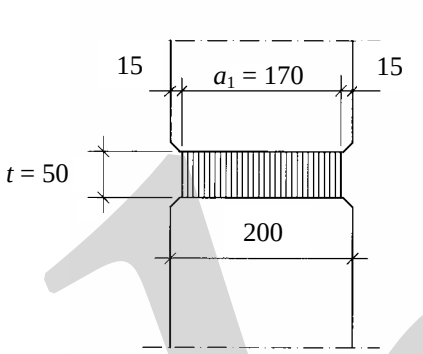

Fig. 6-27: Example: wall connection with mortar joint

A more complete design example is shown in Section 6.7.2

6.4 Hard bearings

Connections are classified as hard bearing connections when they are either without joint material, or with joint material harder than concrete.

6.4.1 Concrete against concrete without joint material

Compressive connections without joint material can be used for short slabs with small support loads, negligible rotation and horizontal forces, see Fig. 6-28.

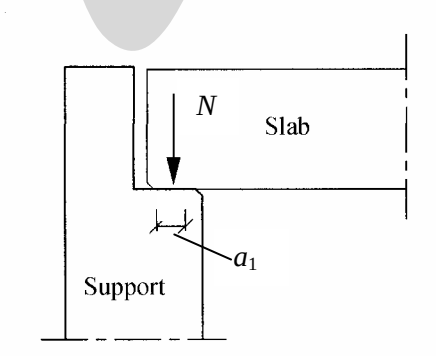

Fig. 6-28: Connection with concrete against concrete

The effective support length a_1 must be adequate, taking into account production and erection tolerances, see Fig. 6-8. The bearing stress $\sigma_m = N/(a_1 \cdot l)$ should be limited to approximately 0,2 - 0,3 N/mm^2. The corner of the supporting member should be chamfered.

6.4.2 Embedded steel

Steel members or plates cast into the concrete members, with various types of steel members or plates in the joint itself, can be designed to accommodate for almost any kind of connection. Some examples are shown in Figs. 6-1 e, g, 6-3 a, b, c, 6-5 b, 6-7 c.

The use is restricted due to high cost, limited rotation ability and high friction coefficient, μ = 0,2 – 0,5. Steel plates are especially used if minimum support areas are aimed at and/or it is desired to transfer horizontal forces by field welding.

There are few test reports concerning load distribution through steel plates. Recommended loading areas are shown in Figs. 6-29 – 6-30, and the bearing capacity is calculated by using eqs. (6-6) – (6-8).

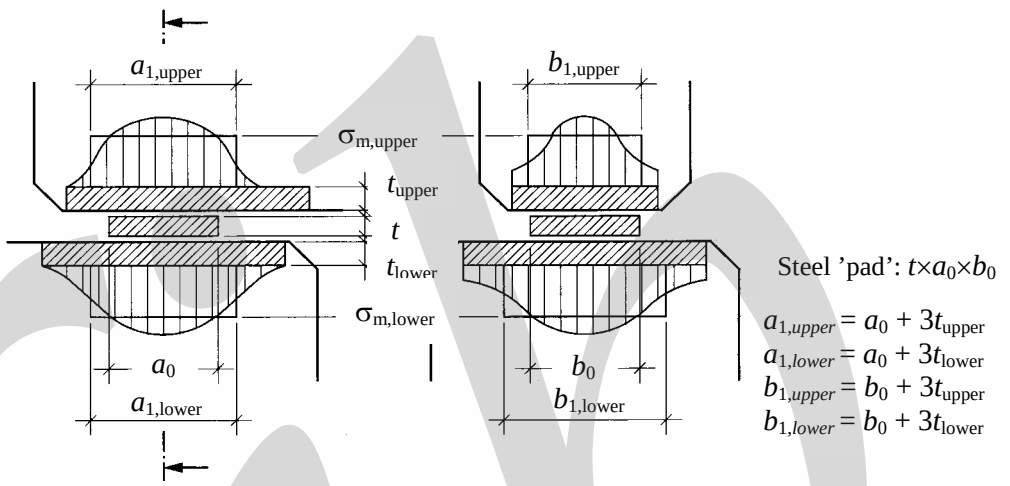

Fig. 6-29: Connections with steel plates and steel 'pad', according to BLF (1995)

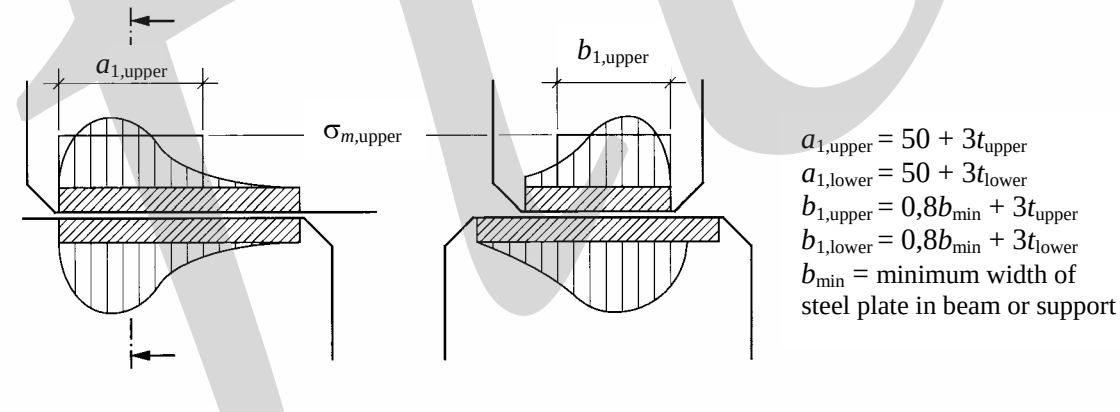

Fig. 6-30: Connections with steel plates without 'pad', according to BLF (1995)

The connection with a steel pad will accommodate ordinary beam rotation in building construction. Normally it is recommended to use a_0 = 50 – 100 mm, maximum a_0 = 150 mm (direction of rotation).

The connection without a pad is recommended for moderate loads with limited rotation, such as the support of prestressed double tees or short prestressed beams. A design example is shown in Section 6.7.1.

Design of column- or frame joints similar to Figs. 6-3 a, b, c has to be co-ordinated with the production and erection tolerances, but the design principles are the same. The capacity can be increased by compressive reinforcement parallel to the load (welded to the steel).

6.4.3 Other steel bearings

There are numerous types of steel bearings, most of them basically developed for the steel construction industry or bridge construction [Rahlwes (1989)]. Design guidelines are given in various codes, by bridge authorities and by the manufacturers. These bearings are expensive, and need maintenance regarding corrosion.

6.5 Soft bearings

6.5.1 General

Many kinds of materials softer than concrete – such as building paper, felt, hardboard, plastics, elastomer, lead, etc – might be suitable for supporting elements, such as slabs, double tees, beams, and single walls. A simple guideline for selecting a proper bearing type and material is given in Section 6.1.3, and the reasons for using bearing pad are seen in Fig. 6-6.

Rubber bearing pads, including natural rubber and synthetic rubber, are usually called elastomeric bearing pads. Neoprene and chloroprene are synthetic rubbers with special resistance to ozone, chemicals, heat and cold. The rubber hardness is normally classified by Shore A. Normally, a 50 to 70 Shore A will be used.

Rubber pads behave quite differently from the other mentioned material, see Fig. 6-31. They are normally designed in the serviceability limit state because of the very large deformations they may undergo at ultimate. Rubber is practically an incompressible material (Poisson's ratio is 0,5) and will therefore show large lateral expansion (bulging) when subjected to compression. If the lateral expansion is restrained, there will be a reduction of the compressive strain, see Section 6.2.1. The lateral expansion is restrained in two ways, namely, by friction in the loaded contact area and by vulcanised reinforcement. The effect of reinforcement varies from negligible (one layer of fibre) to very large (several layers of steel).

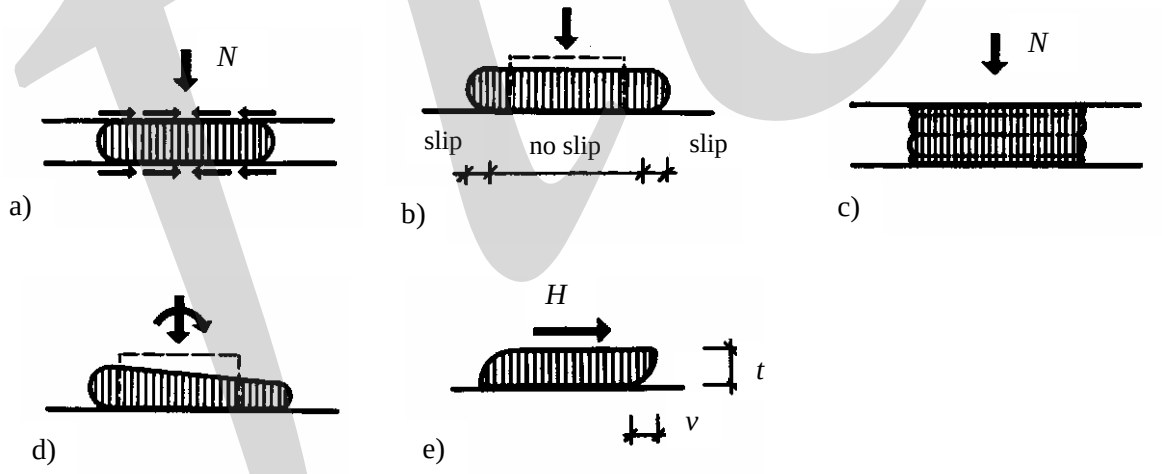

Fig. 6-31: General behaviour of elastomeric bearing pads, according to Vinje (1985a, b), a) compression of plain elastomeric bearing pad, b) deformation of plain pad, c) compression of steel reinforced elastomeric bearing pad, d) combined compression and rotation, e) shear deformation

Therefore, there is no possibility to calculate the compressive strain as a simple function of elastomer hardness or modulus of elasticity. The compressive strain may be expressed as a function of the compressive stress and an empirical shape factor α_S, see Fig. 6-32. The shape factor is defined as:

$$\alpha_S = \frac{\text{Loaded area}}{\text{Surface area free to bulge}}$$

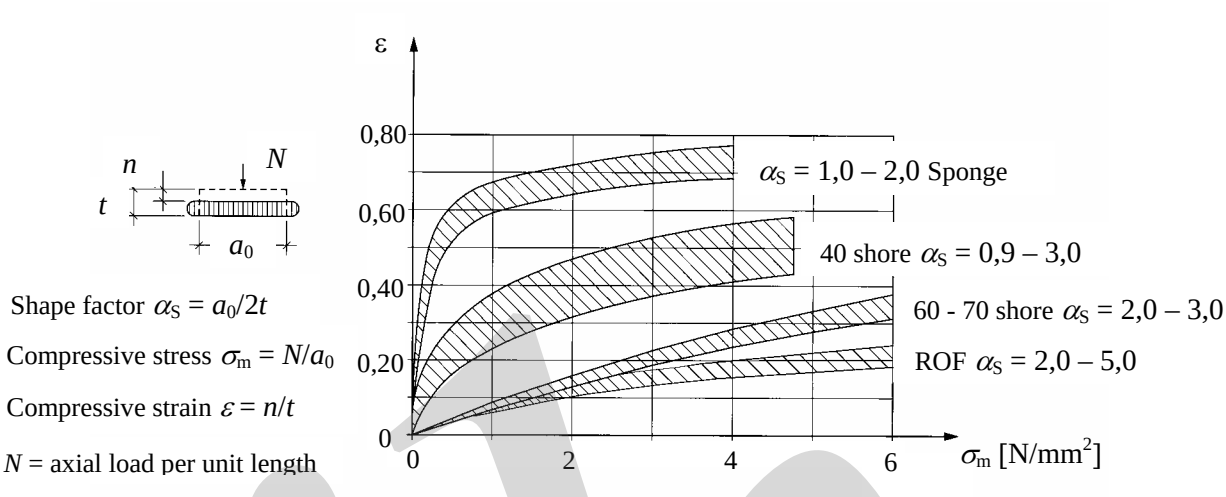

Fig. 6-32: Compressive strain for different types of rubber strips, according to Vinje (1986)

As seen in Fig. 6-32, the resulting compressive strain is very large for soft rubber, and relatively small for harder rubber reinforced with fibre (ROF), and even smaller for rubber reinforced with steel plates.

Due to economic reasons, the softer rubber is used for smaller support loads, such as bearing strips for slabs. The high quality bearing pads reinforced with steel plates are normally used in outdoor construction with large support loads and horizontal movement, for example under bridge beams.

6.5.2 Bearing strips for slabs

Hollow core slabs and compact slabs have normally a support load varying between 10 to 100 kN/m. The compressive stress in the bearing strips in the serviceability limit state, see Section 6.1.4, is normally varying between 0,5 to 3,0 N/mm^2.

Most slabs are supported with inserts or reinforcement for transfer of horizontal forces. Thus the bearing strip is subjected to vertical loads only, see Fig. 6-33.

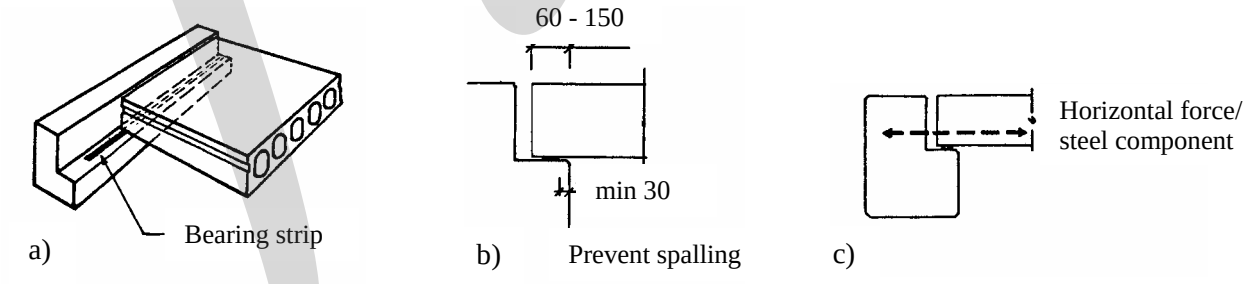

Fig. 6-33: Support connection of hollow core slab

There are many types of bearing strips being used around the world. Most types are composed of various rubber profiles, see Fig. 6-34, produced for the piping industry, but strips of high density plastics are also extensively used.

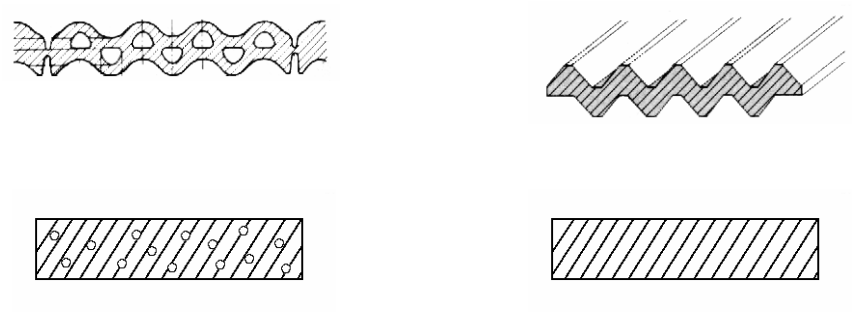

Fig. 6-34: Rubber bearing strips

Typical weight and dimensions of bearing strips for this type of connections are:
weight 0,5 g/cm³
width a_0 = 20 – 30 mm
thickness t = 6 – 10 mm

A design graph for bearing strips of moulded sponge rubber in this range is shown in Fig. 6-35. A complete design guide for bearing strips of moulded sponge rubber (moos gummy) with material quality ethylenpropylen (EPDM) is given in Vinje (1986).

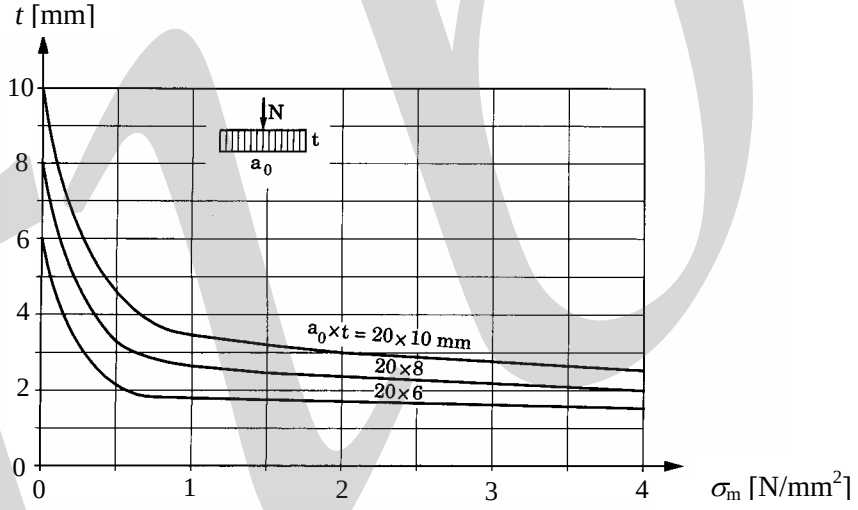

Fig. 6-35: Design graph for bearing strips of moulded sponge rubber, from Vinje (1986)

Worldwide experience indicates that the bearing strips for hollow core floor supports in many cases function primarily as erection levelling strips. Once the slab joints have been reinforced and grouted, uneven support loads are well distributed and transferred through the concrete. This can only be fully documented through FE analysis or full-scale tests of the actual detail.

Experience indicates, however, that regardless a large variety of design guidelines, most hollow core floor supports functions satisfactorily, if the support length is designed based upon the principles shown in Fig. 6-8, which is shown with practical values in Fig. 6-33 b. See also Section 6.2.4 for reinforcement procedures.

Support on steel beams may be designed without bearing strips, if the steel beam is designed for support load at the steel edges.

6.5.3 Bearing pads for single supports

This section is intended for the design of simple support of beams, double tees and single walls. Some examples are shown in Figs. 6-1 a, f, k, 6-2 e and discussed in Section 6.1.3.

Reasons for using bearing pads are shown in Fig. 6-6.

6.5.3.1 Semi hard bearing pads

Many types of semi-hard bearing pads are available, but few of them have data for design. The following values are appropriate for 'rigid smooth oil cured hardboard' and 'hard plastic' (ultrahigh weight polyethylene). Environmental quality must be properly checked.

For beams or double tees with limited rotation:

Lateral movement by gliding with	μ = 0,2 – 0,7 (against concrete)
With two layers	μ = 0,1 – 0,2 (plastic)
	μ = 0,2 – 0,35 (hardboard)
Effective loading area without rotation = size of pad.	
Compressive stress (SLS)	σ_m = 10 N/mm^2 max
Compressive strain	= 5 – 10 % when σ_m = 10 N/mm^2
Minimum edge distance to chamfer:	
Longitudinal (rotation)	= 20 mm (max length of pad = 150 mm)
Transverse	= 5 mm
Tensile force due to lateral effects	$T_{lat} \approx 0$

The effect of rotation must be differently accounted for when placing the support load on the supported member than the supporting member.

Various types of plastic shims are available and suitable for the support of single wall elements, see Figs. 6-1 k, l.

6.5.3.2 Plain elastomeric bearing pads

There are many types of rubber available. Some countries or state authorities have detailed or strict design guides, often too severe for ordinary indoor precast building construction. This often leads to unfavourable large bearing areas requiring larger elements, greater eccentricities and bending moments than are needed.

Vinje (1985a, b) presents a complete design guide for plain elastomeric bearing pads with hardness 60 to 70 shore A, including general background for the design of bearing pads. The following guidelines, taken from Vinje (1985a, b) are valid under the following conditions.

- Hardness: 60 to 70 Shore A
- Maximum area, A = 300 × 400 mm
- Shape factor, α_S = 2 to 7
- Thickness, t = 4 to 10 mm
- Contact surface: concrete
- Reinforcement: maximum of two layers of fibre reinforcing.
- The concrete bearing zone should be designed and reinforced according to Sections 6.2.3 and 6.2.4.

Characteristic dimensions of the bearing pad are defined in Fig. 6-36.

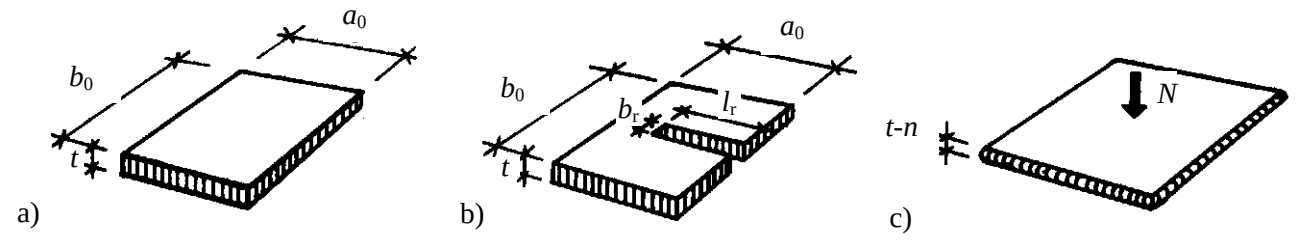

Fig. 6-36: Characteristic dimensions of bearing pads, a) unloaded pad without slot, b) unloaded pad with slot, c) loaded pad

The compressive stress σ_m is defined as the average stress over the actual area of the bearing pad before loading as

$$\sigma_m = \frac{N}{a_0 \cdot b_0 - b_r \cdot l_r} \tag{6-15}$$

The maximum allowable compressive stress is $\sigma_m = 10$ N/mm^2 (SLS), but the stress must often be restricted further due to the following limitations:

- there should be compression over the entire face of the bearing pad
- direct contact between the surfaces of the concrete members should be prevented
- the pad should not protrude from the concrete edges

The compressive strain is defined as

$$\varepsilon = n/t \tag{6-16}$$

where n (the compressive differential) is shown in Fig. 6-37

Typical relations between compressive stress and strain are presented in Fig. 6-37.

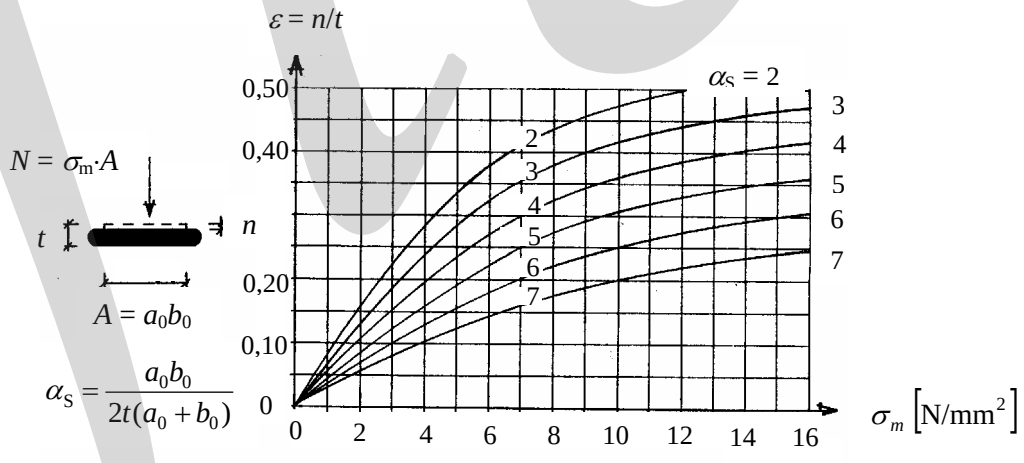

Fig. 6-37: Relation between stress and strain for plain elastomeric bearing pads

The thickness t should be designed so that there will be compression over the entire face of the bearing pad (see Fig. 6-38), that is:

$$t_1 \le t \qquad \varphi \frac{a_0}{2} \le \varepsilon \cdot t \qquad \text{or} \qquad t \ge \frac{\varphi a_0}{2\varepsilon} \tag{6-17}$$

The thickness t must be designed to prevent direct contact between the surfaces of the concrete members:

$$t_2 = t - \varepsilon \cdot t - \varphi \cdot l_e \tag{6-18}$$

The lower limit for t_2 should be chosen judiciously to account for erection tolerances.

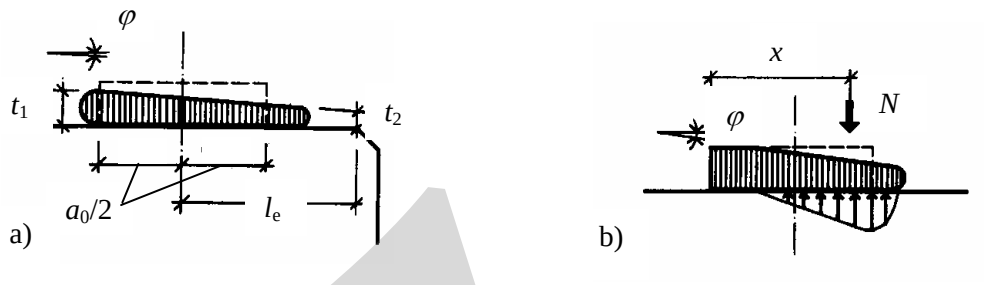

Fig. 6-38: Bearing strip subjected to rotation of supported member, a) combined compression and rotation, b) compressive stress block

When designing for small horizontal movements and low compressive strain values, it is permissible to have compression only over a part of the pad face, see Fig. 6-38 b.

When there is compression over the total pad area, the resulting force will usually be located at $x = 0{,}5a_0$ to $0{,}7a_0$ (depending on the angle of rotation φ). This should be evaluated especially in cases where there are corbels and dapped ends.

The stiffness of the elastomer increases with low temperatures thus reducing its capacity to accommodate rotation at low temperatures.

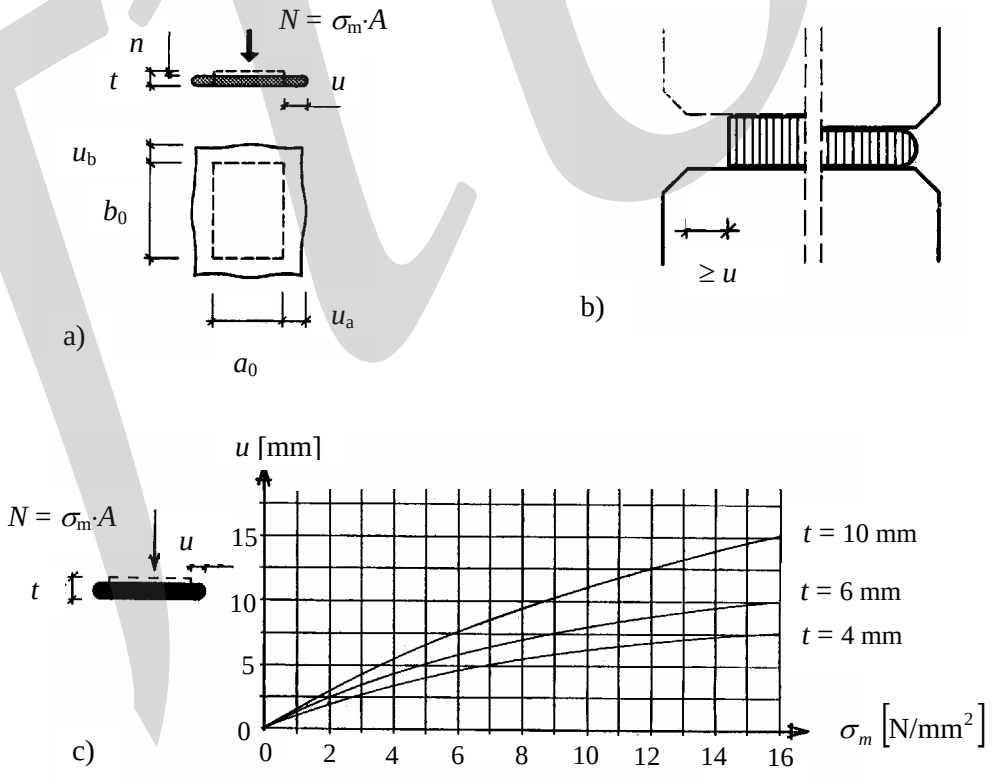

Fig. 6-39: Lateral expansion (bulging) of elastomeric bearing

The lateral expansion u is the maximum lateral expansion for one side of a pad with a specified compressive stress, compared with an unloaded pad of size $a_0 \cdot b_0$, see Fig. 6-39.

The size of the pad ($a_0 \cdot b_0$) should be limited so that the pad will not protrude from the concrete edges when subjected to loading, see Fig. 6-39 b.

Consider, for example, a 10 mm plain elastomeric bearing pad. Assume that σ_m is 10 N/mm^2 and the corresponding lateral expansion is u = 11 mm. As a minimum edge clearance (including chamfer), it would be advisable to use 25 mm in the direction of no rotation and 30 mm in the direction of rotation.

Shear deformation, Fig 6-40, is defined by

$$\tau_m = \frac{H}{A} = G\frac{v}{t} \tag{6-19}$$

where H = horizontal force
A = area of unloaded pad
G = shear modulus for bearing pad
v = shear deformation

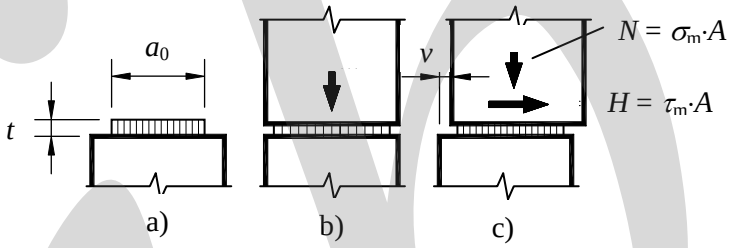

Fig. 6-40: Shear deformation of bearing pad, a) unloaded pad, b) compression, c) compression and shear deformation

Maximum and minimum horizontal resistance against shear deformation (lateral displacement), which depends on the compressive stress σ_m, is found from Fig. 6-41.

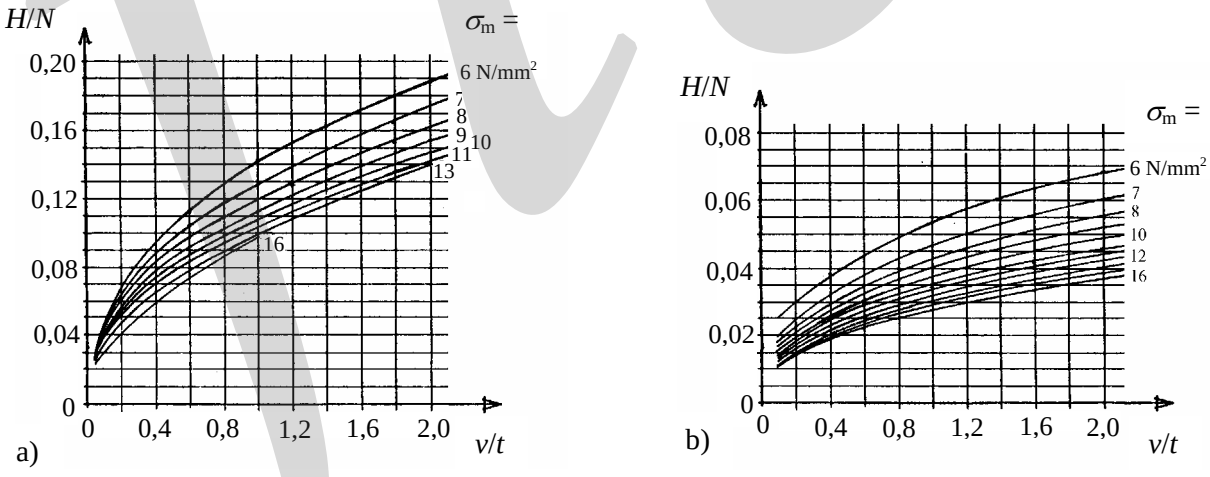

Fig. 6-41: Horizontal resistance against shear deformation, a) maximum resistance, b) minimum resistance

Note that the maximum shear resistance always is smaller than 20 % of the support load, which means it is smaller than the friction coefficient μ = 0,2 – 0,4. Also note that the above values are only applicable at temperatures of +20°C. In general, the shear stiffness increases with low temperatures. It is suggested that the shear stiffness should be corrected with the factor α_T at low temperature, see Fig. 6-42.

$$G_T = \alpha_T \cdot G_{20°C}$$

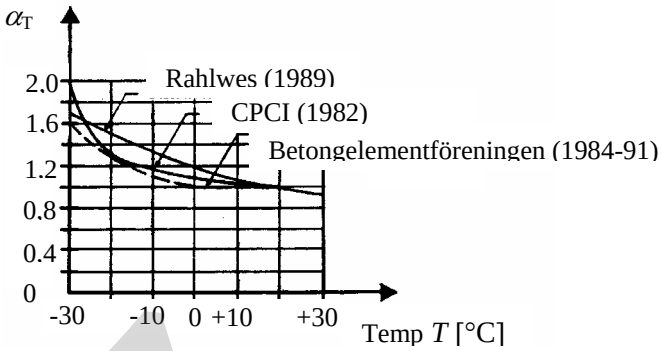

Fig. 6-42: Shear modulus versus temperature, [Rahlwes (1989), CPCI (1982), Betongelementföreningen (1990)]

It is recommended that the maximum allowable shear deformation v is limited for plain elastomeric bearing pads related to pad thickness t and compressive stress σ_m as shown in Fig. 6-43. The limitations for v/t should be based on engineering judgement especially regarding the calculation of the horizontal movement v.

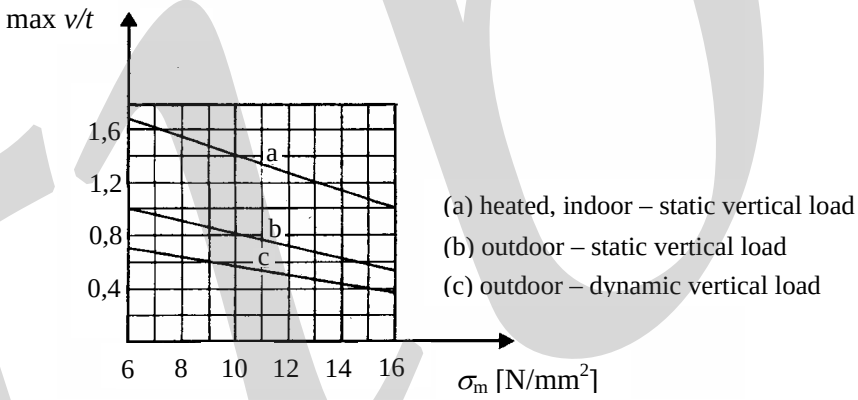

Fig. 6-43: Maximum allowable shear deformation

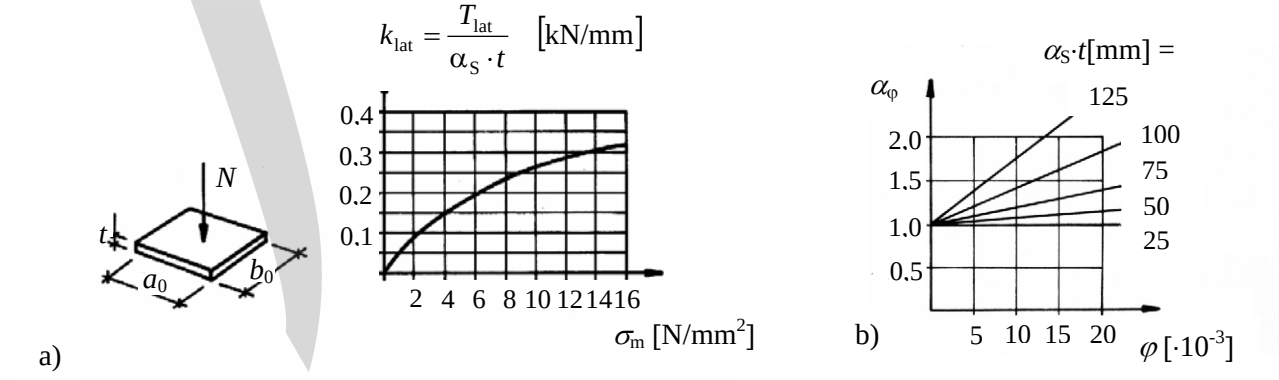

Fig. 6-44: Lateral expansion force from plain elastomeric bearing pad, a) centric load (smooth concrete surface), b) correction factor for rotation

The lateral expansion creates tensile forces in the adjoining concrete members that should be included in the design of the splitting reinforcement, see Section 6.2.4.

$$T_{\text{lat}} = \alpha_{\varphi} \cdot k_{\text{lat}} \cdot \alpha_{\text{S}} \cdot t \quad \text{[kN, mm]} \tag{6-20}$$

Example 6-2

Design a bearing pad for a simply supported prestressed concrete beam. Assume that there is only one span with no movements of the supports. Fig. 6-45 shows the assumed bearing detail.

Length L = 12 m
Width b = 300 mm
Width of supporting member h = 200 mm (for architectural reasons)
Edge distance l_e = 90 mm
N = 300 kN (service load)
Rotation φ = 10 ‰ = 0,01 radians
Horizontal movement of beam ends: 0,5 $\varepsilon_{tot} L$

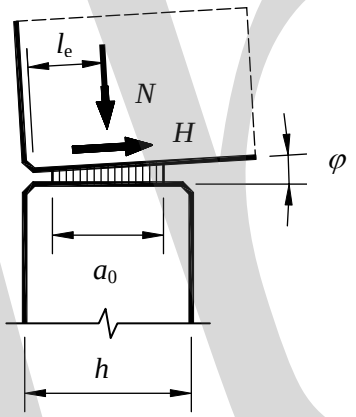

Fig. 6-45: Bearing detail in example

The bearing pad is to be designed for the following two environmental and loading conditions:

Alternative 1, heated building, subject to static vertical load, (Fig 6-43 – condition a):

Try an edge clearance c_a = 30 mm and c_b = 25 mm i.e., pad size $a_0 \cdot b_0$ = 140 × 250 mm

$$\sigma_{\text{m}} = \frac{N}{a_0 b_0} = \frac{300000}{140 \times 250} = 8{,}6 \text{ N/mm}^2$$

Horizontal movement and corresponding need for shear deformation v

$\varepsilon_{\text{tot}} = 950 \cdot 10^{-6}$ (assumed value, calculations not shown here)

$$v = 0{,}5 \cdot \varepsilon_{tot} L = 0{,}5 \times 950 \cdot 10^{-6} \times 12000 = 5{,}7 \text{ mm}$$

Max allowable $\frac{v}{t} = 1{,}5$ (Fig. 6-43, condition a)

Min. required $t = \frac{v}{1{,}5} = \frac{5{,}7}{1{,}5} = 3{,}8$

Try t = 10 mm which is commonly used for beam pads.

Lateral expansion, u = 10 mm (Fig. 6-39) (OK)

$$\alpha_S = \frac{a_0 b_0}{2t(a_0 + b_0)} = \frac{140 \times 250}{2 \times 10(140 + 250)} = 4{,}5$$

Average compressive strain, $\varepsilon = 0{,}31$ (Fig. 6-37)

Maximum allowable rotation regarding compressive stress

$$\varphi \le \frac{2 \cdot \varepsilon \cdot t}{a_0} = \frac{2 \cdot 0{,}31 \cdot 10}{140} = 0{,}044 = 44\ ‰ > 10\ ‰ \text{ (OK)}$$

Edge clearance (see Fig. 6-38 a):

$$t_2 = t - \varepsilon \cdot t - \varphi \cdot l_e = 10 - 0{,}31 \cdot 10 - \frac{10}{1000} \cdot 90 = 10 - 3{,}1 - 0{,}9 = 6{,}0 \text{ mm (OK)}$$

Maximum horizontal resistance (shear) force

$v/t = 5{,}7/10 = 0{,}57$

Max $H = 0{,}09N$ (Fig. 6-41 a)
$= 0{,}09 \times 300 = 27$ kN

The selected pad 140 × 250 × 10 mm is OK. A similar calculation with t = 6 mm gives adequate performance also.

Alternative 2, outdoor building, subject to static vertical load (Fig. 6-43, condition b):

Try again, $a_0 \cdot b_0$ = 140 × 250 mm with t = 10 mm, i.e., σ_m = 8,6 N/mm^2

$\varepsilon_{tot} = 1150 \cdot 10^{-6}$ (assumed value, calculation not shown here)
$v = 0{,}5 \cdot \varepsilon_{tot} \cdot L = 0{,}5 \times 1150 \cdot 10^{-6} \times 12000 = 6{,}9$ mm (need for shear deformation)
$v/t = 6{,}9/10 = 0{,}69 < 0{,}9$ (Fig. 6-43, condition b), which is OK.

Lateral expansion, rotation, edge clearances are the same as before.

Maximum horizontal resistance (shear) force

$H = 0{,}10 \cdot N$ (Fig. 6-41 a)
$= 0{,}10 \times 300 = 30$ kN

If the temperature is -20°C the shear modulus correction factor $\alpha_T \approx 1{,}4$ (Fig. 6-42), which leads to

$$H = 30 \times 1{,}4 = 42 \text{ kN}$$

6.5.3.3 Fibre reinforced elastomeric bearing pads

There are several types of rubber and fibres available for fibre reinforced elastomeric bearings. J. V. Inc offers a design guide for ozone-resistant elastomer with random oriented synthetic fibres (ROF). The ROF pad has a higher elastic and shear modulus than plain pads, and is therefore available with larger thickness.

The fibres offer a higher resistance to internal pad stresses and are therefore more suitable to cyclic loads. The ROF pads are more suitable than plain pads for precast structures with higher vertical loads and horizontal movement, i.e. outdoor parking structures or larger girders.

General pad thickness recommendations:

- non-beam members spanning less than 18 m t = 10 mm
- non-beam members spanning more than 18 m t = 10 - 12 mm
- beams spanning less than 12 m t = 12 mm
- beams spanning more than 12 m t = 16 – 19 mm

The design procedure follows the principle and notations shown for plain pads. All design is in the serviceability limit state. The maximum allowable working load is limited by a maximum compressive strain $\varepsilon = n/t = 0{,}40$ at the pad's extreme edge, or a compressive stress $\sigma_m = 55$ N/mm^2. A standard recommendation is to start with a pad size $a_0 \cdot b_0$ that results in a $\sigma_m = N/(a_0 \cdot b_0) \approx 10$ N/mm^2, without any regards to rotation. The thickness t should be minimum $t = v/0{,}75$ (compare with Fig. 6-43). The average compressive strain without rotation is shown in Fig. 6-46.

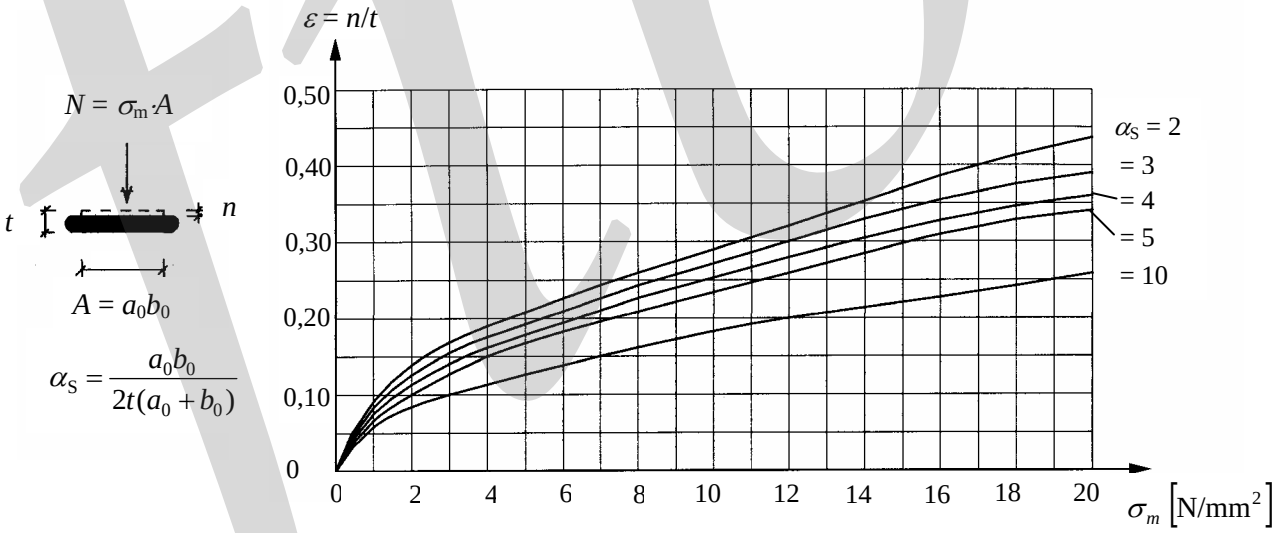

Fig. 6-46: Compressive stress and strain for ROF bearing pads

The angle of rotation φ between the upper and lower bearing surfaces must be calculated. It is recommended to use minimum φ = 0,03 radians (Prestressed slabs and beams with limited deformation have φ = 0,003 – 0,02 plus construction tolerances).

The rotation may lead to a reduced bearing length a_1 in the direction of rotation, see Fig. 6-21, which is permitted in ROF design. Calculate a_1 according to Fig. 6-47 (see also Fig. 6-38).

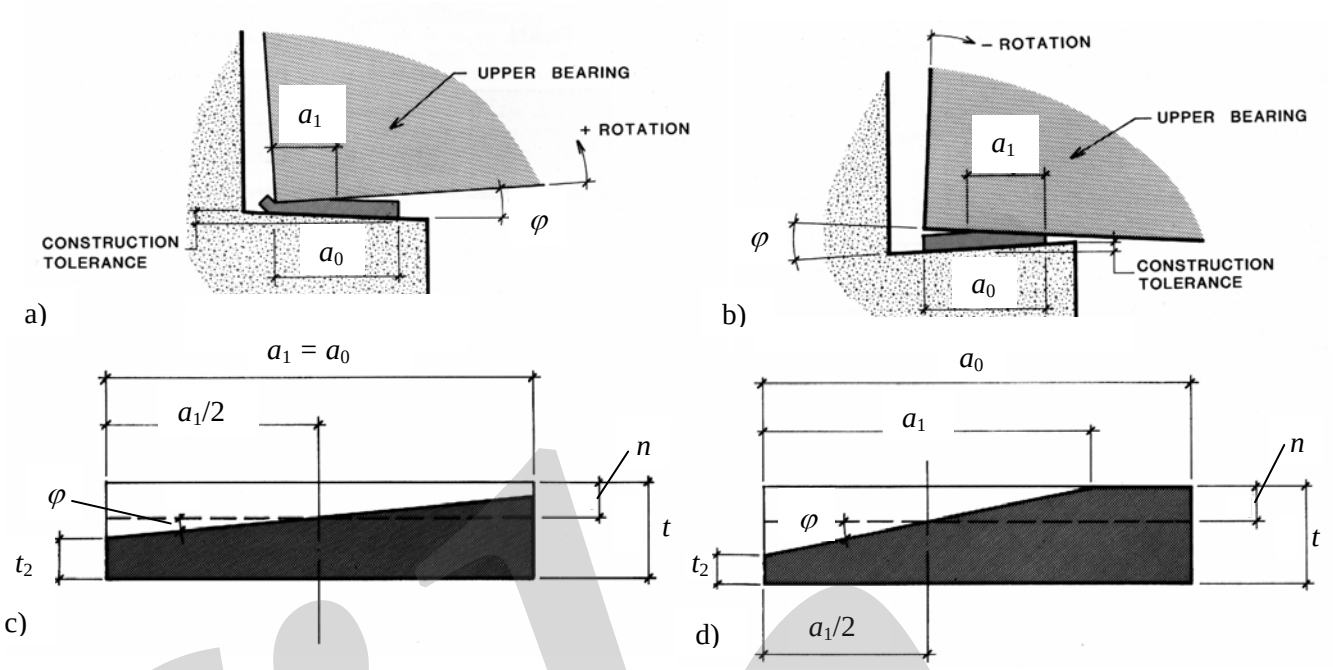

Fig. 6-47: Effective bearing length a_1 for ROF bearing pads, a) maximum camber, b) maximum deflection, c) compression over the whole pad, d) partial compression

The effective compressive stress is now defined as $\sigma_m = N/(a_1 \cdot b_1) \leq 55$ N/mm^2 (a reduction of b_0 to a smaller effective b_1 should be evaluated). Calculate the corresponding average compressive strain $\varepsilon = n/t$ from Fig. 6-46, and the edge compressive strain from Fig. 6-47 c or d, which now should not exceed $\varepsilon_{max} = 0{,}40$.

The horizontal resistance against shear deformation (horizontal movement) is given in Fig. 6-48. The factor H/N is slightly higher than the maximum values for plain pads given in Fig. 6-41 a, but is still smaller than the slipping friction coefficient $\mu = 0{,}2 - 0{,}5$. Lateral expansion is normally neglected, and consequently the lateral tensile force $T_{lat} \approx 0$.

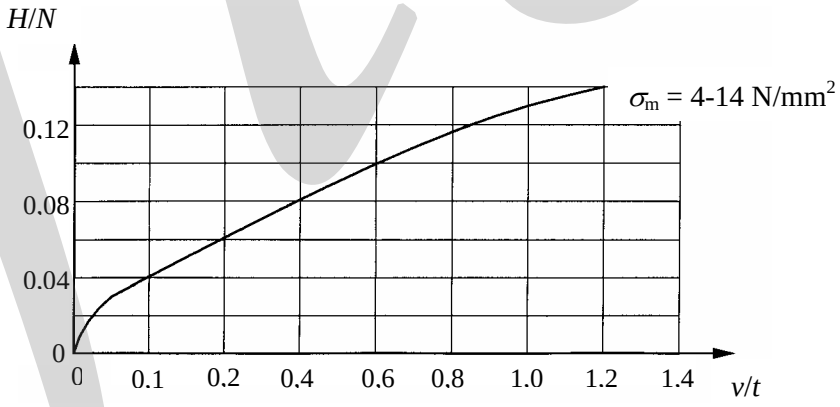

Fig. 6-48: Horizontal resistance against shear deformation for ROF bearing pads

6.5.3.4 Elastomeric bearing pads with steel plates

These pads are composed of multiple rubber layers, see Fig. 6-49, which leads to much smaller lateral expansion and lateral strain than plain pads, see Figs. 6-37 and 6-39. This allows for high compressive stresses even for thick pads, thus accommodating for large horizontal movements.

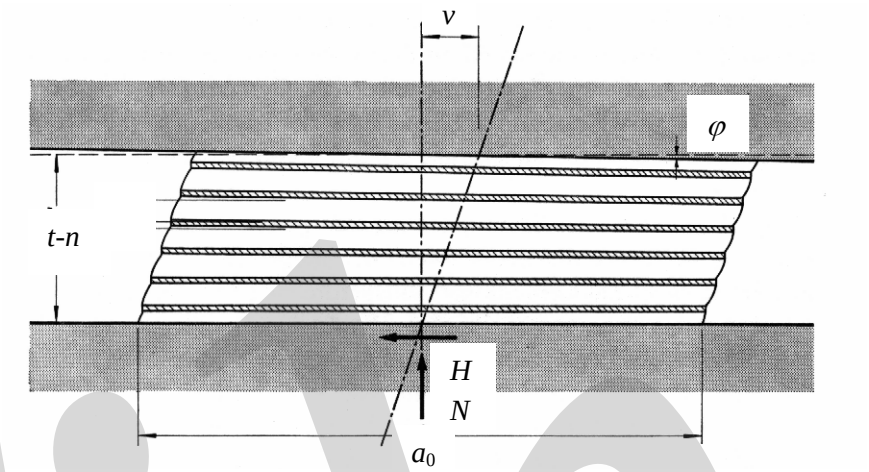

Fig. 6-49: Elastomeric bearing pad with steel plates

These pads are expensive and typical for girders with large support loads and horizontal movement, like bridge girders. The producers have their own design guides and installation procedures. Lateral expansion is not significant, which means that the lateral tensile force $T_{lat} \approx 0$.

6.6 Layered connections

Compression joints where different types of concrete elements are joined together with different types of bearing materials require special analysis. Horizontal loads and concrete member rotation may change the compressive force into tension and/or impose shear forces on the joint, see Section 6.1.2.

An accurate design of these connections requires complex mathematical tri-axial analysis combined with good knowledge of the material properties. Normally there exist three practical alternatives:

- Full scale testing of the existing structure.
- Using FE analyses for tri-axial analysis.
- Using simplified empirical formulas, or conservative strut-and-tie models (compression and tension), see Sections 6.2.3 and 6.2.4.

Figs. 6-50 and 6-51 shows two layered connections with force transfer according to Alternative 3. The connection shown in Fig. 6-50 is illustrated with a ‘complete’ design example in Section 6.7.2.

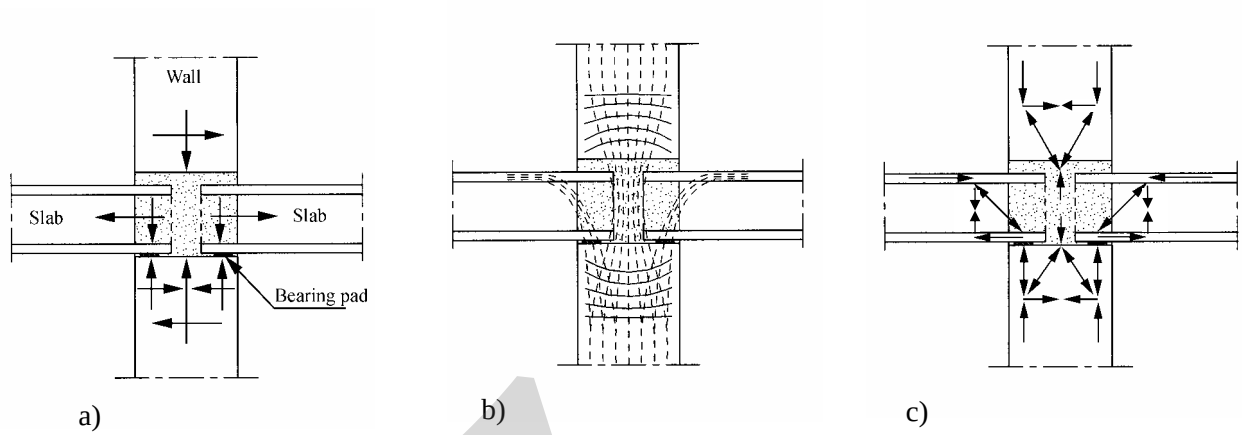

Fig. 6-50: Slab-wall connection, a) forces, b) simplified stress analysis, c) strut-and-tie model

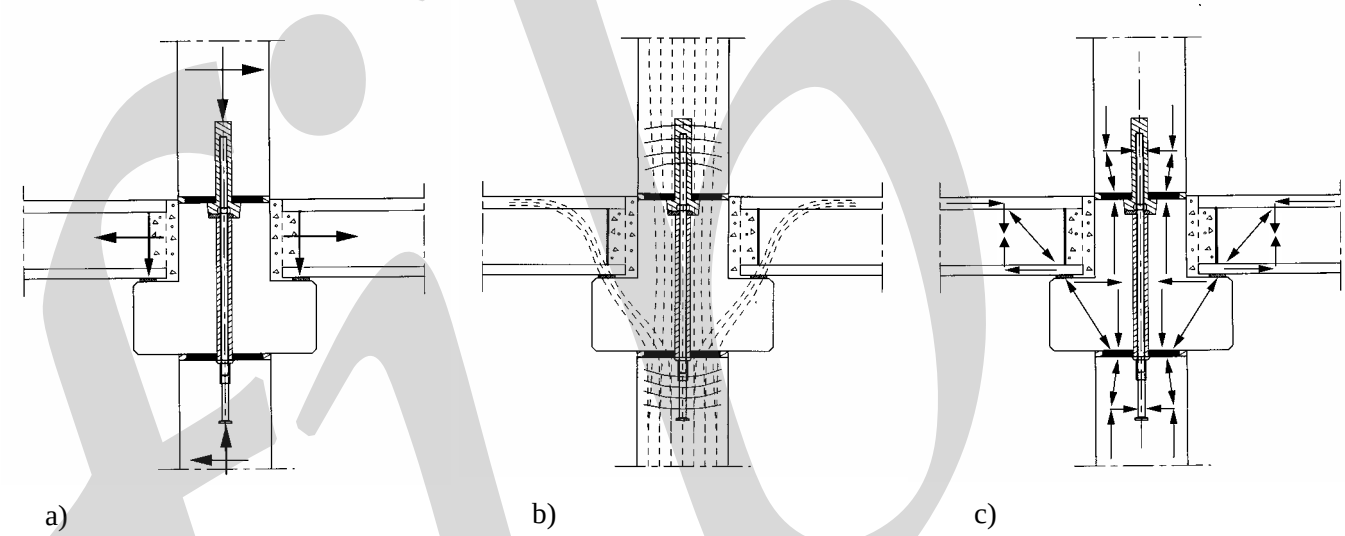

Fig. 6-51: Slab-beam-column connection, a) forces, b) simplified stress analysis, c) strut-and-tie model

6.7 Design examples

6.7.1 Beam-column connection with steel plates

Example 6-3

Two beams are supported by a single column. The beams and the column have embedded steel plates with a steel 'pad' between. The embedded steel plates are provided with anchor bolts, and the pad is welded to both steel plates to transfer the horizontal forces. The geometry and notation are shown in Fig. 6-52.

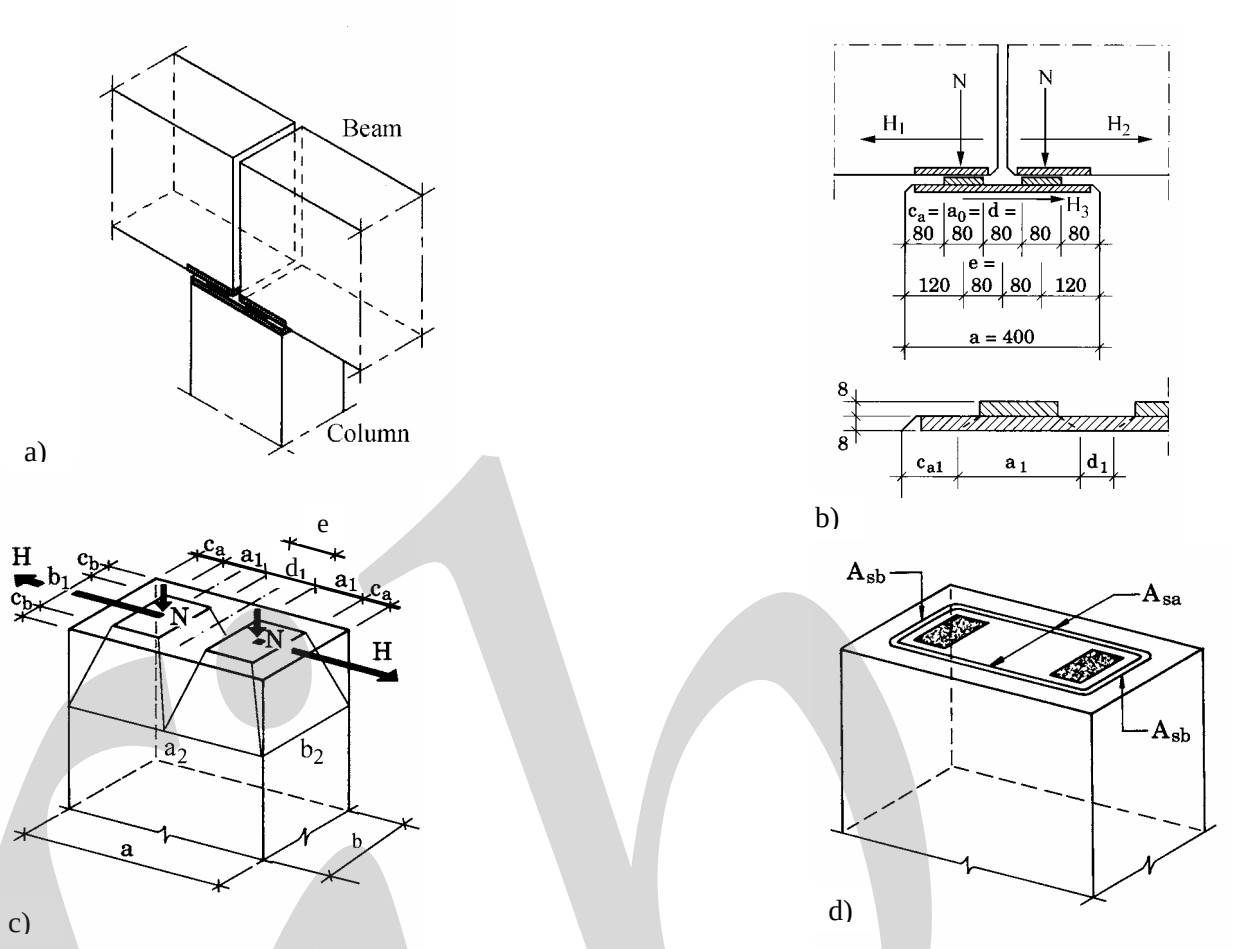

Fig. 6-52: Beam-column connection with steel plates in example, a) overview, b) geometry, c) notation for compression and splitting control, d) notation for splitting reinforcement

The design is made according to Sections 6.2.3, 6.2.4, 6.4.2.

Vertical load (ULS) N = 700 kN
$H_1 = H_2$ = 150 kN = 0,21 N going into the steel plates
H_3 = 50 kN going into the column

Column $a \cdot b = 400 \times 400$ mm
Beam width b = 400 mm
Embedded steel plates: t = 8 mm
Steel 'pad': $t \cdot a_0 \cdot b_0 = 8 \times 80 \times 350$ mm
Concrete design compressive strength: f_{cd} = 20 N/mm^2

Effective loading area in column (Fig. 6-29)

$$a_1 = a_0 + 3 \cdot t = 80 + 3 \times 8 = 104\,\text{mm}$$
$$b_1 = b_0 + 3 \cdot t = 350 + 3 \times 8 = 374\,\text{mm}$$
$$d_1 = d - 3 \cdot t = 80 - 3 \times 8 = 56\,\text{mm}$$
$$c_{a1} = c_a - 1{,}5 \cdot t = 80 - 1{,}5 \times 8 = 68\,\text{mm}$$

a_2 is defined according to Fig. 6-17 c (overlapping loads).

$$\sum a_2 = a = 400\,\text{mm}$$
$$\sum a_1 = 2a_1 = 208\,\text{mm}$$

In the other direction b_2 = 400 mm.

$b_1/a_1 = 374/104 = 3{,}60 > 2{,}0$, which means that

$$f_{cd}^{*} = f_{cd}\sqrt[3]{A_2/A_1} \le 2{,}5\cdot f_{cd} \quad \text{(eq. 6-8)}$$

$$f_{cd}^{*} = f_{cd}\sqrt[3]{400\cdot 400/(208\cdot 374)} = 1{,}27\cdot f_{cd} = 1{,}27\cdot 20 = 25\ \text{N/mm}^2$$

Local compression capacity

$$N_{Rd} = f_{cd}^{*}\cdot a_1\cdot b_1 = 25\times 104\times 374\cdot 10^{-3} = 972\ \text{kN} > N = 700\ \text{kN (OK)}$$

Lateral tensile forces due to two eccentric loads N and horizontal forces in a-direction, using eqs. (6-12) - (6-13)

(6-12): $T_s = 0{,}25\sum N\left(1-\dfrac{\sum a_1}{\sum a_2}\right) = 0{,}25\cdot 1400\cdot\left(1-\dfrac{208}{400}\right) = 168$ kN

T_{lat} = (steel plates) = 0

H_3 = = 50

(6-13): T_{sa} = = 218 kN

Lateral tensile forces in the b-direction are calculated as for one single load, eq. (6-9)

$$T_{sb} = 0{,}25\cdot N\left(1-\frac{b_1}{b_2}\right) = 0{,}25\cdot 700\cdot\left(1-\frac{374}{400}\right) = 11\,\text{kN}$$

Splitting reinforcement required (Fig. 6-52 d), f_{yd} = 400 N/mm². In the a-direction:

$$A_{sa} = \frac{T_{sa}}{2f_{yd}} = \frac{218000}{2\cdot 400} = 273\ \text{mm}^2 \text{ per tie leg} = 4\phi 10 \text{ ties}$$

In the b-direction:

$$A_{sb} = \frac{T_{sb}}{f_{yd}} = \frac{11000}{2\cdot 400} = 13\ \text{mm}^2 \text{ per tie leg}$$

Alternative column head reinforcement is given in Fig. 6-53.

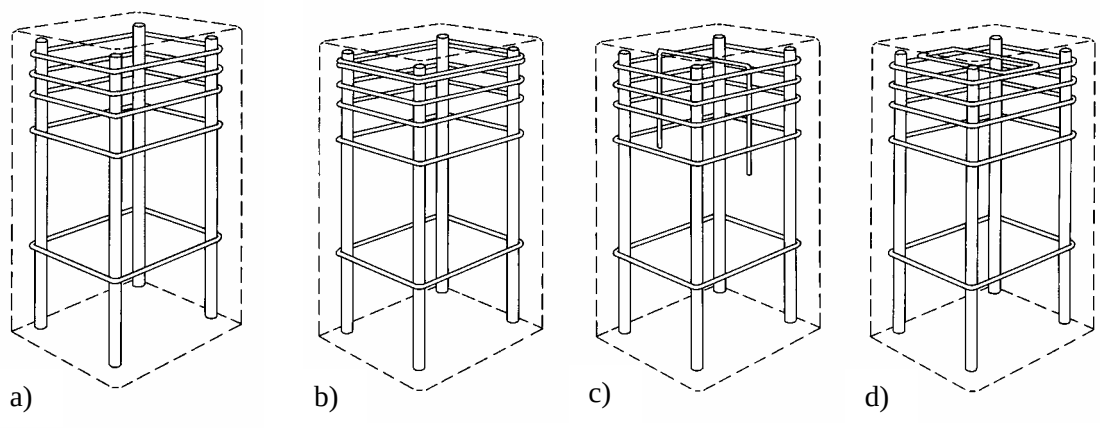

Fig. 6-53: Column head splitting reinforcement, a) normal, b) additional tie, c) U-shaped tie, d) special tie

6.7.2 Hollow core floor – load bearing wall with grout, multi-story building

Example 6-4

The geometry and loads are shown in Fig. 6-54.

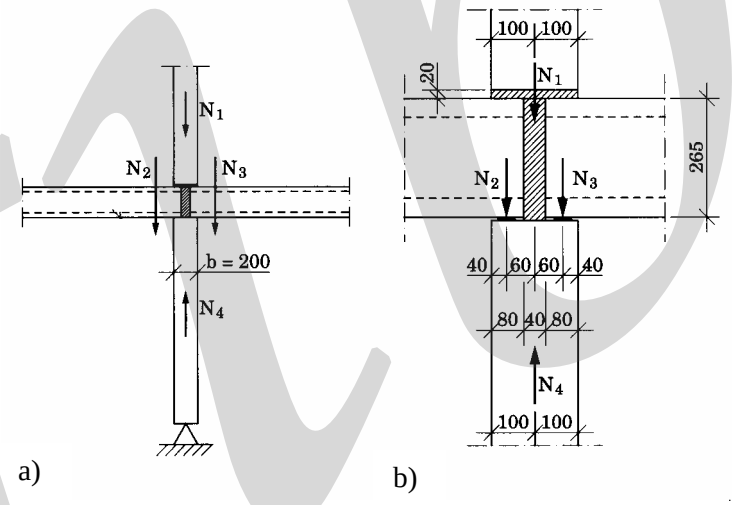

Fig. 6-54: Hollow core floor-wall connection in example, a) overall view, b) connection detail

The force flow is similar to the one shown in Fig. 6-50. Vertical design loads (ULS) are

N_1 = 194 kN/m
N_2 = 32 kN/m
N_3 = 49 kN/m
N_4 = 275 kN/m

Horizontal loads are not shown in this example. Normally the horizontal loads can be treated and reinforced separately from the vertical loads.

Wall strength: $f_{cd,wall} = 20\,\text{N/mm}^2$

Mortar strength: $f_{\mathrm{cd,mortar}} = 12\ \mathrm{N/mm^2}$
Splitting reinforcement: $f_{\mathrm{yd}} = 400\ \mathrm{N/mm^2}$

(1) Lower end of upper wall, see Fig. 6-55.

$N_1 = 194\ \mathrm{kN/m}$

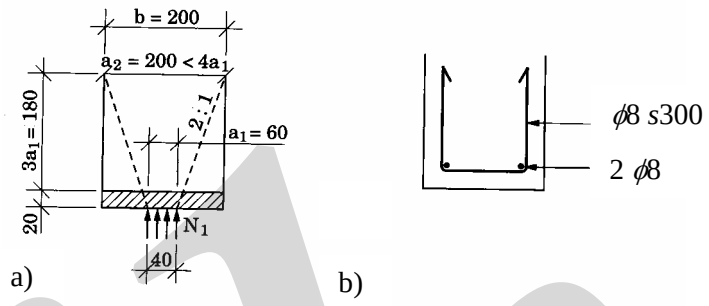

Fig. 6-55: Lower end of upper wall, a) load distribution, b) splitting reinforcement

The mortar joint compressive strength is checked according to Fig. 6-55 a and Fig. 6-26.

$\beta_0 = f_{\mathrm{cd,mortar}} / f_{\mathrm{cd,wall}} = 12/20 = 0{,}6$
$t = 20\ \mathrm{mm}$
$a_{1,\mathrm{mortar}} \approx 0{,}5(60 + 40) = 50\ \mathrm{mm}$
$t/a_{1,\mathrm{mortar}} = 20/50 = 0{,}4$

Fig. 6-26 c gives $\beta = 0{,}85$ and

$$f_{\mathrm{cd,joint}} = \beta \cdot f_{\mathrm{cd,wall}} = 0{,}85 \times 20 = 17\ \mathrm{N/mm^2}$$

Compression bearing capacity for strip loading:

$$f_{\mathrm{cd}}^{*} = f_{\mathrm{cd}} \sqrt[3]{a_2/a_1} = 17 \cdot \sqrt[3]{200/60} = 25\ \mathrm{N/mm^2} \qquad \text{eq. (6-8)}$$

$$N_{\mathrm{Rd}} = f_{\mathrm{cd}}^{*} A_1 = 25 \cdot 10^{-3} \times 60 \times 1000 = 1500\ \mathrm{kN/m} > 194\ \mathrm{kN/m} - \mathrm{OK}$$

Lateral tensile reinforcement:

Lateral expansion force $T_{\mathrm{lat}} \approx 0$, because of the small difference in ν/E for mortar and element, see Section 6.2.1)

Lateral splitting force:

$T_{\mathrm{s1}} = 0{,}25 N_1 (1 - a_1/a_2) = 0{,}25 \times 194 \times (1 - 60/200) = 34\ \mathrm{kN/m}$
$A_{\mathrm{s}} = T_{\mathrm{s1}} / f_{\mathrm{yd}} = 34/0{,}4 = 85\ \mathrm{mm^2/m}$

Use minimum reinforcement $\phi 8\ s\ 300 = 167\ \mathrm{mm^2/m}$.

(2) Top of lower wall, see Fig. 6-56.

$$\sum N = N_1 + N_2 + N_3 = 194 + 32 + 49 = 275 \text{ kN/m}$$

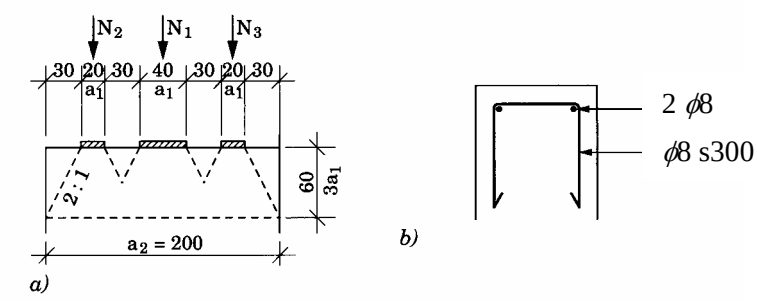

Fig. 6-56: Top of lower wall, a) load distribution, b) splitting reinforcement

Compression bearing capacity, using the same $f_{cd,joint}$.

$$f_{cd}^{*} = f_{cd}\sqrt[3]{a_2 / \sum a_1} = 17 \cdot \sqrt[3]{200/(20+40+20)} = 23 \text{ N/mm}^2$$

$$N_{Rd} = f_{cd}^{*} \cdot \sum a_1 \cdot l = 23 \cdot 10^{-3} \cdot 80 \cdot 1000 = 1840 \text{ kN/m} > N_4 = 275 \text{ kN} - \text{OK}$$

Lateral tensile reinforcement:
- Lateral expansion force $T_{lat1} \approx 0$ (due to N_1)
- Lateral expansion force T_{lat2} and T_{lat3} due to hollow core bearing strips is minimal and is neglected.

Lateral splitting force due to several overlapping loads:

$$T_s = 0{,}25 \sum N \left(1 - \sum a_1 / \sum a_2\right) = 0{,}25 \times 275 \times (1 - 80/200) = 41 \text{ kN/m}$$
$$A_s = T_s / f_{yd} = 41/0{,}4 = 103 \text{ mm}^2\text{/m}$$

Use minimum reinforcement $\phi 8$ $s300$ = 167 mm^2/m.

(3) Joint between ends of hollow core, see Fig. 6-57.

The mortar joint has t/a_1 = 265 / 40 = 6,6 and β_0 = 0,6. According to Fig. 6-26 c this gives β = 0,6 which means that the joint compressive strength is the same as the mortar strength (no lateral expansion resistance effect).

The cores of the hollow core floor units are normally also grouted at the ends as shown in Fig. 6-57. Together with the ends of the hollow core units, this provides enough lateral support to prevent buckling of the mortar joint.

$$N_{Rd,\,joint} = f_{cd,mortar} \cdot A = 12 \cdot 10^{-3} \times 40 \times 1000 = 480 \text{ kN/m} > N_1 = 194 \text{ kN (OK)}$$

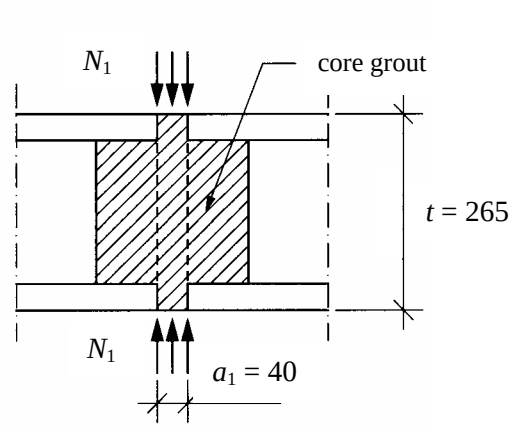

Fig. 6-57: Joint between ends of hollow core elements

This example demonstrates that the joint between ends of hollow core elements is the week part for transferring N_1 according to this simple design method. The theoretical capacity of the connection can be increased by taking into account the fact that the cores of the hollow core slab only amounts to approximately half the cross-sectional area of the slab element. The other half will contribute to the lateral confinement of the grout and results in higher allowable compressive stresses, see Section 6.2.1.4.

The capacity of the connection can be increased by using vertical reinforcement through the joint, by extending the wall to the top of the slab at certain points (‘column joint’), by removing any soft materials between slab and wall etc. This is also partly discussed in Sections 3.5.2 and 3.7.

Normally the joint will have vertical ties from the lower to upper wall, which can be used as compressive reinforcement if required.

7 Transfer of tensile force

7.1 Principles for tensile force transfer

When structural connections are designed to be tensile resistant, it must be presumed that the joint section is cracked. The tensile force acting across the joint should be resisted by certain tie arrangements, e.g. tie bars that are sufficiently anchored at both sides of the joint. The ordinary model for cracked reinforced concrete sections can be applied in the design of the joint section, and the anchorage can often be designed according to standard methods. Furthermore, the tensile forces anchored in the connection zones of the jointed precast units should be linked to the main resisting system of the units in such way that a continuous force path is obtained.

Tie connections (connections with tensile capacity) are often part of overall tying systems that should provide structural integrity and prevent progressive collapse. Such connections should be designed and detailed to have a ductile behaviour. Premature brittle failures must be avoided and it should be possible to obtain rupture of the ductile components of the connection. For this reason enhanced requirements of anchorage may be justified compared to ordinary design at the ultimate limit state. How to provide anchorage to secure a ductile behaviour is treated more thoroughly in the following sections.

In joints that are filled with joint grout or joint concrete, the adhesive bond in joint interfaces may be considerable. Experience from tests shows that the bond strength at joint interfaces may be of the same magnitude as the tensile strength of the joint fill itself [Engström (1992), Bäckström (1993)]. In many cases the cracking resistance of a joint section exceeds the tensile capacity of the ties that are arranged across the joint according to minimum requirements. However, it is not possible to utilise the adhesive bond at joint interfaces in the design, since the bond is unreliable and so are also restraint stresses due to intrinsic deformations. However, the possibility that joints remain uncracked must still be considered, as this in some respects may be unfavourable. For instance, uncracked joints may result in unintended restraint moments in structural elements designed as simply supported, see Section 3.5.2. Because of the bond in joint interfaces larger restraint forces might be transferred through the joint than otherwise supposed in the design of the joint zones and the structural elements.

A tensile resistant connection can be achieved either by ‘continuous’ tie bars that are placed continuously across a joint and anchored in the precast units on each side of the joint, or by ‘protruding’ tie bars or other tensile resistant devices that are anchored in the respective elements and connected in the joint by bolting, welding or lap splicing.

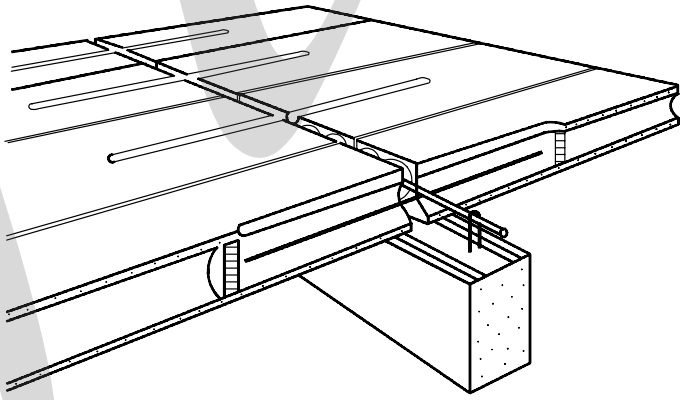

Fig: 7-1: Hollow core floor connection where adjacent spans are connected by continuous tie bars anchored in concreted cores opened from the top. Adjacent hollow core floor units are also connected in the transverse direction by a continuous tie bar in the cast insitu transverse joint

Continuous tie bars, normally made from ordinary reinforcement bars, must be anchored ‘indirectly’ at least in one of the precast units in joints, sleeves, slots, cores or other recesses that are filled with grout or concrete at the building site. Tie connections in hollow core floors are typical

examples of connections where the continuous tie bars are anchored indirectly to the precast units in concreted cores, see Fig. 7-1.

As an alternative to the solution in Fig. 7-1, the longitudinal tie bars can be placed in grouted joints, see Fig. 7-36. However, because of the specific production method normally used for hollow core floor units, extrusion on long tensioning and casting beds, it is not possible to anchor steel details directly in the elements or use protruding reinforcement.

Continuous tie bars can also be cast in place with protruding ends in one of the elements. At erection the next element, provided with sleeves, is placed to match the protruding tie bars, which are anchored indirectly in this element by grout, glue, etc. Examples of connections with this type of continuous tie bars are shown in Fig. 7-2.

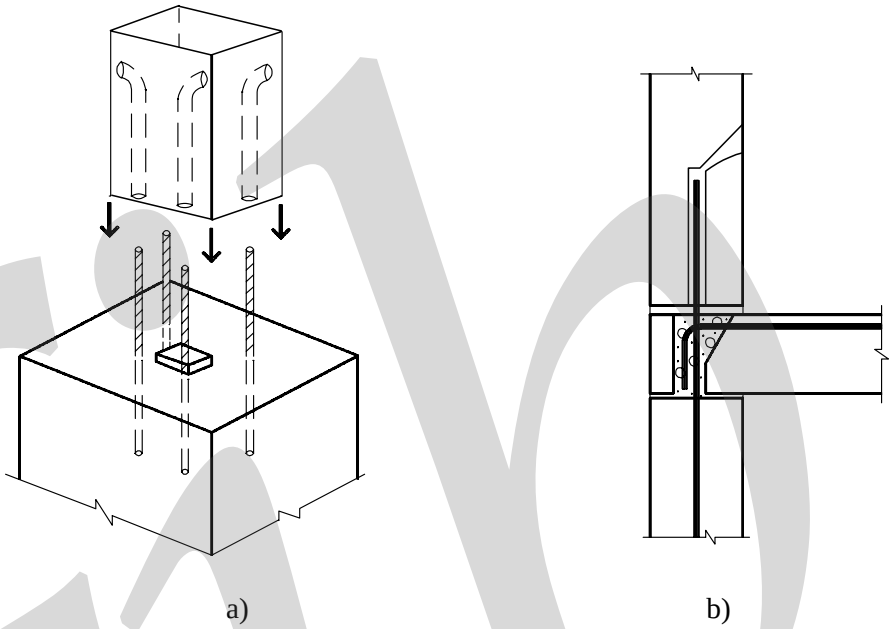

Fig. 7-2: Tensile resistant connections where continuous tie bars are anchored directly in one of the elements and indirectly in sleeves of the connected element, a) connection between column and foundation, b) connection between wall elements

Tensile resistant connections can also be achieved by means of steel details (inserts) that are anchored separately in the respective elements that should be connected. At the site the protruding or naked steel details are connected by welds, bolts or lap splicing in joints that are filled with grout or concrete. The steel details can be cast into the elements originally (direct anchorage), or fixed afterwards in slots, sleeves, cores or recesses by grout or glue (indirect anchorage). The recesses can be made in the fresh concrete by moulding or in the hardened concrete by drilling etc.

Reinforcement bars or loops that are protruding from the respective elements can be connected by lap splicing in the intermediate joint, see Fig. 7-3.

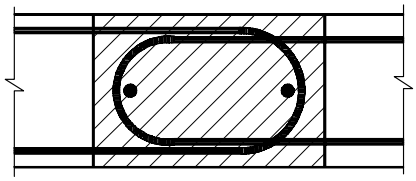

Fig. 7-3: Reinforcement loops, anchored directly in the elements and protruding from the joint faces, are connected by lap splicing in the intermediate joint and filled with concrete or grout on site

The connection is activated as the joint is filled with grout or concrete. Lap splicing of reinforcement loops is a classical way to obtain tensile capacity through joints between precast

elements. The splitting effect is large in the plane of the loop. To prevent premature brittle failure of the connection, transverse reinforcement should be placed through the overlapping part of the loops. With such a solution, a ductile behaviour can be obtained

Fig. 7-4 shows a connection where the ties in the respective elements are connected by bolting or welding.

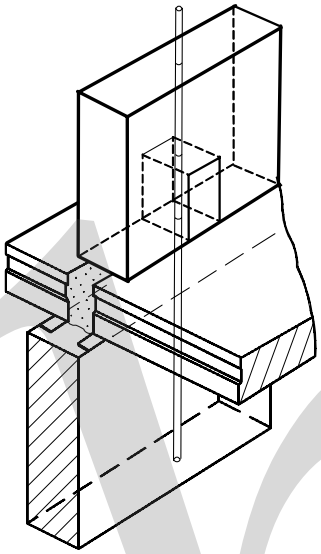

Fig. 7-4: Tensile resistant connection at a horizontal joint of a prefabricated wall. This connection normally transfers compressive forces. However, if the wall is used as a shear wall for stabilisation, tensile forces may appear in some regions of the wall, at least for certain load cases as shown in Fig. 2-7

Bolts with end anchors, for instance anchor heads, can be cast into concrete elements with the threaded end protruding from the joint face. As an alternative, a threaded insert with welded anchor bars can be cast into the element, see Fig. 7-5. At the building site, a threaded bolt or a threaded bar can be fixed to the insert and used to connect adjacent elements.

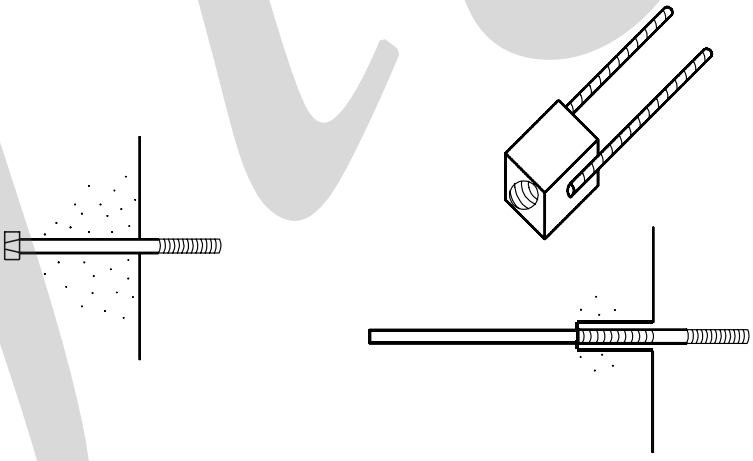

Fig. 7-5: Embedded steel details for bolted connections, a) embedded bolt with end anchor and a protruding threaded end, b) embedded threaded insert with welded anchor bars

The advantage with this solution, compared to the first one, is that protruding details are totally avoided until the connection is made. This is favourable with regard to the production of the elements (no parts need to protrude through the moulds), handling, and transportation (no risk of personal

injuries or damage to protruding steel details). A variety of threaded inserts exist, for light or heavy fastening. To allow some tolerance for geometrical deviations in bolted connections, holes for bolts should have some oversize. Fully anchored cast-in steel sections are necessary to generate large tensile capacity; barrel sockets are not adequate.

The main advantages in using a bolted connection are that an immediate connection is made. The main disadvantage is in the restricted tolerances required for mating, particularly where the bolts resist shear and oversized holes are not permitted. However, designers have overcome these problems with a wide range of fixing devices. Captive bolts or nuts secured to the precast components in the factory assist site operative to locate and fix the bolts, and eliminate the chance of incorrect sizes.

Welded connections can be used to directly connect steel details protruding from the meeting elements, for instance overlapping reinforcement bars, Fig. 7-6. One alternative is to connect the steel details from the meeting elements by welding to an intermediate piece of steel. In this way, the quality of the welded connection can be improved. The intermediate piece of steel can be welded to protruding steel details, Fig. 7-7 a, or to naked weld plates or angles embedded in the joint faces, Fig. 7-7 b.

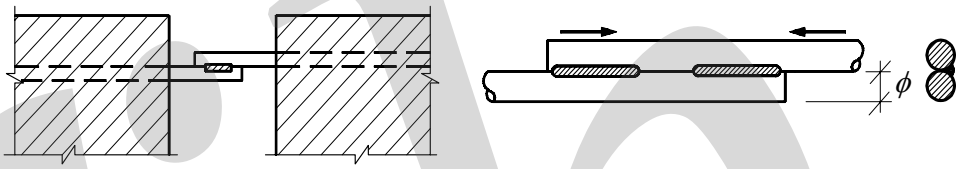

Fig. 7-6: Welded connections with the direct welding between protruding steel details

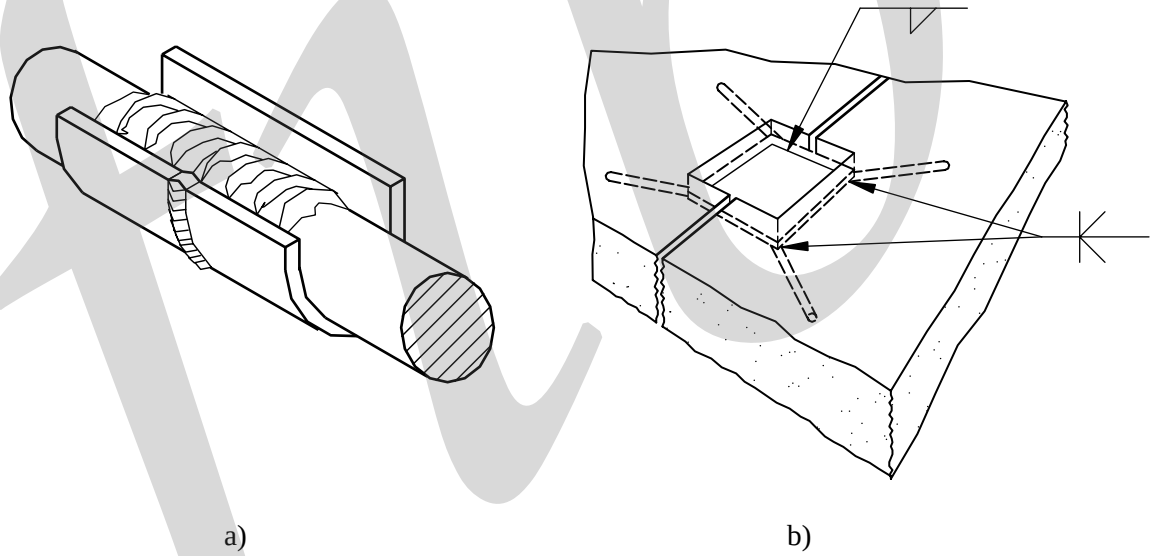

Fig. 7-7: Welded connection with intermediate piece of steel, a) connection between protruding bars, b) connection between embedded and naked weld plates

The tensile capacity of the connection depends on the capacity (strength and dimension) of tie bars, connection details, welds etc., but also on the anchorage of the steel details in the concrete elements. Anchorage can be obtained by bond along ribbed bars or by various types of end anchors. Examples of how embedded weld plates can be anchored by ribbed anchor bars, or smooth bars with end anchors are shown in Fig. 7-8.

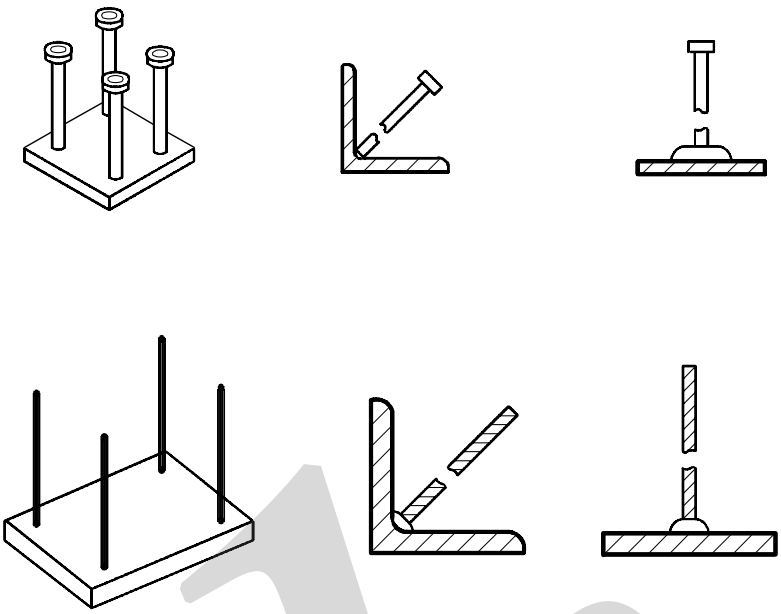

Fig. 7-8: Anchorage of weld plates by ribbed anchor bars or smooth bars with end anchors

When anchor bars are anchored by bond, ordinary ribbed or indented reinforcement bars are normally used. It is also possible to use threaded bars. With regard to bond properties, threaded bars are similar to indented reinforcement bars. In anchorage by bond, tangential tensile stresses appear in the concrete around the bar. By providing sufficient concrete covers and anchorage length, the anchorage capacity can exceed the tensile capacity of the bar. When this is not possible, due to limitations in the geometry, the tensile capacity of the tie connection is determined by the anchorage capacity. The anchorage can be lost by splitting failure in the concrete cover, Fig. 7-9 a, or by pullout failure, Fig. 7-9 b. The anchorage capacity can be estimated by ordinary methods for reinforcing bars. Then the upper limit of the bond strength corresponds to the capacity at pullout failure. In design for ductility, enhanced requirements of the anchorage may be needed, since the anchorage capacity in this case should exceed the tensile capacity of the connection at steel rupture. This may result in increased anchorage lengths, increased concrete cover, or provision of end-hooks, even on ribbed bars.

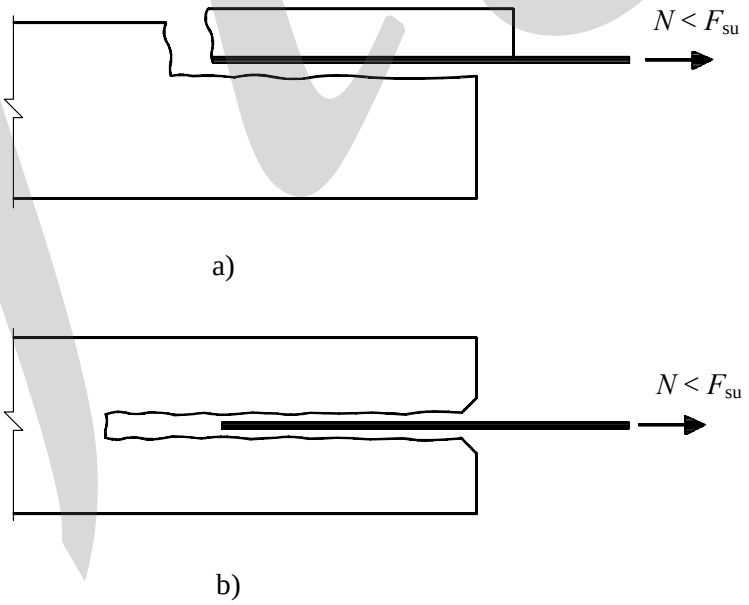

Fig. 7-9: Anchorage failures of ribbed anchor bar, a) splitting failure, b) pullout failure

End anchors can be made as anchor heads, anchor bends, or anchor hooks, see Fig. 7-10.

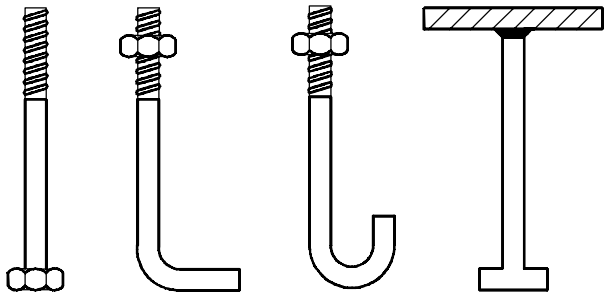

Fig. 7-10: Various types of end anchors

Bolts and studs are provided with anchor heads. Anchor bends and hooks can be used to improve the anchorage of ribbed bars when the space for anchorage is limited. Smooth reinforcement bars must always be anchored by hooks. At the anchor a concentrated force is introduced into the concrete element. This may result in splitting cracks and a brittle anchorage failure.

A variety of special devices for fastening in concrete exist, especially for light fastening, for instance expansion anchors.

The concrete-cone pullout failure, see Fig. 7-11 is typical for anchorage by anchor heads. The concrete-cone failure can be regarded as a tensile failure in the concrete, where a concrete cone on top of the anchor head is separated and released from the concrete element. The anchorage capacity increases with increased concrete strength, anchor depth, and diameter of the anchor head. Placement of the anchor near an edge of the concrete element reduces the anchorage capacity as the volume of the concrete cone decreases in size. When several anchors are placed near each other, a common concrete cone may form and separate for a load, which is smaller than the sum of the capacities of the individual anchors, Fig. 7-11 b.

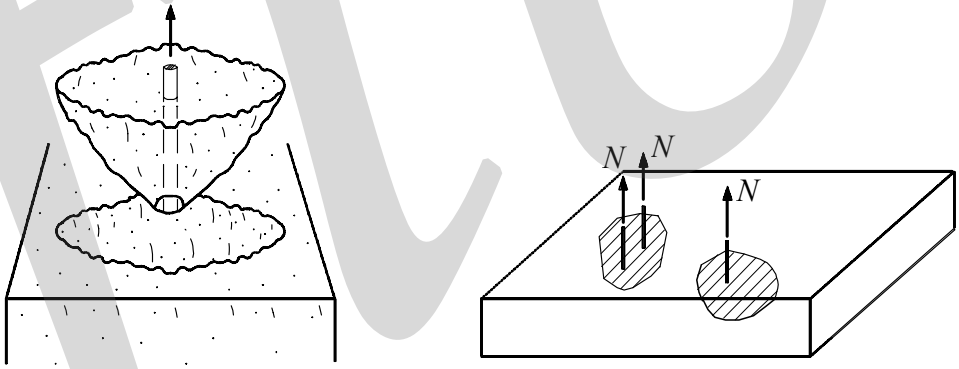

a) b)

Fig. 7-11: Concrete-cone pullout failure may occur in case of anchorage with anchor heads, a) individual anchor, b) reduced capacity in case of placement near free edge, or anchorage in groups

When the concrete element has small dimensions, or the anchors are placed near a free edge, other types of overall splitting failures may occur. In the case of small anchor heads, the head may begin to slip in a pullout mode, without formation of a concrete-cone or overall splitting cracks. The slip is possible as the concrete in front of the anchor head locally experiences plastic deformations or crushes in tri-axial compression. Methods to estimate the anchorage capacity of anchors with anchor heads and other type of fasteners are presented in CEB (1997).

7.2 Anchor bar

7.2.1 Anchorage behaviour and failure modes

For anchor bars provided with ribs, indentations or threads a tensile force applied to the bar is transferred along the steel/concrete interface to the surrounding concrete by bond. This is in general a favourable way to anchor connection details, since the tensile force is transferred successively along the anchorage length and high stress concentrations can be avoided.

No anchorage is perfectly rigid, but the bond transfer results in a certain slip between the anchor bar and the surrounding concrete. It should be noted that the bond stresses along the steel/concrete interface are not normally uniformly distributed and, accordingly, the slip varies along the anchorage length. This means that the slip at the loaded end of the bar exceeds the slip at the passive end. It can even be the case that the active end has a slip, while the passive end is still firmly fixed without any slip at all. Accordingly, the anchor bar should not be regarded as a rigid body.

For an anchor bar subjected to a tensile force N that increases step by step, typical anchorage behaviour is illustrated in Fig. 7-12. At the loaded end of the anchor bar, the whole tensile force is resisted by the bar only. Along the steel/concrete interface the tensile force is transferred to the surrounding concrete by bond stresses τ_b that decreases along the bar. For a small tensile force, see Fig. 7-12 a, bond stresses appear only within a limited length that is shorter than the anchor bar. This 'contributing' length is referred to as the 'transmission length'. The bond stresses are distributed along the transmission length with the maximum value near the loaded end and approach zero at the end of the transmission length. In every section within the transmission length the steel strain exceeds the strain of the surrounding concrete, which means that the bar must elongate and slip in relation to the concrete. The total elongation of the steel bar in relation to the concrete can be recognised as the slip at the loaded end, the so-called 'end-slip'. In the actual case the active end of the bar has a certain slip, but the passive end of the bar has no slip at all.

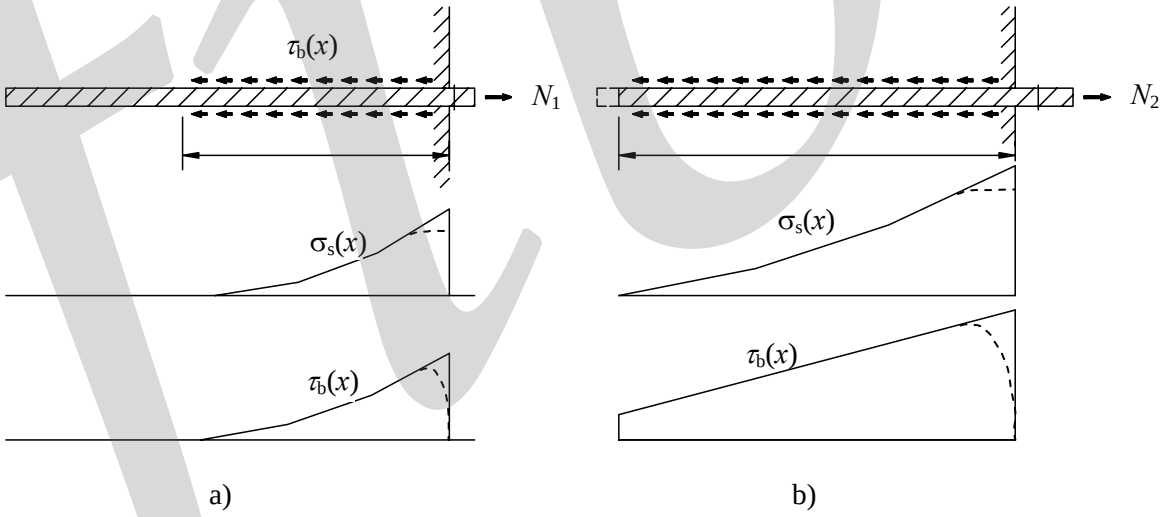

Fig. 7-12: Typical anchorage behaviour of an anchor bar loaded in tension and typical distributions of steel stress and bond stress for a) a small tensile force, b) an intermediate tensile force. Dotted lines indicate possible effect of local concrete failure near the free edge

In Fig. 7-12 b the tensile force has increased and bond stresses appear along the entire anchor bar. This means that the whole anchor bar moves in the concrete, but the slip is greater at the loaded end. It should be noted that while the steel stress always becomes zero at the passive end of the bar, there could still be a considerable bond stress at this end. Its actual value depends on the slip that has occurred at the passive end. When the tensile force increases even more, it results in an increase of the average bond stress and of the overall slip. The bond stress distribution also becomes more uniform.

In design for the ultimate limit state it is generally assumed that the bond stress in each section along the anchorage length reaches the bond strength. However, this assumption of a uniform bond

stress distribution is a simplification of the real behaviour. A uniform bond stress distribution means that the tensile force and the steel stress increase linearly along the transmission length. Various failure modes are possible depending on the actual detailing and material properties.

The failure can take place in the concrete or in the steel. In case of small concrete covers, the anchorage can fail due to splitting of the concrete, see Fig. 7-9 a. If the concrete cover is sufficient to prevent a splitting failure, the anchor bar can loose its grip in the concrete by a shear failure that develops along the interface starting from the loaded end. This failure mode is referred to as a pullout failure, see Fig. 7-9 b. It is generally assumed that a concrete cover greater than about 3 times the bar dimension is sufficient to prevent a splitting failure. In CEB-FIP Model Code 1990 [CEB-FIP (1992)] it is stated that the anchorage condition can be considered as 'well confined', when the concrete cover is 5 times the bar dimension or greater.

In case of a short anchorage length, a pullout failure can occur before yielding of the steel is reached. Ordinary design rules prevent that this would be the case. However, a pullout failure can also occur in the post-yield stage before the steel reaches its ultimate strength due to rupture of the steel. In ordinary design the steel strength is based on the yield strength, but in cases where ductility is important the connection detail should be designed so that the tensile capacity at rupture can be safely anchored. In that case the plastic behaviour of the bar can be fully utilized.

Near the free edge, inclined cracks starting from the ribs of the anchor bar develop towards the edge and may cause a local concrete cone failure as indicated in Fig. 7-13. Such local cone failures have been observed in tests, see Fig. 7-15. The depth of the cone have been about 2ϕ, where ϕ = the anchored bar diameter. When these cracks appear, the bond will be reduced as shown in Fig. 7-13 a. At larger end-slips, when the concrete cone is separated from the concrete element, the bond will be totally lost near the edge, Fig. 7-13 b.

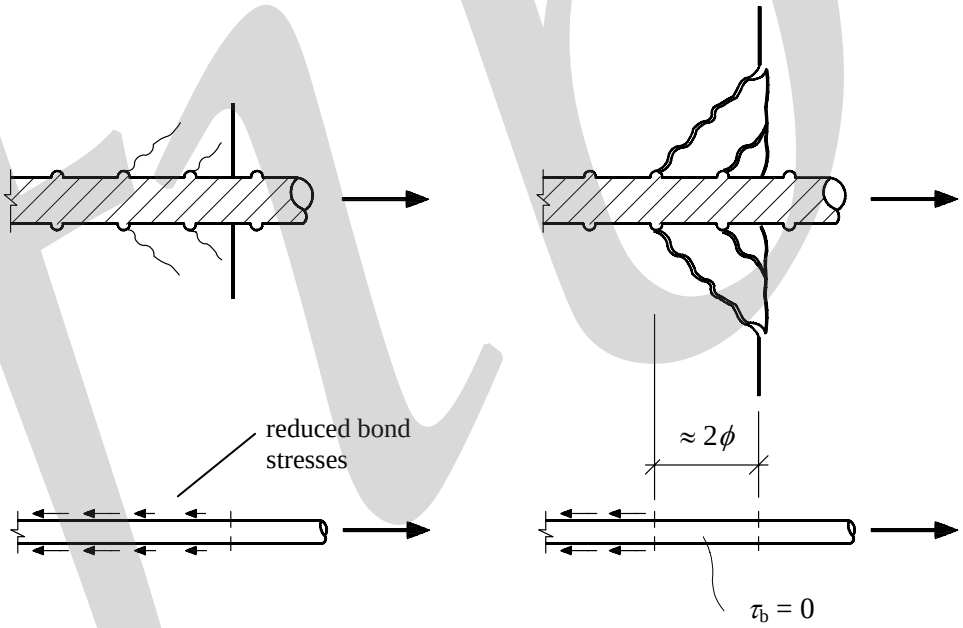

Fig. 7-13: Local bond failure near the free edge because of inclined cracks, a) reduced bond at an early stage of cracking, b) loss of bond due to local concrete cone failure

Fig. 7-14 shows results from pullout tests on anchor bars of various lengths anchored in well-confined concrete (concrete cover not less than 12 times the bar diameter) [Engström *et al.* (1998)]. The anchor bars were ϕ16 mm ribbed hot-rolled bars with characteristic yield strength of 500 MPa. According to tensile tests on samples the average yield capacity was 114 kN and the average ultimate tensile capacity (at steel rupture) was 130 kN.

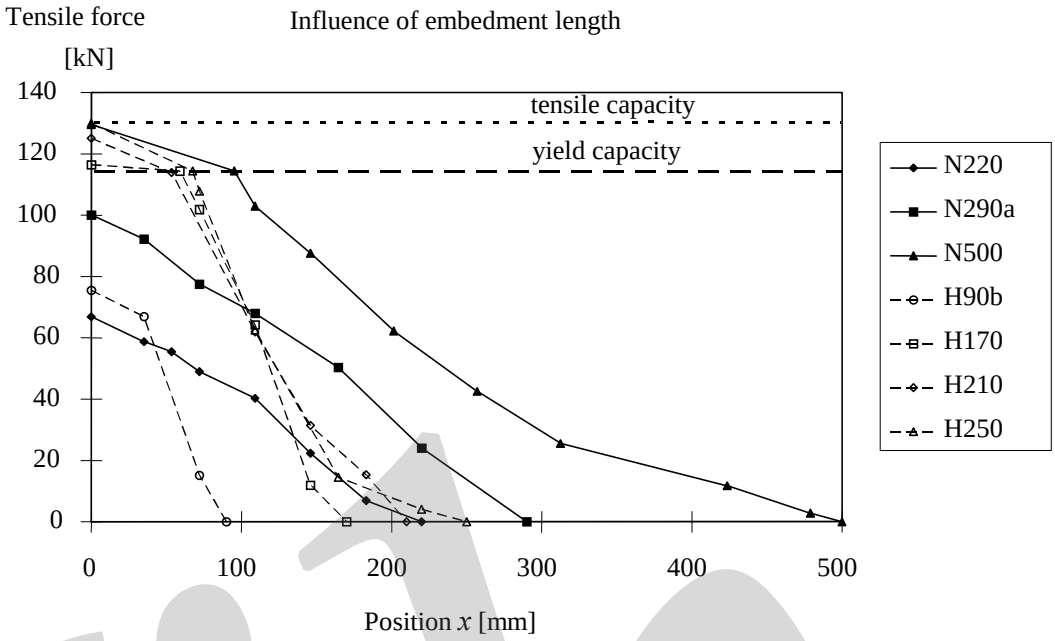

Fig. 7-14: Results from pullout tests on anchor bars anchored in well-confined concrete, according to Engström et al. (1998). Tensile force variation along anchor bars of various lengths in two concrete types just before failure

The figure shows how the tensile force varied along the anchor bar at the maximum load just before failure. Three bars were anchored in normal strength concrete (mean compressive strength about 25 – 30 MPa) and four bars were anchored in high strength concrete (mean compressive strength about 100 – 105 MPa). It appears from the figure that in normal strength concrete an anchorage length of either 220 mm or 290 mm was insufficient to prevent pullout failure before yielding of the bar, while an anchorage length of 500 mm was sufficient to anchor not only the yield capacity but also the ultimate tensile capacity. When this bar ruptured yielding had been reached within a length of about 100 mm from the loaded end. This was the final extension of the plastic zone (yield penetration). For bars anchored in high strength concrete an anchorage length of 90 mm was insufficient to avoid pullout failure. When the anchorage length was 170 mm or 210 mm, pullout failure occurred in the post-yield stage. An anchorage length of 250 mm resulted in rupture of the steel bar. The yield penetration was in that case about 70 mm.

In all of these pullout tests a local concrete cone failure, see Fig. 7-13 b, occurred near the loaded end of the bar. Of a total of seven tests in normal strength concrete the depth of the failure cone varied between 18 and 35 mm with an average value of 26,4 mm, which corresponds to 1,65 times the bar diameter. For seven tests in high-strength concrete specimens the depth of the failure cone varied between 16 and 30 mm with an average value of 27, 0 mm, or 1,68 times the bar diameter.

The response of an anchor bar can be characterised by the relation between tensile force and end-slip. By combining models for the material behaviours, equilibrium and deformation conditions a differential equation that governs the anchorage behaviour can be established, see for instance the CEB-FIP Model Code 1990. If the local relationship between bond stress and slip is known and can be mathematically formulated, it is possible to solve this differential equation analytically and the response can be determined. Bond stress-slip relations are presented in Section 7.2.2 and prediction of the response is shown in Section 7.2.3.

Fig. 7-15: Typical example of a local concrete cone failure at the loaded end, from pullout tests on anchor bars anchored in well-confined concrete [Engström et al. (1998)]

7.2.2 Bond mechanism and bond stress-slip relations

Several mechanisms contribute in a complex way to the bond resistance. For small bond stresses bond can be achieved by adhesion. When the bond stress τ_b increases, the shear-key effect from the ribs will be more important and the adhesion is eventually broken. The shear stress along the interface results in inclined principal tensile and principal compressive stresses in the surrounding concrete. When the principal tensile stress reaches the tensile strength of concrete, inclined cracks form near the tips of the ribs and the bond resistance depends mainly on the action of inclined compressive struts originating from the ribs, see Fig. 7-16.

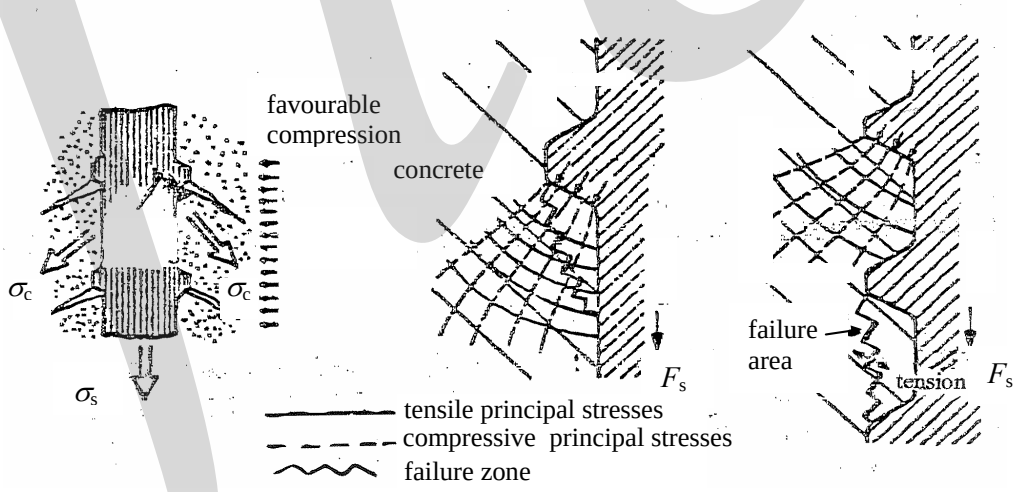

Fig. 7-16: The bond mechanism along ribbed anchor bars results in inclined cracks and inclined compressive forces. The longitudinal component corresponds to the bond stress and the transverse component must be balanced by the surrounding concrete

To keep equilibrium these inclined compressive struts, which act outwards in all radial directions, must be balanced by tensile stresses. These tensile stresses appear in rings around the anchored bar.

When the anchor bar is placed in well-confined concrete, these ring stresses can be resisted by the surrounding concrete and either a pullout failure or rupture of the steel bar will finally result.

According to the CEB-FIP Model Code 90 the anchorage conditions can be considered as confined when the concrete cover is at least 5 times the bar diameter and the spacing between adjacent anchored bars is at least 10 bar diameters. Confined conditions can also be achieved by transverse reinforcement with a total area, across the critical splitting plane, of at least one time the total area of all bars anchored in the same section, or by a transverse pressure that is at least 7,5 MPa.

However, when the concrete cover is small the ring stress might cause the concrete cover to crack and splitting cracks develop through the concrete cover along the bar, see Fig. 7-17. The effect of inclined compressive struts is the same as that of a radial pressure to the surrounding concrete originating form the anchored bar. It is obvious that in case of small concrete covers the resistance to such a pressure is small and the concrete might crack.

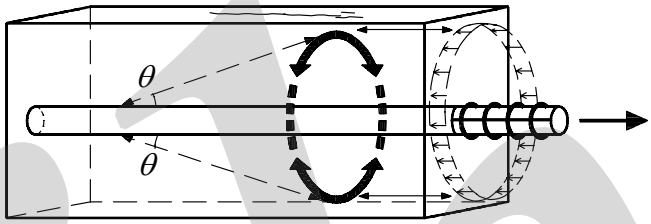

Fig. 7-17: The inclined compressive stresses must be balanced by tangential tensile stresses in the surrounding concrete, according to Tepfers (1973)

This type of longitudinal splitting cracks may result in a sudden brittle type of splitting failure where the concrete cover along the anchorage length splits away, as shown in Fig. 7-9 a. The risk of such brittle splitting failures increases when the anchor bar is located with a small concrete cover especially near a corner, when there is small spacing between adjacent bars and no or small amounts of transverse reinforcement. According to recent test results the tendency for brittle splitting failures is more pronounced in high strength concrete, since the ability for favourable stress redistribution will be smaller when the concrete strength increases [fib (2000b)].

However, if the anchorage zone is confined by stirrups a new state of equilibrium can exist also after occurrence of longitudinal splitting cracks, since the anchorage zone is kept together and the transverse bars are able to resist tangential tensile stresses across the cracks. In that case brittle splitting failures can be avoided and the anchorage capacity will be governed by pullout failure. However, in this case the pullout failure develops in split concrete (with longitudinal cracks) where the pullout resistance is smaller than in well-confined concrete.

Fig. 7-18 shows a typical crack pattern from a pullout test of a 16 mm anchor bar with a small concrete cover c = 16 mm (or $c = 1{,}0 \cdot \phi$), from Engström *et al.* (1998). The anchorage length was 290 mm, the concrete compressive strength was about 20 – 25 MPa, the bar was placed in a mid position in a wide specimen and the specimen was provided with 4 stirrups ϕ 6 mm with constant spacing within the anchorage length and enclosing the anchored bar.

A longitudinal splitting crack appeared rather early during the test, but the tensile force could still be increased. The crack propagated successively when the tensile force continued to increase. Transverse cracks appeared one by one in a 'fishbone' pattern. Due to the confinement from the surrounding concrete in the wide specimen and the transverse stirrups, it was possible to reach the same anchorage capacity as in the comparable tests (N290) in well confined concrete, see Fig. 7-14. Accordingly, the pullout resistance in split concrete was in this case the same as in well-confined concrete without cracks. However, the residual capacity after the peak was smaller in the test with splitting cracks.

Normally in reinforced concrete structures, the main reinforcement is anchored in regions where the concrete cover is as small as possible with regard to minimum requirements. The design rules for anchorage regions assume that the anchorage capacity is governed by splitting cracks. However, in precast concrete structures anchor bars are often placed with considerable concrete covers far away from corners. In such cases the anchorage is often provided in regions, which can be considered as

'well confined'. Confined conditions can be achieved either by a thick concrete cover, great amounts of transverse stirrups or a transverse pressure

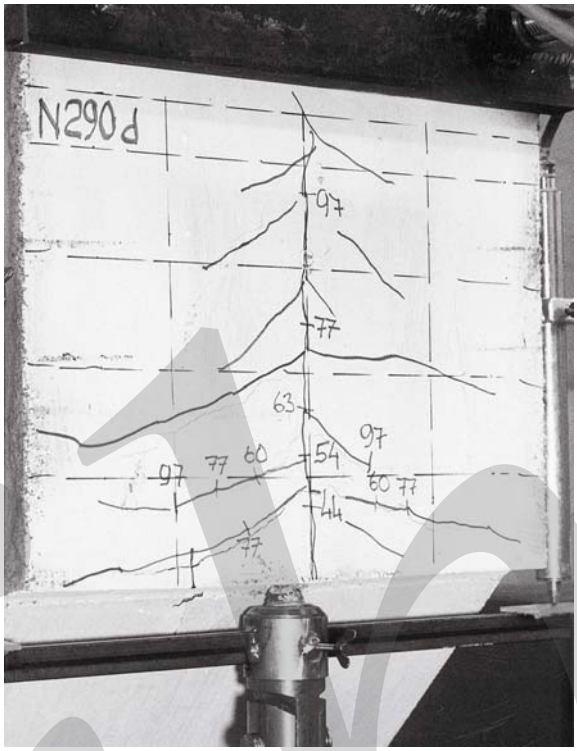

Fig. 7-18: Typical crack pattern from pullout test of an anchor bar placed in a mid position of a wide specimen but with a small concrete cover, according to Engström et al. (1998)

It is stated in CEB-FIP Model Code 1990 that anchorage regions should always fulfil minimum rules with regard to concrete cover and transverse stirrups. Hence, the concrete cover should be at least one bar diameter, and in beams the transverse reinforcement in anchorage regions should have a total area, across the critical splitting plane, of at least one quarter of the cross-sectional area of one anchored bar. In slabs no transverse reinforcement is required. This can be motivated by the fact that in slabs the spacing between bars is normally greater than in beams and almost all of the bars are placed far away from corner regions.

The local relationship between bond stress and slip has been studied experimentally in pullout tests with short embedment lengths, for instance according to the principle shown in Fig. 7-19. In this type of test the bond stress will be rather uniformly distributed along the bonded length l_a since this is very short. Since the bonded length is placed in the interior part of the test specimen, boundary effects are prevented and the anchorage conditions can be considered as confined.

For a certain applied tensile force the (average) bond stress is calculated as

$$\tau_b = \frac{N}{\pi\phi \cdot l_a} \tag{7-1}$$

The slip s_b is assumed to be equal to the measured relative displacement u between the reinforcement bar and the end face of the concrete specimen. Fig. 7-20 a shows some typical examples of relationships between bond stress and slip obtained from pullout tests of ribbed bars with short embedment length in confined concrete, according to Soroushian and Choi (1989). The typical bond behaviour and the bond mechanisms involved are explained in Fig. 7-20 b.

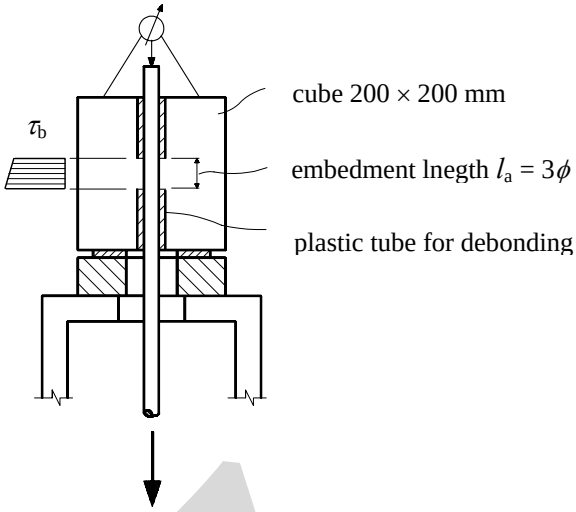

Fig. 7-19: Example of pullout test with short embedment length, according to Losberg and Olsson (1979)

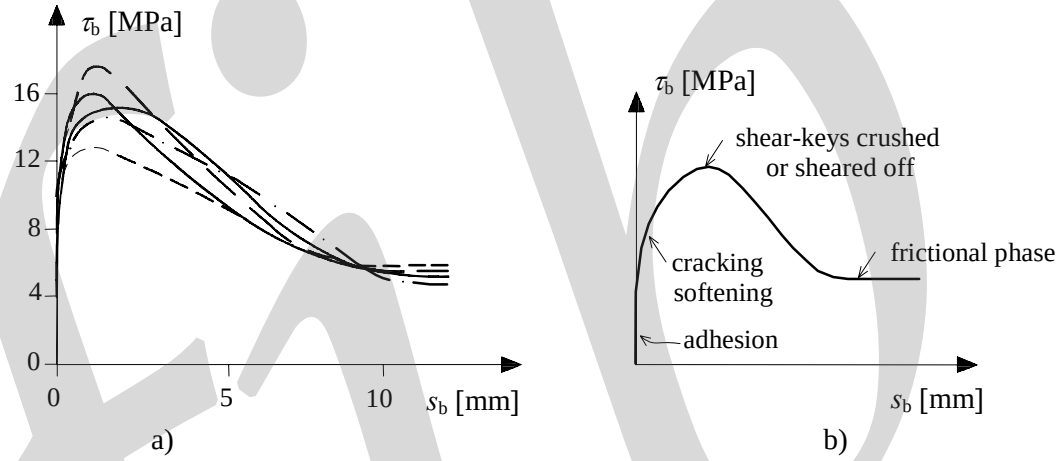

Fig. 7-20: Relationship between bond stress and slip for ribbed bars in confined concrete, a) examples of relationships obtained from pullout tests with short embedment length,[Soroushian and Choi (1989)], b) typical bond behaviour and mechanisms

It should be noted that the relationship between bond stress and slip refers to the local condition. Along an anchor bar the bond stress is normally not uniformly distributed and various sections have developed different slips. However, if the bond conditions are the same for all sections along the bar, all sections will have the same relationship between the bond stress and the local slip, i.e. the total slip developed in that section.

In pullout tests with a short embedment length in well confined concrete the bar is strong in relation to the total bond resistance. Accordingly, a pullout failure caused by shear failure along the tips of the ribs will limit the capacity and occur when the steel stress still is small. The corresponding bond-stress slip relation can be regarded as a virgin curve, which is an upper limit for the bond behaviour that is obtainable in real applications. The total bond resistance increases with the anchorage length. Hence, if the total bond resistance exceeds the yielding capacity of the bar, the bar will start to yield at the loaded end before the maximum bond stress according to the virgin curve is reached. As it was shown by Engström (1992) yielding of the bar results in a drastic decrease of the bond stress for further imposed slip, see Fig. 7-21 a. In cases where the concrete cover is small, longitudinal cracks will occur due to the effect of the radial compressive stresses before the maximum bond stress according to the virgin curve is reached. The maximum bond stress will then be determined by the formation of longitudinal splitting cracks, see Fig. 7-21 b. The post peak behaviour depends on the actual confinement. With little confinement the crack formation might result in a sudden splitting failure of the whole anchorage region. With more transverse stirrups, for example, it

may be possible to achieve a new equilibrium in the cracked concrete. Bond stresses can redistribute along the anchorage length and a stable post-peak behaviour can be achieved where the residual bond stress depends on the actual confinement.

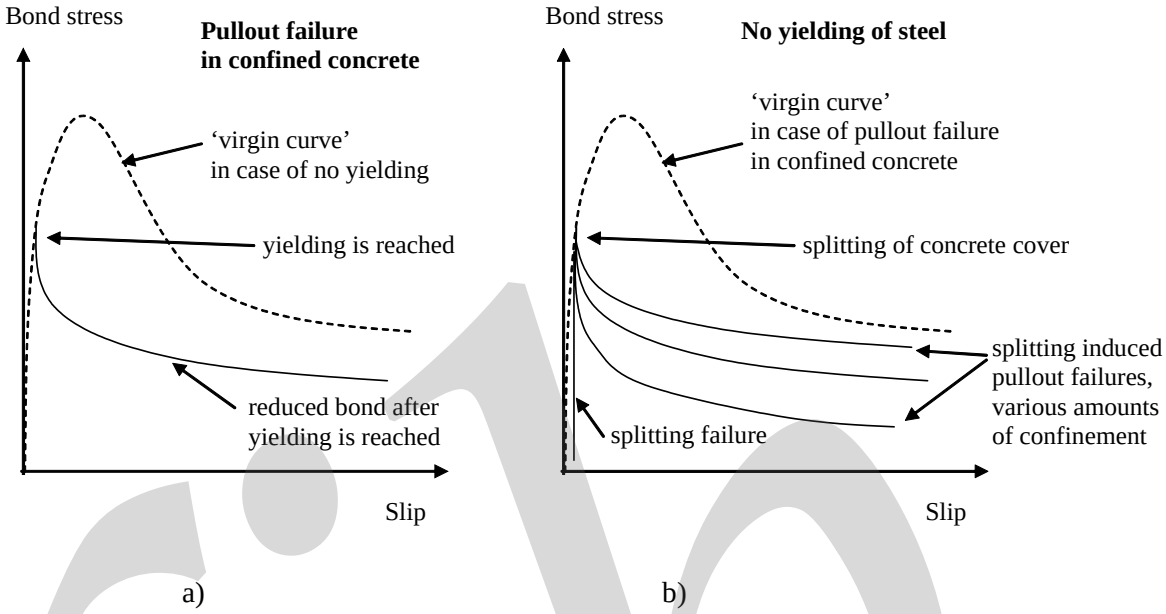

Fig. 7-21: Typical relationships between bond stress and slip, virgin curve valid for anchorage in well confined concrete (dotted curve), a) influence of yielding of the bar, b) influence of longitudinal splitting and various amounts of transverse reinforcement

On basis of results from pullout tests with short embedment length, a schematic local relationship between bond stress and slip is proposed in CEB-FIP Model Code 1990, see Fig. 7-22. This relationship can be used as in-put data in calculations where the local bond slip behaviour needs to be considered. The relationship in the Model Code is valid for normal strength concrete. For high strength concrete reference is made to fib (2000b).

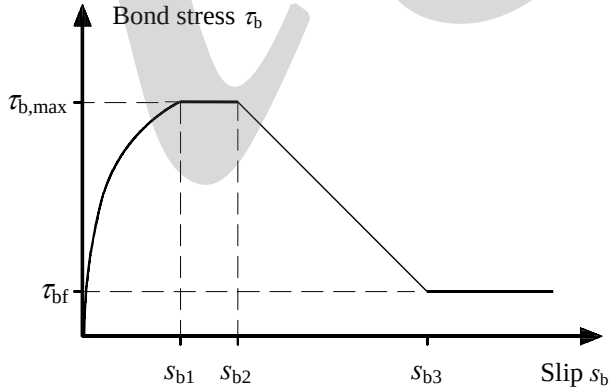

Fig. 7-22: Schematic relationship between bond stress τ_b and local slip s_b according to CEB-FIP Model Code 1990

The idealised bond-slip relationship in Fig. 7-22 can be used for ribbed and smooth reinforcement bars with various anchorage conditions. For each case, appropriate values of the parameters $\tau_{b,max}$, τ_{bf}, s_{b1}, s_{b2}, s_{b3} and α_b are specified in the Model Code.

The ascending branch of the relationship can be expressed by the function

$$\tau_b = \tau_{b,max}\left(\frac{s_b}{s_{b1}}\right)^{\alpha_b} \tag{7-2}$$

For ribbed bars anchored in 'confined' concrete, the specified parameters are listed in Table 7-1. In this context, 'confined' concrete means that the bar should be embedded in concrete in such a way that it is possible to reach the pullout mode, where the concrete is sheared off along the steel to concrete interface without premature splitting failure.

Even in the case of confined concrete, the bond resistance can vary considerably depending on the local bond conditions. Of this reason the actual bond conditions are considered in the Model Code by classification into two categories 'good bond conditions' and 'all other conditions'. The bond conditions can be considered as 'good' when the bar has an inclination of 45° - 90° to the horizontal during concreting, or when the bar has an inclination less than 45° to the horizontal and is placed either within a distance not more than 250 mm from the bottom or within a distance not more than 300 mm from the top of the concrete edge during concreting.

In precast structures the bond conditions of anchor bars are not always easy to define in these terms. It is then assumed that the two cases 'good' and 'all other cases' can be used as upper and lower estimates of the bond behaviour.

Bond conditions	Good	All other cases
s_{b1}	1,0 mm	
s_{b2}	3,0 mm	
s_{b3}	free rib distance	
α_b in eq. (7-2)	0,4	
$\tau_{b,max}$	$2{,}5\sqrt{f_{cc}}$ [1)]	$1{,}25\sqrt{f_{cc}}$ [1)]
τ_{bf}	0,40 $\tau_{b,max}$	

[1)] f_{cc} inserted in [MPa]

Table 7-1: Parameters describing the idealised relationship, Fig. 7-22, between bond stress and local slip for ribbed bars in confined concrete, according to CEB-FIP Model Code 1990

For ribbed bars anchored in 'unconfined' concrete, the corresponding parameters are listed in Table 7-2. Unconfined concrete refers to the case when the failure is of the splitting type and the detailing corresponds to the minimum requirements of concrete cover and transverse confining reinforcement. For intermediate cases it is assumed that appropriate values of s_{b1}, s_{b2}, s_{b3}, $\tau_{b,max}$ and τ_{bf} can be found by linear interpolation between confined and unconfined concrete. If transverse reinforcement, with an area greater than the minimum, is present simultaneously with a transverse pressure, these two effects may be added.

The idealised bond stress-slip relationship defined for confined concrete corresponds to the virgin curve in Fig. 7-21. In the case of unconfined concrete, the bond stress-slip relation is modified by the parameters in Table 7-2 and the resulting bond-slip model simulates the effect of longitudinal splitting cracks shown in Fig. 7-21 b. As shown in the figure the bond-slip response is influenced by the actual amount of confining reinforcement. According to the CEB-FIP Model Code 90 this influence can be taken into account by linear interpolation between the models for confined and unconfined concrete.

However, the Model Code gives no information of how to consider the effect of yielding of the steel, which is shown in Fig. 7-21 a. Consequently, the bond-slip relationship according to Fig. 7-22 is only true as long as the tie bar remains in the elastic range.

Bond conditions	Good	All other cases
s_{b1}	0,6 mm	
s_{b2}	0,6 mm	
s_{b3}	1,0 mm	2,5 mm
α_b in eq. (7-2)	0,4	
$\tau_{b.max}$	$2{,}0\sqrt{f_{cc}}$ [1)]	$1{,}0\sqrt{f_{cc}}$ [1)]
τ_{bf}	0,15 $\tau_{b.max}$	

[1)] f_{cc} inserted in [MPa]

Table 7-2: Parameters describing the idealised relationship, Fig. 7-22, between bond stress and local slip for ribbed bars in unconfined concrete fulfilling minimum requirements of concrete cover and transverse confining reinforcement, according to CEB-FIP Model Code 1990

To simulate the bond-slip behaviour for smooth hot-rolled bars, it is proposed in the Model Code that the two intermediate stages of the idealised relationship in Fig. 7-22 should be removed, which means that $s_{b1} = s_{b3}$. The specified parameters for this case are presented in Table 7-3. These parameters are valid for anchorage in confined concrete as well as for unconfined concrete.

Bond conditions	Good	All other cases
$s_{b1} = s_{b2} = s_{b3}$	0,1 mm	
α_b in eq. (7-2)	0,5	
$\tau_{b,max} = \tau_{bf}$	$0{,}3\sqrt{f_{cc}}$ [1)]	$0{,}15\sqrt{f_{cc}}$ [1)]

[1)] f_{cc} inserted in [MPa]

Table 7-3: Parameters describing the idealised relationship, Fig. 7-22, between bond stress and local slip for smooth bars in confined or unconfined concrete, according to CEB-FIP Model Code 1990

7.2.3 End-slip response

7.2.3.1 Ribbed bars where the transmission length is shorter than the anchorage length

The length of the transmission zone increases with increasing tensile force. Whenever the transmission length is shorter than the available anchorage length the information in this section is valid.

If the anchorage is designed for a tensile load less than the design yield capacity of the bar, the actual pullout resistance should be reduced accordingly. This holds also true in the specific case when joint interfaces of precast connections are subjected to shear sliding, and the pullout resistance of transverse bars is taken into account in design for shear resistance (see Fig. 8-35). Hence, the values of imposed shear displacement according to eqs. (8-35) and (8-36) should be reduced accordingly.

A typical relationship between tensile force and slip at the loaded end of an anchor bar, loaded until rupture of the steel, is shown in Fig. 7-23 [Engström (1992)].

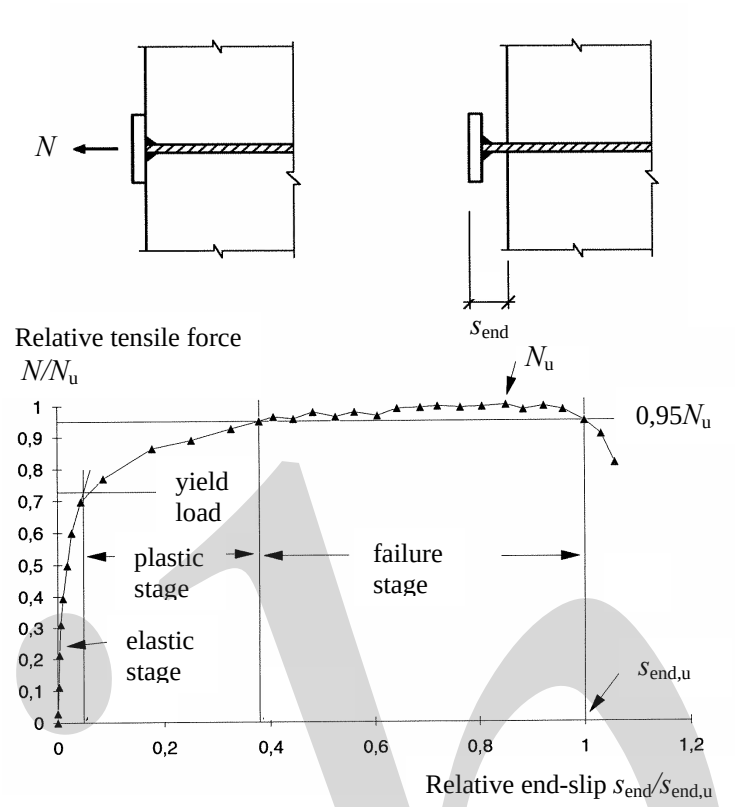

Fig. 7-23: End-slip response of anchor bar a) end-slip, b) typical relationship between relative tensile force N/N_u and relative end-slip $s_{end}/s_{end,u}$ (slip at loaded end) for anchor bars loaded until rupture of the steel and where the transfer length is shorter than the actual anchorage length

The end-slip response can be divided in a stiff almost linear stage until yielding of the bar, a plastic stage with load increase due to strain hardening of the steel, and an extended failure stage with an almost constant tensile force corresponding to the tensile capacity of the anchor bar (at steel rupture). It will be shown in the following how a typical relationship and its characteristics can be predicted depending on the bar diameter and material properties. The presentation is divided in three parts: response before yielding of the anchor bar, ultimate end-slip, idealised load-displacement relationship.

(1) Response before yielding of the anchor bar

In case of 'confined' concrete, according to Table 7-1, the maximum bond stress is obtained for a slip

$$s_{b1} = 1{,}0 \text{ mm} \quad \text{(confined concrete)}$$

In this case the ascending branch of the bond stress-slip relation, according to eq. (7-2) and Table 7-1 can be expressed as

$$\tau_b = \tau_{b,max} \cdot s_b^{0,4} \tag{7-3}$$

where $\tau_{b,max}$ = maximum bond stress, see Fig. 7-22 and Table 7-1
s_b is inserted in [mm]

With this model for the interfacial behaviour the differential equation that governs the anchorage behaviour can be solved analytically, [Tue and König (1991), Engström (1992), fib (2000b)]. Here it is assumed that the concrete is rigid in relation to the steel, which gives a slight overestimation of the

calculated end-slip. The following relation is then obtained between steel stress and end-slip. The relation is valid as long as the bar is in the elastic state and the net end-slip is less than 1 mm.

$$s_{\text{end}} = 0{,}288\left(\frac{\phi \cdot \sigma_{\text{s}}^2}{\tau_{\text{b,max}} \cdot E_{\text{s}}}\right)^{0{,}714} + \frac{\sigma_{\text{s}}}{E_{\text{s}}} \cdot 2\phi \tag{7-4}$$

where ϕ is inserted in [mm]

$\tau_{\text{b,max}} = 2{,}5\sqrt{f_{\text{cc}}}$ for 'good' bond conditions

$\tau_{\text{b,max}} = 1{,}25\sqrt{f_{\text{cc}}}$ for 'all other cases'

where f_{cc} is inserted in [MPa]

The first term in eq. (7-4) corresponds to the end-slip caused by the bond action along that part of the transmission length where bond stresses appear, here denoted as the 'net end-slip' $s_{\text{end,net}}$. The last additional term considers the effect of a local concrete cone failure near the free edge, see Fig. 7-13.

$$s_{\text{end,net}} = 0{,}288\left(\frac{\phi \cdot \sigma_{\text{s}}^2}{\tau_{\text{b,max}} \cdot E_{\text{s}}}\right)^{0{,}714} \tag{7-5a}$$

In case the steel stress is searched for a certain given value of the end slip, for instance imposed by shear wedging, see Section 8.3.4, it is convenient to use the following inversed expression that relates the steel stress to the net end-slip. If the local concrete cone failure needs to be considered, iteration can be used, see Example 8-1 in Section 8.3.5.

$$\sigma_{\text{s}} = 2{,}39\sqrt{\frac{\tau_{\text{b,max}} E_{\text{s}}}{\phi} s_{\text{end,net}}^{1{,}4}} \tag{7-5b}$$

where ϕ is inserted in [mm]

$$s_{\text{end,net}} = s_{\text{end}} - \frac{\sigma_{\text{s}}}{E_{\text{s}}} 2\phi$$

Accordingly, the transmission length is found as

$$l_{\text{t}} = 0{,}583\frac{\phi \cdot \sigma_{\text{s}}}{\tau_{\text{b,max}} \cdot s_{\text{end,net}}^{0{,}4}} + 2 \cdot \phi \tag{7-6}$$

where ϕ is inserted in [mm]

Predictions made by the equations above are illustrated in the following. Fig. 7-24 shows how the end-slip (slip of the loaded end of the anchor bar) develops with increasing steel stress until yielding is obtained in the case of confined concrete of strength C30 and good bond conditions. The influence of various bar diameters is also shown. The calculations are made assuming mean material properties f_{cm} = 38 MPa, $f_{\text{ym}} = f_{\text{yk}}$ = 500 MPa. The corresponding development of the transmission length is shown in Fig. 7-25.

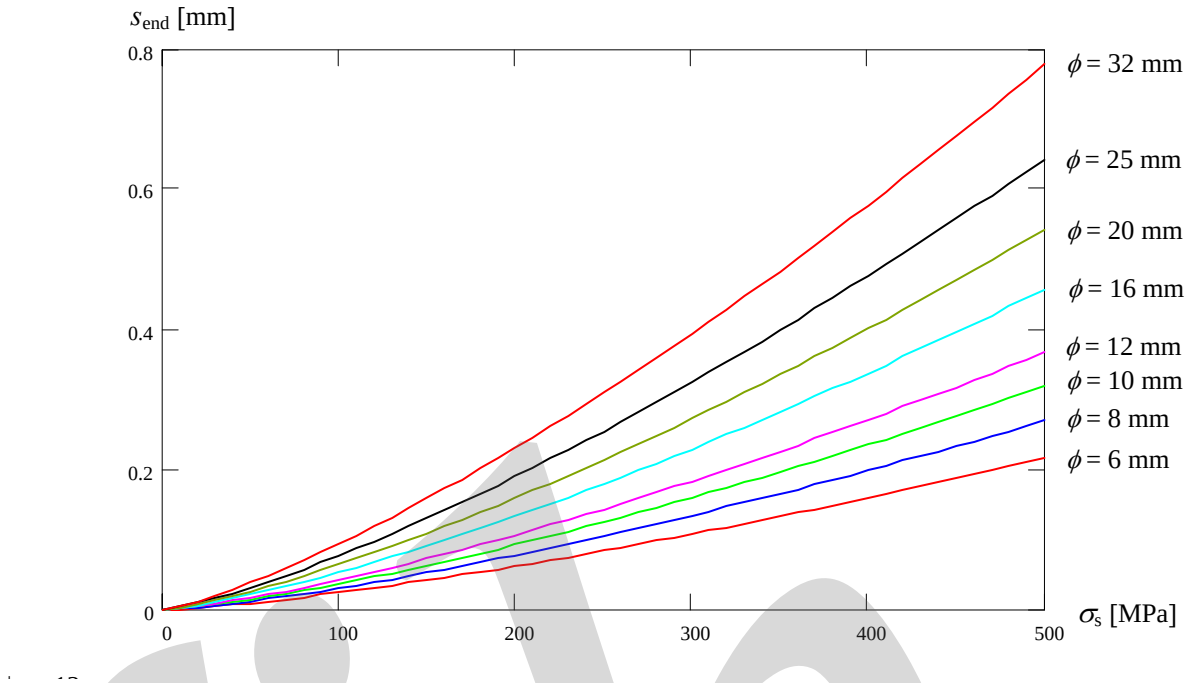

Fig. 7-24: Relationships between end-slip at loaded end and steel stress for anchor bars of various dimensions, 6, 8, 10, 12, 16, 20, 25, 32 mm, anchored in confined concrete of strength class C30 (f_{cm} = 38 MPa), good bond conditions

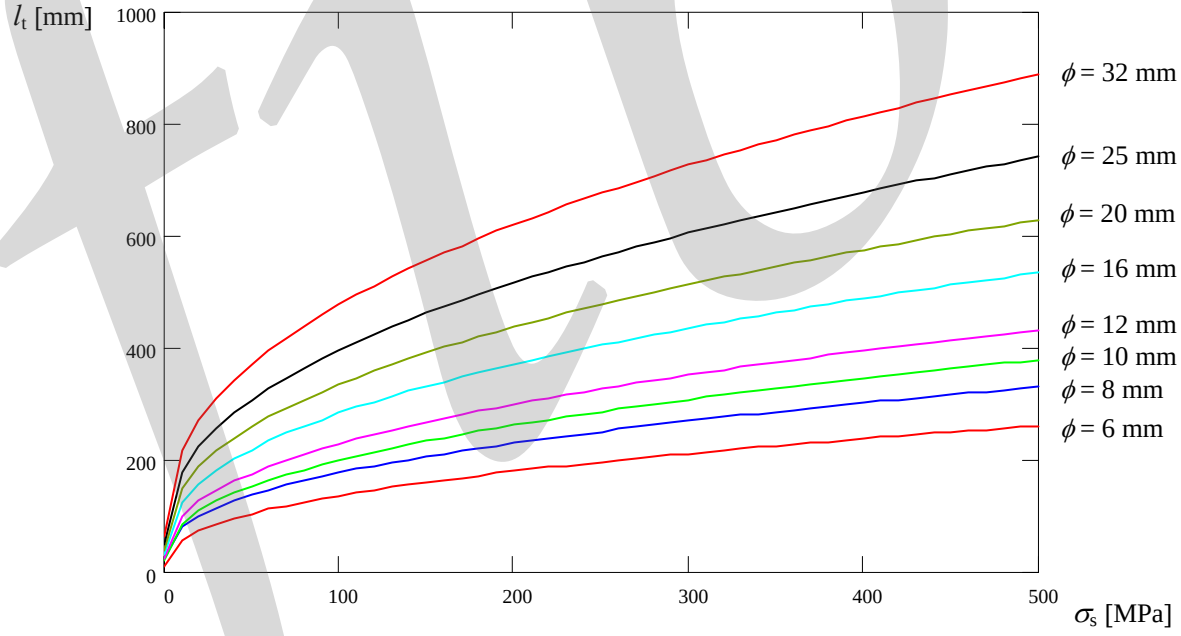

Fig. 7-25: Relationships between transmission length and steel stress for anchor bars of various dimensions, 6, 8, 10, 12, 16, 20, 25, 32 mm, anchored in confined concrete of strength class C30 (f_{cm} = 38 MPa), good bond conditions

It appears from the Fig. 7-24 that in no case the end-slip exceeds the value s_{end} = 1,0 mm, which means that the model presented above is valid. Accordingly, yielding is obtained at the loaded end of the anchor bar before the maximum bond stress $\tau_{b,max}$ according to Fig. 7-22 is reached.

The influence of the concrete strength is exemplified in Fig. 7-26 for a 12 mm anchor bar anchored in confined concrete with good bond conditions.

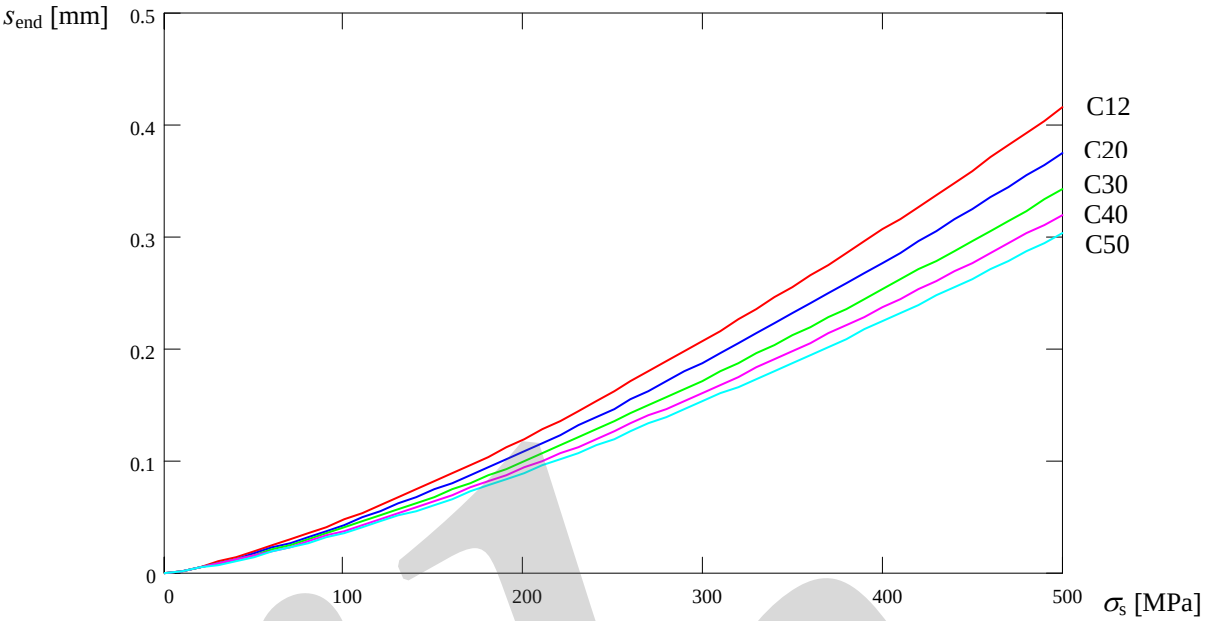

Fig. 7-26: Relationships between end-slip at loaded end and steel stress for a 12 mm anchor bar, anchored in confined concrete of various strength classes C12 (f_{cm} = 20 MPa), C20 (f_{cm} = 28 MPa), C30 (f_{cm} = 38 MPa), C40 (f_{cm} = 48 MPa), C50 (f_{cm} = 58 MPa), good bond conditions

The influence of the bond conditions, 'good' or 'all other cases', is exemplified in Fig. 7-27 for a 12 mm anchor bar anchored in confined concrete of strength class C30.

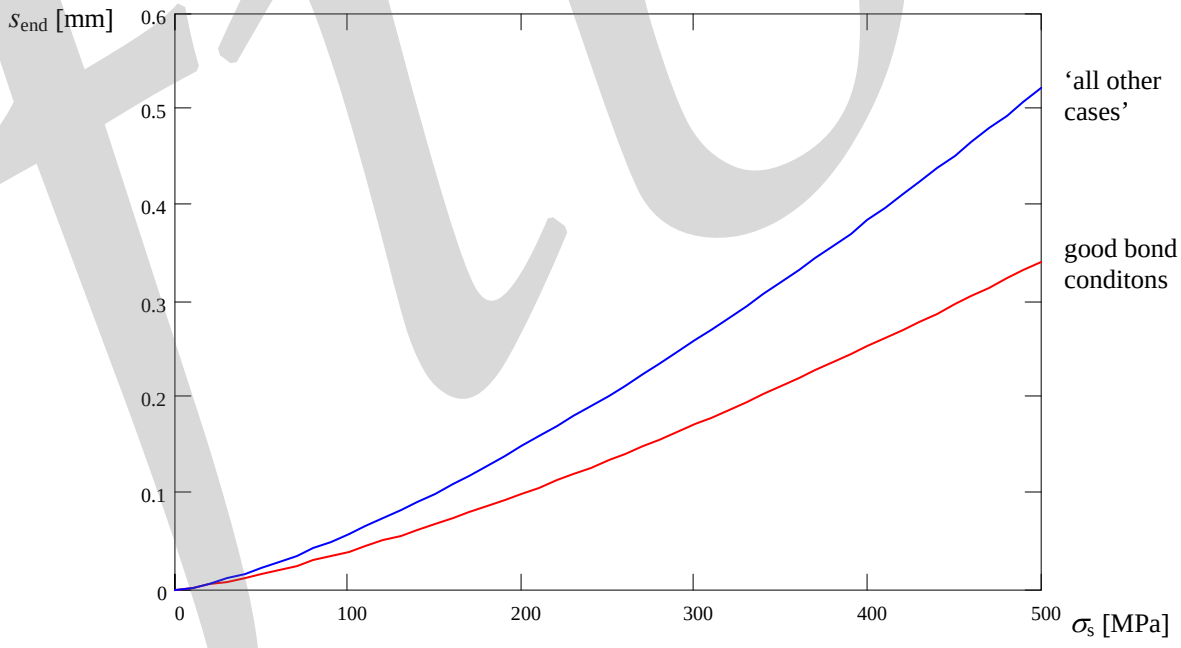

Fig. 7-27: Relationships between end-slip at loaded end and steel stress for a 12 mm anchor bar anchored in confined concrete of strength class C30 (f_{cm} = 38 MPa), with various bond conditions, 'good' or 'all other cases'

It appears from Figs. 7-26 and 7-27 that the bond condition has a stronger influence than a variation of the concrete strength.

The end-slip $s_{end,y}$ and the transmission length l_{ty} when yielding starts can be determined by eqs. (7-4) and (7-6) by inserting a steel stress equal to the yield strength.

The relationship between tensile force and end-slip, before yielding is reached, is non-linear as defined by eq. (7-4). Hence, the pullout stiffness K_a (s_{end}) varies with the end-slip and is in general defined as

$$K_a(s_{end}) = \frac{N(s_{end})}{s_{end}} \tag{7-7}$$

where s_{end} = end-slip

An approximate value for the overall pullout stiffness K_a can be determined on basis of the stiffness just before yielding is reached as

$$K_a = \frac{N_y}{s_{end,y}} \tag{7-8}$$

where N_y = yield load of anchor bar
$s_{end,y}$ is determined by eq. (7-4) for $\sigma_s = f_y$

This expression underestimates the stiffness for small values of the load. For a given range of the tensile force or the end-slip, a more representative stiffness can be calculated by (7-7), see Example 7-4 in Section 7.4.1.

(2) Ultimate end-slip

When the anchor bar starts to yield, the part within the local concrete cone failure, which is not anymore bonded to concrete, can obtain plastic deformations directly. However, in order to achieve yield penetration along the bonded part of the bar, the steel stress at the loaded end must exceed the yield strength. The 'plastic zone' of the transmission length is now defined as the part where the embedded steel bar has reached yielding. Within the plastic zone the bond stress decreases due to yielding, see Fig. 7-21 a. These remaining bond stresses must be equilibrated by an increase of the steel stress.

When the anchorage is sufficient to anchor the tensile capacity of the anchor bar at steel rupture, the plastic zone will reach its maximum extension. Then along the plastic zone the steel stress increases from the yield strength f_y to the tensile strength f_u at the loaded end, see Fig. 7-28.

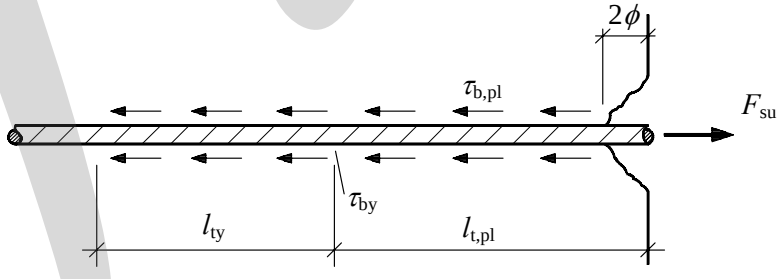

Fig. 7-28: Equilibrium condition for the plastic region of the tie bar just before rupture of the bar

The ultimate extension of the plastic zone $l_{t,pl}$ can be found from the equilibrium condition as

$$l_{t,pl} = \frac{F_{su} - F_{sy}}{\tau_{bm,pl}\pi\phi} = \frac{f_u - f_y}{\tau_{bm,pl}} \cdot \frac{\phi}{4} \tag{7-9}$$

where $\tau_{bm,pl}$ = average bond stress within the plastic zone

For ribbed tie bars of ductile type ('high ductility'), it has been proposed, [Engström (1992)] that the average bond stress in the plastic zone when the bar ruptures, can be estimated as

$$\tau_{bm,pl} = 0{,}27 \cdot \tau_{b,max} \tag{7-10}$$

where $\tau_{b,max} = 2{,}5\sqrt{f_{cc}}$ for 'good' bond conditions

$\tau_{b,max} = 1{,}25\sqrt{f_{cc}}$ for 'all other cases'

where f_{cc} is inserted in [MPa]

When the ultimate extension of the plastic zone is known, the ultimate end-slip can be estimated as

$$s_{end,u} = l_{t,pl} \cdot \varepsilon_{sm,pl} + s_{end,y} \tag{7-11}$$

The average steel strain $\varepsilon_{sm,pl}$ in the plastic zone can be estimated as

$$\varepsilon_{sm,pl} = 0{,}5 \cdot \varepsilon_{su}$$

where ε_{su} = ultimate steel strain (total strain at maximum stress)

It appears from eq. (7-11) that the ultimate displacement increases with increased ultimate extension of the plastic zone. According to eq. (7-9) the plastic zone increases with increased dimension of the anchor bar and decreases with increased concrete strength. From eq. (7-9) the importance of strain hardening is also apparent, as the deformability is proportional to the steel stress increase (f_u - f_y) obtained in the plastic stage.

Typical distributions of the steel force and bond stress just before steel rupture are shown in Figs. 7-29, from Engström (1992).

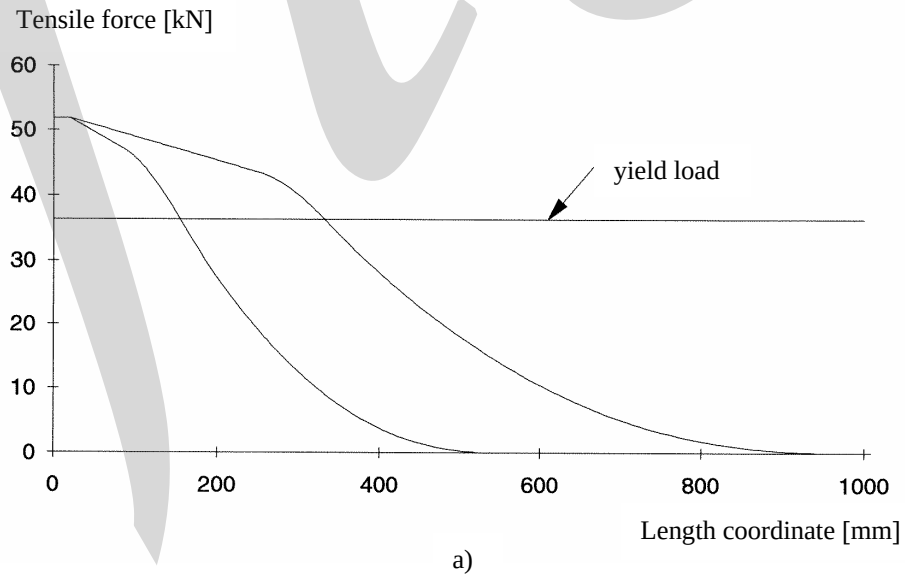

a)

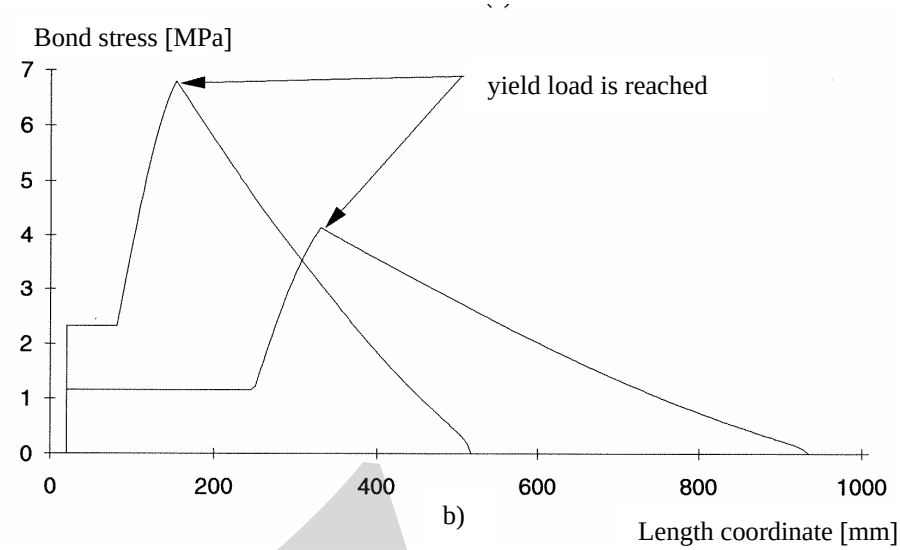

Fig. 7-29: Typical distributions of the tensile force (a) and the bond stress (b) along an anchor bar just before rupture according to numerical simulation assuming 'good' and 'other' bond conditions, from Engström (1992). Ribbed bar of ductile type

It appears from Fig. 7-29 how the bond stress decreases in the areas where the tensile force exceeds the yield load. It is also possible to see how high bond stresses result in an increased rate of the tensile force in the anchor bar. In the areas within the plastic zone where the bond stress is constant (= the residual bond strength), the tensile force increases linearly. As a consequence of this behaviour in the post-yield stage the ultimate end-slip depends mainly on the slip that has occurred in the plastic zone. The contribution to the end-slip from the elastic zone is negligible in comparison, in spite of the fact that the elastic zone is much larger than the plastic one.

(3) Idealised end-slip response

It has been found from parametric studies and tests that the proportions of the load *vs*. end-slip relationship are almost the same as long as the anchor bar is anchored to rupture of the steel. According to Engström (1992) an idealised tri-linear relationship between tensile force and slip at the loaded end can be used to characterise approximately the response of anchor bars loaded until steel rupture, see Fig. 7-30.

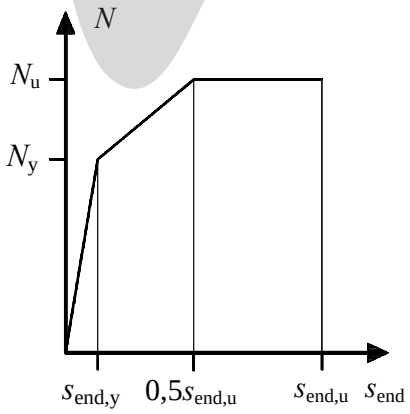

Fig. 7-30: Idealised relationship between tensile force and end-slip (slip at loaded end) for anchor bars loaded until rupture of the steel and where the transfer length is shorter than the actual anchorage length

The behaviour can be divided into an initial stiff stage until yielding is reached, a plastic stage with load increase due to strain hardening of the steel, and an extended failure stage with an almost constant tensile force corresponding to the tensile capacity of the anchor bar (at steel rupture).

The idealised relationship gives a reasonable estimate of the whole end-slip response until rupture of the steel. The procedure is presented in Example 7-1 below. The end-slip $s_{end,y}$, obtained just before yielding, is determined by means of eq. (7-4) with $\sigma_s = f_y$. The ultimate end-slip $s_{end,u}$ is calculated by eq. (7-11). Furthermore, it is assumed that the maximum tensile force is reached for an end-slip $s_{end} = 0{,}5\ s_{end,u}$. It should be noted that the response before yielding is in fact non-linear, see Fig. 7-23, and can be predicted more accurately by eq. (7-4), when it is considered to be necessary.

Example 7-1, prediction of end-slip response of anchor bar

An anchor bar ϕ16 B500 ('high ductility') is anchored with long embedment lengths in 'confined' concrete of strength class C20/25, 'good' bond conditions. For design with regard to progressive collapse (accidental action) the end-slip response is predicted on basis of characteristic steel properties. Furthermore, the pullout stiffness before yielding starts is estimated.

f_{yk} = 500 MPa; $(f_u/f_y)_k$ = 1,08; E_s = 200 GPa; $\varepsilon_{suk} = 50\cdot10^{-3}$

Yield capacity: $N_y = f_{yk}\cdot A_s = 500\cdot10^6\cdot201\cdot10^{-6} = 101\cdot10^3$ N

Tensile capacity (steel rupture): $N_u = 1{,}08\cdot N_y = 1{,}08\cdot101 = 109$ kN

The end-slip $s_{end,y}$ just before yielding starts is estimated according to eq. (7-4). The maximum bond stress, in the bond stress-slip relationship, Table 7-1, is calculated assuming good bond conditions. To make a realistic estimation of the end-slip, the mean concrete strength is used. Otherwise, since the end-slip increases with decreasing concrete strength, the end-slip may be overestimated.

$$\tau_{b,max} = 2{,}5\sqrt{f_{cm}} = 2{,}5\sqrt{28} = 13{,}2 \text{ MPa}$$

where $f_{cm} = f_{ck} + 8 \text{ MPa} = 20 + 8 = 28$ MPa

$$s_{end,y} = 0{,}288\left(\frac{16\cdot(500\cdot10^6)^2}{13{,}2\cdot10^6\cdot200\cdot10^9}\right)^{0{,}714} + \frac{500\cdot10^6}{200\cdot10^9}\cdot2\cdot16 \quad \Rightarrow$$

$$s_{end,y} = 0{,}388 + 0{,}080 = 0{,}468 \text{ mm}$$

where $s_{y,net}$ = 0,388 mm < 1,0 mm OK

The extension of the transmission length just before yielding starts can be calculated by eq. (7-6).

$$l_{ty} = 0{,}583\cdot\frac{500\cdot10^6\cdot16}{13{,}2\cdot10^6\cdot0{,}388^{0{,}4}} + 2\cdot16 = 516 + 32 = 548 \text{ mm}$$

The ultimate crack width, just before rupture of the tie bar is estimated by eq. (7-11). First the ultimate extension of the plastic zone is determined by eq. (7-9).

$$l_{t,pl} = \frac{1{,}08\cdot500\cdot10^6 - 500\cdot10^6}{0{,}27\cdot13{,}2\cdot10^6}\cdot\frac{16}{4} = 44{,}9 \text{ mm}$$

$$s_{\text{end,u}} = 44{,}9 \cdot \left(0{,}5 \cdot 50 \cdot 10^{-3}\right) + 0{,}468 = 1{,}12 + 0{,}468 = 1{,}59 \text{ mm}$$

With these characteristic end-slips and following the principles shown in Fig. 7-30, the end-slip response of the anchor bar can be described by the schematic load-displacement relationship shown in Fig. 7-31.

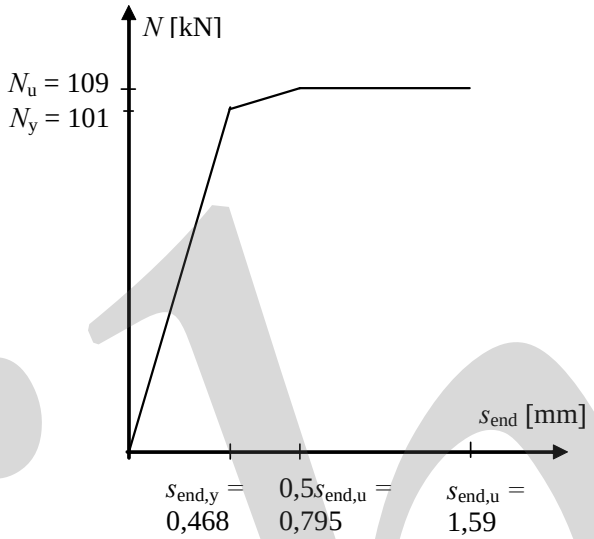

Fig. 7-31: Schematic load-displacement relationship (end-slip response) for the anchor bar in Example 7-1

The pullout stiffness for the stage before yielding is reached can be estimated by eq. (7-8)

$$K_{\text{a}} \approx \frac{N_{\text{y}}}{s_{\text{end,y}}} = \frac{101 \cdot 10^{3}}{0{,}468 \cdot 10^{-3}} = 216 \cdot 10^{6} \text{ N/m}$$

This value of the stiffness gives a reasonable value for the whole range when the load varies from zero to the yield load. The stiffness is higher for small values of the load, compare with Figs. 7-23 and 7-24.

7.2.3.2 Simplified approach to predict the response of anchor bars before yielding

On the basis of the assumptions that the bond stress is constant along the transmission length and not influenced by the tensile load applied to the anchor bar, it is possible to derive a simplified approach to predict the end-slip of anchor bars in the elastic range. Consequently, the steel stress will increase linearly along the transmission length and with the same rate independently of the load as shown in Fig. 7-32. Since the real bond stress distribution is non-linear and the bond stress increases with increasing slip, the assumed constant value τ_{bm} of the bond stress should correspond to a reasonable average value along the transmission length.

A relation between the mobilised transmission length l_{t} and the steel stress at the active end can be derived from an equilibrium condition between the applied tensile force and the total bond resistance.

$$\sigma_{\text{s}} \cdot \frac{\pi\phi^{2}}{4} = \tau_{\text{bm}} \cdot \pi\phi \cdot l_{\text{t}} \qquad \Rightarrow$$

$$l_t = \frac{\sigma_s}{\tau_{bm}} \frac{\phi}{4} + 2 \cdot \phi \tag{7-12}$$

where σ_s = steel stress at the active end
τ_{bm} = average bond stress along the transmission length

The last term in eq. (7-12) considers the influence of a local concrete cone failure near the active end as shown in Fig. 7-13. Since the steel stress and the steel strain vary linearly along the effective transmission length, the end slip can be determined as

$$s_{end} = \frac{1}{2} \frac{\sigma_s}{E_s} \cdot l_t + \frac{\sigma_s}{E_s} \cdot 2 \cdot \phi$$

$$s_{end} = \frac{1}{8} \frac{\sigma_s^2 \cdot \phi}{E_s \cdot \tau_{bm}} \cdot + \frac{\sigma_s}{E_s} \cdot 2 \cdot \phi \tag{7-13}$$

where σ_s = steel stress at active end of anchor bar

Then, for a given end-slip, the corresponding steel stress can be estimated as

$$\sigma_s = \sqrt{\frac{8(s_{end} - \Delta s) E_s \tau_{bm}}{\phi}} \tag{7-14}$$

where $\Delta s = \frac{\sigma_s}{E_s} \cdot 2 \cdot \phi$ (influence of local concrete cone failure)

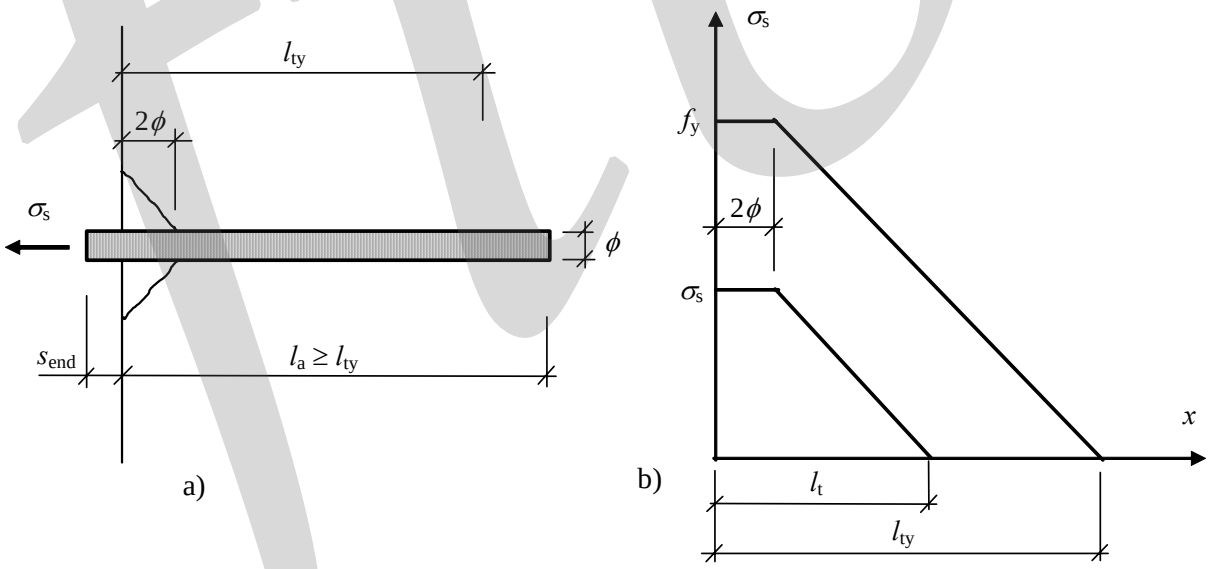

Fig. 7-32: Simplified approach to analyse the end-slip response of anchor bars before yielding, a) anchor bar where the maximum transmission length l_{ty} before yielding is shorter than the actual embedment length l_a , b) steel stress distributions

The difficulty in this simplified approach is to assume an appropriate value of the average bond stress that represents the real behaviour. It is here proposed to estimate the average bond stress as

$$\tau_{bm} = \alpha_t \cdot \tau_{b,max} \tag{7-15}$$

where $\tau_{b.max}$ = maximum bond stress in the relevant bond stress-slip relationship according to Tables 7-1 and 7-2

α_t = factor that considers the bond stress development and distribution and depends on the bar diameter according to Table 7-4

Bar diameter [mm]	6	8	10	12	16	20	25	32
α_t	0,30	0,32	0,34	0,36	0,40	0,42	0,45	0,45

Table 7-4: Reasonable values of the factor α_t to be used in eq. (7-15)

Fig. 7-33 shows one example where results of the simplified approach and the more accurate method in Section 7.2.3.1 are compared.

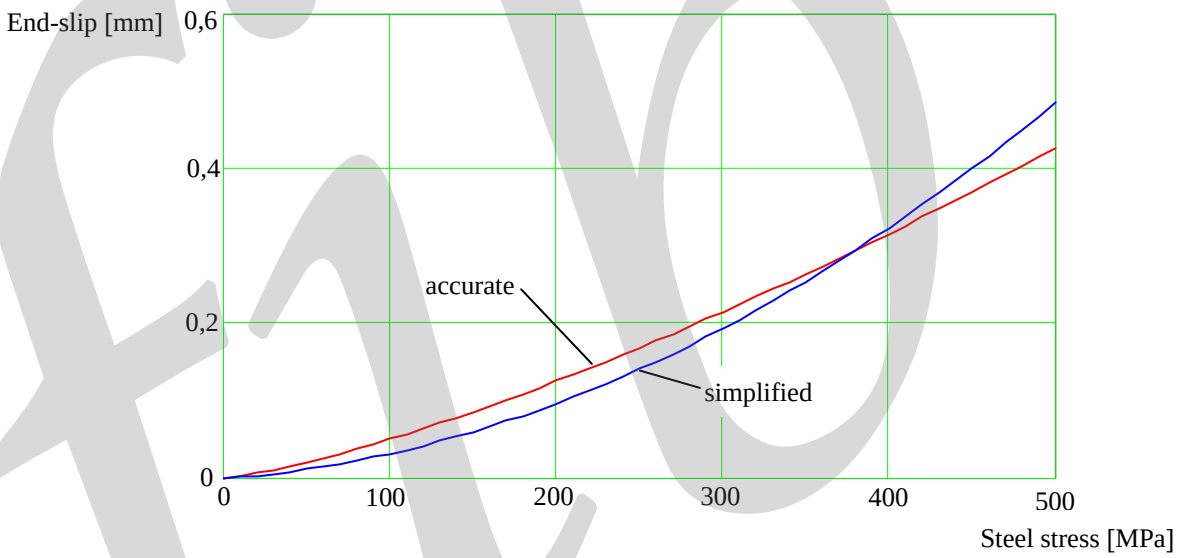

Fig. 7-33: Example of relationship between the steel stress and the end slip at the active end predicted by the simplified approach, eq. (7-13), in comparison with the more accurate method, eq. (7-4). Anchor bar ϕ = 16 mm anchored in confined concrete C30, 'good' bond conditions

The transmission length l_{ty} when yielding starts and the corresponding end-slip $s_{end,y}$ can be determined by eqs. (7-12) and (7-13) by inserting a steel stress equal to the yield strength.

$$l_{ty} = \frac{f_y}{\tau_{bm}} \frac{\phi}{4} + 2 \cdot \phi \tag{7-16}$$

$$s_{end,y} = \frac{1}{8} \frac{f_y^2 \cdot \phi}{E_s \cdot \tau_{bm}} \cdot + \frac{f_y}{E_s} \cdot 2 \cdot \phi = \varepsilon_{sy} \left(\frac{1}{2} l_{ty} + 2 \cdot \phi \right) \tag{7-17}$$

where ε_{sy} = yield strain of anchor bar

The overall pullout stiffness can be estimated on the basis of load and end-slip just before yielding is reached.

$$K_a = \frac{f_y A_s}{s_{end,y}} \tag{7-18}$$

By means of eq. (7-17) and ignoring the influence of the bond free length, the overall stiffness can alternatively be expressed as

$$K_a = 2\frac{E_s A_s}{l_{ty}} \tag{7-19}$$

For prediction of the end-slip after yielding reference is made to the method presented in Section 7.2.3.1.

In the case where the actual embedment length l_a is shorter than the calculated transmission length l_{ty} when yielding starts, the whole length will transfer bond stresses before yielding is reached and the passive end of the bar will begin to slip. The expression (7-13) for the end-slip response is valid as long as the transmission length is less than the embedment length, which yields

$$\frac{\sigma_s}{\tau_{bm}} \cdot \frac{\phi}{4} + 2 \cdot \phi \le l_a$$

$$\sigma_{s,max} = \frac{4 \cdot \tau_{bm}\left(l_a - 2 \cdot \phi\right)}{\phi} \tag{7-20}$$

where $\sigma_{s,max}$ = the maximum steel stress that can be applied to the active end before the passive end starts to slip

l_a = actual embedment length $\le l_{ty}$

Since the end-slip is proportional to the transmission length in square, the corresponding value of the end slip can be determined as

$$s_{end,max} = \left(\frac{l_a}{l_{ty}}\right)^2 \cdot s_{end,y} \tag{7-21}$$

where $s_{end,max}$ = the maximum end-slip obtained before the passive end starts to slip

(1) Cycling loading

The expressions given above are valid for monotonic loading. The effect of cyclic loading on the pullout resistance is not systematically investigated. However, it is reasonable to assume that the reduction of the pullout resistance corresponds to the reduction of the average local bond under cyclic conditions.

However, since fully slip reversals are not expected, it is reasonable to use a less severe reduction factor; thus instead of 1/4 valid for full cycling, according to Tassios (1979) and Moriata and Kaku (1975), a value equal to 1/3 is proposed for design purpose, i.e.

$$\left(\sigma_{s,n}\right)_d \approx \frac{1}{3}\left(\sigma_s\right)_d$$

where $(\sigma_s)_d$ refers to the steel stress at the active end of the anchor bar under monotonic loading determined by eq. (7-14) or (7-20).

Nevertheless, for prevailing cyclic conditions, this subject would necessitate a more detailed investigation.

7.2.3.3 Smooth bars anchored by hooks

As for ribbed bars, the end-slip response of plain hot-rolled anchor bars with end hook depends on the bond behaviour. The idealised bond stress-slip relationship given in CEB-FIP Model Code 1990**,** Fig. 7-22, can be used also in case of smooth hot-rolled bars. However, the characteristic parameters, according to Table 7-3, are quite different compared to ribbed bars. This means that the maximum bond stress is obtained for a local slip of only $s_{b1} = s_{b3} = 0{,}1$ mm and the residual bond strength, when the bar slips in a frictional mode, is the same as the maximum value. This can, in case of 'good' bond conditions, be estimated as

$$\tau_{b,max} = \tau_{bf} = 0{,}30\sqrt{f_{cc}} \quad \text{(with } f_{cc} \text{ in [MPa])} \qquad \text{('good' bond conditions)}$$

In 'all other cases' half this value should be used. Due to the low bond strength it can be assumed that the end-slip at the active end, just before yielding is reached, exceeds the value $s_{b1} = 0{,}1$ mm considerably. Consequently, when yielding is reached the end hook resists a considerable portion of the applied force.

Of this reason it is not possible to establish a similar analytical expression for the end-slip response on the basis of the ascending branch of the bond stress-slip relation as it was for ribbed bars, eq. (7-4). However, ignoring the influence of the adhesive bond and assuming that the residual bond strength τ_{bf} is reached in all sections along the embedment length, the end-slip just before yielding of the anchor bar can be estimated as

$$s_{end,y} = \frac{f_y + \sigma_{sa,y}}{2 \cdot E_s} \cdot l_a \tag{7-22}$$

where $\sigma_{sa,y}$ = steel stress at anchor (end hook) when yielding is reached at the active end
l_a = distance from active end to anchor (end hook)

The total force transferred by bond along the embedment length should equal the decrease of force in the anchor bar. Hence, the force at the anchor (end hook) is determined as

$$\sigma_{sa,y} \cdot \frac{\pi\phi^2}{4} = f_y \cdot \frac{\pi\phi^2}{4} - \tau_{bf}\,\pi\phi \cdot l_a \qquad \Rightarrow$$

$$\sigma_{sa,y} = f_y - 4\frac{\tau_{bf} \cdot l_a}{\phi} \tag{7-23}$$

Probably, the bond resistance along smooth bars is reduced in a similar way as for ribbed bars when the steel begins to yield. However, it is not reasonable to assume that the bond is totally lost at yielding, not even for a smooth bar. It is proposed [Engström (1992)] that the average bond stress in the plastic zone along a smooth bar can be estimated as

$$\tau_{bf,pl} = 0{,}05\sqrt{f_{cc}} \qquad \text{for 'good' bond conditions} \tag{7-24}$$

$$\tau_{bf,pl} = 0{,}025\sqrt{f_{cc}} \qquad \text{for 'all other cases'} \tag{7-25}$$

where f_{cc} is inserted in [MPa]

If the ultimate extension of the plastic zone $l_{t,pl}$ is smaller than the anchorage length l_a (the distance between the active end and the end hook), the length of the plastic zone can be calculated from an equilibrium condition, as was the case for ribbed anchor bars, see Fig. 7-29.

$$l_{t,pl} = \frac{f_u - f_y}{\tau_{bf,pl}} \cdot \frac{\phi}{4} \qquad \text{if} \quad l_{t,pl} \le l_a \tag{7-26}$$

where l_a = distance between crack section and end hook

In this case the ultimate end-slip can be estimated as

$$s_{end,u} = l_{t,pl} \cdot 0{,}5 \cdot \varepsilon_{su} \qquad \text{if} \quad l_{t,pl} \le l_a \tag{7-27}$$

However, for normal embedment lengths, it is more likely that the plastic zone will reach the end hook before rupture of the anchor bar. The steel stress $\sigma_{sa,u}$ at the end hook just before rupture of the bar can be estimated as

$$\sigma_{sa,u} \cdot A_s = f_u \cdot A_s - \pi\phi \cdot \tau_{bf,pl} \cdot l_a \Rightarrow$$

$$\sigma_{sa,u} = f_u - 4\frac{\tau_{bf,pl} \cdot l_a}{\phi} \qquad \text{if} \quad l_{t,pl} \ge l_a \tag{7-28}$$

where $\sigma_{sa,u}$ = steel stress at anchor (end hook) when rupture occurs at the active end

In this case the ultimate displacement can be estimated as

$$s_{end,u} = \frac{\sigma_{sm} - f_y}{f_u - f_y} \varepsilon_{su} \cdot l_a \qquad \text{if} \quad l_{t,pl} \ge l_a \tag{7-29}$$

where $\sigma_{sm} = \dfrac{f_u + \sigma_{sa,u}}{2}$ (average steel stress in the anchorage length)

With the characteristic end-slips determined by eq. (7-22) and either eq. (7-27) or (7-29), a simplified idealised load-displacement relationship can be established following the principles in Fig. 7-33. The approach is presented for a continuous smooth tie bar with end hooks in Example 7-6, see Section 7.4.2.

7.2.4 Design of anchor bars and tie bars

In order to provide safe anchorage of anchor bars and tie bars brittle pullout failures and splitting failures must be prevented in the anchorage regions. Normally the anchorage is designed for the design yield capacity of the bar. When a ductile behaviour is needed it should be possible to anchor the tensile capacity of the bar (at steel rupture). In tie connections composed of several components, a balanced design for ductility should then be applied, see Section 3.6.

7.2.4.1 Anchorage of deformed bars

Pullout and splitting types of anchorage failures, as shown in Fig. 7-9, can be prevented by an appropriate choice of (1) concrete cover and (2) anchorage length. Anchor bars in precast units are often placed in positions far away from edges and corners where the concrete is well confined.

For bars with a small concrete cover, the bond strength at the steel/concrete interface is determined by formation of splitting cracks through the concrete cover. The bond strength increases with increasing concrete cover c until a critical value c_{crit}, for which a further increase of the cover gives no corresponding increase of the bond strength. At this critical value it can be assumed that the failure mode changes from a splitting type of failure to a pullout type and this intermediate state also defines the change from anchorage in unconfined to anchorage in confined concrete.

For smaller concrete cover where splitting cracks can be expected, the bond behaviour can be improved, as illustrated in Fig. 7-21 b, by provision of confining transverse reinforcement.

In the pullout type of anchorage failure, the bond strength is not influenced by the concrete cover but depends only on the shear strength at the steel/concrete interface. The critical concrete cover c_{crit} can be taken to about 3 times the dimension of the considered anchored bar. This is also the value used in MC 90 to determine the maximum confinement effect of the concrete cover.

According to CEB-FIP Model Code 90 the design bond strength of reinforcing bars, in a reference situation fulfilling minimum conditions, is determined as

$$f_{bd} = \eta_1 \eta_2 \eta_3 f_{ctd} \tag{7-30}$$

where $f_{ctd} = \dfrac{f_{ctk,min}}{\gamma_c} = \dfrac{f_{ctk,min}}{1{,}5}$

η_1 = 2,25 (ribbed bars); = 1,4 (indented bars); = 1,0 (plain bars)
η_2 = 1,0 ('good' bond conditions); = 0,7 ('all other cases')
η_3 = 1,0 (for bars with $\phi \le 32$ mm)

For this reference situation the basic anchorage length necessary to transfer the yield load of the bar is found from an equilibrium condition between the applied force and the total bond resistance, compare with the derivation of eq. (7-12).

$$l_b = \frac{f_{yd}}{f_{bd}} \cdot \frac{\phi}{4} \tag{7-31}$$

To determine the necessary design anchorage length $l_{b,net}$ in the specific situation, favourable effects in relation to the reference situation may be taken into account.

$$l_{b,net} = \alpha_1 \alpha_2 \alpha_3 \alpha_4 \alpha_5 l_b \frac{N_{Ed}}{N_{yd}} \ge l_{b.min} \tag{7-32}$$

where N_{Ed} = design tensile load to be resisted ($\le N_{yd}$)
N_{yd} = design yield capacity of bar
α_1 = 1,0 (straight bar); = 0,7 (bar with hook, bend and $c \ge 3\phi$)
α_2 = 1,0 (no welded transverse bars); = 0,7 (bar with welded transverse bars)
α_3 = 0,7 (if $c \ge 3\phi$); = 1,0 (if $c = 1{,}0\phi$ - minimum requirement); $0{,}7 \le \alpha_3 \le 1{,}0$
α_4 = 0,7 (max. effect of transverse reinforcement);
= 1,0 (min. effect of transverse reinforcement); $0{,}7 \le \alpha_4 \le 1{,}0$
α_5 = 0,7 (max. effect of transverse pressure);
= 1,0 (min. effect of transverse pressure); $0{,}7 \le \alpha_5 \le 1{,}0$
$l_{b,min} > \max\{0{,}3 l_b ; 10\phi ; 100 \text{ mm}\}$

In eq. (7-32) the favourable influence of confinement effects, i.e. concrete cover, transverse reinforcement, and transverse pressure, should be limited as

$\alpha_3 \alpha_4 \alpha_5 > 0{,}7$ (for high bond bars)

$\alpha_3\alpha_4\alpha_5 = 1{,}0$ (for plain or indented bars)

For the normal case when straight anchor bars without welded transverse bars are anchored in confined concrete ($c \geq 3\phi$) the design expression, eq. (7-32), can be simplified as

$$l_{b,net} = 0{,}7 \cdot l_b \frac{N_{Sd}}{N_{yd}} \geq l_{b,min} \tag{7-33}$$

According to CEB-FIP Model Code 90 a minimum amount of transverse reinforcement is always required in anchorage regions in beams, but not in slabs. Hence, for single anchor bars located far away from edges and corners, i.e. in well confined concrete, is seems not necessary to provide transverse reinforcement. In anchorage regions where bars are placed together with small spacing and or a small cover, it is recommended to provide transverse reinforcement in the anchorage region. For more information about the design method and how to consider influencing parameters in intermediate situations reference is made to the CEB-FIP Model Code 90.

When a ductile behaviour is needed, the anchorage should be sufficient to balance not only the yield capacity of the anchor bar but also the full tensile capacity at steel rupture. When the load increases above the yield capacity due to strain hardening of the steel, yield penetration takes place along the embedded bar as shown in Fig. 7-28. Along that part of the bar where it yields at ultimate, the bond strength is reduced and can in average be taken as $\tau_{bm,pl}$ according to eq. (7-10). Accordingly, the enhanced anchorage length $l_{b,tot}$ required to balance the tensile capacity of the tie bar at steel rupture can be determined as

$$l_{b,tot} = l_{b,net} + l_{b,pl} \tag{7-34}$$

where $l_{b,net}$ = anchorage length required to anchor the yield load, see eq. (7-32) or (7-33)
$l_{b,pl}$ = additional anchorage length required to allow for yield penetration in the plastic range

The additional anchorage length to allow for yield penetration equals the maximum extension of the plastic zone according to eq. (7-9)

$$l_{b,pl} = l_{t,pl} = \frac{f_u - f_y}{\tau_{bm,pl}} \cdot \frac{\phi}{4} \tag{7-35}$$

where $\tau_{bm,pl} = 0{,}27\tau_{b,max}$

$\tau_{b,max} = 2{,}5\sqrt{f_{cc}}$ for ‘good’ bond conditions in ‘confined’ concrete

$\tau_{b,max} = 1{,}25\sqrt{f_{cc}}$ for ‘all other cases’ in ‘confined’ concrete

where f_{cc} is inserted in [MPa]

If the anchorage length is not increased by this additional amount according to eq. (7-34), there is a risk that a pullout failure occurs in the ultimate state when the bar is yielding, but before the tensile strength of the steel has been reached. In that case it is not possible to take full advantage of the plastic strain capacity of the steel. The principle to provide anchorage for a ductile behaviour is illustrated in Fig. 7-33.

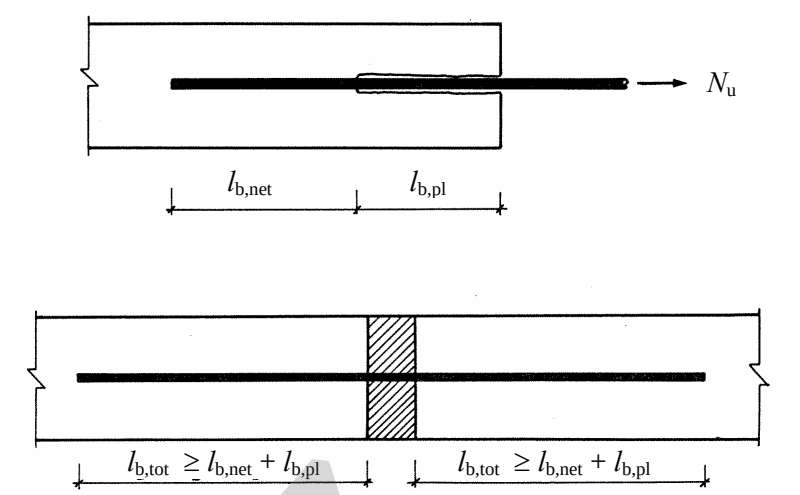

Fig. 7-33: To secure a ductile behaviour in the ultimate state, the anchorage should balance not only the yield capacity of the tie bar but also allow for yield penetration until the bar ruptures. For this an additional anchorage length is required

Furthermore, in order to obtain a ductile behaviour of anchor bars and tie bars it is recommended to prevent splitting cracks by providing a sufficient concrete cover $c \geq c_{crit}$ in the 'effective' anchorage region, Fig. 3-20 a. When of some reasons anchor bars must be placed with a small concrete cover, for example near a transverse joint, one possibility would be to bend down the bar and anchor it in confined concrete, i.e. where $c \geq c_{crit}$, see Fig.3-20 b. A safe approach would then be to ignore that part of the anchorage where the concrete cover is insufficient.

Example 7-2, design of anchorage

The anchorage of a straight anchor bar ϕ16 B500 in concrete C50 should be designed so that a ductile behaviour can be achieved. The bar is placed in a location away from edges and corners and therefore the anchorage region can be considered as 'confined'. With regard to the casting the bond conditions are classified as 'good'.

Concrete: $f_{ck} = 50$ MPa $f_{ctk,min} = 2{,}8$ MPa

$$f_{cd} = \frac{f_{ck}}{\gamma_c} = \frac{50}{1{,}5} = 33{,}3 \text{ MPa} \qquad f_{cd,acc} = \frac{50}{1{,}2} = 41{,}7 \text{ MPa} \qquad f_{ctd} = \frac{2{,}8}{1{,}5} = 1{,}87 \text{ MPa}$$

Reinforcing steel: $f_{yk} = 500$ MPa; $(f_u/f_y)_k = 1{,}08$

$$f_{yd} = \frac{f_{yk}}{\gamma_s} = \frac{500}{1{,}15} = 435 \text{ MPa}$$

Design bond strength according to eq. (7-30):

$$f_{bd} = 2{,}25 \cdot 1{,}0 \cdot 1{,}0 \cdot 1{,}87 = 4{,}20 \text{ MPa}$$

Basic anchorage length according to eq. (7-31):

$$l_b = \frac{435}{4{,}20} \cdot \frac{0{,}016}{4} = 0{,}414 \text{ m}$$

For straight bar in 'confined' concrete the 'net' anchorage length can be determined by eq. (7-33). Since the anchorage should resist the capacity of the bar, the design load is assumed to be equal to the design yield capacity.

$$l_{b,net} = 0{,}7 \cdot 0{,}414 \cdot 1{,}0 = 0{,}290\,\text{m} \quad > \quad l_{b,min} = 0{,}160\,\text{m}$$

This length is required to balance the yield load of the anchor bar. In order to achieve a ductile behaviour an additional length is provided to allow for yield penetration. Since in this case the strain hardening of the steel is unfavourable and the design is related to accidental situations, this additional length is estimated by means of eq. (7-35) assuming 'mean' material properties for the steel and design strength (accidental) for the concrete.

It is assumed that $(f_u/f_y)_m \approx 1{,}3$ and accordingly

$$f_{um} \approx 1{,}3 \cdot f_{ym} \approx 1{,}3 \cdot f_{yk} = 1{,}3 \cdot 500 = 650\,\text{MPa}; \qquad f_{ym} \approx 500\,\text{MPa}$$

The average bond stress in the plastic zone, se eq. (7-35)

$$\tau_{bm,pl} = 0{,}27 \cdot 2{,}5\sqrt{41{,}7} = 4{,}35\,\text{MPa}$$

$$l_{b,pl} = \frac{650 - 500}{4{,}35} \cdot \frac{0{,}016}{4} = 0{,}138\,\text{m}$$

The total anchorage length is found from eq. (7-34) as:

$$l_{b,tot} = 0{,}290 + 0{,}138 = 0{,}428\,\text{m}$$

7.2.4.2 Influence of local weakness of deformed anchor bars

The deformation capacity and the ductility of anchor bars or tie bars can decrease considerably, if the diameter of the tie bar is reduced locally near the loaded end of the anchorage. This could for instance be the case, when a tie bar is provided with a threaded end to fit a threaded insert in an adjacent precast element as shown in Fig. 7-34. The drastic effect on the deformation capacity of such a local reduction of the diameter appears from the following example.

Example 7-3, effect of locally reduced diameter

A tie bar ϕ10 mm is assumed to have a yield strength f_y = 500 MPa, a tensile strength f_u = 650 MPa (1,30·f_y) and an ultimate strain ε_{su} = 0,10. The tie bar is anchored in concrete with compressive strength f_{cc} = 20 MPa and the bond conditions are considered as belonging to 'all other cases'.

First the ultimate end-slip is calculated assuming that the bar has constant diameter along its length, ϕ = 10 mm. The deformation before yielding is ignored. The calculations follow eqs. (7-9) - (7-11).

$$\tau_{bm,pl} = 0{,}27 \cdot \tau_{max} = 0{,}27 \cdot 1{,}25 \cdot \sqrt{20} = 1{,}51\ \text{MPa}$$

$$l_{t,pl} = \frac{f_u - f_y}{\tau_{bm,pl}} \cdot \frac{\phi}{4} = \frac{650 - 500}{1{,}51} \cdot \frac{10}{4} = 248\ \text{mm}$$

$$s_{end,u} = l_{t,pl} \cdot \varepsilon_{sm,pl} = l_{t,pl} \cdot 0{,}5 \cdot \varepsilon_{su} = 248 \cdot 0{,}5 \cdot 0{,}10 = 12{,}4\ \text{mm}$$

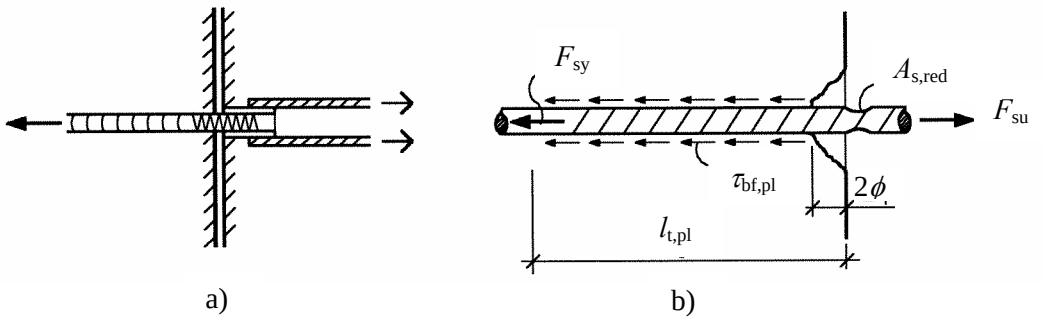

Fig. 7-34 Tie bar with a local reduction of the cross-section in the area where the joint crack appears, a) anchorage in threaded insert, b) model for plastic region

It is now assumed that the tie bar just outside the concrete face has a locally reduced diameter ϕ_{red} = 9 mm due to threading. The cross-sectional area in the threaded region is then $A_{s,red}$ = 63,6 mm^2 (0,81·A_s). In this case the yield penetration along the tie bar depends on the difference between the tensile capacity of the reduced cross-section and the yield capacity of the full cross-section. This appears when the actual case in Fig. 7-34 is compared with the basic case in Fig. 7-28. The ultimate extension of the plastic zone is found by the equilibrium condition of the plastic zone, compare with eq. (7-9).

$$l_{t,pl} = \frac{f_u \cdot A_{s,red} - f_y \cdot A_s}{\tau_{bm,pl} \cdot \pi\phi} = \frac{650 \cdot 63{,}6 - 500 \cdot 78{,}5}{1{,}51 \cdot \pi \cdot 10} = 44{,}1 \text{ mm}$$

$$s_{end,u} = l_{t,pl} \cdot \varepsilon_{sm,pl} = l_{t,pl} \cdot 0{,}5 \cdot \varepsilon_{su} = 44{,}1 \cdot 0{,}5 \cdot 0{,}10 = 2{,}20 \text{ mm}$$

Hence, in this example a local reduction of the cross-sectional area of about 20 % results in a reduction of the deformation capacity with more than 80 % of that of a corresponding tie bar with constant diameter. This drastic decrease of the deformation capacity due to a local weakness near the joint section has been confirmed by test results [Bäckström (1993) and Engström (1992)]. In cases where threads are needed, it is in this respect better to use bars that are threaded all along the length. If in the example above a fully threaded bar is used the deformation capacity is determined as

$$l_{t,pl} = \frac{f_u - f_y}{\tau_{bm,pl}} \cdot \frac{\phi_{red}}{4} = \frac{650 - 500}{1{,}51} \cdot \frac{9}{4} = 224 \text{ mm}$$

$$s_{end,u} = l_{t,pl} \cdot \varepsilon_{sm,pl} = l_{t,pl} \cdot 0{,}5 \cdot \varepsilon_{su} = 224 \cdot 0{,}5 \cdot 0{,}10 = 11{,}2 \text{ mm}$$

In this case the effect of the reduced diameter is less than 10 %.

For tie bars with a smaller hardening ratio f_u/f_y it is even possible that a local reduction of the diameter causes the bar to rupture in the weakened section before yielding is reached in the adjacent part with a full cross-section. In that case no yield penetration is obtained outside the weakened region and the maximum extension of the plastic zone will also be restricted to this region. This results in very small ultimate displacements.

7.2.4.3 Detailing of anchor bars

The purpose of anchor bars is mainly to transfer tensile forces through the connection. The detailing of anchor bars and other connection details should be such that the force path in the ultimate limit state is sound and safe in spite of cracks that might develop, especially in the ultimate state. It

should normally be possible to reach yielding of the anchor bar without premature failures limiting the capacity of the connection. The design approach according to Section 3.6 'Balanced design for ductility' is generally recommended. It means that anchorage lengths, welds etc. should be designed with sufficient overcapacity to control a ductile failure mode. The influence of probable crack locations must be considered.

The concrete cover should be adequate with regard to safe anchorage of the anchor bars, but also sufficient to protect the steel from corrosion and fire exposure. A common difficulty is that forces appearing at the edges of a concrete element should be transferred further into the element by the anchor bars. To achieve this, while keeping a proper concrete cover, the detailing requires careful consideration [Loov (1978)]. The connection details tend to straighten when loaded in tension and this is true also for a chain of details linked together. Bends of bars may cause splitting effects initiating cracks and degradation of the connection zones. Therefore, not only the resistance of details should be selected properly, but the deformed shape of the connection details in the ultimate state should be considered and the equilibrium system should be checked, for instance by a strut and tie model as explained in Section 3,4. As much as possible straight anchor bars without bends and simple straight forward force paths should be preferred. The anchor bars should be designed to act in tension only. Furthermore, welds should be designed, arranged and executed such that the ductility of the connection is not jeopardised.

7.2.5 Indirect anchorage

7.2.5.1 Design principles

Indirect anchorage means that tie bars are anchored in grouted sleeves, recesses, joints etc, instead of being cast and embedded directly into the concrete element or cast *insitu* concrete, such as a foundation structure for instance. It means that the tensile force in the bar has to be transferred by shear to the grout fill and further by shear across the interface between the grout fill and the surrounding concrete. Hence, the tensile capacity of such connections could be determined by pull-out failure of the bar in the grout fill, shear failure along the interface between the grout fill and the surrounding concrete (pullout of grout fill), splitting failure in the surrounding concrete or steel failure of the tie bar.

In general the anchorage capacity of indirectly anchored bars should not be less than of directly anchored bars. This may require an increased anchorage length and other precautions to compensate for less strength of the grout fill, risk of cracks in joints used for indirect anchorage, uncertainties of complete encasing of the projecting bar and quality of execution. However, the design and the procedures at the site should always facilitate a complete encasing of high quality. For instance should the width of sleeves and joints be sufficient to meet deviations in the location of the projecting bars within specified tolerances.

The anchorage of the indirectly anchored tie bar can in many cases be regarded as a lap splice between the tie bar and meeting reinforcement in the surrounding concrete. As in ordinary lap splices subjected to tension the force is transferred from one bar to the other by inclined compression as shown in a simplified way in Fig. 7-35. This is associated with an outward pressure, which must be balanced by tensile ring stresses in a similar way as shown in Fig. 7-17 around a single anchored bar. If the grouted sleeve or joint is well embedded in concrete of substantial dimensions, this concrete confinement can be sufficient to provide support to the outward pressure without a risk of splitting cracks. However, if the sleeve is placed near a free face, splitting cracks may occur through the concrete cover. This could result in an anchorage failure (splitting of the surrounding concrete). Transverse reinforcement around the anchorage zone can be used to provide confinement in concrete in spite of cracks, compare with the bond-stress slip relations in Fig. 7-21 b.

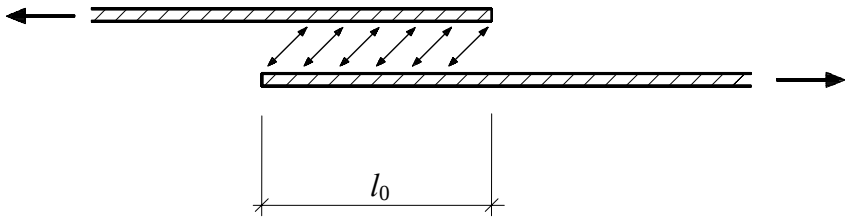

Fig. 7-35 Transfer of forces between bars in lap splice through inclined compression, simplified representation

Indirect anchorage is often a favourable method, because of its simplicity and few details involved. In some applications it is also the only possible way to provide anchorage of tie bars in precast elements. The most common applications with vertical grouted sleeves are column base connections and column splice connections and corresponding connections for wall elements. Indirect anchorage of horizontal tie bars is mainly used in hollow core floors where longitudinal grouted joints or grouted cores of the elements are used. However, indirect anchorage can be used elsewhere when needed.

7.2.5.2 Projecting bar in vertical grouted sleeves

In column base connections and column splice connections the lower concrete element, or the foundation, has projecting reinforcement bars, which fits into sleeves in the upper element as shown in Fig. 7-36 a. The upper element is lowered into position and temporarily braced during grouting. A levelling pad must be provided for correct position in the vertical direction. The detailing and the execution should ensure that in the competed connection there is no concentration of vertical stresses caused by the levelling pad.

The opposite solution is also possible, i.e. the upper element has projecting bars, which fit into sleeves in the foundation, Fig. 7-36 b. The latter solution gives a very simple detailing of the column, since no ducts and no reinforcement splice need to be prepared there. However, the holes in the base must be protected from dirt and water, which could jeopardise the grouting. In both cases temporary bracing is needed.

These connections may be considered in design as monolithic providing the anchorage length (lap length) is sufficient and the bedding joint and grout sleeves are completely filled. For both solutions the number of projecting bar is limited because of the limited space to place sleeves with appropriate spacing and cover to free edges.

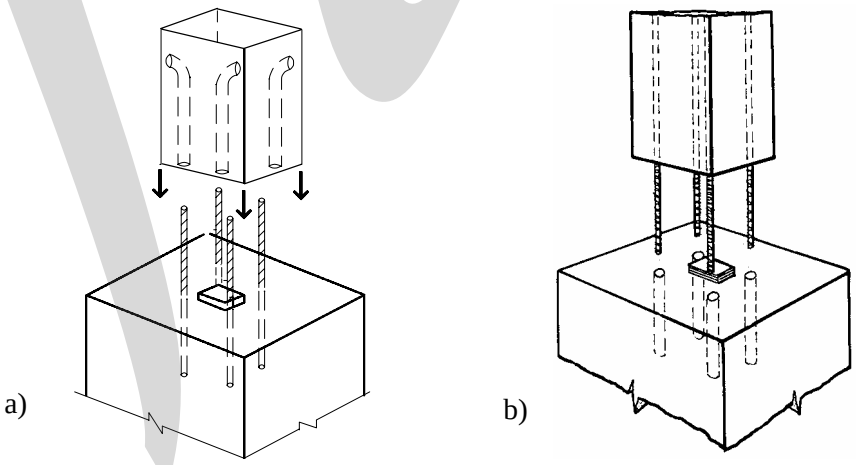

Fig. 7-36 Column base connections with projecting reinforcement bars in grouted sleeves, a) bars projecting from the base, b) bars projecting from the column

When the grouted sleeves are placed in the upper element, the grout can either be poured from the top, as shown in Fig. 7-37 a, or the sleeve if grouted by pressure from the bottom. In the latter case vent holes are needed in the top, see Fig. 7-37 b. The appearance of the grout at the vent hole is also used as an indication of complete filling. When the column has projecting reinforcement bars, the sleeves are filled with grout before the column is lowered into final position.

Various types of grout are possible to use, but the following information refers mainly to cement based grouts. For other types of grouts reference is made to CEB (1997).

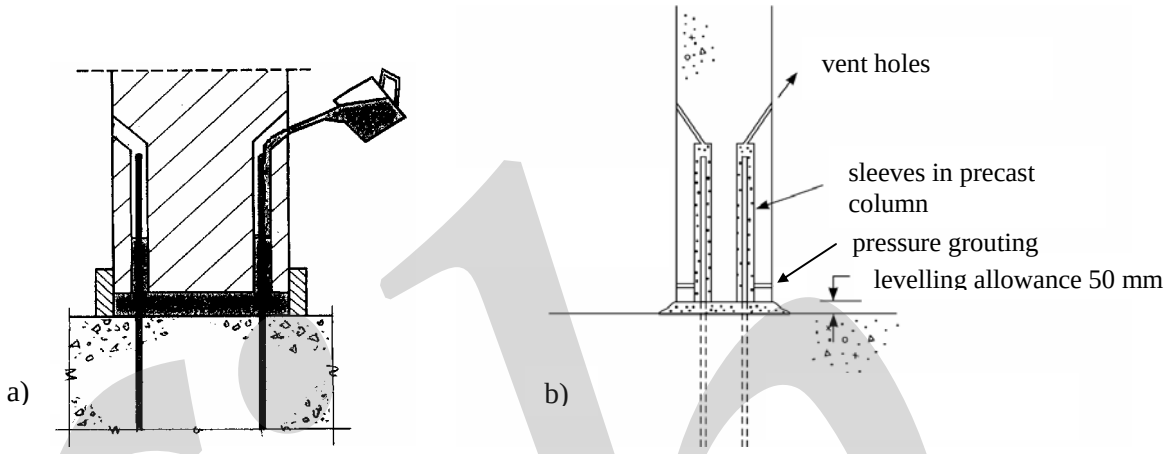

Fig. 7-37 Grouting of sleeves, a) pouring of grout from the top, b) detailing in case of pressure grouting from the bottom

These types of connections require good workmanship. The projecting bar should be completely encased by grout, which is impossible to inspect. Accuracy in erection can be difficult to achieve and it is also difficult to adjust the connection afterwards.

To ensure good bond between the grout fill and the surrounding concrete the surface of the duct should not be smooth. The sleeves, protruding details and element faces should be clean before grouting. The grout should have an adequate fluid consistence to ensure complete filling. Ducts formed by cast *insitu* corrugated steel tubes are preferred. It is recommended that the inner diameter of the duct is at least 30 mm greater than the diameter of the projecting bar to ensure complete encasing of the bar and also to avoid air pockets forming. The tube should have a minimum concrete cover equal to its diameter and the free distance between ducts should not be less.

When precast columns are connected to cast *insitu* foundations, there is also a need for information transfer and interaction between subcontractors in order to have the protruding bar in the correct position for mounting of the columns. An alternative solution is to drill the holes in the cast *insitu* foundation just before the columns are placed.

Basically the same solutions can be used for columns splice connections and to connect wall elements above each other and to the base. Examples of column connections with grouted sleeves are shown in Figs. 9-13, 9-25, 9-31. Fig. 7-38 shows examples of wall connections with projecting bars anchored in grouted sleeves. In these solutions the lower element is provided with a threaded insert and the projecting bar is mounted during erection. In this was the transport and handling of the wall elements are not hindered by protruding details. The connection at the exterior wall in Fig. 7-38 b also includes a horizontal tie bar with indirect anchorage to a hollow core floor unit.

In wall to base connections and wall to wall connections two cases should be distinguished. In the first case the connection should be able to transfer a tensile force with regard to certain load cases which creates tension in a part of the wall or with regard to minimum requirements concerning tying systems as explained in Section 5.2.3. The tie bar should be anchored accordingly and a continuous tying system should be assured. In the other case the connection transfers primarily compression and the bar is used mainly for positioning and simpler fixation. To mobilise shear capacity by dowel action the embedment length can be considerably shorter compared to a tensile resistant connection. Examples of such connections are shown in Figs. 6-2 h, 6-2 i and 6-2 j. In those wall to wall connections the bar has indirect anchorage both upwards and downwards.

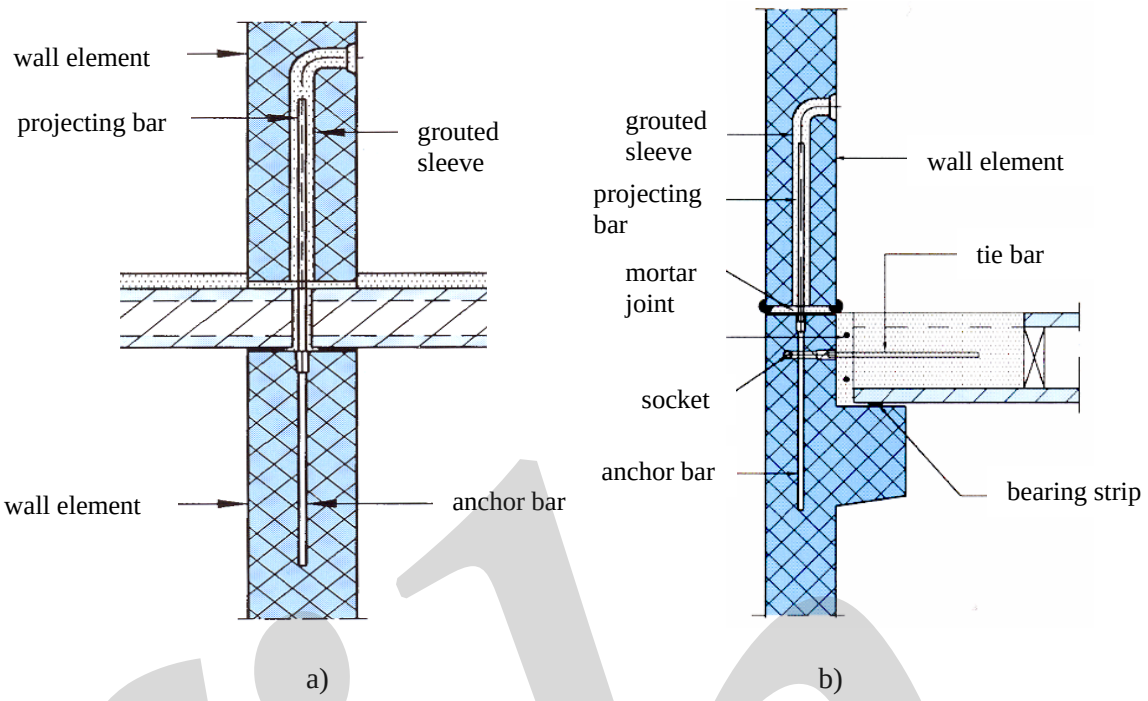

Fig. 7-38 Examples of wall to wall connections with projecting bars in grouted sleeves, a) interior connection, b) exterior connection

7.2.5.3 Anchorage of tie bars in precast hollow core floors

Tie bars indirectly anchored in horizontal joints or sleeves appear in connections between floor elements across transverse joints and between floor elements and exterior supports. The most typical example is connections in hollow core floors where tie bars are anchored either in longitudinal grouted joints, Fig. 7-39 a, or in cores that are opened from the top by a slot, Fig. 7-39 b. At interior supports anchorage in grouted joints is often preferred unless full or partial moment continuity is aimed at, as explained in Section 9.6. At exterior support anchorage in cores is often preferred and Fig. 7-38 b shows one example of this.

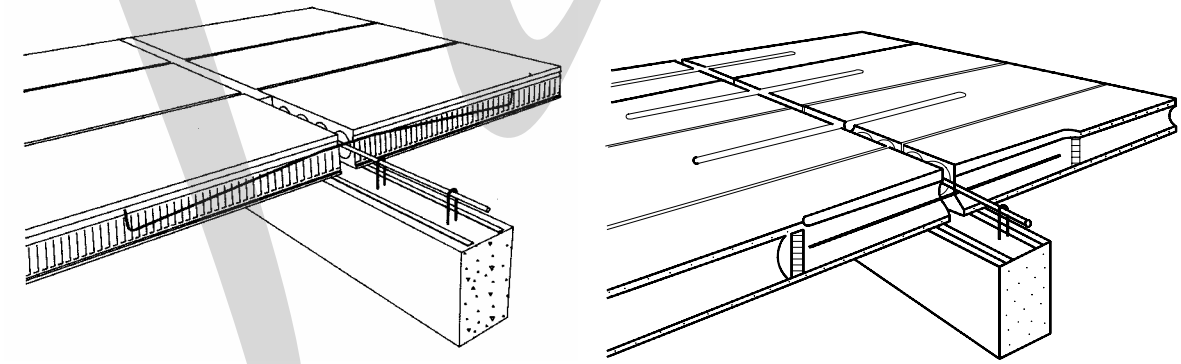

Fig. 7-39 Indirectly anchored tie bars in hollow core floors, a) anchorage in longitudinal joints, b) anchorage in cores opened by a slot in the top

On the basis of experimental results recommendations for arrangement of tie bar in hollow core floors were presented in FIP recommendations for precast prestressed hollow core floors [FIP(1988)].

Anchorage in cores

As always in case if indirect anchorage a complete encasing of the anchored bar should be ensured. Of this reason the bar should never be placed directly at the bottom of the core. At exterior supports a correct level of the tie bar can be ensured by bent-down stirrups or threaded inserts as exemplified in Fig. 7-38 b.

For indirect anchorage of tie bars in cores filled with grout or concrete the interface seems not to be critical for the anchorage capacity. It is rather splitting failure in the surrounding concrete that limits the anchorage capacity. This means that basically the same principles can be adopted as for direct anchorage in concrete elements. The required anchorage length $l_{b,net}$ can be determined according to eq. (7-32). Normally, the concrete cover is well above 3ϕ, which means that eq. (7-33) is applicable. It is recommended to consider the anchorage as a lap splice between the tie bar and the main reinforcement of the hollow core unit and hence increase the anchorage length by a distance equal to the spacing of the spliced units. In design for ductility an additional length should also be provided to allow for full yield penetration according to eq. (7-34). In cases when unintended restraint must be considered, the total length of the infill in the core should not be less than a critical length as defined in Section 3.5.2.2. The reason is to avoid sudden changes of the cross-section in regions where there is a risk of flexural cracks starting from the top.

When considerable tensile forces have been introduced into a hollow core element by tie bars anchored in concreted cores, splitting of the end region of the element has been observed occasionally in tests. The splitting cracks then developed in a horizontal plane along the tie bars. The tensile stresses that may appear in a hollow core element from anchored tie bars will be added to other tensile stresses that exist in the end region due to transfer of the prestressing force, shear, torsion, restraint from the support etc. Therefore, the risk of a splitting failure may be difficult to evaluate accurately. However, it may be assumed that the total transverse force in the vertical direction within the anchorage zone has a magnitude of about half the anchored force. This force has to be resisted by the concrete in a horizontal section including the infill.

For indirect anchorage of tie bars in concreted cores of extruded prestressed hollow core elements with a cross-sectional depth of h = 265 mm, it is recommended in FIP (1988) that the total tensile capacity (determined on basis of the characteristic yield strength) of the anchored tie bars should be limited to

$$\sum f_{yk} A_s \le 160 \text{ kN (in one element)}$$
$$\sum f_{yk} A_s \le 80 \text{ kN (in one concreted core)}$$

Anchorage in joints

When tie bars are anchored in grouted longitudinal joints between hollow core elements additional measures should be taken to ensure an efficient anchorage. To ensure complete encasing of the indirectly anchored tie bar, the bar should not be placed directly at the bottom of the joint. Therefore a minimum distance from the bottom edge of 40 mm is recommended, see Fig. 7-40. Furthermore, the width of the joint at the level of the bar should not be too small. A minimum width of two times the bar diameter, not less than 25 mm, is recommended. The consistence of the joint grout should be fluid enough to ensure a complete filling of the joint and a complete encasing of the tie bar.

When tie bars are anchored in longitudinal joints splitting failure within the joint is a possible failure mode. To ensure sufficient anchorage the bar should be placed with sufficient concrete cover in the vertical direction and be confined by transverse reinforcement (tie beams) in the horizontal direction. To have as good confinement as possible, in order to avoid splitting failure in the joint infill, it is recommended to anchor the bar between the horizontal shear key and the bottom nibs of the joint face as indicated in Fig. 7-40 a. If the shear key is located near the bottom of the hollow core element, the bar should be anchored in the lower half of the joint, see Fig. 7-40 b. At intermediate supports on inverted T-beams for example, it may be necessary to place the bar in a higher a position

above the beam. In such cases the bar should be bent down to be anchored in a safe region and the unsafe zone should be disregarded in the design of anchorage. This design principle is illustrated in Fig. 7.41. The detail shown in Fig. 7-41 facilitates a correct placement of the bar, since the bar is pressed down in the fresh grout until the end hooks disappear below the surface.

Furthermore, to secure the integrity of the longitudinal joint and provide confinement, transverse tie bars should be placed across this joint in the adjacent support joints. The yield capacity of the transverse ties should be at least the same as that of the considered longitudinal tie bar.

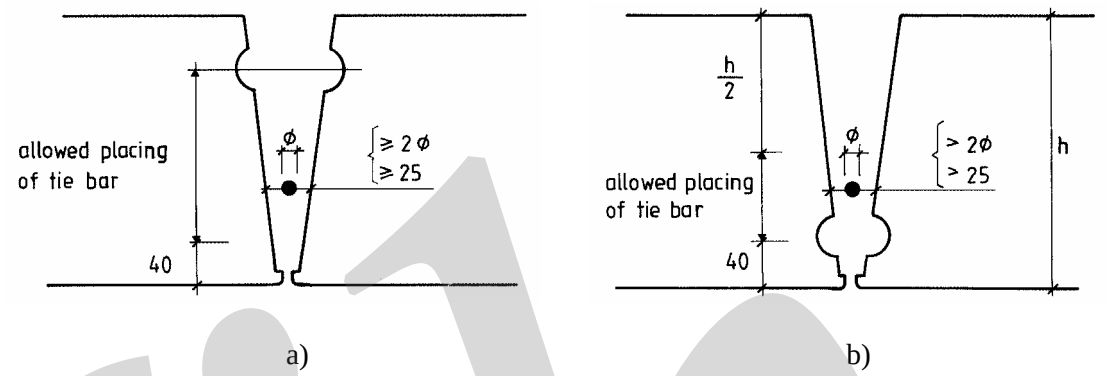

Fig. 7-40 Recommended placing of tie bars anchored in grouted joints between hollow core elements, according to FIP (1988), a) shear key in the upper part, b) shear key in the lower part

It would be possible to calculate the required anchorage length from eqs (7-32) and (7-34) assuming other bond conditions than good and minimum concrete cover in the transverse direction. For a concrete grade of C20 and tie bar with f_{yk} = 500 MPa this would result in an anchorage length $l_{b,net}$ of about 50ϕ. However, with regard to the uncertainties concerning the anchorage capacity in grouted joints, which may be cracked of other reasons, the following anchorage lengths are recommended [FIP (1988)].

$l_{b,tot} \geq 100\phi$ when the tie bar has straight ends

$l_{b,tot} \geq 75\phi$ when the tie bar has end anchors (hooks or bends)

Furthermore, the total tensile capacity of tie bars (determined on basis of the characteristic yield strength) anchored in one grouted longitudinal joint should be limited to

$\sum f_{yk} A_s \leq 80$ kN (in one grouted joint)

End anchors are recommended when the total tensile capacity of the anchored bars in one joint is greater than 40 kN (determined on the basis of the characteristic yield strength) and always in design with regard to progressive collapse. The end anchor provides an extra reserve and should make it possible to take advantage of the full plastic capacity of the bar, i.e. reach rupture of the steel.

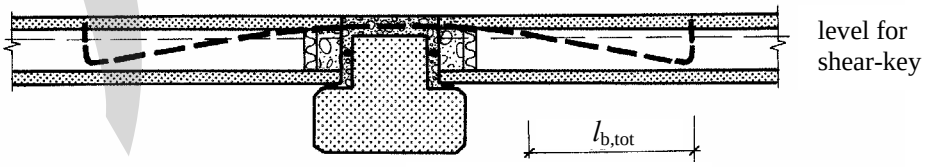

Fig. 7-41: Only the part of the tie bar which is placed in the allowed region, see Fig. 7-41, should be considered in design of the anchorage

7.3 Headed bar

7.3.1 Anchorage behaviour and failure modes

Anchor bars with anchor heads can be made of bolts with a fixed bolt head as anchor head, threaded bars with a threaded nut as anchor head, or studs with coldworked anchor heads. Bolt heads or nuts can be combined with washers and plates to increase the dimension of the effective end anchor. Groups of closely spaced headed bars are typically connected through surface plates or rolled sections, as shown in Fig. 7-8.

The failure due to tensile loading can be rupture of the steel shaft, thread stripping in case of threaded parts, and anchorage failure in the concrete. According to the CEB State of art report [CEB (1994)] anchorage failures can appear as concrete cone failures (Figs. 7-11 and 7-37 a), pullout failures where the anchor head slips in the concrete (Fig. 7-42 b), local 'blow-out' failure or global splitting failure. If the anchor head is placed near a free edge of the concrete member, the radial compressive stresses around the anchor head may cause a local sideway 'blow-out' failure in the concrete cover (Fig. 7-42 c). This failure reminds on the splitting failure around anchored ribbed bars, see Fig. 7-17. However, in case of headed anchors, the splitting effect is localised to the anchor head. The global splitting failure is characterised by splitting cracks in a plane through the anchor bar. This failure can occur when the concrete member has small dimension (Fig. 7-42 d) relative to the headed anchor. The various failure mechanisms and their main influencing parameters are described in the following sections.

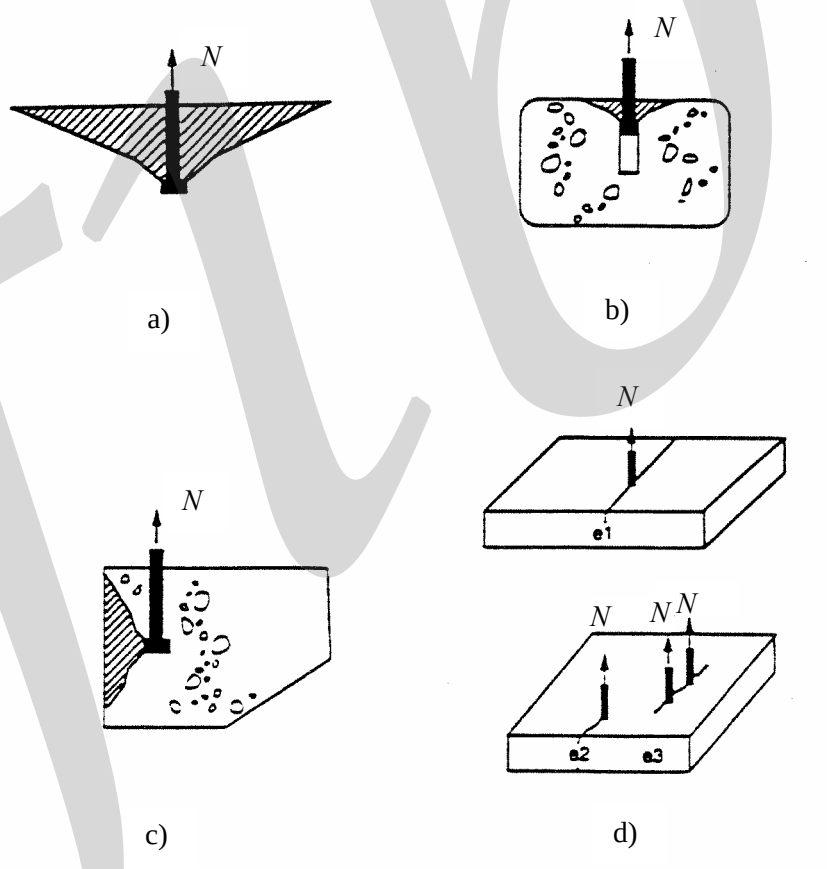

Fig: 7-42: Various types of anchorage failures that are possible for headed anchors, a) concrete cone failure, b) pullout failure, c) splitting failure, local splitting, d) splitting failure, global splitting, adopted from CEB (1994)

Normally anchorages and anchorage zones in structural connections are designed in order to prevent thread stripping, pullout and splitting failures. Anchorage failures can be avoided by a proper choice of the edge distance c_e (transverse distance between anchor bar and free edge), anchorage depth

l_a, diameter ϕ_h of the anchor head, and spacing s between anchors in case of anchor groups. For a headed anchor bar the anchorage depth is defined as the clear distance between the concrete face to the anchor head. Expressions to determine the anchorage capacities for various types of anchorage failures are presented in the following sections.

If a ductile behaviour is required, a balanced design for ductility should be applied. This means for instance that the anchor bar is identified as the ductile component, ductile steel is selected for the anchor bar, and the anchorage, welds and other components of the connection should be designed to obtain an over-capacity relative to the ductile component, compare with Section 3.6.

It should be noted that a design preventing anchorage failures does not ensure a ductile behaviour in the ultimate state, also the steel needs to be of a ductile type.

The end-slip of a well anchored headed anchor bar depends on the elongation of the anchor shaft possibly in combination with a certain displacement of the anchor head due to local crushing under high bearing stresses. The displacement of the anchor head depends on its dimensions, but with normal proportions of headed anchors the design is such that high bearing stresses are utilised. An example of end-slip response of a fully anchored headed anchor of ductile type is presented in Fig. 7-43, which also shows the simultaneous displacement of the anchor head.

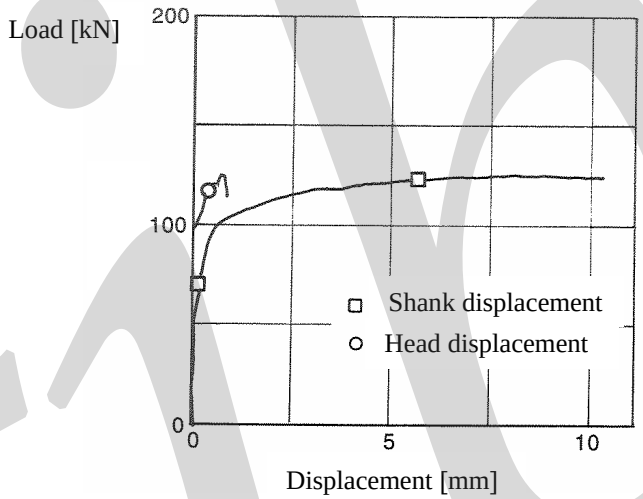

Fig: 7-43: Example of relationship between tensile force and end-slip for a fully anchored headed anchor of ductile type, adopted from Collins and Klingner (1989)

Appropriate and general methods for design of headed anchors with regard to various types of failures have been presented in a CEB Design Guide [CEB (1997)]. The design is based on the 'Concrete Capacity Design (CCD) Approach' [Fuchs, Eligehausen and Breen (1995)]. The method is developed and generalised from the so called 'ψ-method' or 'κ-method' for estimation of the anchorage capacity of headed anchors in case of concrete cone failure. This method, proposed by Eligehausen *et al.* (1987), Eligehausen and Fuchs (1988) and Rehm *et al.* (1988), is based on a large number of test results with various anchorage lengths and concrete strengths. The ψ-method is characterised by the way of considering negative influences on the anchorage capacity by multiplying the basic anchorage capacity of a single anchor in a favourable reference situation with various influence factors ψ. When several influences appear simultaneously, the combined effect is found by multiplying the respective reduction factors for each of the influences. The method has been found to give good agreement with experimental results.

Expressions for the most common cases of headed anchors are given here below. However, for full use of this design method, for instanced in case of other types of anchors, reference is made to the CEB Design Guide [CEB (1997)].

7.3.2 Concrete cone failures

The concrete cone failure can be described as a 'punching' failure resulting from the concentrated force introduced to the concrete by the anchor head. The concrete body released by the 'punching' has a conic shape. The cone angle, i.e. the angle between the centroidal axis of the cone and the crack, is normally about 30° - 40°, see Fig. 7-44 a. Typically, the cone angle is greater, about 45°, near the anchor head, but decreases successively along the crack on its way towards the concrete face. Furthermore, the cone angle seems to be decrease with an increased anchorage depth.

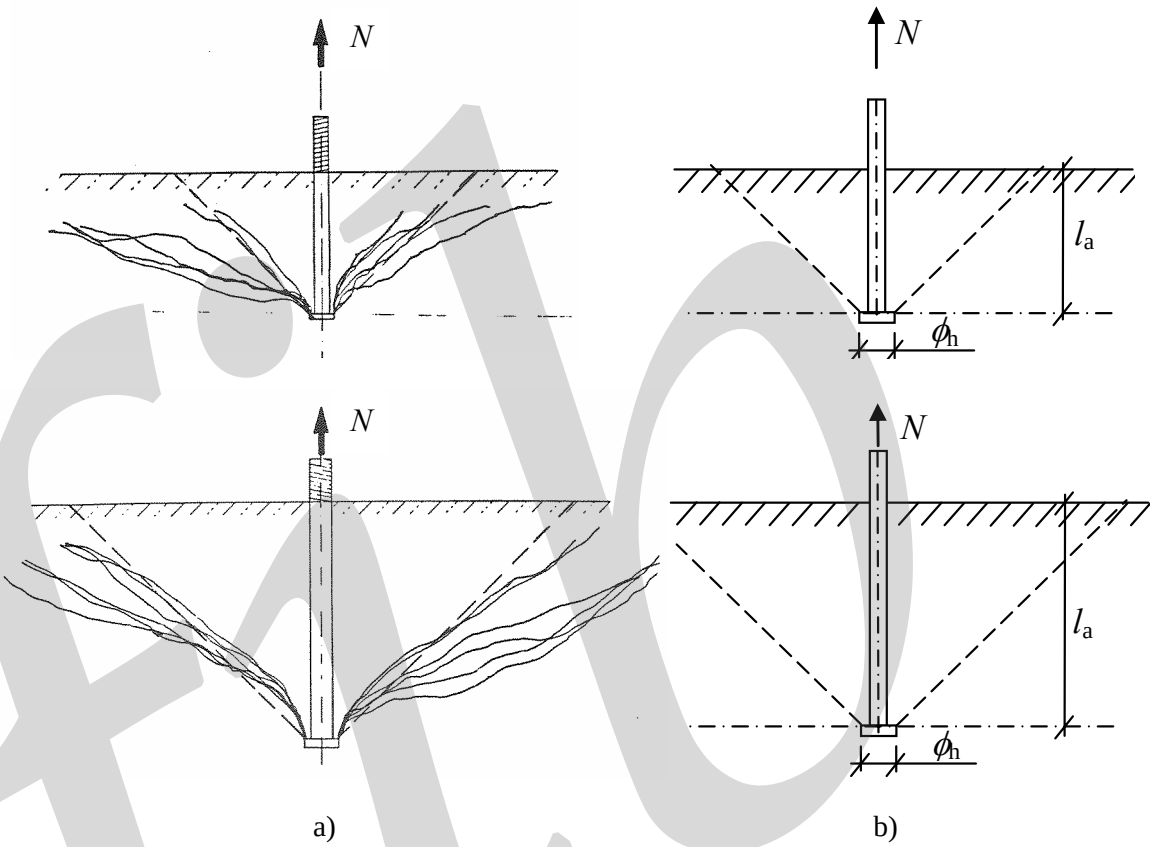

Fig. 7-44: Concrete cone failure for headed anchor bars, a) observed failure cone profiles [Eligehause, Sawade (1989)], b) idealised geometry of concrete cone

The traditional approach to estimate the anchorage capacity is based on the assumption that the cone angle is 45° and that the released concrete body has a perfect conic shape as shown in Fig. 7-44 b. Then the area of the assumed tensioned section A_{ct} can be determined as

$$A_{ct} = \pi \cdot l_a (l_a + \frac{\phi_h}{2}) \sqrt{2}$$

Furthermore, it is assumed that a uniformly distributed tensile stress, equal to the tensile strength, develops perpendicular to the crack just before failure. Then a basic estimation of the anchorage capacity can be determined as the resulting force in the direction of the anchor bar as

$$N_{R,est} = \frac{A_{ct} \cdot f_{ct}}{\sqrt{2}} \tag{7-36}$$

The concrete tensile stress is often assumed to be related to the compressive strength by $f_{ct} = \beta\sqrt{f_{cc}}$ (with f_{ct} and f_{cc} in [MPa]). If this relationship is adopted in eq. (7-36) and the influence of the anchor head diameter on the area of the cracked section is ignored, the anchorage capacity can be expressed as

$$N_{R,est} = \beta \cdot \pi \cdot l_a^2 \cdot \sqrt{f_{cc}} \tag{7-37}$$

However, comparisons with test results [CEB (1994)] have shown that the anchorage capacity is over-estimated by eq. (7-37) when the anchorage length is greater than 200 mm. The poor agreement depends mainly on a too simplified assumption concerning the stress distribution in the cracked section at failure.

According to CEB (1994) analyses based on fracture mechanics show that the failure process in case of concrete cone failures is characterised by a stable and successive crack development along the failure cone. The crack development starts when the tensile force is about 20 - 40 % of the ultimate capacity. When the ultimate load is reached, the crack has only reached about 15 - 20 % of the final failure cone, where the smaller number refers to longer anchorage lengths. The ultimate anchorage capacity depends on the modulus of elasticity E_c and the fracture energy G_f of the concrete. For a certain value of the fracture energy, the anchorage capacity is almost independent of the tensile and compressive concrete strengths. In empirical expressions for the anchorage capacity, both the modulus of elasticity and the fracture energy can be assumed being related to $\sqrt{f_{cc}}$.

Since the concrete cone failure depends on the successive crack development in the concrete, the anchorage behaviour should preferably be analysed by methods based on non-linear fracture mechanics. However, to estimate the anchorage capacity only, it is convenient to apply simplified expressions directly. For normal applications the 'ψ-method' and the 'CCD-approach' give good agreement with test results and better than the traditional approach according to eq. (7-37).

According to the CEB Design Guide [CEB (1997)] it is assumed that the cone angle of the concrete cone is 35°. With this assumption it is found that fully developed concrete cones will develop when the edge distance c_e and the spacing s between adjacent anchors fulfil the conditions

$$c_e \geq c_{e,crit} = 1{,}5 \cdot l_a \quad \text{and} \quad s \geq s_{crit} = 3 \cdot l_a \tag{7-38}$$

For such a **cast-in-place** headed stud or headed anchor bolt, with an anchorage depth $l_a \geq 100$ mm, the design value $N_{Rd,0}$ of the anchorage capacity can be determined as:

$$N_{Rd,0} = 5{,}0 \cdot l_a^{1,5} \cdot \sqrt{f_{ck}} \quad (f_{ck} \text{ in [MPa]}) \quad \text{(for anchorage in cracked concrete)} \tag{7-39a}$$

$$N_{Rd,0} = 7{,}0 \cdot l_a^{1,5} \cdot \sqrt{f_{ck}} \quad (f_{ck} \text{ in [MPa]}) \quad \text{(for anchorage in uncracked concrete)} \tag{7-39b}$$

The design resistance is here calculated assuming a partial safety factor for the resistance, see CEB (1997)

$$\gamma_{Mc} = \gamma_1 \cdot \gamma_2 \tag{7-40}$$

where $\gamma_1 = 1{,}8$ (partial safety factor for concrete loaded in tension, $\gamma_1 = 1{,}2 \cdot \gamma_c$
$\gamma_2 = 1{,}0$ (partial safety factor for installation safety, for cast-in-place headed anchors $\gamma_2 = 1{,}0$ applies as a first indication

If the spacing s between two headed bars is smaller than the critical spacing s_{crit}, eq. (7-38), the failure cones that start from each of the anchor heads will overlap, which results in a decreased capacity, see Fig. 7-45 a. The capacity is also decreased if the headed anchor is placed a distance c_e smaller than the critical distance $c_{e,crit}$ from a free edge because the failure cone will be incomplete

(truncated), see Fig. 7-45 b. For such a design situation the anchorage capacity of an anchor or an anchor group is determined as

$$N_{\mathrm{Rd}} = N_{\mathrm{Rd},0} \cdot \psi_{\mathrm{A}} \cdot \psi_{\mathrm{s}} \psi_{\mathrm{e}} \tag{7-41}$$

where $\psi_{\mathrm{A}} = \dfrac{A_{\mathrm{ct},0}}{A_{\mathrm{ct}}}$

$A_{\mathrm{ct},0} = s_{\mathrm{crit}}^2$ (base area of the concrete failure cone idealised as a pyramid)

A_{ct} = base area of the concrete failure cone, idealised as a pyramid, for the whole group of headed anchors and truncated by free edges, see Fig. 7-45

$$\psi_{\mathrm{s}} = 0{,}3 + \frac{0{,}7 c_{\mathrm{e}}}{c_{\mathrm{e,crit}}} \qquad \leq 1$$

$$\psi_{\mathrm{e}} = \frac{1}{1 + 2\, e / s_{\mathrm{crit}}} \qquad \leq 1$$

e = eccentricity of the resulting tensile force acting on the tensioned anchors relative to the gravity centre of the tensioned anchors

The border lines of the rectangular base area A_{ct} are located at a distance $c_{\mathrm{e,crit}}$ from the corner anchors in the anchor group, but limited by the edges of the concrete member, see Fig. 7-45.

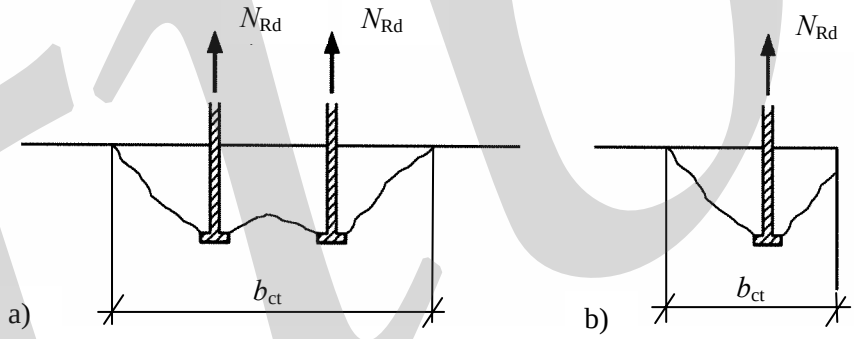

Fig. 7-45: Reduced anchorage capacity for anchor bars and corresponding width b_{ct} of the base area A_{ct},
a) overlapping failure cones in case of small anchor spacing
b) truncated failure cone due to small edge distance

The anchorage capacity for concrete cone failures estimated according to eqs. (7-39) - (7-41) refers mainly to the anchorage capacity of plain (unreinforced) concrete. According to CEB (1994) ordinary surface reinforcement, for instance mesh reinforcement, gives no important increase of the anchorage capacity. In order to obtain a considerable increase of the anchorage resistance specially arranged reinforcement is needed, for instance closely spaced reinforcement loops that anchor the failure cone back to the concrete beneath the anchor head. These reinforcement loops should be placed parallel to the anchor bar and should preferably enclose transverse surface reinforcement. It should be noted that the connection design concerns not only the connecting device, but the force introduced by the headed bar belongs to a force path that must be secured. The connection zone and the structural elements must be designed accordingly. In this respect the design of the connection zone reminds on the case with local compression and strut-and-tie models can be used to design of suitable splitting reinforcement, see Fig. 7-46. With regard to the force transfer into the concrete elements alternative solutions with bonded bars, see Fig. 7-8, should also be considered.

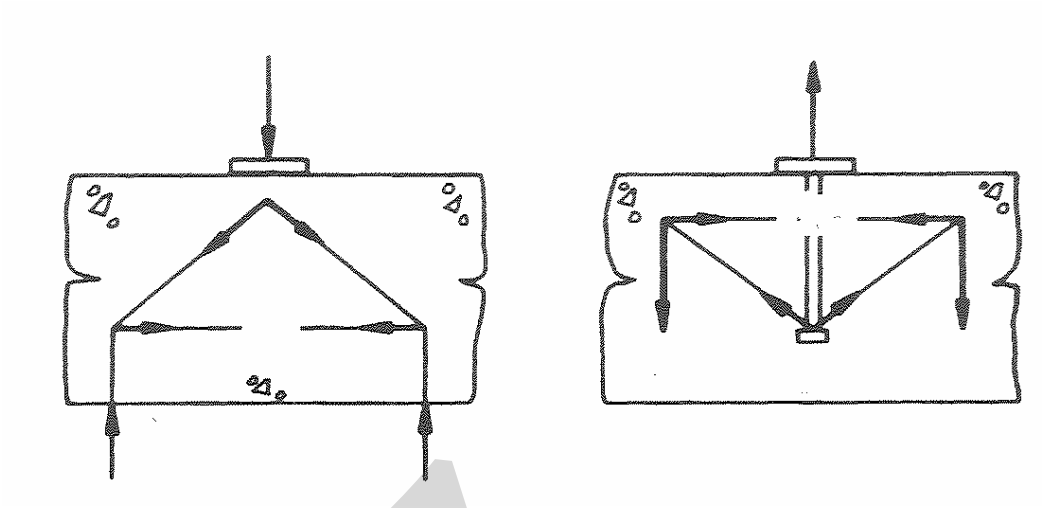

Fig. 7-46: Examples of strut-and-tie models for design of connection zones, a) local compression at the edge, b) local compression at the anchor head, acting towards the free edge and must be tied back into the element

In CEB (1997) there is also possible to consider a reduced anchorage capacity in case of short anchorage depth, less than 100 mm, due to surface reinforcement.

7.3.3 Pullout failures

A pullout anchorage failure (see Fig. 7-42 b) may occur when the dimension of the anchor head is too small relative to the bar diameter and the anchor depth and edge distance and anchor spacing are sufficient to prevent splitting failure. In a deep anchorage, the concrete near the anchor head is well confined and splitting cracks will not develop. In the pullout failure, the concrete in front of the anchor head is subjected to a very high contact pressure that results in pulverisation of the concrete locally in front of the anchor head. Hence, the anchor head will penetrate the concrete and, consequently the headed anchor slips in the concrete under more or less constant load. Since the anchor depth decreases successively, a concrete cone failure will finally develop, as indicated in Fig. 7-42 b.

The contact pressure p_h in front of the anchor head can be estimated as

$$p_h = \frac{N_h}{A_h}$$

where $N_h =$ tensile force applied to the anchor

$$A_h = \frac{\pi(\phi_h^2 - \phi^2)}{4} \qquad \text{(bearing area)}$$

Since the loaded contact area is well encased by confined concrete, a considerable contact pressure can be reached before the anchor head starts to slip. The critical contact pressure $p_{h,crit}$, for which a pullout failure occurs, is not fully known. According to CEB (1994) critical contact pressures evaluated from experiments have been in the magnitude of 12 f_{cc} - 15 f_{cc}, but an influence of the contact area has also been observed.

For a **cast-in-place** headed stud or headed anchor bolt, the design pullout resistance according to CEB (1997) is determined as

$$N_{Rd} = 4{,}2 f_{ck} A_h \qquad \text{(for anchorage in cracked concrete)} \qquad (7\text{-}42a)$$

$$N_{Rd} = 6{,}1 f_{ck} A_h \qquad \text{(for anchorage in uncracked concrete)} \qquad (7\text{-}42b)$$

The design resistance is here calculated assuming a partial safety factor for the resistance according to (7-40)

7.3.4 Local 'blow-out' and splitting failures

The concentrated anchorage force applied to the concrete by the anchor head results in inclined compressive stresses that radiate out from the anchor head towards the free edge. The magnitude of these compressive stresses increases with increased contact pressure in front of the anchor head. In order to keep equilibrium in the anchorage zone, these inclined compressive stresses must be balanced by tangential tensile stresses in the anchorage region. These tensile stresses may cause splitting cracks.

If the transverse distance between the headed anchor and a free edge is too small, splitting cracks may develop transversally from the anchor head towards the free edge. As a result, a local concrete body may be released and split off side-ways, see Fig. 7-42 c. The maximum anchorage capacity for this type of failure is not influenced by the anchorage length, but increases with increased transverse distance from the free edge.

According to CEB (1997) it may be assumed that a local blow-out failure will not occur if the edge distance fulfils

$$c_e > 0{,}5 \cdot l_a$$

For cases where this condition is not fulfilled CEB (1997) presents a method to determine the anchorage capacity.

In properly designed reinforced concrete elements splitting cracks can be accepted if the reinforcement is designed to enable equilibrium with the load in cracked concrete. Hence, it is stated in CEB (1997) that it is not necessary to check the resistance due to splitting failure if the two following conditions are fulfilled.

(1) Reinforcement is present which limits the crack width to a normal value about 0,3 mm, taking into account the splitting effects, see example in Fig. 7-46.
(2) The anchorage resistances for concrete cone failure and pullout failure are determined assuming cracked concrete.

If these conditions are not fulfilled the anchorage resistance due to global splitting failure must be calculated. An appropriated method is given in CEB (1997).

7.4 Continuous tie bars

7.4.1 Ribbed bars

In connections designed and detailed for tensile force transfer, the joint sections are often considerably weaker than the sections through the connected structural elements. This is typically the case for connections that are part of overall tying systems. Hence, when the connection is strained in tension, the first tensile crack can be expected in one of the joint interfaces. When the load increases the capacity of the strained tie bars is in normal cases insufficient to create other cracks in the connection zones. Hence, the deformations will be concentrated to the first crack, which opens up successively for increasing tensile force. This typical behaviour is shown in Fig. 7-47 for a tie connection provided with a continuous tie bar.

The behaviour of this type of tie connections is characterised by the relationship between the tensile force N and the relative displacement w (= the crack width). Examples of such relationships observed in pure tensile tests [Engström (1992)] are shown in Fig. 7-48. In these tests the continuous tie bars were made of ordinary ribbed reinforcement bars of type Ks40 (hot-rolled steel). The bar was cast directly into the two concrete elements separated by a single weak section. The dimension of the tie bars and the compressive strength of the concrete elements varied between the tests. In the tests

presented here, the anchorage capacity was sufficient to balance not only the yield capacity of the tie bars, but also the tensile capacity at steel rupture. This means that the plastic deformability of the steel could be fully used and a very ductile behaviour was obtained.

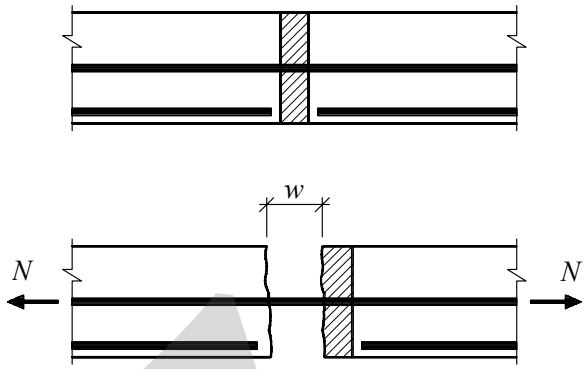

Fig. 7-47: Tie connection with a continuous tie bar. The deformations are concentrated to a single crack, which normally appears in one of the joint interfaces

It appears from the figure that it was possible to obtain a considerable relative displacement of some tens of millimetres before the tie bars fractured. When the anchorage conditions were similar, i.e. the same concrete strength of the concrete elements, the ultimate displacement w_u increased with increased dimension of the tie bar as shown in Fig. 7-48 a. For the same tie bar dimension, the ultimate displacement decreased with increased strength of the concrete elements, Fig. 7-48 b.

In the tests where the tie bars were made of hot-rolled reinforcement bars of type Ks40 (ribbed), Ks60 (ribbed) and Ss26 (smooth bars of mild steel with end hooks) had similar behaviour. This means that the load-displacement relationships were of the same type according to Fig. 7-30. This was true also for some few tests with cold worked reinforcement bars of type Ps50 (indented) and Ks90 (ribbed). In order to obtain steel rupture in the tests with smooth tie bars, these were anchored by end hooks. It was then possible to avoid pullout failure when the steel began to yield.

The crack width w of the joint section depends on the two end-slips s of the tie bar at each side of the crack. Hence, the crack width when yielding is reached w_y and the ultimate crack width at steel failure w_u can be determined as

$$w_y = 2s_{end,y} \tag{7-43 a}$$

$$w_u = 2s_{end,u} \tag{7-43 b}$$

For continuous tie bars the embedment length on each side of the transverse joint normally exceeds the transmission length. Consequently the characteristic values of the end-slip can be determined by the methods presented in Section 7.2.3**.**

In tie connections where continuous tie bars are placed across joints filled with joint grout or joint concrete, the connection contains two critical joint interfaces. It is normally assumed that only one of the two joint interfaces cracks and opens up as shown in Fig. 7-47 and that such tie connections can be treated as ‘single crack’ cases.

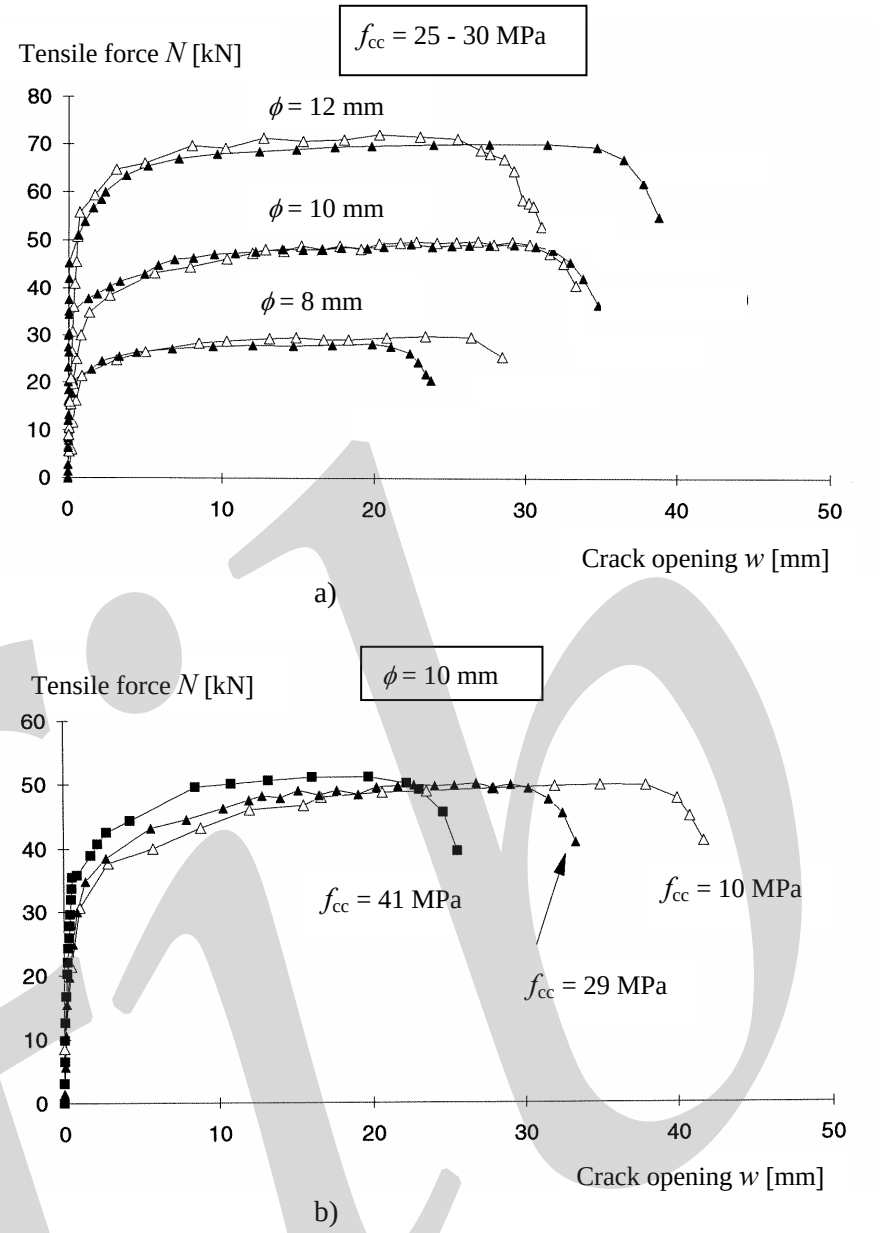

Fig. 7-48: Relationships between tensile force N and crack opening w observed in pure tensile tests on tie connections with continuous tie bars of type Ks40 (ribbed reinforcement bars of hot-rolled steel), a) influence of tie bar dimension, b) influence of concrete compressive strength in the anchorage zone:

In tie connections with more than one tie bar across the critical joint interface, the maximum tensile capacity can be found by adding the capacities of the individual tie bars. Some few tests on tie connections with more than one tie bar of the same type and dimension have shown that the deformation capacity of the connection seems not to be affected by the number of interacting tie bars (in case of tensile load in the tie bar direction). For a tie connection with more than one tie bar interacting, the load-displacement relationship can be estimated by superimposing the corresponding relationships for tie connections with single tie bars. It is assumed that this principle can be applied also in case of tie bars of different types and dimensions. In this case the individual tie bars will rupture for various values of the crack width, see Fig. 7-49 and Examples A1-A2 in Appendix A.

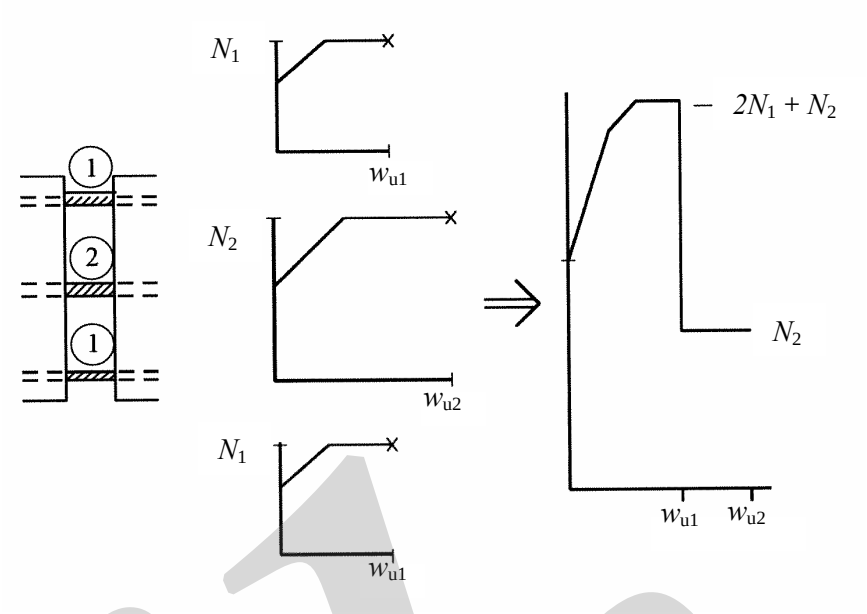

Fig. 7-49: Estimation of the load-displacement relationship of tie connection with interacting tie bars by superimposing the corresponding relationships of tie connections with single tie bars

Example 7-4, estimation of tie beam stiffness

A tie beam along a hollow core floor is reinforced with 2 continuous tie bars ϕ20 B500. The bars are anchored in concrete of strength C20, the concrete is considered as 'confined', but the bond conditions belong to 'all other cases'. When the floor is working under vertical and horizontal load the joint dilatation under shear friction behaviour has been estimated to about $w \approx 0{,}5$ mm. The stiffness of the tie beam will be estimated by different approaches on the basis of characteristic material properties, compare with analysis method in Section 8.5.1.

For a tie beam the deformation in the crack section consists of two end-slips. Hence, the stiffness of the tie beam will be half the stiffness of each anchorage.

The end slip under working conditions is calculated by eq. (7-30):

$$s_{\text{end,max}} = \frac{w}{2} = \frac{0{,}5}{2} = 0{,}25\ \text{mm}$$

For this end slip the corresponding steel stress is determined by eq. (7-4):

$$\tau_{\text{b,max}} = 1{,}25\sqrt{20} = 5{,}59\ \text{MPa}$$

$$0{,}25 = 0{,}288\left(\frac{20\cdot\sigma_s^2}{5{,}59\cdot10^6\cdot200\cdot10^9}\right)^{0{,}714} + \frac{\sigma_s}{200\cdot10^9}2\cdot20$$

$$\Rightarrow \qquad \sigma_s = 191\ \text{MPa}$$

The stiffness is calculated using the maximum tensile force under working conditions and the corresponding crack width. Eq. (7-7) is used but with the crack width in stead of the end-slip.

$$N(s_{\text{end,max}}) = \sigma_s \cdot A_s = 191\cdot10^6\cdot2\cdot314\cdot10^{-6} = 120\ \text{kN}$$

$$w_{\text{max}} = 0{,}5\ \text{mm}$$

$$K_a(w_{max}) = \frac{N(s_{end,max})}{w_{max}} = \frac{120 \cdot 10^3}{0{,}5 \cdot 10^{-3}} = 240 \cdot 10^6 \text{ N/m}$$

Alternatively, the stiffness can be estimated from eq. (7-8) on the basis of the yield load and the corresponding crack width when yielding starts.

$$N_y = f_y \cdot A_s = 500 \cdot 10^6 \cdot 2 \cdot 314 \cdot 10^{-6} = 314 \text{ kN}$$

$$s_{end,y} = 0{,}288 \left(\frac{20 \cdot (500 \cdot 10^6)^2}{5{,}59 \cdot 10^6 \cdot 200 \cdot 10^9} \right)^{0{,}714} + \frac{500 \cdot 10^6}{200 \cdot 10^9} 2 \cdot 20 = 0{,}939 \text{ mm}$$

$$w_y = 2 \cdot s_{end,y} = 2 \cdot 0{,}939 = 1{,}88 \text{ mm}$$

$$K_a = \frac{N_y}{w_y} = \frac{314 \cdot 10^3}{1{,}88 \cdot 10^{-3}} = 167 \cdot 10^6 \text{ N/m}$$

It appears from the calculations that the stiffness determined on the basis of the conditions when yielding starts underestimates the stiffness and consequently also the steel stress under the actual load.

The stiffness is also estimated by means of the simplified approach in Section 7.2.3.3.

The average bond stress according to eq. (7-15), with α_t = 0,42 for ϕ20 mm bar (Table 4-1).

$$\tau_{bm} = \alpha_t \cdot \tau_{b,max} = 0{,}42 \cdot 5{,}59 = 2{,}35 \text{ MPa}$$

The transmission length when yielding starts, according to eq. (7-16):

$$l_{ty} = \frac{f_y}{\tau_{bm}} \frac{\phi}{4} + 2 \cdot \phi = \frac{500}{2{,}35} \cdot \frac{20}{4} + 2 \cdot 20 = 1103 \text{ mm}$$

The stiffness is estimated according to eq. (7-19) considering that the crack width is twice the end slip:

$$K_a = 2 \frac{E_s \cdot A_s}{l_{ty}} = 2 \frac{200 \cdot 10^9 \cdot 2 \cdot 314 \cdot 10^{-6}}{1{,}103} = 228 \cdot 10^6 \text{ N/m}$$

Example 7-5, load displacement relationship of tie connection with ribbed bar

A continuous tie bar ϕ16 B500 with long embedment lengths in 'confined' concrete of strength class C20/25, 'good' bond conditions is anchored on each side of transverse joint. For design with regard to progressive collapse (accidental action) the load displacement relationship is predicted on basis of characteristic steel properties and the ductility is quantified.

The anchorage conditions and the type of bar are the same as in Example 7-1, see Section 7.2.3.1.

f_{yk} = 500 MPa; $(f_u/f_y)_k$ = 1,08; E_s = 200 GPa; $\varepsilon_{suk} = 50 \cdot 10^{-3}$

Yield capacity: $N_y = f_{yk} \cdot A_s = 500 \cdot 10^6 \cdot 201 \cdot 10^{-6} = 101 \cdot 10^3 \text{ N}$

Tensile capacity (steel rupture): $N_u = 1{,}08 \cdot N_y = 1{,}08 \cdot 101 = 109$ kN

The characteristic value of the crack width is determined according to eq. (7-30), using the result from Example 7-1.

$$w_y = 2 \cdot s_{end,y} = 2 \cdot 0{,}468 = 0{,}936 \text{ mm}; \qquad w_u = 2 \cdot s_{end,u} = 2 \cdot 1{,}59 = 3{,}19 \text{ mm}$$

With these values a schematic load-displacement relationship is established following the principles in Fig. 7-30, see Fig. 7-50.

The ductility factor is calculated according to eq. (3-1).

$$\mu = \frac{3{,}19}{0{,}936} = 3{,}4$$

The relative strain energy capacity, i.e. the relative strain energy obtained just before rupture, is calculated according to the definition eq. (3-3).

$$\xi_u = \frac{W_{int}(w_u)}{N_u \cdot w_u}$$

$$\xi_u = \frac{\frac{1}{2} \cdot 101 \cdot 0{,}936 + \frac{101+109}{2}(1{,}595 - 0{,}936) + 109 \cdot (3{,}19 - 1{,}595)}{109 \cdot 3{,}19} = 0{,}835$$

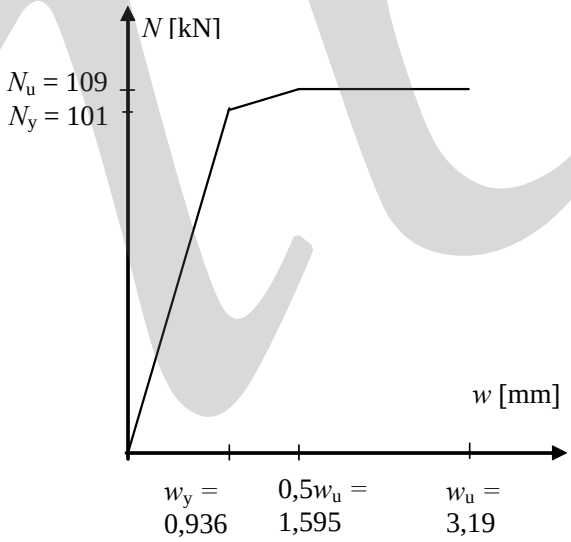

Fig. 7-50: Simplified load-displacement relationship for the tie connection in Example 7-5

The relative strain energy can be determined for any displacement (crack width) during the displacement course. When the crack width is half of the ultimate value ($w = 0{,}5 w_u$), the actual relative strain energy is found from the corresponding part of the load-displacement relationship as

$$\xi(w) = \frac{W_{int}(w)}{N_{max} \cdot w}$$

$$\xi(w) = \frac{\frac{1}{2}\cdot 101\cdot 0{,}936 + \frac{101+109}{2}(1{,}595-0{,}936)}{109\cdot 1{,}595} = 0{,}670$$

7.4.2 Smooth bars of mild steel with end hooks

When smooth bars of mild steel are used as tie bars, the bar must be provided with end hooks. Otherwise, pullout failure would occur when the bar yields, because the bond is almost totally lost at yielding.

Tensile tests on tie connections provided with smooth tie bars of mild steel (Ss26) with end hooks have shown that the load-displacement relationship has the same proportions as for tie connections with ribbed tie bars of ductile type, as long as rupture of the tie bar is reached. However, the deformability in case of smooth bars is much higher.

Typical test results from pure tensile tests [Engström (1992)] are presented in Fig. 7-51. The smooth tie bars had various dimensions but similar properties of steel and concrete. The distance between the end hooks was the same. In these cases the ultimate displacement seemed not to be influenced by the tie bar dimension. However, as appears from Fig. 7-48 a, the effect of the tie bar dimension is pronounced in tie connections with ribbed tie bars. This means that the bond along the smooth tie bar had a very small influence on the results.

The fact that the ultimate displacement was almost the same for the two tests, presented in Fig. 7-51, shows that the two tests had about the same ultimate extension of the plastic zone. According to the strain measurements, the plastic zone propagated at a high rate when yielding was obtained in the crack section. Before the tensile capacity was reached, the plastic zone had developed to the end hooks. Hence, in the two tests the ultimate extension of the plastic zone was determined by the distance between the end hooks, which was the same.

As the load-displacement relationships for tie connections with smooth bars have the same proportions as in the case of ribbed bars, it is possible to describe the behaviour with the same idealised relationships as shown in Fig. 7-30.

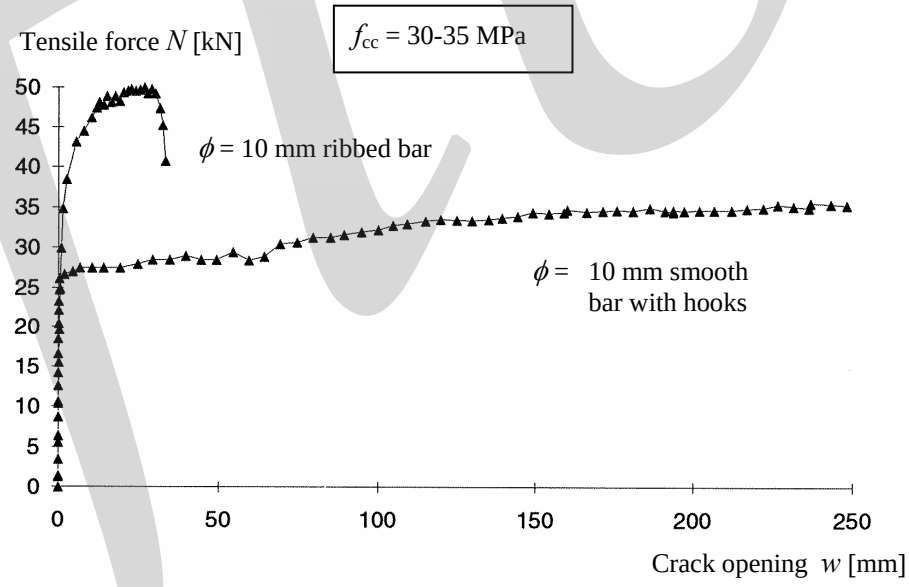

Fig. 7-51: Relationships between tensile force N and relative displacement w observed in pure tensile tests on tie connections with continuous smooth tie bars of mild steel (Ss26) provided with end hooks. The ultimate displacement was not affected by the tie bar dimension, according to Engström (1992)

Example 7-6, load-displacement relationship for tie connection with smooth bar

A tie connection between two precast concrete elements is provided with one plain tie bar ϕ16 of mild steel, anchored in concrete of strength class C20/25 on both sides of the intermediate joint. The joint has a width of 110 mm. The tie bar is anchored by end hooks and the length between the end hooks is 1,50 m, see Fig. 7-52. The bond conditions can be assumed other than good.

Determine the ultimate displacement (crack opening) just before rupture of the tie bar and a simplified load-displacement relationship. The calculations should be based on characteristic steel properties.

f_{yk} = 270 MPa; $(f_u/f_y)_k$ = 1,15; E_s = 200 GPa; $\varepsilon_{suk} = 60\cdot10^{-3}$.

Yield capacity: $N_y = f_{yk} \cdot A_s = 270\cdot10^6 \cdot 201\cdot10^{-6} = 54{,}3\cdot10^3$ N

Tensile capacity (steel rupture): $N_u = 1{,}15 \cdot N_y = 1{,}3 \cdot 54{,}3 = 70{,}6$ kN

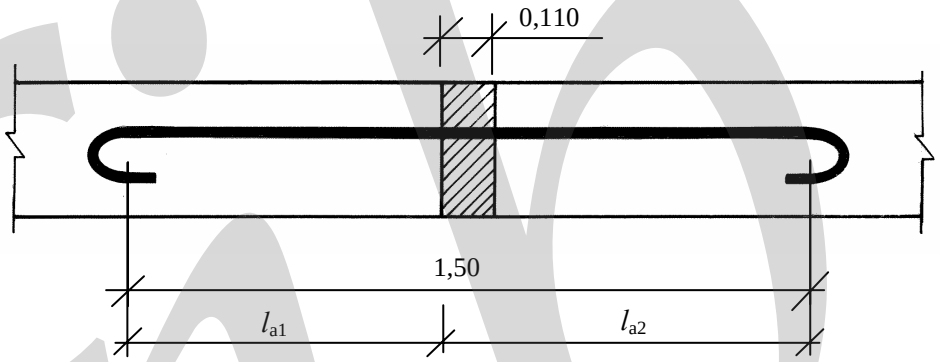

Fig. 7-52: Tie connection with plain tie bar with end hooks in Example 7-3.

Assume that a crack forms in one of the joint interfaces. The distances between the cracked section and the respective end anchors, see Fig. 7-52, are then found as

$l_{a1} = 695$ mm

$l_{a2} = 805$ mm

The displacement just before yielding starts can be calculated by summing up the contributions from each side of the crack. The residual bond stress is calculated according to Table 7-3 assuming bond conditions other than good.

$$\tau_{bf} = 0{,}15\sqrt{f_{cm}} = 0{,}15\sqrt{28} = 0{,}794 \text{ MPa}$$

The steel stresses at the end hooks are then obtained from eq. (7-23)

$$\sigma_{sa,y1} = 270 - \frac{4\cdot0{,}794\cdot695}{16} = 132 \text{ MPa}$$

$$\sigma_{sa,y2} = 270 - \frac{4\cdot0{,}794\cdot805}{16} = 110 \text{ MPa}$$

The crack width when yielding starts becomes, by means of eq. (7-22)

$$w_y = \frac{270\cdot10^6 + 132\cdot10^6}{2\cdot200\cdot10^9}\cdot695 + \frac{270\cdot10^6 + 110\cdot10^6}{2\cdot200\cdot10^9}\cdot805 = 0{,}699 + 0{,}765 = 1{,}46 \text{ mm}$$

The ultimate displacement is estimated differently depending on if the plastic zone reaches the end hooks or not, see Section 7.2.3.4. Assume that the ultimate extension of the plastic zone is less than the respective anchorage lengths. The length of the plastic zone is then estimated according to eq. (7-27). The average bond stress along the plastic zone is determined by eq. (7-25) assuming other bond condition.

$$\tau_{bf,pl} = 0{,}025\sqrt{f_{cm}} = 0{,}025\sqrt{28} = 0{,}132 \text{ MPa}$$

where $f_{cm} = f_{ck} + 8 \text{ MPa} = 20 + 8 = 28 \text{ MPa}$

$$l_{t,pl} = \frac{1{,}15\cdot270\cdot10^6 - 270\cdot10^6}{0{,}132\cdot10^6}\cdot\frac{16}{4} = 1227 \text{ mm}$$

This is greater than both the anchorage lengths provided. In this case the steel stress at the respective end hook can be calculated according to eq. (7-28)

$$\sigma_{sa,u1} = 311 - 0{,}132\cdot695\frac{4}{16} = 288 \text{ MPa} \quad \text{where} \quad f_{su} = 1{,}15\cdot f_{yk} = 311 \text{ MPa}$$

$$\sigma_{sa,u2} = 311 - 0{,}132\cdot805\frac{4}{16} = 284 \text{ MPa}$$

The average steel stress at the respective side of the crack is found as

$$\sigma_{sm1} = \frac{311 + 288}{2} = 300 \text{ MPa}$$

$$\sigma_{sm2} = \frac{311 + 284}{2} = 298 \text{ MPa}$$

The ultimate displacement is calculated by summing up the contributions from each side of the crack, compare with eq. (7-29).

$$w_u = \left[l_{a1}\cdot\left(\varepsilon_{sm,pl}\right)_1 + l_{a2}\cdot\left(\varepsilon_{sm,pl}\right)_2\right]$$

where $\varepsilon_{sm,pl} = \frac{\sigma_{sm} - f_y}{f_u - f_y}\varepsilon_{su}$

$$w_u = 695\cdot\frac{300 - 270}{311 - 270}\cdot60\cdot10^{-3} + 805\cdot\frac{298 - 270}{311 - 270}60\cdot10^{-3} = 30{,}5 + 33{,}0 = 63{,}5 \text{ mm}$$

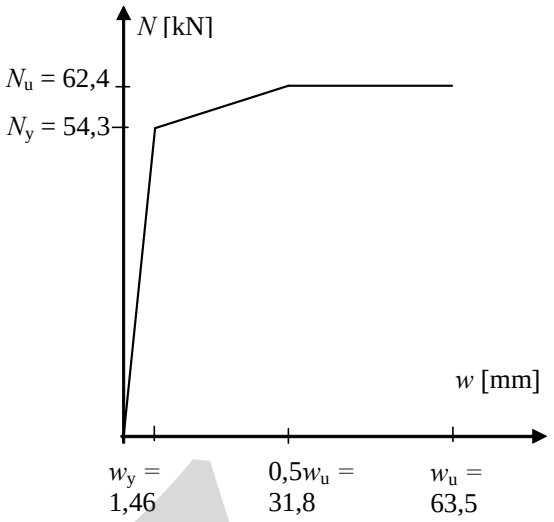

Fig. 7-53: Simplified load-displacement relationship for the tie connection in Example 7-6

7.5 Coupled bars

7.5.1 Loop connections

Loop connections as exemplified in Fig. 7-54, can be used to transfer tensile forces, bending moments and shear forces. It is used between solid slabs where continuity is demanded. However, the production is more difficult due to projecting bars.

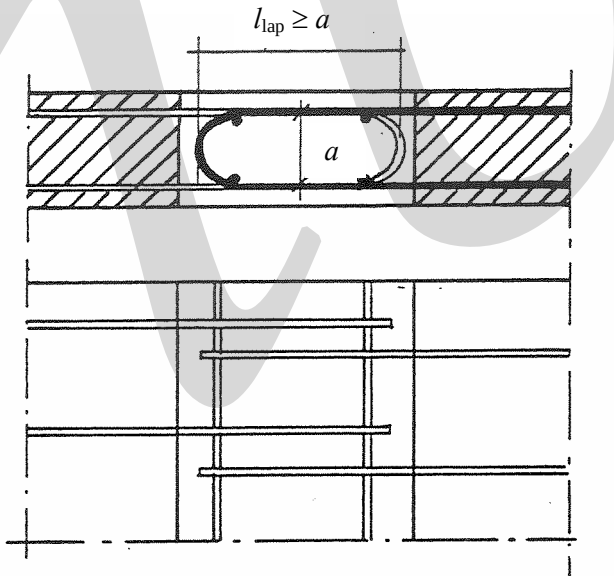

Fig. 7-54: Loop connection

The connection can fail due to rupture of the reinforcement bars, crushing of the joint concrete (mortar) or splitting of the joint concrete in the plane of overlapping loops. The design aims at preventing concrete failures to occur before the reinforcement loops yield. Transverse reinforcement within the overlap is necessary in order to achieve an acceptable behavior. If properly designed the loop connection can exhibit substantial ductility. For the behavior of loop connections reference is made to Dragosavik *et al.* (1975) who reported results from extensive experimental investigations and gave recommendations for design.

The tensile force from one element to the other is transferred by inclined compressive struts between overlapping loops, see Fig. 7-55. The inclined strut originates from radial stresses $\sigma_{c,rad}$ acting against the bend of the loop. The spread of stresses from the loop to the strut causes local splitting stresses due to high bearing stresses inside the loop. Furthermore, the inclination of the strut also gives a transverse tensile force that needs to be balanced. As a consequence of this model the transverse reinforcement needs to be distributed between the two ends of the overlap and be placed inside the loops. The transverse reinforcement can be designed by a simple strut-and-tie model, see Fig. 7-55. The transverse force F_t in the reinforcement at one side of the overlap is calculated as

$$F_t = 2N_y \cot\theta \tag{7-44}$$

where N_y = yield load of one leg of the U-bar
θ = strut inclination

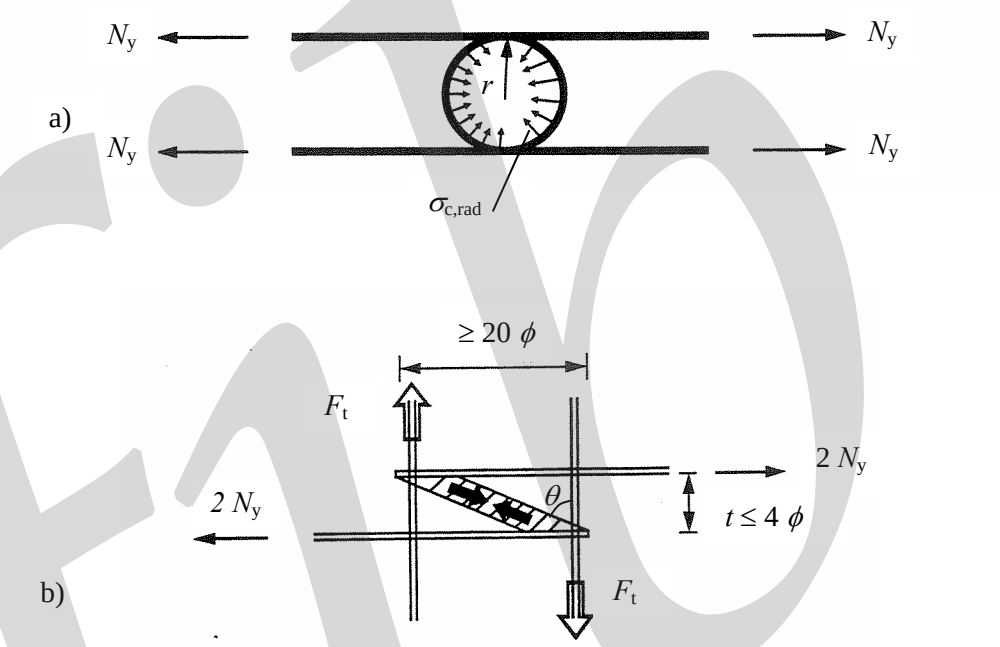

Fig. 7-55: Transfer of forces in loop connection, a) radial stresses against the bend, b) inclined compressive strut between overlapping loops

The tensile force in one U-bar is balanced in the joint by the radial concrete stresses. A horizontal equilibrium for one U-bar gives

$$2r \cdot \phi \cdot \sigma_{c,rad} = 2\frac{\pi\phi^2}{4} \cdot f_y$$

$$\sigma_{c,rad} = \frac{\pi\phi}{4r} f_y \tag{7-45}$$

where r = radius of the bend of the U-bar, see Fig. 7-55
ϕ = diameter of the U-bar

In order to limit the bearing stresses to acceptable values the following condition needs to be fulfilled, according to Basler and Witta.(1966).

$$\sigma_{c,rad} \le f_{cc}\sqrt{\frac{b_i}{\phi}} \qquad \text{not greater than} \qquad 3{\cdot}f_{cc} \tag{7-46}$$

where $b_i = 2\cdot(c_e + \frac{\phi}{2})$ not less than t (transverse spacing of meeting loops)

c_e = concrete cover between U-bar and edge of element, see Fig. 7-56

It is recommended that the detailing should be such that the following condition is fulfilled

$$r \ge \frac{\pi\phi}{4}\frac{f_y}{\sigma_{c,rad}} \qquad \text{not less than} \qquad 8\cdot\phi \tag{7-47}$$

Furthermore, it is recommended that the length l_{lap} of overlap should not be less than the height of the U-bar and greater than 20ϕ, see Fig. 7-54. Furthermore, the straight part of the overlapping loops should be at least 3ϕ. The spacing t between overlapping loops should be less than 4ϕ and it is recommended that the spacing s between loop connections (i.e. between pair of loops) is less than 300 mm.

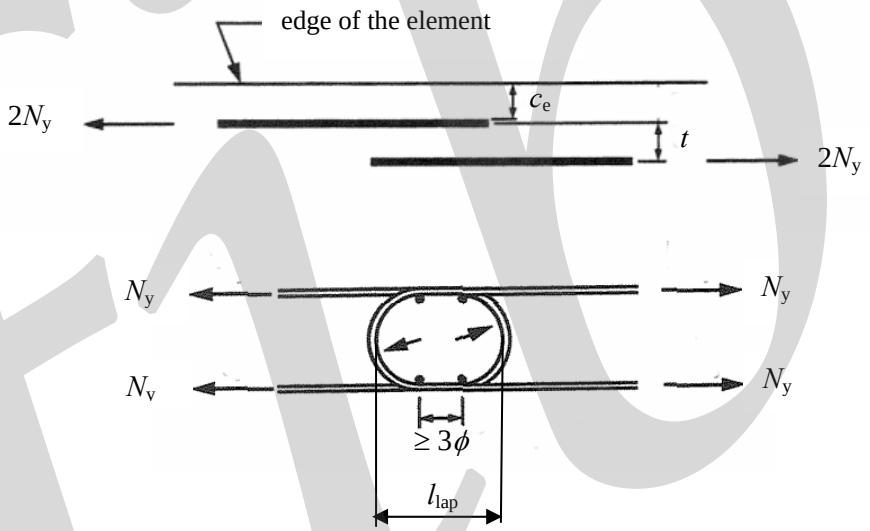

Fig. 7-56: Detailing of loop connection

If the connection is subjected to bending, only the upper bar is in tension, as shown in Fig. 7-57, and the connection can be designed accordingly.

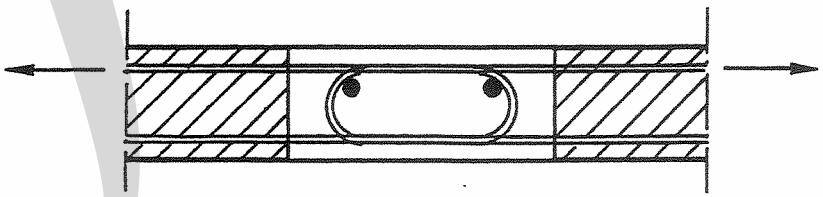

Fig. 7-57: Loop connection subjected to bending only

Example 7-6, design of loop connection

The design of a loop connection should be checked and the transverse reinforcement designed.

Joint concrete C20/25 f_{ck} = 20 MPa; $f_{cd} = \frac{f_{ck}}{\gamma_c} = \frac{20}{1{,}5} = 13{,}3$ MPa

Reinforcement B500 f_{yk} = 500 MPa: $f_{yd} = \frac{f_{yk}}{\gamma_s} = \frac{500}{1{,}15} = 435$ MPa

Geometry:		
	height of slab	h = 200 mm
	spacing between loop connections	s = 150 mm
	spacing between lapping loops	t = 32 mm ($\leq 4\phi$)
	bar diameter	ϕ = 8 mm
	top and bottom concrete cover	c = 20 mm
	cover to edge	c_e = 80 mm

Radius of bend: $r = \frac{200 - 2 \cdot 20 - 8}{2} = 76$ mm

In order to check the radial stress, the 'distribution width' b_i must first be determined, eq. (7-33).

$b_i = 2 \cdot (c_e + \frac{\phi}{2}) = 2 \cdot (80 + \frac{8}{2}) = 168$ mm

but not less than s = 150 mm , which means in this case: b_i = 150 mm

Limitation of radial stress , eq. (7-33): $\sigma_{c,rad} \leq f_{cd}\sqrt{\frac{b_i}{\phi}}$ MPa

check actual value of $\sqrt{\frac{b_i}{\phi}} = \sqrt{\frac{150}{8}} = 4{,}33$ (too large $\Rightarrow$ apply limit value)

$\sigma_{c,rad} \leq 3 \cdot f_{cd} = 3 \cdot 13{,}3 = 39{,}9$ MPa

Check radius of the bend according to eq. (7-34)

$r \geq \frac{\pi\phi}{4} \cdot \frac{f_y}{\sigma_{c,rad}} = \frac{\pi \cdot 8}{4} \cdot \frac{435}{39{,}9} = 68{,}5$ not less than $8 \cdot \phi = 8 \cdot 8 = 64$ mm

Hence, the actual detailing with r = 76 mm is OK

Design of transverse reinforcement:

overlapping length: $l_{lap} = 2 \cdot 76 + 3 \cdot 8 = 176$ mm

spacing between loops: t = 32 mm

assumed strut inclination: $\cot\theta = \frac{32}{176} = 0{,}182$

needed transverse reinforcement per side of the overlap, eq. (7-31)

$F_t = 2N_y \cot\theta = 2 \cdot 435 \cdot 10^6 \cdot 50{,}3 \cdot 10^{-6} \cdot 0{,}182 = 7{,}96$ kN

$$A_{st} = \frac{F_t}{f_{yd}} = \frac{7{,}96 \cdot 10^3}{435 \cdot 10^6} = 18{,}3\,\text{mm}^2$$

This means that 2 ϕ8 mm bar is sufficient on each side of the transverse joint.

7.5.2 Lap splices

Where straight bars are lapped, the bars should be spliced together lengthwise such that a full anchorage length is provided. The lap splice should fulfil ordinary rules for reinforced concrete, as stated in the CEB/FIP Model Code 90. To account for splitting effects, see Fig. 7-35, transverse reinforcement is recommended.

The overlap of the two bars requires however a length which is not always available. Hence, in case of joints with normal strength concrete it is normally advisable to consider a loop connection instead.

In case of special mortars, e.g. epoxy based grouts, or fibre reinforced high strength concrete/mortars the anchorage length can be considerably reduced. Bond lengths to deformed high tensile bars of less than 10 bar diameters are possible with high strength steel fibre reinforced concrete. The necessary splice length must in such cases be determined on the basis of relevant research data.

The design of such connections is based on the principle of balanced design for ductility. The joint is identified as a brittle component and should be given a sufficient overcapacity to guarantee that flexural or tensile cracks occur, not in the joint or along the joint faces, but in the connected elements, where ductility can be achieved by the ordinary reinforcement. An example of a connection designed in this way is shown in Fig. 7-58. Experimental results [Harryson (2002)] confirmed that the joint with lap spliced projecting bars had sufficient overcapacity.

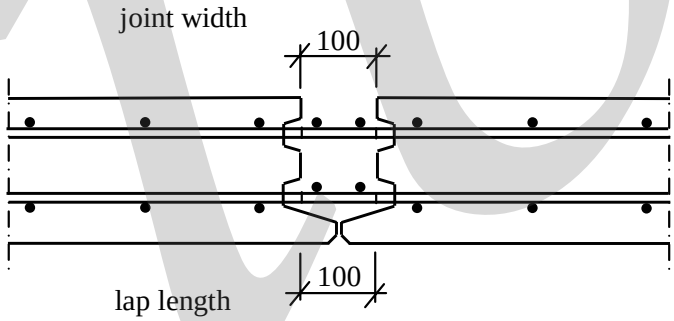

Fig. 7-58: Connection with projecting bars in lap splice in high strength joint, according to Harryson (2002)

7.5.3 Welded connections

Welded connections are found mainly in confined or heavily reinforced areas where the joint length is to be minimised, and immediate structural stability is required (or preferred). Welding is used to connect components through projecting rebars, fully anchored steel plates or rolled steel sections etc.

In the design of connections it is especially important to consider the possibility of welding on the site. The quality of the connection depends not only on accessibility, but also that it is possible to reach the connection in a satisfactory working position to ensure a good result. Underhand welding should be avoided if possible, and the weld should be inspected afterwards. All steel details should be made of steel suitable for welding and the possible negative influence on the concrete elements of the temperature variation should be considered. In the welded connection shown in Fig. 7-59 a small gap

is provided around the weld plates. The reason is to avoid damage to the concrete due to thermal expansion of the steel item during welding.

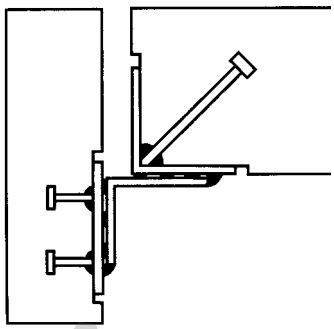

Fig. 7-59: Example of detailing of a welded connection between a façade element and a floor slab. The façade element is fixed to the floor by the connection

The welds should be carefully designed and detailed such that the required capacity of the connection is reached. The thickness and the length of the weld should be calculated and specified. In general the capacity of the connection should not be determined by the resistance of the welds, but a certain overcapacity of the welds is recommended relative to the capacity of tie bars and anchor bars. When ductility is needed or preferred, a balanced design for ductility can be applied, see Section 3.6.

In general concrete elements can be welded together in four different ways. If projecting bars from adjacent elements are meeting side by side, the bars can be welded together along the overlap. This approach is referred to as 'direct welding' of projecting reinforcement bars and is only possible when the meeting bars are parallel and close together. Small tolerances are required, especially when the joint width is small. Otherwise it would be possible to slightly bend the meeting bars in a position where they can be welded. When the connection is loaded the welded part will tend to rotate since the bars are not in line with each other, see Fig. 7-60 a.

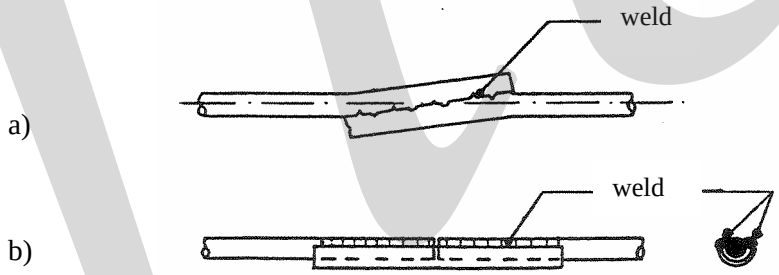

Fig. 7-60: Welded connection between projecting bars, a) direct welding, b) indirect welding

In case of indirect welding the meeting bars are welded to a connecting steel item, e.g. reinforcement bar, steel angle, open channel etc. as exemplified in Fig. 7-60 b. The length of the connecting detail should be determined with regard to the required length of the welds and the gap between the bars considering specified tolerances. For this connection the bars need to meet along the same longitudinal axis, which requires small tolerances. Example of a column splice connection with indirect welding of meeting reinforcement bars is shown in Fig. 9-5 d.

Instead of connecting projecting bars a connection can be achieved using weld plates or steel angles that are partly embedded and fully anchored in the concrete elements. In general larger tolerances can be permitted compared to welding of projecting bars. Also in this case it is possible to distinguish direct and indirect welding. In direct welding the naked steel faces of the two elements are

welded together, while in indirect welding a connecting plate or other connecting steel detail is used between the elements. The connecting plate can easily allow variation of the gap between the elements. Weld plates can be anchored to the concrete elements by ribbed or headed bars. For detailing of anchor bars see Section 7.2.4.3.

Examples of connections with direct welding of embedded steel items are the beam-end column connection with welded plate connector, Figs. 9-19, and the column haunch connection shown in Fig. 9-29 b. The column haunch connection has direct welding at the support joint but indirect welding with a connecting plate in the top. Other examples of indirect welding of embedded weld plates are shown in Fig. 7-61.

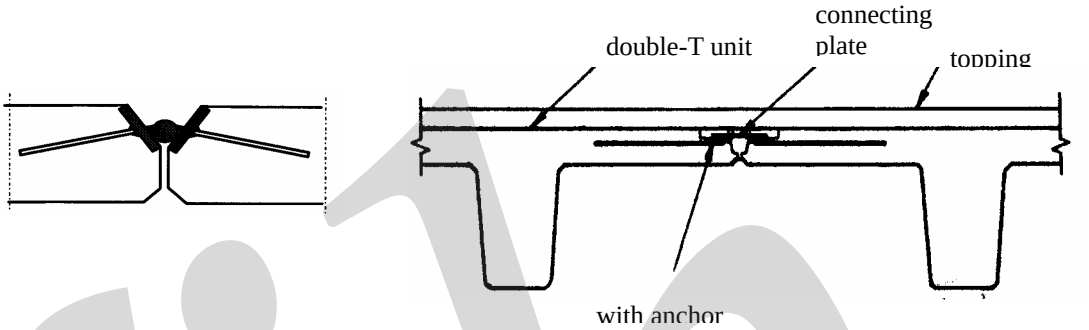

7-61: Examples of welded connections between flanges of double-T units using indirect welding between partly embedded and fully anchored weld plates, a) connecting steel bar between inclined weld plates, b) connecting plate between horizontal weld plates

8 Transfer of shear force

8.1 Principles for shear force transfer

Shear forces can be transferred between concrete elements by adhesion or friction at joint interfaces, shear-key effect at indented joint faces, dowel action of transverse steel bars, pins and bolts, or by other mechanical connection devices. The frictional resistance can be enhanced by the pullout resistance of tie bars properly placed across the joint.

When a joint face has a certain roughness, shear forces can be transmitted by friction even if the joint is cracked, see Section 8.3.3. One condition is, however, that compressive stresses act across the joint, as shown in Fig. 8-1 a. In some joints, for instance horizontal joints in precast walls, the weight of the wall above the joint results in permanent compressive stresses in the joint. Permanent compressive stresses can also be obtained by post-tensioning across the joints. In many applications, external compressive forces of this kind are not available are may not be utilised.

Generally, internal compressive forces are generated across a joint by means of pullout resistance of transverse reinforcement bars, bolts, etc. that are strained when the joint is subjected to shear sliding. This mechanism is further explained in Section 8.3.4. Because of the roughness of the joint faces, the joint will separate a little when shear slip develops along the joint. This separation results in tensile stresses in the transverse bars and the resulting tensile force must be balanced by a compressive force of the same magnitude acting across the joint. This effect of the transverse bars means that the adjacent elements are clamped together when shear slip develops along the joint. This self-generated compressive force contributes to shear transfer, as shown schematically in Fig. 8-1 b and c. The shear force capacity along the joint increases with increased amount of transverse reinforcement and with increased frictional coefficient. In case of a very large amount of transverse steel and depending on the magnitude of the shear action, the concrete at the joint interface may fail in local crushing. This failure mode constitutes an upper limit for the shear capacity by 'shear friction'. The shear capacity can also increase by treatment of the joint faces in order to improve the roughness.

Shear forces along an uncracked joint can be transferred by the adhesive bond between joint grout and the adjacent concrete elements. The adhesive bond, however, depends to a large extent on the workmanship and cleanness of the joint faces during grouting. If the joint faces are dirty from sand, cement or oil wastes, the adhesive bond can be entirely lost. There is also a risk that even well executed joints crack because of restraint actions in the structure.

This means that in practice, it is not possible to rely on adhesive bond for shear transfer, but the joints must be assumed to be cracked and the shear transfer must be secured by shear friction, shear-keys, or mechanical devices. However, in so called 'low shear' applications, where the shear stresses are very small, it may be possible to take account of the adhesive bond at the joint interfaces.

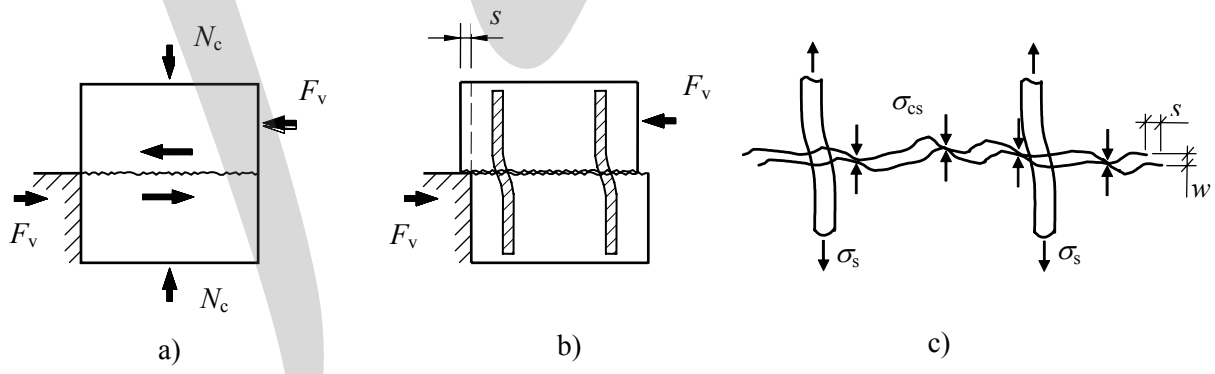

Fig. 8-1: Shear transfer by friction is possible when the joint faces are rough and transverse compression is present, a) external compression across the joint, b) and c) compression is generated by transverse bars across the joint

Shear keys are generally formed by providing the precast members with indented joint faces. An example of an indented joint face is shown in Fig. 8-2. When this type of connection is loaded in shear along the joint, the shear resistance depends on the strength of the shear keys on condition that transverse reinforcement or other tie arrangements are provided. The shear keys work as mechanical locks preventing any significant slip along the joint, see Section 8.4. To function in the intended way, the shear keys must fulfil certain minimum requirements concerning tooth length, tooth depth, and tooth inclination. Such minimum requirements are given in codes and design rules. The joint should also be prevented from uncontrolled joint separation by transverse reinforcement or other transverse tie arrangements. The transverse steel can be distributed along the joint or, under certain conditions, be concentrated to the ends of the joint, according to Fig. 8-2 b-c.

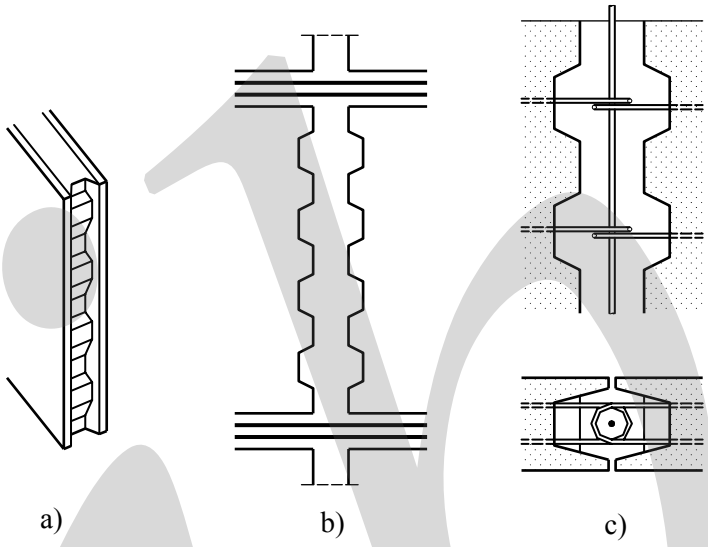

Fig. 8-2: Connection at vertical joint between wall elements, a) indented joint face of wall element, b) transverse, tying reinforcement concentrated to the ends of the wall element (in the horizontal joint), c) transverse, overlapping loops distributed along the joint

A connection with indented joint faces has a very stiff behaviour until the shear-key effect is destroyed by cracking or local crushing at the heaviest loaded contact areas. Various failure modes are possible, from which the most common types are shown in Fig. 8-3. When the shear-key effect decreases due to this degradation of the shear keys, the behaviour changes to a frictional phase associated with a significant shear slip along the cracked section.

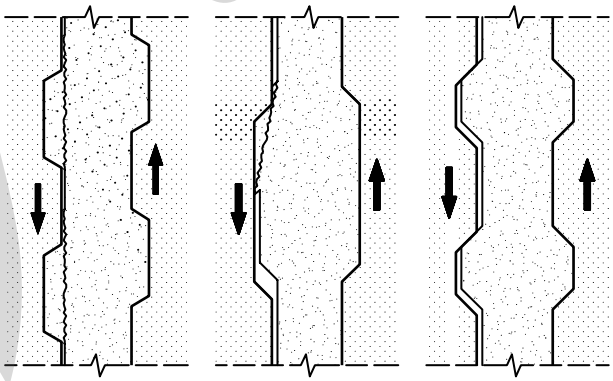

Fig. 8-3: Typical failure modes in connection with indented joint faces, adopted from SBI (1979)

Reinforcement bars, bolts, studs, etc., which are placed across joints, can also contribute to the shear resistance by their dowel action due to imposed shear displacements, see Section 8.2. The typical mode of behaviour is illustrated in Fig. 8-4 a. The 'dowel' is loaded by shear in front of the joint and is supported by a contact pressure along the part that is embedded in the concrete element. This loading condition normally results in considerable flexural deformations and flexural stresses in the 'dowel'. Various failure modes are possible. For normal dimensions and strengths, a collapse mechanism develops by formation of one or more plastic hinges in the dowel. Simultaneously, local crushing occurs in the surrounding concrete where the contact pressure is high, Fig. 8-4 b. For this failure mode the shear capacity increases with increased dimension of the dowel and with increased strengths of steel and concrete. The shear resistance decreases considerably, when the dowel is loaded by a shear force at a certain distance *e* outside the face of the concrete element (= the fixed end of the dowel), see Fig. 8-4. Such eccentric loading should be avoided as much as possible. If the dowel is anchored by bond in the concrete or by an end-anchor, a combined mode of behaviour develops with both dowel and shear friction. Some common types of connections where shear forces are transferred by dowel action in dowel pins and bolts are shown in Fig. 8-5.

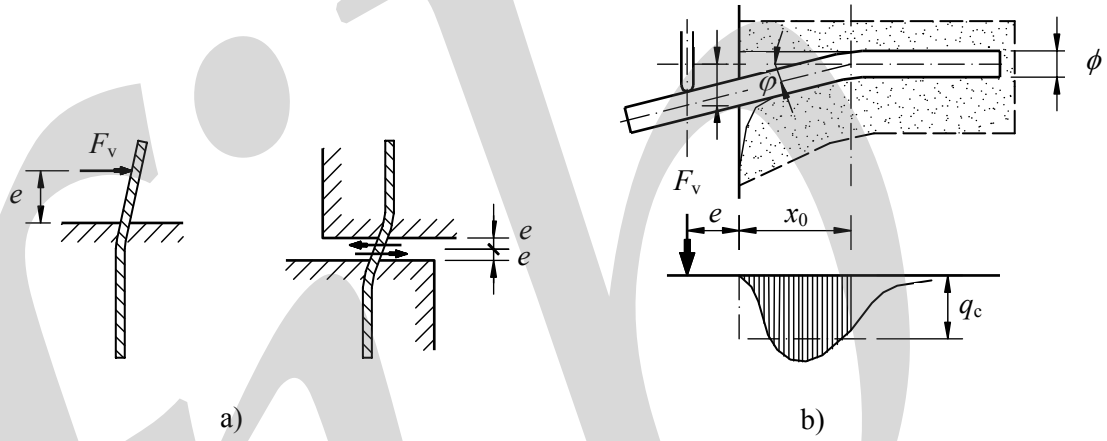

Fig. 8-4: Shear transfer by dowel action in bolt, pin or bar, a) dowel pin with single and double fixation, b) common failure mode with a plastic hinge in the dowel and local crushing in the surrounding concrete

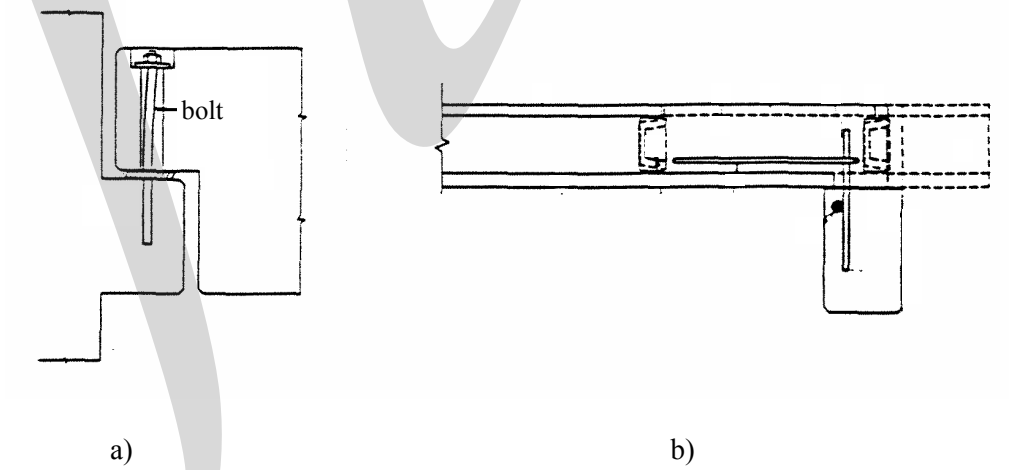

Fig. 8-5: Typical connections where shear forces are transferred by dowel action of bolts and dowel pins, a) bolted connection between beam and support corbel, b) dowel connection between hollow core element and support beam

Through the dowel, high concentrated forces are introduced in the concrete where the dowel is placed and considerable tensile stresses may appear in the area around the dowel. If the dimensions of the concrete element are small, or the dowel is placed near the free edges of the element, splitting cracks may appear even for small shear forces. They can cause premature brittle failures that limit the shear resistance of the shear connection. However, by providing splitting reinforcement in the zone around the dowel, it may be possible to reach the capacity of the dowel, even if splitting cracks appear for a much smaller shear force. The purpose of the splitting reinforcement is to secure equilibrium of the connection zone in case of possible cracking. The splitting reinforcement can be designed by appropriate strut and tie models.

Mechanical devices for shear transfer can be steel details that are welded or bolted to steel plates, which in turn are embedded and anchored in the concrete elements, see Section 8.4.2. Examples of welded shear connections are shown in Fig. 8-6. The weld plates with their anchorage devices must be designed to resist the applied shear force and transfer it into the element. The anchor bars will then be loaded as dowels, see Fig. 8-7.

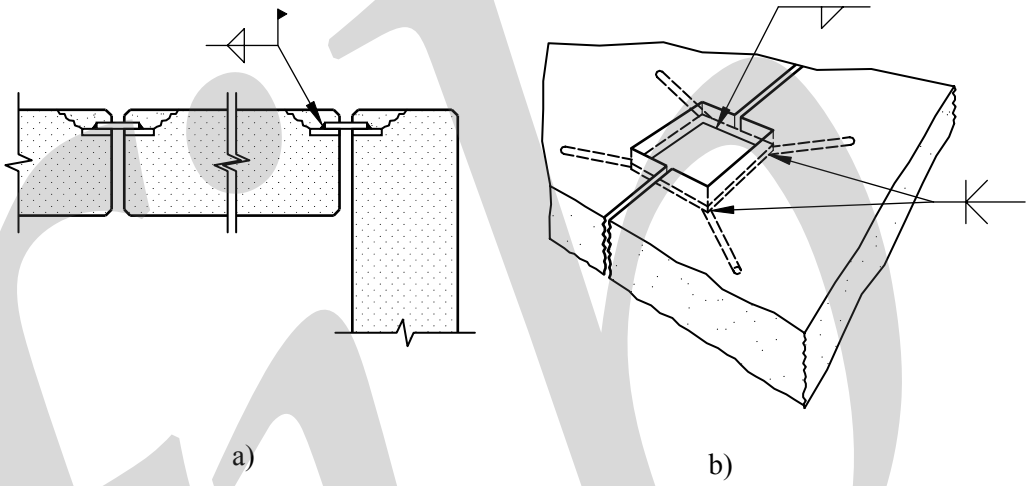

Fig. 8-6: Typical welded connections for shear transfer, a) connection at vertical joint between wall elements in prefabricated shaft, b) connection between double-tee elements

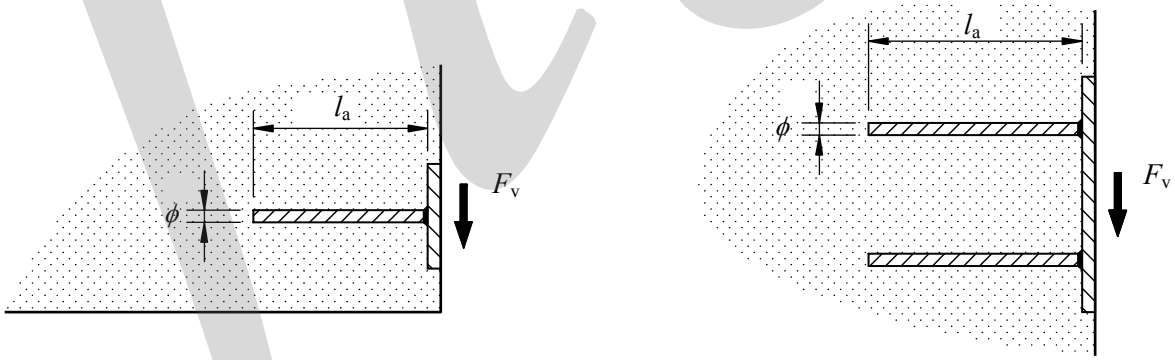

Fig. 8-7: The shear force applied on the anchor plate is resisted by dowel action of the anchor bars

For many connections more than one shear transferring mechanism may contribute to the resistance. When the shear transfer and the load-displacement behaviour of connections are studied experimentally, it is very difficult to distinguish various mechanisms. However, the complex interaction can be described by empirical models and by estimations based on experience. Of this reason, models established in this way, for instance concerning the shear capacity, are only valid for the actual applications and for the actual range of important parameters.

In connections designed using the shear friction effect, the transverse reinforcement contributes to the shear resistance in two ways: by their dowel action and by their resistance to pullout, which generates compressive stresses and in this way contributes to the shear friction, see Section 8.3.4.

8.2 Dowel action

8.2.1 One-sided dowel

8.2.1.1 Possible failure modes

Dowel action of partly embedded steel bars is a basic mechanism in the transfer of shear force. The simplest case is when a bar embedded at one end is loaded by a shear force acting along the joint face or at some distance from the joint face, see Fig. 8-8. When this load case is studied by theory of elasticity as a beam on elastic foundation, see for instance Friberg (1938), the concrete stresses in a plane through the dowel pin vary along the dowel pin as indicated in the figure. As a result there will be high bearing stresses under the dowel pin near the joint face, and the dowel pin will be subjected to a shear force, which changes sign along the dowel pin, and a bending moment with a maximum value at some distance below the joint face.

Depending on the strengths and dimensions of the steel bar and the position of the bar relative to the element boundaries, several failure modes are possible. A weak bar in a strong concrete element might fail in shear of the bar itself. A strong steel bar in a weak element or placed with small concrete cover will more naturally result in splitting of the element itself. However, when the bar is placed in well confined concrete (large concrete covers) or the splitting effects are controlled by properly designed splitting reinforcement, the dowel pin will normally fail in bending by formation of a plastic hinge in the steel bar at some distance below the joint face.

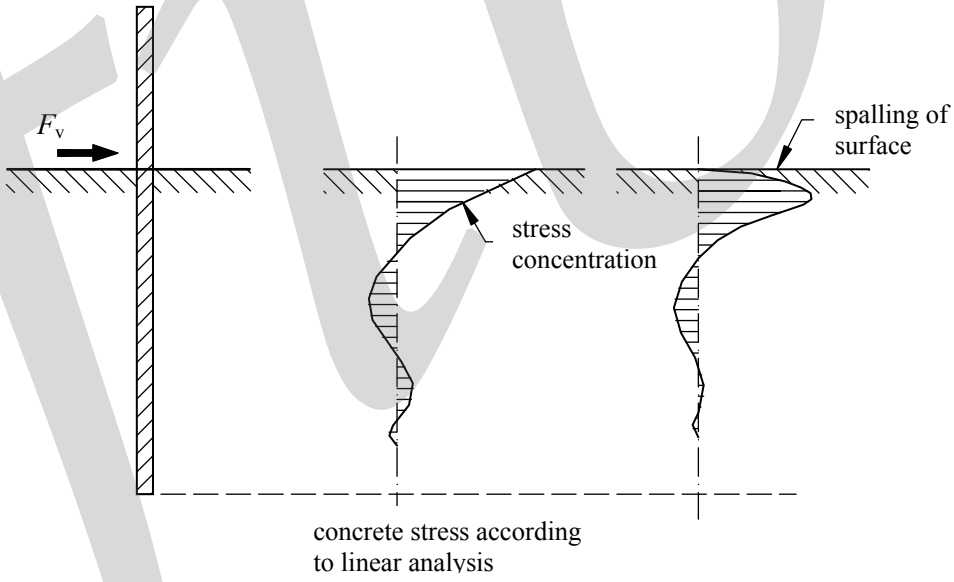

Fig. 8-8: One-sided dowel pin used for transfer of shear force and bearing stresses in the surrounding concrete in the plane through the dowel pin

Failure modes:
- steel shear failure,
- concrete splitting failure,
- steel flexural failure (combined steel/concrete failure).

8.2.1.2 Steel shear failure

The shear capacity of a steel bar loaded in pure shear can be estimated by adopting the yield criterion by von Mieses, which is expressed as

$$F_{vR} = \frac{1}{\sqrt{3}} f_y \cdot A_s \tag{8-1}$$

Experimental results show that von Mieses yield criterion seems to be applicable. In CEB (1991 a) a substantial number of tests results from shear tests of headed anchors were put together and analysed. For headed bars failing in shear the following mean relation was found between the shear capacity and the yield load of the bar.

$$F_{vR,m} = \alpha_y \cdot f_{ym} A_s \qquad \text{with } \alpha_y \approx 0{,}7 \tag{8-2}$$

For tests where the shear capacity was related to the ultimate strength of the steel, the shear capacity could be estimated by

$$F_{vR,m} = \alpha_u \cdot f_{um} A_s \qquad \text{with } \alpha_u \text{ ranging from } 0{,}55 - 1{,}0 \tag{8-3}$$

It is suggested in CEB (1991 a) that the same expressions are applicable also to the shear capacity of bonded bars in case of steel failure. In CEB (1997) it is recommended to determine the shear design resistance of cast-in-place headed anchors without lever arm as

$$F_{vRd} = \alpha_d \cdot f_{yd} A_s \tag{8-4}$$

where $\alpha_d = 0{,}6$ in normal cases
$\alpha_d = 0{,}75$ for anchors welded to the fixture by the stud-welding process

8.2.1.3 Concrete splitting failure

The load case gives rise to a highly concentrated reaction in the concrete under the dowel pin. The connection zone must be designed and detailed so that this concentrated reaction is safely spread and transferred into the element. The concentrated reaction tends to split the element, but the splitting can be controlled by reinforcement designed to establish an equilibrium system in cracked reinforced concrete. The strut and tie method can be used in such design, see Fig. 8-9.

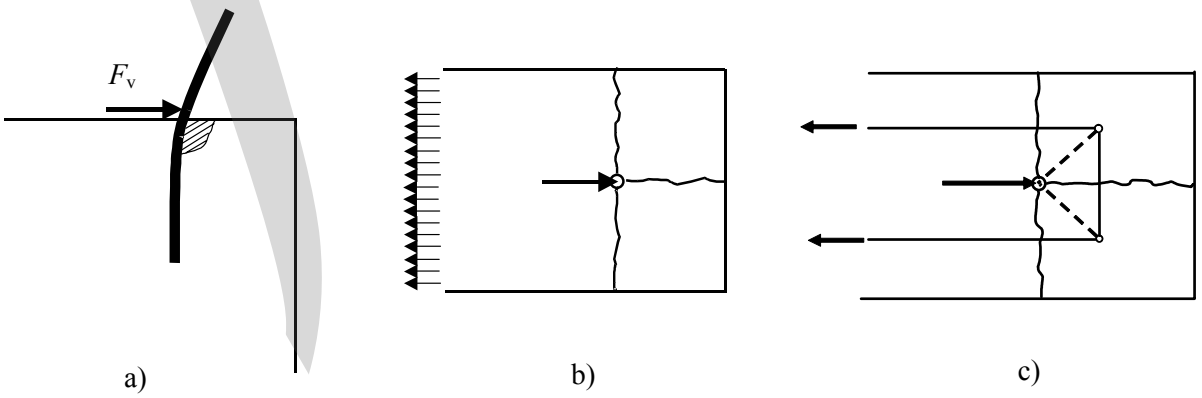

Fig. 8-9: Spitting effects around dowel pin loaded in shear, a) basic load case, b) potential planes of cracking, c) strut and tie model for design of splitting reinforcement

8.2.1.4 Steel flexural failure – no load eccentricity

When the dowel pin is not very weak in relation to the surrounding concrete, the steel bar fails when a plastic hinge is ultimately formed in the section with the maximum bending moment. This failure mode is associated with a significant settlement of the dowel bar in the surrounding concrete that crushes under the high compressive stresses, see Fig. 8-10.

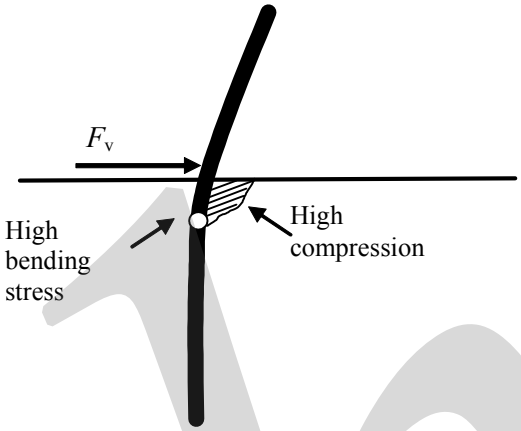

Fig. 8-10: Steel flexural failure with formation of a plastic hinge and settlement of the dowel pin in concrete that crushes locally under the high compressive stresses

For concrete subjected to high bearing stresses under a local loading area, a tri-axial state of stresses is obtained. For such a case compressive stresses can reach values that are several times the uniaxial concrete compressive strength. The following relation is given in CEB-FIP Model Code 90 [CEB-FIP (1992)], see also Section 6.2.2.1.

$$f_{cd}^{*} = 4{,}0 \cdot f_{cd} \tag{8-5}$$

The bearing stress under the dowel pin can be assumed to reach a similar stress level in cases when splitting failure is avoided.

Because both materials reach a plastic behaviour, the state of equilibrium and the resistance in shear can be analysed by adopting theory by plasticity. Such a model was developed by Højlund-Rasmussen (1963), which is presented in the following, see Fig. 8-11.

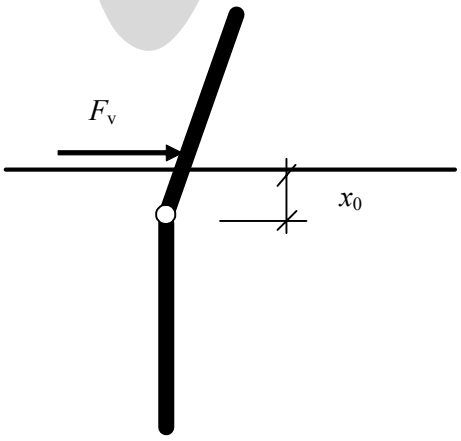

Fig. 8-11: Model for shear capacity of one-sided dowel pin embedded in concrete according to theory of plasticity, adopted from Højlund-Rasmussen (1963).

In the ultimate state the bearing stress in the concrete has reached its maximum value, which with regard to the tri-axial effects is expressed as $\beta_c \cdot f_{cc}$, compare with eq. (8-5). The concrete reaction along the dowel pin per unit length is found as

$$q_c = (\beta_c f_{cc}) \cdot \phi \tag{8-6}$$

where ϕ = diameter of dowel pin

When the maximum load F_{vR} is reached, the section x_0 where the moment is at maximum is found from the condition that the shear force is zero in this section.

$$x_0 = \frac{F_{vR}}{q_c} \tag{8-7}$$

The maximum moment (load effect) is found from a moment equation using eq. (8-7) as

$$M_{max} = F_{vR} \frac{F_{vR}}{q_c} - q_c \frac{1}{2} \cdot \left(\frac{F_{vR}}{q_c} \right)^2 = \frac{1}{2} \frac{F_{vR}^2}{q_c} \tag{8-8}$$

The plastic resistance moment of a dowel pin with homogenous circular section, see Fig. 8-12, is found as

$$M_y = f_y \frac{\pi \phi^2}{8} \cdot \frac{4}{3} \frac{\phi}{\pi} = f_y \frac{\phi^3}{6} \tag{8-9}$$

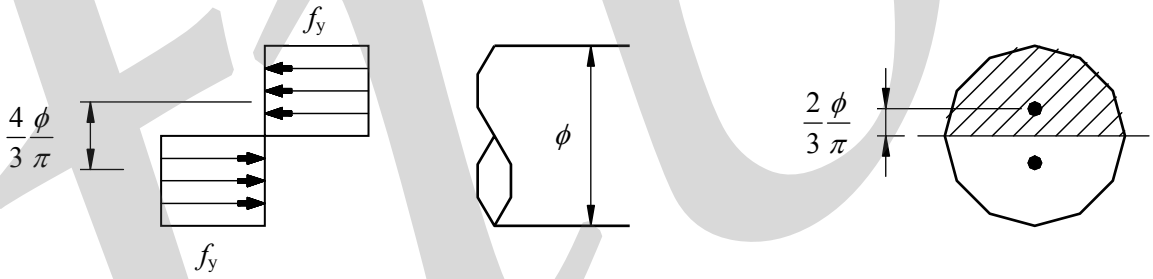

Fig. 8-12: Plastic moment resistance of dowel pin with homogenous circular section

From the condition that the load effect according to eq. (8-8) should be equal to the resisting moment and expressing the concrete reaction by eq. (8-6), the ultimate shear capacity can be solved.

$$\frac{1}{2} \frac{F_{vR}^2}{q_c} = f_y \frac{\phi^3}{6} \qquad \Rightarrow$$

$$F_{vR}^2 = f_y \frac{\phi^3}{6} \cdot 2 \cdot (\beta_c f_{cc}) \phi = \frac{\beta_c}{3} \phi^4 f_{cc} f_y \qquad \Rightarrow$$

$$F_{vRd} = \alpha_0 \phi^2 \sqrt{f_{cd} f_{yd}} \tag{8-10}$$

where $\alpha_0 = \sqrt{\frac{\beta_c}{3}}$ (can be taken as α_0 = 1,0 in design) (8-11)

The distance x_0 from the joint face to the plastic hinge is found as

$$x_0 = \frac{F_{vR}}{q_c} = \frac{F_{vR}}{3\alpha_0^2 f_{cc}\phi} \tag{8-12}$$

Assuming that the relation, eq. (8-5), for local compression is valid also in case of concentrated loading under dowel pins loaded in shear, the coefficient α_0 would be 1,0. The coefficient can also be determined experimentally by assuming that eq. (8-10) is a correct formulation of the failure load and comparing experimental and calculated shear capacities. In tests by Højlund-Rasmussen (1963) on one-sided dowel pins this coefficient was evaluated to 1,16. In tests on double-sided dowels without restraint reported by Dulácska (1972) the coefficient was found to be 1,15 and in tests by Engström (1990) the coefficient was found to be 1,03. In the latter case the tests were controlled by deformations and the failure load was taken as the load when plastic deformations were obtained and not the peak value.

Basically the same model for the shear resistance of dowels is adopted in CEB-FIP Model Code 90, where for design purposes it is recommended to use a global coefficient of $\alpha_0 = 1{,}0$. This value includes a supplementary partial coefficient of $\gamma_{Rd} = 1{,}3$. According to CEB-FIP (1992) the shear displacement s_{max} needed to mobilise the shear capacity can be estimated as

$$s_{max} = 0{,}05 \cdot \phi \tag{8-13}$$

where ϕ = diameter of dowel bar

However, it is obvious that this needed shear displacement will be influenced by the distance x_0 between the plastic hinge and the end face, which in turn depends on the concrete and steel strengths and the bar dimension. In other words, if the bar is strong in relation to the concrete, the distance to the plastic hinge will be greater and a greater shear displacement would be needed to create the plastic hinge.

Based on this reasoning Engström (1990) proposed an alternative approach to estimate the needed shear displacement. It was then assumed that a plastic hinge forms when the overall inclination, see definition in Fig. 8-13, reaches a critical value θ_{crit}. This critical inclination was assumed to be proportional to the curvature of the critical section when yielding is reached

$$\theta_{crit} = k_r \cdot \frac{\varepsilon_{sy}}{\phi} \tag{8-14}$$

where $\varepsilon_{sy} = \frac{f_y}{E_s}$ (yield strain)

k_r = factor that considers the curvature distribution

The shear displacement needed to form a plastic hinge can then be determined as

$$s_{max} = \theta_{crit} \cdot x_0 \tag{8-15}$$

The factor k_r was determined experimentally and was found to be about 1,75 m. However, the experimental basis was rather limited and this value is uncertain.

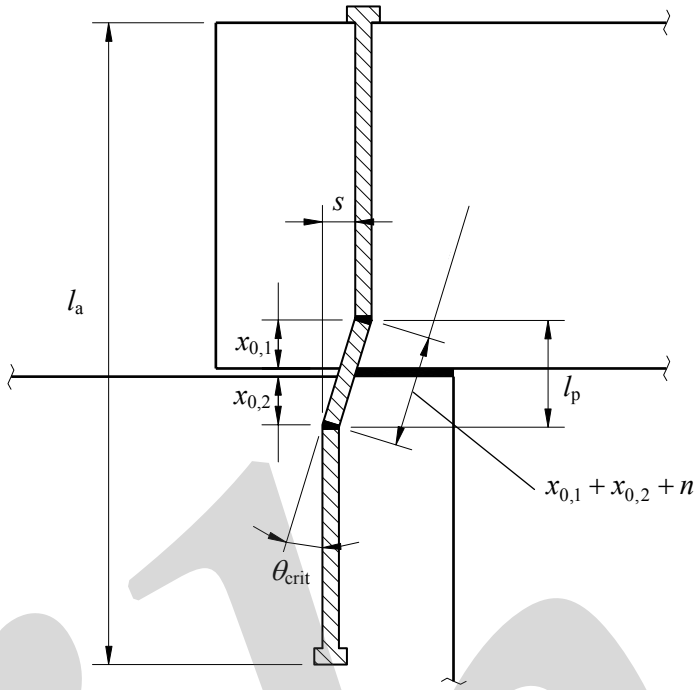

Fig. 8-13: Critical angle needed to create a plastic hinge in a dowel bar

Example 8-1, one-sided plain dowel without end-anchor, parametric study

Consider a one-sided plain dowel, without end anchor and loaded by shear along the joint face (no eccentricity). The bar diameter and steel and concrete properties are ϕ = 24 mm, f_y = 500 MPa, E_s = 200 GPa, and f_{cc} = 50 MPa, assume α_0 = 1,0.

The shear capacity in dowel action is found by eq. (8-10) as

$$F_{vR} = \alpha_0 \phi^2 \sqrt{f_{cc} f_y} = 1{,}0 \cdot 0{,}024^2 \sqrt{50 \cdot 10^6 \cdot 500 \cdot 10^6} = 91{,}1 \cdot 10^3 \text{ N}$$

The distance to the plastic hinge is determined by eq. (8-12) and the critical angle by eq. (8-14) as

$$x_0 = \frac{F_v}{3\alpha_0^2 f_{cc} \phi} = \frac{91{,}1 \cdot 10^3}{3 \cdot 1{,}0^2 \cdot 50 \cdot 10^6 \cdot 0{,}024} = 0{,}0253 \text{ m or } 1{,}05 \cdot \phi$$

$$\theta_{crit} = k_r \cdot \frac{\varepsilon_{sy}}{\phi} = 1{,}75 \cdot \frac{500 \cdot 10^6}{200 \cdot 10^9 \cdot 0{,}024} = 0{,}182 \text{ rad}$$

The shear displacement needed to mobilise the shear capacity is then calculated by eq. (8-15) as

$$s_{max} = \theta_{crit} \cdot x_0 = 0{,}182 \cdot 25{,}3 = 4{,}60 \text{ mm or } 0{,}192 \cdot \phi$$

The bar diameter is now assumed to be ϕ = 20 mm, while the material properties are the same as before f_y = 500 MPa, E_s = 200 GPa, and f_{cc} = 50 MPa. The calculations are repeated and yield the following results:

$$F_{vR} = \alpha_0 \phi^2 \sqrt{f_{cc} f_y} = 1{,}0 \cdot 0{,}020^2 \sqrt{50 \cdot 10^6 \cdot 500 \cdot 10^6} = 63{,}2 \cdot 10^3 \text{ N}$$

$$x_0 = \frac{F_v}{3\alpha_0^2 f_{cc}\phi} = \frac{63{,}2\cdot 10^3}{3\cdot 1{,}0^2\cdot 50\cdot 10^6\cdot 0{,}020} = 0{,}0211 \text{ m or } 1{,}05\cdot\phi$$

$$\theta_{crit} = k_r\cdot\frac{\varepsilon_{sy}}{\phi} = 1{,}75\cdot\frac{500\cdot 10^6}{200\cdot 10^9\cdot 0{,}020} = 0{,}219 \text{ rad}$$

$$s_{max} = \theta_{crit}\cdot x_0 = 0{,}219\cdot 21{,}1 = 4{,}62 \text{ mm or } 0{,}231\cdot\phi$$

The shear displacement associated with the shear capacity is the same as before in absolute terms but in relation to the bar diameter it is greater.

The bar diameter is now assumed to be the same as in the first case, while the material properties are changed so that ϕ = 24 mm, f_y = 500 MPa, E_s = 200 GPa, and f_{cc} = 20 MPa. The calculations are repeated.

$$F_{vR} = \alpha_0\phi^2\sqrt{f_{cc}f_y} = 1{,}0\cdot 0{,}024^2\sqrt{20\cdot 10^6\cdot 500\cdot 10^6} = 57{,}6\cdot 10^3 \text{ N}$$

$$x_0 = \frac{F_v}{3\alpha_0^2 f_{cc}\phi} = \frac{57{,}6\cdot 10^3}{3\cdot 1{,}0^2\cdot 20\cdot 10^6\cdot 0{,}024} = 0{,}0400 \text{ m or } 1{,}67\cdot\phi$$

$$\theta_{crit} = k_r\cdot\frac{\varepsilon_{sy}}{\phi} = 1{,}75\cdot\frac{500\cdot 10^6}{200\cdot 10^9\cdot 0{,}024} = 0{,}182 \text{ rad}$$

The shear displacement needed to mobilise the shear capacity is calculated as

$$s_{max} = \theta_{crit}\cdot x_0 = 0{,}182\cdot 40{,}0 = 7{,}28 \text{ mm or } 0{,}303\cdot\phi$$

The calculations show that the shear capacity, the distance to the plastic hinge and the shear displacement needed to mobilise the shear capacity all vary significantly with variation of the in-put data.

8.2.1.5 Steel flexural failure – eccentric load application

Fig. 8-14 shows a similar load case as before, but the shear force F_v is applied at a distance e outside the joint face. In this case the basic moment equation, eq. (8-8), is modified to

$$M_{max} = F_{vR}\cdot e + F_{vR}\frac{F_{vR}}{q_c} - q_c\frac{1}{2}\cdot\left(\frac{F_{vR}}{q_c}\right)^2 = F_{vR}\cdot e + \frac{1}{2}\frac{F_{vR}^2}{q_c} \qquad (8\text{-}16)$$

By equalising this load effect with the plastic moment resistance, according to eq. (8-9), and inserting eq. (8-6) for the concrete reaction, the shear resistance can be solved as

$$F_{vR}\cdot e + \frac{1}{2}\frac{F_{vR}^2}{q_c} = f_y\frac{\phi^3}{6} \qquad \Rightarrow$$

$$F_{vR}^2 + F_{vR}\cdot e\cdot 2\cdot(\beta_c f_{cc})\cdot\phi - f_y\frac{\phi^3}{6}\cdot 2\cdot(\beta_c f_{cc})\cdot\phi = 0 \qquad \Rightarrow$$

$$F_{vR} = -e \cdot (\beta_c f_{cc}) \cdot \phi \pm \sqrt{e^2 \cdot (\beta_c f_{cc})^2 \cdot \phi^2 + f_y \frac{\phi^4}{3} (\beta_c f_{cc})} \qquad \Rightarrow$$

$$F_{vR} = \sqrt{\frac{\beta_c}{3}} \cdot \phi^2 \sqrt{f_{cc} f_y} \left[\sqrt{1 + 3\beta_c \frac{f_{cc}}{f_y} \frac{e^2}{\phi^2}} - \sqrt{3\beta_c} \sqrt{\frac{f_{cc}}{f_y}} \frac{e}{\phi} \right]$$

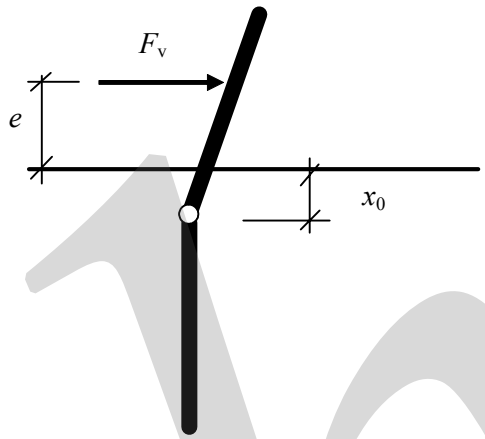

Fig. 8-14: One-sided dowel pin subjected to a shear force with a certain eccentricity e in relation to the joint face. Formation of plastic hinge

An eccentricity factor ε is now defined as

$$\varepsilon = 3 \frac{e}{\phi} \sqrt{\frac{f_{cc}}{f_y}} \tag{8-17}$$

which inserted yields the following expression for the shear capacity in case of eccentric loading.

$$F_{vRd} = \alpha_0 \cdot \alpha_e \cdot \phi^2 \sqrt{f_{cd} \cdot f_{yd}} \tag{8-18}$$

where α_0 = coefficient that considers the bearing strength of concrete

$$\alpha_0 = \sqrt{\frac{\beta_c}{3}} \qquad \text{(can be taken as } \alpha_0 = 1{,}0 \text{ in design)}$$

α_e = coefficient that considers the eccentricity

$$\alpha_e = \sqrt{1 + (\varepsilon \cdot \alpha_0)^2} - \varepsilon \cdot \alpha_0 \tag{8-19}$$

The coefficient that considers the eccentricity is always less than 1 and should be understood as a reduction coefficient. In Fig. 8-15 it is exemplified how the shear capacity is reduced by eccentric loading for two combinations of material strengths, moderate strength concrete with high strength steel, and high strength concrete with moderate strength steel. As appears from the figure, the effect of an eccentricity is significant for both combinations. An eccentricity of the same magnitude as the bar diameter results in a reduction of the shear capacity by about 0,4 – 0,6. Hence, for this type of steel flexural failure an eccentric application of the load reduces the shear capacity significantly and should be avoided when possible.

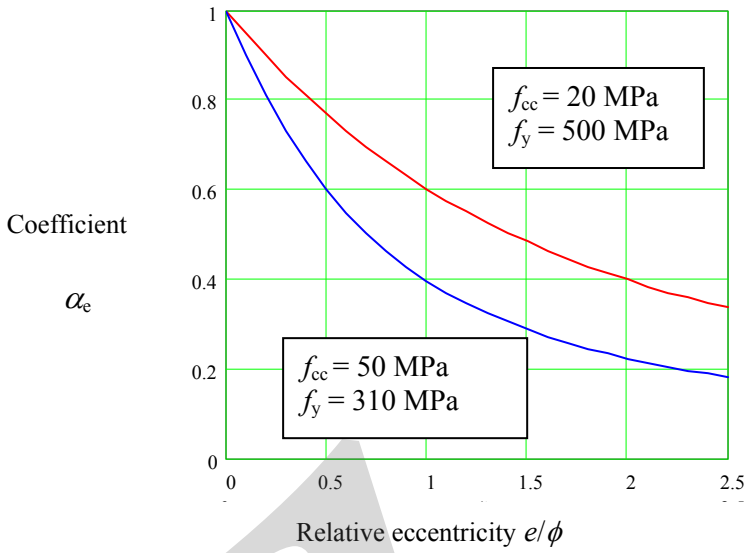

Fig. 8-15: Example of how the coefficient α_e, according to eq. (8-19) that considers eccentric loading varies with increasing relative eccentricity e/ϕ

8.2.1.6 Response of dowel connections

The response $F_v(s)$ of a dowel bar subjected to transverse shear displacement s depends on a number of parameters such as the distance to free edges, the bar diameter and anchorage length, the quality of concrete, the way of loading, etc. When a concrete cover c, adequately larger than the bar diameter ϕ is provided, the dowel transfer mechanism fails due to yielding of the bar and crushing of the surrounding concrete as described above. However, even if a splitting failure is avoided, the distance to free edges may influence the dowel response. For dowel connections failing by development of plastic hinges in the bar, a predicted relationship between shear force F_v and shear slip s is presented in Fig. 8-16, based on research results. [Vintzeleou and Tassios (1985)].

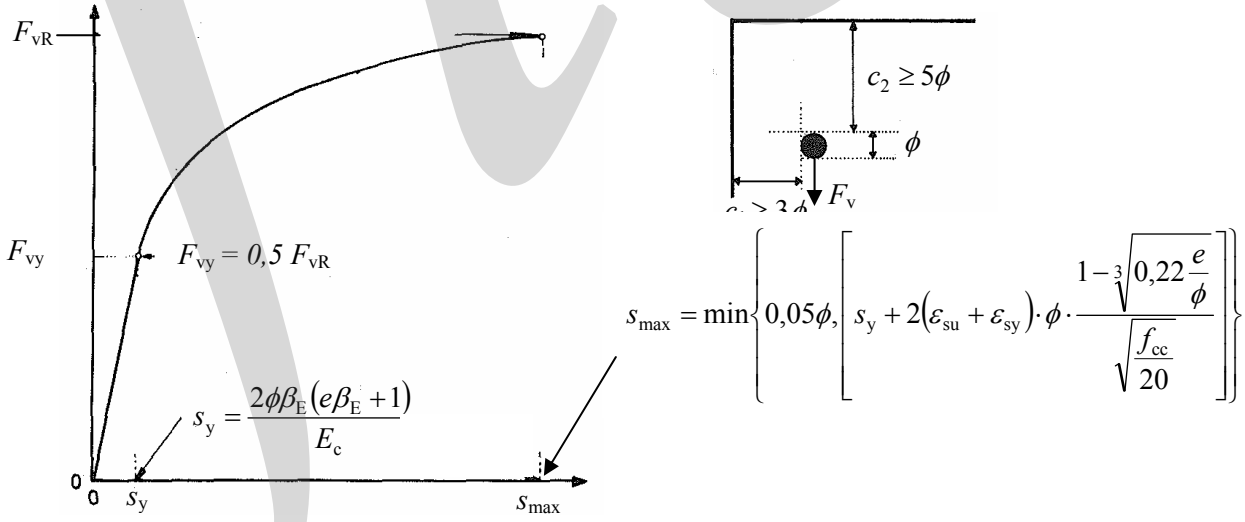

Fig. 8-16: Predicted relationship between shear force F_v and shear slip s for a dowel connection failing due to deformation of plastic hinges in the dowel, according to [Vintzeleou and Tassius (1985)]. Note that s refers to the slip of a one-sided dowel. In case of double-sided dowels with symmetric conditions the figure gives half the shear slip of the connection

In Fig. 8-16 the following main notation are used:

e is the eccentricity of the load, defined according to Fig. 8-14.

$$\beta_E = \left(\frac{E_c}{8 \cdot E_s \cdot I_s} \right)^{0,25} \qquad \text{(stiffness parameter)}$$

where E_s and I_s are modulus of elasticity and second moment of area of the bar, respectively

F_{vR} is the ultimate dowel capacity under monotonic action, with cover conditions as shown in Fig. 8-17.

With regard to combined effects of concrete cover and eccentricity the ultimate dowel capacity under monotonic loading can be predicted by means of the following relationship according to [Vintzeleou and Tassios (1985)].

$$F_{vR}^2 + (10 f_{cc} \cdot \phi \cdot e) F_{vR} - \alpha_c^{\,2} \cdot \phi^4 f_{cc} \cdot f_y = 0 \qquad (8\text{-}20)$$

where the units are mm, N and N/mm^2

α_c is a factor ($\leq$ 1,3) depending on the available concrete cover of the bar in the direction of the shear force. The value of α_c may be estimated as shown in Fig. 8-17 and Table 8-1.

Region in relation to free edges defined according Fig. 8-17	Value of α_c
I	$0,60 + \frac{c_1}{\phi}\left(0,027\frac{c_2}{\phi} + 0,10\right)$
II	$0,90 + 0,03\frac{c_2}{\phi}$
III	$0,60 + 0,233\frac{c_1}{\phi}$
IV	1,3

Table 8-1: The factor α_c that considers the influence of distance to free edges, see Fig. 8-17.

Taking e = 0 the capacity of the dowel connection under monotonic loading, for design purposes, may be estimated as follows, see eq. (8-20) and Fig. 8-16.

$$F_{vRd} = \frac{1}{\gamma_{Rd}} \alpha_c \cdot \phi^2 \sqrt{f_{cd} \cdot f_{yd}} \qquad (8\text{-}21)$$

where $\gamma_{Rd} \approx 1,3$ and the units are mm, N, N/mm^2, and α_c is taken from Table 8-1 and Fig. 8-17.

For a shear force greater than F_{vy} and less than the ultimate capacity F_{vR}, the shear displacement, according to Fig. 8-16, can be calculated by means of the following expression.

$$s = s_y + 1,15 \cdot s_{max}\left[\left(\frac{F_v}{F_{vR}}\right)^4 - 0,5\left(\frac{F_v}{F_{vR}}\right)^3\right] \qquad \text{(for one-sided dowel)} \qquad (8\text{-}22)$$

Note that eq. (8-22) refers to one-sided dowels. For double-sided dowels with symmetrical conditions the expression gives half the shear slip of the joint.

However, for the sake of additional safety, only bars with cover $c \geq 5\phi$ in the direction of the shear force should be taken into account for design purposes, see Fig. 8-17.

According to Vintzeleou and Tassios (1987), the design dowel force under cyclic loading can be taken equal to half the design dowel value under monotonic loading [eqs. (8-21) and (8-22)].

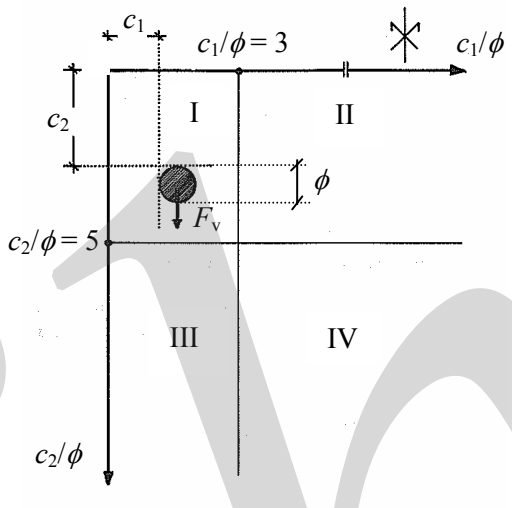

Fig. 8-17: Classification of regions with regard to distance from dowel bar to free edges for estimation of the factor α_c, according to [Vintzeleou and Tassios (1985)]

8.2.2 Double-sided dowel

8.2.2.1 Plain dowel pin without end anchors and no joint gap

For a dowel pin embedded in elements on each side of the joint, plastic hinges will ultimately be formed on each side, Fig. 8-18. The formation of two plastic hinges results in a mechanism in which the shear displacement will increase without control. Hence, the failure of the connection is assumed to take place when such a mechanism is formed

If the dowel pin is plain and without end anchors, the dowel pin is allowed to slide in the concrete, longitudinally, when the connection is subjected to shear displacement, see Fig. 8-18. It means that in the section where the bending moment is maximum there is no overall axial stress, but only flexural stresses.

In case of symmetry, i.e. the same concrete strength in both concrete elements, a point of inflection develops at the joint interface and the two plastic hinges will develop simultaneously and at the same distance x_0 from the joint interface. The shear capacity can be determined by studying the load case where the dowel pin is cut in the plane of symmetry. It appears that in case of no joint width, the load case is basically the same as for a one-sided dowel without eccentricity and the shear capacity can be solved by eq. (8-10).

According to CEB-FIP Model Code 90 the shear displacement needed to mobilise the shear capacity for a shear connection with a double-sided dowel can be estimated as

$$s_{max} = 0{,}10 \cdot \phi \qquad (8\text{-}23)$$

where ϕ = diameter of dowel bar

Alternatively, on basis of the definition of a critical angle θ_{crit}, se eq. (8-14), the needed shear displacement is now determined as

$$s_{max} = \theta_{crit} \cdot 2x_0 \tag{8-24}$$

where $2x_0$ = distance between the plastic hinges

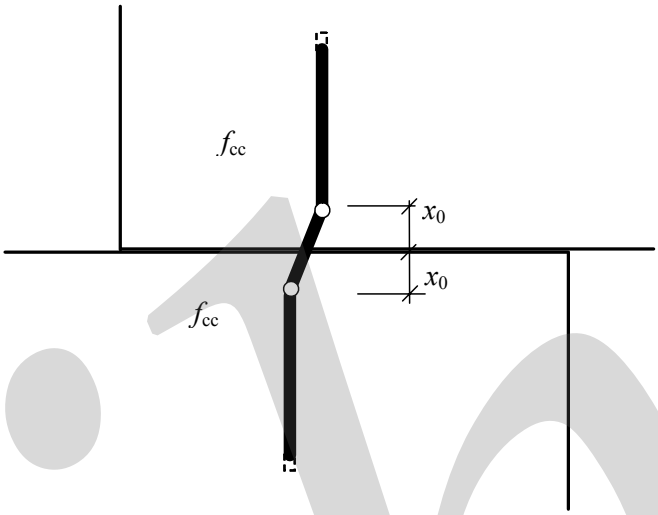

Fig. 8-18: Double-sided plain dowel pin across a joint interface (no joint gap) is equivalent two a one-sided dowel pin with no eccentricity

8.2.2.2 Plain dowel pin without end anchors across a joint of a certain width

When a joint between the two connected elements has a certain width, for instance due to a soft bearing, this may result in eccentric loading of the dowel pin, as shown in Fig. 8-19.

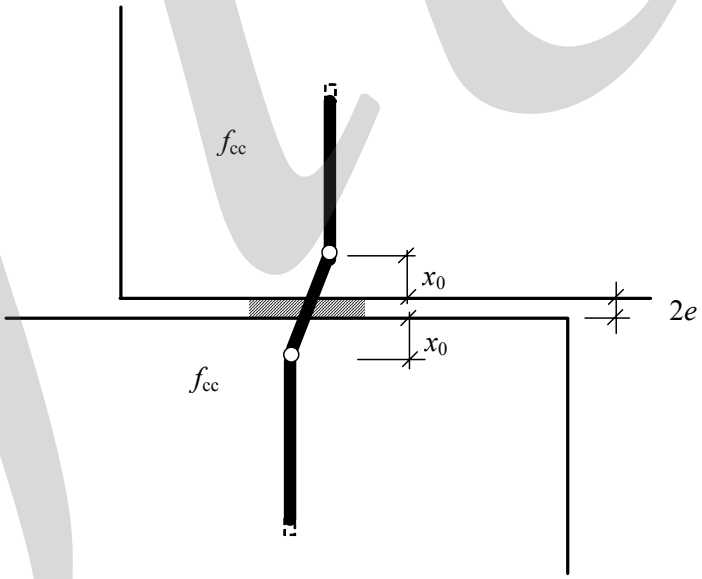

Fig. 8-19: Double-sided plain dowel pin across a joint of a certain width (e.g. due to a soft bearing) is equivalent to a one-sided dowel pin with eccentricity e = half joint width

A soft bearing will give no significant transverse bearing stress to the dowel pin within the joint width and accordingly such transverse support is, on the safe side, ignored. If the conditions are symmetric, the point of inflection will appear in the middle of the joint. A cut through the dowel pin in

this section transforms the actual load case to an equivalent one with a one-sided dowel where the shear force is applied at an eccentricity e = half joint width. Hence, in this case, the shear capacity can be determined by eq. (8-18).

8.2.2.3 Inclined dowel pin

Fig. 8-20 shows a case where a dowel pin is inclined in relation to the joint interface. This situation was studied in tests by Dulácska (1972). The test specimens were provided with two layers of sheet brass, thickness 0,2 mm each, to simulate an initial crack. Due to the loading direction, as shown in the figure, the two parts of the specimen separated during the shear loading and friction along the interface was avoided. The angle varied between 10° and 40° and the shear resistance due to dowel action decreased with increasing angle α.

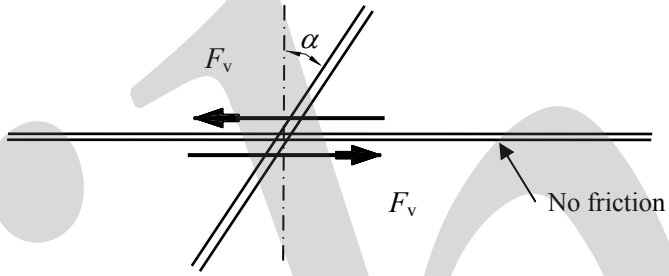

Fig. 8-20: Double-sided plain dowel pin placed in a skew angle in relation to the joint interface, a) positive inclination results in compression of the dowel bar, b) negative inclination results in tension of the dowel bar

On the basis of test results Dulácska (1972) proposed the following expression to determine the shear capacity of inclined dowel bars without contribution from shear friction.

$$F_{vR} = \beta_n \beta_c \sin\alpha \, f_y \phi^2 \left[\sqrt{1 + \frac{f_{cc}}{3\beta_n \beta_c \sin^2 \alpha \, f_y}} - 1 \right] \tag{8-25}$$

where $\beta_n = \left(1 - \frac{N^2}{N_y^2}\right)$

β_c = factor that considers the tri-axial local state of stress of concrete, see eq. (8-6)
α = angle between the dowel bar and the normal plane to the joint interface
N = tensile force in dowel
N_y = yield capacity of bar in tension

For an angle $\alpha = 90°$ and assuming that there is no tensile force in the bar, eq. (8-25) becomes identical with the basic expressions (8-10) and (8-11).

8.2.3 Influence of non-symmetrical conditions

8.2.3.1 Plain dowel pin without end anchors, different concrete strengths

When dowel action is used in practical applications, it happens quite often that the conditions are different on each side of the joint, for instance due to quite different concrete strengths. A typical case is a bolted beam-column connection where the bolt is cast in place in the supporting member and protrudes into a vertical recess in the supported member, where the recess is filled with grout, see Fig. 8-21.

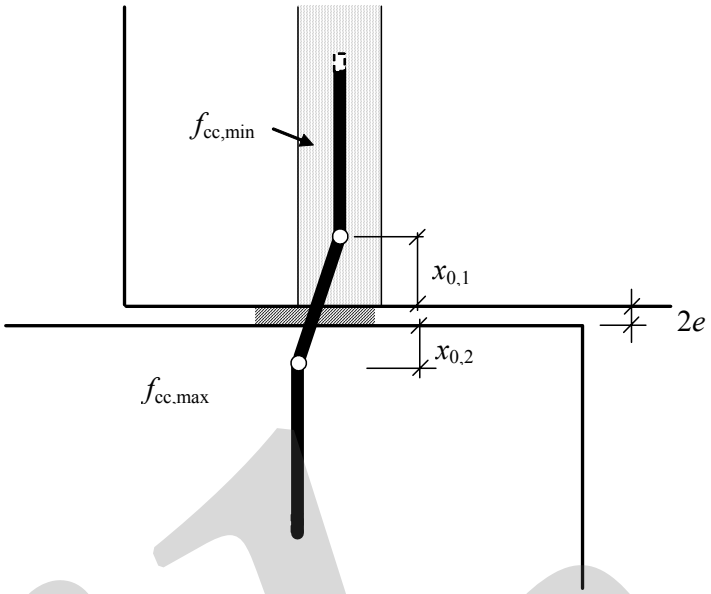

Fig. 8-21: Example of a bolted connection, where the conditions with regard to dowel action are non-symmetrical

This load case is not any longer symmetrical, but the connection has a stronger and a weaker side. Accordingly, the plastic hinges will not develop simultaneously, and the ultimate load is reached at the formation of the second plastic hinge, which turns the resisting system to a collapse mechanism.

It appears from eqs. (8-8) and (8-6) that the maximum bending moment in the dowel pin increases with decreasing concrete strength and from eq. (8-12) that the distance from the joint interface to the plastic hinge increases. This means that for a certain shear force, a plastic hinge is formed in the dowel pin at the weaker side, while the dowel still has an elastic behaviour at the stronger side. Hence, the load can be increased further and not until a plastic hinge is formed also at the other side, a failure mechanism is obtained. However, the stiffness of the shear connection is reduced by the formation of the first plastic hinge.

Since the ultimate capacity of the connection is determined by the formation of the second hinge, the shear capacity in case of no eccentricity can be calculated as

$$F_{vRd} = \alpha_0 \phi^2 \sqrt{f_{cd,max} f_{yd}} \tag{8-26}$$

where $f_{cd,max}$ = design concrete compressive strength at the stronger side

This interpretation of the basic model for dowel action, in case of non-symmetrical conditions, has been confirmed by experimental results of bolted beam-column connections [Engström (1990)]. A typical shear force-shear displacement relationship for a dowel pin with non-symmetrical conditions is shown in Fig. 8-22. The shear force for which the first plastic hinge develops can be estimated by eq. (8-10) with f_{cd} taken as $f_{cd,min}$.

In case of a joint opening between the connected elements (see Section 8.2.2.2), the eccentricity can be taken approximately as half the joint width, in spite of the non-symmetrical conditions, and the ultimate shear capacity of the connection can be determined by eq. (8-10), but with $f_{cd} = f_{cd,max}$.

For cases with non-symmetrical conditions, either with or without a joint gap of a certain width, the shear displacement needed to create the failure mechanism can be expressed by means of the critical angle, see eq. (8-14) and Fig. 8-13, as

$$s_{max} = \theta_{crit} \cdot l_p \tag{8-27}$$

where l_p = distance between the plastic hinges

$l_p = x_{0,1} + x_{0,2} + t_j$

t_j = width of joint gap, if any

$x_{0,i}$ = distance between plastic hinge and joint face of member *i*

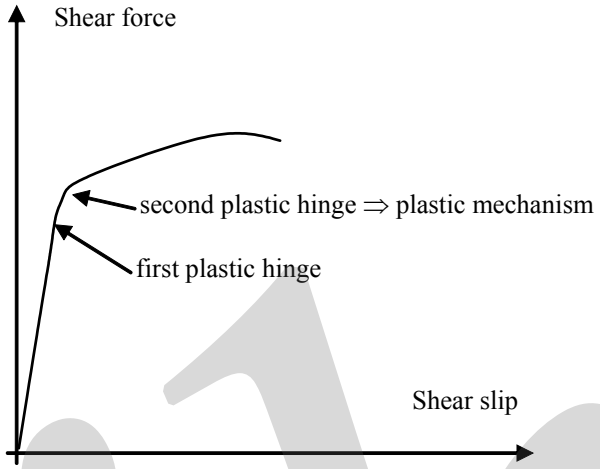

Fig. 8-22: Typical relationship between shear force and shear displacement for bolted connection with non-symmetrical conditions. The formation of the first plastic hinge, on the weaker side, results in a marked reduction of the shear stiffness.

8.2.3.2 Plain dowel pin fixed to steel insert, no joint gap and no end anchor

In order to avoid obstacles with protruding bars during handling and transportation of elements, the dowel pin can be fixed to an insert after mounting of the element. For a dowel pin in an insert, plastic hinges can not develop at the same locations as for a continuous plain bar arranged across the joint. The collapse mechanism still consists of two plastic hinges, but one develops in the section where the dowel bar is fixed to the insert and the other one forms at a certain distance from the joint where the bending moment is maximum, see Fig. 8-23. The restraint from the fixation in the insert will lead to an increased shear capacity of the dowel connection.

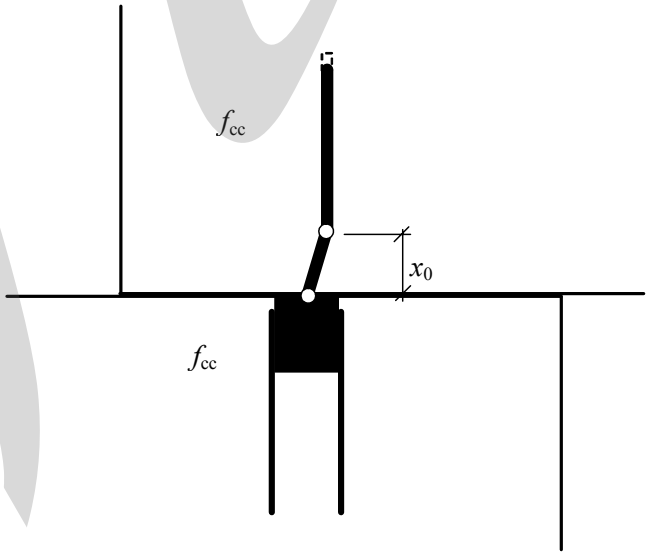

Fig. 8-23: Connection with dowel bar placed in insert, collapse mechanism and calculation model in case of steel flexural failure

The state of equilibrium is studied when the plastic resistance M_y is reached in the section where the dowel bar is fixed to the insert. The basic moment equation, eq. (8-8), is then modified to

$$M_{\max} = F_{\mathrm{vR}} \frac{F_{\mathrm{vR}}}{q_c} - q_{\mathrm{c}} \frac{1}{2} \cdot \left(\frac{F_{\mathrm{vR}}}{q_{\mathrm{c}}} \right)^2 - M_{\mathrm{y}} \tag{8-28}$$

By equalising this load effect with the plastic moment resistance and inserting eq. (8-6) for the concrete reaction, the shear resistance can be determined as

$$\frac{1}{2} \frac{F_{\mathrm{vR}}^2}{q_{\mathrm{c}}} = 2 \cdot f_{\mathrm{yd}} \frac{\phi^3}{6} \qquad \Rightarrow$$

$$F_{\mathrm{vR}}^2 = 2 \cdot f_y \frac{\phi^3}{6} \cdot 2 \cdot (\beta_{\mathrm{c}} f_{\mathrm{cc}}) \phi = 2 \cdot \frac{\beta_{\mathrm{c}}}{3} \phi^4 f_{\mathrm{cc}} f_{\mathrm{y}} \qquad \Rightarrow$$

$$F_{\mathrm{vRd}} = \alpha_0 \sqrt{2} \cdot \phi^2 \sqrt{f_{\mathrm{cd}} f_{yd}} \tag{8-29}$$

where $\alpha_0 = \sqrt{\frac{\beta_{\mathrm{c}}}{3}}$ (can be taken as c_0 = 1,0 in design)

Dowel bars are sometimes placed in threaded inserts. In that case the dowel bar has a threaded end and a reduced plastic moment resistance $M_{y,red}$ at the fixation, see Fig. 8-24. For a general case the shear capacity on the flexural steel failure can be expressed as

$$F_{\mathrm{vRd}} = \alpha_0 \cdot \alpha_{\mathrm{r}} \cdot \phi^2 \sqrt{f_{\mathrm{cd}} f_{\mathrm{yd}}} \tag{8-30}$$

where α_{r} = coefficient that considers the end restraint

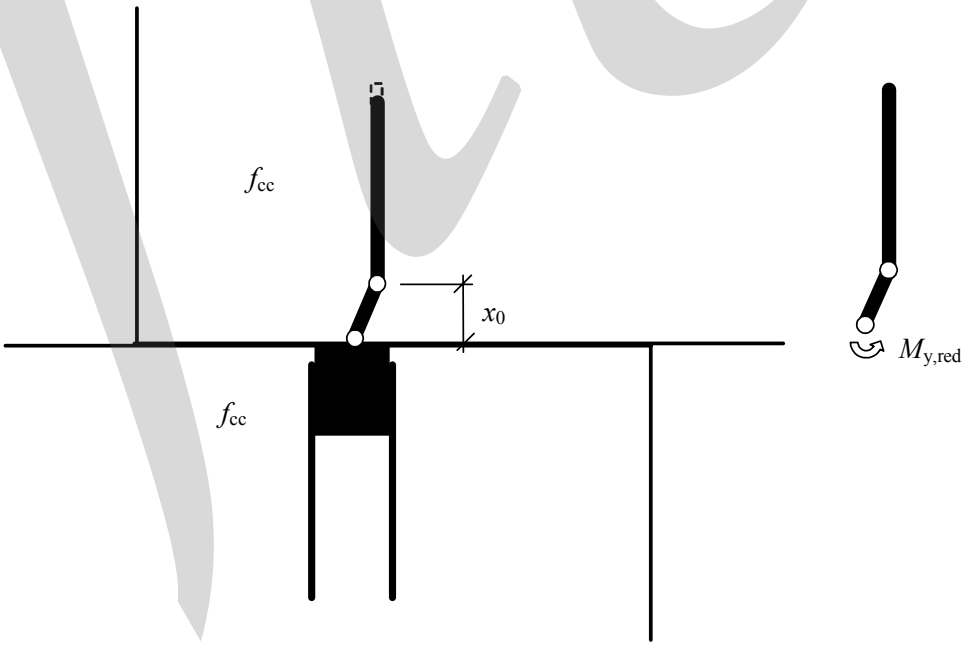

Fig. 8-24: Connection with dowel bar placed in threaded insert, reduced bar cross-section due to threaded end of dowel bar

The restraint factor depends on the reduced plastic moment capacity of the fixed end in relation to that where the other plastic hinge develops. In that case the restraint factor is found as

$$\alpha_r = \sqrt{1 + \frac{M_{y,red}}{M_y}} \tag{8-31}$$

where $M_{y,red}$ = reduced plastic moment capacity of dowel bar at fixation due to threaded end
M_y = plastic moment capacity of dowel bar in general

As in the basic case the distance x_0 from the joint face to the plastic hinge is found as

$$x_0 = \frac{F_v}{q_c} = \frac{F_v}{3\alpha_0^2 f_{cc}\phi} \tag{8-32}$$

It is assumed that the shear displacement needed to create the failure mechanism can be expressed as before by means of the critical angle, see eq. (8-14), as

$$s_{max} = \theta_{crit} \cdot l_p \tag{8-33}$$

where l_p = distance between the plastic hinges

In this case the distance between the plastic hinges is

$$l_p = x_0$$

8.2.3.3 Plain dowel pin fixed to steel insert, across a joint of a certain width

In case of a joint gap, for instance due to a soft bearing, the shear capacity will be influenced by the combined effects of restraint and eccentricity. The load case appears from Fig. 8-25. The dowel bar is cut in the section of fixation and for a general case, with a reduced plastic moment capacity of the fixed end of the bar, the equilibrium condition of the free body yields

$$M_{max} = F_{vR} \cdot e + F_{vR}\frac{F_{vR}}{q_c} - q_c \frac{1}{2} \cdot \left(\frac{F_{vR}}{q_c}\right)^2 - M_{y,red} \tag{8-34}$$

By equalising this load effect with the plastic moment resistance, eq. (8-9), and inserting eq. (8-6) for the concrete reaction, the shear resistance can be solved as

$$F_{vR} \cdot e + \frac{1}{2}\frac{F_{vR}^2}{q_c} = M_y + M_{y,red} \quad \Rightarrow$$

$$F_{vR} \cdot e + \frac{1}{2}\frac{F_{vR}^2}{q_c} = \alpha_r^2 \cdot M_y \quad \Rightarrow$$

$$F_{vR} = \sqrt{\frac{\beta_c}{3}} \cdot \left[\sqrt{\alpha_r{}^2 + (\varepsilon \cdot \alpha_0)^2} - \varepsilon \cdot \alpha_0\right] \cdot \phi^2 \sqrt{f_{cc} \cdot f_y}$$

$\Rightarrow$

$$F_{vRd} = \alpha_0 \cdot \alpha_{e,r} \cdot \phi^2 \sqrt{f_{cd} f_{yd}} \tag{8-35}$$

where $\alpha_0 = \sqrt{\frac{\beta_c}{3}}$ (can be taken as $\alpha_0 = 1{,}0$ in design)

$\alpha_{e,r}$ = factor that considers the combined effect of eccentricity and end restraint

$$\alpha_{e,r} = \sqrt{\alpha_r^2 + (\varepsilon \cdot \alpha_0)^2} - \varepsilon \cdot \alpha_0$$

where ε is determined according to eq. (8-17)

$$\alpha_r = \sqrt{1 + \frac{M_{y,red}}{M_y}}$$

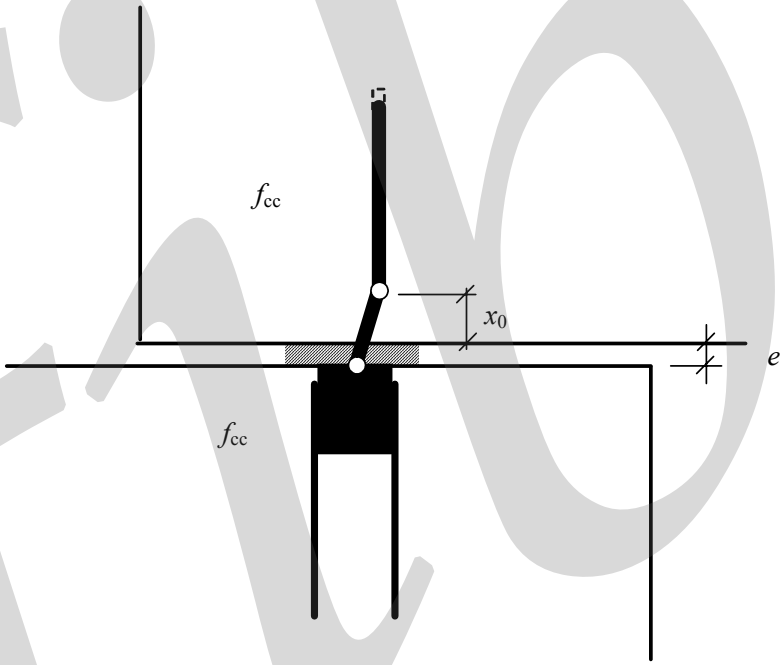

Fig. 8-25: Connection with joint gap and dowel bar placed in threaded insert, collapse mechanism in steel flexural failure

8.2.4 Combination of dowel action and friction

8.2.4.1 Plain dowel pin with end anchors

In a shear connection where the dowel pin is plain and without end anchors, the shear displacement is possible to obtain without any significant axial restraint in the dowel pin. The dowel pin can slide inside the concrete and will successively adapt itself by bending deformations to the actual shear displacement. When the dowel is plain the bond stresses along the dowel can be assumed to be without significance. It means that only flexural stresses will appear in the critical section with the maximum bending moment.

However, for a plain dowel pin with end anchors, a substantial axial restraint develops, when the shear connection is loaded in shear. If the end anchors are firmly fixed in the concrete, the dowel pin must elongate to adapt itself to the shear deformation. It means that overall axial stresses as well as

flexural stresses develop when the connection is loaded in shear. The final failure depends still on a mechanism with plastic hinges, but the dowel capacity is influenced by the axial restraint.

In a general case with non-symmetrical conditions it is assumed that in the ultimate state plastic hinges develop at distances x_{01} and x_{02} from the joint interface as shown in Fig. 8-26. Furthermore, it is assumed that the plastic hinges develop when a critical overall rotation θ_{crit} is reached, see eq. (8-14). Then the elongation of the dowel pin, which is required to reach the failure mechanism, can be calculated as

$$n = \sqrt{l_p^2 + (\theta_{crit} l_p)^2} - l_p = l_p(\sqrt{1 + \theta_{crit}^2} - 1)$$

If this elongation is assumed to be uniformly distributed between the end anchors, i.e. no bond stresses develop, the corresponding axial steel stress can be calculated as

$$\sigma_{sn} = \frac{n}{l_a} E_s$$

where l_a = length of dowel pin between the end anchors

Since this steel stress is used for the overall elongation, it is not any more available for the flexural resistance of the dowel bar and the dowel capacity will be reduced. On the other hand the tensile force in the dowel bar must be balanced by an equal compressive force at the interface and a frictional force develops along the interface, which contributes to the shear resistance.

$$F_{vR} = \alpha_0 \phi^2 \sqrt{f_{cc,max} f_{y,red}} + \mu \cdot \sigma_{sn} A_s \qquad (8\text{-}36)$$

where $f_{cc,max}$ = concrete compressive strength at the stronger side
$f_{y,red}$ = strength available for dowel action
$f_{y,red} = f_y - \sigma_{sn}$

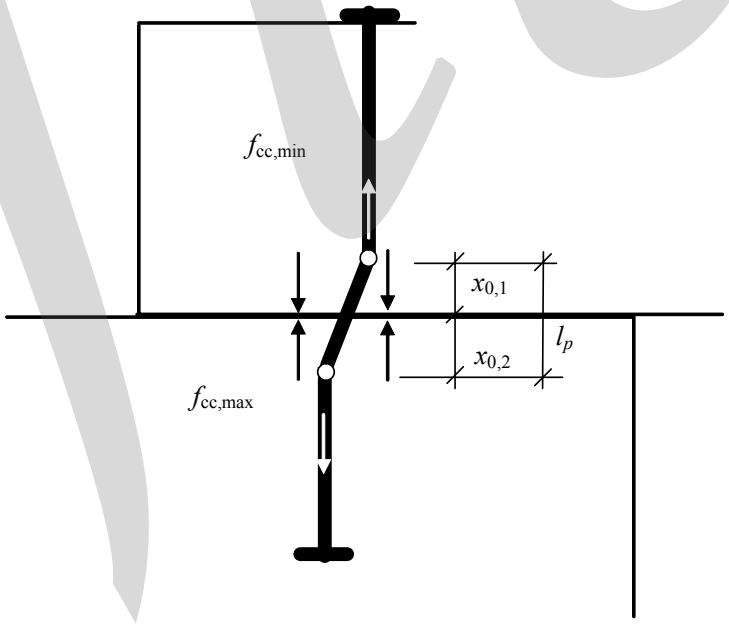

Fig. 8-26: When a dowel bar is provided with end anchors, the shear displacement along the joint interface results in an elongation n of the dowel bar. If the bar is plain this elongation can be assumed to be evenly distributed along the bar between the end anchors

8.2.4.2 Dowel pin anchored by bond

When dowel bars are anchored by bond, for instance by use of ribbed bars, and the connection is loaded in shear along the joint interface, the bars will be subjected to overall tensile stresses in a similar way as shown in Fig. 8-26. However, in this case the necessary elongation corresponding to a certain shear slip can not be assumed to be evenly distributed, but will localize to the region near the joint interface where high tensile stresses will develop in the bar. This is favourable with regard to the frictional component in eq. (8-36), since the compressive stress across the joint will be high for only a small shear slip. On the other hand, the resistance by dowel action will be reduced because of the less tensile strength available. It should also be noted that dowel action requires a significant shear slip before the maximum dowel capacity is reached, see Fig. 8-16.

Now depending on the roughness of the joint interface and the bond characteristics of the bar, various combinations of frictional resistance and dowel resistance are possible when the maximum capacity is reached. In case of a rough interface and high pullout resistance of the dowel bar, the frictional component will dominate and the contribution by dowel action is quite insignificant. This mechanism is referred to as 'shear friction' and this interaction further is explained in Section 8.3.4. When on the other hand the joint interfaces are smooth and the pullout resistance of the bar is small, the contribution by dowel action will dominate, but it develops fully for much greater values of the shear slip. In this case the models given above in Sections 8.2.1 – 8.2.3 are relevant. Intermediate situations are treated in Section 8.3.4.4.

8.3 Shear transfer by concrete-to-concrete friction

One of the basic mechanisms for shear transfer is frictional resistance in joint interfaces, see Fig. 8-1. The resistance depends on concrete-to-concrete friction and the mechanism reminds of shear transfer in cracks due to aggregate interlock. However, in joints to precast elements the roughness of the joint faces may vary and the shear resistance may concern uncracked as well as cracked conditions. The roughness of joint faces can be controlled by treatment of the fresh concrete. Joint faces can be classified with regard to its natural roughness, roughness after special treatment or even specially formed shear keys.

8.3.1 Roughness of joint faces

The shear transfer in joints between concrete elements can increase by treatment of the joint faces to improve the roughness. In this context smooth, rough, and indented joint faces are distinguished. Gustavsson (1981) and FIP (1982) proposed a classification of joint faces, according to the categories listed in Table 8-2. This classification was adopted in CEB-FIP Model Code 1990. The joint faces in Table 8-2 are arranged in order of the unevenness.

Categories		
Smooth	Rough	Indented
type I: a smooth surface, as obtained by casting against a steel or timber shutter	**type VII**: as for (VI), but with more pronounced texturing, as obtained by brushing, by a transverse screeder, by combining with a steel rake or with an expanded metal	**type X**: a surface, which has been provided with mechanical shear keys.
type II: a surface which lies between trowelled or floated to a degree, which is effectively as smooth as (I)	**type VIII**: a surface which has been thoroughly compacted, but no attempt has been made to smooth, tamp or texture the surface in any way, having a rough surface with course aggregate protruding, but firmly fixed in the matrix	
type III: a surface which has been trowelled or tamped in such a way that small ridges, indentations or undulations have been left	**type IX**: where the concrete has been sprayed when wet, to expose the course aggregate without disturbing it	
type IV: a surface achieved by slip-forming or vibro-beam screeding		
type V: a surface achieved by extrusion		
type VI: a surface, which has been deliberately textured by lightly brushing the concrete when wet		

Table 8-2: Classification of joint faces with regard to unevenness, according to CEB-FIP Model Code 90

In practice, however, it is difficult to apply firm borders between the different types of joint faces. In order to determine objectively the roughness of a joint face, the parameter 'unevenness' s_r has been introduced. It is defined in Swedish Standard, SIS (1978).

The distance between the joint face and the average plane of the joint face is measured in a number of points by a special instrument. The tip of the measuring stick should have a radius of 3 mm. Measurements are made in 10 points with an interval of 5 mm on each of 4 lines at the joint face. The measuring lines should be parallel to the expected shear direction in the final application.

For each line n the variance of the differences between measurements in adjacent points is calculated as

$$s_{r,n}^2 = \frac{1}{8}\left[(a_n - b_n)^2 + (b_n - c_n)^2 ..... + (i_n - j_n)^2 - \frac{1}{9}(a_n - j_n)^2 \right] \tag{8-37}$$

where a_n, b_n.....j_n are the measurements in order of measuring

The unevenness s_r is calculated as the estimated standard deviation as

$$s_r = \sqrt{\frac{1}{6}\left(s_{r,1}^2 + s_{r,2}^2 + s_{r,3}^2 + s_{r,4}^2 + s_{r,5}^2 + s_{r,6}^2\right)} \tag{8-38}$$

According to Gustavsson (1981) the joint faces should be regarded as 'smooth' when they are obtained directly by casting without any direct measures to improve the roughness. Formally this corresponds to joint faces of types I - VI in Table 8-2. The unevenness of 'smooth' joint faces is, according to Gustavsson (1981), smaller than s_r = 1 mm. According to the Swedish handbook BBK 94 (1994), a joint face may be considered as 'rough' when the unevenness is not less than s_r = 1,5 mm.

It is not only the unevenness of the joint faces that is important for the shear resistance of shear connections. It is stated by Gustavsson (1981) that the workmanship has at least the same importance. The factors that influence the final result are cleanness of the joint faces, and compaction, curing and wetting of the concrete.

In Eurocode 2 [CEN (2004)] joint faces are classified as 'very smooth', 'smooth', 'rough' or 'indented'. The definitions are presented in Table 8-3.

Category	Description
Very smooth	A surface cast against steel, plastic or specially prepared wooden moulds
Smooth	A slip-formed or extruded surface, or a free surface left without further treatment after vibration
Rough	A surface with at least 3 mm roughness at about 40 mm spacing, achieved by raking or exposing of aggregate or other methods giving an equivalent result
Indented	Indented surface where the geometry complies with Fig. 8-27

Table 8-3: Classification of joint faces according to Eurocode 2 [CEN (2004)]

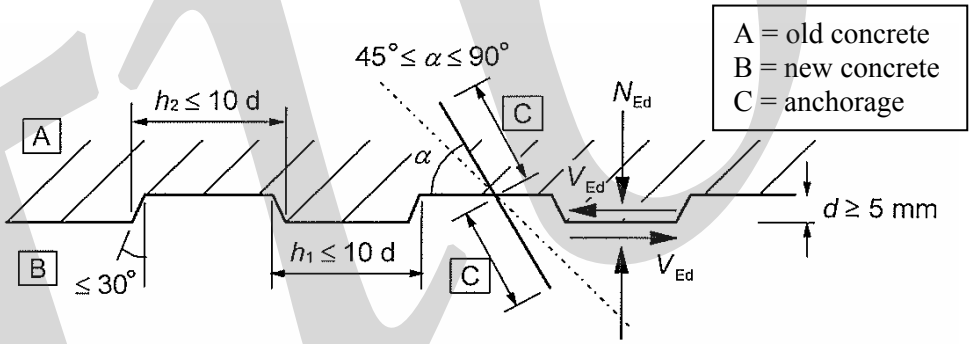

Fig. 8-27: Geometrical requirements on indented joint face according to Eurocode 2 [CEN (2004)]

8.3.2 Shear slip and joint separation

When a shear displacement s is imposed along a joint interface, a lateral dilatancy w is produced due to the irregularities of the joint faces, see Fig. 8-28 a. This joint separation, equal to the crack width, increases with increasing shear slip up to a maximum value w_{max}, which depends on the roughness of the joint faces. Hence, for each joint interface, depending on its surface characteristics, there exists a characteristic relationship between the longitudinal shear slip s and the corresponding lateral separation w.

When the joint faces are displaced along the joint, in contact to each other but without significant transverse compression, a basic relationship is obtained that mainly depends on the original surface geometry. However, if the joint is loaded by transverse compression during the shear slip, the joint separation will be smaller because the irregularities in contact are compressed, crushed and sheared off. Hence, the joint separation decreases with increased compressive stresses across the joint

interface. The typical influence of transverse compression on the relationship between shear slip and joint separation is shown in Fig. 8-28 b.

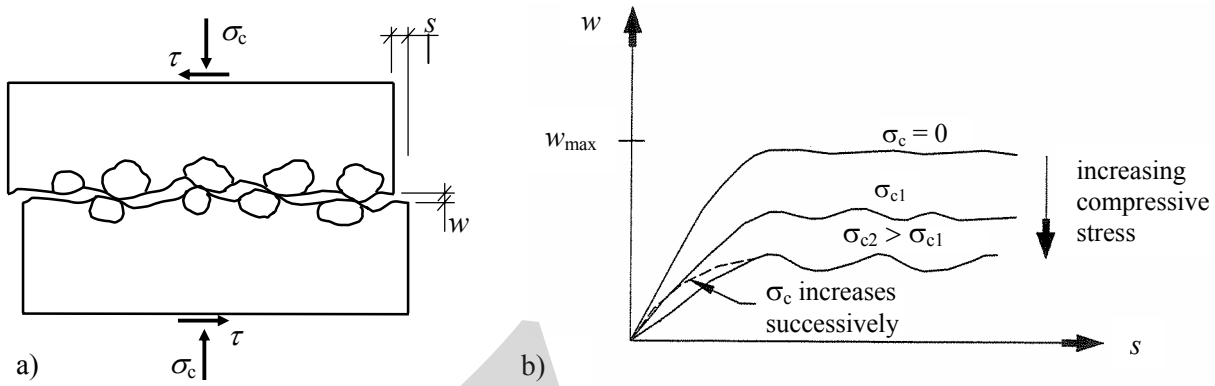

Fig. 8-28: Shear slip s along a rough joint interface results in a lateral joint separation w, a) basic mechanism, b) typical relationships between w and s depending on the transverse compressive stress

In many practical applications, the compressive stress increases, due to pullout resistance of transverse steel for instance, when the shear slip increases. The dotted line in Fig. 8-28 b refers to such a case.

The lateral dilatancy w may be related to shear displacement s in the following empirical relations.

For smooth interfaces:

$$w = 0{,}05 \cdot s \tag{8-39}$$

For rough interfaces, according to CEB-FIP Model Code 90 [CEB-FIP(1992)]:

$$w = 0{,}6 \cdot s^{2/3} \tag{8-40}$$

where the units are in mm.

Note that these relations are valid for $w \le w_{max}$. The relations seem to be valid for values at least up to s = 2,0 mm for eq. (8-39) and s = 2,5 mm for eq. (8-40). When the shear slip increases beyond these limits, the lateral separation can be assumed to remain approximately constant and equal to the maximum value w_{max}.

8.3.3 Resistance due to friction

Shear may be transferred along a concrete interface by means of friction, wherever a normal compressive stress is acting on this interface. Normal compression may be due to an externally imposed load, prestressing or to the pullout resistance of reinforcing bars crossing the interface. In the latter case, which is treated in Section 8.3.4, the compression is generated by the shear mechanism itself.

The shear transfer at a joint interface has often been visualized schematically as shown in Fig. 8-29. The joint interface is thought to be saw-toothed and the tooth inclination is equal to the frictional angle ϕ. The load case with a transverse compressive force N_c and a longitudinal shear force F_v results in contact forces perpendicular to the inclined contact areas. The resultant to these inclined contact forces is denoted F_c and its component along the joint section is then $N_c \cdot \tan\phi$. Hence, the shear resistance can be estimated as

$$F_{vR} = N_c \tan\phi \tag{8-41}$$

where $\mu = \tan\phi$ (frictional coefficient)

By dividing this expression with the area of the interface, the shear strength τ_R is found as

$$\tau_R = \mu\sigma_c \tag{8-42}$$

where σ_c = compressive stress acting across the joint interface

This approach was used by Birkeland and Birkeland (1966) to estimate the shear capacity of joints, where concrete was cast to a hardened concrete surface. Frictional coefficients were evaluated from test results. For ordinary construction joints the frictional coefficient was found to be in the order of $\mu = 0{,}6$ to $\mu = 0{,}8$. For joint faces that were roughened by special measures, the frictional coefficient was found to be about $\mu = 1{,}4$.

The frictional properties of joints between concrete elements not cast to each other, e.g. support joints, were examined by Möllersten and Packalen (1966). When the concrete faces were cast to very smooth moulds, the frictional coefficient was found to vary between $\mu = 0{,}55$ and $\mu = 0{,}70$. For frictional coefficients to be used in design, see below and also Sections 8.3.4.3 and 8.4.3.

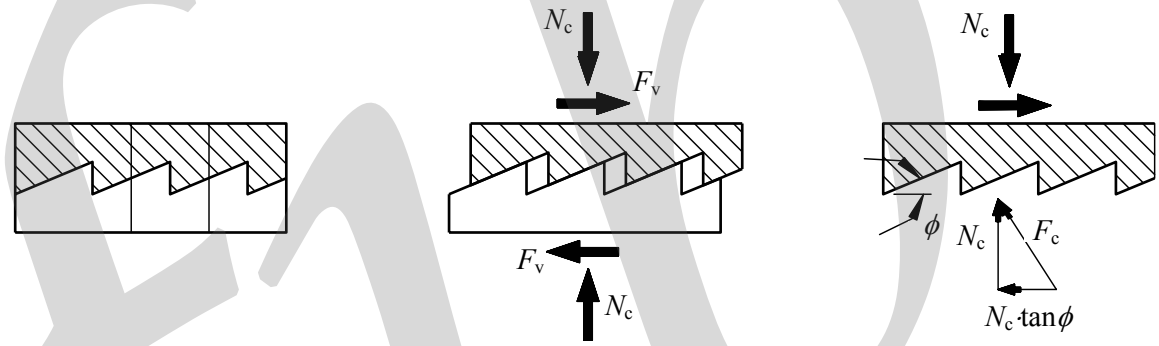

Fig. 8-29: Schematic illustration of shear transfer by friction

This way to visualise the shear behaviour may seem to be very simplified with regard to the non-regular unevenness of real joint faces. However, according to Carlsson (1979), the most pronounced irregularities of the joint face will be loaded first, as they are the most effective 'shear keys'. The concentrated forces acting on these spots will result in local crushing of these irregularities and shear-off of tips and sharp edges. Thereby, there will be a successive degradation of the joint face and the irregularities are levelled out to a more uniform roughness. This successive degradation of the joint face means that the shear stresses will be more uniformly distributed after some shear slip, and the joint face will be more and more like the idealisation shown in Fig. 8-29. The extent of degradation and levelling out depends on the compressive stress across the joint interface, the roughness, and the concrete strength [Carlsson (1979)].

By adding a cohesion term the expression for the shear resistance, eq. (8-42) became more general. This resulted in a better agreement with test results.

$$\tau_R = c + \mu\sigma_c \tag{8-43}$$

On the basis of test results of shear joints with transverse reinforcement Mattock (1974) proposed the values c = 2,8 MPa and μ = 0,8.

Since eq. (8-43) is very general, this form of expression has often been used for design of construction joints and joints between large panels in precast structures. The cohesion term can then be

used to account for bond of uncracked joint interfaces, influence of shear keys in indented joint faces, see Section 8.4.3.

In cases with more pronounced roughness the contribution by 'aggregate interlock' will be significant. It was shown by Walraven (1981) that the shear resistance of cracks in concrete (rough interfaces) was influenced by the concrete strength. A behaviour model was proposed, see Fig. 8-30, by which it was shown how the shear transfer is built up by numerous small forces at contact areas between aggregates and the cement matrix,

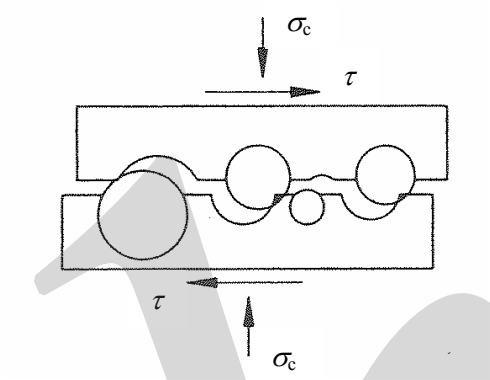

Fig. 8-30: Model for shear transfer by aggregate interlock, according to Walraven (1981)

Design expressions for the shear strength of **smaller joint interfaces** are given in the following in accordance with CEB-FIP Model Code 90. For smooth interfaces the expression is of the same type as eq. (8-42), while for rough interfaces the expression considers the concrete strength. For larger joint faces, as between wall or floor panels, the design approach in Section 8.4.3 is applicable.

(1) Shear resistance of smaller joint interfaces in case of monotonic action

The **design value** of the frictional resistance τ_{Rd} under monotonic action may be estimated as follows. Note that the shear strength in eqs. (8-44) and (8-45) refers to the average strength in the joint section. This should be compared to the calculated average shear stress $\tau = F_v / A_{cc}$, independently of the real contact area, where A_{cc} = concrete area subjected to compression.

For **smooth interfaces** (friction between concrete surfaces which are cast separately)

$$\tau_R = 0{,}4 \cdot \sigma_c$$

$$\tau_{Rd} = 0{,}4 \cdot \frac{\sigma_c}{\gamma_c} \qquad \text{or for } \gamma_c = 1{,}5$$

$$\tau_{Rd} = 0{,}27 \cdot \sigma_c \qquad (8\text{-}44)$$

where σ_c = normal compressive stress at the joint interface

For **rough interfaces**:

$$\tau_R = 0{,}5 \cdot \left(f_{ck}^2 \cdot \sigma_c\right)^{1/3}$$

$$\tau_{Rd} = \frac{0{,}5}{\gamma_{Rd}} \cdot \left[\left(\frac{f_{ck}}{\gamma_c}\right)^2 \cdot \sigma_c\right]^{1/3} \qquad \text{or for } \gamma_{Rd} \approx \frac{4}{3} \text{ and } \gamma_c = 1{,}5$$

$$\tau_{Rd} \approx 0{,}27 \cdot \left(f_{ck}^2 \cdot \sigma_c \right)^{1/3} \tag{8-45}$$

Since eq. (8-45) is derived on the basis of tests with relatively small interface areas, it overestimates the shear resistance due to friction of larger interfaces. In such case the design approach in Section 8.4.3 should be used instead.

For smooth interfaces eq. (8-44) for the shear resistance can be understood as based on the traditional frictional concept, where the coefficient 0,40 corresponds to the so-called frictional coefficient, compare with eq. (8-42). For rough interfaces, there will be a certain shear contribution by shear damage of the joint face and the corresponding expression for the resistance is based on the so-called 'aggregate interlock' concept.

The validity of eq. (8-45) has been checked for concrete strengths up to 65 MPa. For such concretes the major part of the aggregate particles contributes to 'aggregate interlock'. Cracks in high strength concrete become smoother, because the aggregates fracture at the crack formation. This will substantially reduce the shear resistance by friction [Walraven (1997)].

The expressions (8-44) and (8-45) for smooth and rough joint interfaces, respectively, give low estimates of the frictional resistance and should be used when frictional resistance is utilised in design, i.e. when friction has a favourable effect. However, in cases when the effects of friction is unfavourable, for instance with regard to restraint forces, the coefficients should be increased by 50 %.

In Figs. 8-31 and 8-32, schematic relationships for the shear friction stress versus shear displacement are presented for smooth and rough concrete interfaces, respectively [Vintzeleou (1986), Vintzeleou and Tassios (1985)]. According to CEB-FIP Model Code 90 the maximum shear resistance of smooth joint interfaces according to eq. (8-44) is reached for a shear slip s_u, which can be estimated as

$$s_u = 0{,}15\sqrt{\sigma_c}$$

where σ_c is inserted in [MPa] and s_u in [mm]

Also according to CEB-FIP Model Code 90, the maximum shear resistance of rough joint interfaces is reached for a shear slip of approximately 2 mm. However, in this case it must be assumed that the specific value strongly depends on the actual type of roughness.

For increasing shear slip beyond these values the shear resistance can be assumed to remain constant.

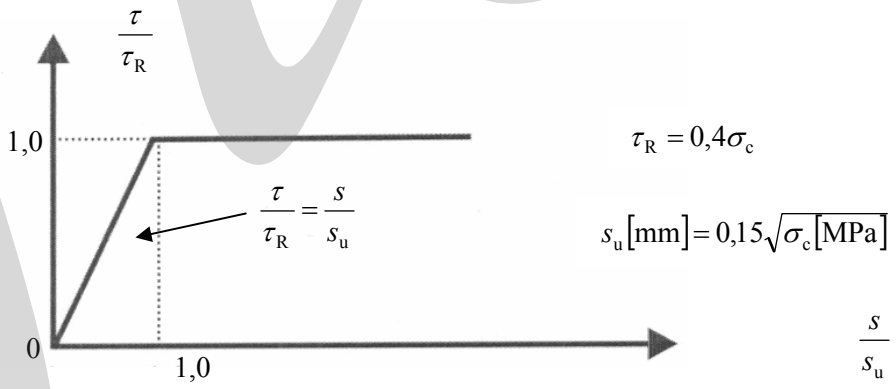

Fig. 8-31: Idealised and normalised relationship between friction-shear stress and shear displacement in case of smooth joint faces, [Vintzeleou (1986), Vintzeleou and Tassios (1985)]

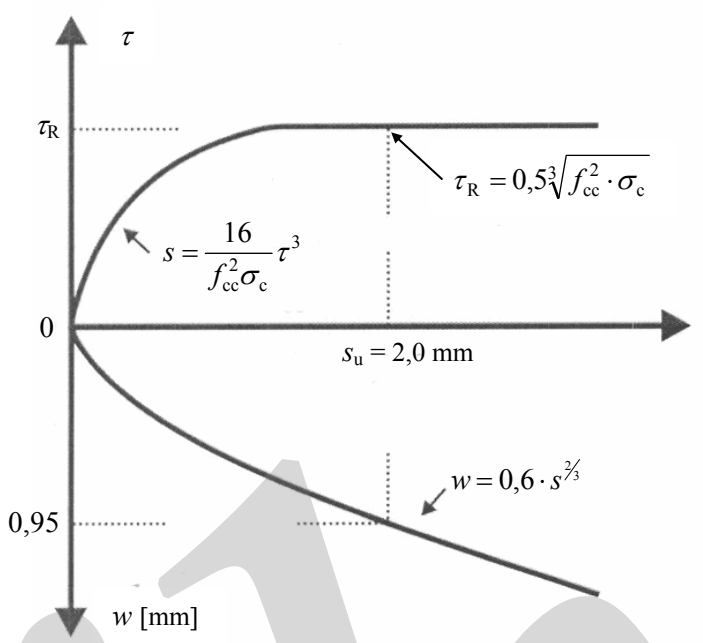

Fig. 8-32: Idealised and normalized relationship between friction-shear stress and shear displacement in case of rough joint faces, [Vintzeleou (1986), Vintzeleou and Tassious (1985)]

In case of rough and wavy joint areas, the real bearing area may be considerably smaller than the total joint area A_{cc}. Though, in the relationship given in Fig. 8-32 this fact has been considered.

(2) Shear resistance in case of cyclic action

Under cyclic fully reversed displacements, the following empirical equations may be used for the estimation of the friction degradation for smooth and rough interfaces. These equations are derived from Tassios and Vintzeleou (1987) and assuming n = 5 cycles, which corresponds to severe seismic conditions:

For smooth interfaces:

$$\frac{\tau_{Rd,n}}{\tau_{Rd,1}} = 0,7 \tag{8-46}$$

For rough interfaces:

$$\frac{\tau_{Rd,n}}{\tau_{Rd,1}} = 1 - 0,2\left[\left(\frac{\sigma_{cc}}{f_{cc}}\right)^{-1}\frac{s_n}{s_{u,1}}\right]^{\frac{1}{3}} \tag{8-47}$$

In the above equations (8-46) and (8-47) are:

$\tau_{Rd,n}$ = the remaining frictional resistance after 5 cyclic fully reserved displacements

$\tau_{Rd,1}$ = the frictional resistance mobilised under monotonic action. It may be taken from eqs. (8-41) and (8-42) for smooth and rough interfaces respectively

$s_{u,1}$ = the shear slip of the interface that corresponds to the maximum mobilised friction under monotonic loading, (see Figs. 8-31 and 8-32)

8.3.4 Influence of transverse steel

8.3.4.1 Self-generated compression by clamping of transverse steel

When under shear loading slip s develops along the joint interface, this will be associated with a certain joint separation w, because of the irregularities of the rough joint face, see Fig. 8-33. If the joint interface is crossed by steel bars that are well anchored on each side of the joint, the steel bars will be tensioned due to this joint separation. The tensile force in the bars must be balanced by compression at the joint interface. Thus, the wedging of the joint caused by the irregularities generates a compression force that makes shear transfer by friction possible even in the case when there is no compression at the interface initially.

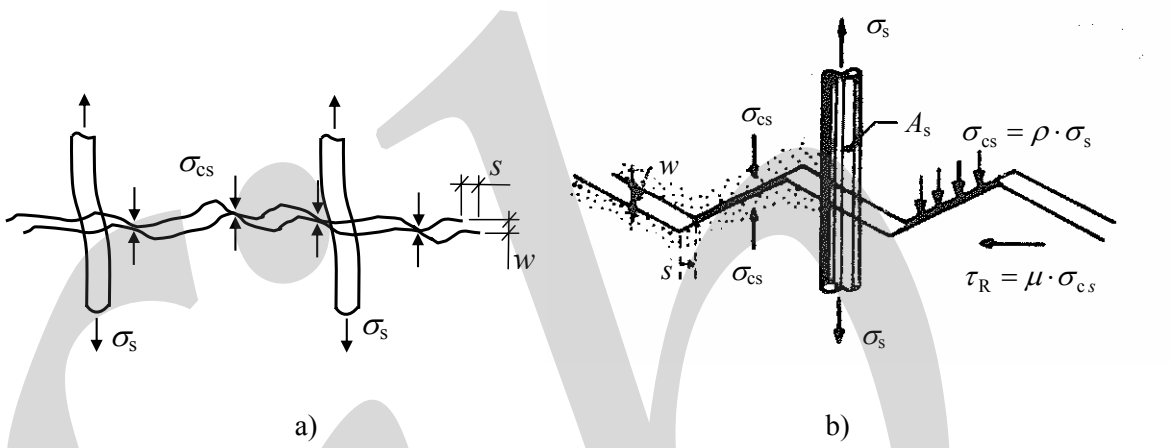

Fig. 8-33: Transfer of shear force by friction due to the pullout resistance of reinforcement across rough joint interfaces, a) general behaviour, b) qualitative description

As a consequence of the joint separation of rough interfaces subjected to shear slip, reinforcing bars A_s crossing the joint area respond, when adequately anchored, with a tensile force, $A_s \cdot \sigma_s$. Consequently, compressive stresses σ_{cs} appear at the concrete interface and subsequently friction is mobilized. This self-generated compressive stress depends on the steel stress and steel ratio.

$$\sigma_{cs} = \rho \cdot \sigma_s$$

where $\rho = \dfrac{A_s}{A_c}$

As described in Section 8.3.2 each type of joint has its characteristic relationship between shear slip s along the joint interface and joint separation w. The joint separation increases with increasing shear slip up to a maximum separation w_{max} when a further joint slip will give no increase in joint separation. The shear slip needed to create the maximum possible joint separation belongs also to the basic joint characteristics, compare with Figs. 8-31 and 8-32.

The force that develops in the steel bars for a certain joint separation depends on the resistance of the bar to bar pullout. In this respect the way the bar is anchored is essential. A plain smooth bar without end anchors will not provide any significant resistance to bar pullout and no compressive forces will be generated by the wedging effect. A plain bar with anchors will be strained due to the joint separation and the corresponding tensile force generates compression at the joint interface. In case of a ribbed bar the tensile strain will localise to the region near the joint interface and high tensile stresses may develop in the bar for very small shear slips.

In the following paragraphs it is exemplified how the concrete compressive stress σ_{cs} at the shear plane, due to 'clamping' of transverse steel, is influenced by various parameters and how it can be estimated. It is assumed that this compressive stress can be considered separately or added to other

compressive stresses acting at the shear plane and, hence, be included in general expressions to determine the shear resistance due to concrete-to-concrete friction. These expressions can have the form according to eqs. (8-42) and (8-43), but the concrete compressive stress due to pullout resistance of transverse steel can also be considered in eq. (8-45).

8.3.4.2 Effect of external transverse bars not embedded in the concrete

Consider two concrete elements in contact along an intermediate joint interface. The elements are connected by external bars that are anchored by anchor plates at the exterior faces of the elements, see Fig. 8-34. The bars are fixed to the anchor plates and tightened, but without imposing any initial tensile stresses in the bars. The bars have a total cross-sectional area A_s and the free distance between the end anchors is l_a.

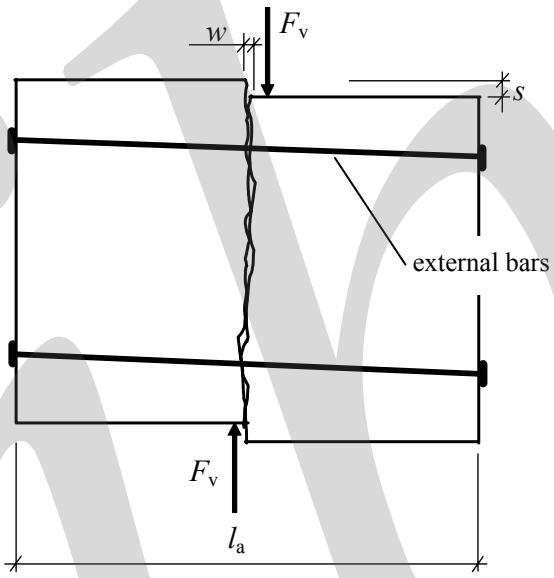

Fig. 8-34: Connection where the elements on each side of the intermediate joint section are connected by external bars

The connection is loaded by a shear force F_v along the joint interface. After a certain shear slip s along the joint, a joint separation w has occurred due to the roughness of the joint faces. Then the tensile rods have got an elongation w that can be assumed to be uniformly distributed between the end anchors. The corresponding steel strain ε_s and stress σ_s in the tensile rods are determined as

$$\varepsilon_s = \frac{w}{l_a} \quad ; \qquad \sigma_s = \varepsilon_s \cdot E_s$$

The total tensile force in the rods $F_s = \varepsilon_s \cdot E_s \cdot A_s$ is resisted by the end anchors and results in a compressive stress of the same magnitude across the joint. The concrete compressive stress due to clamping effect of transverse steel becomes

$$\sigma_{cs} = \frac{A_s}{A_c}\sigma_s = \rho \cdot \varepsilon_s E_s$$

For an increasing shear slip s, the shear force increases until the maximum joint separation is reached. Hence, the shear capacity F_{vR} of the shear connection is determined by the maximum joint separation w_{max} that is characteristic for the specific joint face. When the maximum joint separation is

reached, the strain of the tensile rods is $\varepsilon_{s,max} = w_{max}/l_a$ and the corresponding maximum compressive stress that can be achieved by clamping effect of transverse steel is

$$\sigma_{cs,max} = \rho \cdot \varepsilon_{s,max} E_s \tag{8-48}$$

A further slip along the joint gives no significant increase of the shear stress due to friction since the joint separation will remain more or less constant.

A typical example of the shear stress versus shear slip relationship for connections of this type is shown in Fig. 8-36 a.

8.3.4.3 Effect of transverse reinforcement bars embedded in the concrete

A typical situation of shear transfer along a joint interface is shown in Fig. 8-35. To achieve a high self-generated compression with as little steel amount as possible, the steel should be forced to yield for a very small joint separation. As a consequence a high resistance to bar pullout is required. A ribbed bar is effectively anchored on both sides of the joint face by bond and a small joint separation will result in large tensile strains that appear locally around the joint interface. For such a bar yielding can be obtained for a very small shear slip and before a significant contribution to the resistance is achieved by dowel action. Hence, in the case of good bond, the bar will enable shear transfer by friction and the capacity of the bar is mainly used in bar pullout. On the other hand, in the case of less effective bond a greater shear slip is possible before yielding. With a greater shear slip the bar is forced to act as a dowel and will be loaded more in bending before yielding. In this case the shear resistance is due to a combination of shear friction and dowel action, see further Section 8.3.4.4.

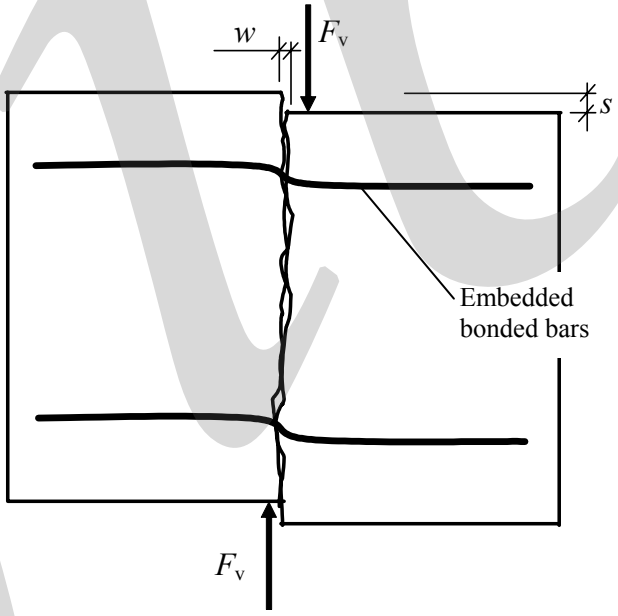

Fig. 8-35: Connection where the adjacent concrete elements are tied together by embedded transverse reinforcement bars anchored by bond

The elongation w that is imposed on the transverse bars at shear slip s along the joint cannot, in this case, be distributed uniformly along the bars. The steel strain will be considerably higher in the vicinity of the joint interface. This means that for the same shear slip and for the same steel area, the self-generated compressive force will be much higher in case of ribbed transverse bars compared to smooth bars. The compressive force that is generated in this case can be estimated by the methods given in Sections 7.4.1 and 7.2.3 for tie bars. The tensile force in the tie bars is then obtained as a function of the crack width w, for instance according to the schematic relationship in Fig. 7-33 for

ribbed tie bars. The shear force increases with increased shear slip until the tie bars reach yielding, or the maximum joint separation is reached.

Normally, the shear capacity of the connection will be determined by the yielding of the transverse tie bars and the maximum concrete compressive stress due to pullout resistance of transverse steel is calculated as:

For $w_y \leq w_{max}$

$$\sigma_{cs,max} = \rho \cdot f_y \tag{8-49}$$

where f_y = yield strength of tie bars
w_{max} = maximum joint separation due to shear slip

The separation w_y, which corresponds to the state when yielding is reached, can be estimated by means of eqs. (7-4) and (7-49a). Reference is made to Section 8.3.4.4 for the cases where the roughness is insufficient to cause yielding of the transverse bars, i.e. when the maximum joint separation w_{max} is less than the crack width w_y when yielding is reached.

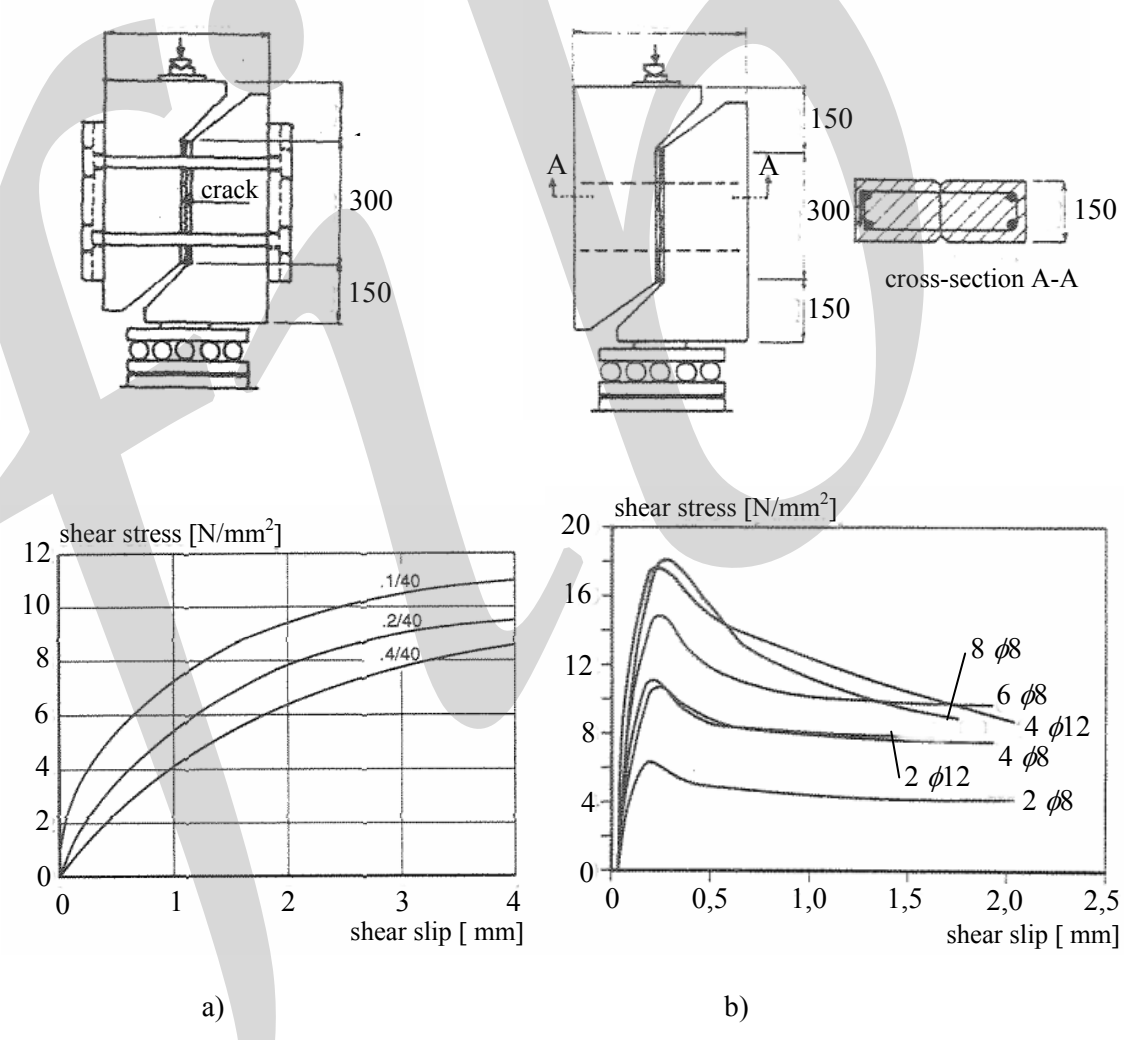

Fig. 8-36: Examples of shear stress-shear slip relations from push-off specimens where the shear plane was cracked before testing (natural crack) according to Walraven (1997), a) test specimens with external bars, b) test specimens with reinforcement across the crack

An increase in shear slip above the value that results in yielding of the tie bars will not give a significant increase to the shear resistance. In this case it is normally not possible to take advantage of

the dowel action of the bars because they begin to yield due to joint separation before the bars have developed considerable flexural deformations. This means that the strength of the steel is already fully used before plastic flexural hinges can form, and no additional capacity is available.

In case of well bonded transverse bars in combination with rough joint interfaces, the compressive stress due to pullout resistance increases rapidly with increasing shear slip. As a result this type of connection will have a stiffer behaviour with a more pronounced peak stress compared to joints clamped by external bars. Typical results of both behaviours are shown in Fig. 8-36.

The relationship between shear stress and shear slip can be assumed to depend on the roughness of the joint faces, the concrete strength, and the dimension, strength and bond properties of the tie bars. A basic relationship between τ and s is given in CEB-FIP Model Code 1990, see Fig. 8-37. This relationship is valid independently of the parameters mentioned above and should be considered to be indicative only.

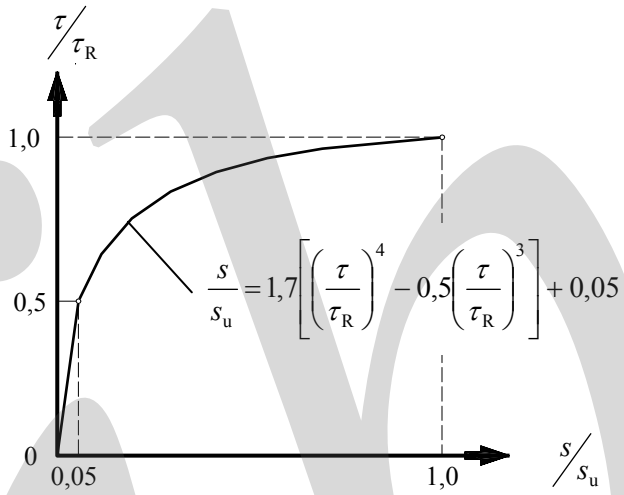

Fig. 8-37: Basic relationship between shear stress τ and shear slip s for connections with rough joint faces and transverse bars anchored by bond, according to CEB-FIP (1992)

Inclined tie bars

When the tie bars are inclined (angle α) with respect to the joint interface, the tensile force in the tie bar can be resolved in components perpendicular and parallel to the joint, see Fig. 8-38.

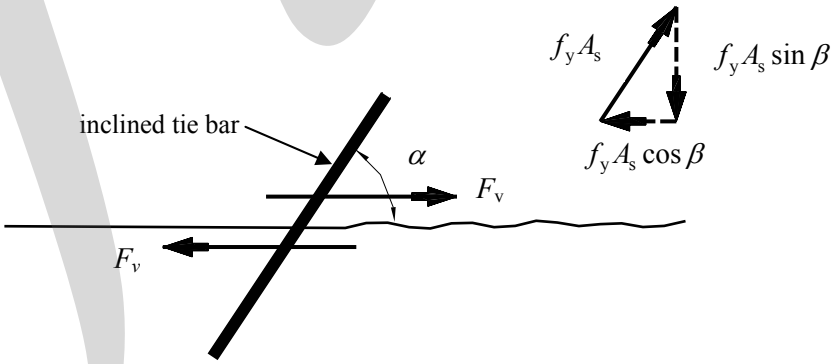

Fig 8-38: Connection at shear interface with inclined tie bars

The parallel component, $f_y A_s \cdot \cos\alpha$, resists some of the shear force in direct tension and can be added to the shear friction resistance. The perpendicular component induces compression in the joint and can be calculated as

For $w_y \leq w_{max}$

$$\sigma_{cs} = \rho f_y \sin\alpha \tag{8-50}$$

Upper limit for the shear capacity

For this type of shear connection designed on the basis of shear friction and self-generated compression, the shear capacity increases with an increased amount of transverse steel, which means that the compressive stress at the joint interface increases. However, in case of very high compression, there is a risk that the concrete crushes at the joint interface. This failure mode constitutes an upper limit for the shear capacity. Hence, this failure also determines the maximum amount of transverse steel that can be used to increase the shear capacity.

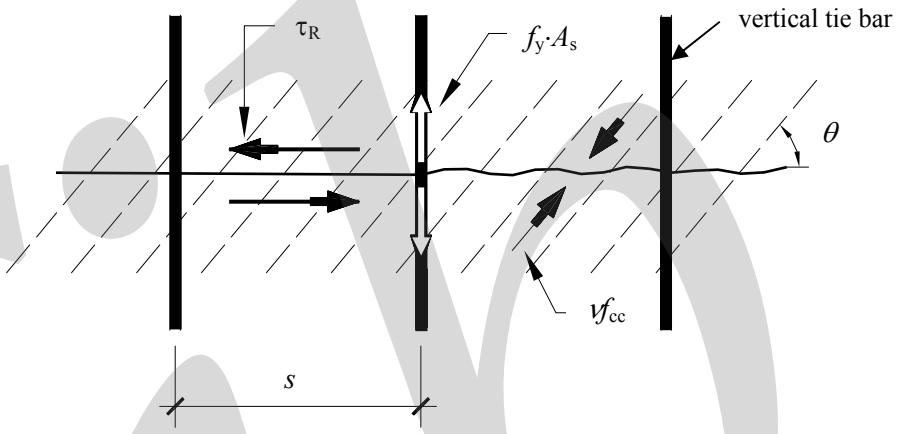

Fig. 8-39: Model for a shear connection in the ultimate limit state, based on theory of plasticity, adopted from Nielsen (1984)

A model for the behaviour in the ultimate limit state of shear connections with self-generated compression is shown in Fig. 8-39. The combined effect of a shear force along the joint interface and tensile forces in the transverse ties, results in an inclined compressive force across the joint interface, compare with Fig. 8-33. This compressive force is transmitted by a series of inclined struts that are balanced by the transverse tie bars. The compressive strength of the struts is reduced with regard to the biaxial state of stresses and expressed as νf_{cc} where $\nu \leq 1{,}0$.

An approach based on the theory of plasticity [Nielsen (1984)] assumes that the strength (plastic behaviour) is reached in both concrete and steel. A vertical equilibrium condition yields

$$\nu f_{cc} \cdot b_j \cdot s \cdot \sin^2\theta = f_y \cdot A_s \qquad \Rightarrow$$

$$\sin^2\theta = \frac{f_y \cdot A_s}{\nu f_{cc} \cdot b_j \cdot s} = \omega \quad ; \qquad \cos^2\theta = 1 - \omega \tag{8-51}$$

where A_s = cross sectional area of one reinforcement unit
b_j = width of the joint section
ω = mechanical steel ratio
s = spacing of transverse bars

At this combined steel/concrete failure the upper limit for the shear strength τ_R is reached. Then a horizontal equilibrium condition for an element with length s is given by

$$\tau_R \cdot b_j \cdot s = \nu f_{cc} \cdot b_j \cdot s \cdot \sin\theta \cdot \cos\theta \qquad \Rightarrow$$

$$\frac{\tau_R}{\nu f_{cc}} = \sqrt{\omega(1-\omega)} \tag{8-52}$$

The inclination of the compressive struts depends on the frictional angle according to the expression

$$\theta = 90° - \phi$$

This means that the compressive struts appear perpendicular to the assumed tooth inclination, see Fig. 8-29. For rough joint faces, the frictional coefficient can be expected to be in the interval $0{,}7 \le \mu \le 1{,}4$ which corresponds to a frictional angle in the interval $35° \le \phi \le 54{,}5°$. The corresponding value of the mechanical reinforcement ratio ω can be determined according to eq. (8-51) and the interval for the upper limit of the shear strength is then determined from eq. (8-52) as

$$0{,}47 \le \frac{\tau_R}{\nu f_{cc}} \le 0{,}50$$

In this case the upper limit corresponds to a frictional angle $\phi = 45°$ ($\mu = 1{,}0$). With the efficiency factor ν about 0,5 - 0,8, the upper limit for the shear capacity will be in the order of

$$0{,}24 \cdot f_{cc} \le \tau_R \le 0{,}4 \cdot f_{cc} \tag{8-53}$$

The maximum amount of reinforcement that is possible to improve the shear resistance can now be determined from eq. (8-51) and is derived as

$$\frac{A_s}{s} = \omega \frac{b_j \cdot \nu f_{cc}}{f_y} \tag{8-54}$$

This risk of compressive failure at joint faces in case of high transverse compression motivates introduction of an upper limit in design expressions for the shear resistance due to shear friction, compare with Section 8.4.3.

Influence of joint roughness

To obtain the favourable contribution due to pullout resistance of transverse steel, according to eqs. (8-49) and (8-50), one condition is that the joint separation due to wedging is large enough to produce yielding of the transverse steel. This means that the roughness of the joint faces must result in a maximum joint separation w_{max} that exceeds the crack width w_y for which the transverse bars begin to yield, see Fig. 8-40 a. For smooth joint faces and/or large diameter bars, the maximum joint separation may be insufficient to generate yielding of the tie bars. From Fig. 8-40 b it appears that in the latter case the maximum concrete stress due to pullout resistance of transverse steel is obtained as:

For $w_y \ge w_{max}$

$$\sigma_{cs,max} = \rho \cdot \sigma_s(w_{max}) \tag{8-55}$$

where $\sigma_s(w_{max}) =$ the tensile stress in the transverse tie bars at maximum joint separation caused by wedging of the joint

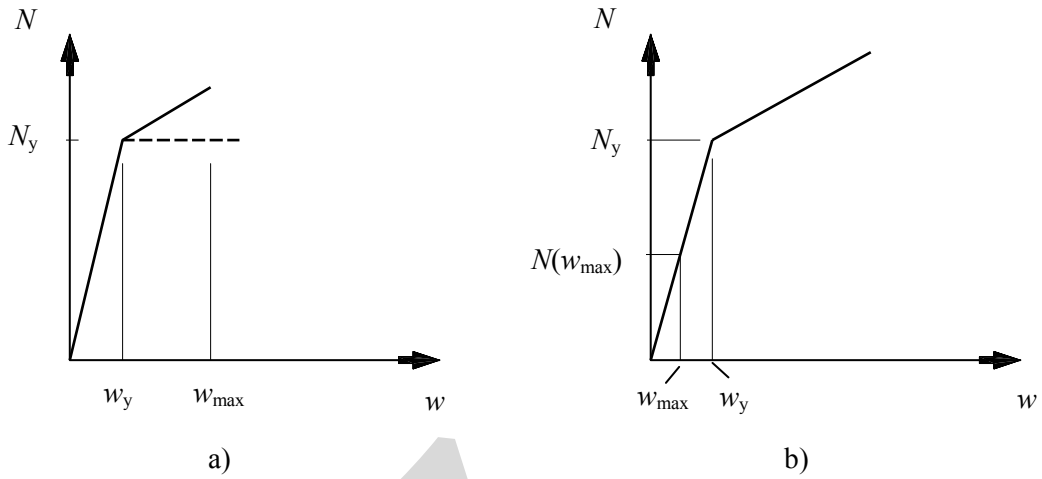

Fig. 8-40: Maximum self-generated compressive force in the joint interface, a) yielding of the tie bars governs ($w_y \leq w_{max}$), b) maximum joint separation is decisive ($w_y \geq w_{max}$)

8.3.4.4 Interaction between pullout resistance and dowel action of transverse bars

If the external bars in Fig. 8-34 are replaced by plain bars embedded in the concrete elements and provided with end-anchors, the connection will be less stiff in shear and it is possible to get a significant contribution by dowel action in the bars as shown in Fig. 8-41 before yielding is reached

However, as the bars are strained in tension due to wedging of the joint, there will also be a frictional resistance due to pullout resistance of the transverse bars. The elongation of the bars can be assumed to be almost evenly distributed between the end-anchors, as for the example with external bars shown in Section 8.3.4.2.

It is reasonable to assume that the maximum joint separation w_{max} due to wedging is reached before the dowel action is fully developed. Hence, dowel action and shear friction will not develop to their respective maximum values simultaneously. With increasing shear slip the dowel action of the bar will increase and contribute further to the shear resistance. This situation is very similar to the bolted beam/support connection shown in Fig. 8-26.

In most cases when reinforcement bars are placed across a joint there will be an interaction between frictional resistance and resistance by dowel action, which is shown schematically in Fig. 8-42. As explained above this interaction will depend on the roughness of the joint faces and the bond and anchorage of the transverse steel.

It should be noted that without anchorage of the bar, resistance by pure dowel action is still possible. It is interesting to see that for the same steel section, and a frictional coefficient about 1,0, the shear capacity due to pure friction will normally exceed the shear capacity obtained by pure dowel action.

For the response of a bar subjected to combined pullout and dowel action (which is the rule), the following criterion may be applied:

$$\left(\frac{\sigma_s}{f_y}\right)^{0,2} + \left(\frac{F_{v,dowel}}{F_{vR,dowel}}\right)^{0,2} \leq 1 \qquad (8\text{-}56)$$

where σ_s = steel stress at the loaded end of the bar due to imposed end slip of the bar
$F_{v,dowel}$ = contribution to shear resistance by dowel action
$F_{vR,dowel}$ = ultimate shear resistance by dowel action without pullout effect

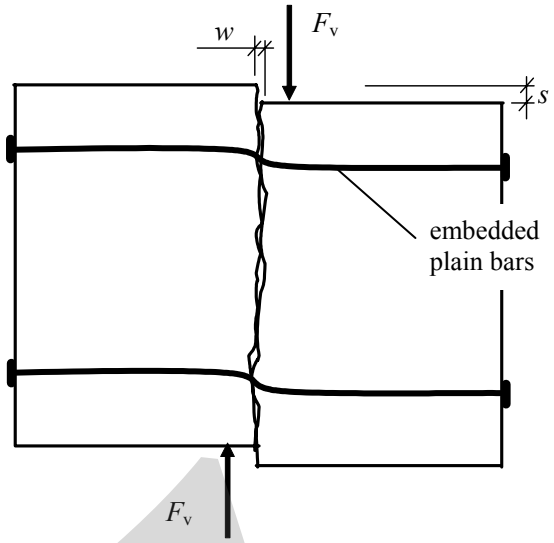

Fig. 8-41: Connection where the elements on each side of the intermediate joint section are connected by plain bars (no bond) embedded in the concrete

8.3.5 Design of connections between linear elements

For design of connections between linear elements, such as beams and columns, the following design principles can be applied, according to Tsoukantas and Tassios (1989).

(1) Ultimate shear displacement

For the ultimate limit state, an ultimate shear slip at the interface of, say, $s_u = 2$ mm is proposed to be taken into account. As seen in Figs. 8-31 and 8-32, for such a shear slip there is not a substantial descending branch of any of the resisting mechanism.

(2) Serviceability limit state

For the serviceability limit state a shear slip equal to $s_{ser} = 0{,}2$ mm is proposed to be adopted. It is assumed that for this magnitude of shear slip, no harmful cracks will appear along the connection. In fact, according to eqs. (8-39) and (8-40), the corresponding maximum dilatancy (due to wedging of the joint) is determined as

$$w_{ser} = 0{,}05 \cdot 0{,}2 = 0{,}01 \text{ mm} \tag{8-57}$$

or

$$w_{ser} = 0{,}6 \cdot 0{,}2^{2/3} = 0{,}2 \text{ mm} \tag{8-58}$$

for smooth and rough interfaces, respectively.

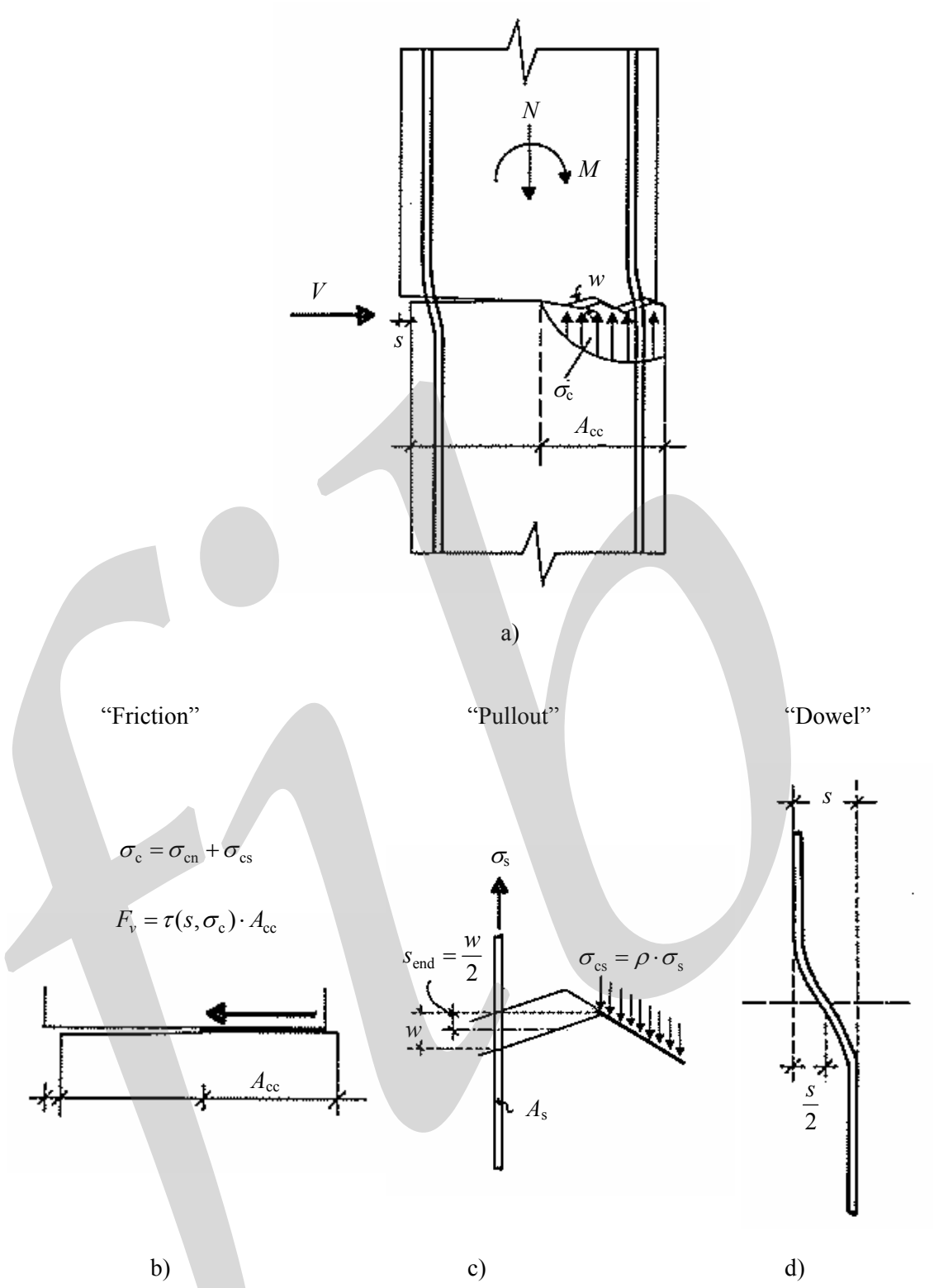

Fig 8-42: Imposed shear slip s mobilizes dowel action and frictional resistance. The transverse bars are strained due to both dowel action (bending) and bar pullout (tension) that results from the joint separation w, a) overview, b) friction, c) pullout, d) dowel action. Adopted from Tsoukantas and Tassios (1989)

(3) Force transfer as a function of imposed shear displacement

As previously stated, due to a given displacement s of an interface, a lateral dilatancy w will appear and the activated shear transfer sub-mechanisms (Fig. 8-42) may be evaluated as follows:

The shear force transferred through dowel action (Fig. 8-42 c) can be estimated taking into account a displacement of a corresponding one-sided dowel $s/2$ and using eqs. (8-21) and (8-22). For the effect of axial stresses simultaneously acting on the bar, eq. (8-56) may be used.

Fig. 8-43, may serve as a guide for the distinction of dowels according to their position in the cross section with regard to shear direction. Note however that in case that bars with $c < 5\phi$ are to be taken into account (in the opposite side of the shear direction), proper transverse reinforcement should be foreseen.

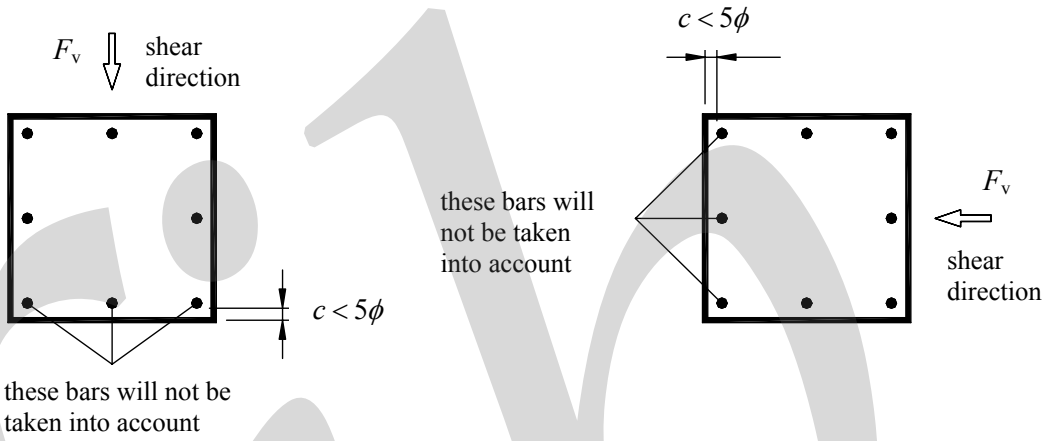

Fig. 8-43: Distinction of dowels according to their position in the cross-section with regard to shear direction

The shear transferred through friction (Fig. 8-42 a) can be estimated taking into account the displacement s, the total compressive stress $\sigma_c = \sigma_{cn} + \sigma_{cs}$, and using eq. (8-44) for smooth and eq. (8-45) for rough interfaces, respectively. Note, however, that the interfaces of connections between prefabricated linear elements tend to be rather smooth, unless roughening is guaranteed during construction (e.g., by means of sand-blasting or indentation, see also Section 8.3.1).

The concrete stress σ_{cn} (average value) is due to the normal action effects M_{Ed} and N_{Ed} whereas the additional concrete compressive stress σ_{cs} is due to the pullout resistance of the reinforcement crossing the compressive area A_{cc} of the interface (Fig. 8-42 b and 8-33).

If $\rho_{cc} = \Sigma\, A_{s,cc}/A_{cc}$ denotes the percentage of this reinforcement, the steel stress σ_s, due to bar pullout, may be estimated by means of eq. (7-4), taking into consideration a pullout end-slip of $s_{end} = 0{,}5w$. The value of w depends on the value of the shear displacement s and the conditions of the interface. Empirical relationships between the shear slip s and w are given in eqs. (8-41) and (8-42) for smooth and rough interfaces, respectively. Under known steel stress σ_s the corresponding concrete compressive stress $\sigma_{cs} = \rho_{cc} \cdot \sigma_s$, is calculated (where ρ_{cc} denotes the ratio of compressed steel area over the compressed concrete area).

It is worth mentioning that the concrete area A_{cc} used in this respect should be taken equal to the entire compressive cross section despite the fact that (Fig. 8-33) less than half of it is expected to be really in contact. This conventional consideration of the entire 'compressed' concrete area A_{cc} is imposed by the fact that the constitutive relationships of Figs. 8-31 and 8-32 are also based on the same consideration.

In conclusion, the shear resistance of a reinforced concrete interface may be estimated according to the following general expression:

$$F_v(s) = F_{v.friction}(s) + F_{v,dowel}(s) \tag{8-59}$$

where $F_{v,friction}(s) = \tau(s, \sigma_c) \cdot A_{cc}$

= the shear frictional resistance of the interface due to the total compressive stress acting on the interface (in correspondence to the imposed shear displacement s)

$F_{v,dowel}(s)$ = the shear resistance due to dowel action.

Example 8-2, frictional resistance of concrete interfaces

Consider the concrete interfaces according to Fig. 8-44, under N = 21,5 kN and M = 237 kNm, subject to shear ship s.

Concrete strength class C20/25 f_{ck}= 20 MPa
Steel grade B500
l_a = available anchorage length of the bars
ϕ = diameter of the bars
$s = s_u$, (shear displacement)
s_u = 2,5 mm for rough interfaces and 2,0 mm for smooth interfaces

Frictional resistance under monotonic loading, according to Fig. 8-44.

$$F_v(s) = \tau(s, \sigma_c) \cdot A_{cc}$$

(a) Rough interfaces

Frictional contribution according to eq. (8-45):

$$\tau_{Rd} = 0{,}27 \cdot \left(f_{ck}^2 \cdot \sigma_c\right)^{1/3}$$

$$\sigma_c = \sigma_{cn} + \sigma_{cs}$$

where σ_{cn} = mean compression stress due to external actions (M, N).
σ_{cs} = additional compressive stress due to pullout of the reinforcement, crossing to compressive area of the interfaces. (in this example 3 ϕ16, see Fig. 8-44)

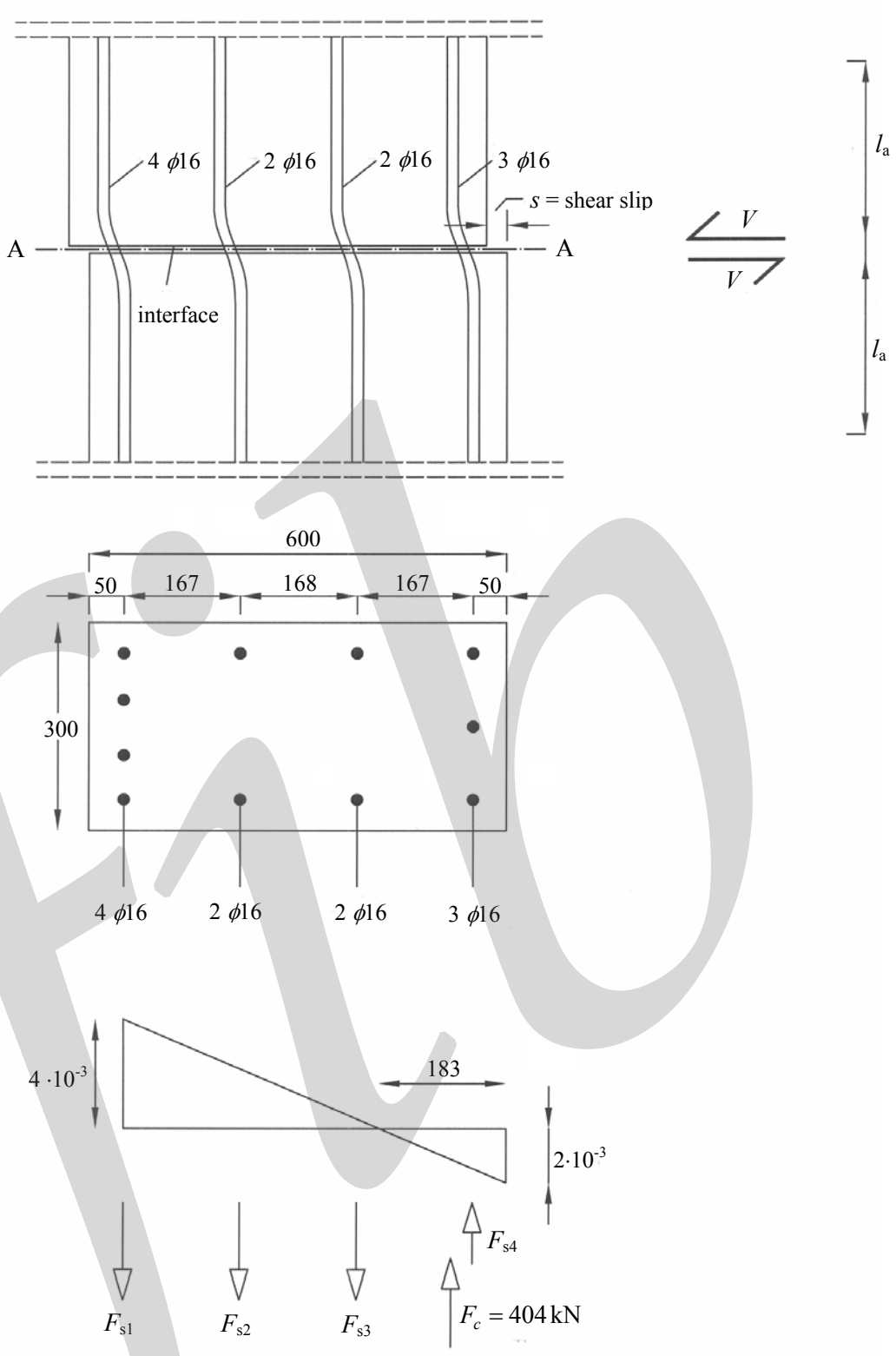

Fig. 8-44: Joint intersection studied in the design example

Mean compression stress due to M and N, see Fig. 8-44:

$$\sigma_{cn} = -\frac{404}{0{,}183 \cdot 0{,}3} = 7481\,\text{kN/m}^2 \approx 7{,}48\ \text{MPa}$$

Compressive stress due to pullout resistance, where 603 mm^2 is the area of 3 ϕ16.

$$\sigma_{cs} = \rho_{cc} \cdot \Delta\sigma_s$$

$$\rho_{cc} = \frac{603 \cdot 10^{-6}}{0{,}183 \cdot 0{,}30} = 10{,}93 \cdot 10^{-3}$$

Under the condition that the reinforcement is fully anchored in relation to the joint section, the following procedure should be followed for the estimation of σ_s, due to bar pullout.

The joint dilatancy is estimated by eq. (8-40) as:

$w = 0{,}6 \cdot s^{2/3} = 0{,}6 \cdot 2{,}5^{2/3} = 1{,}1$ mm

Thus, the end slip s_{end} in eq. (7-4) will be taken:

$$s_{end} = \frac{w}{2} = \frac{1{,}1}{2} = 0{,}55\ \text{mm}$$

The steel stress σ_s of the bars due to wedging effects is calculated using eqs. (7-4) and (7-5). Since the bond has a favourable effect, the maximum bond stress $\tau_{b,max}$ is calculated on the basis of design values. The steel stress is first determined without considering the effect of a local conic concrete failure. The effect on the end-slip of such a local weakening is then considered; hereafter the steel stress is updated.

$$\tau_{b,mmax} = 1{,}25\sqrt{\frac{f_{ck}}{\gamma_c}} = 1{,}25\sqrt{\frac{20}{1{,}5}} = 4{,}56\ \text{MPa}$$

$$\sigma_s = 2{,}39\sqrt{\frac{\tau_{b,max} E_s}{\phi} s_{end}^{1,4}} = 2{,}39\sqrt{\frac{4{,}56 \cdot 200 \cdot 10^3}{16} 0{,}55^{1,4}} = 375\ \text{MPa}$$

$$s_{end,net} = s_{end} - \frac{\sigma_s}{E_s} 2\phi = 0{,}55 - \frac{375}{200 \cdot 10^3} 2 \cdot 16 = 0{,}49\ \text{mm}$$

$$\sigma_s = 2{,}39\sqrt{\frac{\tau_{b,max} E_s}{\phi} s_{end}^{1,4}} = 2{,}39\sqrt{\frac{4{,}56 \cdot 200 \cdot 10^3}{16} 0{,}49^{1,4}} = 346\ \text{MPa}$$

The corresponding concrete compressive stress is:

$$\sigma_{cs} = \rho_{cc} \cdot \sigma_s = 10{,}93 \cdot 10^{-3} \cdot 346 = 3{,}78\ \text{MPa}$$

Thus, the total concrete compressive stress is found as:

$\sigma_c = \sigma_{cn} + \sigma_{cn} = 7{,}48 + 3{,}78 = 11{,}2$ MPa

and the shear resistance can be calculated as:

$$\tau_{Rd} = 0{,}27 \cdot \left(20^2 \cdot 11{,}2\right)^{1/3} = 4{,}45 \text{ MPa}$$

(b) Smooth interfaces

Frictional resistance under monotonic loading is found by means of eq. (8-44):

$$F_v(s) = \tau(s, \sigma_c) \cdot A_{cc}$$

$$\tau_{Rd} = 0{,}27\sigma_c$$

$$\sigma_c = \sigma_{cn} + \sigma_{cs}$$

where $\sigma_{cn} =$ 7,48 MPa (see above)
$\sigma_{cs} = 10{,}93 \cdot 10^{-3} \cdot \sigma_s$

For smooth joints the joint dilatancy is estimated by eq. (8-39) as:

$$w = 0{,}05 \cdot s = 0{,}05 \cdot 2{,}0 = 0{,}1 \text{ mm}$$

and the end slip and the corresponding steel stress is found as:

$$s_{end} = \frac{w}{2} = 0{,}05$$

$$\sigma_s = 2{,}39\sqrt{\frac{\tau_{b,max} E_s}{\phi} s_{end}^{1,4}} = 2{,}39\sqrt{\frac{4{,}56 \cdot 200 \cdot 10^3}{16} 0{,}05^{1,4}} = 70 \text{ MPa}$$

$$s_{end,net} = s_{end} - \frac{\sigma_s}{E_s} 2\phi = 0{,}05 - \frac{70}{200 \cdot 10^3} 2 \cdot 16 = 0{,}039 \text{ mm}$$

$$\sigma_s = 2{,}39\sqrt{\frac{4{,}56 \cdot 200 \cdot 10^3}{16} 0{,}039^{1,4}} = 59 \text{ MPa}$$

The corresponding concrete stress and the total concrete stress are determined as:

$$\sigma_{cs} = 10{,}93 \cdot 10^{-3} \cdot 59 = 0{,}64 \text{ MPa}$$

$$\sigma_c = 7{,}48 + 0{,}64 = 8{,}12 \text{ MPa}$$

Finally, the shear resistance can be calculated as:

$$\tau_{Rd} = 0{,}27 \cdot 8{,}12 = 2{,}19 \text{ MPa}$$

8.4 Connections for shear transfer

8.4.1 Connections between wall elements

8.4.1.1 Concreted and grouted connections

When the dimensions (i.e. length and thickness) of the connection permit it, joints can be provided with specially formed shear keys to increase the shear stiffness and the shear capacity. This is mostly the case in vertical grouted joints of large panel systems, see Fig. 8-45, where the prevailing action is shear force and also in the horizontal joints (mostly under compression) of similar systems where large shear forces are simultaneously expected e.g. under strong wind or seismic actions, Fig. 8-46.

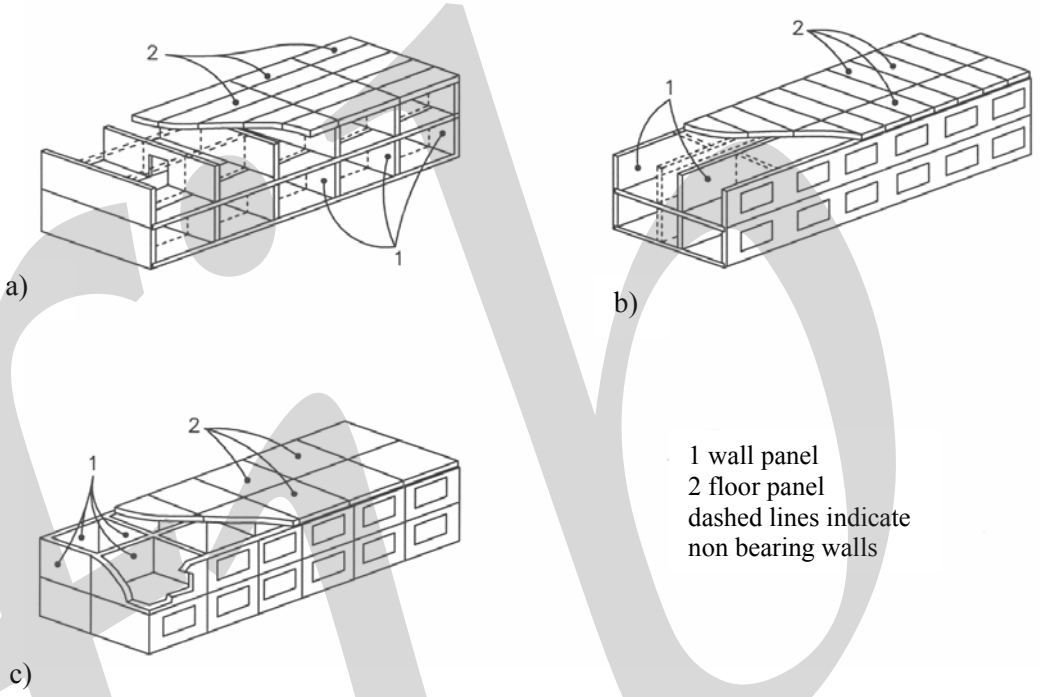

Fig. 8-45: Basic structural configurations of large panel systems, a) cross-wall system, b) long-wall system, c) two-way system

In Fig. 8-46, the structural response of joints between large panels to 'design actions' is presented schematically. In Fig. 8-47, a typical connection with shear keys at a vertical joint between wall elements is shown.

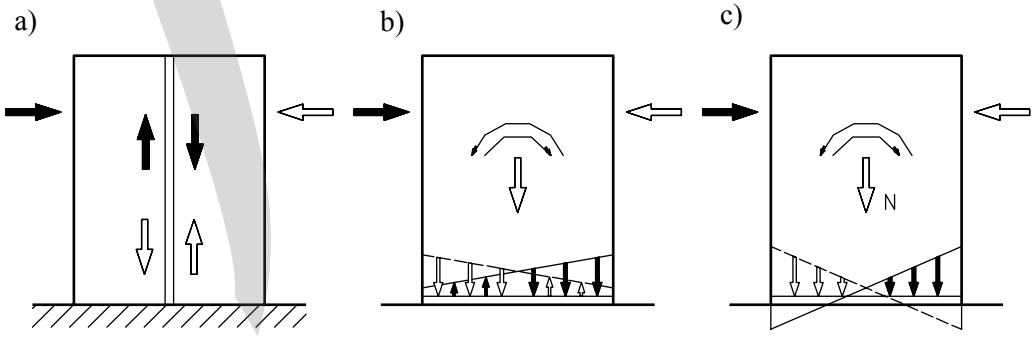

Fig. 8-46: Structural response in joints to 'design actions', a) vertical joints, b) horizontal compression joints under compression entirely, c) partially

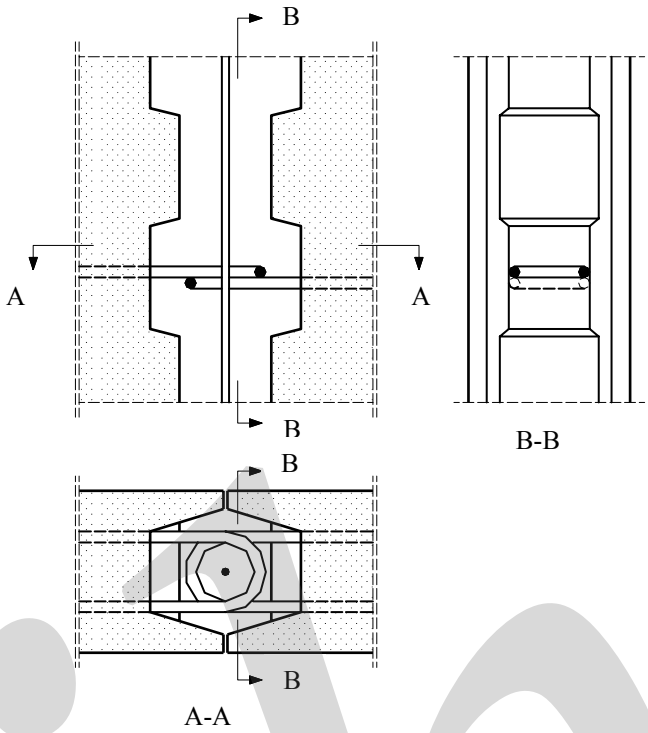

Fig. 8-47: Typical connection with shear keys at a vertical joint between wall elements

As it can be seen in Fig. 8-46, in connections of large panels, shear and normal forces generally have to be transferred between precast panels and the cast *insitu* concrete of the joint. This involves the transfer of forces across the interface of concrete of different ages. Several basic force-transfer mechanisms involving both the concrete and reinforcing steel can generally be identified.

In shear connections with indented joint faces the shear behaviour is initially very stiff. This appears from Fig. 8-48, which shows typical shear stress-slip relationships for concrete connections with plain and tooth shaped joint faces and distributed horizontal reinforcement. The shear stress-slip relations are compared with that for a critical section in monolithic concrete. From such relations the effective stiffness and shear capacity of the shear connection can be evaluated.

The **adhesion** that exists in the interface initially will transfer shear between the two concrete surfaces until it is 'broken' and a crack forms along the interface. Once slippage commences along the crack at the interface, shear is transferred across the crack by a number of other mechanisms.

Fig. 8-49 shows the external actions and the mobilized resisting forces acting on an idealised crack. The normal compressive reaction across the crack will result in shear transfer by **friction** along the crack. Steel reinforcement will transfer additional shear force due to **dowel** action of the steel, while the force induced by pullout resistance (when sliding shear displacements occur along the crack) will increase the shear transferred by friction.

The simplified model of shear transfer of joints with shear keys, presented in Fig. 8-50, may serve as an example of how the mechanisms of shear transfer (which contribute to the strength under monotonic loading) may be taken into account. Direct diagonal compression transfer between keys, friction and dowel action are mobilized due to shear displacements at the interface between the prefabricated concrete panel and the *insitu* joint concrete. The shear keys work as mechanical locks preventing any significant slip along the joint. The horizontal component of the inclined compressive force must be balanced by transverse tensile forces. For this purpose transverse reinforcement must be provided, connected be means of loops or welding, well anchored in the body of the panel. This transverse steel may be concentrated to the ends of the wall element or be distributed along its height.

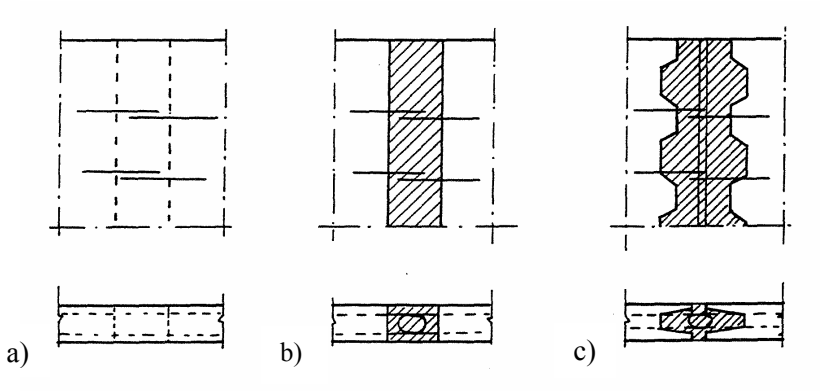

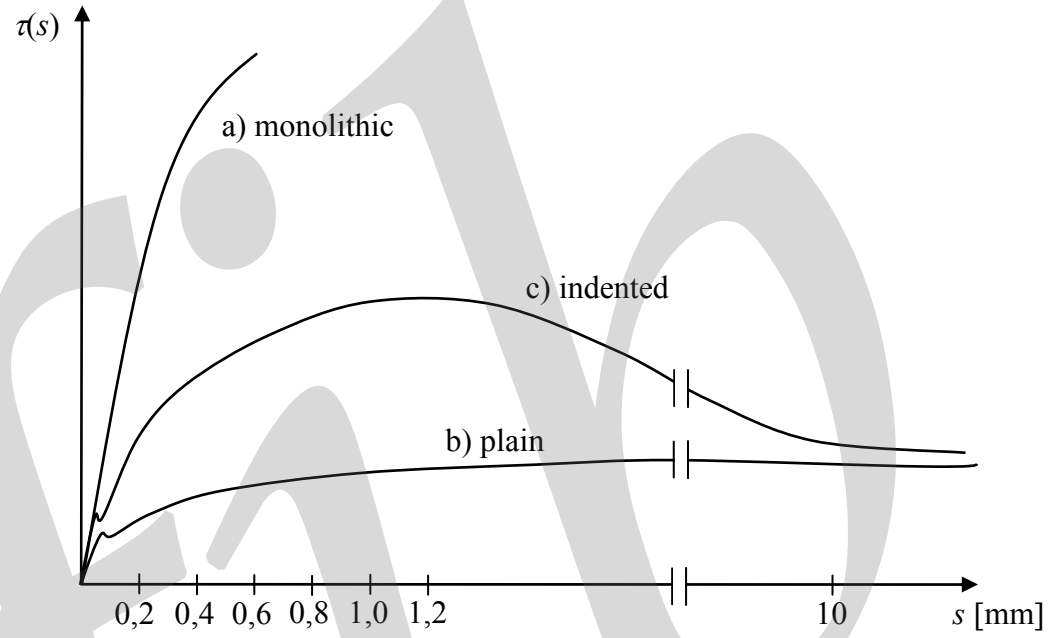

Fig. 8-48: Typical shear stress-slip relationships for wall connections at vertical concrete filled joints with plain or tooth shaped joint faces in comparison with that for monolithic concrete

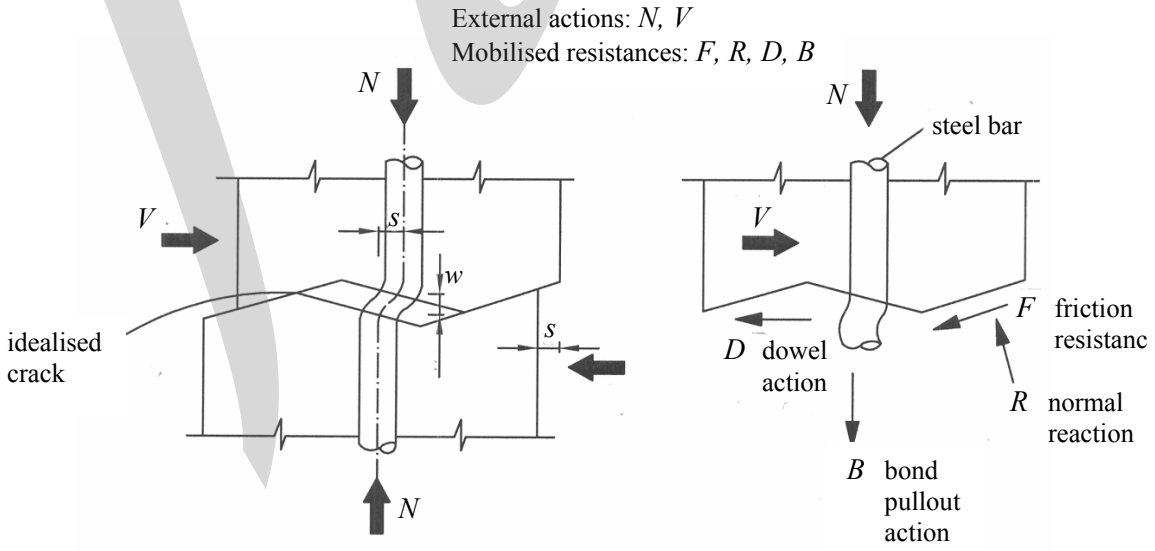

Fig. 8-49: Shear slip along a crack and resisting mechanisms

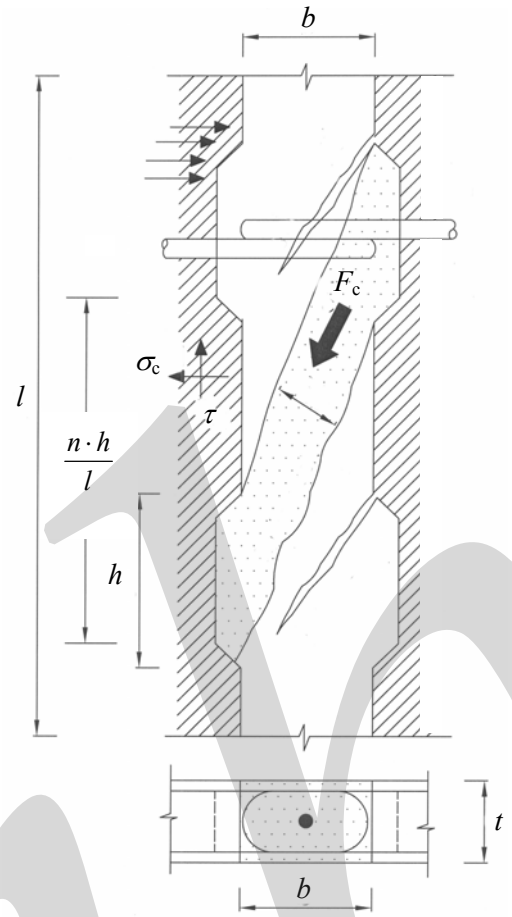

Fig. 8-50: Model for the shear transfer within a large panel reinforced concrete connection [Tassios and Tsoukantas (1978)]

Taking into account a suitable reduction of the compressive strength of the concrete in the diagonal compression struts within the joint (due to compressive stresses acting simultaneously with high shear stresses in the struts) and using suitable models for the estimation of frictional resistance and dowel action, it is possible to estimate the ultimate shear resistance of shear joints and with an equation of the form:

$$\tau_{R,nom} = C + F + D \tag{8-60}$$

where C = the contribution of the diagonal compression struts within the joint
F = the friction mobilized from the pullout resistance of transverse reinforcement (and of an external compressive force if exists)
D = the contribution of dowel action

The maximum shear force is reached when the effect of the shear keys disappears because of failure. Various failure modes are possible as shown in Fig. 8-51

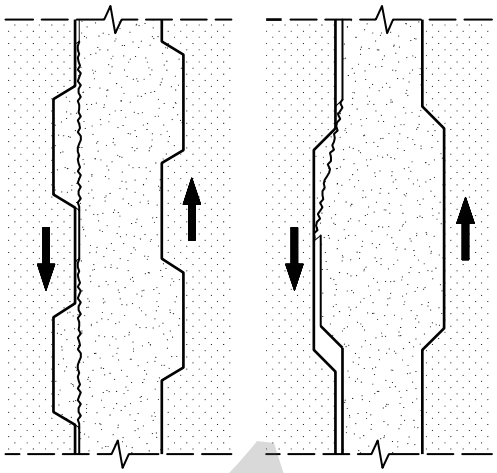

Fig. 8-51: Transfer of shear force by interlocking of shear keys, possible failure modes at peak load

In Fig. 8-52 shear stress-shear slip relationships for shear large-panel connections with or without shear-keys, are presented schematically.

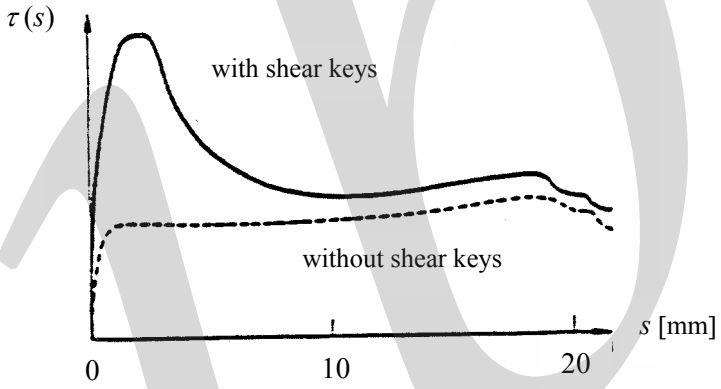

Fig. 8-52: Transfer of shear force by interlocking of shear keys, typical shear-slip response of joints with and without shear keys, adopted from SBI (1979)

The maximum capacity is governed by the failure of the shear-keys. Significant shear slip occurs when the shear-key effect is reduced by shear cracks along the joint or by local cracking or crushing of the shear-key corners. In the residual stage, after destruction of the shear-keys, the shear connection can still transfer considerable shear stresses by shear friction, if the connection is adequately tied together by transverse tie bars. This means that after the initial stiff behaviour, the shear connection will behave more or less like connections without shear-keys.

The shear resistance of this type of connections, with or without shear keys, can generally be explained by models including cohesive and frictional components as shown in eq. (8-43). For the frictional component compressive stresses due to external load and pullout resistance of transverse reinforcement can be utilised according to the principles for the shear friction analogy. With regard to the risk of compressive failure of inclined struts between the keys, an upper limit of the shear resistance needs to be applied, compare with Section 8.3.4.3. A model for design purposes is presented in Section 8.4.3. Normally, the tooth angle of indented joint faces is recommended to be small, typically about $\beta \approx 25°$. According to Eurocode 2, [CEN (2004)] the tooth angle should be less than or equal to 30°.

The behaviour of shear connections with shear-keys depends, according to Eriksson *et al*. (1978), to a large extent on the geometry of the shear-keys, and especially the tooth angle as defined in Fig. 8-53. When this angle is small, the connection initially has a very stiff behaviour and there is a pronounced peak at maximum load. The maximum shear capacity is considerably larger than the residual capacity in the frictional phase. This means that the behaviour at failure is rather brittle. A more ductile behaviour is obtained when the tooth angle increases, Fig. 8-53, but in this case the initial stiffness is considerably reduced.

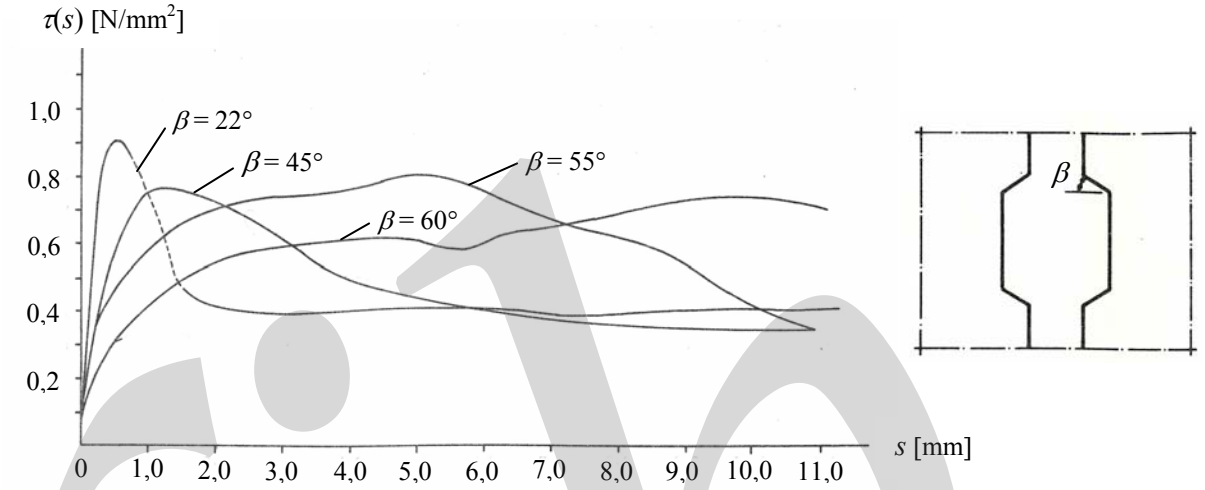

Fig. 8-53: Relationship between shear stress and slip from tests on shear connections with indented joint faces with various tooth angles, according to Eriksson et al. (1978)

8.4.1.2 Welded connections

The detailing of welded connections has a big influence both on the stiffness and the shear resistance of connections between wall elements. The stiffness of the connection is in turn very important for the stiffness of the wall. To illustrate this effect typical shear force – shear slip relations for some types of welded connections are shown in Fig. 8-54, on the basis of research carried out at Delft University of Technology.

In the first type (Fig. 8-54 a) a 10 mm thick connection plate is welded to 6 mm thick weld plates anchored in each wall element by ϕ8 mm anchor bars. The dimensions of the connection plate, weld plats and anchor bars are the same, but the detailing varies slightly. In type 1 the width of the recess is smaller than the width of the weld plate, which is embedded in the concrete element. In type 2 the width of the recess is greater than the width of the weld plate, but otherwise the detailing is the same. In type 3 the width of the recess is also greater than the width of the weld plate, but in this case the weld plate is not embedded in the concrete element but is placed on the face of it. The difference in shear response is significant depending on those small variations.

In the other type (Fig. 8-54 b) two 10 mm thick connection plates, one on each side, are welded to rectangular hollow sections (150×150×10 mm) that are anchored in the respective wall elements by 4 ϕ16 mm bars. The stiffness of this connection is about 10 times greater than of the first type.

In the case of intermittent mechanical connecting devices along a joint, an equivalent stiffness that characterises the joint section can be determined by 'smearing out' the discrete stiffness value over the influencing joint section.

$$K_{eq} = \frac{K_{dis}}{t \cdot s}$$

where K_{eq} = equivalent stiffness
K_{dis} = discrete stiffness of a mechanical connector

t = wall thickness
s = spacing between connectors

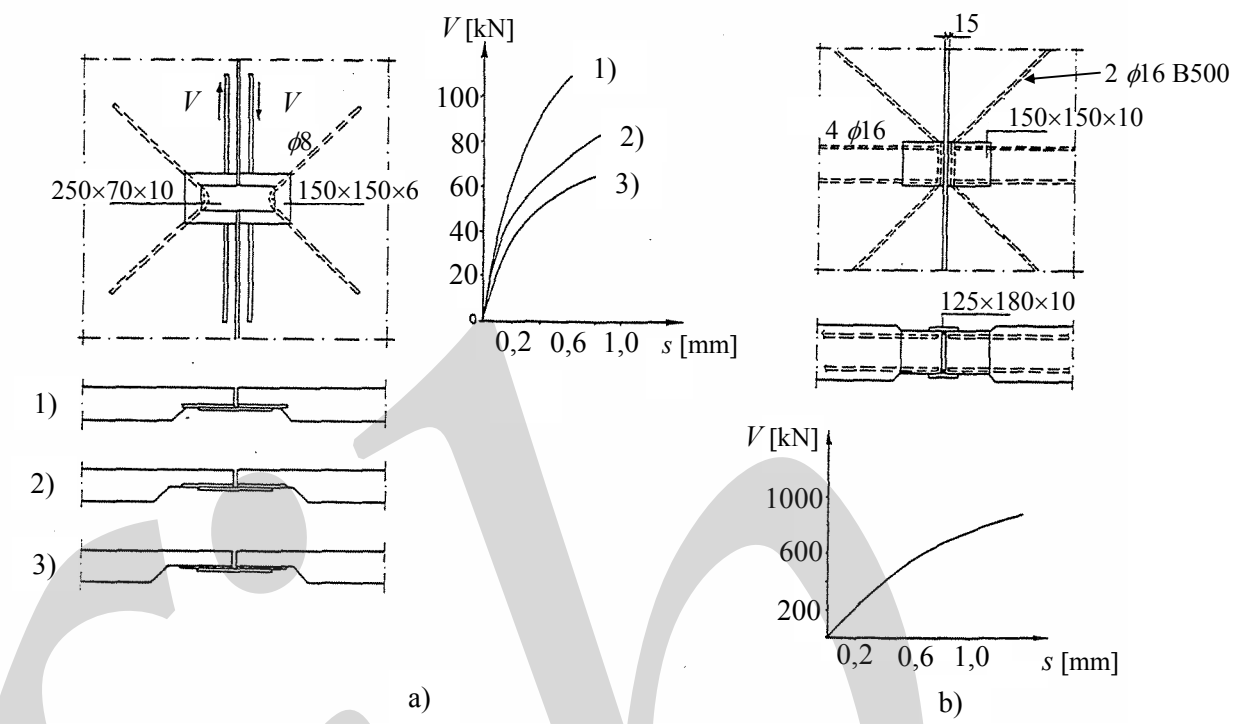

Fig. 8-54: Examples of shear force-slip relationships for welded connections between wall elements, a) steel plate to steel plate, b) steel plate to steel tube, adopted from Vambersky et al (2000)

8.4.2 Connections between floor elements

8.4.2.1 Longitudinal shear transfer in uncracked grouted joints

To study the shear resistance of plain grouted joints between hollow core elements a series of detail tests was carried out at the Delft University of Technology [Reinhardt (1982), Roose *et al.* (1983)]. The test arrangement is shown in Fig. 8-55. The joints were not cracked before the tests started.

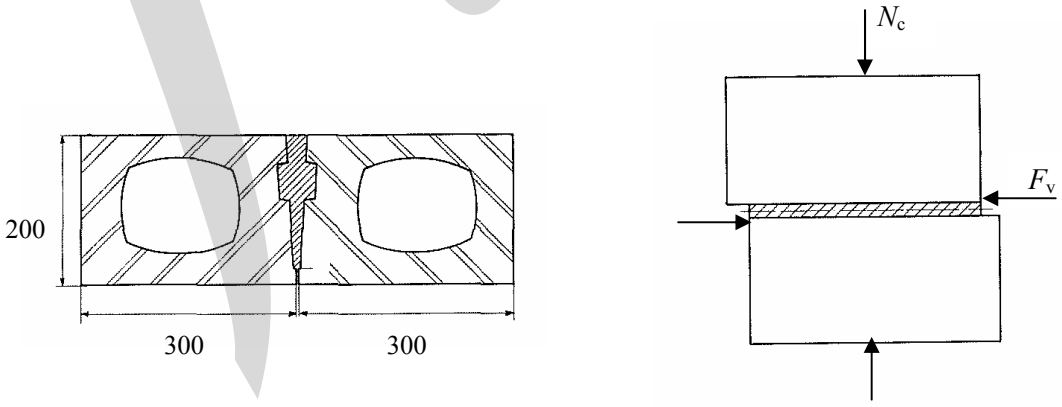

Fig. 8-55: Detail test of shear behaviour of grouted joints between hollow core elements according to Reinhardt (1982)

The test specimens were loaded to failure by shear loading F_v along the joint. In the transverse direction the joint was kept together by a normal force N_c that was applied before the shear loading started and kept constant during the test. The shear capacity of the joints was expressed as the average shear stress τ_{Rm} at joint failure (at maximum load). By parametric variation in the test program it was examined how the shear strength was influenced by the compressive strength of the joint grout, the magnitude of normal stress, and the length of the joint in the loading direction. Examples of test results are shown in Fig. 8-56.

$$\tau_{Rm} = \frac{F_{v,max}}{b_j l_j}$$

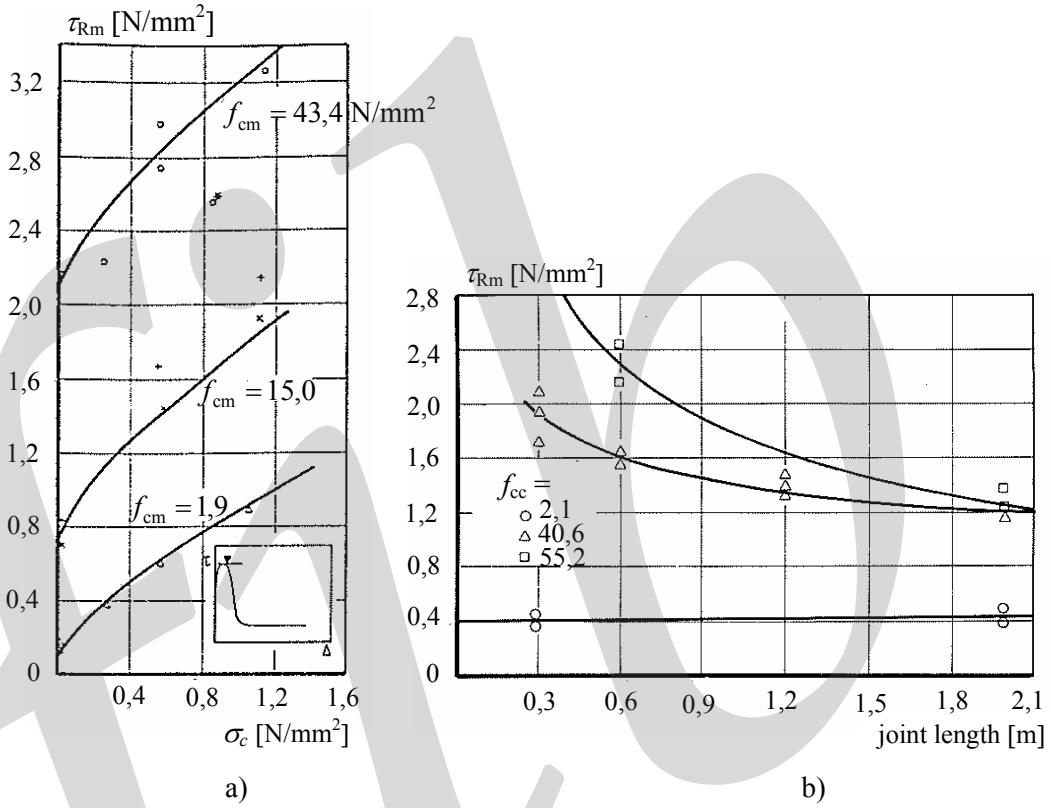

Fig. 8-56 Examples of test results from shear tests on uncracked grouted joints according to Reinhardt (1982) and Roose et al. (1983). Shear strengths of joints with different joint strengths, a) influence of normal stress, b) influence of joint length

From Fig. 8-56 a it appears that the shear strength increased with increased strength of the joint grout and for the same joint grout this increase was almost proportional to the applied normal stress. There was also a significant contribution by cohesion and the results reminds of a model for shear resistance of the type given in eq. (8-43). The dependency of the compressive stress was slightly stronger for joints with higher grout strengths, while the cohesive part of the shear resistance increased significantly with increased strength of the joint grout.

It was not possible to study directly the shear stress distribution along the joints at failure. However, if the average shear stress at failure varies when the joint length varies, this indicates that the shear stress in not uniformly distributed along the joint at failure. The joint length dependency from the tests is shown in Fig. 8-56 b. It appears that for joints with normal strength grout the shear strength was higher for short joints than for long ones. However, when the joint grout had extremely low strength, the shear capacity was not influenced by the length of the joint.

It can be assumed that in case of normal strength grout, high stresses appear near the ends of the joint, but the interior part is less stressed. When the stress at the ends reaches a critical level a joint failure is triggered, while the average stress is still rather small. The joints with extremely low strength

had a more ductile behaviour. Of this reason favourable stress redistribution could take place when the joint failure was approached. By that a more uniform stress distribution was obtained at failure and the whole length of the joint could significantly contribute to the shear resistance independently of the joint length.

In practice it is often not possible to rely on the cohesive part of the resistance. The reason is that grouted joints in floors easily crack due to restraint stresses from shrinkage, thermal actions, cyclic effects, transverse distribution of concentrated loads etc, see Fig. 8-57. According to observations from tests, [Svensson *et al.* (1986), Engström (1992)], such cracks are most likely appearing at the interface between the joint grout and the slab element.

According to Eurocode 2 [CEN (2004)] the possible cohesive part of the resistance of grouted joints between slab or wall elements should be disregarded for smooth and rough joints in cases where the joint may be cracked, which is typically the case for floors acting as diaphragms in the stabilising system. For indented joints the cohesion should be reduced, see Section 8.4.3.

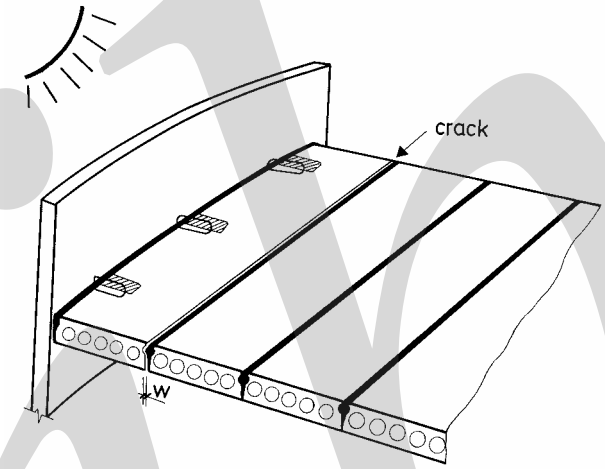

Fig. 8-57 Grouted joints in precast floors should normally be assumed to be cracked due to restraint stresses, diaphragm action etc.

8.4.2.2 Longitudinal shear transfer in cracked grouted joints

It is normally assumed that grouted joints in precast floors crack in the service state due to restraint loading caused by shrinkage, creep, temperature variation etc. Even if not all joints will crack, the risk of cracking must be considered in the design of precast floors. Hence, the shear resistance should be based on the frictional resistance of already cracked joints.

The influence of joint cracks on the frictional resistance of grouted joints between hollow core elements has been studied at Delft University of Technology [Ottolini (1986)]. Joints with plain as well as indented joint faces were studied. The same type of specimen as the one shown in Fig. 8-55 was used. However, in this case the joint was cracked and the crack width was adjusted to a certain value before the joint was loaded in shear. During the test the crack width was kept constant by a variable normal force. Some test results are presented in Fig. 8-58.

From Fig. 8-58 a it appears that in spite of an initial crack with a constant width of 0,15; 0,2; or 0,3 mm, considerable shear stresses could be transferred across the joint. It means that even the 'plain' joint faces had a roughness that was sufficient to obtain contact and shear transfer in the joint. This is in agreement with the shear friction theory where it is assumed that a shear displacement results in a joint separation in case of rough joint faces. Hence, to keep the crack width constant to the predetermined value during the test, a normal force was needed to prevent this natural joint separation, see Section 8.3.2. The needed normal stress increased with increased shear displacement and the shear stress increased in proportion to the applied normal stress. From Fig. 8-58 a it also appears that there

was no clear relation between crack width and shear behaviour, but there was a substantial scatter in the results.

The same typical behaviour was also obtained for the joints with indented joint faces, however, in this case with a much stiffer response, see Fig. 8-58 b. Here it can be assumed that the direct contact between the indentations have been of greater importance. ´

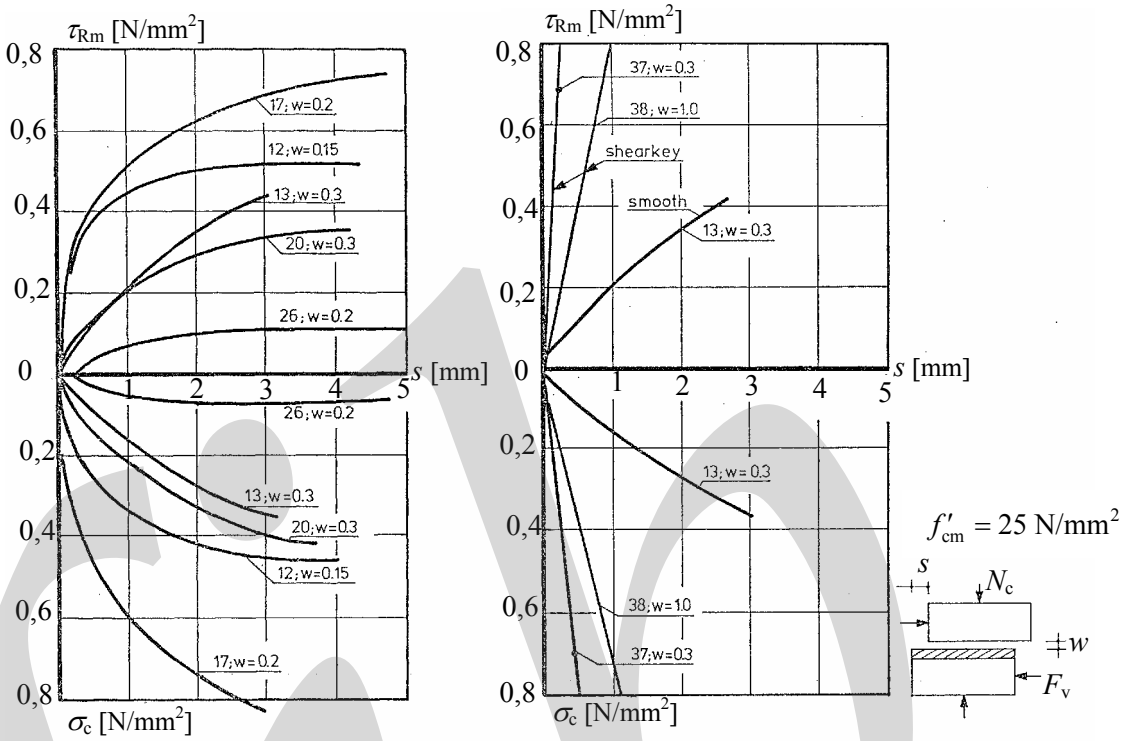

Fig. 8-58: Examples of test results from shear tests on crack grouted joints according to Ottolini (1983). Relations between shear stress, normal stress and crack width, a) joints with plain joint faces, b) joints with indented joint faces

It should be noted that even plain joints can result in significant wedging, if the joint face is long and the width of the element varies due to deviations within tolerances. It has been observed in tests on diaphragm action [Svensson *et al*. (1986)] that the shear stress was transmitted locally on some spots along the joint face, which was explained by such irregularities of the element geometry.

The design resistance of floor connections with regard to longitudinal shear can be determined by the same general model as for wall connections, see Section 8.4.3.

8.4.2.3 Vertical shear transfer in grouted joints

In precast floors a vertical shear resistance is needed to distribute concentrated loads transversally and to enable openings in the floor. To make this shear transfer possible within the short height of the joint, the joint is normally provided with a longitudinal shear key as shown in Fig. 2-22. When this connection is loaded in shear, the joint will crack, if it has not cracked before, and the shear force will mainly be transferred by an inclined compressive strut within the shear key as indicated in Fig. 2-22. To enable the shear transfer a sufficient horizontal 'clamping force' must develop to balance the horizontal component of the inclined compression within the joint.

So far the behaviour of the connection seems to be similar to wall connections with indented joint faces. However, there are some important differences. In wall connections the shear force is distributed on several inclined struts and hence 'smeared out' along the joint. Furthermore, the transverse steel is distributed, either within the height of the wall element or in the horizontal joints. In the floor connection the shear is transmitted by one single strut that develops in the vicinity of free edges of the floor elements and the transverse steel may be arranged far away.

For wall connections the shear resistance can be estimated by the general expression given in Section 8.4.3 considering concrete-to-concrete friction. For the floor connection several failure modes are possible as indicated in Fig. 8-59.

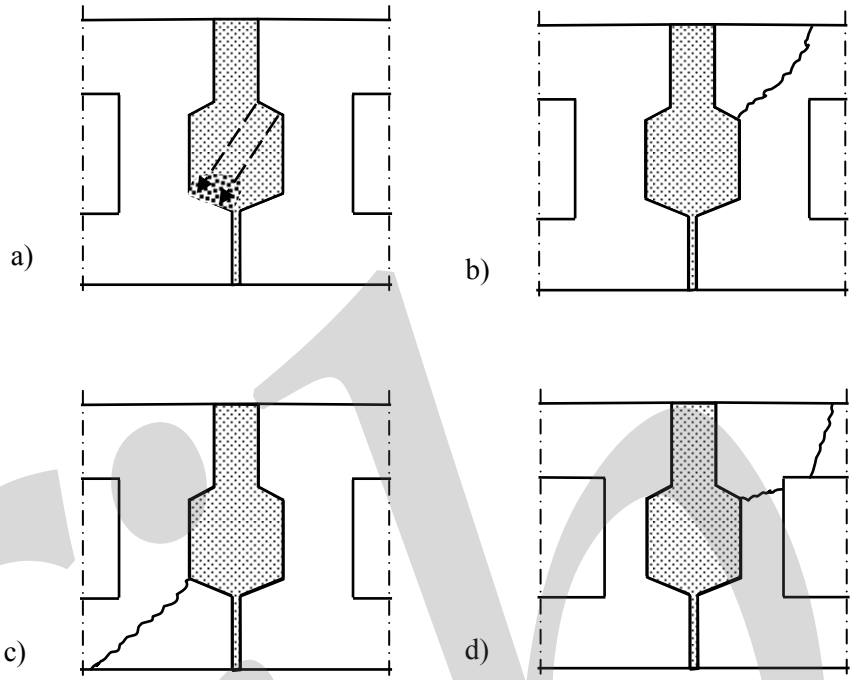

Fig. 8-59: Possible failure modes at longitudinal floor connections subjected to vertical shear, adopted from Walraven (1990), a) crushing of joint grout, b) failure in upper corner of slab element, c) failure of lower corner of slab element, d) failure influenced by core

If the horizontal clamping is insufficient the floor elements will drift apart and, consequently, a shear failure is reached by shear sliding along the joint faces. If the clamping is appropriate, the adjacent floor elements can fail due to cracking of the corners or the inclined strut in the joint grout may fail due to crushing. Cracking in the hollow core elements may also be influenced by the location and geometry of the cores. It is obvious that there exists no general expression for the shear resistance, but each geometry must be analysed separately.

This example shows again that it is not meaningful to define a shear resistance of the 'joint' itself. Instead the whole connection must be considered including the connection zones of the adjacent precast elements and the transverse steel arranged far away from the major part of the joint.

8.4.3 Design of connections with concrete-to-concrete interfaces

The following general expression, adopted from Eurocode 2 [CEN (2004)], may be used for the estimation of the design shear resistance of shear joints under monotonic loading. The same expression is applicable for interfaces between concrete cast at different times, such as joints in composite sections, and for grouted or concreted joints between precast elements. In the latter case the expression refers to the joint interface between the precast element and the *insitu* concrete in the joint.

$$\tau_{\mathrm{Rdj}} = c \cdot f_{\mathrm{ctd}} + \mu \cdot \sigma_{\mathrm{n}} + \rho \cdot f_{\mathrm{yd}} \left(\mu \sin\alpha + \cos\alpha \right) \leq 0{,}5 \cdot \nu f_{\mathrm{cd}} \tag{8-61}$$

where c = coefficient according to Table 8-4
f_{ctd} = design tensile strength for the concrete grade of the *insitu* concrete or the precast unit, whichever is lower

$$f_{ctd} = \frac{f_{ctk\,0,05}}{\gamma_c} \text{ (basic value)}$$

f_{ctd} = 0 if the joint is subjected to transverse tension
μ = coefficient of shear friction according to Table 8-4
σ_n = stress per unit area of external normal force across the joint interface, positive for compression and negative for tension, however $\sigma_n \le 0{,}6\, f_{cd}$
ν = strength reduction factor ($\nu = 0{,}6 - f_{ck} / 200$)
ρ = A_s / A_j
A_s = area of reinforcement (if any) crossing the joint, at an angle α defined in Fig. 8-60 and limited by $45^\circ \le \alpha \le 90^\circ$
A_j = area of joint interface ($A_j = l_j\, b_j$)

Shear reinforcement at the joint, should be provided with adequate anchorage on both sides of the interface. The effect of the angle α is explained in Section 8.3.4.3.

The longitudinal shear resistance of grouted joints between slab or wall elements; can be calculated according to eq. (8-61). However, in cases where the joint can be significantly cracked (e.g. in floors acting as diaphragms), c should be taken as 0 for smooth or rough joints and 0,125 for indented joints.

Furthermore, in joint sections between slab elements the average longitudinal shear resistance τ_{Rdj} should be limited to 0,1 N/mm^2 for very smooth surfaces and 0,15 N/mm^2 for rough surfaces.

Type of surface [1]	c	μ
monolithic [2]	0,62	1,0
indented surface	0,5	0,9
rough surface	0,45	0,7
smooth	0,35	0,6
very smooth surfaces	0,25	0,5

[1] *For roughness of joint faces, Table 8-3 is valid*
[2] *Adopted from ENV 1992-1-3.*

Table 8-4: Values of the coefficients c and μ

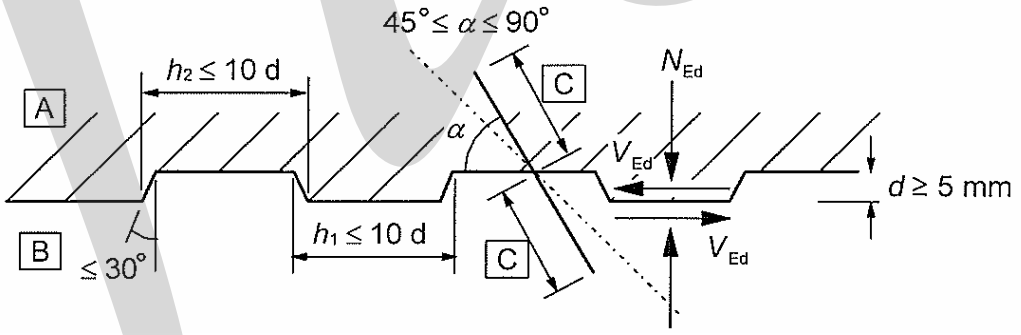

Fig. 8-60: Definition of shear key geometry

The definition of the shear keys in indented surfaces is presented Fig. 8-60.

8.5 Examples of applications

8.5.1 Connections in hollow core floors

8.5.1.1 Specific features for modelling the shear transfer in hollow core floors

In fib (2000a) A. Cholewicki and K.S. Elliott considered in detail the design rules for the connections of hollow core slabs, this approach is briefly presented below.

The shear transfer mechanism of the connections of hollow core slabs is influenced by the following specific features (Figs. 8-61 – 8-62):

- due to the relatively long spans of slabs, the tying reinforcement has a considerable spacing (the distances between the tie beams can approach 12 m, even more),
- the edges of the slabs are due to the way of manufacturing relatively smooth, however the long groove increases the probability of higher shear strengths,
- certain discrepancies in the width of slabs, (dimensional deviations in width are in the range of ± 5 mm), paradoxically contribute to a better shear transfer mechanism compared to the idealistic case of no deviation of dimensions,
- cracks along the interfaces of slabs due to temperature and shrinkage effects cannot be avoided. However, their width can be well controlled and restrained by the tying reinforcement,

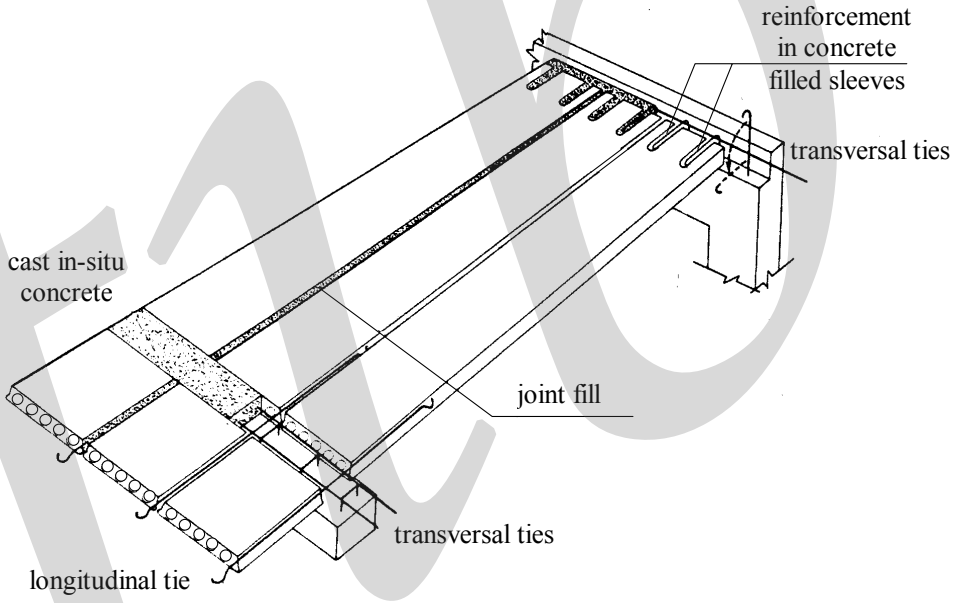

Fig. 8-61: Longitudinal joints of hollow core slabs with transverse tying reinforcement at the perimeter and in internal joint

- moreover, the units have edge profiles which permit the placement of grade C25-C30 *insitu* concrete in the longitudinal joints between adjacent units. Thus joints may be considered 'plain' and reinforced in a concentrated manner,
- for economical reasons all the gaps to be filled on site have limited sizes (in order to save the material and workmanship), for the same reasons the structural topping appears only in specific design situations.

Fig. 8-62: Edge surface at longitudinal joint face. Photo: authors

8.5.1.2 Shear transfer mechanism

Various structural models can be applied to describe the shear transfer mechanism between the individual slabs and between the diaphragm and the bracing elements. The behaviour of a precast hollow core floor diaphragm is different from that of a solid slab, because the precast unit has large in-plane stiffness relative to that of the joints. Small shrinkage cracks appear at the interface between the precast and *insitu* concretes, and the width of this crack influences the effective shear area in the joint. An initial crack width of 0,1 to 0,2 mm may be adopted for use in the calculations if the width of the hollow core unit is no more than 1.2 m, see Table 8-5.

Age of precast unit when *insitu* concrete is cast (days)	Precast unit width (mm)	Width of longitudinal joint (mm)	Initial crack width w_i (mm)
< 7	1200	25	0,215
		50	0,230
	600	25	0,115
		50	0,130
28	1200	25	0,135
		50	0,150
	600	25	0,075
		50	0,090
90	1200	25	0,095
		50	0,110
	600	25	0,055
		50	0,070

Notes. 1. Infill concrete is of medium to high workability with a water to cement ratio of less than 0.6.
2. Linear interpolation permitted.

Table 8-5: Initial crack widths w_i to be used in the calculation of diaphragm strength and stiffness [Elliott et al. (1992)]

The shear resistance τ_R is the result of aggregate interlock in cracked concrete, by so-called 'wedging action' and 'shear friction' (Fig. 8-63 a). The pullout resistance of the steel enables a normal compressive stress σ_{cs} to 'clamp' the units together.

The relationships (Fig. 8-63 b), plotted on the basis of experimental results, describe the shear wedging mechanism. The first quarter of the diagram (Fig. 8-63 b) shows the shear force-displacement relationship. The shear displacement is accompanied by the wedge like enlargement of the joint width that is called wedging (second quarter). Consequently, due to the wedging, tensile force in the tying reinforcement (third quarter) and shear friction resistance occur (fourth quarter). This relationship can be described analytically and thus the shear displacement s is

$$s = \frac{V}{K_s} \tag{8-62}$$

where K_s = the shear stiffness of the joint

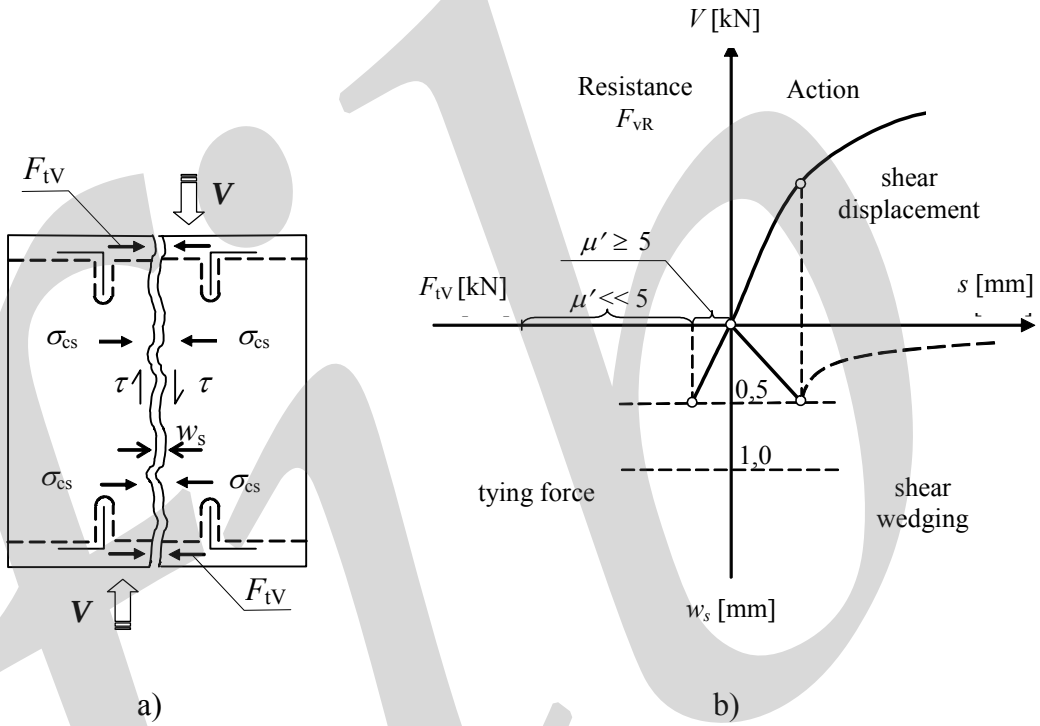

Fig. 8-63: Aggregate interlock (wedging) mechanism, a) shear wedging, b) constitutive relationships between shear force V, transverse tie force ΣF_{tV}, longitudinal slip s and transverse displacement w

The wedging factor ν_w which is equal to

$$\nu_w = \frac{w}{s} \tag{8-63}$$

remains $1 < \nu_w < 2$ within the limited range of w values, approximately within $w \leq 0{,}5$ mm.

The ν_w values drastically drop down after certain values of w are exceeded, as the experiments [Elliott *et al.* (1992)] have showed when $w > 1$ mm the ν_w value approaches even 0,1, compare with w_{max} in Fig. 8-28. It also appears from Fig. 8-32 and Fig. 8-37 that the wedging effect decreases for increasing values of the shear slip. Of this reason it is reasonable for design purpose to choose a maximum value of w, which is smaller than the maximum, according to Fig. 8-37 and eq. (8-40), and for which the wedging effect still is significant. This conservative approach is also supported by the experimental results from the actual application [Elliott *et al.* (1992)].

Friction factor μ', defined in eq. (8-64), (not to be confused with the commonly known friction coefficient μ) achieves, within named range of w, very large values, even $\mu' >> 5$ [Elliott *et al.* (1992)], see second and third quarter on Fig. 8-63 b.

The magnitude of tying forces ΣF_{tV} (indicated in Fig. 8-63 a) is expressed by the formula

$$\Sigma F_{tV} = \frac{V}{\mu'} \tag{8-64}$$

Consequently it can be observed that the total tying force is $\Sigma F_{tV} << V$ within the range of w displacement limited to 0,5 mm.

In the approach presented here no attention has been paid to shear transfer through the so called dowel action mechanism. The appearance of this mechanism is possible within the range of relatively large shear displacements s exceeding 10 mm, see Section 8.2.1.4.

8.5.1.3 Shear transfer mechanism – design rules and formulae

Calculations for the capacity of the longitudinal joint, due to aggregate interlock, should prove that the two following requirements are satisfied:

$$\tau = \frac{V}{A_{j,eff}} \le \tau_R \tag{8-65}$$

$$w = \frac{F_{tV}}{K_t} + w_i \le w_{max} = 0{,}5 \text{ mm} \tag{8-66}$$

where τ = applied shear stress
$A_{j,eff}$ = effective shear transfer area
τ_R = shear strength (maximum permitted design shear stress)
w_i = initial crack width (see Table 8-5)
w_{max} = limiting crack width for aggregate interlock
F_{tV} = maximum tie force in the tie beam which has maximum tensile force
K_t = axial stiffness of the tie beam

Eq. (8-66) should ensure that the tying bars are fully effective and that the shear transfer is accompanied by well-controlled shear displacements. If any of the above specified requirements are not satisfied, the shear resistance of the longitudinal joint should be increased. Technical measures are specified in Section 8.5.1.4. The simplest measure to satisfy eq. (8-66) is to increase the cross section of tying reinforcement A_s.

The axial stiffness of the tie beam, subjected to maximum tensile force, see eq. (8-67), should be large enough to consider that the equivalent bond transmission length $l_{t,eq}$ is smaller than the width of a slab multiplied by coefficient 0,8, e.g. $l_{t,eq} \le 0{,}8 \times 1{,}2 = 0{,}96$ m. This distance, which is conservative, allows for the interaction of shear transfer in the adjacent longitudinal joint.

Axial stiffness of the tie beam can be estimated according to following formula:

$$K_t = \frac{A_s E_s}{l_{t,eq}} \tag{8-67}$$

where E_s = modulus of elasticity for tie steel,
taken as 200 kN/mm^2 for bar and 190 kN/mm^2 for strand
A_s = area of tie bars

The equivalent transmission length $l_{t,eq}$ can be taken as the minimum of:

$$l_{t,eq} = 30\,\phi\,\frac{\sigma_s}{f_y} \quad \text{for high tensile ribbed bar} \tag{8-68}$$

and

$$l_{t,eq} = 0{,}8\, b \tag{8-69}$$

where b = the width of the hollow core unit
ϕ = the diameter of the bar

Alternative approaches to estimate the stiffness of tie beams are given in Example 7-4, Section 7.4.1.

When computing τ, the effective depth of the diaphragm can only be taken as the depth of the effective joint interface, i.e. h - 30 mm, in most types of hollow core slabs (where h is the full height of the slab cross section). The reason for this derives from observations made on the compaction of the *insitu* concrete in the joint [Davies *et al.* (1990)]. It is found that grout loss occurs in the bottom of the joint and that the lower 10 to 15 mm effectively remains ungrouted. Secondly, the lip at the bottom of the units, typically 10 to 15 mm deep, prevents full penetration. The value also recognises that differential camber will be present - further reducing the net contact depth.

In many cases the point of maximum shear will coincide with minimum bending moment and therefore the full length l_j of the longitudinal joint (equal approximately to the diaphragm width) may be used in calculating τ as follows:

$$A_{j\,eff} = l_j\,(h - 30) \text{ (mm units only)} \tag{8-70}$$

The limiting value of τ_{Rd} is given in Eurocode 2 [CEN (2004)], see Section 8.4.3. In general the design strength is determined by eq. (8-61) with due regard to the possibility that the joints being cracked due to diaphragm action of the floor. Furthermore, joint sections between slab elements with smooth joint faces the average longitudinal shear resistance should be limited to 0,1 N/mm, see Section 8.4.3.

Other examples from codes are

τ_{Rd} = 0.23 N/mm^2 according to BS 8110, [BSI (1985)]
τ_{Rd} = 0.275 N/mm^2 according to ACI 318, [ACI (1995]

In the case of significant bending moments in the plane of diaphragm (Fig. 8-64 a, b) the conditions eq. (8-66) and eq. (8-70) will change as shown below. The effective cross sectional area of the diaphragm will be reduced to:

$$A_{j\,eff} = z\,(h - 30) \text{ (mm units only)} \tag{8-71}$$

where z = internal lever arm, see Section 2.3.1
h = height of the cross section of the slab

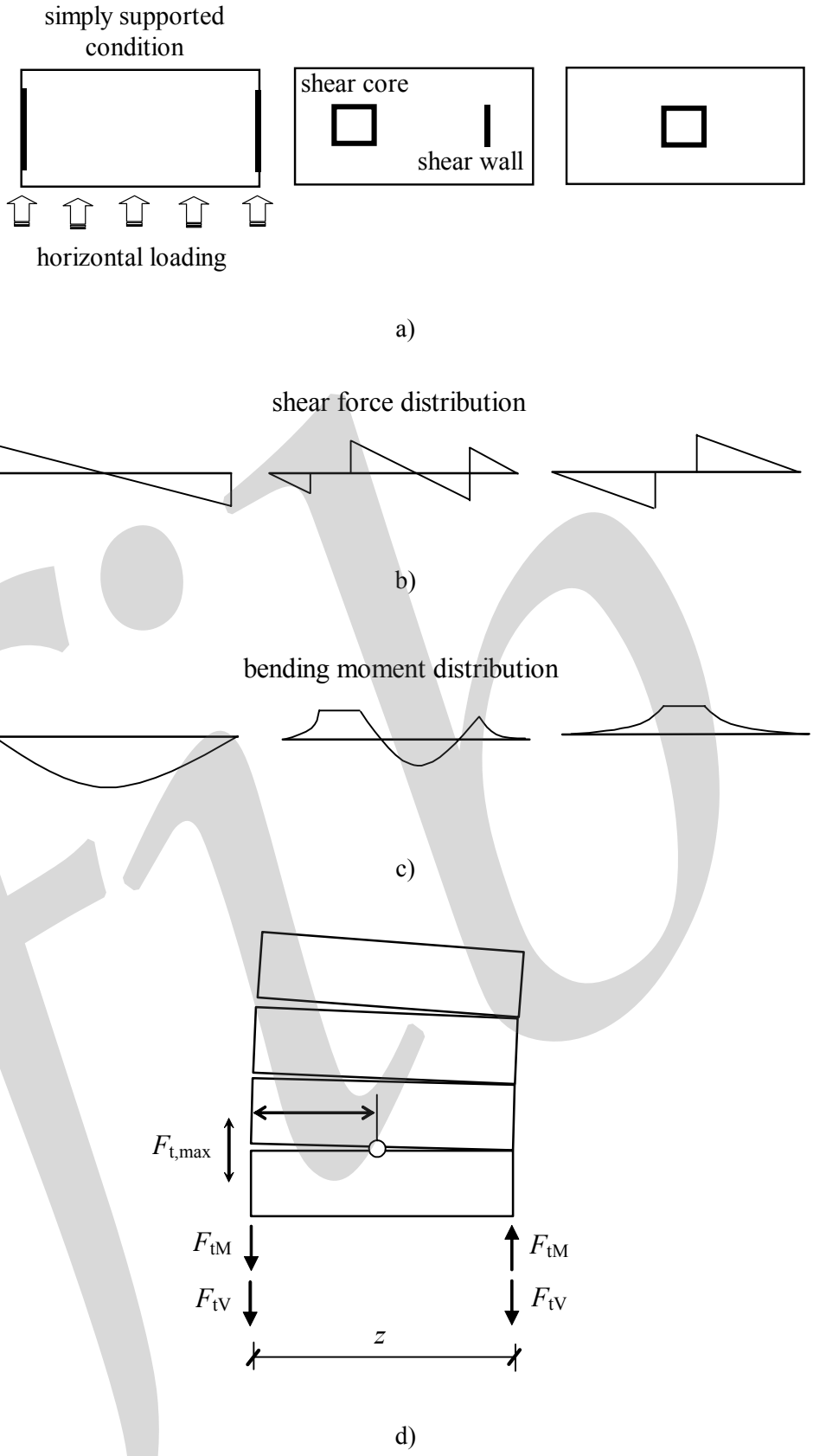

Fig. 8-64: a) plan geometry of floor diaphragms, b) shear force distribution, c) bending moment distribution, d) point of control of maximum total transverse displacement

The maximum lateral dilatancy w_{max} may then be checked at a certain distance from the tie beam with the maximum tensile force (Fig. 8-64 d).

$$w_{VM} = \frac{F_{tV} + F_{tM}\left(0{,}8 - \frac{1}{n_t\sqrt{\mu'}}\right)}{K_t} + w_i \le w_{max} = 0{,}5 \text{ mm} \tag{8-72}$$

provided that

$$\frac{F_{tV} + F_{tM}}{A_s} \le f_y \tag{8-73}$$

where n_t = number of tie beams
f_y = strength of steel

For the case of a diaphragm supported on two ending walls, the location of the section where $F_t = F_{t,max}$ can be found by means of the following formula

$$x_0 = \frac{L}{2} - \frac{z}{n_t} \tag{8-74}$$

where x_0 = distance from the left hand corner of diaphragm

In the case of other models the following condition can be used in order to determine the position of $F_{t,max}$:

$$\frac{dF_t}{dx} = 0 \tag{8-75}$$

The second line of defence would be the fulfilment of the safety condition, checked for the most highly stressed tie beam:

$$F_{t,max} \le \mu A_s f_y \tag{8-76}$$

where μ = friction coefficient, see eq. (8-61) (not the friction factor)

8.5.1.4 Technical solutions applied for the improvement of the shear transfer mechanism

Menegotto (1988, 1994) studied diaphragm action using precast units with undulated edge profiles, see Fig. 8-65, for the specific purpose of application to slabs in seismically active zones.

The typical loading sequence was:

- first, five cycles of small amplitude (slip displacements ± 1mm)
- second, five larger displacements (± 10mm)
- finally, cycles of ± 20mm.

The most important conclusions from this series of tests were:

- the average shear stress developed for displacements of ± 10mm, in case of undulated profiled edges, was about 0,5 N/mm^2,
- very low figures characterise the strength and stiffness of the plain joints; the cyclic loading significantly degrades the wedging mechanism.

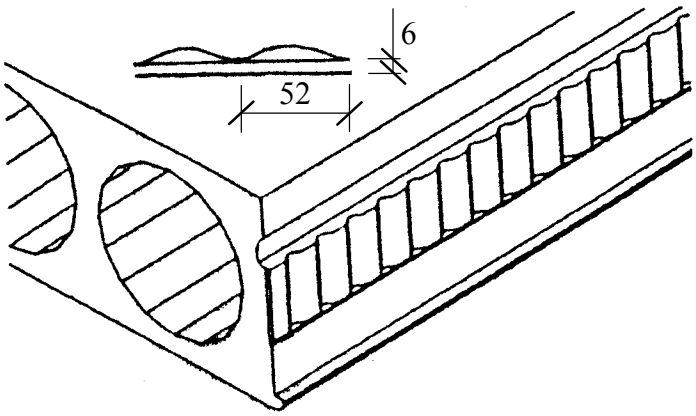

Fig. 8-65: Slab with undulated sinusoidal edge according to tests byMenegotto (1994)

The tests showed that it was possible to use untopped deck with grouted unduluted joints as rigid diaphragms even under severe conditions (seismic action). The behaviour of longitudinal joints between slabs was sufficiently ductile and characterised by low sensitivity to cyclic fatigue. This type of joint behaviour was guaranteed by the sinusoidaly profiled slab edges and by the tie reinforcement bars, which can be determined in accordance with the following:

– pure friction coefficient $\mu = 0{,}35$ (parallel to the waves)
– friction factor (incorporating improved wedge effect in case of sinusoidal profilation) $\mu' = 0{,}50$.

The improved wedge effect in this case ensures limited values of shear displacements at the ultimate limit state. Thus, the full capacity of tying reinforcement can be used for design. The shear resistance of that type of joint is then

$$F_{vR} = \mu' \Sigma A_s f_y \tag{8-77}$$

Internal beams (Fig. 8-61) can be thought of as so-called **large shear keys** and can effectively contribute to the shear transfer mechanism. The principle of equal shear displacements of the longitudinal joint and the local large shear key is the basis for adding both shear resistances in order to calculate the total shear resistance of the joint.

In mixed systems where steel sections are used for beams the contribution of those elements can be dominant in the shear transfer mechanism.

Elliott *et al.* (1992) did not hesitate to recommend the use of prestressing wires as the main perimeter reinforcement for the diaphragm. It is natural that the yield point of the prestressing steel will be reached at free elongation of the tendons in the range of 3-4 mm per joint. In real structures, in which the floor units are much longer than the tested specimens (2 to 4 m), besides the local roughness, the global unevenness of slab edges (due to technological inaccuracies or not ideally split surfaces between the slab edge and grout in the joint) may also occur; therefore this 4 mm crack opening may not be critical with respect to the shear wedging mechanism. Generally, however, the shear displacements of the longitudinal joints should be taken into account in considerations aimed at fully utilising the carrying capacities of the prestressing wires.

The application of structural topping on precast hollow slabs can create a cast in place membrane, which connects all slabs into an integrated diaphragm and which ensures an additional shear transfer mechanism along the individual longitudinal joints.

The simplest approach is to design the reinforcement in cast structural layer providing the condition that the steel bars, along the direction perpendicular to the joints, are the only elements, which transmit shear force V, and horizontal bending moment M.

In more complex calculations the interaction of both parts of the diaphragm i.e. the tying reinforcement placed within the depth of the slabs and the one placed in the structural topping can be

taken into account. The principle for the interaction (superposition of the capacities of the two types of reinforcement) should be equality of shear displacements imposed by V (accompanied by M) on the real joint and its projection into the topping layer.

8.5.2 Connections in composite beams

8.5.2.1 Introductory remarks

The integrity of composite construction relies on the long-term continuity between precast beam and *insitu* concrete or precast floor.

The interface connection fulfils the important structural function, it determinates the transmission of the shear flow forces (shear forces expressed per unit of the connection length) (Fig. 8-66); these shear forces generate a so-called coupling moment M_v.

$$M_v = F_v \cdot a \tag{8-78}$$

where F_v = sum of the unit shear force along half the span of the beam
a = distance between centroidal axes of part 1 and part 2

Maximum possible value of that moment guarantees that the model of the composite beam can be comparable to the model of a corresponding homogeneous structure. The contemporary technological methods enable to achieve satisfactory roughness of the horizontal interface (top surface) of beam to cast the *insitu* part of the connection (Fig. 8-66 b). Ties projecting through that surface (so-called interface shear reinforcement) are designed according to rules settled in the standard documents, like Eurocode 2 [CEN (2004)].

The assumption of this approach is that the interface reinforcement (Fig. 8-66 b) guarantees that the shear stiffness K_s fulfils the condition

$$K_s > K_{s,min}$$

where $K_s = \dfrac{F'_v}{s}$ (shear stiffness) (8-79)

F'_v = shear force at the interface per unit length (Fig. 8-66)
s = shear displacement (Fig. 8-28)
$K_{s,min}$ = minimum value of shear stiffness

When the shear stiffness exceeds the minimum value $K_{s,min}$ the corresponding shear displacement s (shear slip) has negligible effects on the distribution of internal forces in the composite beam.

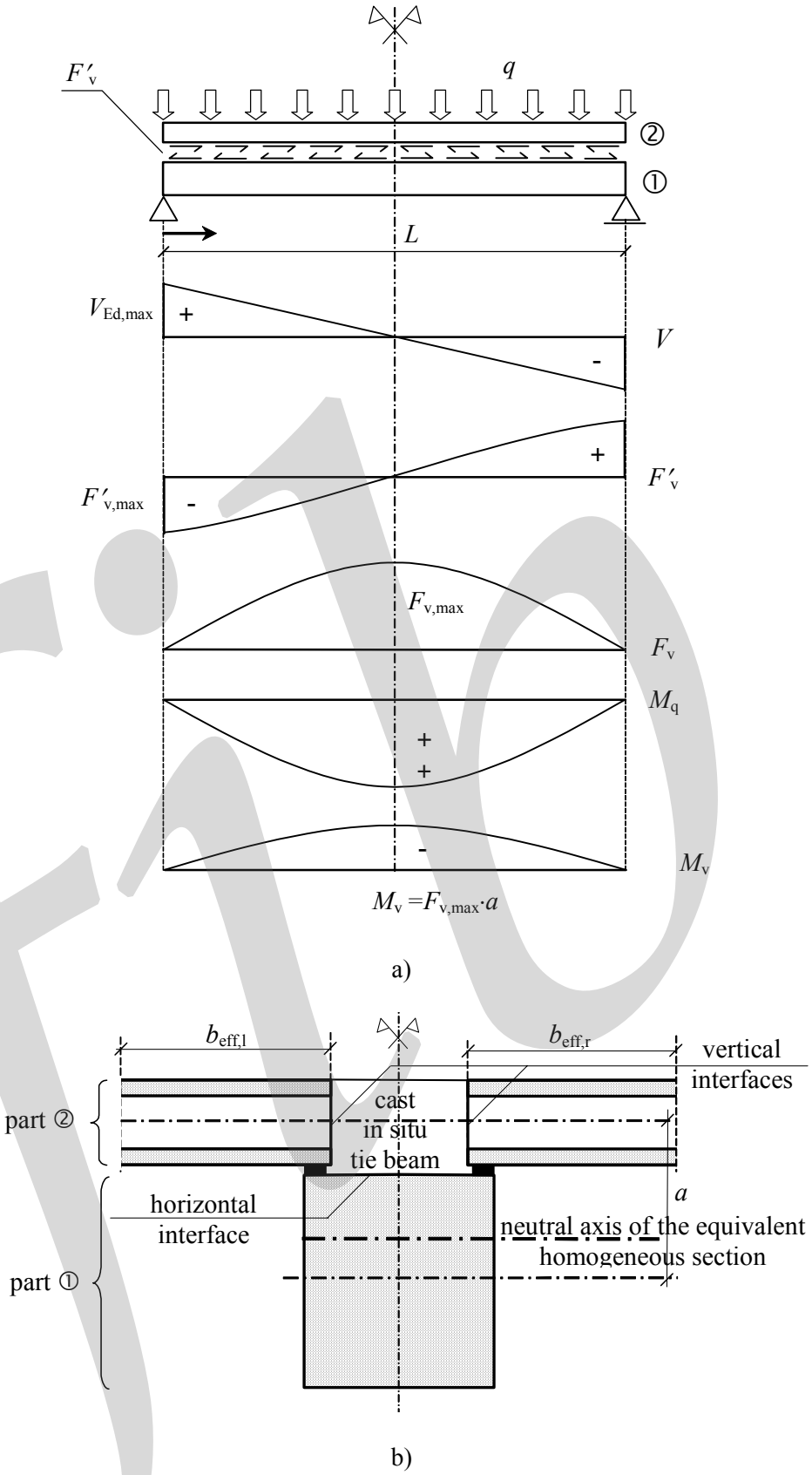

Fig. 8-66: 'Two-beam model' of a composite simply supported beam, a) distributions of moments and shear forces, b) cross-section

Consequently, according to Eurocode 2 [CEN (2004)], the design shear stress at the interface is calculated as

$$\tau_{\mathrm{Edj}} = \frac{F_{\mathrm{cj}} \cdot V_{\mathrm{Ed,max}}}{F_{\mathrm{c}} \cdot z \cdot b_{\mathrm{j}}} \tag{8-80}$$

where F_{cj} = the axial force (compressive) transferred through that part of the composite beam which is located above the interface
$V_{\mathrm{Ed,max}}$ = design value of the shear force at the support section
F_{c} = total value of the axial compressive force
z = internal lever arm in the section through the homogenous structure
b_{j} = width of the interface area of the connection

The maximum shear force per unit length is determined as

$$F'_{\mathrm{v,max}} = \tau_{\mathrm{Edj}} \cdot b_{\mathrm{j}} = \frac{F_{\mathrm{cj}} \cdot V_{\mathrm{Ed,max}}}{F_{\mathrm{c}} \cdot z} \tag{8-81}$$

Composite action of beams with precast floors supported on them creates a potential enhancement of the flexural capacity; in the most favourable case the equivalent width b_{eff} of the flange can be assumed like in corresponding cast *insitu* reinforced concrete structures.

Very widely used types of precast flooring are now either hollow core slabs or double-T panels. Presently the first ones may reach the thickness even of 1000 mm. When these floor units are supported on precast beams, composite action is preconditioned by the following:

- efficient shear transfer, i.e. the shear transfer path should be safe, not only through the horizontal interface, but also **through the vertical ones**,
- the full flange should remain either in the compression zone of the section (Fig. 8-66 b) or, if tensile forces appear, they should be safely transferred by reinforcement,
- the compressive force should be safely transferred through well grouted longitudinal joints of the floor slabs

Cholewicki (2000) has proposed to apply the 'two-beam model' for two purposes:

- easy check of consequences of shear deformability of the joints at horizontal and vertical interfaces,
- easy evaluation of minimum values of shear stiffness, $K_{\mathrm{s,min}}$ of the horizontal interface and $K_{\mathrm{sv,min}}$ of the vertical interfaces.

If the shear stiffness K_{s} is less than the minimum value $K_{\mathrm{s,min}}$, the qualitative consequence is an increase of the bending moments M_1 in the beam part and M_2 in the upper part of the composite section (above the level of the horizontal interface), see Fig. 8-67 a. The consequence of a shear stiffness K_{sv} less than $K_{\mathrm{sv,min}}$ may be disintegration of the interacting floor slabs due to insufficient compression, which would mean $M_2 \rightarrow 0$, see Fig. 8-67 b.

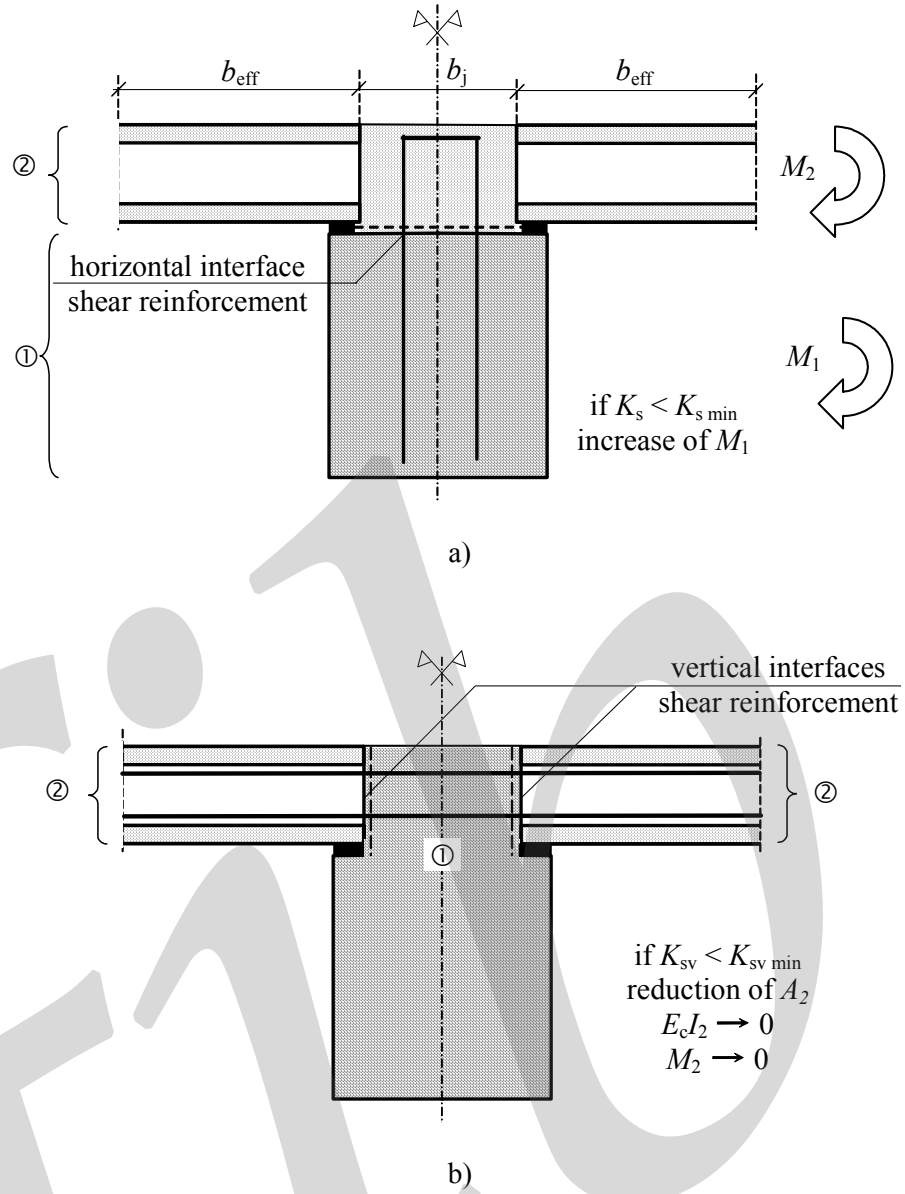

Fig. 8-67: Consequences of insufficient shear stiffness of the connection, a) increase of M_1 at horizontal interface , b) disappearing of M_2

8.5.2.2 Interaction in a composite structure according to the 'two-beam model'

The 'two-beam model' (Fig. 8-66) was applied by some authors, e.g. König (1981), Cholewicki (2000), in order to determine the distribution of unit shear forces F_v', the sum $F_{v,max}$ of those forces in the mid section of the span of the beam, and the coupling moment $F_{v,max} \cdot a$. Table 8-6 contains coefficients η'_{max} and η_m, necessary for the derivation, which is related to the following characteristic value

$$\frac{\alpha L}{2} = \frac{L}{2}\sqrt{\left(\frac{1}{E_{c1}A_1} + \frac{1}{E_{c2}A_2} + \frac{a^2}{E_{c1}I_1 + E_{c2}I_2}\right)K_s} \tag{8-82}$$

where E_{c1}, E_{c2} = concrete modulus of elasticity in parts 1 and 2, respectively
A_1, A_2 = cross-section areas of parts 1 and 2, respectively
I_1, I_2 = moments of inertia of parts 1 and 2, respectively

a = distance between the centroids of parts 1 and 2.
L = span of the beam,
K_s = shear stiffness, see Section 8.5.2.3

Table 8-6 was elaborated on the basis of tables published by Rosman (1968) for the calculation of shear walls, see also Cholewicki (1985).

The maximum shear force per unit length for a simply supported beam is

$$F'_{v,max} = V_{Ed,max} \frac{\psi}{\alpha^2} \eta'_{max} \tag{8-83}$$

The sum of the unit shear forces along the half the span of beam, i.e. along the portion from the support to the mid section, is

$$F_{v,max} = 0{,}5\, V_{Ed,max} \frac{\psi}{\alpha^2} L\, \eta_m \tag{8-84}$$

where $V_{Ed,max}$ = design shear force at the support
η'_{max} and η_m = coefficients according to Table 8-6

The ratio $\frac{\psi}{\alpha^2}$ is

$$\frac{\psi}{\alpha^2} = \frac{\dfrac{a}{E_{c1}I_1 + E_{c2}I_2}}{\dfrac{1}{E_{c1}A_1} + \dfrac{1}{E_{c2}A_2} + \dfrac{a^2}{E_{c1}I_1 + E_{c2}I_2}} \tag{8-85}$$

If $E_{c1} \approx E_{c2}$ then

$$\frac{\psi}{\alpha^2} = \frac{S}{I} \tag{8-85}$$

where S = first moment of area of the part of the section above the joint related to the neutral axis
I = moment of inertia of the whole composite section related to the neutral axis

In case of a negligible effect of the connection shear deformability, i.e. when $\eta'_{max} \approx 0{,}9$ the value of $F'_{v,max}$ according to eq. (8-83) is:

$$F'_{v,max} = V_{Ed,max} \frac{S}{I} \tag{8-86}$$

where S and I are area moments, which if $E_{c1} \neq E_{c2}$ are calculated on the basis of a transformed section (equivalent dimensions)

The 'two-beam model' helps to illustrate the positive effect of composite action; the total sectional moment can be subdivided into three parts, i.e

$$M = M_{beam} + M_{floor} + F_{v,max} \cdot a \quad \text{or} \quad M_{beam} + M_{floor} = M - F_{v,max} \cdot a \tag{8-88}$$

where M_{beam} = moment transferred by the beam (part 1 in Fig. 8-66 a)

M_{floor} = moment transferred by the part of the structure lying either above the horizontal joint interface or lying outside the beam if the vertical interfaces are assumed to be deformable shear joints

$\alpha L/2$	η'_{max}	η_m	$\alpha L/2$	η'_{max}	η_m
0,50	0,076	0,047	5,25	0,810	0,464
0,75	0,154	0,095	5,50	0,818	0,467
1,00	0,238	0,148	5,75	0,826	0,470
1,25	0,419	0,199	6,00	0,833	0,472
1,50	0,397	0,244	6,25	0.840	0,474
1,75	0,462	0,284	6,50	0,846	0,476
2,00	0,518	0,316	6,75	0,852	0,478
2,25	0,566	0,344	7,00	0,857	0,480
2,50	0,605	0,366	7,25	0,862	0,481
2,75	0,640	0,385	7,50	0,867	0,482
3,00	0,669	0,400	7,75	0,871	0,483
3,25	0,694	0,413	8,00	0,875	0,484
3,50	0,715	0,423	8,25	0,878	0,485
3,75	0,733	0,432	8,50	0,883	0,486
4,00	0,750	0,440	8,75	0,886	0,487
4,25	0,764	0,446	9,00	0,889	0,488
4,50	0,778	0,452	9,25	0,892	0,488
4,75	0,800	0,456	9,50	0,895	0,489
5,00	0,800	0,461	9,75	0,898	0,489
			10,00	0,900	0,490

Table 8-6: Coefficients η'_{max} and η_m. The table has been elaborated on basis of tables published by Rosman (1968) for the calculation of bearing wall structures, see also Cholewicki (1985)

The third part in eq. 8-88 is the coupling moment. Examples of calculations show that if $\alpha L/2 \geq 5$ the shear stiffness K_s has no meaningful importance either for the summed shear force $F_{v,max}$ or the distribution of unit shear forces F'_v (this one is close to a triangular one). These two groups of forces are then only approximately the same as according to the equations given in documents Eurocode 2 [CEN (2004)] and FIP (1998).

Negligence of the effects of shear deformability although leads to overestimation of the maximum unit shear force (this is safe), results in an underestimation of the normal stresses in the composite parts of the structure (this is not safe!).

The 'two-beam model' was applied by Cholewicki and Szule (2006) to determine the minimum shear stiffness $K_{s,min}$, which is necessary to guarantee that the part 2 of the section (Fig. 8-67) remains fully in a state of compression under simultaneous action of the bending moment M_2 and normal compressive force $F_{cj} = F_{v,max}$. The following expression for $K_{s,min}$ was obtained

$$K_{s,min} = \frac{121}{L^2} \cdot \frac{E_{c1}}{\frac{1}{A_1} + \frac{E_{c1}}{E_{c2}} \frac{1}{A_2} + \frac{a^2}{I_1 + \frac{E_{c2}}{E_{c1}} I_2}} \tag{8-89}$$

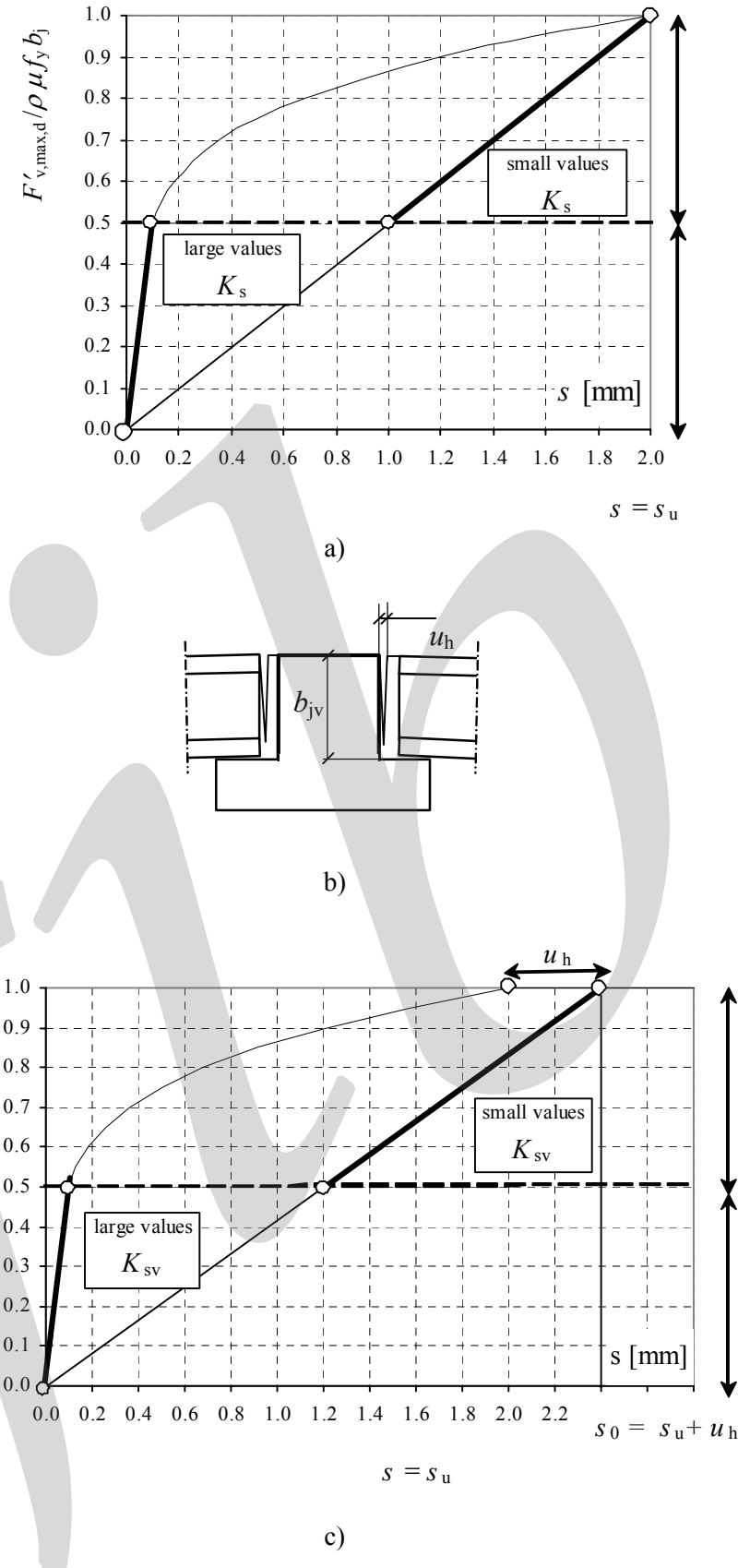

Fig. 8-68: Shear stiffness K_s and K_{sv}, a) approximate values to calculate the shear stiffness K_s of the connection at the horizontal interface, b) peculiar features of the beam-slab connection with vertical interfaces and support rotation, c) shear stiffness K_{sv} of the connection at the vertical interfaces

The same two-beam model can be applied in the case when two vertical shear interfaces are assumed to be deformable shear joints characterized by the shear stiffness K_{sv}, see Section 8.5.2.3 and Fig. 8-68. The formula (8-88) then changes into:

$$M = M_{b+tb} + M_{floor} + (F_{v,l} + F_{v,r})a \tag{8-90}$$

where M_{b+tb} = moment transferred by the beam together with a cast *insitu* tie beam (part 1 of the cross-section)
M_{floor} = moment transferred by the two parts of the floor (part 2)
F_{vl} = sum of shear forces along the left vertical interface, Fig. 8-69
F_{vr} = sum of the shear forces along the right vertical interface, Fig. 8-69

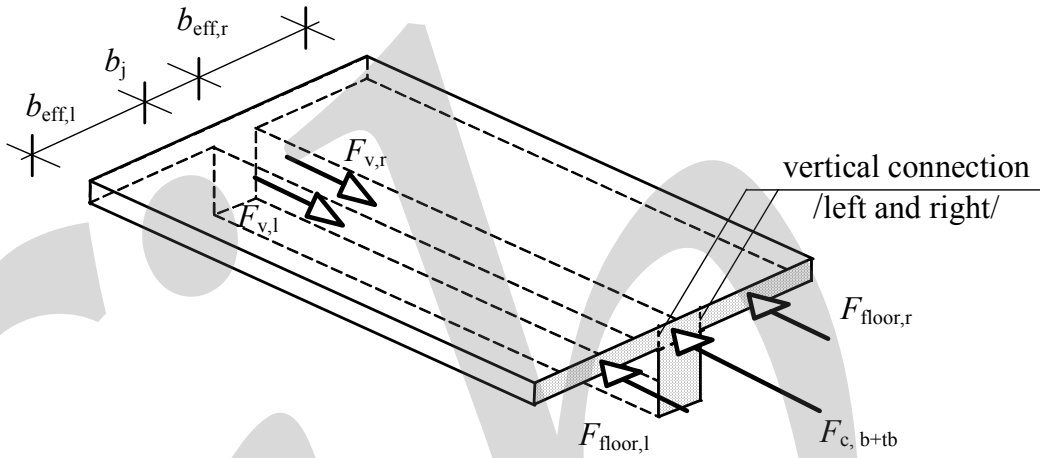

Fig. 8-69: Distribution of the total shear force F_v on three longitudinal forces (above the horizontal interface)

Eqs. (8-82) and (8-85) change into:

$$\frac{\alpha L}{2} = \frac{L}{2}\sqrt{\left(\frac{1}{E_{c1}A_{b+tb}} - \frac{1}{E_{c2}A_{floor}} + \frac{a^2}{E_{c1}I_{b+tb} + E_{c2}I_{floor}}\right)2K_{sv}} \tag{8-91}$$

and

$$\frac{\psi}{\alpha^2} = \frac{\dfrac{a}{E_{c1}I_{b+tb} + E_{c2}I_{floor}}}{\dfrac{1}{E_{c1}A_{b+tb}} + \dfrac{1}{E_{c2}A_{floor}} + \dfrac{a^2}{E_{c1}I_{b+tb} + E_{c2}I_{floor}}} \tag{8-92}$$

The values of A_{floor} and I_{floor} in eqs. (8-91) and (8-92) should be determined for a floor width equal to $2b_{eff}$ (Fig. 8-68).

Assuming that the neutral axis of an equivalent homogenous section lies below the floor slab surfaces (Fig. 8-66 b) and that $E_{c1} \cong E_{c2} = E_c$, the expression for $K_{sv,min}$ can be derived, which means that the whole equivalent floor section with the width $2b_{eff}$ remains in the compression state, then:

$$K_{s,min} = \frac{60}{L^2} \cdot \frac{E_c}{\dfrac{1}{A_{b+tb}} + \dfrac{1}{A_{floor}} + \dfrac{a^2}{I_{b+tb} + I_{floor}}} \tag{8-93}$$

Values of $F_{V,l}$ and $F_{V,r}$ in eq. (8-90) can be determined, in case of symmetrical cross-section, according to eq. (8-84) in which 0,25 replaces 0,5.

8.5.2.3 Estimation of shear stiffness

The basic relationship, according to CEB-FIP Model Code 90 [CEB-FIP (1992)] between shear stress τ and shear slip s, for connections with rough interfaces (Fig. 8-32) can be adopted for the estimation of design values of the shear stiffness K_s. The maximum value of the shear displacement has been assumed to s_u = 2 mm. The τ-s relationship can be simplified to a bilinear curve (Fig. 8-68 a).

The reliable connection characteristic along the horizontal interface can be determined respectively to the maximum shear force $F'_{v,max,d}$, which is calculated by means of

$$F'_{v,max,d} = F'_{v,max} - cf_{ctd} b_j - \mu \sigma_c b_j \tag{8-94}$$

where $F'_{V,max}$ can be found according to eq. (8-81)
σ_{cc} = compressive stress acting across the interface

The shear stiffness K_s can be determined as

$$K_s = 5000 \rho \mu f_{yk} b_j \qquad \text{when} \qquad \frac{F'_{v,max,d}}{\rho \mu f_{yd} b_j} \le 0{,}5 \tag{8-95}$$

$$K_s = 500 \rho \mu f_{yk} b_j \qquad \text{when} \qquad \frac{F'_{v,max,d}}{\rho \mu f_{yd} b_j} \ge 0{,}5 \tag{8-96}$$

where ρ = reinforcement ratio, see Section 8.4.3
μ = friction coefficient, see Section 8.4.3
f_{yk} = yield strength of the tie bars, characteristic value

It should be noted that the shear stiffness is 10 times smaller in cases where the tie reinforcement is insufficient to keep the composite cross-section homogenous.

The shear stiffness of the connection at the vertical interface (Fig. 8-68 c) can be calculated with allowance for reduction due to possible opening u_h (Fig. 8-68 b) of the cracks along the vertical interfaces, imposed by the support rotation of the floor slabs. The eqs. (8-95) and (8-96) change into:

$$K_{sv} = \frac{1}{0{,}0002 + u_h} \rho_v \mu f_{yk} b_{jv} \qquad \text{when} \qquad \frac{F'_{v,max,d}}{\rho_v \mu f_{yd} b_{jv}} \le 0{,}5 \tag{8-97}$$

$$K_{sv} = \frac{1}{0{,}002 + u_h} \rho_v \mu f_{yk} b_{jv} \qquad \text{when} \qquad 0{,}5 \le \frac{F'_{v,max,d}}{\rho_v \mu f_{yd} b_{jv}} \le 1{,}0 \tag{8-98}$$

where $F'_{v,max,d} \approx F'_{v,max,l,d}$ or $\approx F'_{v,max,r,d}$
ρ_v = ratio of reinforcement projecting through the vertical interfaces
b_{jv} = height of vertical shear interface as defined in Fig. 8-68 b

The values of $F'_{v,max,d}$ can be determined according to eq. (8-80) provided that

$$\frac{F_{cj,l}}{F_c} = \frac{b_{eff,l} \cdot h_{eq.}}{A_c} \qquad \text{or} \qquad \frac{F_{cj,l}}{F_c} = \frac{b_{eff,r} \cdot h_{eq.}}{A_c} \tag{8-99}$$

where $b_{eff,l}$ = effective widths of interacting floor part, left side
$b_{eff,r}$ = effective widths of interacting floor part, right side
h_{eq} = equivalent height of floor cross-section, see Fig. 8-68
A_c = area of the cross-section being compressed in a homogeneous model

8.5.2.4 Design of transverse steel

The design shear resistance τ_{Rdj} at the horizontal interface can be determined by the general expression given in eq. (8-61) according to Eurocode 2 [CEN (2004)], see Section 8.4.3.

Interface shear reinforcement, see Fig. 8-66 b, is required in areas where the design shear stress exceeds the resistance without the pullout resistance from transverse steel, i.e. when

$$\tau_{Edj} > c\, f_{ctd} + \mu\, \sigma_n \tag{8-100}$$

For simplicity reasons the value of maximum shear stress τ_{Edj} can be determined according to eq. (8-80), i.e. ignoring a certain reduction resulting from the shear deformability along the interface, see Section 8.5.2.2.

The reinforcement should have a total area and a distribution along the member axis approximately corresponding to the variation of the net shear stress. A distribution of the shear reinforcement corresponding to the diagram in Fig. 8-70 is acceptable. The net shear stress is determined as

$$\tau_{Edj,net} = \tau_{Edj} - (c\, f_{ctd} + \mu\, \sigma_n) \tag{8-101}$$

More conservative recommendations concerning the design of shear reinforcement are given in British Standard BS 8110 [BSI (1985)] according to which, if the case expressed by eq. (8-100) takes place, the reinforcement should be designed to transfer the entire shear force, found according to eq. (8-80).

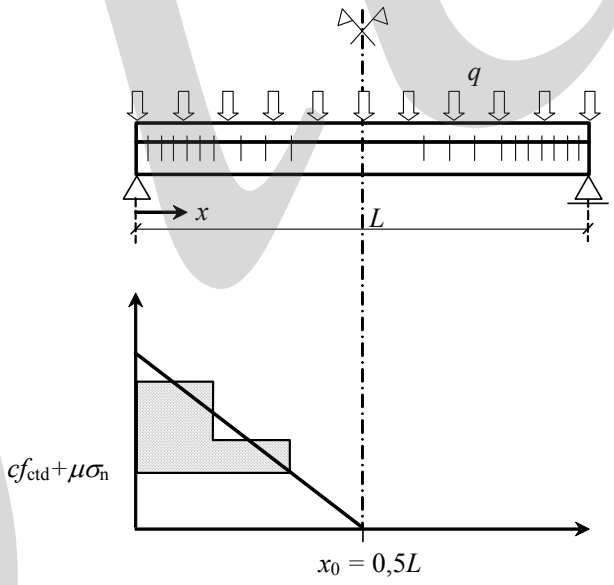

Fig. 8-70: Design of shear reinforcement across the horizontal interface

The next step in design is the decision, either to accept a shear stiffness K_s which is less than the minimum value $K_{s,min}$, or to increase the amount of shear reinforcement such that the minimum value is exceeded. It should be noted that an increase of the shear reinforcement ratio (even very slight) may be very favourable, since the shear stiffness can be determined by eq. (8-95) instead of the much

smaller value according to eq. (8-96). This means that the shear stiffness is increased 10 times. This recommendation does not meet commonly applied practice and the recommendations of Eurocode 2, in which the shear stiffness of a connection is uncontrolled.

The shear reinforcement can be arranged as projecting loops or dowels well anchored in the cast *insitu* part of the composite beam, see Fig. 8-66 b. In case of a structural topping it is recommended to connect the loops with the reinforcement mesh, see Fig. 8-71. It is not satisfactory to provide loops in the top of inverted T-beams, if the cast *insitu* layer is too small, see Fig. 8.72.

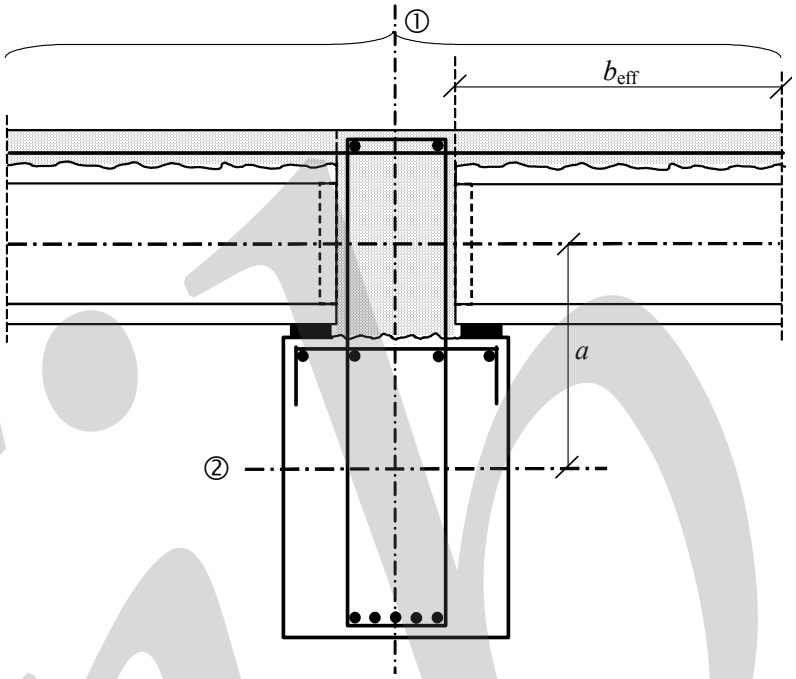

Fig. 8-71: Shear reinforcement anchored in structural topping

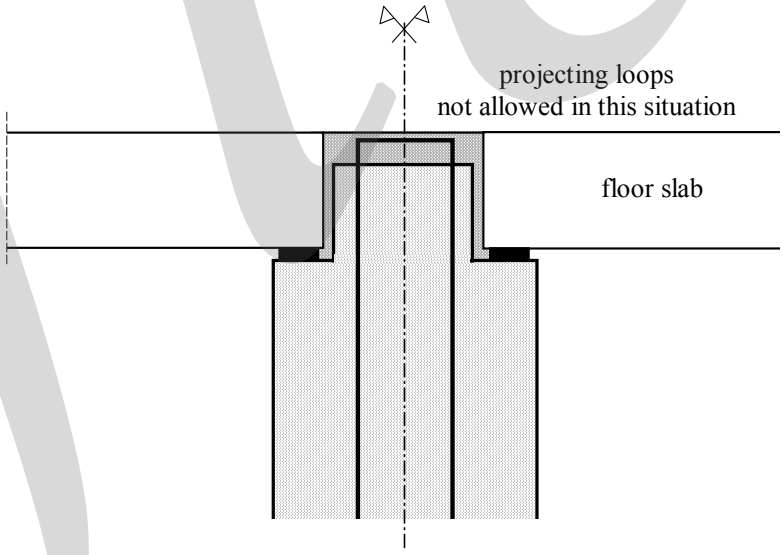

Fig. 8-72: Projecting loops from inverted T-beams cannot be anchored satisfactory, if the cast insitu layer is too small

8.5.2.5 Composite beam with hollow core floor units

In the case when the neutral axis of the composite beam cross-section (assumed as homogenous structure) lies below the bottom surface of the floor (Fig. 8-66 b), the full effective width can be considered provided also the full height h of the floor section. The advantage of floor interaction is preconditioned however, by a shear stiffness K_{sv} greater than the minimum value $K_{sv,min}$, eq. (8-93). If the shear stiffness is less than the minimum value, the lower part of the floor section should be ignored in design according to eq. (8-80) as it is shown in Fig. 8-73 a.

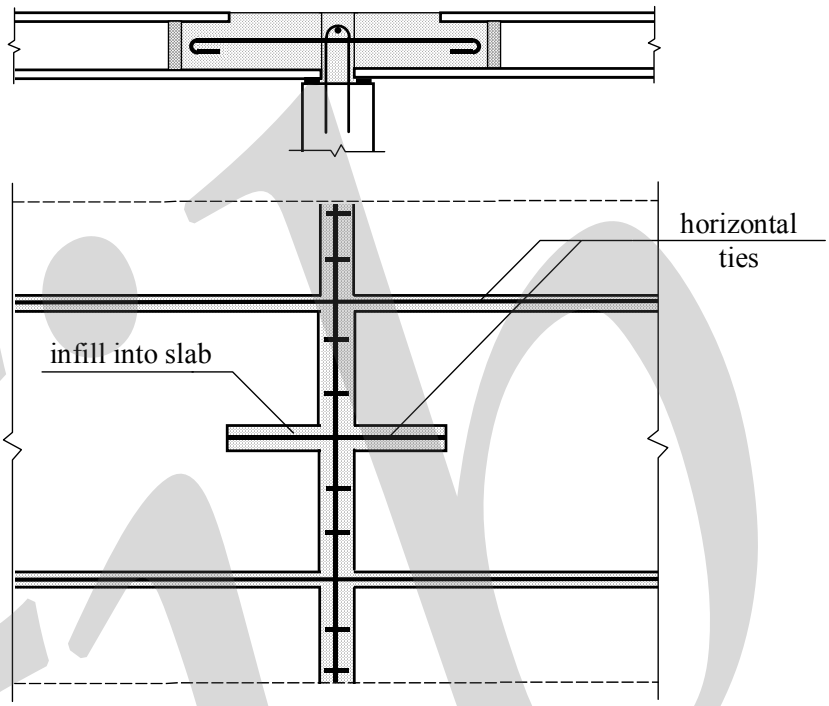

Fig. 8-73: Composite beam with precast hollow core floors, a) cross-section, b) arrangement of horizontal ties

Arrangement of the shear reinforcement across the vertical shear interfaces is shown in Fig. 8-73 b, where projecting bars are placed into the floor, either into opened cores or in joints between the hollow core units.

In the case when the neutral axis of the composite beam cross-section lies within the height of the floor section (Fig. 8-74), the lower part of the floor should be ignored in design. The shear transfer mechanism becomes more complex in this case. This is particularly the case with inverted T-beams. It may happen then that the horizontal interface disappears totally and the composite section is subdivided in two parts like in Fig. 8-74.

Based on the results of full-scale tests [Pajari (1995)] the following reduced value $b_{eff,d}$ of the effective width of were recommended for design [FIP (1998)].

$$b_{eff,d} = b_{eff,ref}\,\frac{L}{5} \tag{8-102}$$

where $b_{eff,ref}$ = reference value corresponding to the effective width for a beam with a span of 5 m, see Table 8-7

L = span of simply supported beam in m

h [mm]	Voids circular	non-circular	$b_{eff,ref}$ [mm]
200	x		150
265	x		185
320		x	270
400		x	400

Table 8-7: Values of $b_{eff,ref}$ in mm upon the floor heights h mm according to Pajari (1995)

The tests of Pajari showed that the floor units themselves did not participate in the transfer of the bending moment, even those with the highest investigated depth equal to h = 400 mm. It means that the component M_{floor} according to eq. (8-84) was not observed.

8.5.2.6 Other cases of composite beams

(1) Beams bearing double-T floor units

Composite beam design is usually not carried out where double-T floor units with a relatively thin screed are used [Elliott (1996)]. However, the position of the centroid of the composite section lies below the flange, even if the beam has inverted T-profile as shown in Fig. 8-75. It means that the flange of the slab together with the structural screed can potentially interact in the composite beam. By means of the formulas given in Section 8.5.2.2 the effectiveness of the interaction mechanism can be checked. The shear stiffness of the horizontal interface connection on the top of the beam may be assumed to be infinitively high. The shear stiffness of the connection at the vertical interfaces, shown in Fig. 8-75, should be, on the contrary, determined as for a cracked medium. Because of possible rotations of the slab ends at the support, this stiffness should be even more reduced.

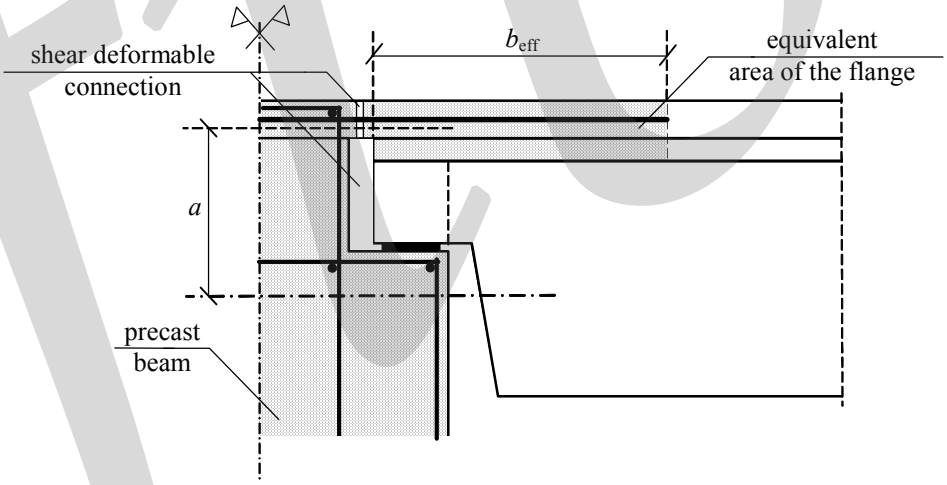

Fig. 8-75: Beam bearing the double-T floors – equivalent dimensions for the check of composite action of the structure

Eqs. (8-84) and (8-85) can be combined into the following expression

$$\frac{\psi}{\alpha^2} = \frac{1}{\left(1+\frac{A_2}{A_1}\right)\frac{I_1+I_2}{A_2 a}+a} \tag{8-102}$$

The area A_1 of half the beam cross-section is well defined. The area A_2 (cross section of the flange) can, because of the lack of experimental data, be estimated approximately as for an equivalent width $b_{\text{eff}} = 0{,}1L$ (Fig. 8-72). Even smaller value of $F_{\text{v,max}}$ can contribute effectively to resist the bending moment M, because the distance a is relatively big in case of double-T units.

The reinforcement bars, which help to transfer the force F'_{v}, should be designed for the simultaneous action of the tensile force, if the beam and the adjacent structure take a negative moment from the floor.

(2) Beam bearing solid plates of floor plate floors

Very good conditions can be established in order to ensure composite action of beams with solid plates or) floor plate floors. Similarly like in the former presented cases the horizontal connection can be assumed to be infinitively stiff, whereas the shear deformability of the vertical connections should be taken into account in order to design the whole structure as a composite one.

(3) Interface shear in edge beams

The horizontal shear stresses at an interface between floor slabs and an edge beam can be generated not only due to flexure but also due to asymmetrical floor loads, according to Elliott (1996). In case of beams with higher upstands, the frame may participate in the transfer of loads to which the building is subjected later, and then additional shear stresses along the interfaces occur.

9 Transfer of bending and torsional moment

9.1 Basic considerations in design of moment resisting connections

This chapter is concerned with the design and construction of moment-resisting connections, and of their influence on the behaviour of precast concrete structures. The positions where moment resisting connections may be used, or where they should be avoided, are identified. The effects on frame stability and structural integrity are assessed.

Moment resisting frames and cores incorporating precast elements may be used to resist horizontal wind or seismic loading. Connections are placed in critical regions and the approach is to use strong connections possessing stiffness, strength and ductility approaching that of cast *insitu* construction. Moment connection can lead to significant economies in certain situations, e.g. the size of precast columns in portal sway frames connected at the eaves is directly related to the stiffness of the moment resisting connections there.

Moment resisting connections are used mainly to:

- stabilise and increase stiffness of portal and skeletal frames, see Section 2.3.3,
- reduce the depth of flexural frame members,
- distribute second order moments in to beams and slabs, and hence reduce column moments,
- improve the resistance to progressive collapse.

For moment resisting connections used in seismic design reference is made to fib (2003b).

Fig. 9-1: Moment resisting perimeter frame (Courtesy BFT Journal)

One of the most important factors in this respect is to ensure that the safety of the connection is not jeopardised by faulty workmanship on site, and that site operations are as simple as possible, sufficient to ensure the safety of the components being fixed. In all cases the important operations should be carried out in the factory where quality control is assured. The role of full scale testing should not be dismissed as a method of design, particularly where composite action between interacting components may lead to complex force fields and stress redistribution.

Moment resisting connections are used primarily in column foundations, column splices and at beam-column connections. Common methods to achieve moment resisting connections are grouting of projecting reinforcement, and bolting or welding of anchored steel details. These methods can be used

in various combinations in one connection. The connection should be designed so that the rigidity is maintained for all loading conditions. This is particularly important where a small quantity of cast *insitu* or infill grout is placed adjoining precast concrete cast surfaces. Some guidance is given later in this chapter on surface preparation.

Moment resisting connections should be proportioned such that ductile failures will occur and that the limiting strength of the connection is not governed by shear friction, short lengths of weld, plates embedded in thin sections, or other similar details which may lead to brittleness. Many of the principles behind these requirements have evolved through years of seismic R & D, and the common practice in the U.S., Japan and New Zealand is often to design and construct moment-resisting connections in the perimeter of the frame, where there are less size restrictions on beams and columns. Moment resisting portal frames, such as the multi-legged U-frames shown in Fig. 9-1 may be used to provide peripheral framework to what is otherwise a pinned-jointed structure. Deep spandrel beams with ample space for this purpose are specified as moment resisting frames, whilst the interior frames connections are all pinned-jointed shallow beams.

Fig. 9-2 shows how precast U-beams may be used to form moment connections by making the trough continuously reinforced across the column line. A similar approach is made using post tensioning in the trough of a precast inverted-tee beam as indicated in Figs. 9-3 and 9-4. In these cases the connections are designed as pinned-jointed for self weight loads, and moment resisting for imposed floor and horizontal loads. The sagging bending moments induced by horizontal sway loads are, by comparison, smaller than the hogging moments caused by gravity loads, but they still must be considered in the design.

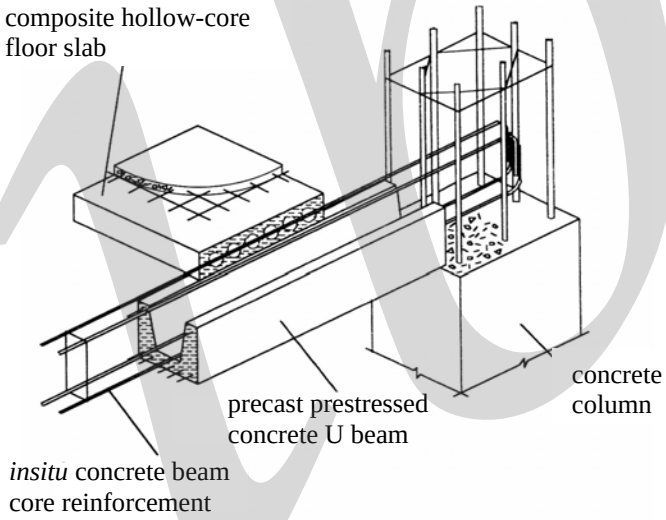

Fig. 9-2: Mixed precast and insitu concrete used to form moment resisting connections (Courtesy New Zealand Concrete Society)

The following sections present guidance on the design and construction of moment resisting connections. The main design criteria are:

- strength,
- stiffness,
- ductility and a ductile failure mode,
- ease of construction.

If moment resisting connections are to be used purposefully, either in reducing sagging moments in beams, or increasing the global strength and stiffness in frames, moment capacities of at least 50 to 100 kNm are usually required. If the moment capacity is less than this, then it is probably better to design the connection as pinned-jointed. In order to avoid localised stress concentrations in the connection, a lever arm of about 150 mm to 250 mm is required between the compressive and tensile forces, which generate the moment. Moment capacities in the region of 200 to 400 kNm (or greater) may be required at column foundations, for example in sway and portal frames.

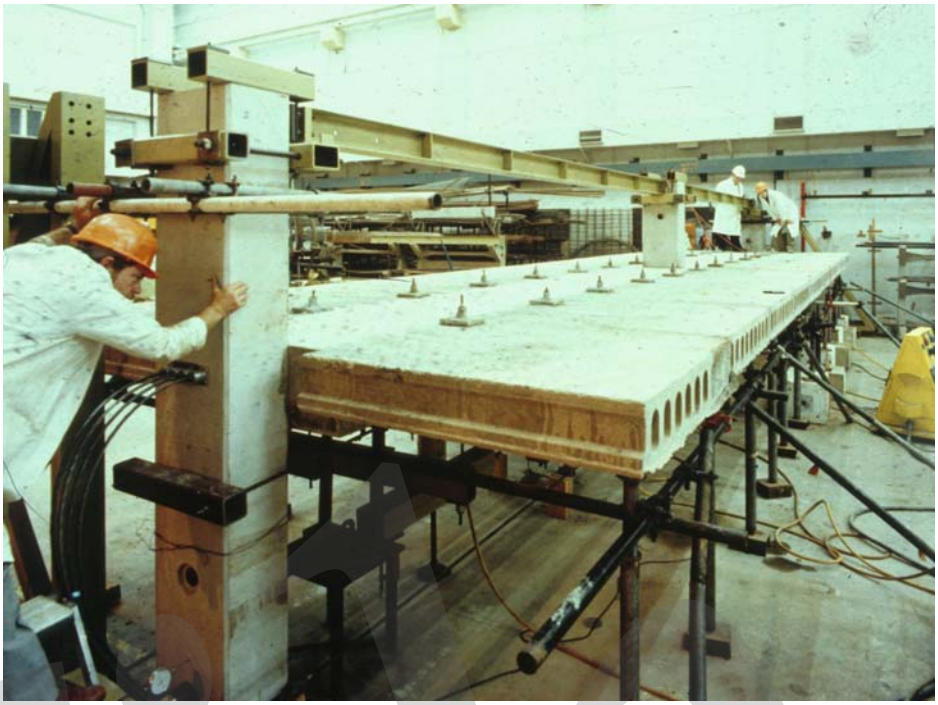

Fig. 9-3: Full-scale tests demonstrated that post-tensioned inverted-tee beams provide negative moment continuity at columns

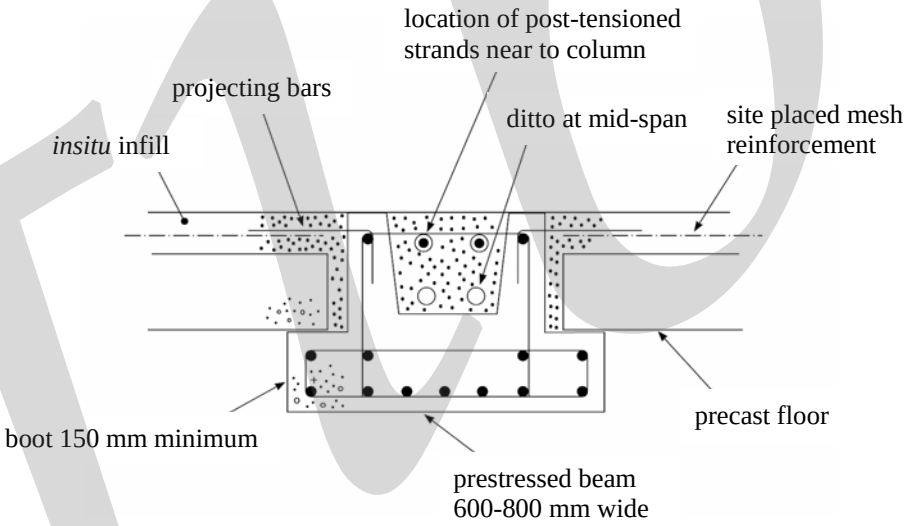

Fig. 9-4: Post tensioning of prestressed inverted-tee beams increases sagging moment capacity as well as providing negative moment continuity at columns

The methods used to achieve this involve one or more of the following methods:

- Grouting to projecting rebars, or steel sections, Fig. 9-5 a. The grout may contain small coarse aggregates and additives.
- Bolting between steel sections, plates etc., Fig. 9-5 b. The bolts may be friction bolts if shear forces are present. *Saw-tooth* plate washers may achieve similar means.
- Threaded bars to couplers, cast-in sockets, or to nuts and plate washers, Fig. 9-5 c. The bars may be threaded rebars, threaded *bright drawn* or *black* dowels, or long length bolts (e.g. holding down bolts).
- Welding to steel sections, plates, rebars etc., Fig. 9-5 c.

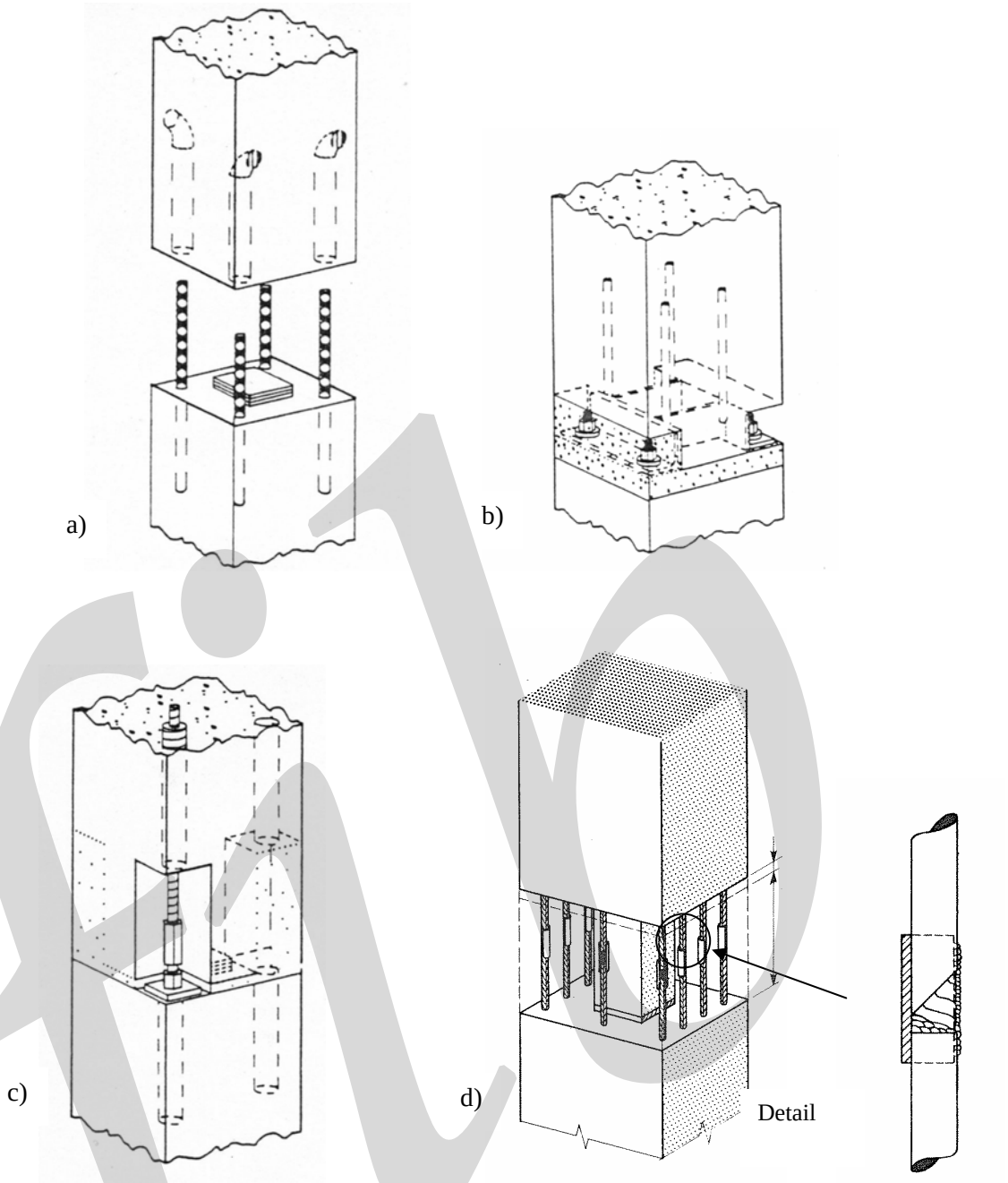

Fig. 9-5 Examples of connection methods, a) grouted sleeve – projecting rebar connection, b) bolted connection, c) threaded coupler connection, d) welded connection. Comments on various connection methods are given in Table 9-1. Courtesy 'PCI Design Manual on Connections' (Figs. 9-5 a – c), Stupre report 'Structural Connections' (Fig. 9-5 d)

The choice of connection system should be compatible with the design of the structural system, and be consistent throughout the building. In an ideal situation only one connection method should be used in a building. However the most common situation is where one method is used to make vertical connections and another different method is used to make horizontal connections. Table 9-1 gives guidance on this subject.

In all cases the effects of internal movements must be considered, for reasons such as thermal expansion/contraction, creep, shrinkage, imposed elastic deformation. The forces that are resisting bending moments should also be capable of being generated in the precast components in combination with other forces such as end shear.

Connection identification	On site jointing action	Advantages	Disadvantages	Approximate max. moment capacity*
Column base plate	Bolted	Immediate column stability.	High accuracy in setting bolt position. Cost of bolts	400 kNm
Column pocket	Grouted	Low cost of foundation and column. No additions to column	Temporary propping required	250 kNm
Column grouted sleeve	Grouted	Low cost of foundation. Easy to construct	Accuracy in projecting rebar positions. Temporary propping required	150 kNm
Coupled column splice	Coupler	Immediate column stability.	Expensive. Difficult to construct	100 kNm
Welded plate column splice	Bolted	Immediate column stability. Easy to construct	Expensive	50 kNm
Grouted sleeve column splice	Grouted	Low cost. Easy to construct	Accuracy in projecting rebar positions. Temporary propping required	100 kNm
Grouted sleeve coupler splice	Grouted	Easy to construct. Splice length short	Expensive. Temporary propping required. Pressure grouting	100 kNm
Steel shoe column splice	Bolted	Immediate column stability. Easy to construct. Grout quantity small	Expensive	175 kNm
Welded plate beam connector	Welded	Immediate fixity. Large tolerances	Site weld inspection. Large volume of grout	300 kNm **
Steel billet beam connector	Bolted	Immediate fixity. Easy to fix. Grout quantity small	Tolerances	200 kNm **
Bolted plate beam connector	Bolted	Immediate fixity. Grout quantity small	Expensive. Relatively difficult to fix. Tolerances	250 kNm **
Portal frame eaves connection	Bolted	Inexpensive. No grouting.	Tolerances	150 kNm
Wall to floor connection	Grouted	Inexpensive. Large tolerances. Grout quantity small	Wet bedding and temporary propping required.	50 kNm/m

* based on members up to about 400 x 400 mm in cross section. ** includes 200 mm deep floor slab and ties.

Table 9-1: Guidance on choice of method for moment resisting connections

Connection capacity is derived from accepted, codified, load transfer mechanisms and conditions of equilibrium. Strength reduction factors are developed either from experimental evidence or knowledge of strain compatibility, particularly where several precast components are involved. The main reason for this is the force limitations and slippage between certain parts of the connection. Other reduction factors are due to local deformations at precast-*insitu* concrete interfaces, and large strain gradients across thin sections. Many of the equations presented below have been derived empirically using full or model scale experimental data. A brief commentary on moment resisting connections is given by Elliott (1996) and Elliott (2002).

Moment resisting connections may be formed at the following locations:
- beam-column connections, Section 9.3
- column splices, Section 9.4
- column-base connections, Section 9.5
- floor connections, Section 9.6

Beam-to-beam moment resisting connections are not used in order to avoid torsion in the receiving beam. Edge beam-to-floor slab moment resisting connections are treated in Section 9.7.

The large flexibilities of many prestressed floor slabs, e.g. hollow core and double-tee slabs which have low stiffness-to-strength ratios, cause significant end rotations at the connection, and these are better left as pinned-joints.

9.2 Various types of moment resisting connections

A connection can be designed to transfer bending moment by means of a force couple of tensile and compressive forces, see Fig. 9-6. Reinforcement bars, bolts or other steel components with tensile capacity are arranged and anchored in such a way that an internal force couple can be developed when the connection is subjected to imposed rotation. On the opposite side of the connection, transfer of the corresponding compressive force through the joint must be ensured. (In such connections various regions, parts and components will be subjected to compression and tension and Chapters 6 and 7 are applicable for the behaviour and design of the individual parts.). Full scale testing by Ferriera *et al.* (2003), Fig 9.7 has shown that the negative moment capacity of precast concrete beams made continuous with high tensile rebars placed in topping is at least 85% of the moment of resistance of a fully monolithic connection.

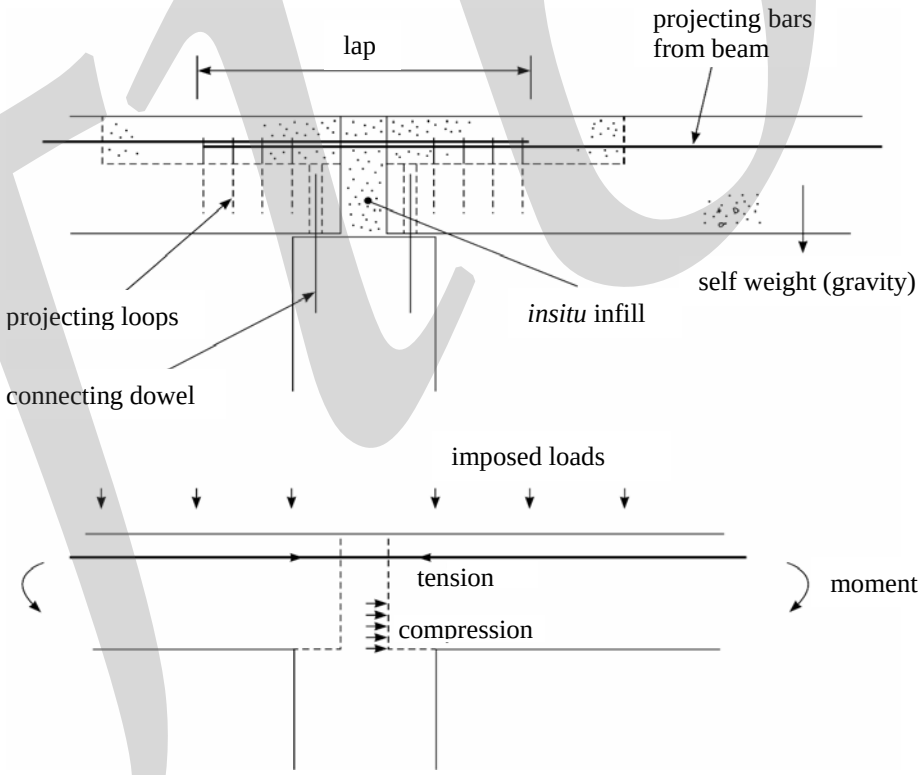

Fig. 9-6: Principle of moment resisting connections in precast frames. Moment continuity exists only for imposed loads after the insitu infill has matured to full strength

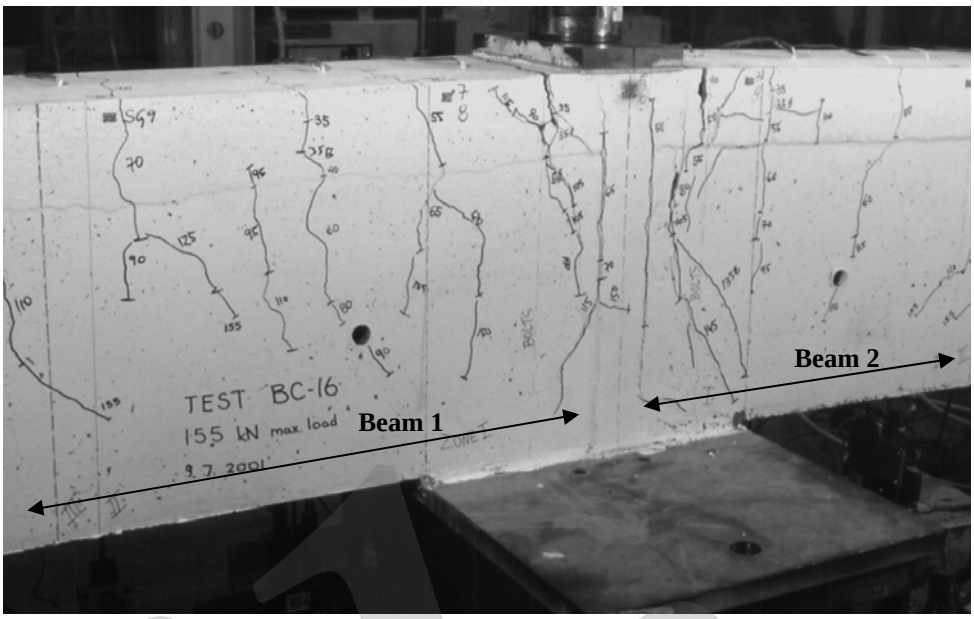

Fig. 9-7: Full scale testing of support continuity between precast concrete beams with reinforced insitu topping, Ferreira (2002)

The magnitude of the transferred moment depends on the magnitude of the tensile and compressive resultants at the actual rotation and the internal lever arm as

$$M_R = F_t \cdot z = F_c \cdot z \tag{9-1}$$

where F_t = actual tensile force
F_c = actual compressive force
z = actual internal lever arm

The tensile capacity of the tensile components as well as the strength of the compressed region of the connection can determine the flexural resistance M_R of the connection in bending.

Alternatively, a moment capacity can be achieved by force couples of compressive and/or shear forces. A common example of this is the pocket type of column-base connection, as shown in Fig. 9-8, where the bending moment at the column base is resisted by a force couple of horizontal compressive forces in the foundation pocket. Under certain conditions it would also be possible to add the effect of vertical shear forces (force couple) acting along the compressed parts of the vertical joint interfaces.

When a connection in a floor is activated after the erection of the floor, it will give continuity only for that part of the load that is added after erection, and, if the bending moment capacity is limited, only for a part of this additive load, see Fig. 9-9. Cases with partial continuity will require certain consideration in design, since standard methods are not applicable.

A certain moment capacity can be obtained as a secondary effect. Typical examples are connections in floor slabs. The floor elements are designed to be simply supported, but, due to requirements of minimum tensile capacity within floors and between floors and their supports, a certain amount of tie bars is provided. Together with the jointing with grouts and cast *insitu* concrete, the tie connections will attain a certain bending moment capacity that was not aimed at by purpose. The moment capacity depends on the position of the tie bars in relation to the sign of the acting moment. This secondary moment capacity can be favourable in case of accidental situations, since it provides ductility and facilitates force redistribution.

However, such a secondary bending moment capacity could also have an unfavourable effect, because of the restraint that it causes. A floor element that is designed to be simply supported could be subjected to a negative moment that it is not prepared for, due to unintended restraint at the supports. As a result, flexural cracks could appear in positions where they could be dangerous with regard to the load-carrying capacity of the elements, see Section 3.5.2.

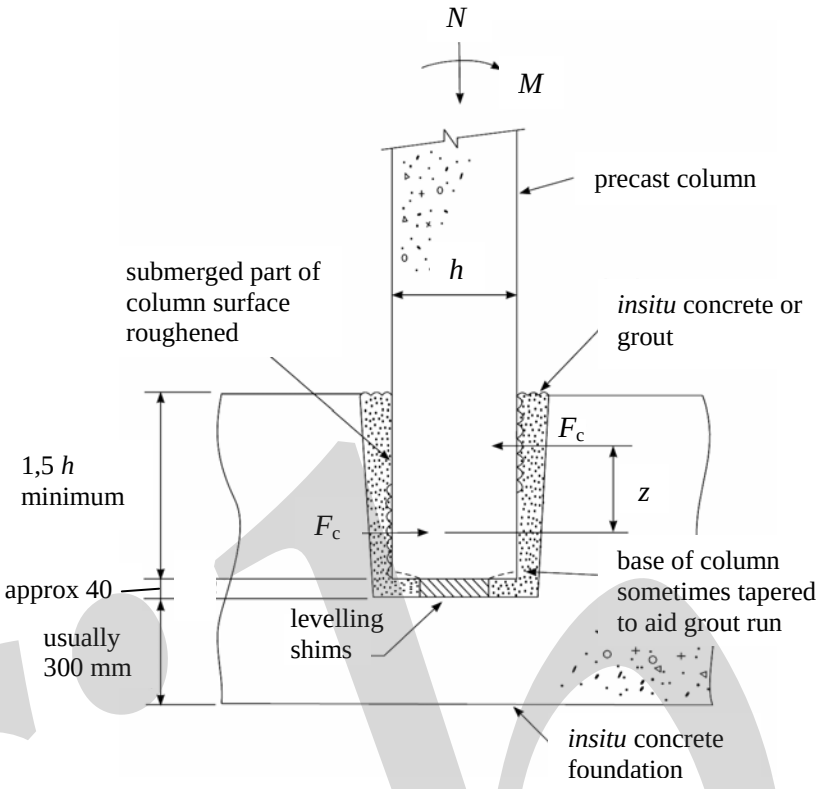

Fig. 9-8: Connections for transfer of bending moment at a column foundation pocket

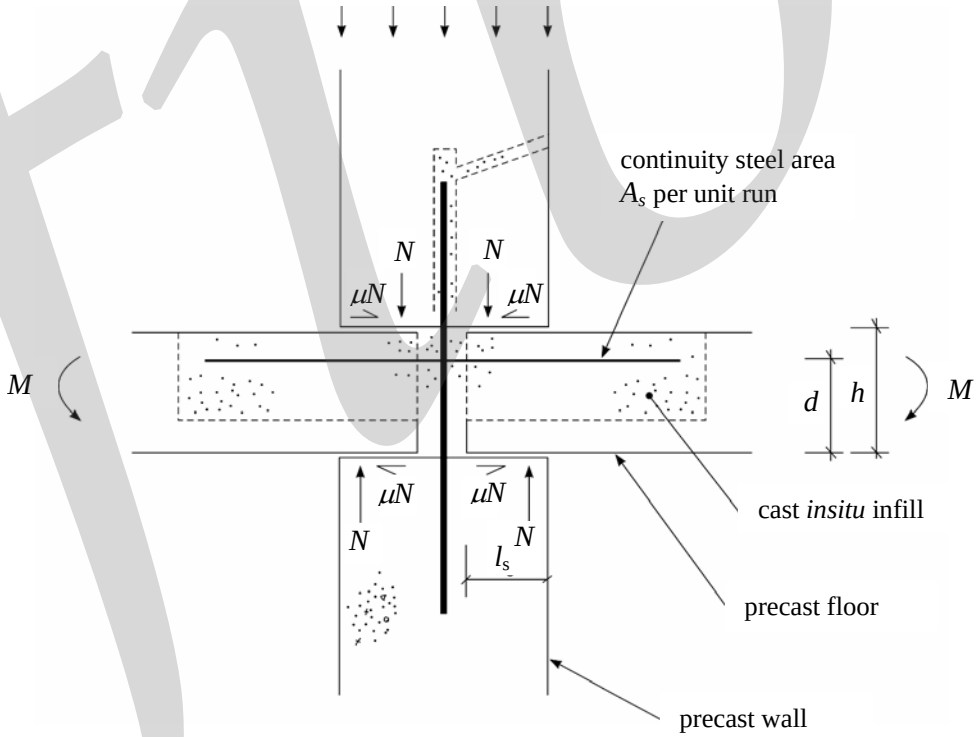

Fig. 9-9: Typical example of floor-wall-floor connection designed to have full or partial capacity for moment in the floor

The mechanical behaviour can vary considerably depending on how the connection is designed. For this reason it is essential to distinguish the following two extreme cases.

In a connection where the joint sections, with regard to their bending moment capacity, are weak in relation to the adjoining elements, the imposed rotation θ will concentrate to such a section, see Fig. 9-10 a. This is typical for connections that are not designed to be moment-resisting, but where single tie bars are placed across the joint. In such connections the ultimate rotation θ_u will be determined by the elongation capacity or the anchorage of the tie bars. The compressive side of the connection will not be influenced in a critical way.

However, in a connection that has a significant moment capacity, which is of the same order as that of the adjoining elements, a high bending moment will result in flexural deformations that are spread in the whole connection region, including the connection zones of the elements. In the ultimate state plastic deformations can be expected in the whole connection regions, see Fig. 9-10 b. The rotation θ of the connection depends mainly on the curvature distribution within the plastic region and its extension. The ultimate tensile strain in the steel as well as the ultimate compressive strain in the concrete can limit the ultimate rotation θ_u.

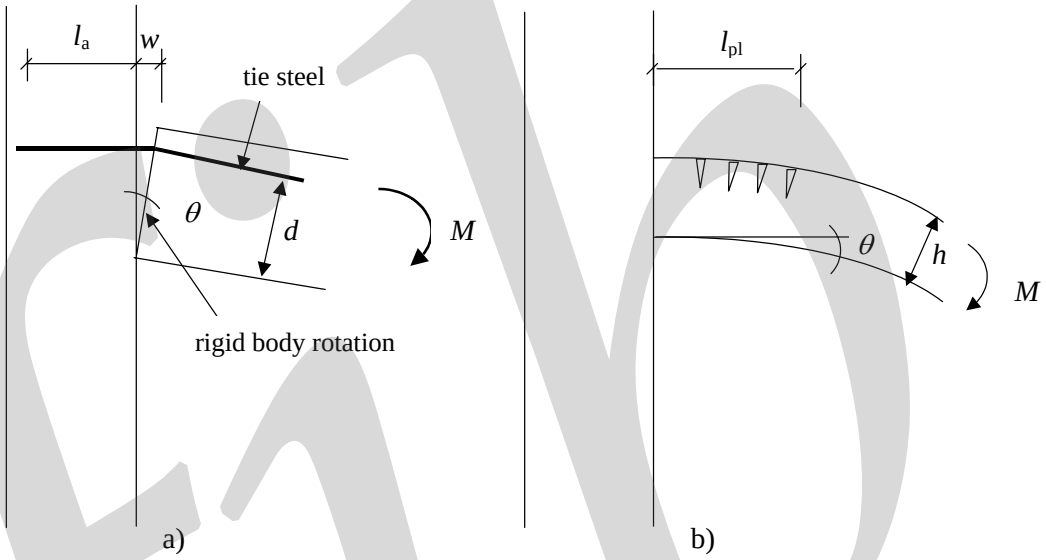

Fig. 9-10: Extreme cases with regard to the mechanical behaviour, a) connection provided with single tie bars only and where the rotation concentrates at the weak joint section, b) connection with a moment resistance that is about the same as in the elements and where the flexural deformations are spread in the whole connection region

Example 9-1

In the analysis of tests on hollow core floors [Broo *et al.* (2004)] it was found that the support connection at the end support gave a certain rotational restraint. The floor was fixed to a cast *insitu* tie beam, which in turn was tied by reinforcement bars to a rigid support beam, see Fig. 9-11. The response of the hollow core floor was modelled by non-linear FE analyses. When assuming that the floor was simply supported, the predicted response was too stiff compared to the observed. Hence, it was assumed that the end restraint needed to be considered in the analysis.

The cast *insitu* concrete filled the ends of the hollow cores to a certain distance from the end, which means that the connection between the tie beam and the floor was assumed to be rigid. However, the connection between the cast *insitu* tie beam and the support beam was much weaker and consequently it was assumed that the tie beam could rotate as a rigid body relative to the support beam, in a similar manner as shown in Fig. 9-10 a. Then the vertical reinforcement bars provide rotational restraint by their pullout resistance. Hence, the relation between moment and rotation at the end depends directly on the relation between tie force and crack opening. This relation was modelled as a non-linear spring according to the principles in Sections 7.2.3.1 and 7.4.1. When the so defined

non-linear spring was adopted into the FE analysis, there was a good agreement between the predicted and the observed responses.

Since the rotation was very small, it was sufficient to model the response of the connection before yielding of the bar. The bars were anchored on each side of the joint that opened. Therefore, the bars were treated as continuous tie bar, which was approximate because the anchored length was short. By means of eqs. (7-30) and (7-4) the non-linear spring was modelled as

$$w(\sigma_s) = 2 s_{end}(\sigma_s)$$

where $$s_{end}(\sigma_s) = 0{,}288\left(\frac{\phi \cdot \sigma_s^2}{\tau_{b,max} \cdot E_s}\right)^{0{,}714} + \frac{\sigma_s}{E_s} \cdot 2\phi$$

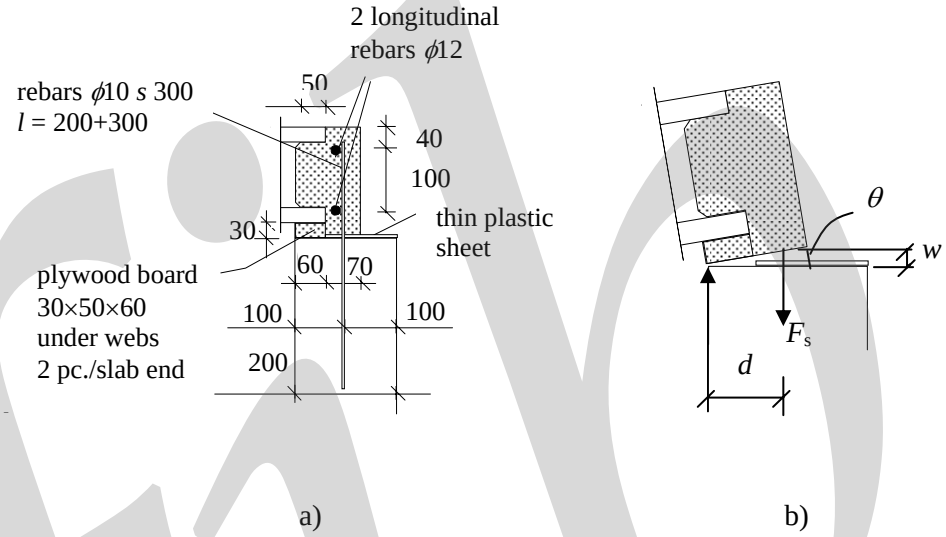

Fig. 9-11: Connection at the end support of hollow core floors analysed by Broo et al. (2004) a) detail of tested specimen, b) model. The end restraint was modelled assuming a stiff rotation between the transverse tie beam and the support beam with the vertical reinforcement bars acting as non-linear springs

9.3 Beam-column connections

There is a very wide range of beam-column connections, varying in complexity, cost and structural behaviour. Referring to Fig. 9-12 there is a major sub-division in that either:

- the vertical member is *continuous*, and horizontal components are framed into it. This is termed a "beam end" connection.
- the vertical member is *discontinuous* (only in construction terms) and the horizontal components are either structurally continuous or separate across the junction. This is termed a "column head" connection.

These two cases will be dealt with separately because of the differences in structural behaviour. Typical examples of internal moment resisting beam column connections are shown in Fig. 9-13. The connection in Fig. 9-13 a is of type I B (beam end to corbel on continuous column) and the connection in Fig. 9-13 b is of type II C (discontinuous column and separate beams). The figure also shows column splice and column base connections, both with grouted sleeve.

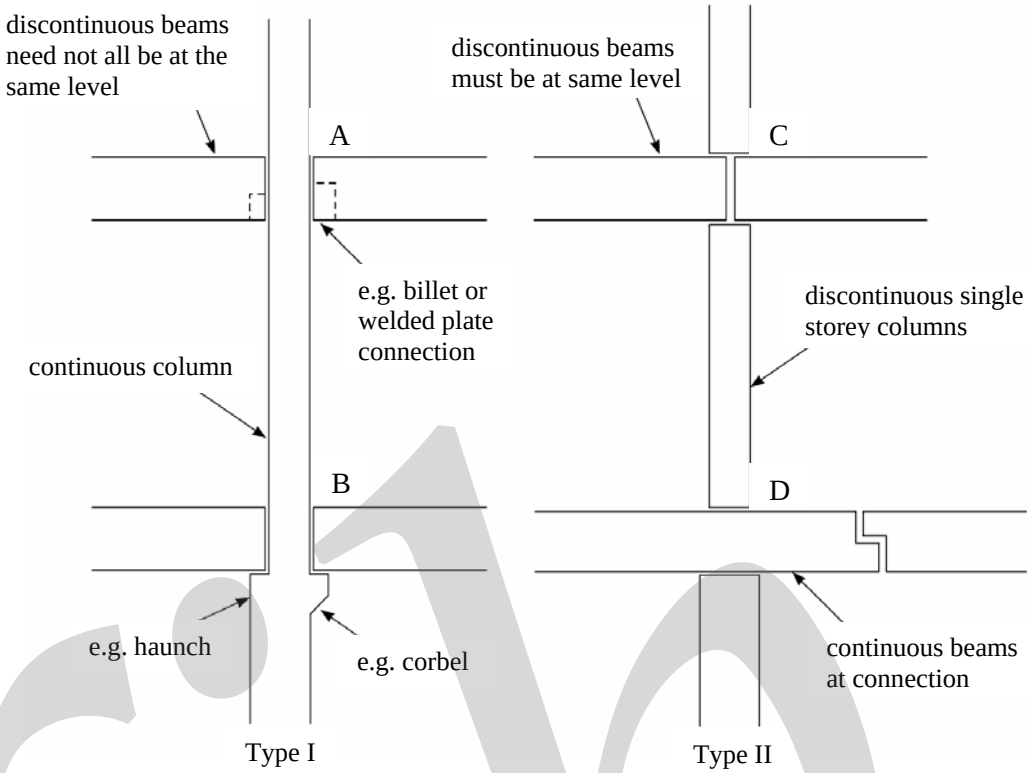

Fig. 9-12: Generic types of beam-column connections, A: beam end hidden connection to continuous column, B: beam end to column corbel, C: discontinuous beam and column, D: column to continuous beam

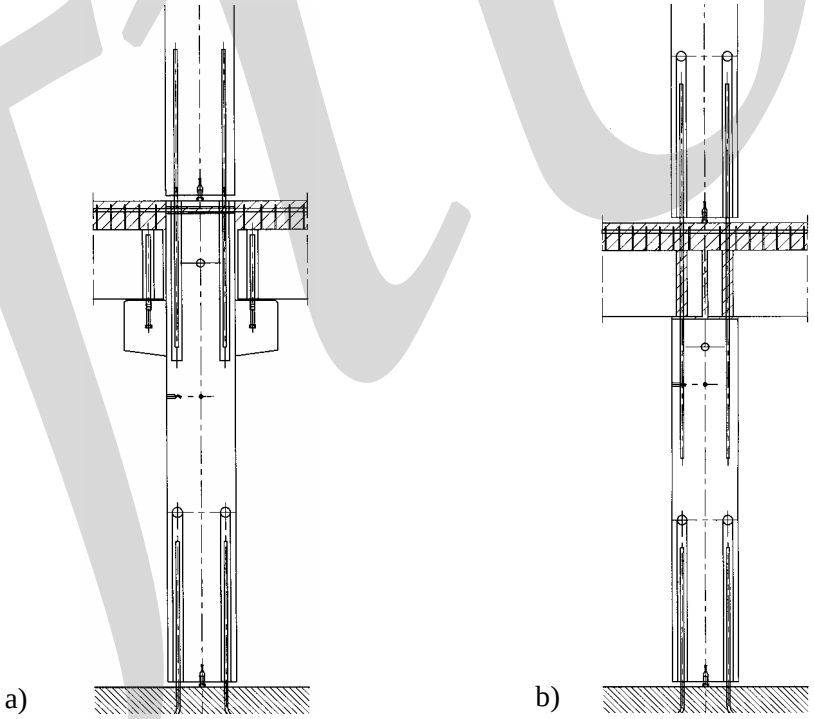

Fig. 9-13: Examples of internal moment resisting beam column connections, a) beam end connection to continuous column with corbels, b) beam to column head connection with discontinuous beam and column

9.3.1 Beam end connection to continuous column or wall

This type of connection has been the subject of a large number of experimental and analytical investigations [Martin and Korkosz (1982), Pillai *et al.* (1981), Park (1986), Stanton *et al.* (1987), Cheok and Lew (1990, 1993), Elliott *et al.* (1993a, 1997, 1998, 2003, 2004, 2005), Ferriera *et al.* (2003), Nakaki *et al. (*1994), Loo and Yao (1995), Englekirk (1995)]. In many cases connections that have been designed as pinned joints, have, following the introduction of the floor slab and stability tie steel, demonstrated considerable strength and stiffness. Although many such joints may be referred to as *semi-rigid*, in that the moments of resistance are accompanied by beam-to-column rotations, the stiffness is sufficiently large that the connection is effectively fully rigid. In many cases the rotational ductility of the connection is equal to or greater than the curvature capacity of the beams and columns.

The basic structural mechanism for beam end connections is shown in Fig. 9-14.

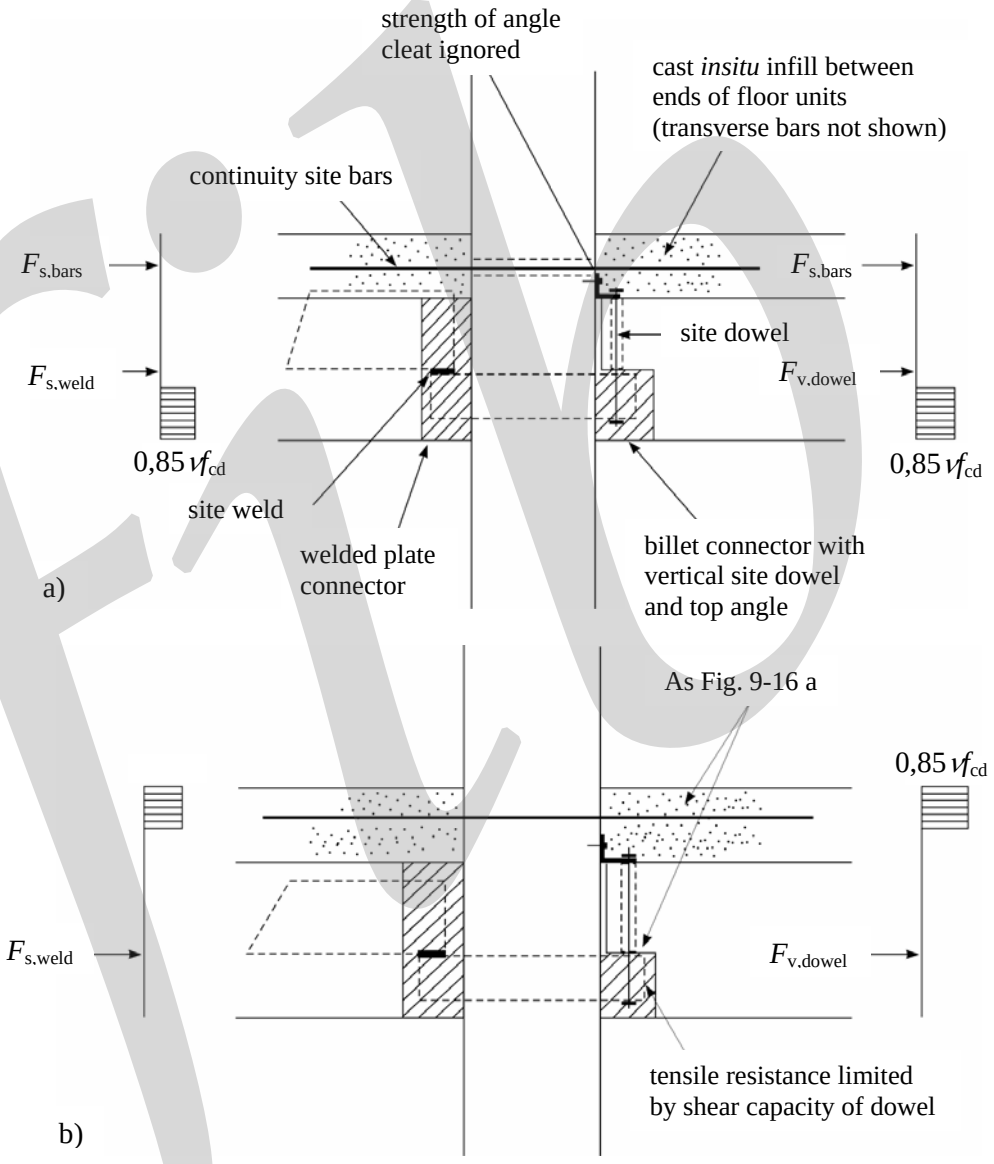

Fig. 9-14: Load transfer mechanism through beam end to column connection, a) hogging moment, b) sagging moment

Considering first a hogging moment the compression zone at the support on the right side of Fig. 9-14 a is concentrated in a contact region at the edge of the support, typically within $^1/_5$ of the depth of the beam/column interface. Here the shear force from the beam is combined with the vertical force couple resisting the support moment. This zone must be reinforced against horizontal splitting

using closed links at not more than 25 mm beneath the seating. A small steel plate, typically 150 x 150 x 12 mm in size, cast in to the column beneath the bearing is preferred to a highly reinforced region.

Sagging moments, Fig. 9-14 b, are less easy to deal with, particularly if uplift develops at the edge of the column. Continuity tie steel in the bottom of the beam must be fully anchored across the column. A bolted or welded detail is usually the only means of achieving this. Thus, connections are sometimes designed as pinned-jointed where sagging moments arise.

There are two major sub-divisions to this connection, namely:

- *in-plane*, where the tie steel runs parallel with the beam and the floor slab direction is perpendicular to the span of the beam, Fig. 9-14. In this case composite action between the floor slab and structural screed may be considered in the calculation.
- *out-of-plane*, where the slab is spanning perpendicular to the span of the beam in the same direction of the bending moment. Fig. 9-15 shows two alternative mechanisms for moment transfer – flexural moment between floor and beam, and torsional moment between beam and column.

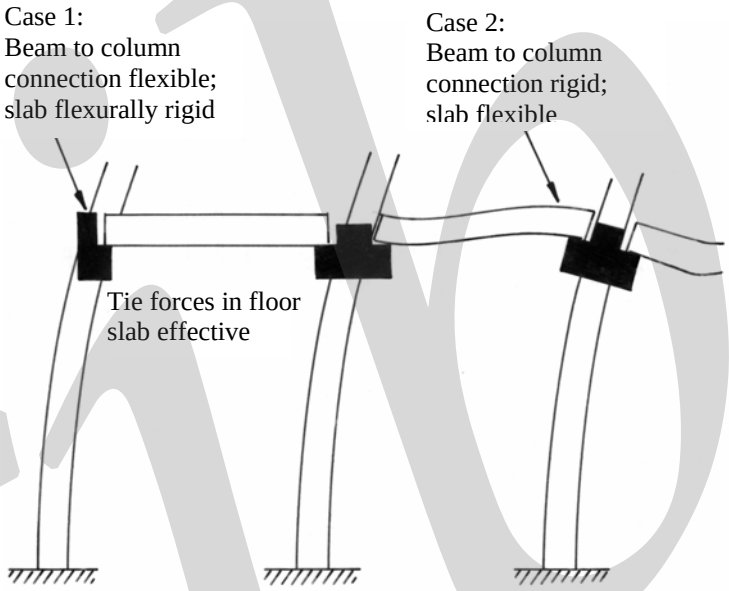

Fig. 9-15: Alternative methods for out-of-plane moment transfer

In the in-plane case, the tie steel must be fully anchored to the column, either by mechanical devices, such as threading into cast-in inserts, or by anchorage bonding through grouted sleeves etc. in the manner shown in Fig. 9-16. It is not sufficient to continue the tie steel around the column. Full scale testing [Elliott, *et al.* (1998)] has shown that the force in the tie steel is not fully mobilised, achieving only about 25 per cent of the yield value, and that the capacity of the connection is equal to that of the beam end connector.

The major types of moment resisting beam end connections and the results of experimental tests to determine the moment capacities are shown in Figs. 9-17 to 9-22. The most favourable situation is to design the connection to resist hogging moments only, and to class the sagging mode as pinned. In all but high sway load cases, the hogging moment resulting from gravity beam loads will dominate, and the connection may never experience sagging moments. The hogging moment of resistance for these connections is calculated as follows:

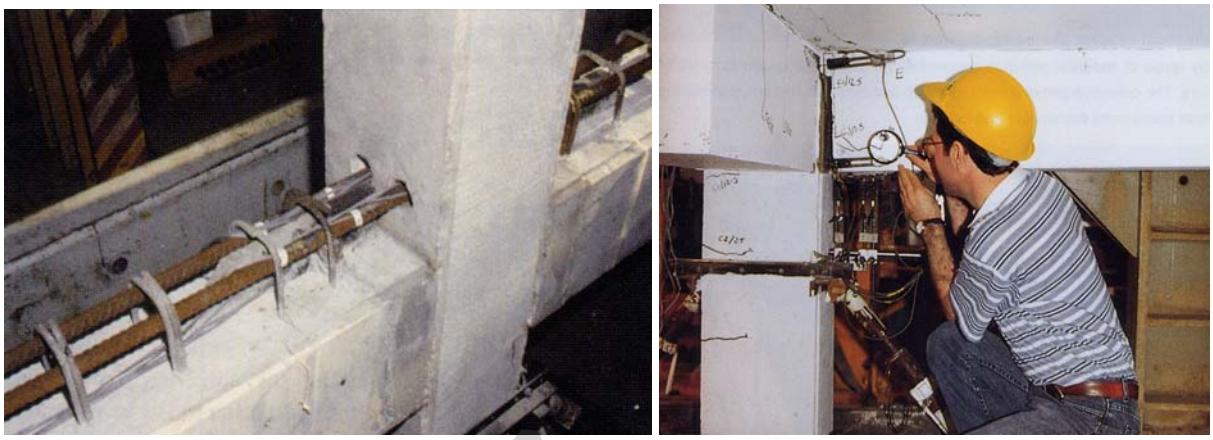

a) b)

Fig. 9-16: Beam end to column connection, a) continuity of tie steel passing through sleeves in columns, b) measurement of beam-column rotation provides the data to determine semi-rigidity of the connection.

9.3.1.1 Concrete corbel

Projecting dowels from the corbel seating are site grouted through location holes in the beams and can be additionally secured to a steel angle (or similar) at the top of the beam, see Fig. 9-17.

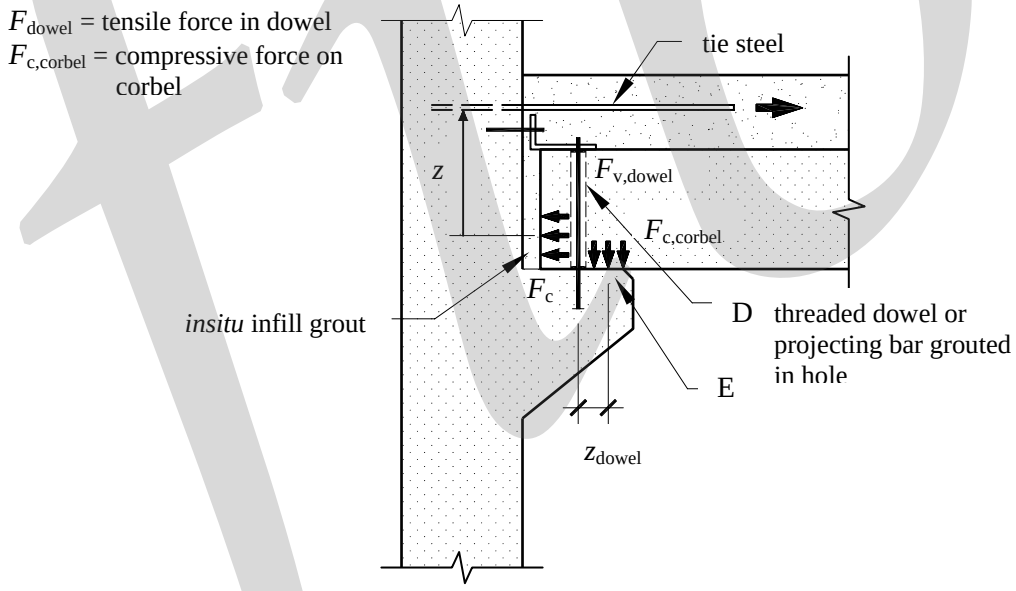

Fig. 9-17: Structural mechanism for the beam end connection with concrete corbel

The gap at the end of the beam, which should be at least 50 mm to ensure good compaction, is site grouted enabling full compressive strength to develop. Corbels are mainly used to resist hogging moments by providing fixity to the column near to, or at the top of the beam. This may be in the form of bolts into cast-in sockets, welded bars or plates, or a grouted lap joint. The latter is more suited to internal connections where the lap bars may be sited through holes in the column, see Fig. 9.13 a. The compressive strength of the concrete at the bottom of the beam is limited by the strength f_{cd} of the infill concrete. Depending on the dimensions of the corbel and the position of the dowel, an additional

moment can be resisted due to the tensile force in the dowel (D) and the compressive force on the corbel (E), this contribution is generally ignored. Horizontal equilibrium yields

$$F_c = 0{,}85\nu f_{cd} \cdot b \cdot x\,; \qquad F_s = f_{yd} A_s\,; \qquad F_c = F_s$$

where $\nu = 1 - f_{ck}/250$ (f_{ck} in [MPa])
A_s = cross-sectional area of horizontal tie steel

Hence, x and z can be determined and the moment resistance can be calculated as

$$M_{Rd} = F_c \cdot z \left(+ F_{dowel} z_{dowel}\right)$$

Example of reinforcement arrangement in corbel is shown in Fig. 9-18.

Fig. 9-18: Reinforcement arrangement for corbel

9.3.1.2 Welded plate connector

The thin plate is anchored to the beam using large diameter rebars, typically 25 mm high tensile. The plate is site welded to a projecting steel billet. Expansive infill concrete is used to fill the gap, see Fig. 9-19.

Horizontal bars (two on each side of the column) are for temporary means only. Tie bars (A) arranged within the column width can be assumed to be fully stressed at the ultimate limit state, if they are fully anchored to the column, or are continuous through the column (as describe above). The beam plate is fully anchored such that the weld at the billet (B) is also fully effective. The compressive strength of the concrete at the bottom of the beam (C) is limited by the strength f_{cd} of the infill concrete. The contribution of the solid steel billet is ignored. Then

$$F_c = 0{,}85\nu f_{cd} \cdot b \cdot 0{,}8x\,; \qquad F_s = f_{wd} l_w t_w + f_{yd} A_s \quad \text{and} \quad F_c = F_s$$

where $\nu = 1 - f_{ck}/250$ (f_{ck} in [MPa])
f_{wd} = yield strength of weld, design value
l_w = length of weld

t_w = width of weld
A_s = cross-sectional area of tie bars

Hence, x and z may be determined, giving the lever arms z_1 and z_2 to the tie steel and weld, respectively.

$$M_{Rd} = A_s f_{yd} \cdot z_1 + f_{wd} l_w t_w \cdot z_2 \qquad (9\text{-}2)$$

where z_1 and z_2 = internal lever arms, defined in Fig. 9-19

Interface shear links should be provided between the beam and floor slab and be capable of resisting the force $A_s f_{yd}$ of the tie steel. It is suggested that the links should be distributed over a distance beyond the end of the connector equal to 1,5 d, where d = effective depth of the beam.

An example of an internal beam column connection under construction is shown in Fig. 9-20.

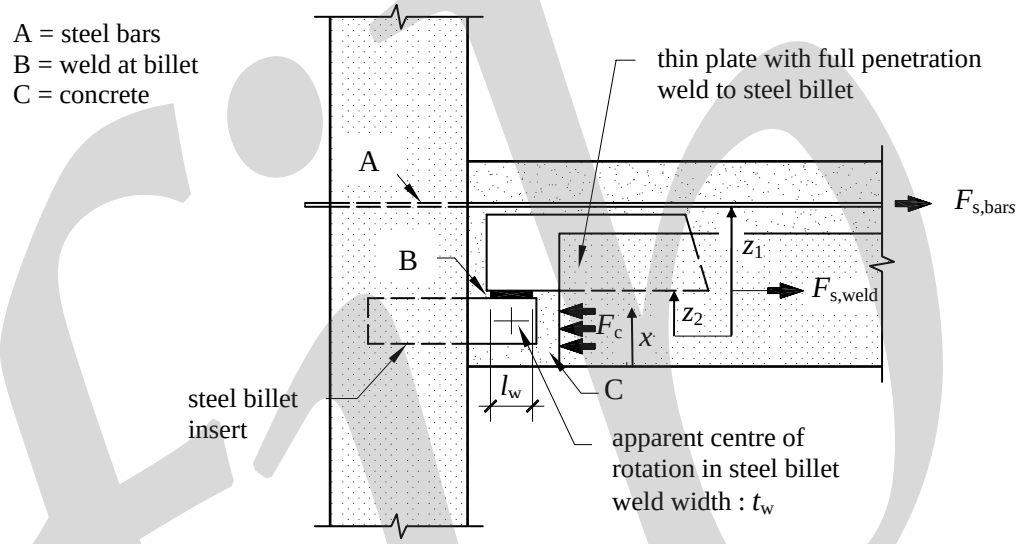

Fig. 9-19: The structural mechanism for the beam end connection with welded plate connector

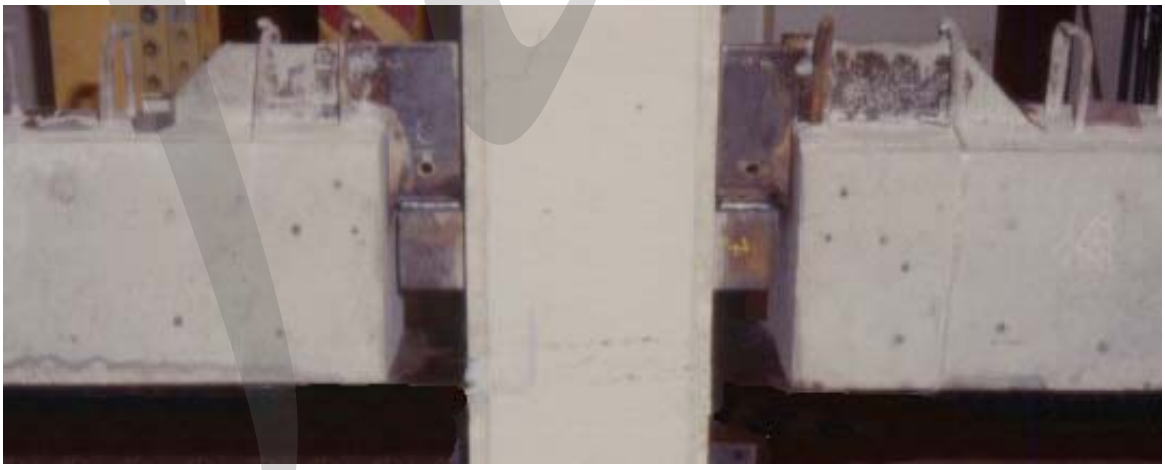

Fig. 9-20: Construction of a double sided welded plate connection

9.3.1.3 Steel billet connector

The arrangement of a single beam column connection with steel billet appears from the model shown in Fig. 9-21.

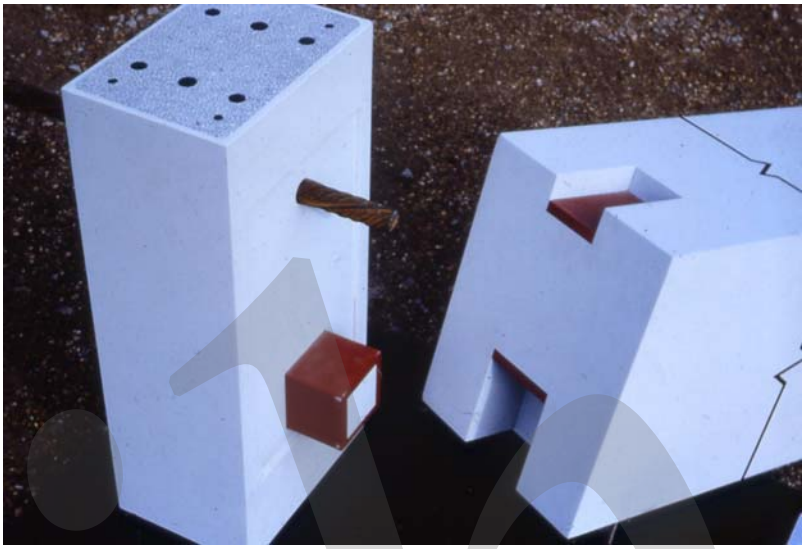

Fig. 9-21: Model construction of a single sided billet connection with welded top bar (bolted cleat or grouted joint options possible)

A threaded rod or dowel is site fixed through a hole in the beam and supporting steel billet and secured to a steel angle (or similar) at the top of the beam, see Fig. 9-22. The annulus around the billet is site grouted. If the tie steel is fully anchored as described above, the tie steel bars are fully stressed at the ultimate limit state. The shear strength of the vertical dowel (A) is ignored due to the negligible strength of the bolted angle (B). Although a shear force in the vertical dowel (at C) is present, its contribution is ignored due to a lack of ductility.

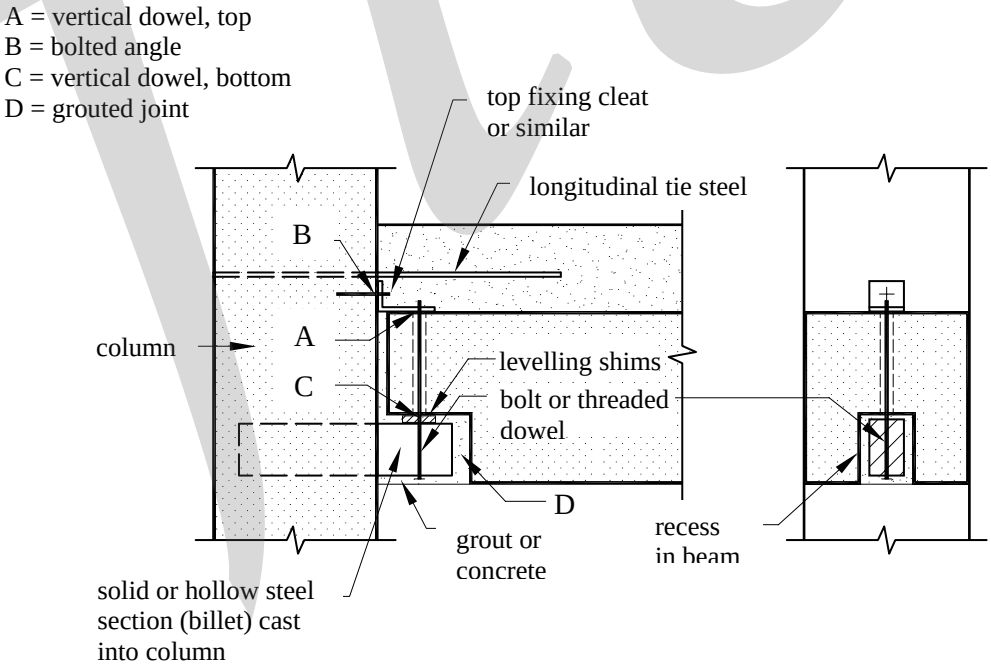

Fig. 9-22: Structural mechanism for the beam end connection with steel billet connector

The compressive strength of the concrete at the bottom of the beam is limited by the strength f_{cd} of the narrow grouted joint (D). The contribution of the steel billet is ignored. Then

$$F_c = 0{,}85\nu f_{cd} \cdot b \cdot x; \quad F_s = f_{yd} A_s; \qquad F_c = F_s$$

where $\nu = 1 - f_{ck}/250$ (f_{ck} in [MPa])

Hence, x and z are determined as before

$$M_{Rd} = A_s f_{yd} \cdot z \tag{9-3}$$

Horizontal interface links should be specified as above.

9.3.2 Experimental verification

Results from full-scale tests carried out on in-plane sub-assemblages comprising the welded plate and steel billet connectors, together with 300 × 300 mm precast beams and columns, and 200 mm deep hollow core slabs containing 2 no. T25 mm diameter tie bars are shown in Fig. 9-23 [Elliott *et al.* (1998)].

Tests ref. TW1 and TB1 are internal connections with fully continuity tie steel, whilst TW2 and TB2 are external connections where the tie steel is not anchored in the column. The design moment capacity of the connections, including the shear capacity of 16 mm dia. high tensile dowels in the billets tests, was 240 kNm. The intersection of the moment-rotation curve with the *beam-line* (shown as a solid line where no PSF are applied to the materials, and dashed with PSF) gives the point at which the response of the connection and beam are compatible in terms of rotation and strength. The results in Fig. 9-23 b show that the hogging moment of resistance, with PSF, at this point is about 200 kNm for the internal connections and up to 120 kNm for the external ones.

To use the beam-line method the flexural stiffness *EI/L* of the connecting beam must be known. A very conservative lower bound to the data gives connection stiffness [in units of kNm/rad] = 25-40 times the moment capacity [in units of kNm]. Connection stiffness may therefore be used to determine the end rotations due to joint rotation subjected to hogging moments.

Full scale test result of a concrete corbel connection supporting 400 mm deep x 300 mm wide precast beams with a 100 mm deep reinforced *insitu* concrete is shown in Fig. 9-24, [de Chefdebien 1998]. The sub-assemblage tested is an internal connection where continuity is provided by screwing the tie steel into inserts cast into the column and linked face to face by high strength bars. Two no. T 16 mm diameter tie bars are placed in the *insitu* concrete. The dowels are made by two 24 mm high tensile threaded bars. The design moment of resistance including the tensile resistance of the dowels was 96 kNm.

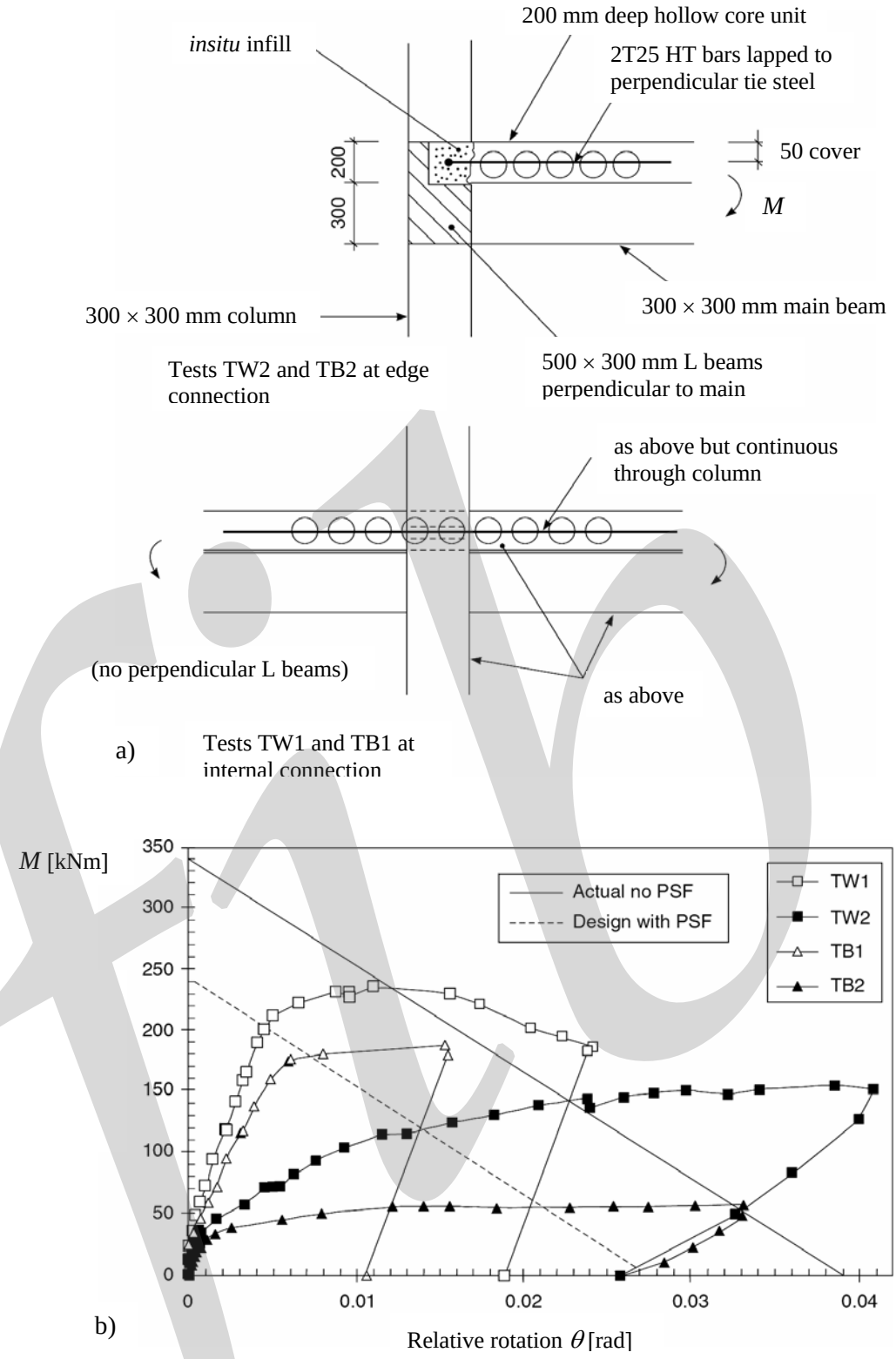

Fig. 9-23: Beam column connection tests at University of Nottingham [Elliott et al. (1998)], a) general test arrangement, b) the moment-rotation results

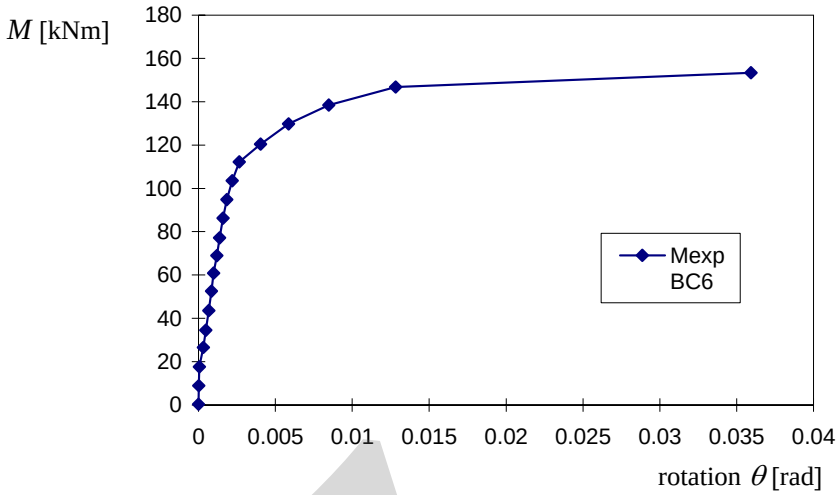

Fig. 9-24: Moment-rotation results from tests on beam-column corbel connections, [de Chefdebien 1998]

9.3.3 Beam to column head connection

This connection is used mainly in portal frames, it may be used in skeletal frames where continuous (or cantilevered) beams are required, as shown in Fig. 9-25. Unlike the discontinuous beam end connections described in Section 9.3.1, the column head connection may be designed with, or without contributions from floor slabs and tie steel. The basic structural mechanism for column head connections is shown in Fig. 9-26 and an internal connection under construction is shown in Fig. 9-27.

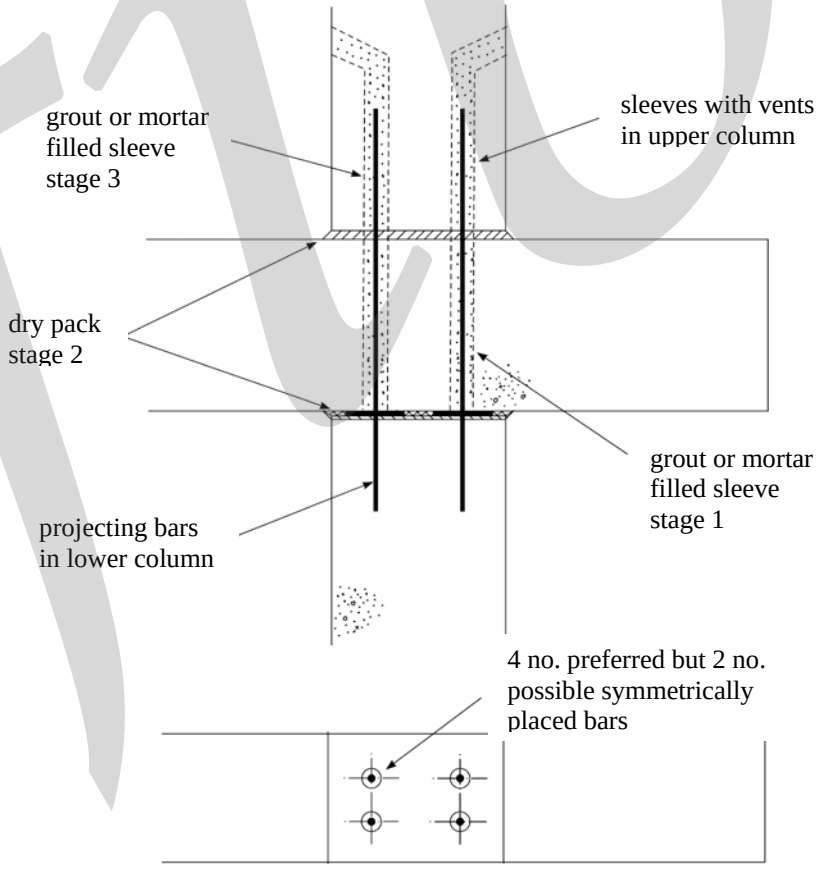

Fig. 9-25: Continuous cantilever beams at column head

This type of connection has been the subject of a number of experimental and analytical investigations [Comair and Dardare (1992), Lindberg and Keronen. (1992), Lindberg (1992), Keronen (1996), deChefdebien and Dardare (1994)], even though the number of variants in use is small.

In the case of discontinuous beams the effects of wind loading, creep and possible temperature reversals in prestressed beams may lead to sagging bending moments. Thus the connection should be designed for equal hogging and sagging moment capacity. This does not apply to continuous beams.

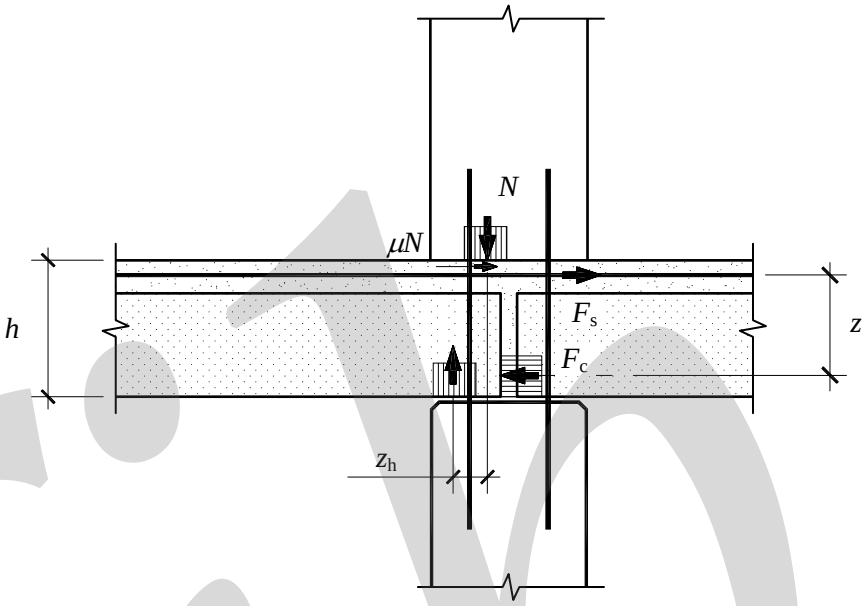

Fig. 9-26: Beam-column head connection, a) overview, b) structural mechanism of beam-column head connection

Fig. 9-27: Construction of beam-column head connection

The detail at the beam end should allow for projecting beam reinforcement to be fully anchored according to the details given in Section 7.5.2. This may be achieved in a number of ways depending on the cross section of the column. The gap between the ends of the beams should be filled with a well-compacted expanding grout or a fine concrete depending on the size of the gap. The beam should be solidly wet bedded on a 3 mm minimum thickness cohesive sand/cement mortar of strength equal to the strength of the column. The floor slab should not interrupt the joint at the top of the beam, where the upper column should also be wet bedded onto the beams. A nominal thickness of 10 - 30 mm should be allowed here to allow for deviations in beam level. If the precast beams are not topped by *insitu* reinforced concrete, steel plates should be placed at the top corners of the beam in order to avoid spalling due to the vertical forces transmitted by the upper column. The projecting reinforcement in the lower column should be grouted or connected to the upper column to form a column splice as given in Section 9.4.2.

The moment capacity is based on the lowest value obtained at the beam end joint or column head; the contribution of dowel can generally be neglected. Then

$$M = \mu N \cdot h + N \cdot z_h + F_s z \tag{9-4}$$

where μ = coefficient of concrete-to-concrete friction, which can generally be taken as 0,7, compare with Sections 8.3.3 and 8.4.3.

At the column head, column *M-N* interaction charts may be used to determine the moment capacity given the axial force *N* and the joint parameters.

9.3.4 Column haunch connection

The connection has the potential of developing a hogging moment of considerable magnitude by the use of extended bearings and reinforced *insitu* concrete in composite action with the precast beam. Fig. 9-28 shows the basic principles involved in this and examples of solutions are presented in Fig. 9-29. Careful detailing and specific instructions to site are prepared to ensure composite action at the ultimate design load. The main requirement is for a rigid bottom connection that does not rely on horizontal shear transfer to the column. If the beams are connected rigidly at the top, but not at the bottom, temperature movement etc. will cause rotations reducing the stiffness and possibly the strength of the connections.

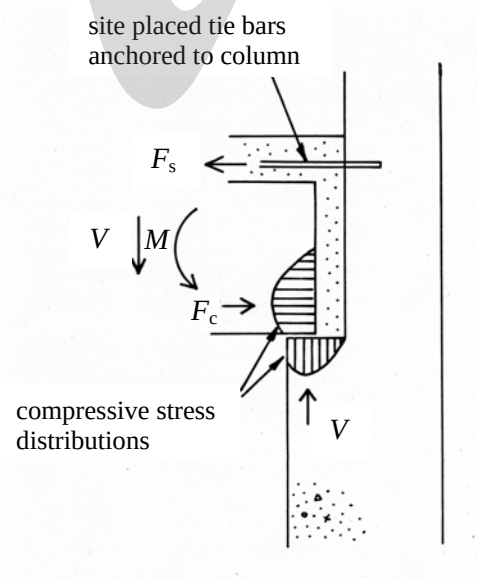

Fig. 9-28: Principle of moment resisting column haunch connection

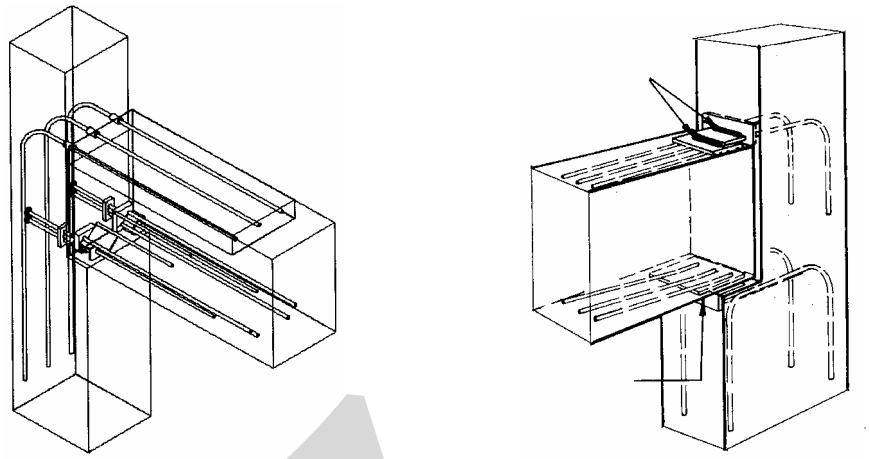

a) b)

Fig. 9-29: Examples of column haunch connections, a) threaded bars and bolting, b) weld plates (PCI Design Manual on Connections)

9.4 Column splices

A column *splice* is the general term for a connection between a column and another precast component. The base member is usually a column, but it may also be a wall, structural cladding panel or beam. It does **not** include the connection to bases or other foundations. The choice of splice is often dictated more by site erection considerations than by structural needs. It is very important that the temporary stability of a structure is not placed at risk in using a connection, which relies heavily on friction, wedging or other physical actions.

Column to column splices are made either by coupling or bolting mechanical connectors anchored into the separate precast components, or by the continuity of reinforcement through a grouted joint. The compressive capacity of the splice is made equal to that of the parent columns by confining the *insitu* concrete placed into the joint. Although the 'design' strengths of the precast and *insitu* concrete are equal, it is almost certain that the 'actual' strengths will differ - the precast concrete being greater.

9.4.1 Coupled joint splice

The coupled joint shown in Fig. 9-30 provides a mechanical tie between the precast components, which is capable of axial load and bending moment interaction. This connection requires absolute **precision** (to about ±3 mm) in placing projecting threaded bars and should only be used if the designer is satisfied that such tolerances can be achieved both in the factory and on site. The other main drawback is in connecting all couplers simultaneously. The projecting reinforcement in the upper and lower columns is threaded to opposite hands, or else the coupler is provided with opposite threads. A sufficient threaded length of bar within the coupler is assured by turning the coupler down to predetermined marks on the reinforcement.

The strength of the splice may have to be down-rated due to problems in the strain compatibility between the ordinarily reinforced precast components and the less ductile behaviour of the threaded coupler. Links are provided in the infilled region to provide stability to the compression reinforcement and to increase the strength of the infill by confinement.

The strength of the *insitu* infill is at least equal to the design strength of the column. A proprietary expanding agent is added to the cement/sand/6mm aggregate mix to prevent shrinkage cracking between the different concretes. The height of the splice is generally less than 200 mm and is

structurally adequate if the *insitu* connection is made in one pour. In dealing with larger volumes (greater than 0.05 m^3) or greater height (exceeding 300 mm) it is necessary to concrete in two stages by leaving a narrow 10 to 15 mm gap and dry packing with a 2:1 sand / cement mortar at a later date.

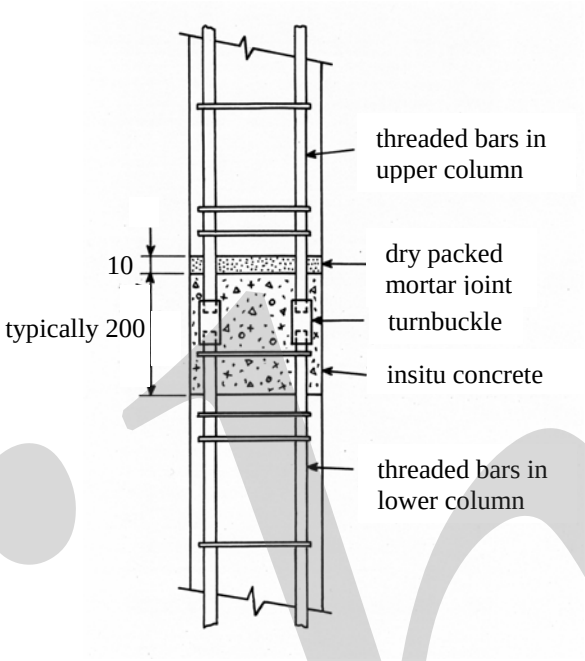

Fig. 9-30: Coupled joint splice

9.4.2 Grouted sleeve splice

One of the most popular (and easily the most economical) column splice detail is the grouted splice sleeve, Fig. 9-31 a.

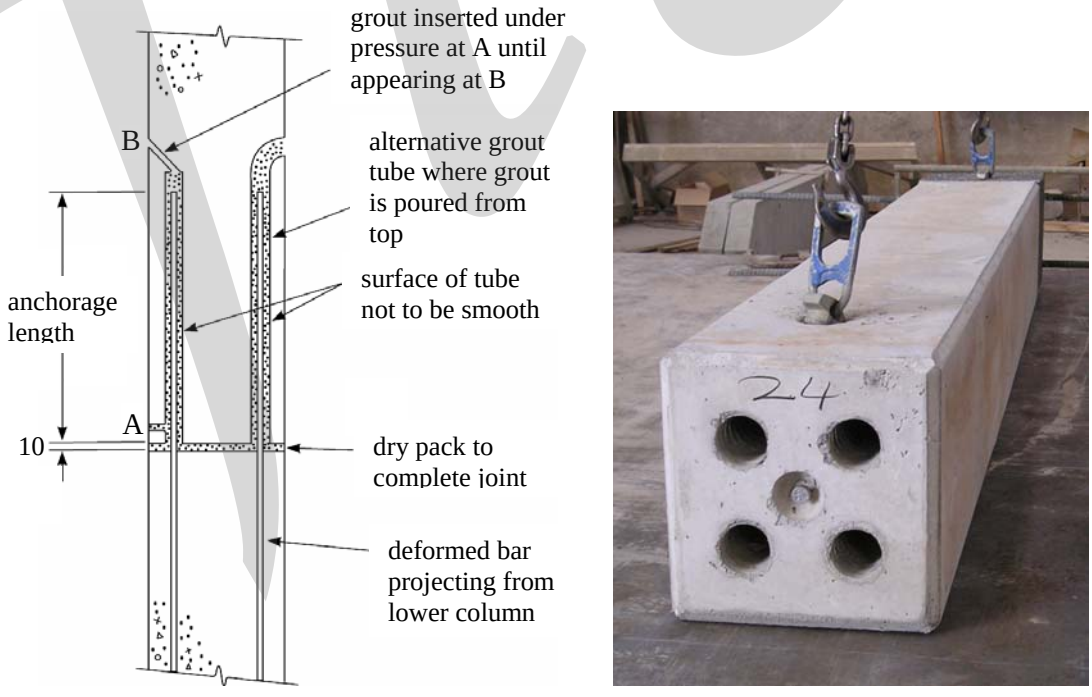

Fig. 9-31: Grouted sleeve splice, a) alternative methods b) corrugated steel tubes in column

Full-scale tests [Kuttab and Dougill (1988)] have shown that the axial load - bending moment interaction characteristics of this connection are equal to those of the parent column. The connection possesses most of the advantages (confinement of concrete, thin dry packed joint, continuity of high tensile reinforcement, easy to manufacture and fix) and few of the disadvantages (need for temporary propping and accuracy in projecting bar position) associated with precast construction methods. Splices may be made in this way at virtually any level in the frame and are not restricted to column-to-column connections. The grout sleeves may be formed in smooth or corrugated steel tubes, for example as shown in Fig. 9-31 b.

9.4.3 Grouted sleeve coupler splice

Reinforcing bars to be connected are inserted end to end into a steel sleeve and pressure grouted. The grout contains small steel fibres (e.g. melt extract) and additives such as silica fume. The splice detail shown in Fig. 9-32 may be used for compression and tension, and is equally suited to horizontal as well as vertical (or inclined) splices.

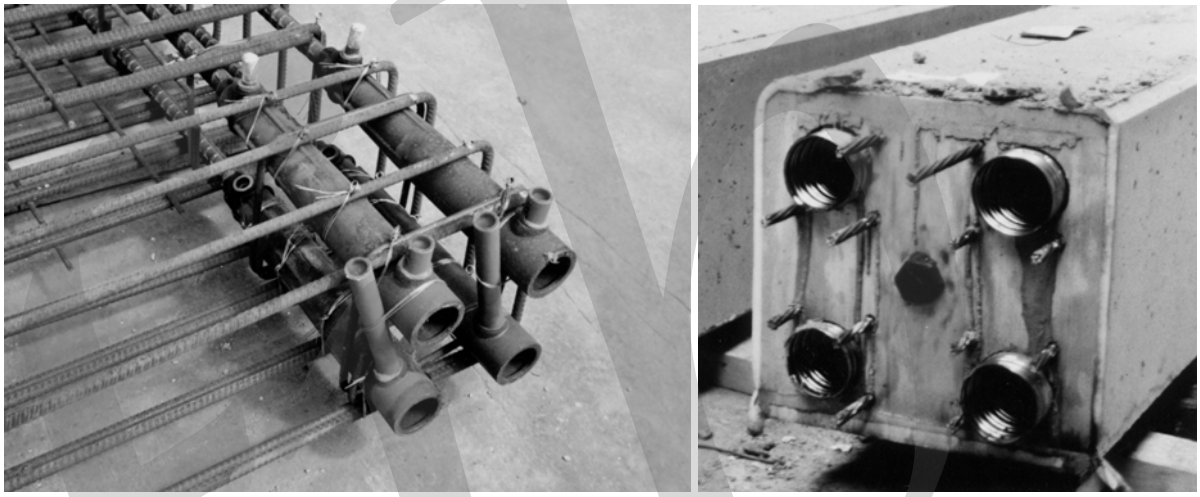

a) b)

Fig. 9-32: Details for grouted sleeve coupler, a) splice sleeve couplers for columns and walls, b) corrugated splice sleeve in a column

The principle is that the bond length of the bars may be reduced to about 8 × diameters because the grout inserted into the annulus between the bars is confined by the tapered and ribbed inside face of the sleeve. The annulus is approximately 8 mm minimum thickness, but special large opening sleeves may be used where site tolerances need to be greater than the standard practice. The sleeve contains a stop formed at its centre to ensure that each bar is embedded the correct length. The bars may be of different diameter.

9.4.4 Steel shoe splice

Prefabricated steel shoes, Fig. 9-33, are used where it may be necessary to generate bending moment and tensile forces in splices. The so-called 'column shoe' may also be used at foundation connections. It is an attractive alternative to the welded splice plate in large cross-sections (greater than say 400 × 400 mm) where large plates may be wasteful. In all four shoes are used, one at each corner of a rectangular column. Modified versions of the standard shoe are possible for non-rectangular columns. The connectors are expensive in terms of materials and manufacture, but compensate for this by providing a very rapid and structurally safe fixing on site, accommodating large tolerances. Positioning errors of up to 10 mm are possible by the use of cleverly designed

eccentric hole plate washers. The arrangement of column splice shoes at the bottom end of a column is shown in Fig. 9.34.

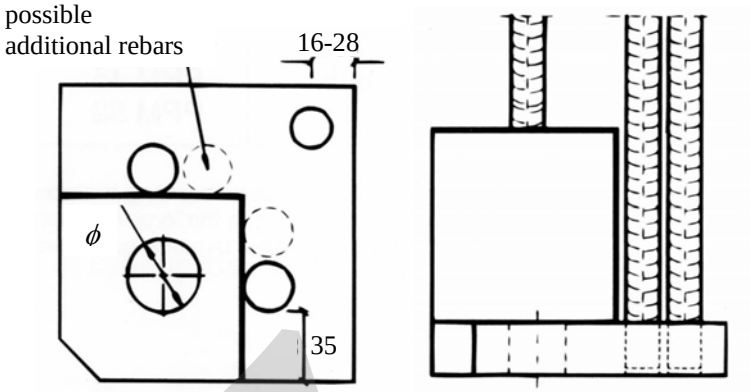

Fig. 9-33: Column splice shoe – plan and elevation

Fig. 9-34: Column splice shoes cast into the bottom ends of a column (or wall)

Base plate size [mm]	Bolt diameter [mm]*	Tension capacity [kN]**
110×110×12	M16	69
120×120×18	M20	108
140×140×25	M24	182
170×170×35	M30	275

* bolt grade 8.8 ** values subject to national partial safety factors

Table 9-2: Tensile capacities of column shoe (Courtesy Terrespeikko Oy, Finland)

Each consists of a thick (grade 50) steel plate, typically 12 mm to 40 mm thick and 100 mm to 150 mm square, joined to a thin plate metal shroud forming a (approx.) 80 mm open box cube, and 3 no. rebars in a triangular formation. The bars, which are typically 16 mm to 40 mm in diameter, provide the bond force to the concrete column. The base plate has a punched hole at its centre, which is there to receive the threaded bars from the adjoining column (similar to the welded plate splice detail). The

column shoe may be recessed in the column if the splice connection is exposed; otherwise the edge of the base plate is made flush with the column.

The tensile capacity of these connectors is always governed by the strength of the threaded portion of the coupler bar, and never by the bond strength of the rebars. Table 9-2 gives typical dimensions and tensile force capacities (per shoe).

9.5 Column base connections

Moment resisting connections of columns to pad footings and other *insitu* (or precast) concrete foundations (e.g. retaining wall or ground beam) are of three main types:

(i) grouted pocket,
(ii) base plate; greater or equal in plan dimension than the dimensions of the column,
(iii) grouted sleeve.

Methods (i) and (ii) are most commonly used. The base plate has the advantage that the column may be stabilised and plumbed vertical by adjusting the level of the nuts to the holding down bolts. This is particularly important when working in soft ground conditions where temporary propping may not provide adequate stability alone.

9.5.1 Columns in pockets

The use of column pockets is restricted to situations where fairly large concrete pad footings can easily be established. Either precast or *insitu* concrete pad footings can be used. The *insitu* concrete foundation is cast using a tapered box shutter to form the pocket. The gap between the pocket and the column should be at least 75 mm at the top of the pocket. The basic precast column requires only additional links to resist bursting pressures generated by end bearing forces, and a chemical retarding agent to enable scrabbling to expose the aggregate in the region of the pocket, see Fig. 9-35. To increase the shear capacity along the vertical interfaces, the pocket and the column can be provided with castellations, see Fig. 9-36.

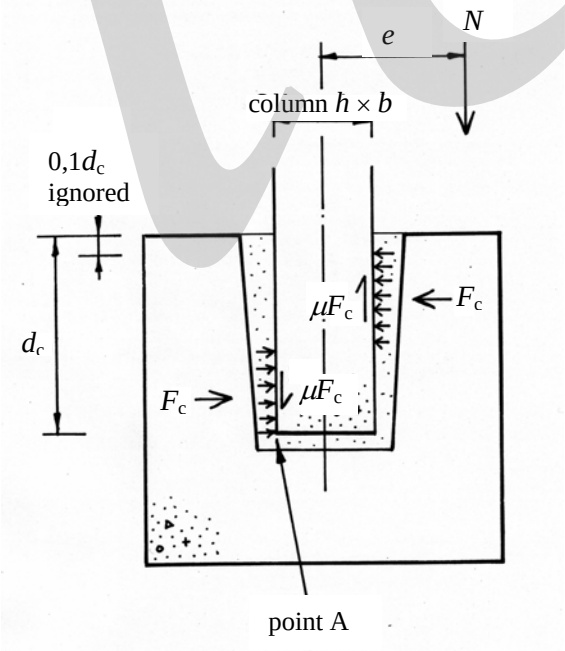

Fig. 9-35: Column in pocket foundations, mechanical behaviour

If overturning moments are present half of the skin friction is conservatively ignored due to possible cracking in all of the faces of the precast/*insitu* boundary. Ultimate load design considers vertical load transfer by end bearing based on the strength of the gross cross-sectional area of the reinforced column and equal area of non-shrinkable sand/cement grout. The design strength of the infill grout is usually $f_{cd,} = 40$ N/mm^2 and the specification is the same as for the grout used in splices.

There is a lack of analytical or experimental data on the real behaviour of pocketed connections, but this is most probably due to an almost total absence of failures. The only research on this topic has been limited to considering the prevention of concrete splitting in the sides of the pocket, particularly where the cover thickness is less than about 200 mm [Korolev and Korolev (1962)]. Results on the moment rotation behaviour of such connection and on the rotation capacity of the column under cyclic loading are available in Saisi and Toniolo (1998) and a design model based on experimental results is presented by Canha *et al.* (2007).

The depth of the pocket is governed by the bond length of the column reinforcement. This should be a full tension bond length if the column is designed at the balanced section. However it is most unlikely that this will be the case in multi-storey frames and so strictly speaking one should calculate the actual tensile stress in the bar and provide a corresponding bond length. In order to avoid using very deep pockets when using large diameter bars it will be necessary to provide a hook to the bottom of the bar. The minimum bond length, and hence pocket depth, should not be less than 12 x bar diameters.

Fig. 9-36: Precast concrete column pocket foundations, with castellations for enhanced bond to the column

The depth d_c of the column in the pocket is related to the ratio of the moment M and the axial force N as follows [Brüggeling and Huyghe (1991)]:

If $M/N < 0{,}15\ h$, then $d_c > 1{,}2\ h$

If $M/N > 2{,}00\ h$, then $d_c > 2{,}0\ h$ (9-11)

Intermediate values may be linearly interpolated; in the case of high friction interfaces (indented surfaces) these values can be reduced.

The failure mode may be by diagonal - tension shear across the corner of the pocket, in which case links are provided around the top half of the pocket. Several small links, say T8 to T12, are preferred to larger bars in order to keep the corner bend radii small. Another mode of failure is crushing of the *insitu* concrete in the annulus. This is guarded against by using an ultimate stress of $0{,}85\nu f_{cd}$ working over a width equal to the precast column only, i.e. ignoring the presence of the 3rd dimension. Horizontal shear and overturning moments are dealt with as shown in Fig. 9-35. Compressive contact

forces generate the vertical frictional resistance μF_c (using μ = 0,7), and a horizontal friction μN underneath the bottom of the column. Horizontal forces F_c in the contact region are distributed to the pad footing using horizontal links, and particular attention should be paid to this if the edge cover is less than the smaller dimension of the column. The recommended minimum depth of pocket d_c is equal to 1,5 times to the breadth of column, even though analysis may suggest values for $d_c < h$ for columns with small bending moments. The depth should not be less than h because of the need to develop a diagonal compressive strut in the column to resist shear forces. Castellations to the sides of the column are frequently used in large cross sections to reduce the penetration depth to h. The root depth is 40 mm minimum.

The moment M and axial force N may be resolved into a single force acting at a distance $e = M/N$ from the centre line of the column. The moment is transferred from the column to the foundation by a set of diagonal compressive struts. The shear stress acting in the sides of the pocket is equal to the sum of the skin friction resisting part of the axial force (assuming a rectangular column) and that resulting from μF_c. The critical interface is where the overturning moment is attempting to lift the column upwards out of the pocket - it would be unlikely to puncture the bottom of the base of the pocket.

The design assumes that a force couple $F_c \cdot z$ is generated between forces acting on opposite faces of the column. The analysis is for uniaxial bending only. There is no method for dealing with biaxial bending, but the method for dealing with biaxial bending in columns may be adopted here, i.e. an increased moment in the critical direction is considered as a uniaxial moment. The force F_c acts such that a force couple $F_c \cdot z$ is generated over a distance

$$z = (d_c - 0{,}1d_c)/2 = 0{,}45d_c \qquad \text{or} \tag{9-12}$$

$$z = (d_c - c)/2 \tag{9-13}$$

where c = concrete cover

which ever is greater. This is because the top $0{,}1d_c$ of the pocket is ignored within the cover zone, typically 50 mm to 60 mm. Thus, referring to Fig. 9-35 and taking moments about A:

$$N \cdot e - \mu F_c \cdot h - 0{,}45F_c \cdot d_c = 0 \tag{9-14}$$

Then

$$F_c \le 0{,}85\nu f_{cd} \cdot b \cdot (0{,}45d_c) \tag{9-15}$$

where f_{cd} = strength of infill

Simplifying for $d_c = 1{,}5h$ only and assuming $\mu = 0{,}7$ and we get a limiting value for e:

$$e = \frac{0{,}93 \cdot (0{,}85\nu f_{cd}) \cdot bh^2}{N} \tag{9-16}$$

Similar equations may be derived for other values of d_c/h, but the mode of action in shallow pockets will inevitably change from the above model where skin friction underneath the column will dominate. In reality the skin friction will also act over the sides of the column parallel to the direction of the moment, and so eq. (9-16) will be conservative in the presence of large axial forces.

The reinforcement around the pocket must be capable of carrying the horizontal reaction force F plus the lateral force due to the taper in the pocket = $N \tan 5^\circ$. Hence links A_{sv} are provided in the top half of the pocket such that:

$$A_{sv} = \frac{F_c + N \tan 5^\circ}{f_{yd}} \tag{9-17}$$

9.5.2 Columns on base plates

Base plates, which are larger than the size of the columns, are used where a moment resisting connection is required. Fig. 9-37 shows the structural mechanism for this type of connection. A base plate before casting the column is shown in Fig. 9-38 and examples column ends provided with base plates are shown in Figs. 9-39 – 9-40.

The disruption to manufacture of the precast column may be considerable because the plate cannot be contained within the internal confines of the mould. On the other hand base plates provide immediate stability when fixing the column on site, and the depth of the foundation is not excessive.

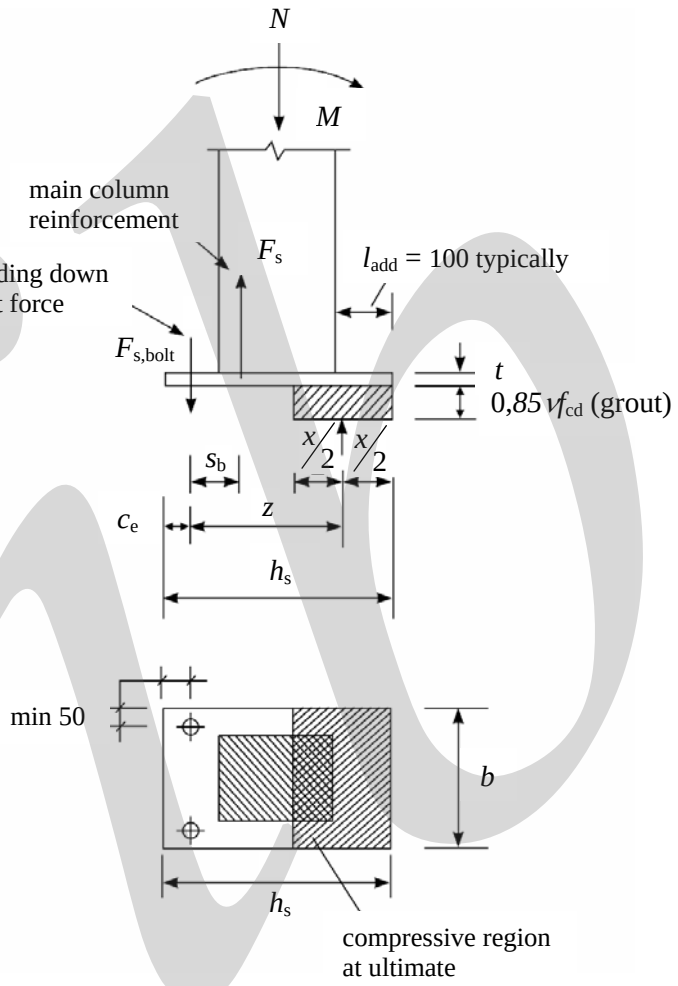

Fig. 9-37: Design principle for base plate connection

The following design method may be used to calculate the base plate thickness in the completed structure. Referring to Fig. 9-37 and resolving vertically, if $F_{s,bolt} > 0$

$$F_{s,bolt} + N = 0{,}85\nu f_{cd} b \cdot x \tag{9-18}$$

where x = depth of compressive zone
$\nu = 1 - f_{ck}/250$ (f_{ck} in [MPa])

Taking moments about centre line of compressive stress block

$$M = F_{s,bolt}(h_s - c_e - 0{,}5x) + N(0{,}5h_s - 0{,}5x) \tag{9-19}$$

also, $M = N\,e$, such that

$$\frac{N(e+0{,}5h_s-c_e)}{0{,}85\nu f_{cd} b h_s^2}=\frac{x}{h_s}\left[1-\frac{c_e}{h_s}\right]-0{,}5\left(\frac{x}{h_s}\right)^2 \qquad (9\text{-}20)$$

from which x/h_s and $F_{s,bolt}$ may be calculated. If $x/h_s > N / 0{,}85\nu\ f_{cd}\ b\ h_s$, then $F_{s,bolt}$ is positive. Assume n number bolts each of root area A_b and ultimate strength f_{byd} to be providing the force, then

$$A_b=\frac{F_{s,bolt}}{n\cdot f_{byd}} \qquad (9\text{-}21)$$

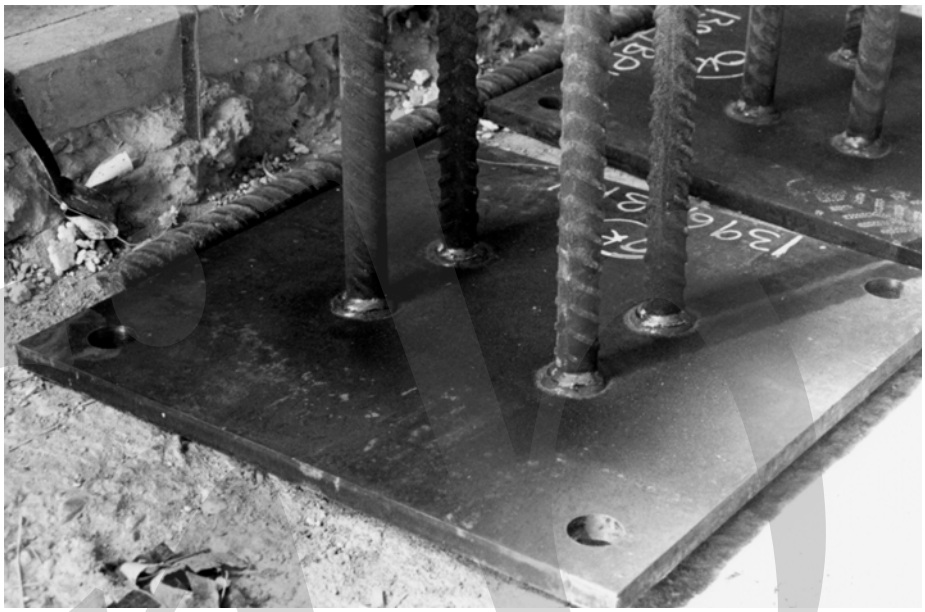

Fig. 9-38: Base plate prepared with high tensile starter bars welded to the plate

The length of the anchor bolt is typically 375 mm to 450 mm for 20 mm to 32 mm diameter bolts. The bearing area of the bolt head is increased by using a plate, nominally 100×100×8 mm. The bottom of the bolt is a minimum of 100 mm above the reinforcement in the bottom of the footing. Confinement reinforcement (in the form of links) around the bolts is usually required, particularly where narrow beams and/or walls are used and where the edge distance is less than about 200 mm. The steel is designed on the principle of shear friction but should not be less than 4 no. R 8 links at 75 mm centres placed near to the top of the bolts. To err on the side of caution anchor loops are usually provided around the bolts in order to achieve the full strength of the bolt if the horizontal edge distance is less than about 200 mm.

Larger compressive forces beneath plates, which project beyond the column face in two directions cause biaxial bending in the plate. The maximum projection of the plate is therefore usually restricted to 100 mm, irrespective of size. Use a base plate of thickness t, which is the greatest of:

$$t=\sqrt{\frac{0{,}85\nu f_{cd} l_{add}^2}{f_{pyd}}} \quad \text{(based on compression side)} \quad \text{or} \qquad (9\text{-}22)$$

$$t=\sqrt{\frac{4F_{s,bolt}\cdot s_b}{b\cdot f_{pyd}}} \quad \text{(based on tension side)} \qquad (9\text{-}23)$$

where l_{add} = overhang of plate beyond column face
s_b = distance from centre of bolts to centre of bars in column
f_{pyd} = yield strength of the plate, design value. Steel grade 43 or 50 is used.

Reinforcement is fitted through holes in the base plate and fillet welded at both sides. The design strength of the column is therefore determined using mild steel reinforcement, which occasionally leads to cumbersome detailing. Additional links are provided close to the plate, as is the practice at splices.

Fig. 9-39: Flush base plate for column splicing or pinned-jointed foundation

Fig. 9-40: Construction of steel base plate, showing starter bars are welded through holes in the plate

9.5.3 Columns to foundation shoe connection tests

Bolted column to foundation connections were studied experimentally in bending tests [Bergström (1994)]. The type of connection studied is shown in Fig. 9-41 a.

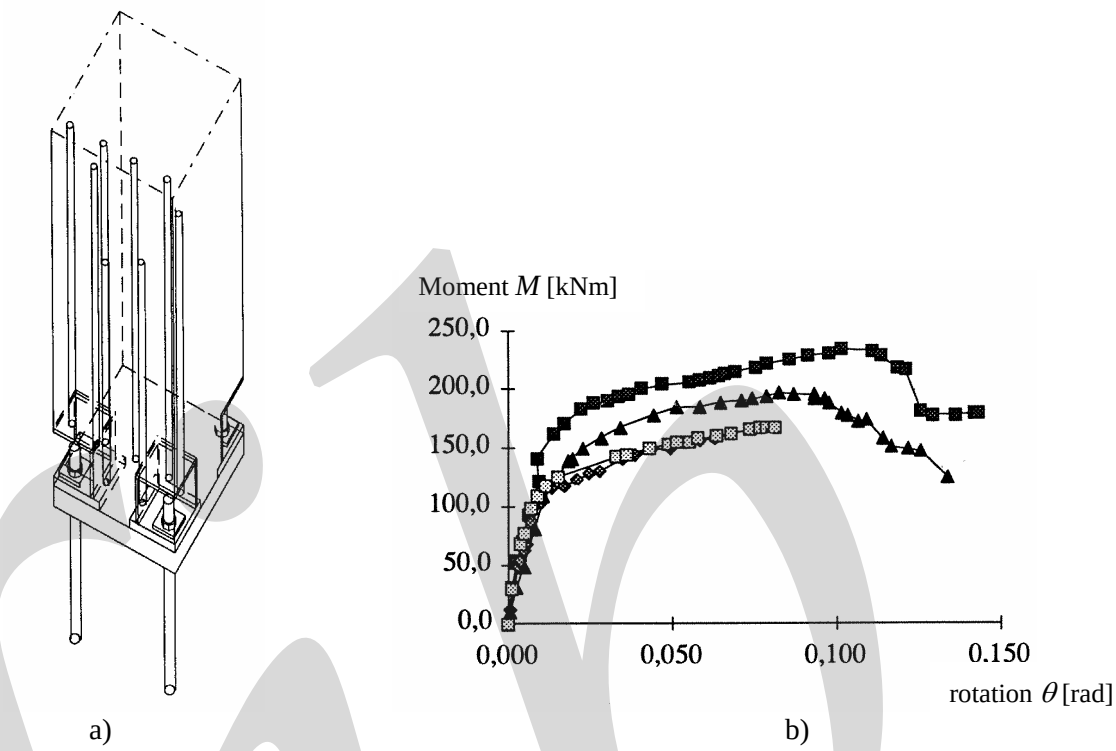

Fig. 9-41: Tests on column-base connections with steel shoes, a) connection type, b) moment-rotation relationships for various detailing, according to Bergström (1994)

Each steel "shoe" was made by a steel angle with top and bottom plates welded to it in such a way that a recess was formed at the corner of a 400×400 mm column. Each base plate, 20 or 25 mm thickness, was anchored by two bars welded to the main column reinforcement. The joint between the (grade 50) column and the foundation was filled with grade C40 grout. The column was subjected to an overturning moment M and the rotation of the base of the column was measured. The resulting moment-rotation relationships are shown in Fig. 9-41 b. The moment capacity varies from 150 to 250 kNm, whilst the stiffness is in the range from 11 to 22 kNm/rad. For M < 200 kNm the local pull-out deformation of the bolt was small (less than 1 mm).

9.5.4 Columns in grouted sleeves

The design of these connections is identical to the grouted sleeve splice shown in Fig. 9-31. Full compression or tension anchorage lengths are provided in both the precast column and *insitu* foundation. High tensile deformed reinforcing bars are left protruding from the foundation, Fig. 9-42, something that is quite difficult to achieve with any accuracy. This is the main disadvantage in using this connection. The tendency is for the bars to be touching the sides of the sleeves in the precast column thus preventing a full envelopment of grout around the bar. Also, the grouting cannot be inspected afterwards and so there is no guarantee that the bar is fully bonded. Therefore the internal diameter of the duct should not be too small, a minimum diameter of ϕ_{bar} + 30 mm is recommended. Furthermore, measures should be taken to ensure accurate position of the projecting reinforcing bars. Nominal cover to the tube and the minimum distance between tubes should be at least 75 mm.

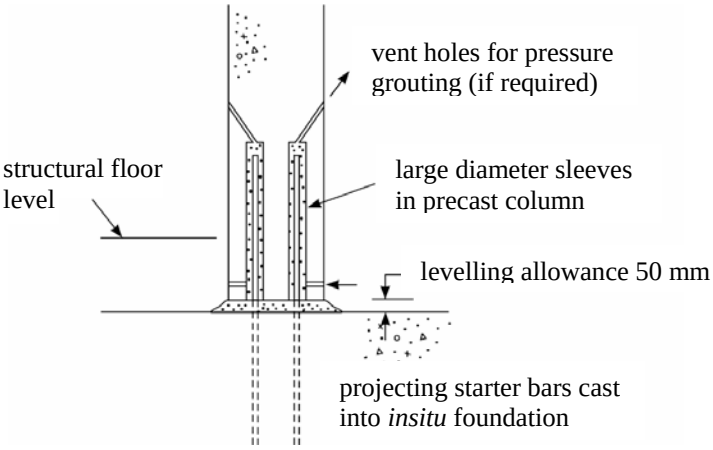

Fig. 9-42: Column-base connection with grouted sleeves, projecting reinforcement at column foundation

The connection may be considered in design as monolithic providing the bedding joint and grout sleeves are completely filled with grout to the satisfaction of the site engineer. Tests results [Kuttab and Dougall (1988)] show that the axial force-moment interaction characteristics of the connection are equal to the column itself. An added bonus is that high tensile reinforcement is used throughout.

An alternative solution of a grouted connection is shown in Fig. 6-2 b where the column has projecting reinforcement bars which are grouted into preformed holes in the foundation. Corrugated steel pipes are preferred. The holes are filled with grout before the column is placed. In this case the problem with tolerances is smaller, but there is a risk of getting dirt, water and ice in the holes during construction. Therefore the holes should be protected during construction, inspected and cleaned (if needed) before grouting.

9.6 Floor connections – moment continuity across supports

9.6.1 Introduction

Precast floor slabs, such as hollow core units and floor plates (also known as half-slab) are normally designed and constructed as simply supported and one-way spanning. The reinforcement, in the form of rebars or pretensioned tendons, is positioned in the bottom of the units to give a sagging (positive) moment of resistance. Top reinforcement is sometimes provided in hollow core units to guard against flexural cracking due to handling, and to cater for shrinkage and thermal effects, etc., but otherwise is not provided for negative moment continuity at supports. This must be facilitated by placing site reinforcement across the support and filling the gaps and joints at the ends of the units with structural grade cast *insitu* concrete, as shown in Figs. 9-43 and 9-44.

Positive continuity reinforcement may also be required at the ends of prestressed units to restrain against the effects of creep and elastic relaxation in order to ensure that the displaced diagram of the positive moment is covered, particularly in case of a composite support.

Moment continuity will provide the following benefits:

1. reduce the magnitude of positive sagging moments due to imposed loads, both in the serviceability (SLS) and ultimate (ULS) limit states, leading to shallow floor depths and/or greater spans;
2. reduce deflections and crack widths at SLS due to the negative moment restraint;
3. increased structural integrity between floor units and supports;
4. improved diaphragm action in resisting horizontal wind loads and earth pressures.

Fig. 9-43: Negative moment continuity reinforcement placed into top opened cores in precast hollow core units. Transverse reinforcement parallel with the beams also provides moment continuity through the column (Courtesy APE and GRUPPO CENTRO NORD)

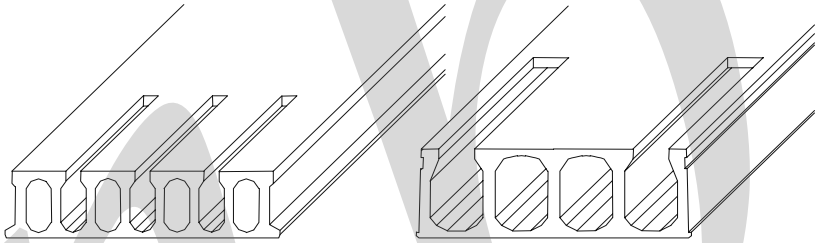

Fig. 9-44: Opened cores in hollow – core units at support

The reinforcement details necessary to achieve moment continuity are shown in Figs. 9-45 and 9-46. These depend on the degree of continuity required and the support conditions as follows:

1. Direct support of the precast floor slab on a wall or a beam, Fig. 9-45. The structural connection may be designed to transfer forces and moments or not (continuity or simple support), according to the design requirements by means of suitable additional *insitu* reinforcement and concrete, connecting the slab end at the support.
2. Composite support, Fig. 9-46. There is no direct support under the precast floor slab. The cast *insitu* beam and the ends of the floor slab require temporary propping, which is removed after hardening of *insitu* concrete. In this case the structural composite connection should be capable to transfer all forces and moments according to the continuity scheme, by means of suitable additional *insitu* reinforcement and concrete to prevent failure in the ultimate limit state.

In case of non rigid supports, as it may occur with steel or prestressed/reinforced concrete beams of moderate stiffness (shallow or flat beams), the curvature of the beam introduces stresses in the transversal direction of the slab which reduces the shear capacity of the floor unit. This is to be considered in the design as stated in *fib* (2000a).

In case of direct support it is not always necessary or desirable for the connection to be fully rigid. Partial interaction is possible. The connections may therefore be classified as follows:

1. Fully restrained. The slab is treated as continuous over the supports in both SLS and ULS.
2. Partially restrained. The slab is treated as continuous over the supports in SLS, but simply supported in ULS.

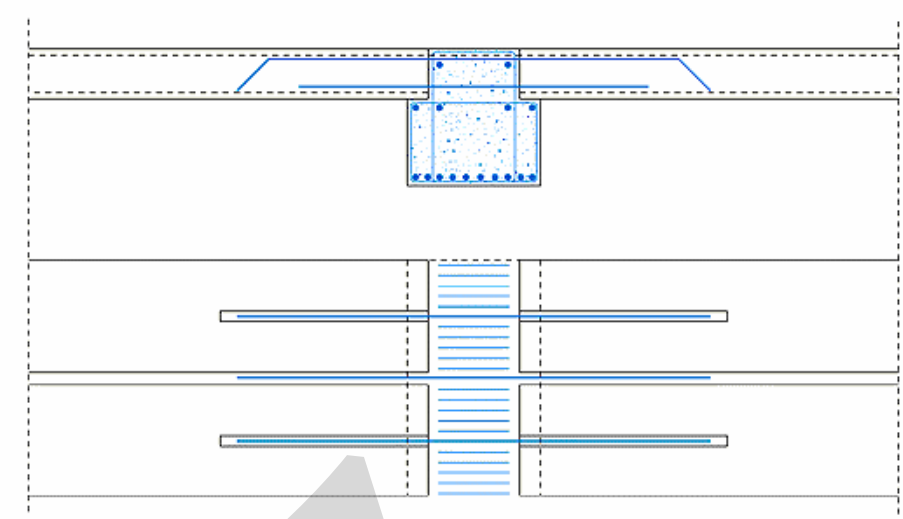

Fig. 9-45: Restrained connection with direct support

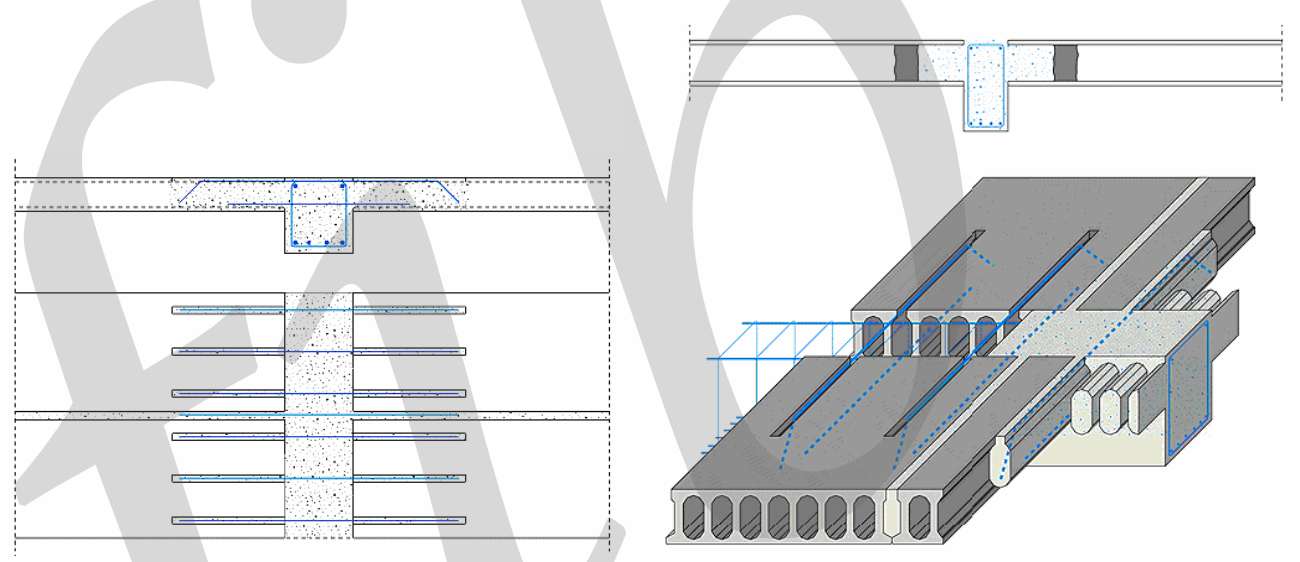

a) b)

Fig. 9-46: Restrained connection with composite support, a) sections, b) view

In case of restrained connections with composite support the length-to-depth ratio for the floor slabs should not exceed 35 as stated in *fib* (2000a). This is to ensure that sufficient end rotation takes place in the floor unit to fully mobilise the forces in the continuity bars. To limit shear and spalling stresses, and to limit the prestressing and the corresponding spalling stresses, the total width of the webs in the floor unit should be greater than 380 mm (per 1.2 m wide unit) according to *fib* (2000a).

9.6.2 Connections with unintended restraint

In many cases in practice, due to the particular construction conditions, 'unintended' restraint appears in the connection between the floor and the support, as explained in Section 3.5.2. This has to be taken into account by the designer. Typical examples are shown in Figs. 9-47 – 9-48 and reasons for the unintended restraint could be:

- floor slab restrained between lower and upper wall
- multispan floor slabs with reinforced (continuous wire – mesh) structural topping
- floor slab restrained at the support of a wall or a beam with protruding steel reinforcement
- floor slab restrained as a consequence of extensive tie bar systems
- floor slab restrained as a consequence of large tensile strength of the *insitu* concrete cast at the support and within the floor slab

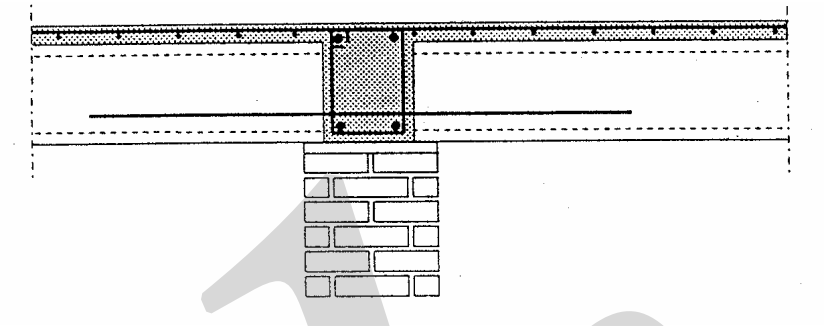

Fig. 9-47: Unintended floor continuity

A negative consequence of such unintended restraint may be that, still in the service state, the concrete tensile strength is reached and suddenly a large crack occurs in the floor unit. Such a large crack may not only be unsightly in the floor finishing, but also be dangerous if it occurs in an unfavourable location, see Fig. 3-10.

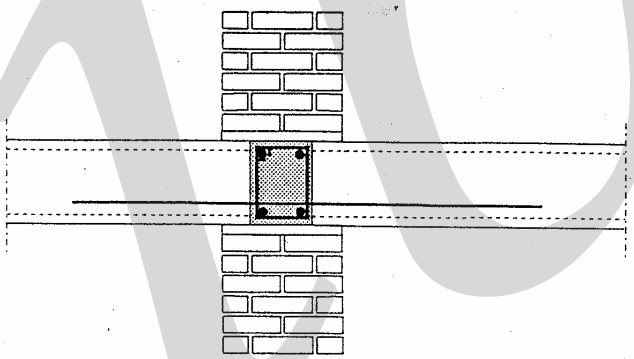

a)

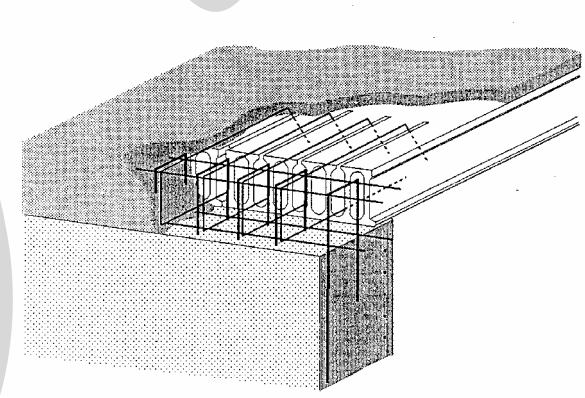

b)

Fig. 9-48: Unintended wall restraint, a) interior support, b) exterior support

9.6.3 Simply supported connections without restraint

Basically this type of connection shall be capable to transfer horizontal forces between the floor and the tie beams or two adjacent floor bays to meet floor diaphragm requirements, but with negligible moment resistance and therefore no restraint of the precast floor slab at the support, see Fig. 9-49.

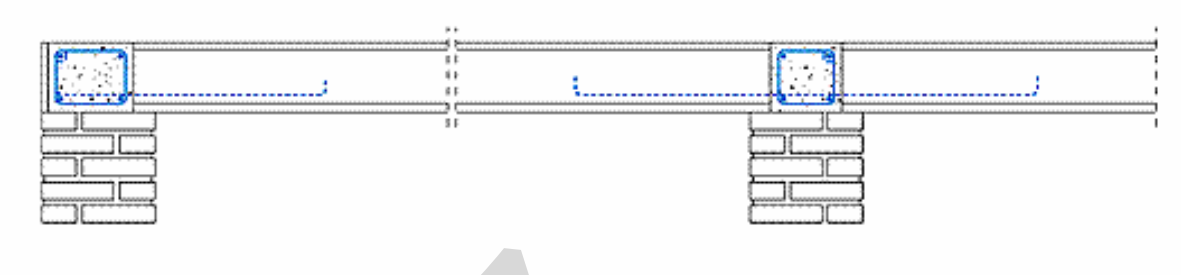

Fig.9-49: Tie bar reinforcement in unrestrained connection

The tie bars have to be grouted in suitable positions of the precast floor slab (in longitudinal joints or in opened cores in hollow-core slabs) or in the structural topping, when topping is specified. The tie bar has to be positioned as low as possible (possibly in the lower third of the section) in the transversal section at the support in order to avoid unintended restraint and to permit free rotation of the slab end under the superimposed load according to the simple bearing scheme as indicated in Fig. 9-49.

In case of tie bars placed in the structural topping, as shown in Fig. 9-50, the end section of the precast unit at the support should have a minimum free allowance below the neutral axis in order to allow the end rotation. This normally occurs in case of double-tee ribbed units without any special provisions; in case of hollow-core slabs or similar precast units, 1÷2 cm of soft material (as polystyrene or similar) has to be interposed between the lower parts of slab end sections and the beam or tie beam concrete in order to avoid unintended negative moment at the connection.

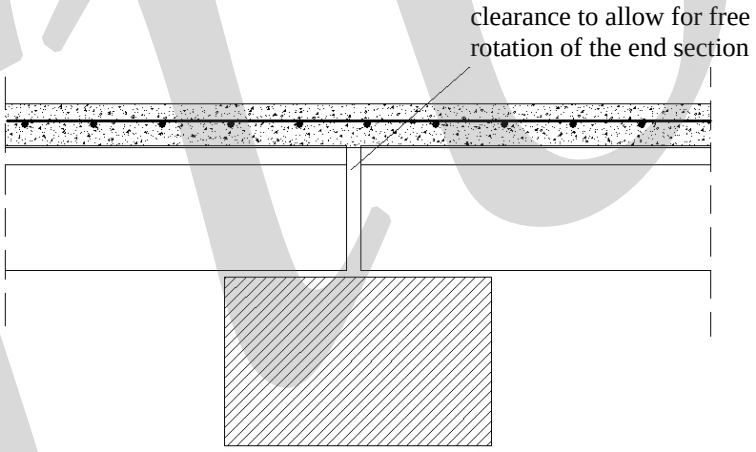

Fig. 9-50: Unrestrained connection of double-tees units

A solution with a structural topping, Fig. 9-51, is appropriate to avoid unsightly and even dangerous large cracks in the topping above the support in the service state and at the same time allow free rotation according to the intended simply supported condition.

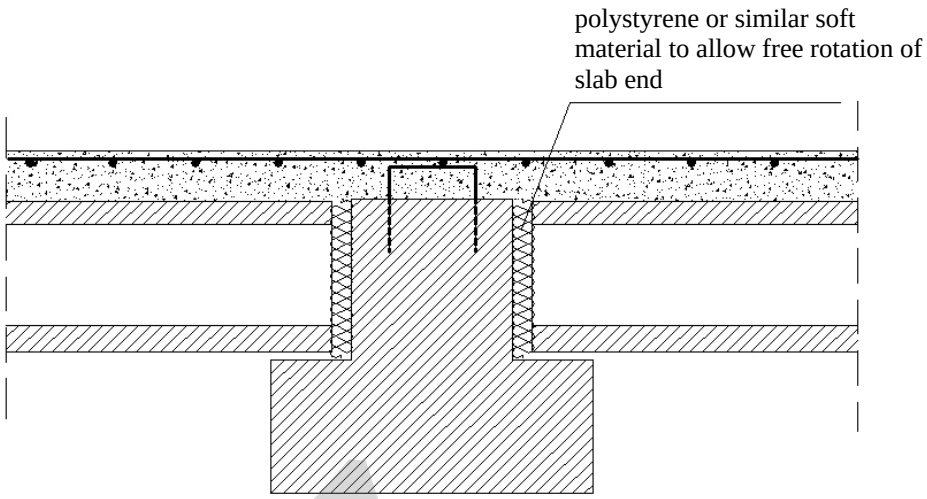

Fig.9-51: Unrestrained connection of hollow-core slabs or similar

9.6.4 Connections with full continuity

This structural connection is recommended and applicable for residential buildings, underground car parks and also seismic buildings with a monolithic structural behaviour, or where other particular construction or architectural requirements call for it. This type of connection is strictly required in case of composite supports of hollow core floors, but not in floors with ribbed double-tees or similar precast units.

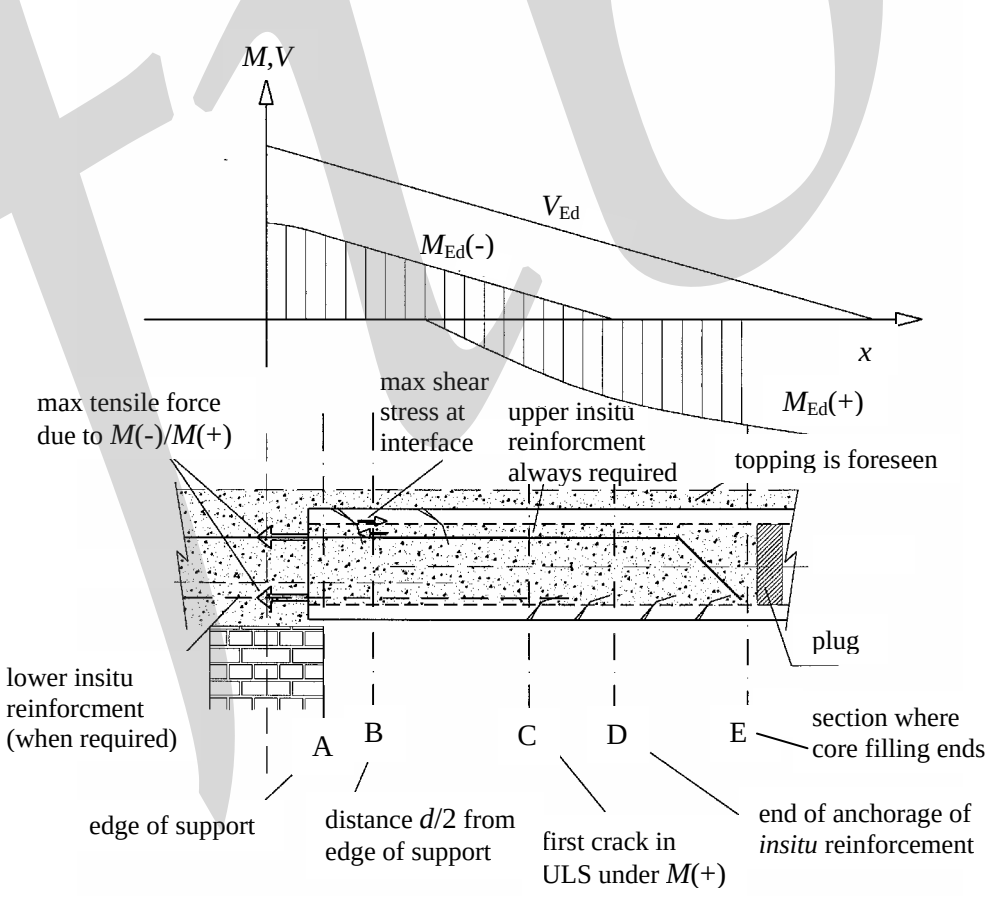

Fig. 9-52: Critical sections of a composite restrained connection

The longitudinal cross section and the associated design moment diagram are shown in Fig. 9-52. Calculation models for the moment and shear resistance at the sections A to E are given in *fib* (2000a).

The *insitu* concrete is required to fill milled slots (called opened cores) in the precast hollow core unit for a distance equal to the dimensions given in Table 9-3. The moment capacity of the connection is limited either by the ultimate strength of the negative continuity reinforcement, or by the compressive strength of the concrete in the bottom of the precast unit or the *insitu* infill. Compressive stresses due to the negative moment are additive to those induced by prestressing and may be critical.

The area of negative moment reinforcement is determined for the ultimate limit state, assuming imposed floor loads, which act only after the *insitu* infill has hardened, and taking also into account long term effects of creep and shrinkage. The cover of the bars should satisfy the normal fire and durability requirements. No shear links are required.

In particular the following specific design checks shall be carried out for the structural connections with full continuity:

- anchorage capacity of the *insitu* reinforcement in filled cores
- shear capacity of the interface between the *insitu* and the precast concrete
- shear capacity of the composite member and the *insitu* concrete
- bending capacity of the composite member at the support under the design negative moment
- effects of creep and differential shrinkage between precast and cast *insitu* concrete

The shear capacity of the composite member under the negative moment close to the support (sections A-B) has to be calculated without contribution from the prestressing. The bending capacity of the composite member at the support shall be evaluated considering the ordinary *insitu* reinforcement together with the effective prestressing steel in the considered section, provided that anchorage failure of the prestressing steel is prevented.

The additional *insitu* reinforcement should be well distributed, to avoid stress concentration and the length of the reinforcement bars should be correlated to the design M(-) diagram, and often sized in 2 or 3 lengths with the minimum not less than the transfer length of the prestressing force.

The maximum diameter of the reinforcement should be limited with regard to the shear resistance at the interface between the concreted core and the precast concrete.

It is also recommended to provide suitable plugs at the end of each core to be filled with *insitu* concrete in order to ensure adequate compacting of concrete.

In addition to the general recommendations given for the 'direct' supports, it is necessary, in case of no direct support under the precast slab, to provide additional *insitu* reinforcement at the bottom level of the connection, with adequate anchorage length. The *insitu* concrete should fill all the cores, including those without additional reinforcement bars, over a length l_c at least equal to the total depth of the slab, with suitable plugs to ensure good compaction of *insitu* concrete, see Fig. 9-53.

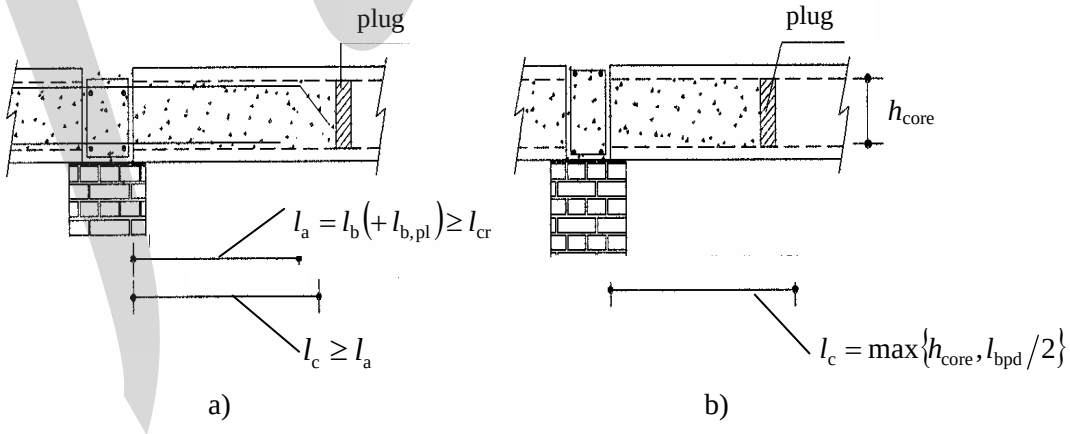

Fig. 9-53: Arrangement of restrained "composite" connection, a) cores with additional continuity reinforcement, b) cores without continuity reinforcement

The span/depth ratio of the hollow-core slab has to be limited (normally $L/h \leq 30\text{-}35$) and the total web width increased (normally $\sum b_w \geq 380$ mm) to limit the spalling stress and shear stress so that the resulting value will not exceed the design value of concrete tensile strength in ULS.

The calculation of the shear capacity at the edge of the restrained connection may require adding ordinary shear reinforcement in the cast *insitu* cores, see Fig. 9-54.

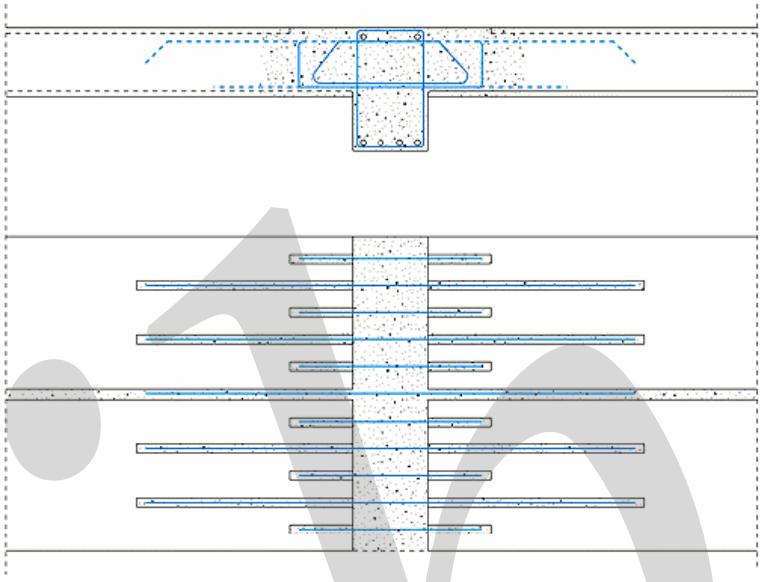

Fig. 9-54: Specific shear reinforcement of insitu concrete

9.6.5 Connection with partial continuity in the serviceability limit state

This type of connection, which is designed for negative moment continuity in the serviceability limit state only, is only applicable in case of direct support of a precast floor on a wall or a beam. In the ultimate limit state the floor unit is designed as simply supported. This solution may be selected if the ultimate moment of resistance of the floor unit is much greater than the service moment or in the case where SLS deflections govern. Continuity is not considered in the ultimate limit state, because no significant restraint exists.

Partial restraint can also be achieved using a reinforced structural topping. No additional reinforcement is placed in the cores or joints between the floor units. Horizontal shear stresses at the interface to the topping must be checked, as well as the rules regarding cover and durability.

In all situations, the top reinforcement is limited to about one-half of the value compared to the connection for full continuity.

9.6.6 Simplified rules

For preliminary design of floors and restrained floor connections, the following recommendations and simplified rules, given in Table 9-3, are valid in case of a uniformly distributed load between 4,0 kN/m^2 and 8,0 kN/m^2. The shear force and moment distributions are determined for the serviceability limit state before redistribution.

Data per 1.2 m wide hollow core unit	Full restraint Normal support	Full restraint Composite support	Partial restraint Normal support
Minimum number of reinforced cores and joints: Span < 6.0 m Span < 10.0 m Span > 10.0 m	 2-3 3 3-4	 3 3-4 4	 2 2-3 3
Number of additional cores filled but not reinforced	Nil	All remaining for 300/400 mm	Nil
Length of bars projecting into opened cores or joints: Span < 6.0 m Span > 6.0 m	1000 mm in opened cores 1400 mm in joints 1200/1500 mm in opened cores 0,20/0,25 x floor span in joints		
Site placed top reinforcement (mm^2)	0.005 *M/h*		0.0025 *M/h*
Maximum diameter of top reinforcement (mm)	The lowest of	6 + *h*/25 *c*/3 *c*-20	
Site placed bottom reinforcement (mm^2)	Nil	0.005 *V*	Nil
Maximum diameter of bottom reinforcement (mm)	Nil	2 + *h*/25	Nil
Site placed reinforcement in *insitu* structural topping (mm^2)	0,005*M*/(*h*+*t*)		0.0025*M*/(*h*+*t*)
Maximum diameter of reinforcement in *insitu* structural topping (mm)	The lowest of	6 + (*h*+*t*)/25 *t*/3	

M = negative hogging bending moment due to imposed loads at SLS (Nmm units), *V* = support shear force due to imposed loads at SLS (N units), *h* = slab depth (mm), *t* = topping thickness (mm), *c* = core width or joint width (mm).

Table 9-3: Simplified rules for moment continuity in floors across supports, [fib (2000a)]

9.7 Transfer of torsional moment

9.7.1 Torsional interaction, equilibrium and compatibility conditions

With regard to the effect of torsion it is appropriate and common to distinguish equilibrium torsion (or primary torsion) and compatibility torsion (or secondary torsion). In the first case the torsional moment and its distribution along the structural member in question only depend on equilibrium conditions. This means that the problem is statically determinate and the structural member is free to twist without any other restraint than from its supports where the torsional moment is balanced. Compatibility torsion occurs when the twisting in one structural member is a result of interaction with adjacent structural members that deform under load. This problem is statically indeterminate and the actual torsional moment and its distribution along the structural member depend on the rigidity of the interacting elements and their connections within the system. In a completed precast structure, equilibrium torsion will rarely occur, since the structural elements are normally connected to each other so that one element can not twist freely without interfering with adjacent elements. This means that with regard to torsion, compatibility torsion is the normal case. Torsion seldom appears alone, but almost always together with shear and bending.

However, during erection and before the elements are fully connected into a completed system, equilibrium torsion could occur. A typical case is when a deep simply supported beam (roof girder)

mounted on columns is subjected to horizontal load, e.g. wind load or impact (accidental) load. The horizontal load is resisted at the support joints by friction or connection details. If the load and the reaction act at different levels, the beam is subjected to torsion, besides the transverse bending and transverse shear. To prevent tilting of the beam the connections at the supports must be arranged so that the corresponding torsional moment can be resisted. Also during erection of elements, equilibrium torsion could occur in beams when the load from the supported element acts with an eccentricity relative to the shear centre of the beam cross-section. A typical case is erection of a precast floor on an edge beam with L-shaped section. Before the floor and its connections are completed, the dead weight from the floor elements give rise to torsional moment in the ledge beam and corresponding twisting and need for torsional restraint at the supports. However, as soon as both ends of the floor elements are placed on support beams, the beams can not deform independently, but a certain interaction takes place due to restraint from the floor/beam connections, e.g. due to friction at the support joints. The interaction between the beams and the floor elements becomes more and more developed, when more elements have been placed and the connections within the structure have been fully completed, see Fig. 9-55. When the floor elements are connected to the beam, more or less firmly, the end rotation will be partly restrained and the ledge beam will be forced to twist.

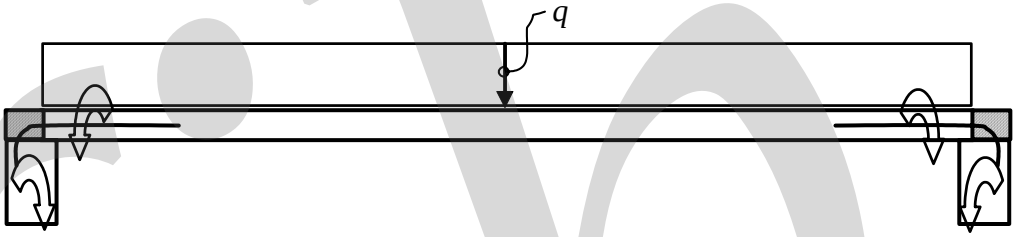

Fig. 9-55: Transfer of moment through support connections

When beams with an asymmetric cross-section, like an L-section, is loaded eccentrically and is free to deform, it will deflect vertically, twist, but also undergo horizontal deflection. This horizontal deflection takes place because the principal axis of inertia does not coincide with the vertical and horizontal axes. In full scale tests on deep spandrel beams that were allowed to deform freely when loaded on the ledge, the horizontal deflection has been the dominant behaviour [Klein (1986), Lundgren (1995)]. When ledge beams are connected to floor elements, this horizontal deflection is restrained. However, according to the experiments by Klein (1986) and Lundgren (1995) this restraint did not substantially reduce the torsion.

In the completed system the actual torsional interaction depends on a number of parameters involving the rigidity of the structural members, their supports and the characteristics of the structural connections between the elements within the system. The analysis is a complex non-linear, three-dimensional problem. In a specific case weak and stiff components can be identified. In general the stiff components attract load and deform further due to the flexibility of the weak elements, while the weak components are stiffened by the stiffer ones.

The complexity of the system is illustrated by Fig. 9-56. When the floor element is loaded, it will deflect and this deflection is associated with a certain end rotation at the floor support. This end rotation is transferred to the ledge beam, which will be loaded in torsion and twist. However, the torsional stiffness of the ledge beam might reduce the end rotation of the floor compared to a simply supported floor. Since the twist varies along the beam, all floor elements cannot have the same end rotation, which gives rise to another restraint within the system. The torsional load on the ledge beam is distributed between its supports where the corresponding torsional moments must be resisted by the support connections. However, even if these connections are rigid with regard to torsion, tilting of the beam ends cannot be fully prevented, since the restraint depends on the flexural rigidity of the columns, which in turn has to balance the torsional moment. When the torsion is transferred to the columns, they will deflect out of the plane of the wall. This deflection may have a negative influence of the columns with regard to buckling.

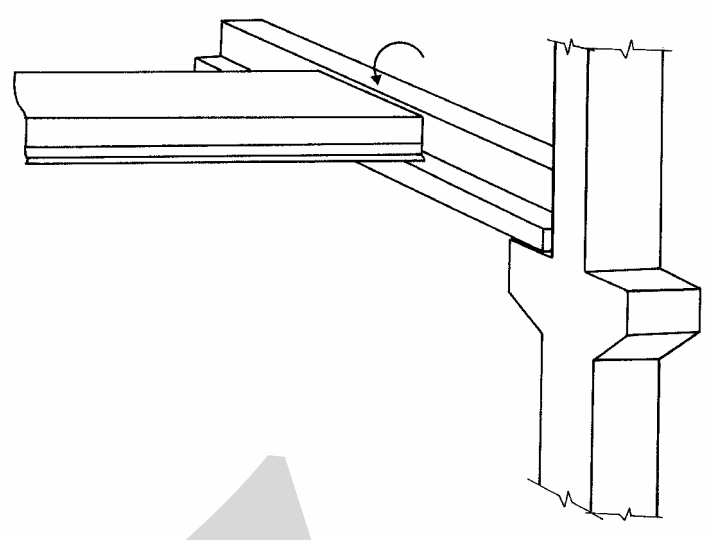

Fig. 9-56: Exterior edge beam subjected to torsion

In a system with weak columns (with regard to bending out of the plane of the wall) and/or weak beams (with regard to torsion), the twisting of the beams could be reduced by the floor, if the tendency for end rotation of the floor is less than the tendency for twist of the ledge beam. However, in a system where the floor is slender, and the columns and/or the beam are stiffer, the situation could be the opposite, so that the torsion of the beam increases due to the deflection of the floor. Hence, each case is unique and requires careful considerations to evaluate the torsional interaction and its consequences with regard to design measures.

In the traditional classification of torsional interaction, it is assumed that compatibility torsion is associated with full continuity between the connected elements and hence that the connection is rigid. However, in a precast structure the compatibility conditions may be significantly influenced by the connection behaviour, since the deformations can be localised to the joints.

With regard to torsional interaction in precast concrete structures the following design problems can be identified:

(1) The twist and corresponding deformations (e.g. transverse deflection) of support beams and tilting at the beam supports may cause difficulties during erection of floor elements
(2) The twist of support beams relative to floor elements may look harmful in the service state with regard to aesthetical demands
(3) Torsional cracks in support beams may require precautions with regard to aesthetical demands
(4) The torsional moment that occurs under the design load in the ultimate limit state must be resisted by properly designed connections and precast elements
(5) Torsional moments resisted at beam end connections must also be further resisted by the vertical elements and the corresponding induced deformations must be considered, e.g. with regard to buckling of columns.

9.7.2 Eccentric loading of beam-floor connections

There are two fundamental approaches to consider eccentric loading on beams. In both cases the aim is to avoid a complex behaviour by applying simple support conditions, either at the beam-floor connection or at the beam supports.

(A) The floor is simply supported on the beam, see Fig. 9-57 a. The torsion that results from the eccentric loading must be resisted by the beam and the resulting torsional moment must be carried at the beam support. In this case no special reinforcement is needed in the connection to take up the eccentric loading.
(B) The floor is firmly connected to the beam and the beam is considered as an integrated part of the floor, which means that the floor span increases as shown in Fig. 9-57 b. The beam-floor

connection is designed for the eccentric loading. In this case the support of the beam should not be able to resist torsion but be free to rotate around its centroidal axis.

In practice intermediate situations may occur, which results in a more complex behaviour as discussed in Section 9.7.1.

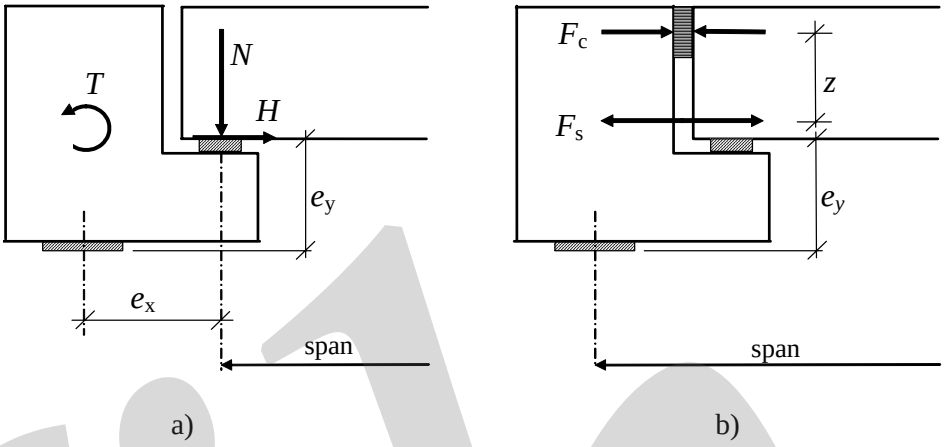

Fig. 9-57: Fundamental ways to consider eccentric loading on beams, a) the floor is simply supported on the beam, design approach (A), b) the floors firmly connected to the beam, which is free to rotate at its supports, design approach (B)

A typical example of a beam-floor connection designed according to design approach A is shown in Fig. 9-58. The connection is, however, able to transfer a tensile force from the floor to the beam to fulfil demands on structural integrity. When the floor is loaded the floor elements rotate, but this rotation is not transferred to the beam. However, since the beam is connected for tension transfer, in-plane deflection of the beam is prevented and it cannot deform fully freely.

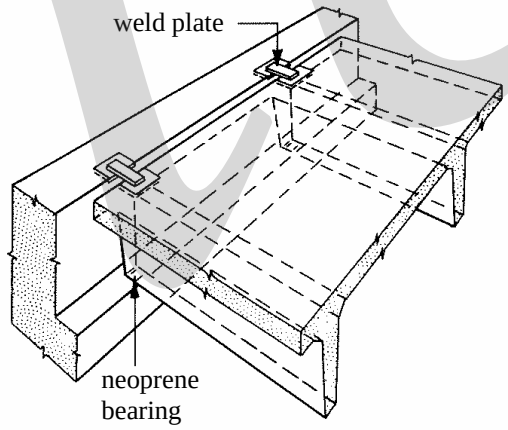

Fig. 9-58: Connection between double-T floor element and edge beam where there is no significant torsional restraint but where the horizontal deflection of the beam is restrained

Typical examples of connections designed according to design approach (B) are given in Fig. 9-59. The intention is that when the connection is completed, the floor and the beam should interact compositely. Temporary propping of the floor beam is absolutely needed during erection and casting of the in-situ joint concrete

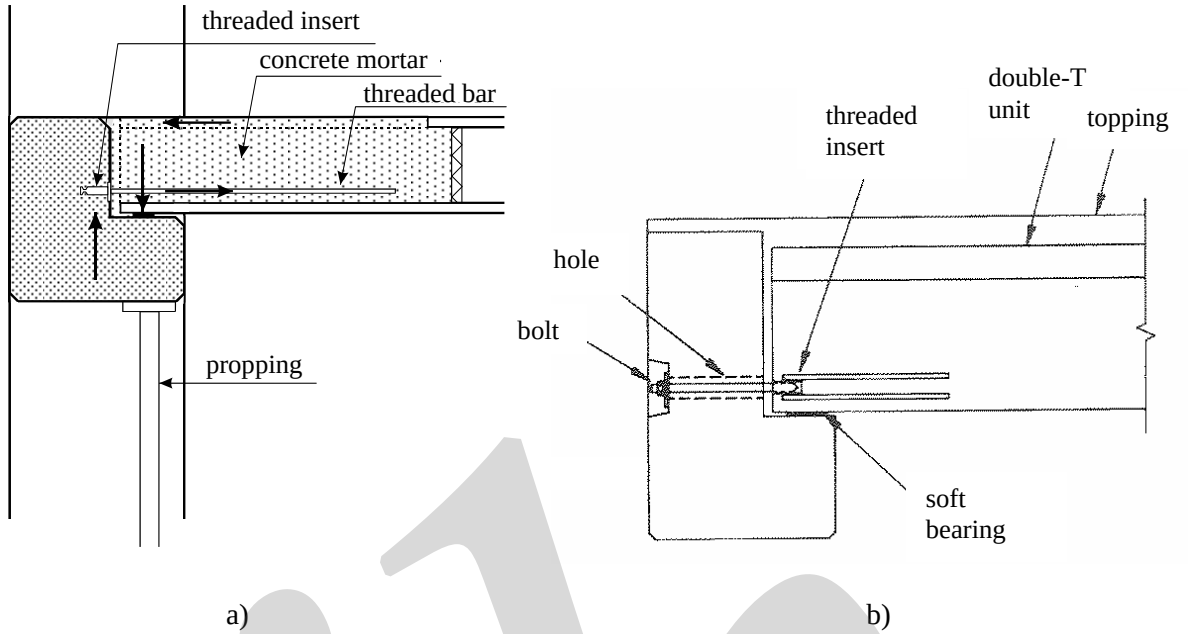

Fig. 9-59: Connection between floor slab and ledge beam providing torsional restraint, a) hollow core floor, b) double-T floor

In this case the floor-beam connection is designed and detailed to establish a force couple that counteracts the action from the eccentric vertical load from the floor. The connection is in the bottom part provided with devices that are able to transfer the tensile force in the force couple, see Fig. 9-59. These force transferring devices could be weld plates, anchor bars or loops from reinforcing bars that are anchored by grouting in recesses and cores. The compressive force transfer can be realised by steel plates, inserts or wedges placed in the joint between the floor element and the web of the beam or the joint can be filled with joint concrete or grout. The tensile force capacity provided between the floor and the support beam should also account for diaphragm action in the floor and possible restraint forces due to shrinkage, temperature effects etc. The common design approach is to calculate the horizontal force couple so that it counteracts the moment from the vertical load relative to the shear centre of the beam.

If the beam cannot rotate freely at its supports, a substantial moment can be transferred through the connection from the floor to the beam and result in compatibility torsion. The interaction depends on the rigidities within the structural systems and is influenced by cracking of the precast elements and the connections. The moment-rotation characteristics of the floor-beam connection are essential and it should be noted that the responses in positive and negative bending could be different, compare with Fig. 9-61.

Examples of the bending moment-rotation behaviour of connections between hollow core floor elements and ledge beams are shown in Figs. 9-60 – 9-61, from Bäckström (1993) and Lundgren (1995). Three different connections were loaded either in positive or negative bending. All connections were provided with a tying device fixed to the ledge beam and anchored by concrete in the mid core of the hollow core element. In connection type a (tests Nos. 1, 3 and 4) a bolt was fixed to a threaded insert in the ledge beam and spliced to a reinforcement loop anchored in the hollow core element with a cross bar inside the loop, see Fig 9-60 a. In connection type b (tests Nos. 2 and 5) a reinforcement bar with a threaded end was fixed to a threaded insert in the ledge beam, see Fig. 9-60 b. In connection type c (test No. 6) a reinforcement loop protruding from the beam was bent into a core where it was anchored by cast *insitu* concrete, Fig. 9-60 c. All the connections had a behaviour that could be characterised as ‘semi-rigid’. Before cracking the connection had a rigid behaviour. The cracking capacity of the joint could be significant and much greater than the capacity of the cracked connection.

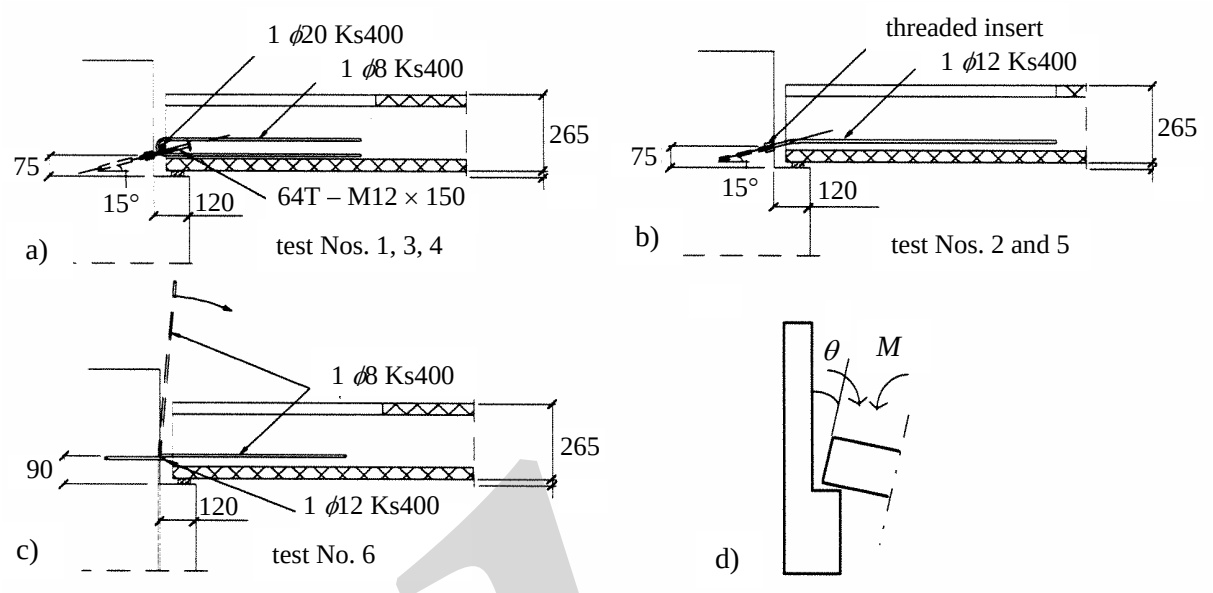

Fig. 9-60: Various support connections between hollow core floor elements and ledge beam, tested by Bäckström (1993), a) bolt in threaded insert spliced to loop, b) bar in threaded insert, c) projecting loop bent into recess, d) test procedure

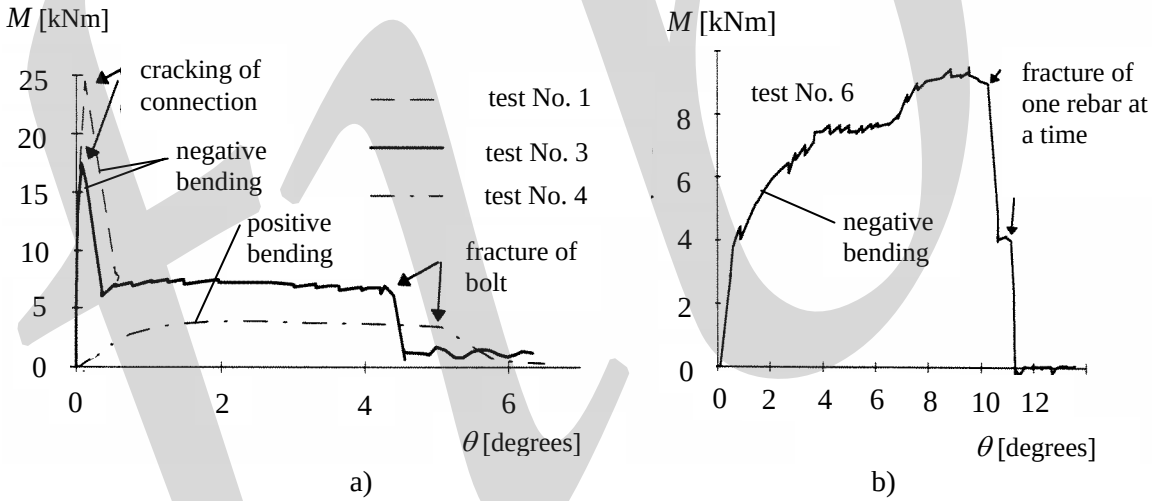

Fig. 9-61: Examples of bending moment-rotation relations from tests on support connections between hollow core floor element and ledge beam [Bäckström (1993), Lundgren (1995)], a) bolt in threaded insert spliced to loop, negative and positive bending, b) projecting loop bent into recess

An alternative type of floor/beam connection is shown in Fig. 9-62. Here tie bars anchored in two cores per hollow core unit are tied to stirrups that protrude from the support beam. This type of "composite connection" was tested by Elliott *et al.* (1993b).

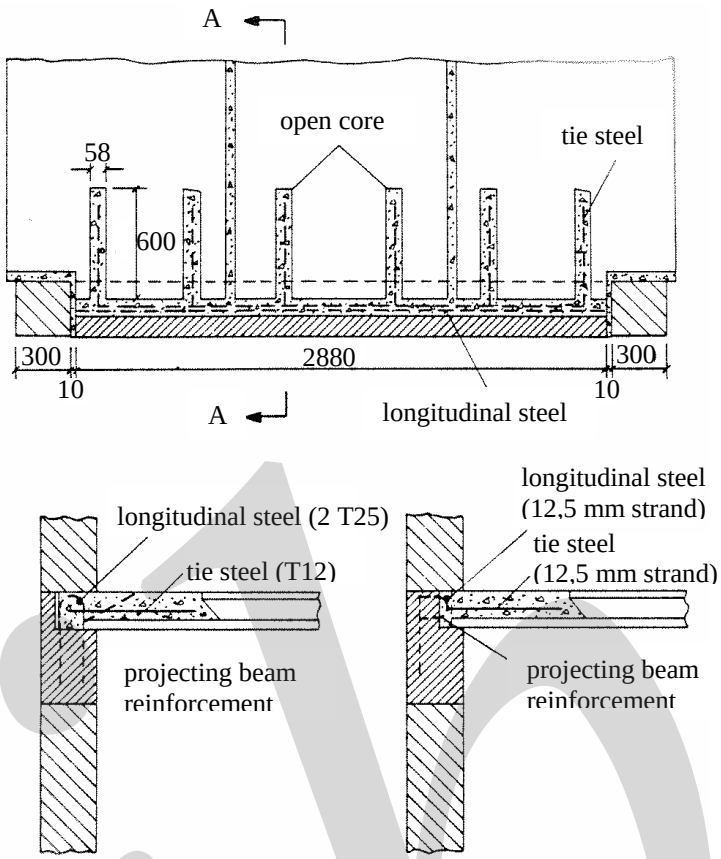

Fig. 9-62: Composite type of connection between hollow core floor and ledge bream [Elliott et al. (1993b)]

9.7.3 Eccentric loading of beam at support

In design approach (A), defined in Section 9.7.2, the beam support must be able to resist the torsional moment at the beam end. This means simple calculations of equilibrium torsion, which is statically determinate.

In design approach (B) the free rotation is often not fully developed. When using hidden steel corbels placed in the rotation centre of the beam and/or week columns the conditions can be regarded as 'free to rotate'. In these cases the calculation model is simple.

If the rotation is partially restrained at the beam supports, a more complex situation appears and a more advanced analysis is needed. This problem is statically indeterminate and the actual torsional moment and its distribution along the structural member depend on the rigidities of the interacting elements and their connections within the system as described in Section 9.7.1.

When torsion appears in beams, the beam itself should have sufficient torsional capacity and the resulting torsional moments at the ends of the beam must be resisted at the supports. However, in compatibility torsion the torsional moment depends on the rigidities and decreases when the beam cracks in torsion.

There are various alternatives to resist a torsional moment at beam end supports. In case of wide beams it might be possible to balance the torsional moment by an eccentricity of the reaction force in the support, see Fig. 9-63. In case of one-sided ledge beams this means that the support reaction might act mainly on the ledge itself, see Fig. 9-64. The connection zones of the supporting as well as of the supported elements must be designed and detailed accordingly to withstand the reaction in this eccentric location. The strut and tie method is appropriate for this purpose. The reaction is of course associated with small deformations in the support connection, which means that the tilting is not fully prevented.

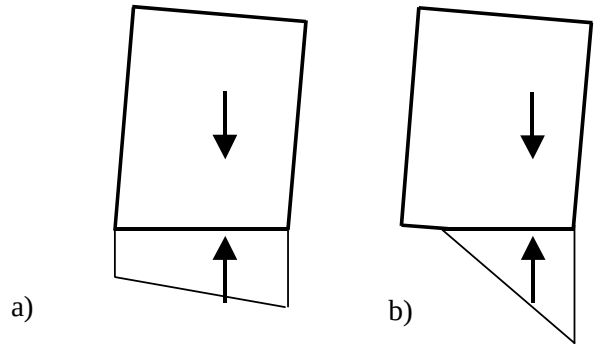

Fig. 9-63: A moderate torsional moment can be balanced at the beam support by an eccentric support reaction, a) support fully in compression, b) support partially in compression

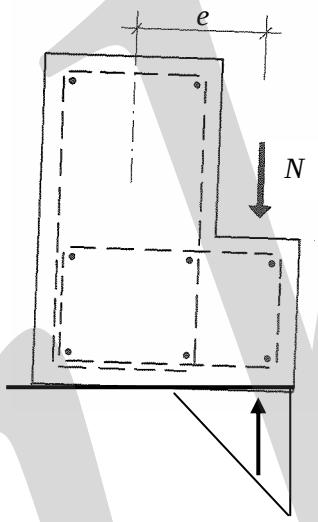

Fig. 9-64: At ledge beams the reaction might be concentrated towards the ledge, which must be considered in the design and detailing of the beam end

If the support joint is provided with a soft bearing, an eccentricity of the reaction force might result in an unacceptable or undesirable tilting of the beam at the support due to the flexibility of the bearing. To obtain a stiffer torsional restraint the connection can for instance be provided with eccentrically arranged bolts, see Fig. 9-65.

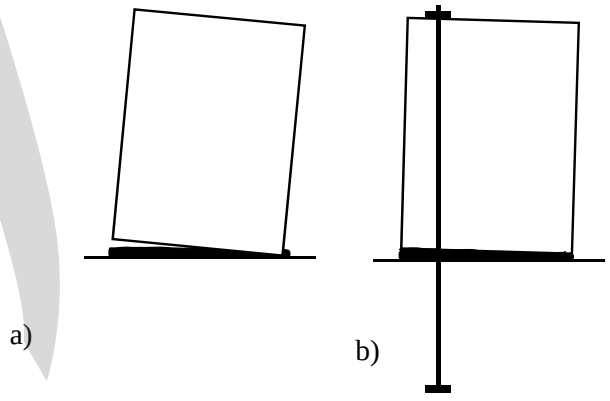

Fig. 9-65: Eccentric bolt increases the torsional restraint at the support and reduces the tilting of the beam even if the bolt is not needed with regard to the torsional resistance, a) tilting of beam without bolt, b) tilting prevented by bolt

In case of greater torsional moments and/or more narrow beams, it might be impossible to resist the torque just by an eccentric reaction. Instead the connection must be designed so that a force couple can be established to balance the torque. Force couples can be established by compressive, tensile or shear forces established by the basic force transfer mechanisms described in Chapters 6, 7, and 8. Some examples will be presented in the following.

On column heads the only possibility is to establish a force couple by vertical forces. A simple and common solution is to use a support bolt in an eccentric position or twin bolts as shown in Fig. 9-66 a. With this solution the beam can still move rather freely in relation to the support in the longitudinal direction. Alternatively the beam can be connected by welds between weld plates, see Fig. 9-66 b. In this case longitudinal movements are restrained and the corresponding restraint forces must be considered in the design.

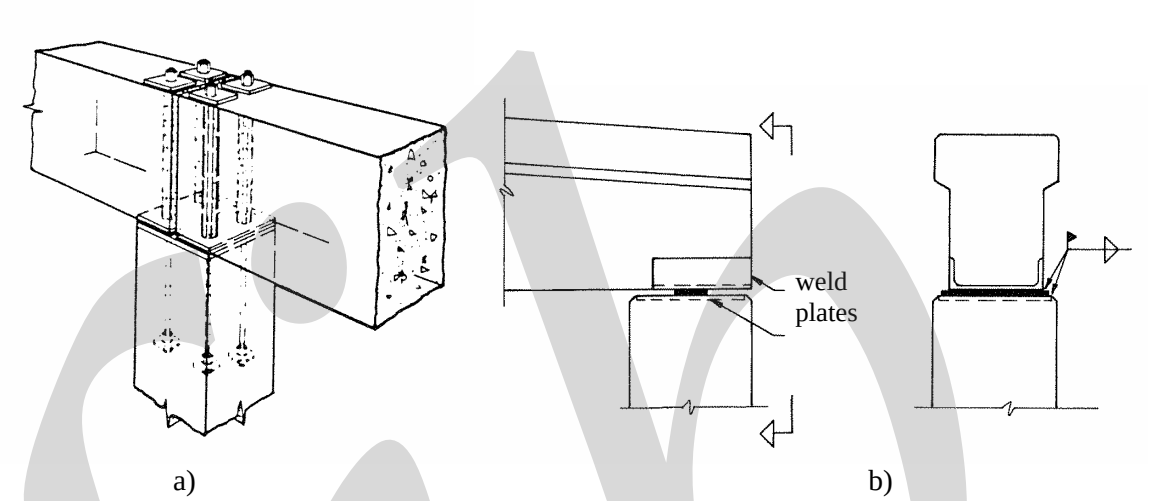

Fig. 9-66: Examples of torsion resistant connections at beam supports where a vertical force couple balances the torsional moment, a) eccentric bolts (Courtesy 'PCI Design Manual on Connections'), b) weld plate and eccentric welded joints

In case of beam supports on corbels, the column, which passes behind the beam end, gives a possibility to establish torsional transfer by horizontal forces in a force couple. Fig. 9-67 shows examples where a steel plate or a hollow steel section protrudes from the column face into a recess in top of the beam.

The steel plate, which is welded to the column, can slide in the 'tray' in order to prevent negative moments from developing. The horizontal force caused by the torsional moment is resisted by edge pressure between the plate welded to the column and the 'tray' in the top of the beam, and further on through the weld to the column. The balancing force couple consists of the contact force between the beam and the protruding steel detail and an opposite horizontal force developing at the support joint. This solution is only possible in case of smaller forces. Instead of a steel plate and a 'tray', the connection can be made by using hollow steel sections, where the one welded to the columns fits tightly into the one embedded in the beam.

Beam-column supports with a hidden support knife require special considerations with regard to transfer of torsional moments. Even if the support knife itself has a large capacity for torsion, the beam end might tilt slightly due to the clearance for the support knife in the recess. To prevent this tilting a permanent torsion resistant connection could be provided using the solution above, see Fig. 9-67 b. Depending upon the magnitude of the torsional moment, the hidden support knife can resist the opposite horizontal force in the force couple, or a similar solution must also be provided in the bottom of the beam. When the beam and column are large enough, double knifes could be used to balance torsion.

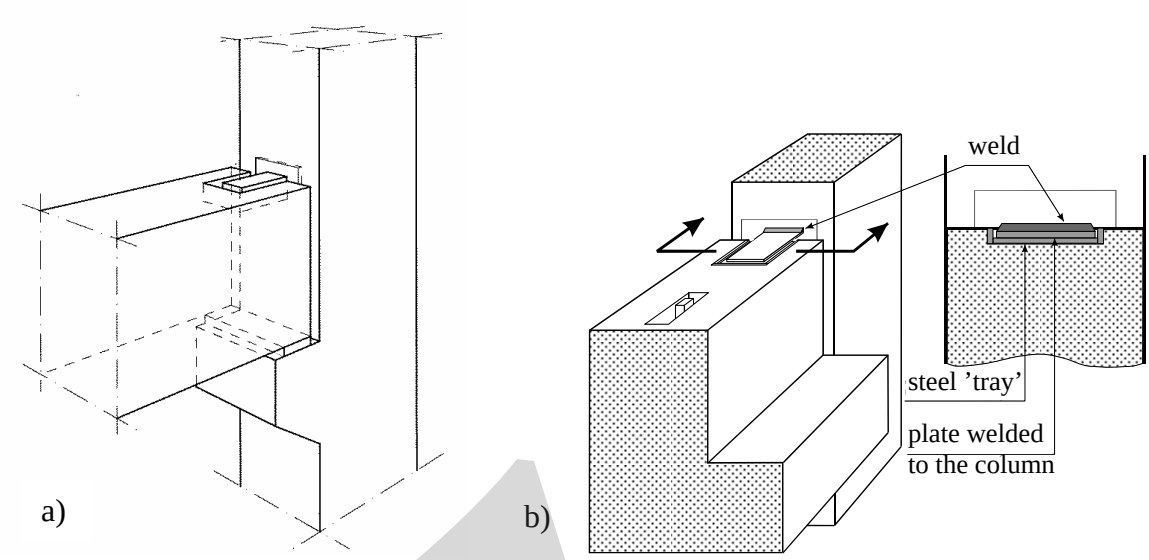

Fig. 9-67: Examples of torsion resistant connections at beam support where a horizontal force couple balances the torsional moment, a) beam support on corbel, b) beam support with hidden 'support knife'. In case of greater forces hollow steel sections should be used instead of steel plates

9.7.4 Considerations during erection

To prevent problems during erection and significant twist of support beams relative to the floor, the following alternative measures could be taken depending on the actual combination of influencing parameters.

(1) Propping or other stabilisation of the support beam during erection of the floor, establishment of rigid floor/beam connection (to avoid relative deformations), if necessary establishment of torsion resistant connections at the beam supports, removal of propping.

(2) Establishment of temporary torsion resistant connections at the beam supports (to avoid tilting of the beam ends during erection of the floor), erection of the floor, establishment of rigid floor/beam connection (to avoid additional relative deformations), removal of temporary connections.

(3) The same procedure as (2) but where permanent torsion resistant connections are provided at the beam ends instead of temporary ones.

In alternative (1) the beam is prevented from twisting relative to the floor by fixation in the floor/beam connection. In alternatives (2) and (3) the beam is allowed to twist in relation to the floor during erection. In both cases the beam will be subjected to torsion in the completed structure when the floor is loaded. Depending on the magnitude of the torsional moment and the corresponding twist, it might be necessary to design the beam and its supports for the torsion. In all the alternatives the torsion in the completed structure is of type "compatibility torsion" and the torsional moment in the beam is reduced when the beam cracks in torsion and/or the floor/beam connections crack.

In the first case tilting and twisting of the beam relative to the floor is prevented during erection along its whole length. The purpose is mainly to avoid problems during erection and to avoid that the beam becomes twisted in relation to the floor. The procedure is that the beam is placed and propped, see Fig. 9-68. Then the floor elements are placed and connected to the beam.

In alternatives (2) and (3) the beam is placed and fixed to the supports so that the torsional moment that arises during erection of the floor can be resisted there by temporary or permanent connection devices. The beam is not propped or stabilised by other means. When the floor elements are placed the beam twists and the corresponding torsional moments are balanced at the supports. Hence, the beam will get some twist relative to the floor. After erection the floor elements are connected to the beam.

In all the alternatives mentioned above, the beam/floor connection is designed to provide a torsional restraint between the beam and the floor and by that prevent or reduce the relative

deformation. In alternative (1) relative deformation for both dead weight and live load is prevented, but in alternatives (2) and (3) relative deformation under the dead weight is permitted.

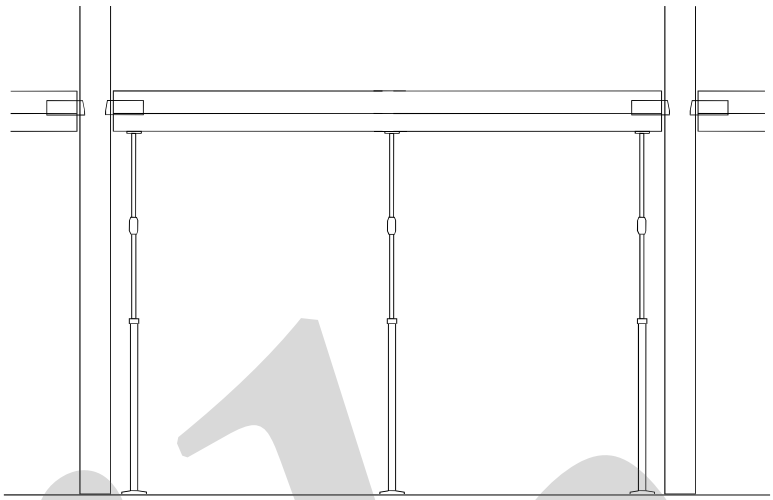

Fig. 9-68: Temporary propping of beam is used to prevent tilting and twisting of the beam during erection of floor slab

In cases when a torsion resistant connection is not required in the completed structures, temporary stabilization of the beam might be needed during erection of the floor to prevent tilting at the beam supports. Fig. 9-69 shows examples of temporary solutions for beams with a hidden support knife.

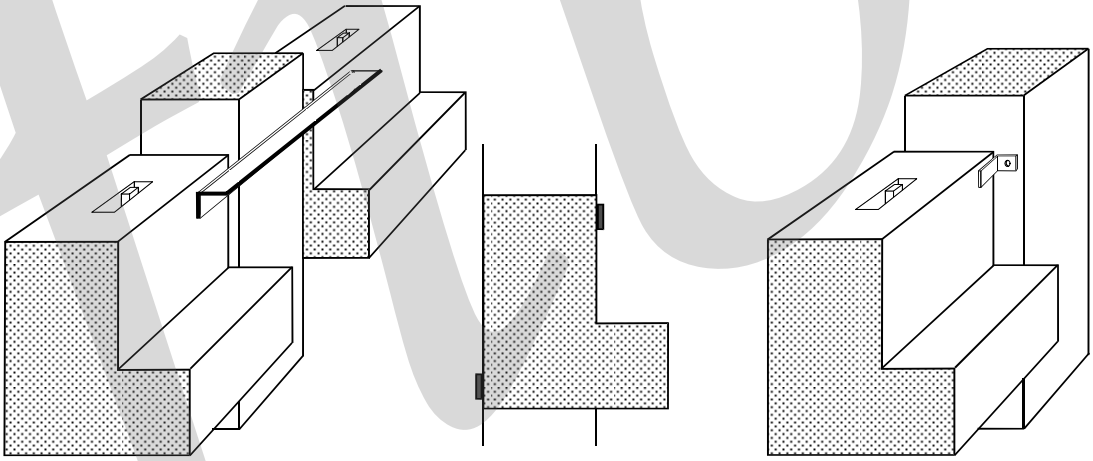

Fig. 9-69: Example of temporary torsion resistant connections at beam support with a hidden support knife, a) same width of column and beam web, b) different widths

Here temporary clamps of steel plates or angles are attached to the column. The connection to the column is established with short bolts in inserts, or longer bolts going through holes in the columns. The solution only requires one plate or angle at the top and bottom of the beam, on opposite sides. The disadvantage is that the columns must have threaded inserts or holes, which complicate the production. In case of small forces, the counteracting horizontal force can be resisted by the hidden support knife.

References

ACI (1995): *Building code requirements for structural concrete (ACI 318-95) and Commentary (ACI 318R-95)*. American Concrete Institute, Farmington Hills, 1995, 369 pp.

Basler and Witta (1966): Basler, E. and Witta, E., *Grundlagen für kraftschlussige Verbindungen in der Vorfabrikation.* (Basics of structural connections in prefabrication. In German). Technische Forschungs- und Beratungsstelle der Schweizerischen Zementindustrie, Wildegg, 1966.

BBK 94 (1995): *Boverkets handbok om betongkonstruktioner, Band 1 Konstruktion.* (Handbook on concrete structures, Vol. 1 Design. In Swedish). National Board of Housing, Building and Planning (Boverket), Karlskrona, 1998, 166 pp.

Bergström (1994): Bergström, S., *Inspänning av betongelementpelare med grundskruv och stålfot.* (Fixation of precast concrete columns with bolts and steel feet. In Swedish). Chalmers University of Technology, Division of Concrete Structures, Master's thesis 94:1, Göteborg, 1994.

Betongelementföreningen (1990): *Anslutningar*. (Structural connections. In Swedish). Swedish Precast Concrete Federation, Publication No. 41, Bromma, 1990.

Birkeland and Birkeland (1966): Birkeland, P.W. and Birkeland, H.W., Connections in precast concrete construction, *ACI Journal*, 1966.

BLF (1994-1997): *Betongelementboken, Bind A-F.* (Design manual for precast concrete, Vol. A-F. In Norwegian). Betongindustrins Landsforening, Oslo 1994-1997.

BLF (1995): *Betongelementboken, Bind B.* (Design manual for precast concrete, Vol. B. In Norwegian). Betongindustrins Landsforening, Oslo 1995, 296 pp.

BLF (1996): *Betongelementboken, Bind C.* (Design manual for precast concrete, Vol. C. In Norwegian). Betongindustrins Landsforening, Oslo 1996, 293 pp.

BLF (1997): *Betongelementboken, Bind D* (Design manual for precast concrete, Vol. D. In Norwegian). Betongindustrins Landsforening, Oslo 1997, 127 pp.

Bljuger (1987): Bljuger, F., *Design of precast concrete structures*. Ellis Horwood, Chichester, 1987, 296 pp.

Brüggeling and Huyghe (1991): Brüggeling, A.S.G. and Huyghe, G.F., *Prefabrication with concrete*. Balkema, Rotterdam, 380 pp.

BSI (1985): *British Standard 8110, Part 1*, *The structural use of concrete*. British Standard Institution, London, 1985.

Bäckström (1993): Bäckström, M., *Anslutningar vid ändupplag för hålelement.* (Connections at end support of hollow core units. In Swedish). Chalmers University of Technology, Division of Concrete Structures, Master's thesis 93:1, Göteborg, 1993.

Canha *et al*. (2007): Canha, R.M.F., El Debs, A.L.H. and El Debs, M.K., Design model for socket base connections adjusted from experimental results. *Structural Concrete*, Journal of *fib*, Vol. 8, No. 1, March 2007, pp. 3-10.

Carlsson (1979): Carlsson K.-I., *Skjuvningskapacitet hos armerade fogar i betong-konstruktioner*. (Shear capacity of reinforced joints in concrete structures. In Swedish). Royal Institute of Technology, Department of Bridge Engineering, Notice 3/79, Stockholm 1979.

CEB (1985): *Draft guide for the design of precast wall connections, contribution to Sesion Plenere de CEB Rotterdam*. Comite Euro-International du Beton, Bulletin d'Information No. 169, June 1985.

CEB (1991): *Fire design of concrete structures*. Comite Euro-International du Beton, Bulletin d'Information No. 208, Lausanne, July 1991.

CEB (1994): *Fastenings to concrete and masonry structures*. Comite Euro-International du Beton, Bulletin d'Information No. 216, Lausanne, July 1994.

CEB (1997): *Design of fastenings in concrete*, *Design Guide – Parts 1 to 3*. Comite Euro-International du Beton, Bulletin d'Information No. 233, Thomas Telford, London. 1997.

CEB-FIP (1992): *CEB-FIP Model Code 1990, Design Code*. Comite Euro-International du Beton, Bulletins d'Information Nos. 203-205, Thomas Telford, London. 1993.

CEN (2004): *EN 1992-1-1, Eurocode 2: Design of concrete structures – Part 1-1: General rules and rules for buildings*. European Committee for Standardization, Brussels, 2004, 225 pp.

CEN (2005): EN1992-1-2. Eurocode 2: *Design of concrete structures – Part 1-2: General – Structural fire design*. European Committee for Standardization, Brussels, 2005,

Cheok and Lew (1990): Cheok, G.S. and Lew, H.S., *Performance of one-third scale model of a precast concrete beam-column connection subjected to cyclic inelastic loads*. 1st Meeting of Joint Technical Coordinating Committee on Precast Seismic Structural Systems, Proceedings, San Diego, Nov. 1990, p. 104.

Cheok and Lew (1993): Cheok, G.S. and Lew, H.S., Model precast concrete beam-column connections subjected to cyclic loading. *PCI Journal*, Vol. 38, No. 4, July-Aug. 1993, pp. 80-92.

Cholewicki (1985): Cholewicki, A., *Analysis of shear walls*. Swedish Council for Building Research, Document D4:1985.

Cholewicki (2000): Cholewicki, A., *Tying in precast framed buildings made with hollow core floors – specific problems of design*. Second International Symposium on Prefabrication, Cement Concrete Association, Helsinki, May 2000.

Cholewicki and Szule (2006): Cholewicki, A. and Szule, J., *Model of composite beam for analysis of the interaction of precast floor slabs*. (In Polish). Building Research Institute, Quartely No. 2 (138), Warsaw, 2006.

Cholewicki and Szule (2007): Cholewicki, A., Szule, J., Interaction in precast composite beams. *Beton+Fertigteiltechnik*, No. 5, 2007.

Collins *et al.* (1989): Collins, D.M., Klingner, R., Polyzois, D., *Load-deflection behaviour of cast-in-place and retrofit concrete anchors subjected to static, fatigue, and impact loads.* University of Texas at Austin, Center for Transportation Research, Report No. 1126-1, 1989.

Comair and Dardare (1992): Comair, F. and Dardare, J., *Model testing of precast concrete semi-rigid connection*. COST C1, Proceedings of the first state of the art workshop, Semi-rigid behaviour of civil engineering structural connections, E.N.S.A.I.S., Strasborg, pp. 99-119.

COST C1 (1998): *Control of the semi-rigid behaviour of civil engineering structural connections*. COST C1, Proceedings of the international conference, Liége, September 1998.

CPCI (1982): *Metric design manual, precast and prestressed concrete*. Canadian Precast Concrete Institute, Ottawa, 1982.

CUR (1988): *Ontwerp en betrouwbaarheid van demontabele betonconstructies*. (In Dutch). Civieltechnisch Centrum Uitvoering Research en Regelgeving, CUR-report 88-1, Gouda, 1988.

Daschner (1980): Daschner, F., *Schubkraftübertragung in Rissen von Normal- und Leichtbetong*. (Transfer of shear force in cracks in ordinary and light-weight concrete. In German). Technical University of Munich, Preliminary Report, March 1980, 93 pp.

Davies *et al.* (1990): Davies, G., Elliott, K.S., Omar, W., Horizontal diaphragm action in precast hollow core floors. *The Structural Engineer*, Vol. 68, No. 2, 1990.

deChefdebien and Dardare (1994): deChefdebien, A. and Dardare, J., *Experimental investigations on current connections between precast concrete components*. COST C1 Proceedings of the second state of the art workshop, Semi-rigid behaviour of civil engineering structural connections, Prague, pp. 21-30.

Dragosavić *et al.* (1975): Dragosavić, M., van den Beukel, A., Gijsbers, B.J., Loop connections between precast concrete components loaded in bending. *Heron*, Vol. 20, No. 3, 1975.

Dulácska (1972): Dulácska, H., Dowel action of reinforcement crossing cracks in concrete. *ACI Journal*, Vol. 69, No. 12, 1972, pp. 754-757.

Eligehausen *et al.* (1987): Eligehausen, R., Fuchs, W., Mayer, B., Loadbearing behaviour of anchor fastenings in tension. *Betonwerk + Fertigteil – Technik*, No. 12, 1987, pp. 826-832, No. 1, 1988, pp. 29-35.

Eligehausen and Fuchs (1988): Eligehausen, R.and Fuchs, W., Loadbearing behaviour of anchor fastenings under shear, Combined tension and shear or flexural loading. *Betonwerk + Fertigteil – Technik*, No. 2 1988, pp. 48-56.

Elliott *et al.* (1992): Elliott K.S., Davies, G., Omar, W., Experimental and theoretical investigation of precast hollow cored slabs used as horizontal diaphragms. *The Structural Engineer*, Vol. 70, No. 10, May 1992.

Elliott *et al.* (1993a): Elliott, K.S., Davies, G. And Mahdi, A.A., Semi-rigid connections in precast concrete frames. *Betonwerk und Fertigteil-Technik*, Vol. 59, No. 9, pp. 79-94.

Elliott *et al.* (1993b): Elliott, K.S., Davies, G., Adlparvar, M., Torsional behaviour of precast concrete edge beams and connections. *Magazine of Concrete Research*, Vol. 45, No. 164, Sept. 1993, pp. 157-168.

Elliott (1996): Elliott, K.S., *Multi-storey precast concrete framed structures*. Blackwell Science, Oxford, 1996, 624 pp.

Elliott *et al.* (1997): Elliott, K.S., Davies, G., Gorgun, H., Semi-rigid connections in precast concrete frames. *FIP Notes*, Vol. 1997/4, pp. 6-12.

Elliott *et al.* (1998): Elliott, K.S., Davies, G., Gorgun, H., Adlparvar R., Stability of semi-rigid precast concrete structures. *PCI Journal*, Vol. 43, No. 2, pp. 42-60.

Elliott (2002): Elliott, K.S., *Precast concrete structures*, Butterworth-Heineman, Oxford, April 2002, 380 pp.

Elliott *et al*. (2004): Elliott, K.S., Ferriera, M., El Debs, M., *Classification methods for semi-rigid connections in precast concrete building structures*. CONCET 2004, 8th International Conference on Concrete Technology, Malaysia, April 2004, CD no pages.

Elliott *et al*. (2005): Elliott, K.S., Ferriera, M., de Aranjo, D., El Debs, M., *Analysis of multi-storey precast frames considering beam-column connections with semi-rigid behaviour*. *fib* Symposium 'Keep Concrete Attractive', Proceedings, Budapest, May 2005, pp. 496-501.

Englekirk (1995): Englekirk, R.E., Developing and testing of a ductile connector for assembling precast concrete beams and columns, *PCI Journal*, Vol. 40, No. 2, March-April 1995, pp. 36-51.

Engström (1990): Engström, B., Combined effects of dowel action and friction in bolted connections. *Nordic Concrete Research*, The Nordic Concrete Federation, Publication No. 9, Oslo 1990, pp. 14-33.

Engström (1992): Engström B., *Ductility of tie connections in precast structures*. Chalmers University of Technology, Division of Concrete Structures, Publication 92:1, Göteborg. 1992, pp. 452.

Engström *et al.* (1998): Engström, B., Magnusson, J., Huang, Z., *Pull-out bond behaviour of ribbed bars in normal and high-strength concrete with various confinements*. Bond and Development of Reinforcement – A Tribute to Dr. Peter Gergely, ACI SP-180, February 1998, pp. 215-242.

Eriksson *et al.* (1978): Eriksson, A., Kärrholm, G., Petersson, H., *Ductile shear key joints in large panel structures*. RILEM-CEB-CIB Symposium on mechanical and insulating properties of joints of precast reinforced concrete elements, Proceedings, Nat. Techn. Univ. of Athens, 1978.

Ferriera *et al.* (2003b): Ferriera, M.A., El Debs, M.K., Elliott, K.S., *Analysis of multi-storey precast frames with semi-rigid connections*. Brazilian Conference on Concrete, IBRACON 2003, 45th Brazilian Concrete Congress, Brazilian Concrete Institute – IBRACON, Victoria, Brazil, August 2003, CD no pages.

fib (2000a): *Special design considerations for precast prestressed hollow core floors*. Guide to good practice, fédération internationale de béton, Bulletin 6, Lausanne 2000.

fib (2000b): *Bond of reinforcement in concrete*. fédération internationale de béton, Bulletin 10, Lausanne 2000.

fib (2003a): *Environmental issues in prefabrication*. State-of-the-art report, fédération internationale de béton, Bulletin 23, Lausanne 2003.

fib (2003b): *Seismic design of precast concrete building structures*. State-of-the-art report, fédération internationale de béton, Bulletin 27, Lausanne 2003.

Fintel *et al.* (1976): Fintel, M., Schulz, D., Iqbal, M., *Philosophy of structural response to normal and abnormal loads*. Design and construction of large-panel concrete structures – report 2, Portland Cement Association, Skokie, 1976.

FIP (1982): *Shear at the interface of precast and in-situ concrete*. Guide to good practice, FIP/9/6, London, 1982.

FIP (1988): P*recast prestressed hollow core floor*. FIP Recommendations, Thomas Telford, London, 1988.

FIP (1998): *Composite floor structures*. FIP Guide to good practice, FIP, May 1998.

Friberg (1938): Friberg, B.F., Design of dowels in transverse joints of concrete pavements. *American Society of Civil Engineers, Proceedings*, Vol. 64, No. 2, November 1938, pp. 1809-1828.

Fuchs *et al*. (1995): Fuchs, W., Eligehausen, R., Breen, J.E., Concrete Capacity Design (CCD), Approach for fastening to concrete. *ACI Structural Journal*, Jan.-Feb. 1995, pp. 73-94.

Furche and Eligehausen (1990): Furche, J., Eligehausen, R., *Lateral blow-out of headed studs near the free edge*. ACI – convention, Toronto, 1990.

Gustavsson (1981):Gustavsson, K., *Fogar i samverkande betongkonstruktioner med tunn pågjutning.* (Joints in composite concrete structures with thin topping. In Swedish). Chalmers University of Technology, Division of Concrete Structures, Report 81:7, Göteborg 1981.

Harryson (2002): Harrysson, P., *Industrial bridge construction – merging development of process, productivity and products with technical solutions*. Chalmers University of Technology, Department of Structural Engineering – Concrete Structures, Publication 02:1, Göteborg 2002.

Højlund-Rasmussen (1963): Højlund-Rasmussen, B., Betoninstöbte, tvaerbelastade boltes og dornes baereevne. (Resistance of embedded bolts and dowels loaded in shear. In Danish).

Bygninsstatiske Meddelser, No. 34, 1963.

IABSE (1981): *General principles on quality assurance for structures*. IABSE, Joint Committee on Structural Safety, Zürich, 1981.

J.V. Inc.: *Design guide for masticord structural bearing pad*

Keronen (1996): Keronen, A., *Effect of semi-rigid connections in reinforced precast portal frame – load tests*. Tampere University of Technology, Report 69, Tampere, Finland, 1996.

Klein (1986): Klein, G.J., Design of spandrel beams. *PCI Journal*, Sept.-Oct. 1986, Vol. 31, No. 5, pp. 76-124.

Korolev and Korolev (1962): Korolev, L.V. and Korolev, H.V., *Joint between prefabricated reinforced column and foundation*. Promyshlennoe SroitelÕstvo, Vol. 16, No. 9, 1962.

Kuttab and Dougill (1988): Kuttab, A. and Dougill, J.W., Grouted and dowelled jointed precast concrete columns, behaviour in combined bending and compression. *Magazine of Concrete Research*, Vol. 40, No. 144.

König (1981): König, J., *The composite beam action of cold-formed sections and boards*. Swedish Council for Building Research, Document D14, 1981.

Leon (1998): Leon, R.T., *Developments in the use of partial restraint frames in the United States*. COST C1, Control of the semi-rigid behaviour of civil engineering structural connections, Proceedings of the international conference, Liége, September 1998.

Leonhardt (1975): Leonhardt, F., *Vorlesungen über Massivbau – Zweiter Teil, Sonderfälle der Bemessung im Stahlbetonbau*. (Lectures in Concrete Structures – Second Part, Special Cases of Calculations. In German). Springer-Verlag, 1975.

Leskelä and Pajari (1995): Leskelä, M.V. and Pajari, M., *Reduction of the vertical shear resistance in hollow-core slabs when supported on beams*. Concrete 95 Conference, Brisbane, Australia, 4-7 September 1995, Proceedings, pp. 559-568.

Lindberg and Keronen (1992): Lindberg, R. and Keronen, A., *Semi-rigid behaviour of a RC portal frame*, COST C1 Proceedings of the first state of the art workshop, Semi-rigid behaviour of civil engineering structural connections, E.N.S.A.I.S., Strasborg, pp. 53-63.

Lindberg (1992): Lindberg, R., *Beam-to-column connections in storey height concrete frame.* Tamepre University of Technology, Report 57, Tampere, Finland, 104 pp.

Loo and Yao (1995): Loo, Y.C. and Yao, B.Z., Static and repeated load tests on precast concrete beam-to-column connections. *PCI Journal*, Vol. 40, No. 2, March-April 1995, pp. 106-115.

Loov (1978): Loov, R.E., *Welds and bending details for precast concrete connections*. Course Manual for seminar presented for COMPA International pte ltd, Singapore, September 25-27, 1978, pp. 32-41.

Losberg and Olsson (1979): Losberg, A. and Olsson, P.-Å., Bond failure of deformed bars based on longitudinal splitting effects on the bars. *ACI Journal*, No. 1, Vol. 76, 1979, pp. 5-18.

Lundgren (1995): Lundgren, K., *Slender precast systems with load-bearing façades*. Chalmers University of Technology, Division of Concrete Structures, Publication 95:2, Göteborg, 1995.

Martin and Korkosz (1982): Martin, L.D. and Korkosz, W.J., *Connections for precast prestressed concrete buildings including earthquake resistance*. National Science Foundation, Washington and PCI, Chicago, 1992.

Mattock (1974): Mattock, A.H., *Shear transfer in concrete having reinforcement at an angle to the shear plane*. ASCE, SP 42 'Shear in reinforced concrete', Michigan 1974, pp. 17-42.

Menegotto (1988): Menegotto, M., *Hollow core floor tests for seismic action*. FIP Symposium, Proceedings, Jerusalem, 1988.

Menegotto (2000): Menegotto, M.: *Precast floors under seismic actions*. The second International Symposium on Prefabrication, Proceedings, Helsinki, Finland, May 2000.

Menegotto and Monti (2005): Menegotto, M. and Monti, G., Waved joint for seismic-resistant precast floor diaphragms. *ASCE Journal of Structural Engineering*, Vol. 131, No. 10, October 2005.

Moriata and Kaku (1975): Morita, H. and Kaku, T., *Cracking and deformations of R.C. prisms subjected to tension*. CEB-CIB-FIP-IASS-RILEM Symposium on behaviour in service of concrete structures, Proceedings, Vol. 2, University of Liege, 1975, pp. 583-594.

Möllersten and Packalen (1966): Möllersten, N.B.I. and Packalen, J.M., *Experimentell undersökning av friktionen vid upplag för förtillverkade balkar* (Experimental study of friction at supports of precast beams. In Swedish). Royal Institute of Technology, Department of Bridge Engineering, Master's thesis 129, Stockholm 1966.

Nakaki *et al.* (1994): Nakaki, S.D., Englekirk, R.E., Plaehn, L., Ductile connectors for a precast concrete frame. *PCI Journal*, Vol. 39, No. 5, Sept.-Oct. 1994, pp. 46-59.

Nielsen (1984): Nielsen, M.P., *Limit analysis and concrete plasticity*. Prentice-Hall, New Jersey, 1985.

Odgård (1976): Odgård, A , *Strength of locally damaged walls consisting of large prefabricated concrete panels*. Byggeteknisk Konstruktionsforsknings Central, Report 54, Lyngby, 1976.

Ottolini (1986): Ottolini, P.: *Shear resistance of joint between hollow-core slabs*. Notes, 1986.

Pajari (1995): Pajari, M., *Shear resistance of prestressed hollow core slabs on flexible supports*. Technical Research Centre of Finland, VTT Publication No. 218, 1995.

Pajari and Koukkari (1998): Pajari, M. and Koukkari, H.,Shear resistance of PHC slabs supported on beams, I: Tests. *Journal of Structural Engineering*, Vol. 124, No.9, September, 1998, pp.1050-1061.

Pajari (1998): Pajari, M., Shear resistance of PHC slabs supported on beams, II: Analysis. *Journal of Structural Engineering*, Vol. 124, No. 9, September, 1998, pp. 1062-1073.

Park (1986): Park, R., *Seismic design considerations for precast concrete construction in seismic zones*. Seminar on precast concrete construction in seismic zones, Japan Society for the promotion of science & U.S. National Science Foundation, Proceedings, Vol. 1, pp. 1-38, Tokyo.

Paschen and Zillich (1980): Paschen, H. and Zillich, V., The butt jointing or precast concrete columns. *Betonwerk + Fertigteil – Technik*, Nos. 5-6, 1980.

Paschen *et al.* (1981): Paschen, H., Stockleben, V.C., Zillich, V., Transverse tensile stress in mortar joints due to transverse strain and partial area loading. *Betonwerk + Fertigteil – Technik*, No. 7, 1981.

Pillai *et al.* (1981): Pillai, S.U. and Kirk, D.W., Ductile beam-column connections in precast concrete. *ACI Journal*, Nov.-Dec. 1981, pp. 480-487.

Rahlwes (1989): Rahlwes, K., Lagerung und Lager von Bauwerken. (Bearings and joints in building structures. In German). *Beton-Kalender* 1989, Vol. 2.

Reinhardt (1982): Reinhardt, H.W., Length influence on bond shear strength of joints in composite precast concrete slabs. *The International Journal of Cement Composites and Light-weight Concrete*, Vol. 4, No. 3, August 1982.

Rehm *et al.* (1988): Rehm, G., Eligehausen, R., Mallée, R., Befestigungstechnik. (Fixation technique. In German). *Beton-Kalender* 1988, Vol. 2, Berlin, 1988, pp. 564-663.

Rosman (1968): Rosman R., *Statik und Dynamik der Scheibensysteme des Hochbaues*.(Statics and dynamics of large panels systems for high buildings. In German). Springer Verlag, Berlin, 1969.

Roose *et al.* (1983): Roose, L.W., Reinhardt, H.W., Huyghe, G.F., Onderzoek naar de eigenshappen van voegen tussen gepraficeerde kanalplaten zonderm druklaag. (Investigation of the properties of joints between prefabricated hollow core units subjected to compression. In German). *Cement* XXXV, No. 1, 1983.

SBI (1979): Skivebygningers stabilitet 2, Beregningsmetoder. (Stability of large panel buildings, calculation methods. In Danish). Statens byggeforskningsinstitut, SBI report 115, Danmark, 1979.

Schäfer (1999a): Schäfer, K., *Deep beams and discontinuity regions*, Section 7.3 in Structural Concrete, Vol. 3. fédération internationale de béton, Bulletin 3, Lausanne 1999, pp. 141-184.

Schäfer (1999b): Schäfer, K., *Nodes*, Section 4.4.4 in Structural Concrete, Vol. 2. fédération internationale de béton, Bulletin 2, Lausanne 1999, pp. 257 – 275.

Schleich and Schäfer (1991): Schleich, J. and Schäfer, K., Design and detailing of structural concrete using strut-and-tie models. *The Structural Engineer*, Vol. 69, No, 6, March 1991.

Stanton *et al.* (1987): Stanton, J.F., Anderson, R.G., Dolan, C.W., McCleary, D.E., *Moment resistant connections and simple connections*. Final Report to PCI, Specially funded R&D projects Nos. 1 & 4, 1986, and *PCI Journal*, Vol. 32, No. 2, pp. 62-74.

SIS (1978): *Betongytor, bestämning av ytojämnhet.* (Concrete surfaces, determination of unevenness. In Swedish). Byggstandardiseringen, Swedish Standard 812005, Stockholm 1978.

Soroushian and Choi (1989): Soroushian, P. and Choi, K.-B., Local bond of deformed bars with different diameters in confined concrete. *ACI Structural Journal*, Vol. 86, No. 2, March-April 1989.

Svensson et al. (1986): Cederwall, K., Engström, B., Svensson, S., Diaphragm action of precast floors with grouted joints. *Nordisk Betong*, No. 1-2, 1986.

Tassios and Vintzeleou (1987): Tassios, T.P., Vintzeleou, E.N., Concrete to concrete friction. *Journal of Structural Engineering*, ASCE, Vol. 113, No. 4, 1987, pp. 832-849.

Tassios (1979): Tassios, T.P., *Properties of bond between concrete and steel under load cycles idealising seismic actions*. Comité Euro-International du Beton, Bulletin d´Information No. 131, Paris 1979, pp. 65-122.

Tassios and Tsoukantas (1978): Tassios, T.P. and Tsoukantas, S.G., *Serviceability and ultimate limit-states of large panel connections under static and dynamic loading*. RILEM-CEB-CIB Symposium on mechanical and insulating properties of joints of precast reinforced concrete elements, Proceedings, Nat. Techn. Univ. of Athens, 1978.

Tepfers (1973): Tepfers, R., *A theory of bond applied to overlapped tensile reinforcement splices for deformed bars*. Chalmers University of Technology, Division of Concrete Structures, Publication 73:2, Göteborg 1973.

Tsoukantas and Tassios (1989): Tsoukantas, S.G., Tassios, T.P., Shear resistance of connections between linear elements. *CIB Structural Journal*, May-June, 1989.

Vambersky and Walraven (1988): Vambersky, J.A., Walraven, J.C., The bearing capacity of unreinforced mortar joints loaded in compression. *Betonwerk + Fertigteil – Technik*, No. 7, 1981.

Vambersky *et al.* (2000): Vambersky, J.N.J.A., Walraven, J.C. , Straman, J.P., *Designing and understandning precast concrete structures in buildings*. Delft University of Technology, Division of Concrete Structures, Delft 2000.

Vinje (1985a): Vinje, L., Bemessung von unbewehrten Elastomer-Lagern in Betonfertigteilbauten. (Behaviour and design of plain elastomeric bearing pads in precast structures. In German). *Betonwerk + Fertigteil – Technik*, Nos. 5-6, 1985.

Vinje (1985b): Vinje, L., Behaviour and design of plain elastomeric bearing pads in precast structures. *PCI Journal*, Nov.-Dec., 1985.

Vinje (1986): Vinje, L., Bearing pads for prestressed hollow core slabs. *Betonwerk + Fertigteil – Technik*, No, 10, 1986.

Vintzeleou (1986): Vintzeleou, E.N., *Mechanisms of load transfer along concrete interfaces under monotonic and cyclic actions*. (In Greek). National Technical University of Athens, Department of Civil Engineering, PhD thesis, 1986, 359 pp.

Vintzeleou and Tassios (1985): Vintzeleou, E.N. and Tassios, T.P., Mechanisms of load transfer along interfaces in reinforced concrete, Prediction of shear force vs. shear displacement curves. *Studie Ricerche*, No. 7, Corpo di Perfezionamento per le Construzioni in Cemento Amato, Italcementi Societa per Azioni (S. p: A), Bergamo, 1985, pp. 121-161.

Vintzeleou and Tassios (1987): Vintzeleou, E.N. and Tassios, T.P., Behaviour of dowels under cyclic deformations. *ACI Structural Journal*, Vol. 84, No. 1, Jan.-Feb., 1987, pp. 18-30.

VTT (2002): Experimental research on wall-slab connections, VTT Technical Research Centre of Finland, Research report No. RTE77/02, Espoo 2002.

VTT (2003): Experimental research on wall-hollow core slab connections. VTT Technical Research Centre of Finland, Research report No. RTE3960/03, Espoo 2003.

Walraven *et al.* (1979): Walraven J.C., Vos, E., Reinhardt, H.W., *Experiments on shear transfer in cracks in concrete, Part 1: Description of results*. Delft University of Technology, Report No. 5-79-3, 1979, 89 pp.

Walraven (1981): Walraven, J.C., Fundamental analysis of aggregate interlock. *ASCE Journal of the Structural Division*, Vol. 11, November 1981, pp. 2245-2270.

Walraven (1990): Walraven, J. C., *Transmission of vertical shear forces across longitudinal joints between prestressed hollow core slabs*. Notes, 1990.

Walraven and Stroband (1997): Walraven, J. and Stroband, J., *The behaviour of cracks in plain and reinforced concrete subjected to shear*. 5th International Symposium on Utilization of High Strength/High Performance Concrete, 20-24 June 1999, Sandefjord, Proceedings, Vol. 1, pp. 701-708.

Westerberg (1999): Westerberg, B., *Stabilisation of buildings*. Compendium, Stockholm, 1999.

A Examples of analysis of accidental collapse mechanisms

A.1 General assumptions

In the design of alternative load-bearing systems it is possible to take advantage of large displacements and a ductile behaviour. For such a system the resistance can be expected to be considerably affected by dynamic effects during the transition to the alternative mode of action, and the non-linear behaviour of the strained connections. In an appropriate model for the design and analysis these effects must be considered. A simplified approach for such analysis was proposed by Engström (1992) and is presented in the following. The model is applied on alternative bridging systems where the resistance is determined by the action of tie connections loaded mainly in tension. However, the basic principles can be adopted also in the analysis of other types of collapse mechanisms where the deformations are localised to ductile connections, e.g. joint slip mechanisms.

In order to simplify the analysis of the collapse mechanism the following assumptions are made:

1) The supporting member is assumed to be removed instantly due to the accidental action.
2) At the support removal the collapse mechanism is assumed to be loaded by gravity forces only, i.e. the weight of the elements and dead loads.
3) The elements under displacement are assumed to be perfectly rigid.
4) In a unit of several interacting elements the intermediate connections are assumed to be perfectly rigid.
5) The resistance of the bridging system depends only on the action of certain critical connections that are strained during the displacement of the system. In the initial state when the support is removed these connections are assumed to be unstrained.

The gravity forces on the system are represented by the resultant $Q = m \cdot g$ acting in the centre of gravity. The actual position of the system is determined by the displacement a_q of the centre of gravity and a rotation φ, where a_{qz} is the vertical component of the displacement. By means of the assumptions 3) and 4) it is possible to find a simple geometrical relationship between the displacement a_{qz} of the system and the displacements w_i of the ductile connections. For each tie connection i the behaviour is described by a characteristic load-displacement relationships $N_i(w_i)$, see Section 7.4.1.

Immediately after the support removal there is no resistance against displacement, since the ductile connections are unstrained (assumption 5). Consequently, the system is under acceleration. The bridging effect of the alternative can be regarded as a resistance R, defined as the ability to balance a force acting in the gravity centre. The resistance can be defined as static or dynamic. The static resistance varies with the displacement and can be described by a resistance function $R_{stat}(a_{qz})$ that depends on the load-displacement relationships of the ductile connections and the geometry and displacement of the system.

For a certain displacement a_q and rotation φ of the moving system the condition of energy equilibrium yields

$$\frac{m}{2}\left(\frac{da_q}{dt}\right)^2 + \frac{I_m}{2}\left(\frac{d\varphi}{dt}\right)^2 = m \cdot g \cdot a_{qz} - \sum_i \int_0^{w_i} N_i(w_i)\,dw_i \qquad \text{(A-1)}$$

where I_m = mass-moment of inertia

Here the two terms at the left side express the kinetic energy W_k due to translation and rotation respectively. The first term on the right side expresses the release of potential energy and the last term the absorbed strain energy of the ductile connections. In order to obtain a deflected state of equilibrium, the motion must cease entirely. At this state the kinetic energy has the value $W_k = 0$ and the maximum values of the vertical displacement $a_{qz,max}$ of the gravity centre and of the connection displacements $w_{i,max}$ are assumed to be reached. Hence, a necessary condition for a deflected state of equilibrium can be expressed as

$$Q \cdot a_{\mathrm{qz,max}} = \sum_i \int_0^{w_{\mathrm{i,max}}} N_{\mathrm{i}}(w_{\mathrm{i}})\, dw_{\mathrm{i}} \tag{A-2}$$

where $a_{\mathrm{qz,max}}$ = the vertical displacement of the driving force when the downward motion ceases
$w_{\mathrm{i,max}}$ = corresponding displacement of connections *i*

The strain energy of the tie connections can be expressed by means of the relative strain energy capacity as

$$\xi(w) = \frac{W_{\mathrm{int}}(w)}{N_{\mathrm{u}} \cdot w} \tag{A-3}$$

where $W_{\mathrm{int}}(w) = \int_0^w N(w)\, dw$

Hence, the condition in eq. (A-2) of energy equilibrium can also be expressed as

$$Q \cdot a_{\mathrm{qz,max}} = \sum_{\mathrm{i}} \xi_{\mathrm{i}}(w_{\mathrm{i,max}}) N_{\mathrm{i,u}} \cdot w_{\mathrm{i,max}} \tag{A-4}$$

When the motion ceases the system is probably not in static equilibrium. In addition to eq. (A-4) the following condition must be fulfilled for the state of maximum displacement.

$$R_{\mathrm{stat}}(a_{\mathrm{qz,max}}) \geq m \cdot g \tag{A-5}$$

If the static resistance at this maximum displacement exceeds the driving force, the system will start to move upwards and a deflected state of equilibrium is found after some cycles of mainly elastic deformations. When eq. (A-5) is not fulfilled the assumed state of displacement is not the correct one. This may happen in systems with several interaction tie connections, if some of the connections fail during the displacement.

By means of the conditions in eqs. (A-4) and (A-5) it is possible to check whether a deflected state of equilibrium is possible to obtain for a certain assumed collapse mechanism. Hence, the dynamic resistance R_{dyn} of the bridging system can be determined as the maximum driving force $Q = m{\cdot}g$, which can be bridged in case of an instant support removal. It appears from eq. (A-4) that the dynamic resistance must be related to a certain state of displacement, defined by the maximum vertical displacement $a_{\mathrm{qz,max}}$ of the gravity centre. The value of $a_{\mathrm{qz,max}}$ can be chosen with due regard to free space for displacements of the system, deformation capacities of the ductile connections. Accordingly, the dynamic resistance can be expressed as a function $R_{\mathrm{dyn}}(a_{\mathrm{qz,max}})$ of the maximum displacement that can be tolerated.

A.2 Identification of collapse mechanisms

Consider a wall element in an area just above a primary damage. An alternative load-bearing system can be obtained by cantilever action of this wall element. The cantilever system is formed immediately at the accidental removal of the support. The dead weight of the wall element and dead load on it, for instance from an adjacent floor, are represented by the resultant force Q that results in sectional forces $V = Q$ and $M = Q{\cdot}e$ at the adjacent vertical joint, see Fig. A-1. The shear force is resisted by the shear capacity of the vertical joint. The moment is resisted by a force couple, tensile force in a horizontal tie connection at the top of the wall element and the corresponding compressive force across the bottom part of the vertical joint. Depending on the resistance of the respective joint

connections, all connections remain in the elastic stage or plastic displacements are obtained. In case of an entirely elastic response, a collapse mechanism is not developed. If a plastic stage is reached, the collapse mechanism can be described as a joint slip mechanism, a rotation mechanism or a combined slip-rotations mechanism, see Fig. A-1.

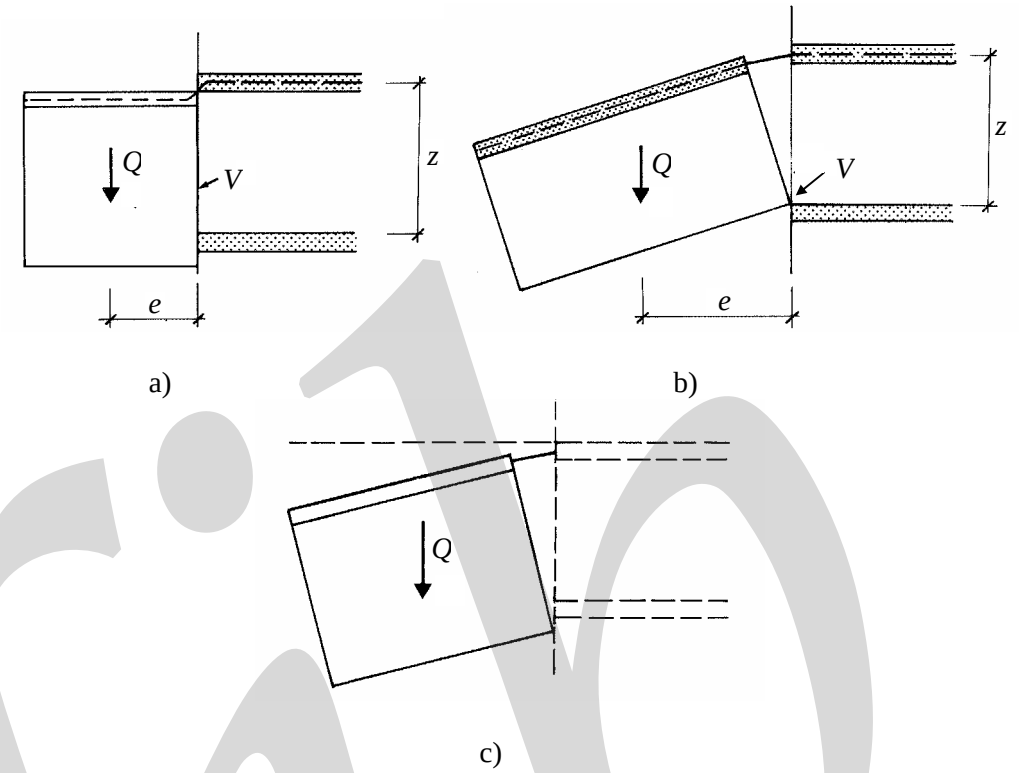

Fig. A-1: Examples of collapse mechanisms for a cantilevering wall element above a damaged area, a) joint slip mechanism, b) rotation mechanism, c) combined slip-rotation

The connection at the vertical joint is assumed to have a non-linear response in shear, characterized by the shear-slip relationship $V_R(s)$. Up to the yield capacity V_y the behaviour is assumed to be ideally linear elastic. The limit of elasticity is reached for a joint slip s_y. Then an elastic response can be expected if

$$V < \frac{V_y}{2}$$

The reduction by 2 follows from the condition of energy equilibrium in eq. (A-2), where $N(w)$ and w are replaced by $V_R(s)$ and s, and with the maximum joint slip limited to $s_{max} = s_y$. Concerning the bending moment transfer, a condition for an elastic response can be expressed accordingly.

$$M < \frac{M_y}{2}$$

Conditions for various possibilities of collapse mechanisms are put together in Table A-1. For other bridging systems alternative collapse mechanisms can be evaluated in similar ways.

If a precast wall element at the edge of a precast multi-storey wall is totally destroyed by accident, the damaged area can be bridged by cantilever action. Depending on the shear resistance at the horizontal joint interfaces, the wall elements above the damage may interact as a combined multi-storey cantilever, as in Fig. A-2 a, or individual cantilevers are formed by the wall elements at each floor as in Fig. A-2 b. The assumption of no shear slip (plastic displacement) or no shear transfer in

the horizontal joints can be considered as two extreme cases. It is assumed that the principle, which is exemplified in Table A-1, can be used to distinguish the two mechanisms.

Expected collapse mechanism	Conditions
Elastic response	If $V < V_y/2$ and $M < M_y/2$
Joint slip mechanism	If $V > V_y/2$ and $M < M_y/2$
Rotation mechanism	If $V < V_y/2$ and $M > M_y/2$
Combined slip-rotation mechanism	If $V > V_y/2$ and $M > M_y/2$

Table A-1: Conditions for various possibilities of collapse mechanisms for cantilever systems, see Fig. A-1

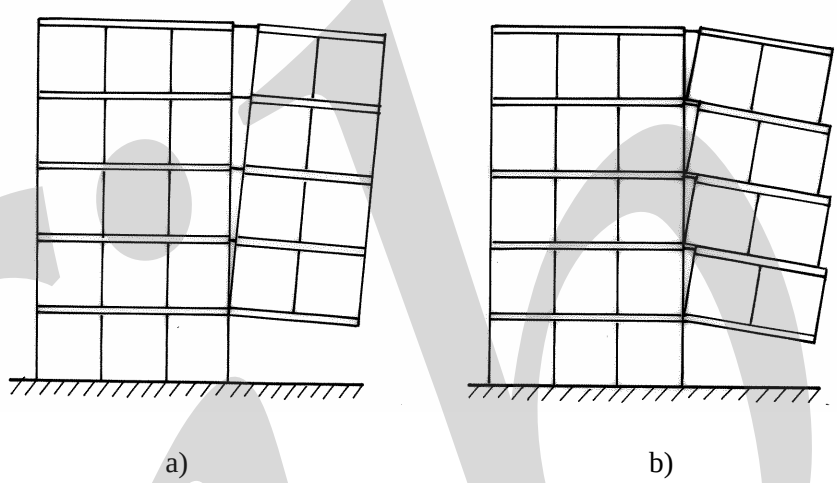

Fig. A-2: Possible rotation mechanisms after damage in a multi-storey precast wall, a) composed multi-storey cantilever, b) individual cantilevers at each floor

According to Fintel et al. (1976), the expected behaviour of the rotation mechanism is in practice somewhere in between these two extreme cases, which give lower and upper bounds to the resistance of the tie connections.

If the shear capacity of the lower joint interface is insufficient to keep the integrity of the system, a collapse mechanism with combined rotation and shear slip in the horizontal joint can be expected. This behaviour has been observed in tests reported by Odgård (1976), see Fig. A-3. In such a case the present model for rotation mechanisms, presented in Section A.3 is not applicable.

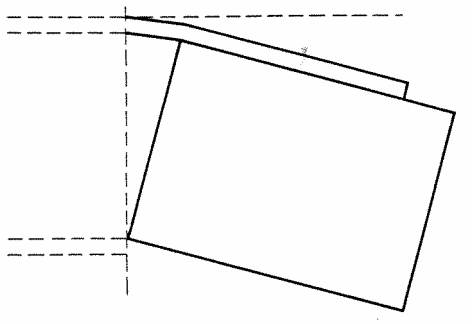

Fig. A-3: Combined collapse mechanism with rotation and joint slip in the horizontal joint, according to Odgård (1976). The present method for analysis of rotation mechanisms is not applicable

A.3 Rotation mechanisms – cantilever action

Consider a pure rotation system like the one illustrated in Fig. A-4. For a small rotation φ of the pure rotation mechanism, the displacement of a tie connection *i* can be expressed approximately as

$$w_i \approx l_i \cdot \varphi \tag{A-6}$$

where l_i = radial distance between the rotation axis and tie connection *i*

and the vertical displacement of the driving force as

$$a_{qz} \approx l_{qx,0} \cdot \varphi \tag{A-7}$$

where $l_{qx,0}$ = horizontal projection of the radial distance between the rotation axis and the driving force *Q* in the undeflected system

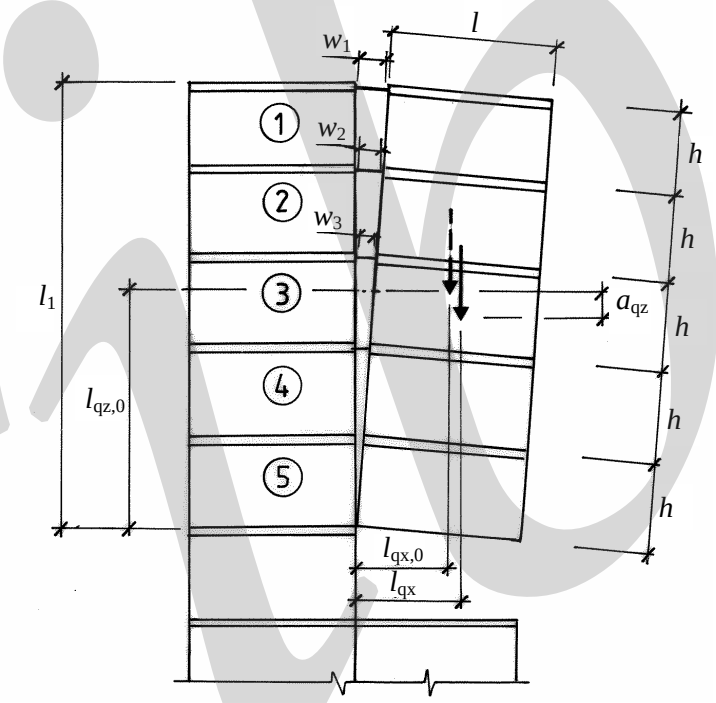

Fig. A-4: Rotation mechanism for a multi-storey wall cantilever above a local damage

As follows from eqs. (A-6) and (A-7) there is a simple geometric relationship between the vertical displacement of the driving force and the displacement of each tie connection.

$$w_i \approx \frac{l_i}{l_{qx,0}} a_{qz} \tag{A-8}$$

For plane cantilevers with a depth to length ratio of $h/l \leq 2$ this expression gives satisfactory accuracy for rotations $\varphi \leq 0{,}3$ rad. For a ratio $h/l = 10$ the rotation should be limited to about $\varphi \leq 0{,}03$. These conditions are normally satisfied for applications in ordinary building structures and also in the case of multi-storey cantilevers.

For a certain small rotation φ of the multi-storey cantilever the condition of static equilibrium yields

$$Q \cdot l_{qx} = \sum_i N_i(w_i) \cdot l_i$$

where l_{qx} = actual horizontal distance between the rotation axis and the driving force Q
w_i is determined by (A-6)

The static resistance of the cantilever system expresses the ability of the system to balance a driving force in the centre of gravity. Since the tie forces develop with the rotation, the static resistance varies with the rotation and can be expressed as a function of the vertical displacement of the driving force as

$$R_{stat}(a_{qz}) = \frac{1}{l_{qx}} \sum_i N_i(w_i) \cdot l_i \tag{A-9}$$

For estimation of the dynamic resistance it is convenient to introduce a formal value of the maximum static resistance in the undeflected state. It is obtained from eq. (A-9) by replacing the actual tensile forces N_i with the tensile force capacity $N_{i,u}$ of each tie connections independently of the actual displacements, and l_{qx} by $l_{qx,0}$.

$$R_{max} = \frac{1}{l_{qx,0}} \sum_i N_{i,u} \cdot l_i = \sum_i R_{max,i} \tag{A-10}$$

where $R_{max,i}$ = contribution to R_{max} from tie connection i

This value is 'formal' since the tie connections are contributing with maximum capacities simultaneously and without any displacement of the cantilever system. In the real system the tie connections may rupture one after the other depending on their locations and deformation capacities.

For a certain tolerable value of the maximum displacement $a_{qz,max}$ of the cantilever system the corresponding dynamic resistance $R_{dyn}(a_{qz,max})$ can be determined by means of the energy equilibrium in eq. (A-4).

$$Q \cdot a_{qz,max} = \sum_i \xi_i(w_{i,max}) N_{i,u} \cdot w_{i,max} \tag{A-11}$$

where $w_{i,max}$ is determined by eq. (A-8) for $a_{qz} = a_{qz,max}$

Eq. (A-11) expresses the maximum load Q that can be bridged by cantilever action in case of a sudden support removal. This is the dynamic resistance of the system. Hence, the dynamic resistance is a function of the vertical displacement $a_{qz,max}$ that is used to slow down the motion

$$R_{dyn}(a_{qz,max}) = \sum_i \xi_i(w_{i,max}) \frac{l_i}{l_{qx,0}} N_{i,u} \tag{A-12}$$

or by means of eq. (A-10)

$$R_{dyn}(a_{qz,max}) = \sum_i \xi(w_{i,max}) R_{max,i} \tag{A-13}$$

Hence, the dynamic resistance can be regarded as a reduced value of the maximum static resistance according to eq. (A-10), where the contributions from the respective tie connections have been reduced by factors $\xi_i(w_{i,max})$. The relative strain energy will always, according to the definition in eq. (A-3), be less than or equal to 1. The actual value depends on to what extent the elongation capacity $w_{i,u}$ of the respective tie connections is used.

It is important to note that the displacements $w_{i,max}$ of the respective tie connections are related by the geometry of the system and should be determined for the same maximum rotation of the bridging system. It is convenient to carry out the analysis of a rotation mechanism according to the following steps:

1) Choice of maximum vertical displacement $a_{qz,max}$ of the driving force with due regard to free space for displacements and elongation capacities of the tie connections.
2) Calculation of the corresponding maximum displacements $w_{i,max}$ for the connections by means of eq.(A-8).
3) Calculations of the corresponding relative strain energy $\xi_i(w_{i,max})$ for the tie connections according to the relevant load-displacement relationships, see Section 7.2.
4) Calculation of the maximum static resistance R_{max}, formal value in the undeflected state, according to eq. (A-10)
5) Calculation of the dynamic resistance R_{dyn} by means of the condition of energy equilibrium in eq. (A-13).
6) Check of static equilibrium in the state of maximum displacement according to eq. (A-9).

This approach to analyse collapse mechanisms where tie connections are strained in the plastic range was confirmed by tests on precast floor specimens subjected to sudden support removal, see Fig. A-5, [Engström (1992)].

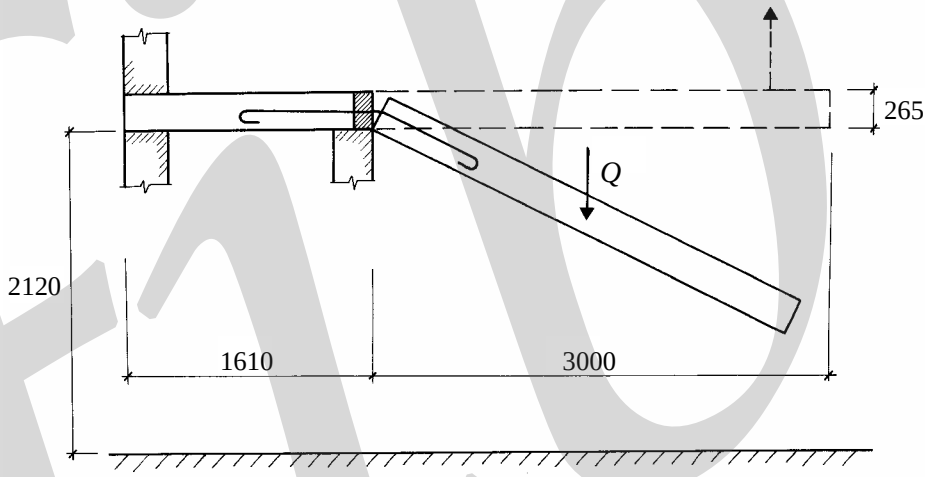

Fig. A-5: Tests on a collapse mechanism in a precast floor with various types of tie connections, according to Engström (1992)

Example A-1, two-wall system – cantilever action

A load-bearing precast wall consists of 6 wall elements arranged in three stories, see Fig. A-6. The possibility that one of the bottom elements is totally damaged by accidental action should be considered in the design against progressive collapse. Check if it is possible to bridge over the damaged area by cantilever action of the wall elements above the damaged area, either as separate wall cantilevers, or as a combined two-storey cantilever. Rotation mechanisms can be assumed. Each wall elements is loaded by the dead weight G = 80 kN and a uniformly distributed load from the floor q = 40 kN/m (gravity load). The horizontal joints are provided with two tie bars ϕ16 B500 anchored in concrete of strength class C20/25, 'good' bond conditions (the same connection as in Examples 7-1 and 7-5).

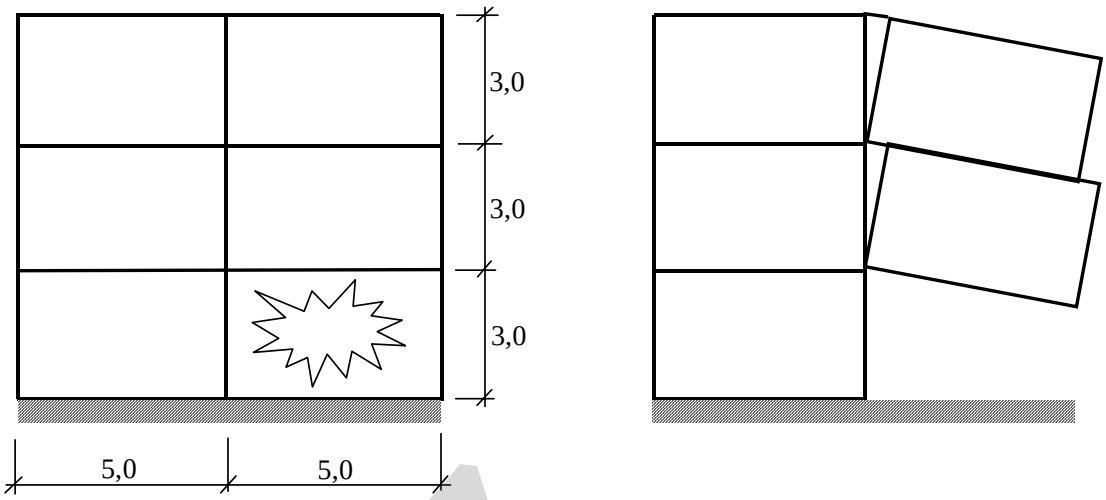

Fig. A-6: Analysis of alternative load-bearing system in a precast wall in Example A-1, a) location of damaged area, b) collapse mechanism of separate wall cantilevers

Separate wall cantilevers:

The resultant Q, considered as a gravity load, and its position (gravity centre) in the undeflected system is determined as, see Fig. A-7.

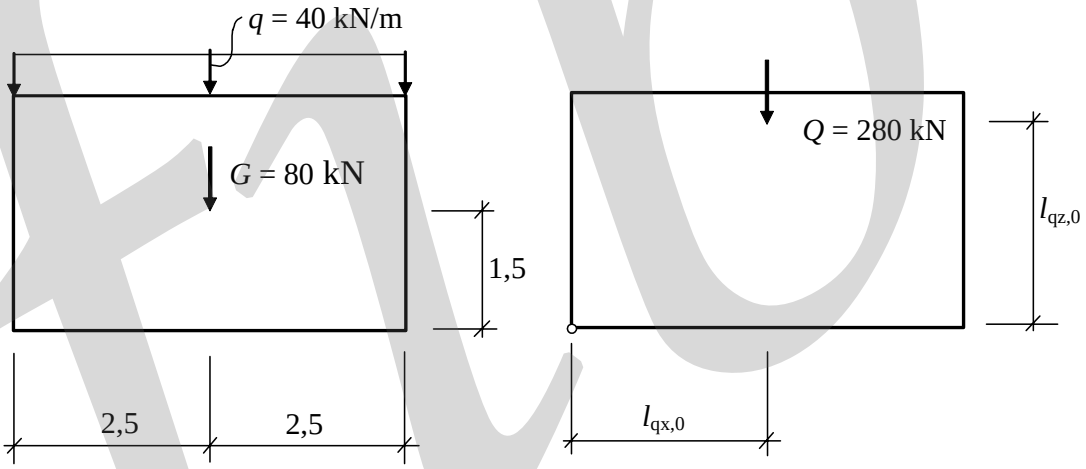

Fig. A-7: Resultant driving force Q and its location on single-storey cantilever

$$Q = G + q \cdot l = 80 + 40 \cdot 5{,}0 = 280 \text{ kN}$$

$$l_{qx,0} = 2{,}5 \text{ m}; \qquad l_{qz,0} = \frac{80 \cdot 1{,}5 + 40 \cdot 5{,}0 \cdot 3{,}0}{80 + 40 \cdot 5{,}0} = 2{,}57 \text{ m}$$

The tie connection across the vertical joint consists of two tie bars ϕ16 and has a total yield capacity of N_y = 202 kN and an ultimate capacity of N_u = 218 kN. The schematic load-displacement relationship of the tie connections has been determined according to Sections 7.2.3 and 7.4.1 (Example 7-5) and is shown in Fig. A-8. On basis of the schematic relationship the relative strain energy has been determined to $\xi(w_u) = 0{,}835$ for the maximum displacement, and $\xi(0{,}5w_u) = 0{,}670$ for half the maximum displacement, see Example 7-5.

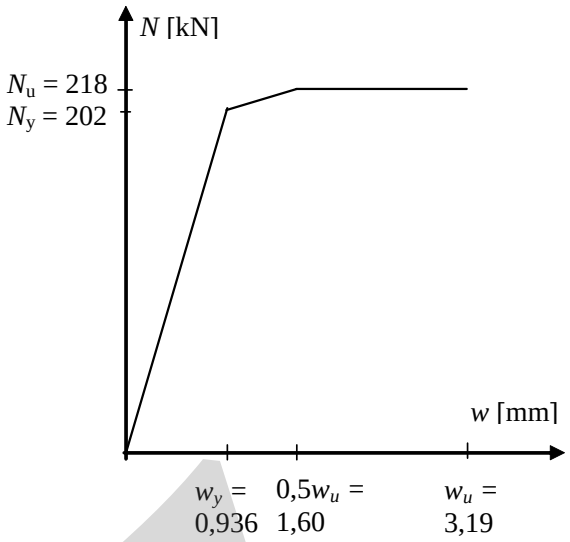

Fig. A-8: Schematic load-displacement relationship of the tie connections

The maximum rotation of the wall cantilevers is determined with regard to the deformation capacity of the tie connections. Hence, the maximum displacement of the tie connection is chosen as $w_{max} = w_u = 3{,}19$ mm. The corresponding rotation is shown in Fig. A-9 and the maximum vertical displacement of the gravity centre is calculated according to eq. (A-8)

$$a_{qz,max} = \frac{l_{qx,0}}{h} w_u = \frac{2{,}5}{3{,}0} 0{,}00319 = 0{,}00266 \text{ m}$$

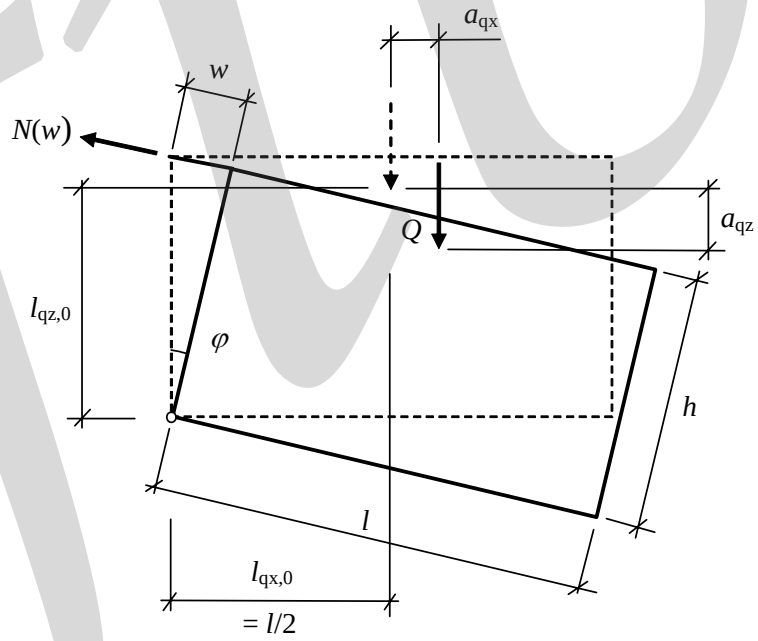

Fig. A-9: Assumed maximum rotation of the single-storey wall cantilever

The condition of energy equilibrium yields

$$Q \cdot a_{qz,max} = \xi(w_{max}) N_u \cdot w_{max}$$

where $\xi(w_{\max}) = \dfrac{W_{\text{int}}(w_{\max})}{N_{\text{u}} \cdot w_{\max}}$

$$R_{\text{dyn}}(a_{\text{qz,max}}) = \frac{w_{\max}}{a_{\text{qz,max}}} \xi(w_{\max}) N_{\text{u}} = \frac{0{,}00319}{0{,}00266} \cdot 0{,}835 \cdot 218 = 218 \text{ kN} < Q = 280 \text{ kN}$$

Accordingly, the dynamic resistance is insufficient. Alternatively the dynamic resistance can be determined by means of the formal value of the maximum static resistance according to eq. (A-13). The condition of static equilibrium yields

$$Q \cdot l_{\text{qx}} = N(w) \cdot h$$

where $l_{\text{qx}} \approx l_{\text{qx,0}} + l_{\text{qz,0}} \cdot \varphi = l_{\text{qx,0}} + l_{\text{qz,0}} \cdot \dfrac{w}{h}$

and the static resistance can be expressed as, compare with eq. (A-9),

$$R_{\text{stat}}(a_{\text{qz}}) = \frac{h}{l_{\text{qx,0}} + l_{\text{qz,0}} \dfrac{w}{h}} \cdot N(w)$$

Hence, the maximum static resistance, formal value, can be calculated as

$$R_{\max} = \frac{h}{l_{\text{qx,0}}} N_{\text{u}} = \frac{3{,}0}{2{,}5} \cdot 218 = 262 \text{ kN}$$

The dynamic resistance can then be calculated according to eq. (A-13) as

$$R_{\text{dyn}}(a_{\text{qz,max}}) = \xi(w_{\max}) \cdot R_{\max} = 0.835 \cdot 262 = 218 \text{ kN}$$

Combined 2-storey wall cantilever:

Each wall cantilever is loaded by its dead weight and the load from the adjacent floor. The resultant Q, considered as a gravity load, and its position (gravity centre) in the undeflected state is determined as, see Fig. A-10.

$$Q = 280 + 280 = 560 \text{ kN}$$

$$l_{\text{qx,0}} = 2{,}5 \text{ m}; \qquad l_{\text{qz,0}} = \frac{280 \cdot 2{,}57 + 280(2{,}57 + 3{,}0)}{2 \cdot 280} = 4{,}07 \text{ m}$$

The maximum rotation of the combined wall cantilever is determined with regard to the deformation capacity of the tie connections. In this case tie connection (1), the upper one, has twice as large displacement as tie connection (2). Hence, the maximum displacement of the top tie connection is chosen as $w_{1,\max} = w_{1,\text{u}} = 3{,}19$ mm. The corresponding rotation is shown in Fig. A-11.

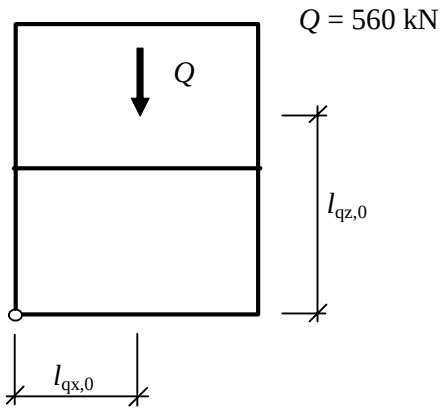

Fig. A-10: Resultant driving force Q and its location on combined two-storey cantilever

The compatibility condition yields

$$w_1 = \varphi \cdot l_1; \qquad a_{qz} = \varphi \cdot l_{qx,0}; \qquad a_{qx} = \frac{l_{qx,0}}{l_1} w_1$$

$$a_{qz,max} = \frac{l_{qx,0}}{l_1} w_{1,max} = \frac{2{,}5}{6{,}0} 0{,}00319 = 0{,}00133 \text{ m}$$

$$w_2 = 0{,}5 w_1; \qquad w_{2,max} = 0{,}5 \cdot w_{1,max} = 0{,}5 \cdot 0{,}00319 = 0{,}00160 \text{ m}$$

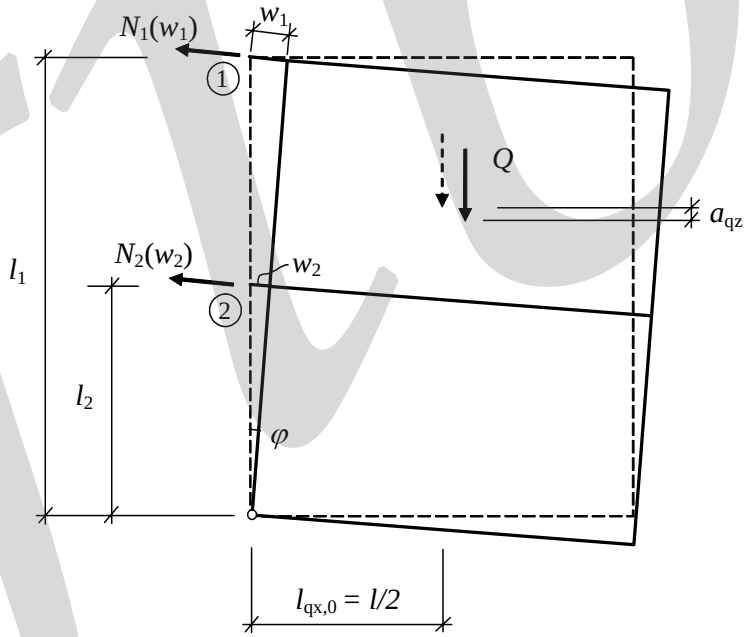

Fig. A-11: Assumed maximum rotation of the two-storey wall cantilever

In this case the condition of energy equilibrium yields

$$Q \cdot a_{qz,max} = \sum_i \xi(w_{i,max}) N_{i,u} \cdot w_{i,max}$$

$$R_{\mathrm{dyn}}(a_{\mathrm{qz,max}}) = \frac{1}{a_{\mathrm{qz,max}}}\left[\xi_1(w_{1,\mathrm{max}})N_{1,\mathrm{u}}w_{1\mathrm{max}} + \xi_2(w_{2,\mathrm{max}})N_{2,\mathrm{u}}w_{2\mathrm{max}}\right]$$

$$R_{\mathrm{dyn}}(a_{\mathrm{qz,max}}) = \frac{1}{0{,}00133}\left[0{,}835\cdot 218\cdot 0{,}00319 + 0{,}670\cdot 218\cdot 0{,}00160\right] = 612 \text{ kN}$$

> 560 kN

Alternatively the dynamic resistance can be determined by means of the formal value of the maximum static resistance according to eq. (A-13). This formal value is obtained by introducing the maximum tie forces $N_{\mathrm{i,u}}$ in the condition of static equilibrium for the undeflected state.

$$Q\cdot l_{\mathrm{qx},0} = N_{1,\mathrm{u}}\cdot l_1 + N_{2,\mathrm{u}}\cdot l_2 \qquad \text{(undeflected state)}$$

From this condition the respective contributions from the two tie connections to the maximum static resistance are distinguished.

$$R_{\mathrm{max}} = R_{\mathrm{max},1} + R_{\mathrm{max},2} = \frac{l_1}{l_{\mathrm{qx},0}}N_{1,\mathrm{u}} + \frac{l_2}{l_{\mathrm{qx},0}}N_{2,\mathrm{u}}$$

$$R_{\mathrm{max},1} + R_{\mathrm{max},2} = \frac{6{,}0}{2{,}5}218 + \frac{3{,}0}{2{,}5}218 = 523 + 262 \text{ kN}$$

$$R_{\mathrm{dyn}}(a_{\mathrm{qz}}) = \sum_{\mathrm{i}}\xi_{\mathrm{i}}(w_{\mathrm{i,max}})R_{\mathrm{max},1} = 0{,}835\cdot 523 + 0{,}670\cdot 262 = 612 \text{ kN}$$

When it is confirmed that the dynamic resistance is sufficient, the static resistance in the state of maximum deflection should be checked, see Fig. A-11. The conditions of static equilibrium yields

$$Q\cdot l_{qx} = \sum_{\mathrm{i}}N_{\mathrm{i}}(w_{\mathrm{i,max}})\cdot l_i$$

where $l_{\mathrm{qx}} \approx l_{\mathrm{qx},0} + l_{\mathrm{qz},0}\cdot\varphi = l_{\mathrm{qx},0} + l_{\mathrm{qz},0}\cdot\dfrac{w_{1,\mathrm{max}}}{l_1}$

and the static resistance can be expressed as, see eq. (A-9),

$$R_{\mathrm{stat}}(a_{\mathrm{qz,max}}) = \frac{1}{l_{\mathrm{qx},0} + l_{\mathrm{qz},0}\dfrac{w_1}{l_1}}\cdot\left[N_1(w_{1,\mathrm{max}})\cdot l_1 + N_2(w_{2,\mathrm{max}})\cdot l_2\right]$$

$$R_{\mathrm{stat}}(a_{\mathrm{qz,max}}) = \frac{1}{2{,}5 + 4{,}07\dfrac{0{,}00319}{6{,}0}}\left[218\cdot 6{,}0 + 218\cdot 3{,}0\right] = 784 \text{ kN} > Q = 560 \text{ kN}$$

When the rotation reaches its maximum value, the static resistance exceeds the driving force. This means that the rotation goes back until after some cycles in the elastic range static equilibrium is obtained.

From this example it is obvious that, with regard to the dynamic resistance, it is favourable to let the wall elements interact in a combined cantilever system. It is assumed that the formation of the collapse mechanism to a certain extent can be controlled by the design and detailing. To keep the integrity of the two-storey cantilever, the shear capacity of the horizontal joints must be sufficient to

avoid a joint separation by large horizontal shear slips. Furthermore, the to get a pure rotation mechanism, the shear capacity of the vertical joint must be sufficient to avoid a shear slip mechanism here. Accordingly, the connections at the horizontal and vertical joint should be designed so that they can remain within the elastic range, when the desired collapse mechanism is formed. The principles given in Table A-1 can be used for this design. Fig. A-12 shows the necessary shear capacities of the horizontal and vertical joints according to this principle

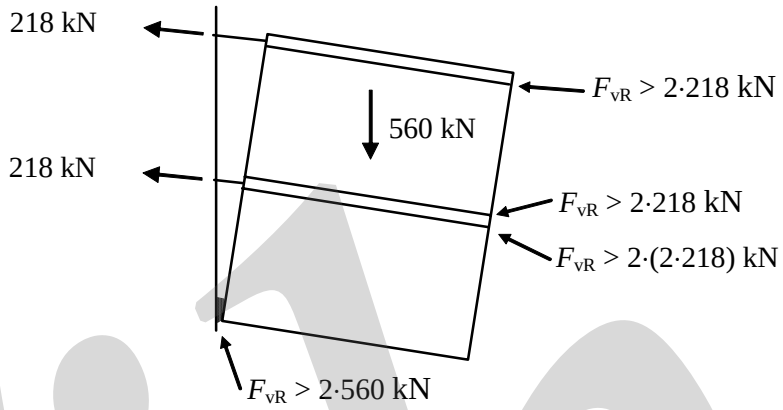

Fig. A-12: Demands on shear capacities on horizontal and vertical joints to get the desired collapse mechanism

Example A-2, single wall system with two tie connections – cantilever action

A corner of a prefabricated wall should be analysed with regard to a collapse situation where the bottom wall element is assumed to be totally damaged by accidental action, see Fig. A-13 a. The wall element above the damaged area is assumed to act as a cantilever in a rotation mode. The tie connections at the top of the element (connection 1) and mid depth (connection 2) contribute to the resistance of the alternative load-bearing system. The characteristic load-displacement relationships of the various connections are shown in Fig. A-13 b, c. Determine the dynamic resistance of the alternative load-bearing system, expressed as the maximum value of the gravity load Q that can be accepted in the centre of the wall elements.

The position of the driving force in the undeflected system is defined as

$$l_{qx,0} = 3{,}0 \text{ m}; \qquad l_{qz,0} = 2{,}25 \text{ m}$$

For a small rotation φ the condition of compatibility yields the following geometrical relations, see Fig. A-14.

$$w_1 = \varphi \cdot l_1; \qquad a_{qz} = \varphi \cdot l_{qx,0}; \qquad \Rightarrow \qquad a_{qz} = \frac{l_{qx,0}}{l_1} w_1; \tag{A-14}$$

$$w_2 = \varphi \cdot l_2; \qquad \Rightarrow \qquad w_2 = 0{,}5 \cdot w_1 \tag{A-15}$$

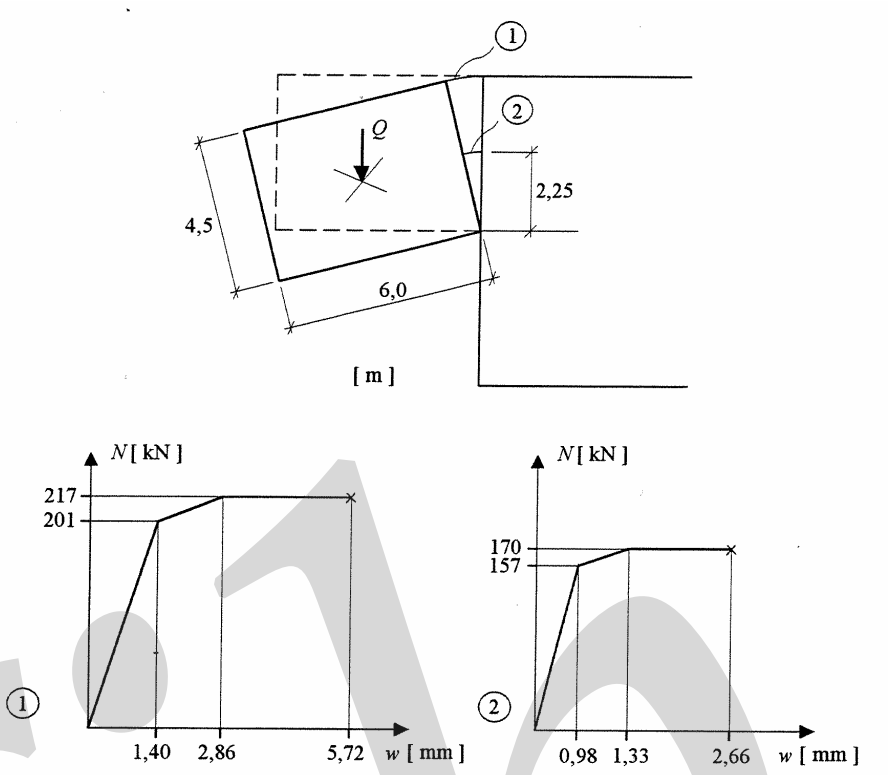

Fig. A-13: Analysis of an alternative load-bearing system in a precast wall in Example A-2, a) location of damaged area and collapse mechanism, b) characteristic load-displacement relationship of tie connection 1 (top), c) characteristic load-displacement relationship of tie connection 2 (mid depth)

For a small rotation of the collapse mechanism the condition of static equilibrium yields

$$Q \cdot l_{qx} = N_1(w_1) l_1 + N_2(w_2) l_2$$

where $l_{qx} = l_{qx,0} + a_{qx} = l_{qx,0} + l_{qz,0} \dfrac{w_1}{l_1}$

and the static resistance can be solved as

$$R_{stat}(a_{qz}) = \frac{N_1(w_1) \cdot l_1 + N_2(w_2) \cdot l_2}{l_{qx,0} + l_{qz,0} \dfrac{w_1}{l_1}} \tag{A-16}$$

The maximum static resistance, formal value, is found from eq. (A-16) by introducing the maximum tensile capacities in the undeflected state.

$$R_{max} = R_{max,1} + R_{max,2} = \frac{l_1}{l_{qx,0}} N_{1,u} + \frac{l_2}{l_{qx,0}} N_{2,u} \tag{A-17}$$

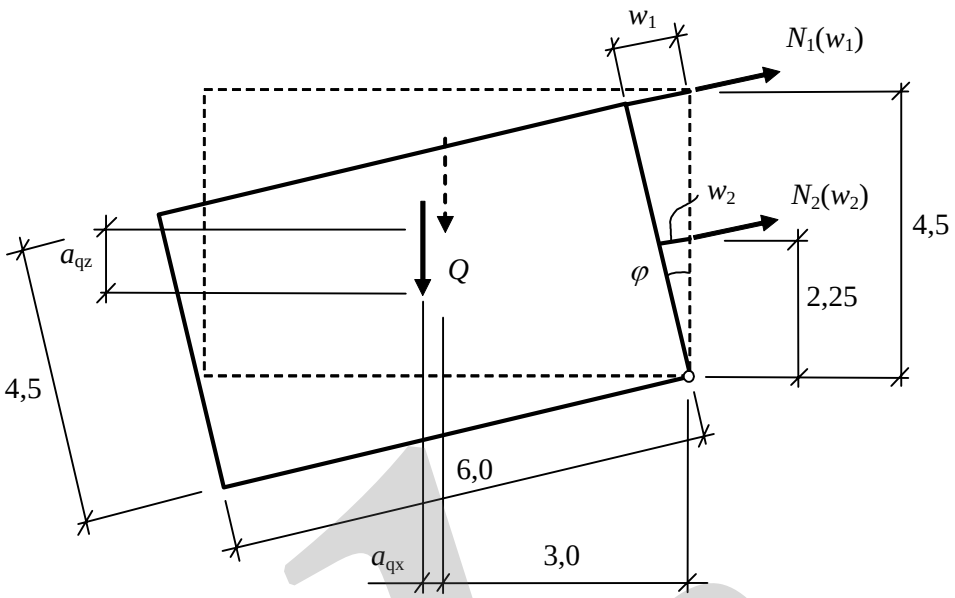

Fig. A-14: The collapse mechanism in a deflected state

Alternative 1, the full deformation capacity of tie connections 1 is used:

The state of maximum displacement is defined with regard to the elongation capacity of tie connection 1.

$$w_{1,\max} = w_{1,u} = 5{,}72 \text{ mm}$$

The corresponding maximum displacements in the collapse mechanism are found by (A-14) and (A-15).

$$a_{qz,\max} = \frac{3{,}0}{4{,}5} \cdot 0{,}00572 = 0{,}00381 \text{ m}$$

$$w_{2,\max} = 0{,}5 \cdot 0{,}00572 = 0{,}00286 \text{ m} \qquad > w_{2,u} = 0{,}00266 \text{ m}$$

This means that the full strain energy capacity of tie connection 2 will be used, but the connection fractures before the maximum displacement is reached. The condition of energy equilibrium yields

$$Q \cdot a_{qz,\max} = \xi_1(w_{1,\max}) N_{1,u} \cdot w_{1,\max} + \xi_2(w_{2,\max}) N_{2,u} \cdot w_{2,\max}$$

$$R_{dyn}(a_{qz,\max}) = \frac{\xi_1(w_{1,\max}) N_{1,u} \cdot w_{1,\max} + \xi_2(w_{2,\max}) N_{2,u} \cdot w_{2,\max}}{a_{qz,\max}}$$

The respective values of the relative strain energy are determined from the characteristic load-displacement relationships, compare with Example 7-5.

$$\xi(w) = \frac{W_{int}(w)}{N_u \cdot w}$$

$$\xi_1(w_{1,\max}) = \frac{\frac{1}{2} \cdot 201 \cdot 1{,}40 + \frac{1}{2}(201 + 217)(2{,}86 - 1{,}40) + 217(5{,}72 - 2{,}86)}{217 \cdot 5{,}72} = 0{,}859$$

$$\xi_2(w_{2,\max}) = \frac{\frac{1}{2}\cdot 157\cdot 0{,}98 + \frac{1}{2}(157+170)(1{,}33-0{,}98) + 170(2{,}66-1{,}33) + 0(2{,}86-2{,}66)}{170\cdot 2{,}86} = 0{,}741$$

$$R_{\text{dyn}}(a_{\text{qz,max}}) = \frac{0{,}859\cdot 217\cdot 0{,}00572 + 0{,}741\cdot 170\cdot 0{,}00286}{0{,}00381} = 374 \text{ kN}$$

Hence, to stop the downward motion within a displacement of the driving force of 3,81 mm, the driving force must not exceed 374 kN. For this maximum displacement the static resistance is checked by eq. (A-16).

$$R_{\text{stat}}(a_{\text{qz,max}}) = \frac{217\cdot 4{,}5 + 0}{3{,}0 + 2{,}25\dfrac{0{,}00572}{3{,}0}} = 325 \text{ kN}$$

Since tie connection 2 has fractured, this will not contribute to the static resistance in the state of maximum displacement. Even if the motion ceases at this state of deflection, the system is under acceleration and the motion will start again downwards.

Alternative 2, the full deformation capacity of tie connections 2 is used:

The state of maximum displacement is defined with regard to the elongation capacity of tie connection 2.

$$w_{2,\max} = w_{2,\text{u}} = 2{,}66 \text{ mm}$$

The corresponding maximum displacements in the collapse mechanism are found by eqs. (A-14) and (A-15).

$$w_{1,\max} = 2{,}0\cdot 0{,}00266 = 0{,}00532 \text{ m}$$
$$< w_{1,u} = 0{,}00572 \text{ m}$$

$$a_{\text{qz,max}} = \frac{3{,}0}{4{,}5}\cdot 0{,}00532 = 0{,}00355 \text{ m}$$

This means that the full strain energy capacity of tie connection 1 will not be fully used. The respective values of the relative strain energy are determined from the characteristic load-displacement relationships.

$$\xi_1(w_{1,\max}) = \frac{\frac{1}{2}\cdot 201\cdot 1{,}40 + \frac{1}{2}(201+217)(2{,}86-1{,}40) + 217(5{,}32-2{,}86)}{217\cdot 5{,}32} = 0{,}849$$

$$\xi_2(w_{2,\max}) = \frac{\frac{1}{2}\cdot 157\cdot 0{,}98 + \frac{1}{2}(157+170)(1{,}33-0{,}98) + 170(2{,}66-1{,}33)}{170\cdot 2{,}66} = 0{,}797$$

The dynamic resistance is found as

$$R_{\text{dyn}}(a_{\text{qz,max}}) = \frac{0{,}849\cdot 217\cdot 0{,}00532 + 0{,}797\cdot 170\cdot 0{,}00266}{0{,}00355} = 378 \text{ kN}$$

For this maximum displacement the static resistance is checked by eq. (A-16).

$$R_{\text{stat}}(a_{\text{qz,max}}) = \frac{217 \cdot 4{,}5 + 170 \cdot 2{,}25}{3{,}0 + 2{,}25\dfrac{0{,}00532}{3{,}0}} = 452 \text{ kN}$$

The static resistance exceeds the driving force and the assumed maximum displacement can be accepted. Hence, the maximum gravity load that can be bridged in case of a sudden support removal is 378 kN.

Example A-3, wall-floor corner system - cantilever action

A cross-wall structure damage at the corner of the building can also be bridged by a three-dimensional single-storey cantilever with a wall element and a floor span in interaction, see Fig. A-15. Here the cantilever system is assumed to rotate around the axis (3)-(4). The rotation is counteracted by tie connections at the locations (1) and (2) in the figure. The driving force is divided in two resultants, which are assumed to act in the centre of each unit, Q_1 in the wall unit (1) and Q_2 in the floor unit (2). The forces are related by factors α_i to a common load parameter.

$$Q_i = \alpha_i \cdot Q$$

For a small rotation φ the displacement of the tie connections are calculated as

$$w_1 = \frac{l_2\sqrt{l_1^2 + h^2}}{\sqrt{l_1^2 + l_2^2 + h^2}}\varphi$$

$$w_2 = \frac{h\sqrt{l_1^2 + l_2^2}}{\sqrt{l_1^2 + l_2^2 + h^2}}\varphi$$

and the vertical displacement of the driving forces

$$a_{q1z} = \frac{l_1 \cdot l_2}{2\sqrt{l_1^2 + l_2^2 + h^2}}; \qquad a_{q2z} = 0 \tag{A-18}$$

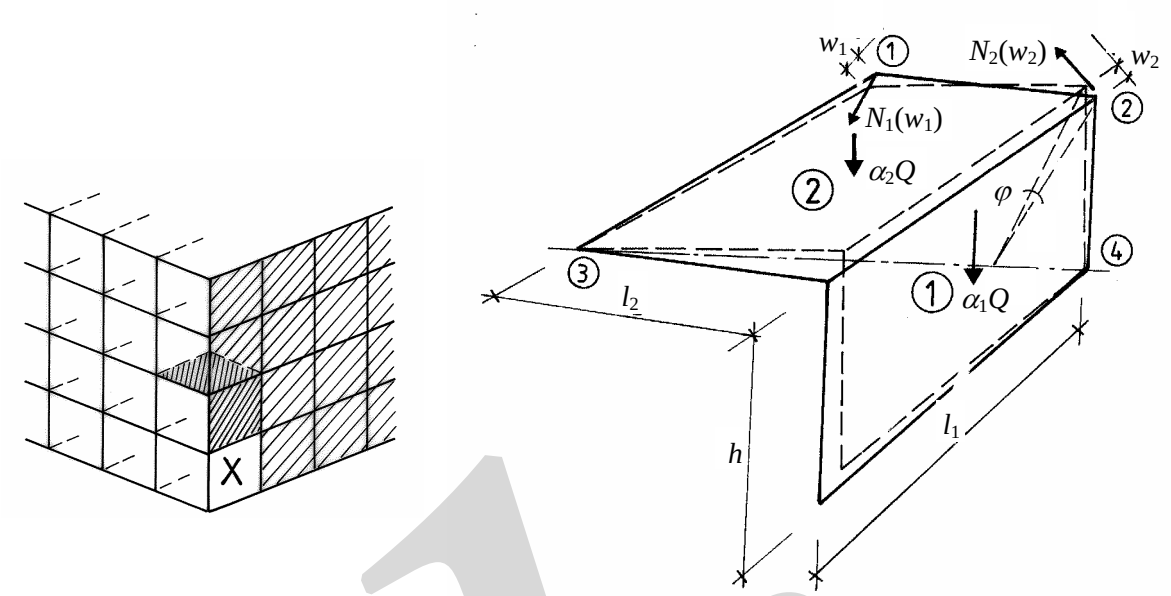

a) b)

Fig. A-15: Composed cantilevering system at the corner of a building. A wall panel and a precast floor interact in the system, a) location in building, b) model

The vertical displacement of the system is represented by one common parameter

$$a_{qz} = a_{q1z}$$

With $\varphi = w_1/h$ the condition of static equilibrium for the deflected state can be expressed as

$$\frac{l_1 \cdot l_2}{2}(\alpha_1 Q + \alpha_2 Q w_1) = N_1(w_1) l_2 \sqrt{l_1^2 + h^2} + N_2(w_2) h \sqrt{l_1^2 + l_2^2}$$

The static resistance with regard to the common load parameter Q is solved as

$$R_{stat}(a_{qz}) = \frac{2}{l_1 \cdot l_2(\alpha_1 + \alpha_2 w_1)}\left[N_1(w_1) l_2 \sqrt{l_1^2 + h^2} + N_2(w_2) h \sqrt{l_1^2 + l_2^2} \right] \quad \text{(A-19)}$$

The formal value R_{max} of the maximum static resistance in the undeflected state is now derived as

$$R_{max} = R_{max,1} + R_{max,2} = \frac{2}{l_1 \cdot l_2}\left[N_{1,u} l_2 \sqrt{l_1^2 + h^2} + N_{2,u} h \sqrt{l_1^2 + l_2^2} \right] \quad \text{(A-20)}$$

With the maximum static resistance determined the dynamic resistance is found as

$$R_{dyn}(a_{qz,max}) = \sum_i \xi_i(w_{i,max}) R_{max,i} \quad \text{(A-21)}$$

A.4 Floor - catenary action

In rotation mechanisms the bridging effect depends on the tensile capacity and the ductility of the tie connections but not directly on the elongation capacity. In alternative load-bearing systems where catenary or membrane action is used the resistance also depends on the displacement of the system.

Therefore, the resistance of such systems is directly affected by the elongation capacities of the tie connections. This is illustrated by the following example.

Consider a precast floor with equal spans. An internal support is totally destroyed by accidental action. In order to prevent debris loading the precast floor should be designed to form a bridging system by catenary action. According to the general assumptions, see Section A.1, the floor elements are considered to be perfectly rigid.

Immediately after the removal of the mid support the floor elements start to rotate at the adjacent supports. During the displacement several modes of action can be distinguished, arch action, beam action and catenary action.

In the following a model for the pure suspension mechanism will be presented, according to Engström (1992). The model is applicable on a longitudinal strip of a precast floor when effects in the transverse direction are neglected. Initial effects of arch or beam action are not considered in the model.

It is supposed that all three tie connections in the catenary system are of the same type with the same characteristics. For any state of deflection it is assumed that the three tie connections have the same tensile force and, because of the characteristic load-displacement relationships, the same elongations. For each floor element the weight and the dead load are represented by the resultant *Q*, which is assumed to be placed in the centre of the element. The state of deflection is defined by the vertical displacements a_{qz} of the driving force, see Fig. A-16.

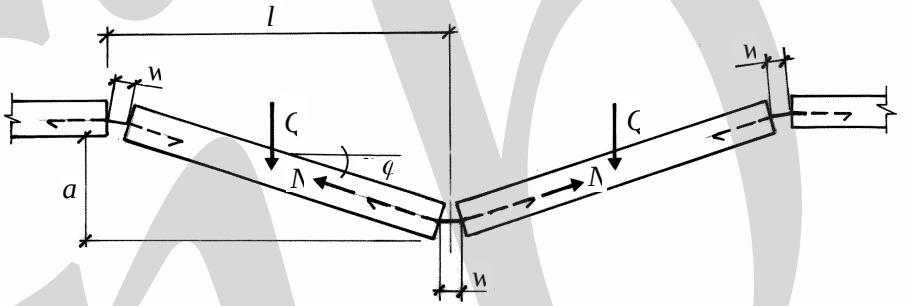

Fig. A-16: Catenary action in strip of a precast floor after removal of an interior support

For a certain displacement *w* of the three tie connections in the system the vertical displacement a_{qz} of the driving forces can be calculated approximately as

$$a_{qz} = \frac{\sqrt{3lw}}{2} \tag{A-22}$$

where l = length of floor elements

The condition of static equilibrium in a deflected state yields

$$Q \cdot \frac{l}{2} = N(w) \cdot 2a_{qz}$$

By means of (A-22) the static resistance can be expressed as

$$R_{stat}(a_{qz}) = 2N(w)\sqrt{\frac{3w}{l}} \tag{A-23}$$

As for rotation mechanisms it is now convenient to introduce a formal value of the maximum static resistance. However, as the resistance directly depends on the deflection this formal value should

now be related to the state of maximum displacement $a_{qz,max}$ for which the downward motion should stop.

$$R_{max}(a_{qz,max}) = 2N_u\sqrt{\frac{3w_{max}}{l}} \tag{A-24}$$

The strain energy of the deflecting floor depends on the elongations of the three tie connections in the system. The condition of energy equilibrium for the doubled span yields

$$2Qa_{qz,max} = 3\xi(w_{max})N_u w_{max}$$

By introducing (A-22) and (A-24) in this expression the dynamic resistance is obtained as

$$R_{dyn}(a_{qz,max}) = \frac{1}{2}\xi(w_{max})R_{max} \tag{A-25}$$

From (A-24) and (A-25) it is obvious that the dynamic resistance of the catenary system not only depends on the tensile capacity and the ductility of the tie connections, but also directly on the elongation capacity. When eq. (A-25) is compared with the corresponding expressions for rotation systems, eq. (A-13), it is observed that a factor 1/2 now is introduced. This can be considered as a response factor for the catenary system. Even if the tie connections would have an ideally plastic response, the static resistance of the catenary system increases linearly with increased displacements.

Example A-4, catenary action in precast hollow core floor

A strip of a precast hollow core floor is now analysed with the proposed model. The width is 1,2 m and the length of the elements is l = 6,0 m. Only the weight of the elements of 4,2 kN/m is considered. Thus, the driving force acting on each element is $Q = 6{,}0 \cdot 4{,}2 = 25{,}2$ kN. The floor elements are connected in the longitudinal direction by tie connections embedded in concrete of strength class C20/25. The mid-displacement is not allowed to exceed 3,0 m (free distance to the next floor). Various tie connections are examined.

Alternative 1, two ribbed tie bars ϕ16 B500, ductility class B:

This tie connection was examined in Examples 7-1 and 7-5 and it has the following characteristics

$N_y = 202$ kN $\qquad N_u = 218$ kN

$w_y = 0{,}936$ mm; $\qquad w_u = 3{,}19$ mm; $\qquad \xi(w_u) = 0{,}835$

The full deformation capacity of the tie connections is used, which means

$w_{max} = w_u = 3{,}19$ mm;

For this maximum elongation of the tie connections, the corresponding values of the maximum vertical displacement, the maximum static resistance (formal value) and the dynamic resistance are found according to eqs. (A-22), (A-24) and (A-25) as

$$a_{max} = 2a_{qz.max} = 2 \cdot \frac{\sqrt{3 \cdot 6{,}0 \cdot 0{,}00319}}{2} = 0{,}240 \text{ m}$$

$$R_{max} = 2 \cdot 218\sqrt{\frac{3 \cdot 0{,}00319}{6{,}0}} = 17{,}4 \text{ kN}$$

$$R_{dyn}(a_{qz,max}) = \frac{1}{2} \cdot 0{,}835 \cdot 17{,}4 = 7{,}26\,\text{kN}$$

This capacity is quite insufficient. It is obvious from eq. (A-24) that the dynamic resistance depends on the maximum displacement. Hence, tie connections with a high deformation capacity should be selected in this case.

Alternative 2, two ribbed tie bars ϕ16 B500, ductility class S:

This tie connection is similar to the one examined in Example 7-5, but the deformation capacity and the ductility are improved. The load-displacement relationship for one fully anchored tie bar is determined in accordance with Example 7-1.

f_{yk} = 500 MPa; $(f_u/f_y)_k$ = 1,15; E_s = 200 GPa; $\varepsilon_{suk} = 60 \cdot 10^{-3}$

Yield capacity: $N_y = f_{yk} \cdot A_s = 500 \cdot 10^6 \cdot 201 \cdot 10^{-6} = 101 \cdot 10^3\,\text{N}$

Tensile capacity (steel rupture): $N_u = 1{,}3 \cdot N_y = 1{,}3 \cdot 101 = 131\ \text{kN}$

The end-slip $s_{end,y}$ just before yielding starts is estimated according to eq. (7-4).

$$\tau_{b,max} = 2{,}5\sqrt{f_{cm}} = 2{,}5\sqrt{28} = 13{,}2\ \text{MPa}$$

where $f_{cm} = f_{ck} + 8\ \text{MPa} = 20 + 8 = 28\ \text{MPa}$

$$s_{end,y} = 0{,}288\left(\frac{16 \cdot (500 \cdot 10^6)^2}{13{,}2 \cdot 10^6 \cdot 200 \cdot 10^9}\right)^{0{,}714} + \frac{500 \cdot 10^6}{200 \cdot 10^9} \cdot 2 \cdot 16 \quad \Rightarrow$$

$$s_{end,y} = 0{,}388 + 0{,}080 = 0{,}468\ \text{mm}$$

where $s_{end,net} = 0{,}388$ mm < 1,0 mm OK

The ultimate crack width, just before rupture of the tie bar is estimated by eq. (7-11). First the ultimate extension of the plastic zone is determined by eq. (7-9).

$$l_{ty} = \frac{1{,}3 \cdot 500 \cdot 10^6 - 500 \cdot 10^6}{0{,}27 \cdot 13{,}2 \cdot 10^6} \cdot \frac{16}{4} = 168\ \text{mm}$$

$$s_{end,u} = 168 \cdot \left(0{,}5 \cdot 60 \cdot 10^{-3}\right) + 0{,}468 = 5{,}04 + 0{,}468 = 5{,}51\ \text{mm}$$

Hence, for the actual tie connection with two tie bars

$N_y = 2 \cdot 101 = 202\ \text{kN}$ $N_u = 2 \cdot 131 = 262\ \text{kN}$

The crack width is two times the end slip

$w_y = 2 \cdot 0{,}468 = 0{,}936\ \text{mm}$ $w_u = 2 \cdot 5{,}51 = 11{,}0\ \text{mm}$

The relative strain energy capacity is found as

$$\xi(w_u) = \frac{\frac{1}{2}202 \cdot 0{,}936 + \frac{202+262}{2}(5{,}51 - 0{,}926) + 262(11{,}0 - 5{,}51)}{262 \cdot 11{,}0} = 0{,}901$$

With this tie connection, when the full deformation capacity is utilised, the dynamic resistance is found as

$$a_{max} = 2a_{qz.max} = 2 \cdot \frac{\sqrt{3 \cdot 6{,}0 \cdot 0{,}011}}{2} = 0{,}481 \text{ m}$$

$$R_{max} = 2 \cdot 262 \sqrt{\frac{3 \cdot 0{,}011}{6{,}0}} = 38{,}9 \text{ kN}$$

$$R_{dyn}(a_{qz,max}) = \frac{1}{2} \cdot 0{,}901 \cdot 38{,}9 = 17{,}5 \text{ kN}$$

The dynamic resistance is still insufficient. However, the minor change of the ductility properties of the tie connection had a significant influence on the resistance, which was more than doubled.

Alternative 3, three plain tie bars ϕ16 with end hooks:

This tie connection was examined in Example 7-6 and it has the following characteristics

$N_y = 3 \cdot 54{,}3 = 163$ kN $\qquad N_u = 3 \cdot 62{,}4 = 187$ kN

$w_y = 1{,}46$ mm $\qquad w_u = 63{,}5$ mm $\qquad 0{,}5w_u = 31{,}75$ mm

$$\xi(w_u) = \frac{\frac{1}{2}163 \cdot 1{,}46 + \frac{187+163}{2}(31{,}75 - 1{,}46) + 187(63{,}5 - 31{,}75)}{187 \cdot 63{,}5} = 0{,}956$$

With this tie connection, when the full deformation capacity is utilised, the dynamic resistance is found as

$$a_{max} = 2a_{qz.max} = 2 \cdot \frac{\sqrt{3 \cdot 6{,}0 \cdot 0{,}0635}}{2} = 1{,}07 \text{ m}$$

$$R_{max} = 2 \cdot 187 \sqrt{\frac{3 \cdot 0{,}0635}{6{,}0}} = 66{,}6 \text{ kN}$$

$$R_{dyn}(a_{qz,max}) = \frac{1}{2} \cdot 0{,}956 \cdot 66{,}6 = 31{,}8 \text{ kN} > Q = 25{,}2 \text{ kN}$$

In this case the dynamic resistance is sufficient to stop the downward motion and prevent the collapse form spreading.

The example shows the influence of the deformation capacity of the tie connections in case of a catenary mechanism. It appears that alternative bearing by catenary action in a precast floor requires a considerable tensile capacity of the tie connections. However, even if a deflected state of equilibrium is not obtained, the energy absorption of ductile connections may be sufficient to prevent collapse of the next floor.